Investigating predation by the predatory bacterium *Bdellovibrio bacteriovorus* at the interface between predatory bacteria, pathogenic prey, and the host immune response

A thesis submitted to the University of Nottingham for the degree of Doctor of Philosophy

Callum Clark

Supervisors: Professor Liz Sockett &

Dr Jess Tyson

Funded by the Wellcome Trust
Antimicrobials & Antimicrobial Resistance
Doctoral Training Programme

Abstract

Bdellovibrio bacteriovorus is a Gram-negative predatory bacterium that is able to prey upon and kill other Gram-negative bacteria, including bacterial pathogens that are resistant to antibiotic treatment. This suggests that *B. bacteriovorus*, or components of its predatory lifecycle, may be of great use in the continued treatment of bacterial infection, as novel antimicrobial therapies. However, before *B. bacteriovorus* can be applied to these scenarios, we must understand how the eukaryotic immune response may alter the efficacy of predation.

B. bacteriovorus has been postulated to be less immunogenic than other Gram-negative bacteria, in part due to its outer membrane containing a modified Lipid A head group that reduces detection by host pattern recognition receptors and interactions with bactericidal antimicrobial proteins, two key components of the innate immune response. However, the interactions between *B. bacteriovorus* and the cells of the immune system have still not been fully characterised.

In the first part of my PhD, I aimed to characterise how predation by *B. bacteriovorus* proceeds, and may be affected, within a host. Building on previous lab findings, I discovered that, in the context of large changes in transcription, transcriptional upregulation of some major surface components by the pathogen *Serratia marcescens,* whilst in human serum, led to resistance to predation. The main outer membrane component implicated in this resistance period was Lipid A, which had been modified with an L-Ara(4)N sugar to reduce its negative charge. Disruption of this LPS modification pathway, through directed gene deletion, did delay the development of resistance to predation in serum, but did not abrogate it entirely, suggesting that other surface components or factors also contribute to this resistance phenotype. This work demonstrates that host environmental factors can modify Gram-negative pathogen behaviour and therefore impact the efficacy of predation by *B. bacteriovorus.*

In the second part of my PhD, I focus on the interactions between *B. bacteriovorus* and macrophages, which are a key component of the mammalian innate immune system, asking what molecular factors allow *B. bacteriovorus* to temporarily survive for approximately 24 hours inside macrophages. This is relevant to understanding and enhancing the efficacy of predation within a human host.

Focusing on genes related to oxidative stress tolerance, that are involved in prolonging the survival of pathogens within the phagosomes of macrophages, I asked whether these genes contribute to the temporary tolerance of phagosomal conditions, extending *Bdellovibrio* survival, and whether these genes also play a role in tolerating the oxidative stresses experienced by *Bdellovibrio* throughout predation. I discovered that two alkyl hydroperoxide reductase proteins and a "survival associated" chaperone protein were essential for predation, whilst a single superoxide dismutase (SodC) enzyme contributed to both predation and macrophage survival.

Finally, I take a wider view on how *Bdellovibrio* is perceived and processed by macrophage of the host immune response asking, through investigation of the macrophage transcriptional response to engulfed *Bdellovibrio*. whether *Bdellovibrio* is recognised, phagocytosed, and destroyed in a similar way to well-characterised Gram-negative bacterial pathogens. I discovered that, although *Bdellovibrio* does induce a proinflammatory immune response and is subsequently killed by host macrophage after 24-48 hours, no discernible transcriptional response is initiated towards the LPS of *Bdellovibrio*, in stark contrast to the detection of other Gram-negative bacteria, where LPS detection forms a cornerstone of the initial immune response. This may, in part, explain the relatively low immunogenicity of *Bdellovibrio* seen in animal studies. This understanding can inform future applications of *B. bacteriovorus* as a novel antimicrobial therapy within a human host.

The work presented in this thesis has further characterised the immune response to *Bdellovibrio* and informs us on potential considerations of, and barriers to, predation within a human host.

Acknowledgements

What brought me to C15, and the University of Nottingham, was the project, but what kept me here was the people.

Firstly, I would like to thank Professor Liz Sockett for her professional and personal support throughout my PhD and (no doubt!) beyond! I have found my PhD project fascinating, so thank you for allowing me to investigate the niche and novel, whilst still giving me the freedom to stray into the dark side that is immunology every once in a while! The opportunities you have given me throughout this PhD far surpass anything that I could have expected.

Jess, I couldn't have done this without you! But, more than that, I **wouldn't** have done this without you! A PhD is a scientific and a personal journey in equal measure, and both have been enormously shaped by you! The last four years have been a pleasure and a privilege that I will never forget! Thank you for never letting me lose sight of The Goal.

Rob, you are undoubtably the workhorse that keeps the lab running, without which I would not have been able to have achieve half as much as I did! But you have always been much more than that! During the COVID pandemic, I (like everyone else) really struggled at times. Sometimes, even finding the motivation to go into work was a battle. Seeing you and Jess every day and knowing that however I felt and whatever I needed, both of you would always be there to help me, really gave me the lift that I needed! Your ability to open a bar of chocolate and not consume it instantly, still amazes and eludes me (How?!?), but this does also mean that you were always happy to share on the occasions that I have been furiously typing away in the office. Thank you!

Paul, thank you for all of your cloning expertise and macrophage whispering. In a room full of microbiologists, having an immunologist at my side is what made this project possible from the start!

Emma, seeing someone in the same position as me, working and persevering to get everything they could out of their PhD, it was the target that I wanted and needed to aim for. The amount that you achieved will always be a testament to the amazing scientist that you are.

Dr Carey Lambert has contributed a wealth of scientific support and knowledge throughout my PhD. The microscopy and predation assays that have formed a significant part of my PhD project would not have been possible without his support. Beyond that, we have spent many years chucking ourselves around a badminton court (and regretting it the day after)! No matter how bad a day we may have had in the lab, or how busy we were, the time spent on those courts, and the people I have met because of it, will always be a personal highlight of my PhD.

I'd like to thank the C3 Prep Room Technicians, Julie and Emma, for their technical support. The stability of a functional lab is invaluable. However, they have also been a cherished support throughout all my dumb days and glum days, and have always been there for a chat, leaving me happier than when I arrived. Thank you!

During my PhD, I had the privilege of supervising 3 amazing MSci students. Laura, Evelyn and Syawal each taught me something different about the person I am, and the scientist I wish to become. They also bolstered the importance of communication, and diverse ways of thinking, and how scientific research would be worthless without it. Their part in my PhD journey will always remain with me.

This PhD was funded by the Wellcome Trust Antimicrobials and Antimicrobial Resistance Doctoral Training Programme (Studentship Number: 220105/Z/20/Z, Programme Number: 108876/Z/15/Z). I would like to thank the Wellcome Trust for funding this project, and for their wider academic and scientific support throughout.

COVID impact statement

My research, like every researcher, was significantly impacted by the COVID-19 pandemic. It reduced my ability to collect data and limited the analysis I could perform on data already collected, it limited my access to lab time, resources, and individual people's expertise, due to working on opposing shift patterns or having to isolate from others, whose health were more vulnerable.

Regarding the work presented in Chapter 3, I had only been working on this project since October 2019, prior to the COVID pandemic in March 2020. Prior to lockdown, I had constructed gene deletion mutants for genes of interest and had gathered preliminary data on how gene deletion would impact susceptibility to predation within human serum. Due to the COVID-19 pandemic, I was not able to continue with this project owing to further batches of human serum not being available. Due to this, and the time lost during the pandemic, the decision was made by my primary supervisor and I to not continue with this project and to re-focus our efforts on the projects discussed in Chapters 4 and 5. The intended work would have characterised the gene deletion mutants, and their susceptibility to predation within human serum further, with different types of sera. It would also have characterised the difference in composition between differing batches of human sera further and would have aligned these changes in composition with any differences in phenotype seen.

Regarding the work presented in Chapters 4 and 5, this work would have been followed up further, if it was not for the time lost during the COVID pandemic, whereby the genes of interest identified in Chapter 5 would have been followed up with further gene deletions and fluorescent tagging experiments (as described in Chapter 4). Further method development to test protein expression throughout macrophage occupation would also have been performed, further informing me of the relative roles and importance of each of these protein candidates.

To mitigate against the impacts of COVID, a significant part of my thesis is bioinformatic analysis of the transcriptional expression of bacterial predator and human macrophage, in response to one another (detailed in Chapter 5). This allowed me to continue working if another pandemic or lockdown was imminent. I aimed to experimentally validate the main emerging themes from this bioinformatic analysis, experimentally, but this was curtailed by the COVID-19 pandemic. Although further work to characterise the roles of these genes in *Bdellovibrio* interactions with macrophage would have been desirable, I believe I have still mitigated for the impacts of COVID as best as I could, with the timeframes and resources available.

Within this thesis is a summation and celebration of the work I could perform within my PhD.

Table of Contents

Table of Figures

Chapter 3

Chapter 4

Table of Tables

Chapter 1: Introduction

1.1. Thesis scope

This thesis concerns the natural invasive predator of Gram-negative bacterial pathogens, *Bdellovibrio bacteriovorus* HD100. This predatory bacterium has been used in some *in vivo* experimental treatments of Gram-negative infections inside animal hosts. In some of those studies, it was clear that the host immune system interacted with the predatory killing of pathogens by *Bdellovibrio*, and that *Bdellovibrio* could persist temporarily inside macrophages (1, 2).

My thesis has taken those studies further and mainly centres upon testing what proteins might allow *Bdellovibrio* to persist inside macrophages, whether they are associated with resisting oxidative stresses and whether such proteins have a dual role in surviving predatory invasion of live bacteria. I also test the surface epitopes of one pathogenic bacterium for *Bdellovibrio* recognition. Finally, I ask what transcriptional responses are induced in the macrophage by the presence of engulfed *Bdellovibrio*, using these to help understand whether an inflammatory or other response is mounted to the bacterial predator. These data illuminate how predatory bacteria will survive and succeed in reducing pathogen numbers in an animal host.

I will begin my thesis by a consideration of Gram-negative pathogens and how they interact with the mammalian host immune system to serve as a background and comparison to *Bdellovibrio bacteriovorus*, which are not pathogenic to animal hosts, but which can kill pathogens inside animal hosts.

1.2. Gram-negative pathogens

1.2.1. Burden of Gram-negative bacterial disease

Antimicrobial agents have been a vital part of human health for decades, both in their predominant role in the treatment of infectious disease and in enabling the implementation of surgical interventions for cancer treatment, organ transplantation and other medical interventions. However, the development and spread of antimicrobial resistance, combined with a decrease in the number of new antimicrobials that have been discovered, threatens this paradigm (3, 4). An increase in the dissemination of antimicrobial resistance threatens the health of individuals around the world (Figure 1.2.1), whilst also having a significant economic cost, through its impacts on the agricultural industry and food security, and the burden it places on healthcare systems. It is estimated that globally, 4.25 million people died of antimicrobial resistant infections in 2019, with 1.27 million of these deaths being attributable to antibiotic resistant bacterial infections (5, 6).

This number is estimated to rise to 10 million people by 2050 (5, 6), therefore new approaches to treating infectious disease and multidrug resistant infections are clearly needed. Amongst the greatest concern bacterially are the ESKAPE pathogens (*Enterococcus faecium, Staphylococcus aureus, Klebsiella pneumoniae, Acinetobacter baumannii, Pseudomonas aeruginosa* & *Enterobacter spp.*), where multidrug resistance, especially within a clinical setting, is particularly prevalent (7). There is therefore a desperate need for the development of novel antimicrobial agents to stem the tide of antimicrobial resistance and allow for the continued treatment of infection and other disease. The majority of these bacterial pathogens are Gram-negative bacteria, which are a great concern due to their high levels of resistance to antimicrobial agents, Therefore, the development of novel antimicrobial therapies that target Gram-negative bacteria, such as *Bdellovibrio* predation (8), are of great interest and importance.

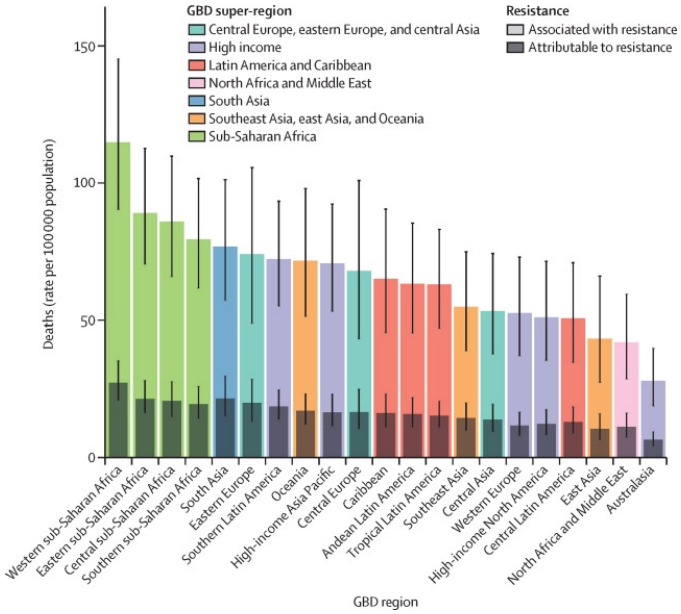

Figure 1.2.1: Rate of deaths attributed to, or associated with, bacterial antimicrobial resistance in 2019. Figure taken from Murray et al., 2022. Error bars show 95% uncertainty intervals.

My PhD studentship was funded by the Wellcome Trust, as part of the Antimicrobials and Antimicrobial Resistance Doctoral Training Programme. This programme aimed to support the research careers of the next generation of multidisciplinary scientists, supporting our research into the study of the molecular and chemical mechanisms of antimicrobial drugs, and how bacterial pathogens become resistant to them, whilst also measuring the impact and dissemination of antimicrobial resistance. Throughout my studentship, I have studied the interactions of the predatory bacterium *Bdellovibrio bacteriovorus* with the human host immune response, with the aim that characterising these interactions will assist in our understanding of how *B. bacteriovorus* may be used as a novel antimicrobial treatment of the future.

1.3. What is a Gram-negative pathogen?

Gram-negative bacteria are some of the main causative agents of antimicrobial resistant bacterial infections. The Gram-negative bacterial surface acts as the first contact between the bacteria and the host, or the environment. Understanding the components of the outer surface is critical as it contains many of the outer membrane proteins and components important for bacterial survival within hostile environments, virulence, and pathogenesis, as well as conferring antimicrobial and host immune resistance (Figure 1.3.1).

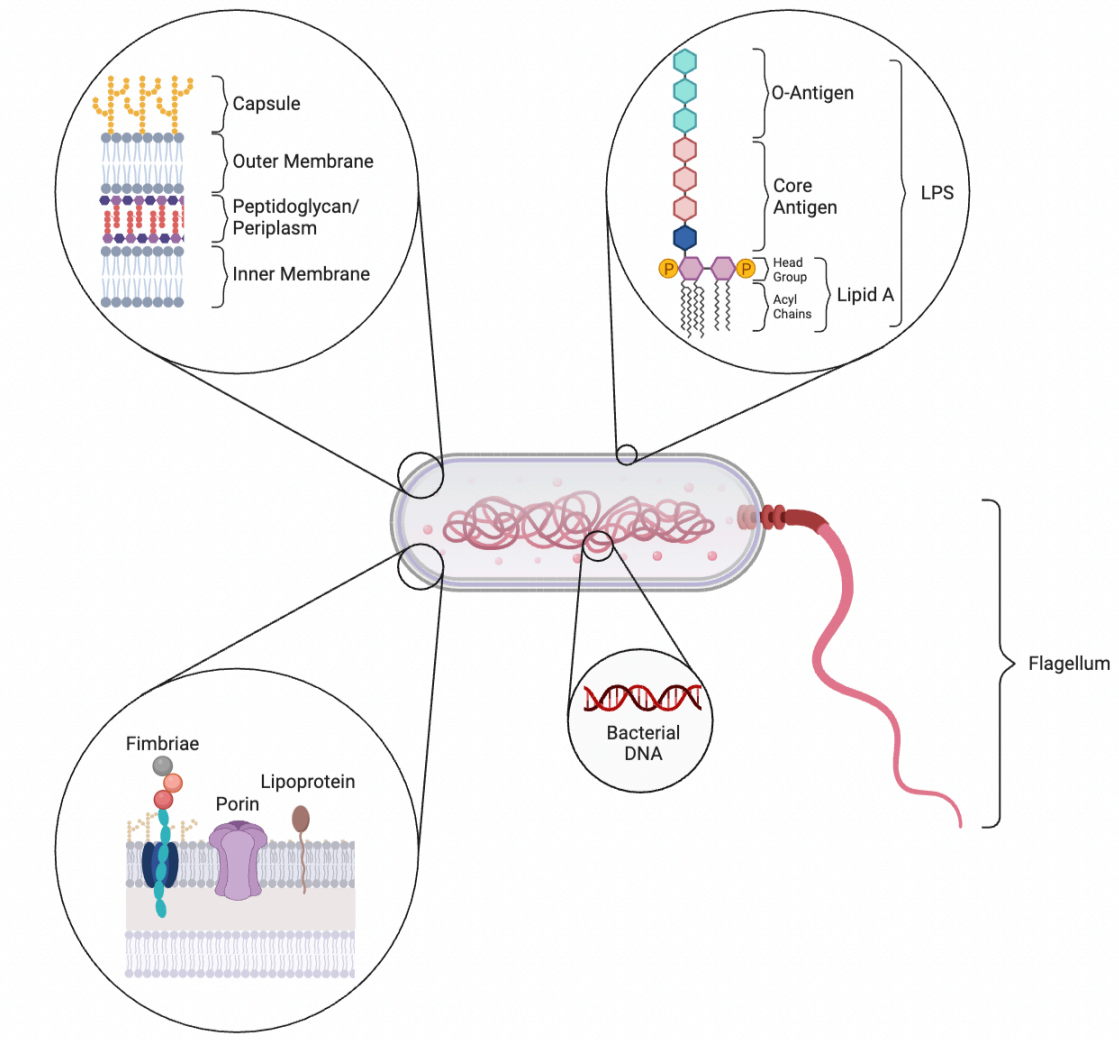

Figure 1.3.1: A typical Gram-Negative bacterium. A diagrammatic representation of a typical Gram-negative bacterium, showing the outer surface components and intracellular components typically present within a Gram-negative bacterium.

1.3.1. Lipopolysaccharide (LPS) outer membrane

On the outermost surface of a Gram-negative bacterium is the outer membrane, whose inner leaflet is phospholipid but whose outer leaflet consists of Lipopolysaccharide (LPS) molecules, complexes of diverse carbohydrate O- and core-antigens, covalently linked to a glucosamine disaccharide Lipid A core (9). Lipid A is one of the main immunogenic components of the Gram-negative bacterial cell and is one of the first components that the host immune response encounters (10). The LPS outer membrane aids the repulsion of antimicrobial agents, due to the overall negative charge inferred on it by the 1' and 4' phosphate groups within Lipid A and Kdo_2 carboxyl groups within the core polysaccharide region (11, 12), and acts as a barrier to drug entry (13, 14). Gram-negative bacteria also have an inner, symmetrical, phospholipid cytoplasmic membrane, which also acts as a barrier and regulates the cytoplasmic environment. Between the inner and outer lipid membranes is the periplasm, where large amounts of protein folding, prior to secretion, and metabolic processes occur (15).

1.3.2. Peptidoglycan cell wall

Within the periplasm, Gram-negative bacteria have a peptidoglycan cell wall polymerised from N-acetyl-Glucosamine (GlcNAc) and N-acetyl-Muramic Acid (MurNAc), crosslinked by peptides of L- and D- amino acids and the amino acid DAP (D-glutamyl-meso-diaminopimelic acid), which is almost exclusively found in Gram-negative bacteria, although some exceptions exist (16). The peptidoglycan cell wall confers strength and rigidity to the bacterial cell, making it a target for classes of antimicrobial agents, such as penicillins, which kill bacteria by disrupting their cell wall and triggering osmotic lysis (Figure 1.3.2). How bacterial peptidoglycan is sensed by the mammalian immune response is further detailed in Section 1.4.3.2.

Other surface features of Gram-negative bacteria may include a polysaccharide capsule, fimbriae and/or pili, other Outer Membrane Proteins (OMPs) and porins, and flagella. I will cover each of these components in more detail below.

1.3.3. Capsule

The bacterial capsule is a polysaccharide layer that may be differentially expressed, and which can surround the bacterial cell, comprised predominantly of polysaccharides interlinked with other peptides and sugars (Figure 1.3.2) (17). The capsules of Gram-negative bacteria are important mediators of protection from the innate immune system, conferring resistance to complement-mediated killing, opsonisation, and phagocytosis (18-20). Capsules do not provide protection against predation by *Bdellovibrio bacteriovorus*, unlike in bacteriophage predation, where predation is inhibited by the capsule (21).

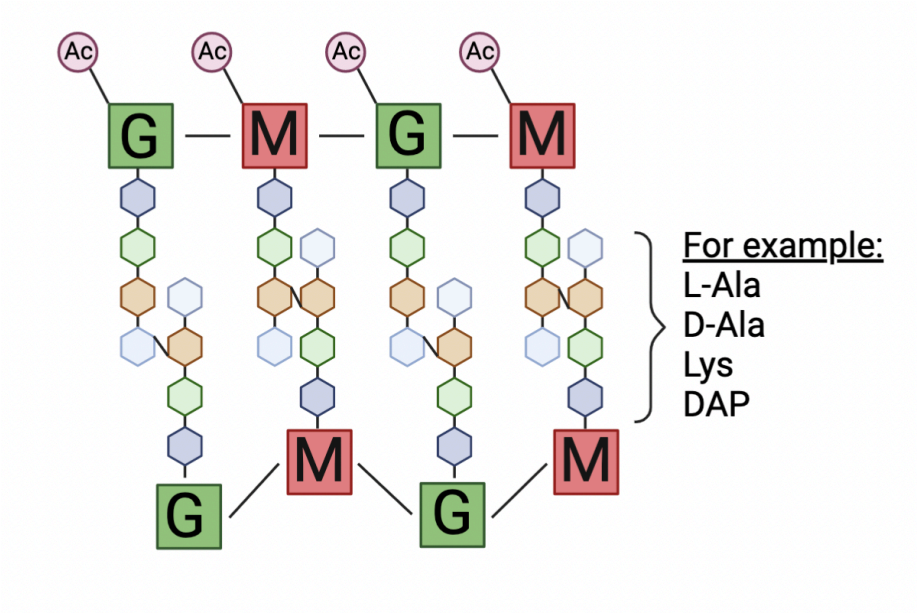

Figure 1.3.2: Peptidoglycan Structure. A schematic showing the polymerisation of Peptidoglycan monomer subunits into a higher order Peptidoglycan structure. G and M glycans are linked into a backbone by short peptides between 1' and 4' residues. Glycan monomers are further crosslinked by bonds between the 3, 4- or 3, 3- residues of the peptides. The peptides that form these crosslinks may vary. Ac represents acetylation; G represents N-acetyl Glucosamine/GlcNAc; M represents N acetyl Muramic Acid/MurNAc; L-Ala represents L-Alanine; D-Ala represents D-Alanine; Lys represents Lysine; DAP represents Diaminopimelic Acid.

1.3.4. S-layer

The bacterial S-layer is comprised of protein and glycoprotein subunits that form a paracrystalline layer, common to a large number of a taxonomic groups of Gram-negative bacteria (22). S-layers provide selective uptake and protection against harmful molecular species, whilst aiding with cellular adhesion and surface recognition. S-layers may also provide structural stability, determining cell shape and division (22). S-layers also have important immunomodulating activities, masking some immunogenic surface residues, to avoid recognition by the host, and providing protection against host-derived antimicrobial proteins (23). S-layers prevent the binding to, and recognition of, immunogenic surface residues by host Pattern Recognition Receptors (PRRs). Analogous to this, S-layers sterically mask the exposure of the outer membrane receptor(s) required for *Bdellovibrio* attachment, rendering bacteria expressing an S-layer non-susceptible to predation by *B. bacteriovorus*. However, once an area of the outer membrane is exposed, due to the lack of localised S-layer expression, *Bdellovibrio* are able to attach, invade and prey upon the Gram-negative bacterium (24).

1.3.5. Fimbriae

Fimbriae are long, proteinaceous fibres that protrude beyond the capsules of some bacteria, aiding binding to and colonisation of biological surfaces. Fimbriae are comprised of major and minor subunits, which assemble under the direction of periplasmic chaperone and outer membrane usher proteins, once secreted across the cytoplasmic membrane, to assemble in a highly specific order to form the longer fimbriae filaments (25).

Details of how fimbriae are recognised by the host immune response are detailed in Section 1.4.3.3.

1.3.6. Pili

In contrast, pili are shorter proteinaceous fibres comprised of individual pilin monomers (26). These monomers are assembled via a similar mechanism to fimbriae, via the Chaperone-Usher pathway (27). Pili have important roles in molecular secretion, cell movement and adhesion, representing a key virulence factor in bacterial infection. Chaperone usher pili are widespread amongst bacteria (Gram positive and Gram-negative) (28), where they facilitate binding to other bacteria, host cells and abiotic surfaces, with important implications for biofilm formation (29, 30). As with most bacterial cell surface factors, the structure and function of pili may vary based on different stresses reflecting adaptation to differing microenvironmental conditions (31).

Type IV pili, a subset of pili distinct from Chaperone-Usher pili, are involved in twitching motility in *Pseudomonas aeruginosa* and other Gram-negative bacteria (32, 33). Type IV pili may also extend and retract to facilitate cell movement, as is seen in *Myxococcus xanthus* (32, 33).

The roles of Type IV pili in bacterial predation by *B. bacteriovorus* are explained in Section 1.6.2.4.

Details of how pili are recognised by the host immune response are detailed in Section 1.4.3.3.

1.3.7. Flagella

Flagella are proteinaceous appendages that, through their rotation, enable bacterial motility. Flagella are comprised of flagellin monomers, polymerised into a flexible, thread-like appendage. The N- and C- termini of flagellin are highly conserved between bacteria, encompassing a variable region in between both termini, which forms the outer, environment-facing surface of the flagellin monomer (34, 35). The flagellin polymer is anchored into the cytoplasmic membrane of the bacterium by the basal body (34). The flagellum is comprised of many other proteins also, but the main immunogenic ligand that is recognised by the host TLR-5 receptor is flagellin (36). Conservation of the N and C termini of flagellin, despite a variable central region, facilitates recognition by TLR-5, across a wide range of bacterial species.

The role of the flagella in bacterial predation by *B. bacteriovorus* are explained in Section 1.6.2.5.

1.3.8. Outer membrane proteins and porins

In addition to the fimbriae proteins extending from the Gram-negative cell membranes, other outer membrane proteins (OMPs) also decorate the outer membrane, with extensive roles in nutrient acquisition, membrane permeability, i.e. the selective exclusion of toxic or harmful products, and multidrug resistance. (37). OMPs may be peripheral, where they are secreted from the bacterial cell but tethered to the outer membrane by their N-terminal domain, or integral, where they are embedded in the outer membrane, a trait exclusive to Gram-negative bacteria (37).

The OMP variety and composition within the outer membrane varies widely between Gram-negative bacteria, conferring differing degrees of virulence and antimicrobial resistance (38). Common groups of OMPs that feature predominantly within the outer membrane include porins and polysaccharide exporter proteins responsible for capsular polysaccharide export (forming the capsule layer) and LPS export (replenishing the outer membrane itself) (39).

1.4. The host immune response to Gram-negative pathogens

1.4.1. Overview

The human host is constantly exposed to microorganisms through inhalation, ingestion or traumatic inoculation. Therefore, the host must provide a barrier to bacterial infection and bacterial establishment. This role is mainly encompassed by the host immune response, which consists of an innate system, which provides a rapid and non-specific response to microorganisms and prevents the establishment of infection in the first instance, and an adaptive system, which confers specificity and memory to the immune response, preventing and providing protection from infection in the longer term, but this response is not immediate.

1.4.2. The innate immune system

The innate immune system forms the first line of defence against bacterial infection, providing a rapid response to bacterial incursion through both cell-dependent and cell independent mechanisms.

Briefly, the immune system consists of serum components, containing antimicrobial peptides and complement components, and a range of innate and adaptive immune cell types including macrophages, neutrophils, dendritic cells, T cells and B cells. A key cell type, in bacterial immune responses, is the macrophage (discussed in more detail below). Macrophages participate in innate immune recognition of bacterial cells, their engulfment and, in many cases, their killing. After bacterial killing, antigen presentation educates and activates the adaptive immune system.

Prior to exploring further, the partitions of the immune response, I will first outline how Gram-negative bacterial pathogens are recognised by the host's innate immune response, as this has implications for both the cell-independent and cellular responses to bacterial infection and for the interaction of the immune system with predation during *in vivo* predation tests of pathogen killing.

1.4.2.1. The cells of the innate immune response

1.4.2.1.1. Overview

A range of different cell types contribute to the immune response, each with differing functions and roles, dependent on their local microenvironment and the different chemotactic signals that they receive to ascribe their function. Within each cell type, some cells e.g., macrophage undergo further differentiation into specific, tissue resident subsets with more specific and specialised surface receptor profiles and functions within the host (40, 41).

The cellular immune response consists of several key players, all with vastly different but overlapping roles in recognising microorganisms, killing them, and then amplifying and alerting the wider immune response to the risk of infection. Multiple cells contribute to the innate immune response, including epithelial cells (which act as a barrier to microorganisms and have some basic recognition functions), basophils and eosinophils (which secrete enzymes and cytokines to stimulate immune cell growth and activation), natural killer cells (which trigger apoptosis in infected cells) and lymphoid cells (42). However, as I am focusing on the innate immune response, of which macrophages and neutrophils are two key components thereof, I will focus on the roles of macrophages and neutrophils. I will also discuss dendritic cells, as they play an important role in the initial signalling to the adaptive immune response.

1.4.2.1.2. Macrophages

Macrophages are phagocytic cells that engulf bacteria and kill them through multiple killing pathways (Figure 1.4.1). Macrophage also play a key role in antigen presentation and proinflammatory (e.g. IL-1β, IL-6 and TNFα) and anti-inflammatory (e.g. IL-10) cytokine release, educating other cells of the immune response to recognise and respond to specific microbial ligands, amplifying the immune response. Macrophages are typically tissue resident, leading to wide ranges of heterogeneity within macrophage populations, depending on their local microenvironment (41, 43). Further details on how macrophage recognise microbial stimuli and how they contribute to the host immune response are covered below.

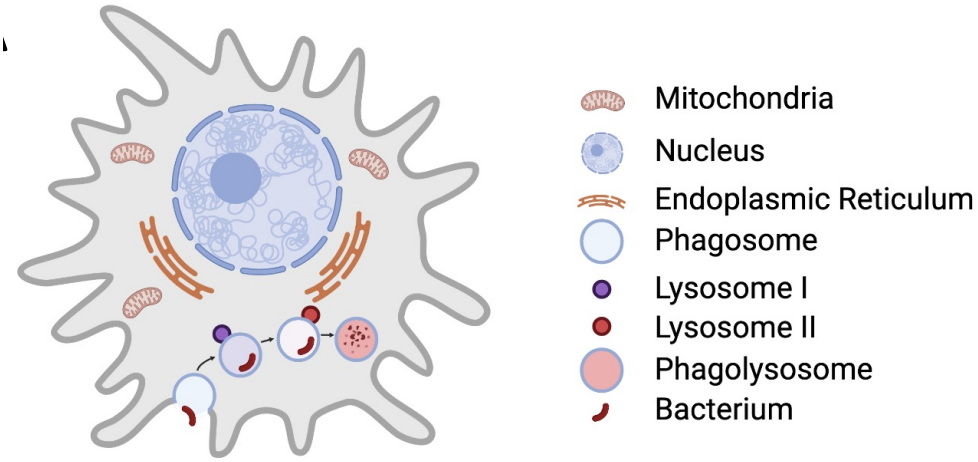

Figure 1.4.1: A Typical Macrophage Cell. Macrophages are nucleated cells that undergo global changes in gene expression in response to microbial stimuli. Microbial ligands, or whole organisms, may be phagocytosed into a phagosome, which subsequently fuses with lysosomes, maturing into a phagolysosome. These processes require extensive transcription of genes (nucleus) and translation of mRNA into proteins (at the Endoplasmic Reticulum). Phagocytosis, protein production and export are all energy expensive processes. These process, and others, are powered by mitochondrial ATP production.

1.4.2.1.3. Neutrophils

Neutrophils are phagocytic cells, with a predominant role in microbial killing, mainly through phagocytosis, and the subsequent generation of ROS and Nitric Oxide. However, neutrophils can also take part in the suicidal construction of extracellular traps in NETosis. These NETs (Neutrophil Extracellular Traps) trap pathogenic bacteria in web-like chromatic structures, preventing pathogen escape and dissemination, whilst killing them through the localised release of antimicrobial proteins and granule-associated hydrolytic enzymes, including cathepsins, cathelicidins and neutrophil elastase (44-46).

Neutrophils provide an immediate response to infection and are often the first immune cell at the site of infection, recruited by cytokine and chemokine messengers (44). Owing to their highly destructive and damaging nature, neutrophils are short-lived, rapidly killing microorganisms and then promptly dying, unless they receive further signals from other immune cells to prolong their survival (44).

1.4.2.1.4. Dendritic cells

The primary role of dendritic cells is in antigen presentation, activation of naïve T cells and bridging the gap between the innate and adaptive immune responses. Even their physical cell structure is specialised for this function. Dendritic cells engulf microbial antigens, subsequently presenting them on Major Histocompatibility Complexes (MHCs), which are recognised by and activate T cells of the adaptive immune response (47, 48). Naïve dendritic cells are also important for promoting tolerance within the host, where they aid in distinguishing self from non-self (47, 48).

In my work, I will focus on the actions of macrophage, because of their roles in innate immune recognition and because culturable experimental systems, i.e., cell lines, exist, which makes my research less dependent on animal models and primary cells.

1.4.3. Innate recognition of Gram-negative bacterial pathogens

As discussed above, the surface of the Gram-negative bacterium is key for understanding the host innate immune response to (Gram-negative) bacterial infection, as it is the first point of contact and recognition. I will explore each of the external surface components mentioned above, in addition to internal microbial ligands, and how they are recognised by the host immune response below.

The interface between the host immune response and pathogens is dictated initially through the recognition of surface moieties. However, little is known about how the alteration of the surface due to microenvironmental changes affects the interactions between host immune cells and the pathogen, therefore further clarification regarding the exact roles of each PRR and microbial ligand in the immune response is needed.

Bacterial recognition, by the cellular and non-cellular components of the innate immune response, relies on the recognition of a bacterial ligand (or Pathogen Associated Molecular Pattern/PAMP) by PRRs. Toll-like receptors (TLRs) are one of the main PRRs involved in detecting and responding to an initial microbial stimulus (49-53). TLRs are expressed by innate immune cells, including macrophage, neutrophils and dendritic cells, but also on non-immune cells, including epithelial cells (51) at low and differing levels. Different PRRs are responsible for the recognition of different microbial ligands, upon which TLR expression is upregulated, along with downstream signalling (Figure 1.4.2).

Surface TLRs (TLRs -1, -2, 4, -5 and -6) detect the main surface ligands on bacteria and initiate the immune response (52), recruiting other cell surface receptors e.g. scavenger receptors, that initiate cytoskeleton and membrane rearrangement, leading to phagocytosis (54). Once phagocytosed, endosomal TLRs (TLR -3, -7, -8 and -9) are trafficked to the phagosome where they sample the contents of the phagosome further to give a more tailored and specific immune response (52). The innate immune response typically gains momentum and becomes increasingly pro-inflammatory over time (Figure 1.4.2).

The role of each PRR in the developing immune response is highly dependent on the ligand, the activation state of the cell, the cell type and the cytokine/chemokine signals that the cell has received (49, 50, 52, 55).

In macrophages, ligation of TLRs with microbial ligands initiates TLR dimerization and the recruitment of other signalling receptors, co-receptors, and adaptor proteins at the host cell surface (or endosomal surface, in some instances). Assembly of these signalling complexes in phagocytes induces signal transduction to transcription factors, including NFκB, which upregulate the transcription of genes encoding antimicrobial peptides and other bactericidal factors (leading to bacterial killing) and proinflammatory cytokines (leading to immune cell recruitment and activation) (49, 50, 52).

In dendritic cells, TLR ligation induces dendritic cell maturation and upregulates antigen presentation (47). Other cell types, e.g., epithelial cells, do not have phagocytic capabilities, but they can signal and activate other (immune) cells in response to microbial stimuli. TLR ligation eventually culminates in microbial killing, degradation, and antigen presentation, educating and activating the adaptive immune response.

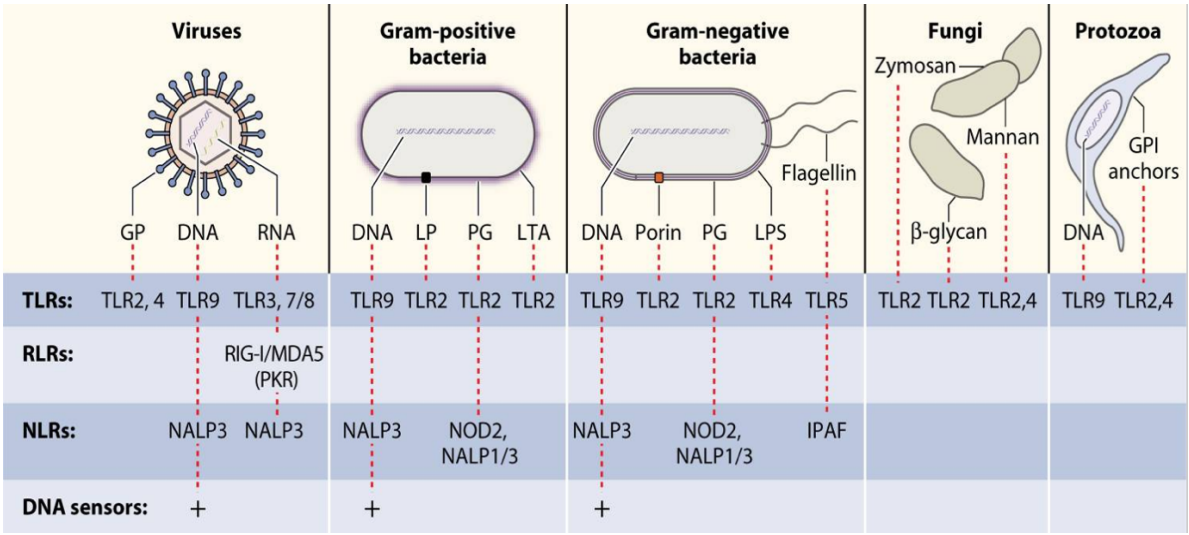

Figure 1.4.2: Recognition of the main Pathogen Associated Molecular Patterns by different Pattern Recognition Receptors in various microorganisms. The detection of PAMPs by host PRRs is what triggers the initiation of the innate immune response, whether this be towards viruses, bacteria, fungi or protozoa. The major PAMPs for each class of microorganism are shown, along with the host cell PRRs that detect their presence. TLRs are expressed by innate immune cells, including macrophage, neutrophils and dendritic cells, but also on non-immune cells, including epithelial cells. N.B. Lipoproteins are also present in Gram-negative bacteria and may be detected by TLR-2. GP, surface glycoproteins; LP, lipoproteins; PG, peptidoglycan; LTA, lipoteichoic acid; LPS, lipopolysaccharide; GPI, glycophosphatidylinositol; TLR, Toll-like receptors; RLR, RIG-1 like receptors; NLR, Nod-like receptors. Figure taken from Mogensen et al., 2009.

1.4.3.1. Recognition of lipopolysaccharide

As mentioned above, LPS consists of a Lipid A core, a core oligosaccharide chain, and a more variable O-antigen polysaccharide chain. Whilst these oligosaccharides may be recognised by the host immune response, and will certainly impact how LPS is recognised as a whole, the main component of LPS that is recognised by the host is Lipid A.

On macrophage, TLR-4, in complex with LBP (Lipopolysaccharide Binding Protein), CD14 and MD2 (Myeloid Differentiation 2) detects LPS in the Gram-negative outer membrane (52). LBP binds LPS, subsequently forming a transient complex with CD14. This enhances the sensitivity of the TLR-4:MD-2 complex to LPS (56, 57). The acyl chains of Lipid A bind inside a hydrophobic pocket within the TLR-4:MD-2 multimer, altering the structural conformation of Lipid A and facilitating the interaction of the phosphate groups present within the Lipid A head group, with TLR-4 (58). This induces dimerization of TLR-4, triggering the recruitment to of adaptor proteins and initiating downstream MyD88 and NFκB signalling. TLR-4 would usually be expected to the one of the first TLRs to detect Gram-negative bacterial exposure, owing to LPS being the major component of the outer membrane surface. TLR-4 may detect LPS at the cell surface or within endosomes, owing to it cycling between both interfaces, signalling through two separate pathways (56, 58, 59). The negative charge of Lipid A, within LPS, is key for TLR-4 binding and stimulation of the immune response (60).

The LPS of Gram-negative bacteria can be modified to prevent recognition by the immune response. Modification of acylation of the Lipid A component, or the addition of positive charged carbohydrate groups to the phosphate groups within Lipid A, alter the overall negative charge of the Lipid A molecule, reducing TLR-4 binding and recognition by the immune response, and reducing outer membrane permeability to AMPs (61, 62). Variation of the composition of the O-antigen also contributes to evasion of the host immune response, preventing the deposition of C3 (Complement protein 3) and causing membrane attack complexes (MACs) to form away from the outer membrane, whilst delaying recognition by PRRs (62). Modification of Lipid A, to prevent host recognition, is further detailed in Maldonado et al., 2016 (62).

Variation of O-antigen length and composition may impact *Bdellovibrio* predation. *Vibrio cholerae* deficient in O-antigen production were more susceptible to predation by *B. bacteriovorus*. *V. cholerae* expressing O-antigen were preyed upon with reduced efficiency, likely due to the masking of target receptors (sterically or through altered charge interactions) by O-antigen chains (63, 64). Variation of the charge of the Lipid A molecule was not thought to affect *Bdellovibrio* predation, although my results (presented in Chapter 3) explore this further. As the target within the outer surface of Gram-negative bacteria that *Bdellovibrio* recognises in predation, is unknown, it is difficult to further detail how LPS modifications would impact predation efficiency. As predation susceptibility varies within the same bacterial species, but all Gram-negative bacteria are susceptible to predation, it is likely that phenotypic variation in LPS and cell surface components determines susceptibility to predation (64).

1.4.3.2. Recognition of peptidoglycan

TLRs. TLR-2 is known to work in combination with TLR-1 and TLR-6, on professional phagocytes including macrophage, to detect triacylated and diacylated lipoproteins respectively (65, 66), along with NAG (N-acetyl glucosamine) and NAM (N-acetyl muramic acid) subunits of peptidoglycan and outer membrane proteins (65, 67). Peptidoglycan is usually masked from detection by TLR-2 due to LPS outer membrane so there is typically a delay in response to peptidoglycan, until non-specific lysis of bacteria in serum, or upon uptake, exposes peptidoglycan fragments.

NOD-Like Receptors. Peptidoglycan may also be detected by cytosolic NLRs (NOD-Like Receptors) NOD-1 and NOD-2, which detect peptidoglycan within macrophage and respond to intracellular bacterial infection (68-71) after peptidoglycan ligands have been internalised/phagocytosed by host cell surface receptor, e.g. scavenger receptor, recognition and binding, inducing actin cytoskeleton remodelling and uptake (54). NOD-1 and NOD-2 respond to both the amino acid DAP (D-glutamyl-meso-diaminopimelic acid) and the backbone muramic acid attached to the peptide MDP (muramyl dipeptide) respectively (69-74).

NOD1 and NOD2 have been shown to sense intracellular bacteria, including *S. flexneri* (70), *L. monocytogenes* (72, 75, 76), *S. pneumoniae (77)*, *M. tuberculosis* (78) and a range of other Gram-negative bacteria (79) but the role of NOD1/NOD2 in the resolution of infection is still poorly understood (80).

Peptidoglycan Recognition Proteins. Macrophage, and other cells of the innate immune response, secrete Peptidoglycan Recognition Proteins (PGLYRPs) that recognise and bind to bacterial peptidoglycan MurNAc-Peptide fragments (81). PGLYRP-1, -3 and -4 lyse peptidoglycan and exert a bactericidal effect (81), in some cases amplifying the immune response. For example, PGLYRP1 activates TNF in *Listeria monocytogenes* infection (82), exerting a bactericidal effect but limiting the proinflammatory response to commensal microbiota (83).

Peptidoglycan Recognition Protein 2 (PGLYRP2) lyses peptidoglycan into biologically inactive fragments that are less well recognised by TLRs -1, -2 and -6. PGLYRP-2 cleaves the sugar backbone from the peptide chain, thus cleaving and removing the ligands for NOD-1 and -2 (70, 84). Recognition and cleavage of peptidoglycan centres around the recognition of N-acetyl Muramic Acid (MurNAc) within the peptidoglycan backbone, along with other D-isoform peptides as these are recognised as bacterial and foreign by the immune response, rather than L-isoforms and N-acetyl Glucosamine (GlcNAc) which are less well recognised owing to their high similarity to host/self-amino acids (85).

1.4.3.3. Recognition of Flagellin and other bacterial surface proteins

TLR-5 recognises bacterial flagellin that has been internalised by host cells (86). TLR-5 detects conserved dipeptides at the N- and C-termini of bacterial flagellin, that are key to flagellar assembly and motility and are therefore indispensable, even if the rest of the flagellar composition is highly variable (87-89). The main recognition site on bacterial flagellins (for TLR5 recognition) lies between amino acids 89 and 96 (see Figure 1.6.2) (36).

Fimbriae are predominantly recognised by TLR-2, whose main ligands are diacylated and triacylated lipoproteins. FimA, the major fimbrial protein of *Porphyromonas gingivalis*, and CsgA, a major subunit of *Salmonella* Typhimurium curled fimbriae, are recognised by TLR-2 (90-96).

Interactions with other TLRs, including TLR-4, also play a role in fimbriae recognition. For example, the FimH tip adhesin of Type I fimbriae of Uropathogenic *E. coli* binds directly to TLR-4 (97, 98).

As with fimbriae recognition, pili are recognised by the PRR TLR-2 (99, 100), although recognition of *Moraxella cattarhalis* pili by TLR-5 has also been documented, enhancing immune-mediated clearance (101).

1.4.3.4. Recognition of bacterial nucleic acids

Historically, TLR-3 was thought to detect viral dsRNA. Increasing evidence suggests that TLR-3 may also detect bacterial RNA. TLR-3 is an endosomal PRR, therefore it is not involved in the initial recognition of microbial stimuli, but will sample the contents of the endosome after initial bacterial uptake and lysis, to detect bacterial RNA (52, 102).

TLRs -7, -8 and -9 are endosomal, so they recognise nucleic acids within the cytosol of the cell (52). TLR-7 responds to synthetic viral components, but may also recognise bacterial RNA in lysosomes, initiating the interferon response and targeting mitochondria to phagolysosomes to induce increased reactive oxygen species (ROS) production and autophagy (38, 103, 104). TLR-8 also recognises bacterial RNA, inducing IFN-β expression through IRF-7 -dependent signalling in response to *Borrelia burgdorferi* phagocytosis and infection (105, 106).

TLR-9 responds to unmethylated CpG containing ssDNA, therefore amplifying the response to bacteria further (107).

The recognition of bacterial ligands by host TLRs is summarised in Figure 1.4.3. below.

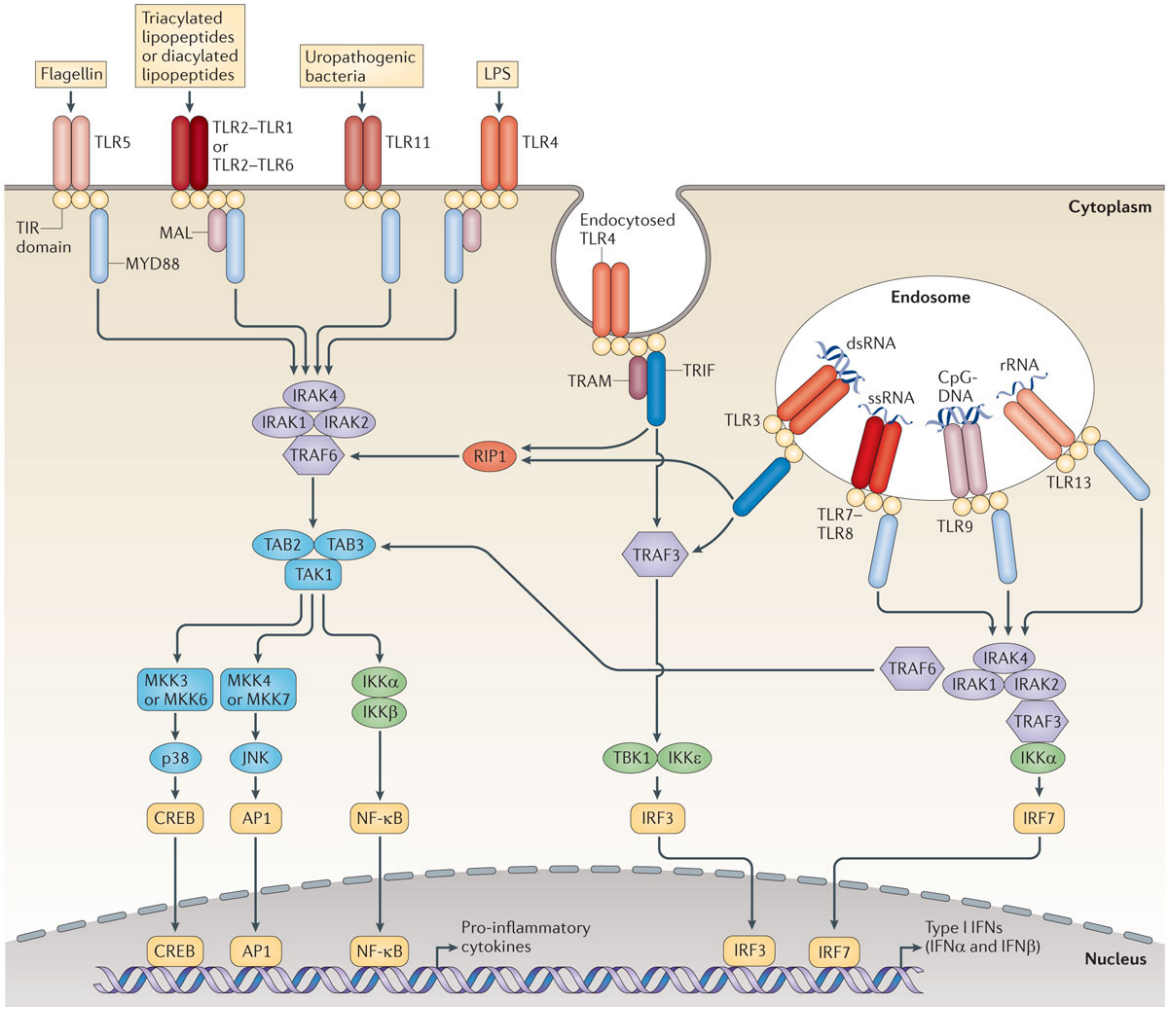

Figure 1.4.3: The role of Toll-Like Receptors (TLRs) in the sensing of microbial ligands. Figure taken from O'Neill et al., 2013; Nature Reviews Immunology. Toll-like receptors (TLRs) are one of the first Pattern Recognition Receptors (PRRS) involved in sensing microbial stimuli. Surface TLRs, TLRs -1, -2, -4, -5, -6 and -11 bind to microbial ligands at the cell surface. Endosomal TLRs, TLRs -3, -4, -7, -8, -9 and -13, sense microbial ligands that have been internalised within endosomes. Upon ligand binding to a TLR, dimerization occurs triggering the recruitment of adaptor proteins to the signalling complex. These adaptor proteins are MYD88 (Myeloid Differentiation Primary Response Protein 88) and MAL (MYD88 adaptor like protein) or TRIF (TIR-domain containing adaptor protein inducing IFN-β) and TRAM (TRIF-related adaptor molecule). Upon assembly of this signalling complex, other adaptor and accessory proteins are recruited to the signalling pathway, including IRAKs (IL-1R-associated Kinases) and TRAFs (TNF Receptor Associated Factors), inducing the activation of MAPKs (Mitogen Associated Protein Kinases), JNK (JUN N-terminal Kinase) and p38. This leads to activation of the downstream transcription factors NFκB (Nuclear Factor kappa B), IFRs (Interferon Regulatory Factors), CREB (Cyclic AMP-responsive element binding protein) and AP1 (Activator Protein 1), and expression of transcription factor regulated genes, predominantly proinflammatory cytokines. dsRNA: double stranded RNA; IKK: Inhibitor of NFκB Kinase; LPS: Lipopolysaccharide; MKK: MAP Kinase Kinase; RIP1: Receptor Interacting Protein 1; rRNA: Ribosomal RNA; ssRNA: Single Stranded RNA; TAB: TAK1-Binding Protein; TAK: TGF-β activated Kinase; TBK1: TANK-binding Kinase 1.

1.4.3.5. Recognition of bacterial ligands by other PRRs

Scavenger receptors are involved in tissue homeostasis within the host, as they bind modified host lipoproteins and apoptotic cells (108, 109). They are typically expressed by myeloid cells, with their expression being controlled by the presence of proinflammatory cytokines and other host cell cues such as oxidative stress, in turn inducing ligand internalisation, NFκB activation and respiratory burst and proinflammatory cytokine activation/production (109). Scavenger receptors also bind microbial glucan ligands, and therefore play a role in the detection and phagocytic uptake of microbial stimuli in the host (109).

C-Type lectin receptors (CTLRs), such as the mannose receptor, are typically Calcium-dependent PRRs that bind carbohydrates (110). CTLRs aid phagocytosis and presentation of opsonised microbial ligands, but also contribute to phagocytosis, ROS and proinflammatory cytokine production (110).

Whilst these, and other types of PRR contribute to the innate immune response (111, 112), my focus is predominantly on the microbial ligands of *Bdellovibrio* that are recognised by host TLRs within this study.

1.4.4. Cell independent factors

To prevent infection, the host must present an exceptionally hostile environment to inhabit and persist in for pathogens, whereby they are quickly set upon by components of the host immune response to restrict infection. Many soluble components of the host immune response are found in plasma. Plasma, the non-cellular component of blood, is where the majority of the initial immunological and bactericidal exchanges between the cells of the host immune response and pathogen occur, during infection. It is also where injected, therapeutic *Bdellovibrio* would encounter bacterial pathogens and so it is important to consider the status of pathogenic bacteria in blood plasma.

Plasma contains two predominant microbicidal mechanisms which target bacterial surfaces, as the key component of the host-pathogen interface, **the complement deposition system, and antimicrobial proteins/peptides,** both of which mediate killing through bacterial cell lysis. One key group of virulence traits that allows human pathogens to persist and cause disease is serum resistance, the ability to survive within the serum of the host alongside numerous antimicrobial proteins, antibodies and bactericidal mechanisms (113). The mechanisms behind complement and antimicrobial protein mediated killing, and how pathogens resist these mechanisms are important to my studies of bacterial predation in host environments as an antimicrobial therapy and will now be explored further.

1.4.4.1. Antimicrobial proteins/peptides

Antimicrobial peptides are small, helical polypeptides, disproportionally highly abundant in positive/cationic, hydrophobic amino acids. Other regions of antimicrobial peptides also contain hydrophilic or ampiphilic amino acids. These net-positive peptides are attracted to the negatively charged bacterial outer membrane with a high affinity (114, 115), although they have a broad spectrum of action, acting on a wide range of microorganisms (bacteria, fungi, viruses and protozoa) (116). AMPs induce pore formation and the dysregulation of membrane solubility to exert their bactericidal/antimicrobial effect.

Antimicrobial peptides (AMPs), freely circulating in human plasma and actively secreted by (bacterially) stimulated immune cells such as macrophages and neutrophils, are an important component of the host innate immune response, whereby they bind to and quickly respond to the presence of pathogens and control infection in various organs and systems of the body, through the modulation of the immune system (117-120). AMPs are thought to be the first line of defence against microbial incursion as they are distributed throughout the bloodstream, distributed in the plasma, and in tissues that first encounter microorganisms, such as the lungs (121).

1.4.4.1.1. Mechanism of action

In Gram-negative bacteria, antimicrobial proteins typically bind to the outer membrane LPS via the electrostatic attraction between the negatively charged phosphate groups and moieties in lipid A and the core oligosaccharide (61, 122, 123), and their positive side chains, after which they are taken up via a self-promoted uptake pathway across the outer membrane and periplasm, and integrate into the inner membrane in between the hydrophilic head groups and fatty acyl chain tails, where pore formation occurs and barrier function and structural integrity is negated, promptly resulting in bacterial cell death and lysis (115, 124). Antimicrobial proteins represent one of the predominant forms of innate immune defence against pathogens within the host (125, 126).

1.4.4.1.2. Resistance to antimicrobial peptides

The structure of LPS is well-recognised by the immune system as a PAMP and as a key signature of Gram-negative bacterial infection (see Section 1.4.3.1). Variation in the structure of LPS results in differing levels of recognition by the innate immune system and impacts the bactericidal effects of cationic antimicrobial peptides (both host and synthetic such as polymyxin B) and human serum sensitivity within the innate immune system (127).

Cationic antimicrobial peptide (CAMP) resistance had previously been attributed to the increased steric hindrance of the O-antigen, where, in *E. coli,* longer oligosaccharide chains were observed to confer increased resistance, presumably by preventing CAMP binding to the bacterial outer membrane (128). Increased incorporation of glycine into the core oligosaccharide, increased N-acetyl glucosamine incorporation into the capsule and the ratio of Galactose to D, D-Heptose in the O-polysaccharide, all of which possess no charge, have also been implicated in conferring CAMP resistance in *Yersinia pestis* (127). However, the most prominent mechanism of CAMP resistance is the incorporation of 4-amino-4-deoxy-L-arabinose (L-Ara(4)N), and to a lesser extend ethanolamine, into the LPS. This alters the overall negative charge of the LPS and negates the binding of cationic antimicrobial peptides, conferring polymyxin and CAMP resistance (129-131). This phenomenon has also been observed in many Enterobacteriaceae including *Salmonella typhimurium* (122, 124, 132-135), *Escherichia coli* (136-138), *Proteus mirabilis* (139), *Chromobacterium* violaceum (140), and *Burkholderia cenocepacia* (141), representing a significant mechanism of resistance to antimicrobial proteins of the innate immune response.

1.4.4.2. The complement system

The complement system is a key host defence against infection within the bloodstream. Various cell types, including leukocytes and epithelial cells, throughout the body synthesise soluble complement proteins into the bloodstream, where they then act to recognise, bind to, assemble upon and permeabilise bacterial membranes. Leukocytes and epithelial cells respond to complement proteins via membrane bound complement receptors (142, 143). It consists of three pathways: the classical activation pathway, the alternative activation pathway, and the lectin-mediated pathway (144, 145).

1.4.4.2.1. Mechanism of action

Classical activation: The classical pathway of complement activation is antibody mediated, predominantly through the deposition of immunoglobulin (Ig) G and M clusters on the bacterial surface when surface antigens are recognised. Initially, complement receptor Clq recognises and binds to the conserved Fc region of IgG and IgM complexes (146). Clq acts as a receptor for two proteases, Clr and Cls, to bind to Clq, activating them (147, 148). Cls proteolytically cleaves C4, another complement protein, into two subunits, a and b, resulting in the deposition of C4b onto the surface of the pathogen through a process termed opsonisation. C4b deposition subsequently cleaves C2 into two subunits, releasing a convertase that cleaves C3, upon which C3b is activated and feeds into the alternative pathway of complement activation, initiating downstream effector functions such as pro-inflammatory cytokine release and phagocyte recruitment (Figure 1.4.4) (149). C3a, an anaphylatoxin, is also released during C3 cleavage, latterly binding to C3aR and triggering the oxidative burst in macrophages (150).

Lectin pathway of activation: Host Mannose Binding Lectin (MBL) binds to carbohydrates, including N-acetyl Glucosamine, mannose and N-acetyl mannosamine, on the pathogen surface, after which MASP1/2 (MBL Associated Serine Protease 1/2) are recruited to MBL to form a cleavage complex (151). This complex subsequently cleaves C4, resulting in C4b deposition on the bacterial cell surface, after which it follows the same pathway as the classical and alternative pathways of complement activation (Figure 1.4.4) (152, 153).

Alternative pathway of activation: The alternative pathway of complement activation differs as it is comprised of three separate pathways of activation, rather than a single, linear pathway (154, 155). Despite being termed the alternative pathway, this pathway likely accounts for between 80% and 90% of complement pathway activation (156). C3 is the chief mediator of the alternative complement pathway, which is hydrolytically cleaved to form the two subunits and activate the protein. The C3b subunit of C3 is highly active, whereby it binds to foreign amine and carbohydrate groups on the pathogen surface and tags them for targeting and destruction.

C3b tagging also occurs on some host cells, however the protein is short-lived and is quickly turned over by the host to prevent self-targeting. Complement Factor D (CFD) cleaves Complement Factor B (CFB) which is attached to C3b, forming the C3bb C3 convertase. Positive feedback on C3b-tagged pathogen components results in further complement tagging and complement protein binding (155, 157). C3b recruits and binds to C5, cleaving its active subunit in the process, which acts as a signal for C7, C8 and C9 recruitment to the cell surface. C3 and C5 convertase complex formation, and the precursors of MAC formation are stabilised by a Complement Factor Properdin (CFP) accessory protein (158). This ultimately results in lytic pore formation through the formation of membrane attack complexes (MAC) which damage and permeabilise bacterial cell membranes (Figure 1.4.4) (159).

Throughout the complement pathway, C3a and C5a anaphylatoxins are released (through C3 and C5 cleavage respectively), binding to membrane bound receptors in an array of immune and non-immune cell types. C3a and C5a binding induces the oxidative burst in macrophage and neutrophils (160, 161), and induce histamine release from mast cells (162). C3a induces IL-6 and TNFα production in B cells and monocytes (163, 164). C5a also acts as a powerful chemoattractant, inducing macrophage (165), neutrophil (166), activated B cell (167) and T cell (168) migration (150),

In summary, the complement pathway contributes to the immune response through the recruitment of leukocytes, the opsonisation of bacteria (facilitating bacterial uptake), and bacterial killing through MAC/pore formation.

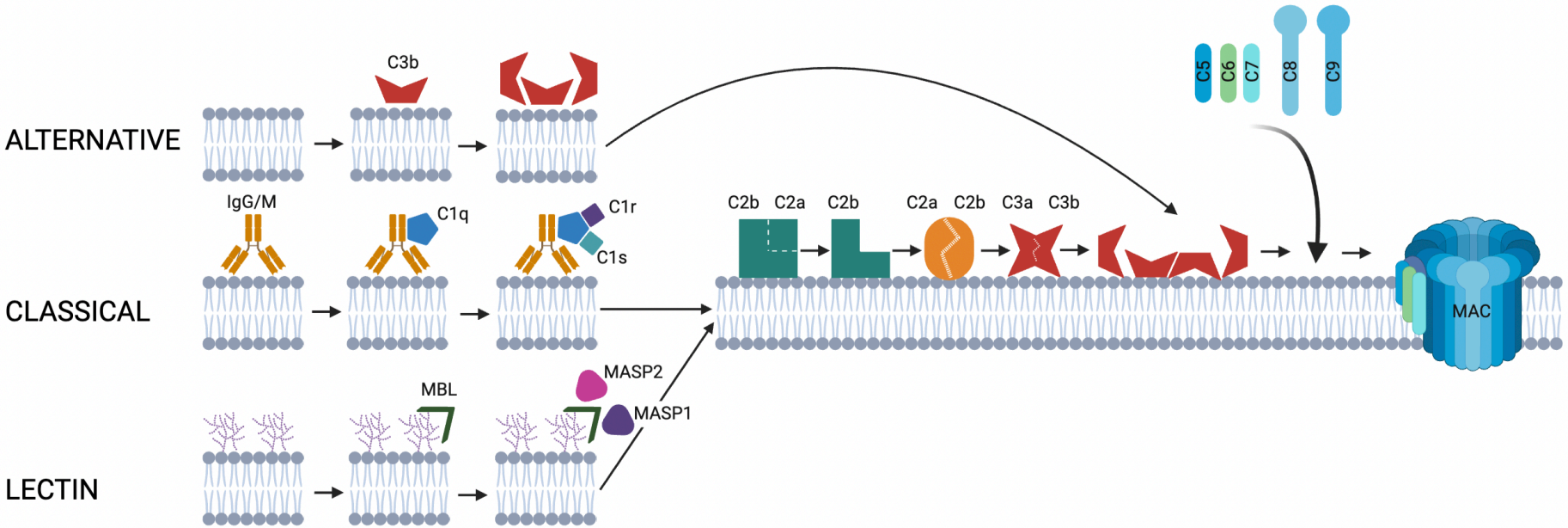

Figure 1.4.4: A schematic depicting the three pathways of complement activation. Binding of IgG or IgM antibodies to the bacterial surface acts as a scaffold for C1q binding, triggering C1r and C1s binding. C1s attracts and cleaves C4, leading to the deposition of C4b on the bacterial cell surface. C4b cleaves C2, causing C2b deposition and subsequent C2b-mediated C3 cleavage. C3b is deposited on the bacterial cell surface, triggering the recruitment of C5, C6, C7, C8 and C9 which subsequently form the Membrane Attack Complex (MAC), forming a pore in the bacterial outer membrane and lysing the cell (**Classical**). C3 molecules may spontaneously cleave and deposit C3b on the surface of host and bacterial cells. Host cells rapidly degrade and turnover C3b, preventing downstream complement activation. C3b deposition on bacterial cells triggers the recruitment of C5, C6, C7, C8 and C9 which subsequently form the MAC (**Alternative**). Mannose Binding Lectin (MBL) binds to carbohydrates on the bacterial cell surface, after which MASP1/2 (MBL Associated Serine Protease 1/2) bind to MBL. This complex subsequently cleaves C4, subsequently following the same route as the classical pathway of complement activation (**Lectin**). Figure drawn and adapted from Lambris et al., 2008.

1.4.4.3. Resistance to complement.

The capsule and LPS are both considered to be important in complement resistance, through their blocking of epitope recognition by host antibodies through O-antigen extension and through steric hindrance of MAC integration, causing MACs to form away from the bacterial outer membrane (169).

The predominant form of resistance to complement-mediated killing is upregulation of capsular polysaccharide synthesis and export, which is believed to decrease complement protein binding and prevent MAC formation in the outer membrane, whereby acapsular mutants of Uropathogenic *E. coli* and *Burkholderia pseudomallei* exhibit increased serum sensitivity and survival due to complement-mediated killing (170, 171).

Other forms of decreased sensitivity to complement include modification of the composition of the O-polysaccharide, where longer O-antigens sterically hinder MAC formation in the outer membrane, and incorporation of less immunogenic residues such as sialic acid, reducing proinflammatory responses and complement activation (172-176). Although there has been some debate regarding the importance of O-antigen length in serum resistance (177), which is likely to vary based on the specific pathogen and killing mechanisms studied, the consensus is that capsule production plays the most important role in decreased susceptibility to complement-mediated killing.

Cleavage of complement proteins by alkaline phosphatases, to prevent complement cascade activation, and masking of the bacterial surface by accumulating host complement factor proteins, such as Factor H or sialic acid (172), to prevent further complement deposition, also represent two mechanisms to resist complement-mediated killing.

As *Bdellovibrio* has an altered Lipid A structure and charge, it is possible that it will be less susceptible to complement protein action, although this remains to be confirmed. This is further covered in Section 3.3.4.

1.4.5. Microbial killing of bacteria internalised by macrophage.

1.4.5.1. Introduction to macrophage activation responses

As detailed above, macrophage are phagocytic cells that recognise, uptake and kill microorganisms, prior to digesting them and presenting their immunogenic components as antigens on the macrophage cell surface to educate and inform the other cells of the innate and adaptive immune response.

Although the predominant focus of this section is the infection associated, inflammatory activation of macrophages, to amplify the immune response and upregulate bacterial killing, it is important to consider that this Type I inflammatory state of macrophages is not the only activation state a macrophage may exist in, even within an infection scenario. Macrophage may also exist in a less inflammatory state, typically associated with Type 2 inflammatory responses and parasitic infection, or an anti-inflammatory state, associated with tissue remodelling and wound healing (40). This latter subtype highlights another important role of macrophage, outside of infection, where they phagocytose or degrade other, typically defective, host cell types to prevent other, non-infectious disease within the host. Although I refer to M1 (classically activated) and M2 (alternatively activated) macrophage within this thesis, it is important to note that recent developments in the field have suggested a shift away from this classification, as a diverse array of macrophage activation types exist (40). However, as I am mainly focused on the inflammatory actions of macrophage, and a lot of literature still refers to these two subtypes, I will use this nomenclature. The contrasting activation states of macrophage are further explored in Chapter 5, Section 5.5.9.

1.4.5.2. Macrophage engulfment and phagocytosis

Engulfment by phagocytes with subsequent phagosomal maturation and bacterial destruction, a process called phagocytosis, is one of the main initial forms of combatting infection in the host, through their actions in internalising and destroying microorganisms or microbial ligands and amplifying the immune response against infection.

1.4.5.2.1. Recognition

As I explained earlier in Section 1.4.3, phagocytosis is initiated when PRRs within the phagocyte membrane bind microbial ligands e.g., PAMPs (non-opsonic phagocytosis), or host receptors bind host proteins that have been deposited on the microorganisms' surface e.g., complement proteins or antibodies (opsonic phagocytosis) (178). The specific combinations of receptors that interact with the microbial stimuli will determine the exact pathway with which phagocytosis proceeds and the ultimate response to the microorganism. Once bound, TLRs dimerise and associate with other co-receptors and signalling molecules, recruiting further cell surface receptors, such as scavenger and mannose receptors (54), to induce a signalling cascade that promotes cytoskeletal rearrangement and particle uptake (52).

Fc-mediated phagocytosis is initiated by Fc receptors, embedded in the membranes of phagocytes, binding the Fc region of antibodies on opsonised particles. Fc receptors alone cannot initiate signal transduction and endocytosis, so they associate with other receptors and co-receptors to initiate signalling (179).

Complement-receptor-mediated phagocytosis precedes in a similar way whereby, if the complement activation pathway does not lyse bacteria, complement receptors bind to C3b, C4b and C3b(i) on the pathogen surface and, if done in combination with a secondary cue such as proinflammatory cytokine activation or other PRR binding, will internalise the opsonised particle (142).

1.4.5.2.2. Uptake

Receptor binding triggers the second stage of phagocytosis, whereby cytoskeletal rearrangement within the phagocyte results in dynamic membrane and actin cytoskeleton (180) remodelling and the uptake and internalisation of the microorganism, whereby it will reside within a membranous vesicle termed the phagosome (178).

1.4.5.2.3. Phagosomal maturation

The microorganism within the phagosome is then degraded in the third phase of the phagocytic process. This degradation process is the result of various membrane fusion events whereby endosomes, vesicles and lysosomes deliver further, highly specific host receptors to sample the contents of the phagosome, latterly triggering the delivery of vesicles containing degradative enzymes and other microbicidal products and complexes (178) (Figure 1.4.5). The delivery of each vesicle is choreographed by the visibility of certain early and late endosomal protein markers on the surface of the phagosome, co-ordinating the process.

Bacterial killing is due to a combination of oxidative and non-oxidative killing mechanisms. To facilitate the various killing mechanisms within the phagosome, the localised environment within the phagosome cycles between highly acidic and more neutral pH, providing the optimum conditions for hydrolytic enzyme action (178). Acidification is achieved through the actions of V-ATPases, protein complexes in the phagosomal membrane which pump H+ protons into the phagosome (181). Not only does the low pH facilitate the activation of various hydrolytic enzymes, including lipases, proteases, hydrolases, lysozymes and cathepsins, and aid the production of superoxide and reactive oxygen and nitrogen species, it also disrupts the metabolism of the pathogen and prevents the utilisation of nutrients within the phagosome (182-184). The presence of antimicrobial proteins and hydrolytic enzymes also contributes to the hostile environment within the phagocyte, disrupting the various membranes resulting in microbial killing (185).

The phagolysosome is also highly restricted in nutrient availability to prevent the growth and active metabolism of the microorganism, facilitated through the release of various high affinity ion chelators and scavenger molecules e.g., lactoferrin which chelates and restricts iron availability, the ions of which are important in the active sites of many metabolic enzymes (185).

Finally, the lysosome is flooded with reactive oxygen and nitrogen species and various other superoxide molecules e.g., NADPH oxidase is inserted into the membrane, reducing NADPH to form superoxide (O2•), all of which damage cellular components including proteins, lipids and nucleic acids, resulting in cell death (183, 186, 187). Production of these reactive intermediates is upregulated through further proinflammatory signalling and release of proinflammatory agonists via inflammasome assembly and activation (188).

Ultimately, phagocytosis terminates in the formation of a phagolysosome, through the fusion of the phagosome with lysosomes, a highly microbicidal and hostile microenvironment within which microorganisms are killed and certain microbial ligands are processed and presented by antigen presenting cells to tailor the immune response acting against infection further (178).

The release of cytokines and chemokines throughout phagocytosis activates neighbouring immune cells and amplifies the immune response. The main contribution of macrophage to immune learning is the presentation of microbial antigens on the macrophage cell surface throughout and after bacterial killing, which also activates neighbouring immune cells, but in a more/highly specific manner, contributing to the activation of the adaptive immune response.

Throughout phagocytosis, bacteria may also be recognised further, either through the exposure of new bacterial ligands, due to non-specific bacterial lysis, or by the growth and division of bacteria within the phagosome or macrophage, by host septin proteins.

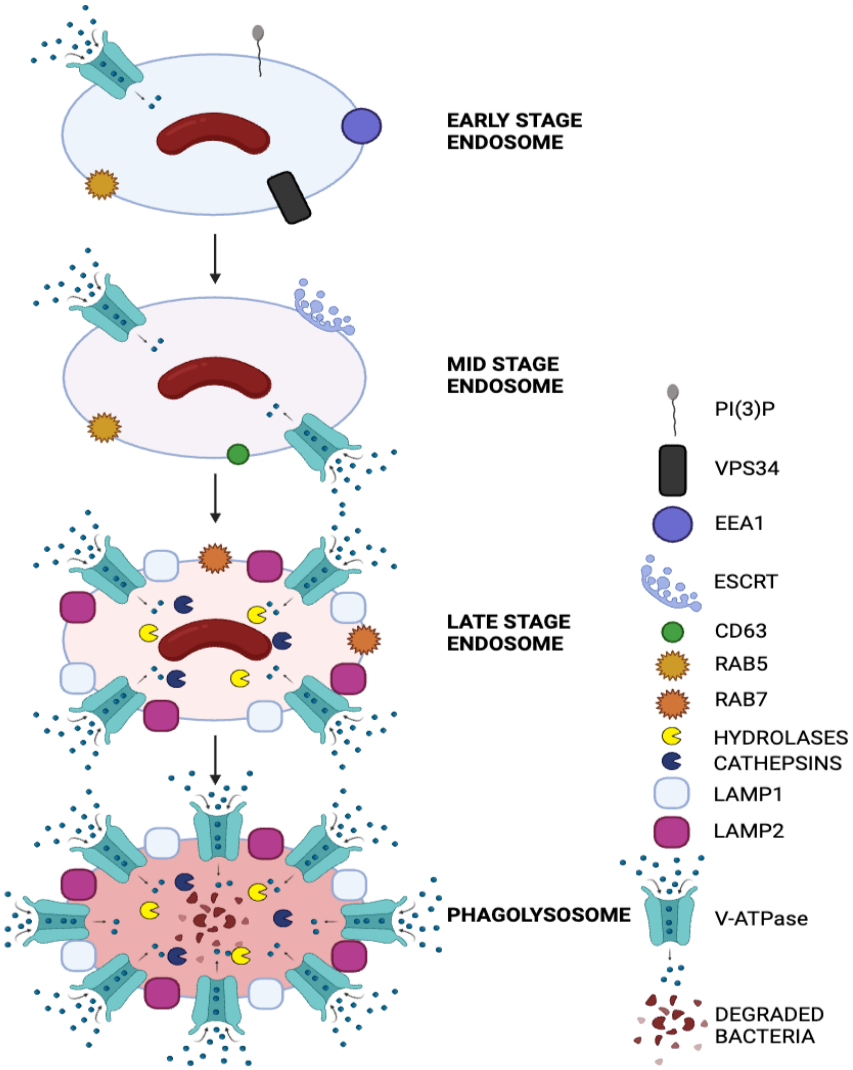

Figure 1.4.5: A schematic depicting the different stages of phagocytosis and phagosomal maturation. After bacterial uptake, maturation of the phagosome is choreographed by diverse surface membrane markers, coordinating the fusion of lysosomes containing various antimicrobial factors, eventually culminating in the formation of a highly acidic, bactericidal phagolysosome. Blue to red shift indicates a shift towards a more acidic pH. PI(3)P: Phosphatidylinositol 3-Phosphate; VPS34: Phosphatidylinositol 3-Kinase Catalytic Subunit Type 3; EEA1: Early Endosomal Antigen 1; ESCRT: Endosomal Sorting Complex Required for Transport; CD63: Cell Differentiation 63; RAB5/7: Ras-related protein 5/7; LAMP1/2: Lysosomal Associated Membrane Protein 1/2; V-ATPase: Vacuolar ATPase. Figure drawn and adapted from Flannagan et al., 2009.

1.4.6. Avoidance of the innate immune response

Microorganisms can avoid the immune response by altering their recognition, preventing phagosomal maturation, or suppressing the onwards signalling.

1.4.6.1. Preventing microbial recognition

Bacteria can prevent recognition by the host immune response either by hiding their surface antigens, or by varying them to prevent repeated recognition by a host that has previously encountered them.

1.4.6.1.1. Masking surface ligands.

To hide their immunogenic surface ligands from detection by the host immune response, some bacteria, including *Streptococcus pneumoniae, Haemophilus influenzae, Escherichia coli* and *Neisseria meningitidis,* express a polysaccharide capsule on their surface (189). As mentioned above, the capsule prevents antibody opsonisation and complement deposition on the bacterial cell surface, thus minimising recognition by the immune response (190, 191). Fimbriae and pili can protrude from the capsule; therefore, the bacterium can still adhere to host cells without exposing its surface (191). *Pseudomonas aeruginosa* expresses alginate to mask the expression of antigens on the bacterial surface (192).

As mentioned above, some bacteria can modify Lipid A in their outer membrane to avoid lysis by antimicrobial peptides. Similar modifications to Lipid A can also minimise recognition by TLR-4, resulting in a significant reduction in TLR-4 activation and NFκB activation (193, 194), as seen in *Helicobacter pylori* (195)*, Salmonella typhimurium* (194) and *Yersinia spp.* (196).

Other bacteria, such as *Listeria monocytogenes*, secrete peptidoglycan hydrolases when internalised within host macrophage, lysing peptidoglycan fragments to prevent recognition by host NOD2 receptors (197, 198).

1.4.6.1.2. Modification and utilisation of host proteins to prevent recognition.

Bacterial pathogens may also secrete proteins that interfere with host signalling molecules or opsonins to prevent opsonisation or complement cascade activation (190, 199).

Streptococcus pneumoniae (200-202)*, Neisseria spp.* (203) and *Staphylococcus aureus* (204) cleave immunoglobulins by secretion immunoglobulin proteases, preventing the formation of effective Fc receptor complexes and uptake by host phagocytes (199). *Neisseria* also sequesters Factor H onto its outer surface, which prevents complement activation (205, 206), as well as incorporating sialic acid onto its surface in an attempt to mimic the host cell surface (Crocker et al., 2005).

Campylobacter jejuni and *Helicobacter pylori* produce flagella enclosed in a membranous sheath, which prevents recognition by TLR-5 (36).

1.4.6.1.3. Variation of surface ligands.

Bacteria can vary their surface antigens to prevent repeated recognition by the host, either through expressing multiple different copies of a surface ligand, or by having a highly variable recognition domain within the ligand, that is constantly changing (191). *Neisseria spp.* are key examples of this, where they can alter the combinations of terminal sugars that it expresses in its lipooligosaccharide outer membrane, through different carbohydrate biosynthesis genes, to avoid detection (207). *Neisseria* also have multiple copies of outer membrane Opa proteins, all of which have a slightly different immunogenicity. By expressing various combinations of these Opa proteins, *Neisseria* can minimise immune recognition (207).

Once taken up, some bacterial pathogens still employ mechanisms to minimise further recognition by the immune response.

Salmonella enterica encodes a two component regulator system, with PhoQ that senses starvation of essential nutrients, phagosome acidification and the presence of cationic antimicrobial peptides (208-210) phosphorylating the cytoplasmic response regulator PhoP in response to hostile environmental stimuli, subsequently altering the protein (structural components, virulence associated secretion systems, flagellar apparatus and membrane transport systems) and lipid (LPS and glycerophospholipid) content of the outer membrane to render the bacterium resistant to the effects of the phagosome and also less immunogenic.

PhoPQ alters the outer membrane by activating pag (PhoP activated gene) expression. These genes encode OMPs, including a protease similar to *S. enterica* PgtE, which promotes CAMP tolerance, and a UDP-glucose dehydrogenase that performs the first step of the L-Ara(4)N Lipid A modification pathway linked to polymyxin resistance (211-213), intracellular type 3 secretion system regulators, including *Salmonella* Pathogenicity Island 2 (SPI2) (214, 215), ATP synthase transport inhibitors, to buffer cytosolic pH (216), and enzymes that covalently modify the outer membrane barrier components (217), e.g. PagL lipase, which deacetylates Lipid A, reducing the negative charge of the outer membrane and decreasing TLR-4 stimulation (58, 218).

These outer membrane components may be modified by decreasing O-antigen chain length (219), acylating/deacylating and hydroxylating lipid A (decreasing TLR-4 recognition and CAMP sensitivity) (217, 220), derivating lipid A and core oligosaccharide with cationic groups (214, 221-224), palmitoylating peptidoglycan molecules in the cell wall (225), increasing cardiolipin content and increased protein synthesis, masking the LPS negative charge and decreasing outer membrane permeability to CAMPs (213, 226, 227), all of which allows for survival within the acidified phagosome.

1.4.6.2. Preventing microbial uptake into macrophages

Bacteria may inject effectors into the host cell to modulate cell signalling and hijack phagosomal maturation and the immune response. This is covered in detail in (191), (190) and (199), and is outside the scope of this project, therefore I will not discuss this further here.

1.4.6.3. Preventing oxidative killing within phagolysosomes

Mechanisms of stalling phagosomal maturation, by preventing the accumulation of the cell surface markers that choreograph maturation and trigger lysosome fusion, or even escaping the phagosome completely, are expertly reviewed in Smith et al., 2013 (178) and so will not be covered here. I will focus on the mechanisms that bacterial pathogens use to **tolerate** conditions within the phagosome, especially oxidative stress.

Bacteria typically encode several oxidative stress tolerance enzymes within their own genome, owing to the need to detoxify reactive oxygen species, hydrogen peroxide and other oxidative species that are generated through their own aerobic respiratory chain, via the high rates of electron transfer that occur via flavoenzymes in the electron transport chain (228). Some bacterial pathogens have subsequently evolved to upregulate the expression of these oxidative stress tolerance genes to counteract the oxidative stresses within the phagosome and promote bacterial survival. These enzymes include, but are not limited to, superoxide dismutases, catalases and peroxidases.

1.4.6.3.1. Superoxide dismutases

Superoxide dismutases catalyse the conversion of oxygen radicals into diatomic oxygen and hydrogen peroxide (Figure 1.4.6). Hydrogen peroxide is then metabolised further by bacterial peroxidases and catalases, neutralising the products of the macrophage oxidative burst.

Burkholderia pseudomallei produces a superoxide dismutase enzyme, SodC, which deactivates superoxide molecules within the phagosome and is essential for survival and virulence (229). Other pathogens, including *Streptococcus agalactiae*, need phagosomal maturation to occur as the acidification triggers the expression of virulence genes, including *sodA* and the oxygen metabolite scavenger glutathione which protects the bacterium against oxidative stress by soaking up oxygen radicals (230-233).

1.4.6.3.2. Peroxidases & catalases

Catalases work in combination with superoxide dismutases to counteract the macrophage respiratory burst. They convert hydrogen peroxide into water and oxygen, effectively negating the antimicrobial effects of reactive oxygen species generation by host phagocytes (Figure 1.4.7).

Other examples of peroxide neutralising enzymes are alkyl hydroperoxide reductases (Ahp), scavengers of intracellular hydrogen peroxide that would otherwise damage cellular lipids and proteins, resulting in bacterial cell death and therefore they play a critical role in the response to oxidative stress (234). Ahp proteins scavenge hydrogen peroxide at lower concentrations whereas catalases are the predominant scavenger at higher concentrations (234). Other pathogens may utilise urease to convert microbicidal reactive species to less harmful by-products such as hydrogen peroxide and ammonia, which are then further broken down by catalases (185).

In *Helicobacter pylori*, a catalase enzyme and SodB convert superoxide to harmless by-products, whilst arginase RocF depletes nitric oxide and AhpC neutralises reactive nitrogen species (235-238).

In summary, bacteria encode multiple classes of oxidative stress tolerance genes within their genome, which may provide a survival benefit and assist in tolerating phagosomal conditions within a host, contributing to the establishment of bacterial infection. These mechanisms overlap and may compensate for one another, highlighting the important role of these proteins.

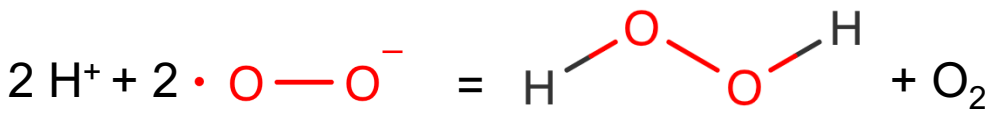

Figure 1.4.6: A schematic showing the chemical reaction of the detoxification of superoxide molecules into hydrogen peroxide and diatomic oxygen, which is catalysed by SOD enzymes. Figure generated using information from UniProt.

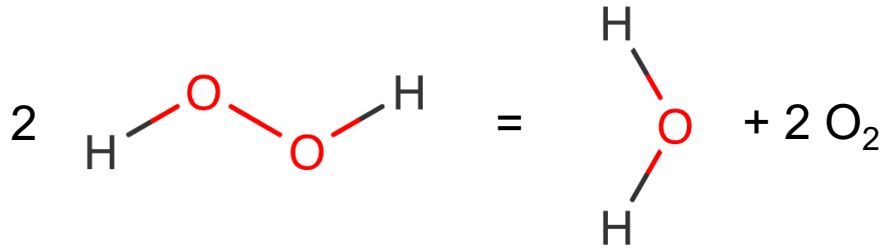

H_2O_2 + Fe(III)-E -> H_2O + O=Fe(IV)-E

H_2O_2 + O=Fe(IV)-E -> H_2O + Fe(III)-E

*Fe-E represents heme group attached to catalase

Figure 1.4.7: A schematic showing the chemical reaction of the detoxification of hydrogen peroxide into water and diatomic oxygen, which is catalysed by catalase enzymes. Figure generated using information from UniProt.

1.5. Antibacterial agents within a host

There are now multiple different classes of antibiotics which have been discovered and are in use for the treatment of bacterial infection. These classes differ in their target range i.e., broad spectrum vs. narrow spectrum, their target site, and their mechanism of action. Bacteriostatic antibiotics inhibit bacterial cell growth but do not kill, usually through the interruption of cellular process such as DNA replication, translation, and transcription. Bactericidal antibiotics kill bacterial cells by inducing lethal structural changes in their peptidoglycan cell walls or phospholipid membranes, resulting in a loss of cellular structural integrity and cell death.

These classes of antibiotics have been well characterised *in vitro* and are greatly effective. The modes of action and resistance are expertly reviewed in (239) so I will not discuss them here.

But, of course, antibiotic treatment occurs within a living host, therefore we must consider the efficacy of antimicrobial treatments in a host setting. The use of *Bdellovibrio bacteriovorus* as an antimicrobial therapy will result in bacterial pathogen lysis, amplifying the proinflammatory immune response due to the release of multiple immunogenic bacterial cell fragments. Many antibiotics also induce bacterial cell lysis; therefore, we can draw parallels between the impact of antibiotic-mediated bacterial lysis on the immune response, and the potential implications of *Bdellovibrio*-mediated bacterial lysis on the host immune response.

1.5.1. Bacterial death (*in vivo*) during cell-wall targeting antibiotic treatment.

Penicillins and other cell wall targeting antibiotics kill bacterial cells by interfering with peptidoglycan crosslinking, resulting in osmotic lysis of the bacterial cell. This is attributed to an imbalance between peptidoglycan synthases and peptidoglycan hydrolases (240) that, through the inhibition of transpeptidase enzymes by penicillins, induces the depletion of peptidoglycan precursors and therefore prevents further peptidoglycan synthesis, whilst also upregulating hydrolase-induced degradation of the remaining peptidoglycan (241). This results in lysis of the bacterial cell and the release of a significant amount of highly immunogenic cell fragments, which are subsequently detected by the host immune system.

This made me consider how bacterial lysis, through antibiotic use or other antimicrobial treatments, may amplify the immune response.

Other forms of bacterial cell lysis within the host, for example lysozyme action, can inform us about the potential effects of bacterial cell lysis on the immune response. Lysozymes trigger bacterial cell lysis by hydrolysing cell wall peptidoglycan or cationically integrating into the bacterial membranes to form pores (242). The actions of lysozymes, and how bacterial pathogens can resist lysozyme action, are reviewed further in Ragland & Criss, 2017.

The actions of lysozymes have clear implications for the host immune response, whereby lysozyme-containing vesicles bind with the phagosome, degrading the internalised bacteria and activating downstream NOD1/2 receptors (via binding of MDP), TLRs and inflammasome assembly, resulting in NFκB activation and proinflammatory cytokine release (242-244). Lysozyme inhibition in macrophages decreases the activation of the inflammasome (245, 246), whilst insoluble peptidoglycan but not soluble peptidoglycan activates the inflammasome (245), supporting the idea that lysozyme does enhance the immune response to peptidoglycan.

Increased lysozyme-mediated degradation does lead to an enhanced inflammatory response (245), but lysozyme action also contributes to peptidoglycan degradation, reducing inflammation (242, 247-249). Smaller peptidoglycan fragments have been shown to be more stimulatory to NOD2 (85, 250, 251), but cleavage by lysozymes reduces the recognition of some peptidoglycan fragments, reducing immune recognition (242).

Interestingly, macrophage and neutrophils are poorly responsive to extracellular MDP (252) and only respond at high concentrations (253), compared to MDP release within the phagosome which phagocytes seem optimised to respond to (242). Additionally, extracellular, soluble peptidoglycan fragments are not effective at activating phagocytes (242).

Studies of phage therapy treatment of a *Pseudomonas aeruginosa* bone infection correlated the release of bacterial cells or cell fragments into the bloodstream with a marked upregulation of innate immunity and transient fever, suggesting that bacterial lysis does induce an inflammatory immune response (254).

Putting this in the context of antibiotic-induced lysis, the release of a large amount of peptidoglycan alone may not induce an excessive and potentially damaging proinflammatory immune response. However, bacterial lysis will also release fragments of lipid A, which is highly immunogenic, flagellins and other bacterial surface proteins and bacterial nucleic acids, suggesting there is still potential for an excessive inflammatory response. The consequences of antibiotic induced lysis of bacterial cells, and the subsequent potential upregulation of the immune response, still require further exploration.

As *Bdellovibrio* uses and re-utilises a large proportion of the components of the Gram-negative prey cell, to produce its own progeny, it is possible that *Bdellovibrio* predation may induce less of an inflammatory immune response than antibiotic-induced lysis, although this would require further investigation.

1.5.1.1. Where do bacteria encounter antibiotics in vivo?

When administered, antibiotics must cross multiple membranous barriers within the host before they can target bacteria. This is further complicated in some bacterial infections by the uptake of bacteria by host phagocytes, meaning that antibiotics must access a further subcellular compartment before they can act on the bacterium. One such example of this is *Mycobacterium tuberculosis*, which is well known to be phagocytosed by macrophage and subsequently escape the phagosome, residing within the privileged subcellular environment of the macrophage (255).

One study of the anti-tubercular drug Bedaquiline showed that antibiotics accumulated within host cells, within lipid droplets. This increased the local antibiotic concentrations and acted as a both a drug trafficking mechanism into the cell, towards the bacterium, and a reservoir of antibiotic that, when the lipid droplet was metabolised and consumed by the tuberculosis bacterium, killed it (256). It is also suggested by Greenwood and co-workers that other intracellular pathogens may interact with lipid droplet reservoirs of other antimicrobial drugs via a similar mechanism, improving drug efficacy (256).

This highlights how drug efficacy is highly reliant on the bacterial localisation when the treatment is administered (256, 257)

For some pathogens, the interactions between bacteria and the host immune response is a well-established field. Whereas for *Bdellovibrio bacteriovorus*, a lot of the interactions with the host immune response were largely unknown, until they began being unpicked in Willis et al., 2016.

1.5.2. Alternatives to antibiotics

Antibiotic resistance mechanisms within bacteria are often costly, therefore, to reduce antimicrobial resistance development and spread, the ideal solution would be to not use antimicrobial agents or to advocate stewardship to limit their use. However, this is unrealistic, as they are a vital part of the treatment of infectious disease, without the treatment of which many more individuals would die. Instead, we must find alternatives to current antibiotics, either through chemical modification of existing antibiotics, discovery of new antibiotics or development of entirely novel, non-chemical, antimicrobial therapies that do not fall foul to the widespread, naturally occurring resistance mechanisms found in the environment. What is needed is a shift away from conventional antibiotics that target a single molecule, towards a more complex, multi-target approach that isn't so readily defeated by the evolution of resistance.

Various classes of alternatives to antibiotics are briefly summarised below.

1.5.2.1. Adjuvants

Adjuvants, other pharmacological modifiers of bacterial growth and function, represent one potential tool which may help to extend the lifespan of conventional antibiotics whilst novel antimicrobial therapies are developed. These chemicals typically have little antimicrobial activity themselves but enhance the efficacy of antibiotics by increasing drug uptake (efflux pump inhibitors inhibit the export of antibiotics from the cell; Loperamide makes the bacterial membrane more permeable to antibiotics) or targeting resistance mechanisms (Clavulanic acid cleaves the TEM β-lactamase, restoring β-lactam sensitivity) (258). However, resistance to adjuvants has already been seen in a clinical setting, suggesting the utility of adjuvants is limited by resistance formation, much like their antibiotic counterparts.

1.5.2.2. Vaccination

Vaccination represents another approach to curtail antimicrobial resistance, by preventing bacterial infection in the first instance. This may have a large impact in the treatment of human infectious disease and animal disease in an agricultural setting (259). The treatment of *Haemophilus influenzae* infection with vaccination reduced β-lactamase prevalence within the *Haemophilus* population and reduced *Haemophilus* infection, demonstrating the utility of vaccination as an approach to combatting antimicrobial resistance (260, 261). However, resistance may evolve to current vaccines and new strains may emerge due to selection pressures against others, such has been the case for the *Streptococcus pneumoniae* Type A vaccine (261), suggesting that vaccines will need to be constantly modified to cover further serotypes and remain effective.

1.5.2.3. Anti-virulence factors

Anti-virulence factors prevent the establishment of infection by inhibiting bacterial mechanisms of colonisation or effector molecule release e.g., Type 3 Secretion System or Quorum Sensing inhibition (262-264). Drawbacks of anti-virulence factors are that they have a narrow spectrum, meaning that clinical diagnostics would need to advance to make their implementation most efficacious, they rely on a functional host immune system to eradicate the pathogen, which may not always be the case if treating immunocompromised individuals, and they only target actively growing cells that are expressing the virulence factor in question so do not eradicate all of the bacterial load as they are not effective against dormant/non-growing cells (265-268). They also have a single target typically, suggesting that the evolution of resistance mechanisms would also limit their effectiveness (269).

1.5.2.4. Bacteriophage therapy

Bacteriophage target and infect bacteria in a highly receptor-specific manner, making them an effective, narrow-spectrum antimicrobial for targeting biofilm and planktonic bacterial populations (270-272). Bacteriophage attack bacteria when they are modifying their cell wall or peptidoglycan, potentially in response to the microenvironmental conditions within a human or animal host, giving a level of complexity to their antimicrobial action that requires further investigation to be fully understood.

This raises the subject of how bacteriophage-mediated pathogen killing is impacted within a host or within host phagocytes due to the host environment induced modifications to the bacterial pathogens surface. Due to this high specificity, large libraries of bacteriophage would be needed, and diagnostic tools would need to improve to make bacteriophage a viable antimicrobial treatment option. Although receptor site mutation may provide resistance to bacteriophage entry in some cases, the live nature of this therapy may mean that co-evolution of both bacteriophage and pathogen may slow resistance formation (270-272).

1.5.2.5. Enzybiotics

Use of the bacteriostatic and bactericidal compounds, such as peptidoglycan hydrolases, phospholipases and other hydrolytic enzymes, that bacteriophage utilise as part of their lifecycle may also represent potential, novel antimicrobials (270, 273-276). Enzymes from the predatory lifecycle of *Bdellovibrio bacteriovorus* may also be of some use as enzybiotics for the treatment of bacterial infection (277).

Bdellovibrio bacteriovorus has a broad host range, preying on a range of Gram-negative bacteria, with predation not being impacted by a capsule, unlike some phage therapy (21). The use of *B. bacteriovorus* as a potential, novel antimicrobial therapy will require an in-depth analysis of the immune response to *Bdellovibrio* itself, and predation, whilst also assessing the efficacy of, and barriers to, predation within a host environment. Current knowledge, from 60 years of laboratory studies and initial *ex-vivo* and *in-vivo* studies, is summarised below.

1.6. *Bdellovibrio bacteriovorus*

1.6.1. Background

Bdellovibrio bacteriovorus is a small (0.3 μm x 1 μm) Gram-negative bacterium, vibroid in shape, belonging to the delta proteobacteria (278) (Figure 1.6.1). It is found within the environment, in soil and water, where it preys upon other Gram-negative environmental bacteria completing its predatory cycle and multiplying (278). *B. bacteriovorus* has a wide host range, preying on all known Gram-negative bacteria without discrimination due to capsule synthesis or LPS modifications, two common forms of immune response and antibiotic resistance.

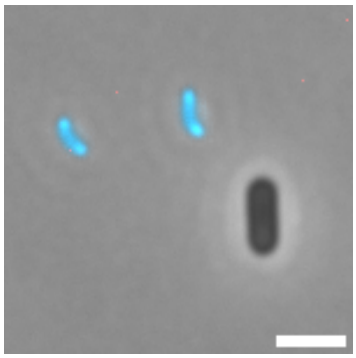

Figure 1.6.1: *Bdellovibrio bacteriovorus* is a small Gram-negative bacterium. Shown are two attack phase *B. bacteriovorus* bacteria (illuminated in blue due to a constitutively expressed cytoplasmic protein, Bd0064, being tagged with an mCerulean fluorescent tag) alongside an *E. coli* S17-1 prey bacterium (Dark). Phase: Exposure 250 ms; mCerulean: Exposure 10 s, Excitation 420-450 nm, Emission 460-500 nm. White scale bar represents 2 μM.

1.6.1.1. Genomic diversity

Of the three well-studied species of *B. bacteriovorus*, all of which belong to the same phylogenomic lineage, *B. bacteriovorus* HD100 is by far the best studied, owing to the availability of a complete genome sequence. *B. bacteriovorus* 109J is also studied, with predation being slower and progeny being shorter and fatter, with the genomic reasons behind this diversity in morphology remaining unknown.

B. bacteriovorus HD100 has a predominantly predatory lifecycle, with host-independent growth on rich carbon sources remaining rare (1 in 10^7 bacteria), whereas *B. bacteriovorus* Tiberius (isolated from the carbon rich river Tiber) exhibits both host-dependent and host-independent lifecycles, likely due to the high amount of carbon and nutrients present (279). This increased bias towards host-independent growth, compared to HD100, is independent of the mutation associated switch to host-independent growth within the Host Interaction locus (detailed in Section 1.6.4) of *B. bacteriovorus* HD100 (279).

The genomes of *B. bacteriovorus* Tiberius and *B. bacteriovorus* HD100 are highly syntenic. Minor differences between *B. bacteriovorus* Tiberius and *B. bacteriovorus* HD100 include an increase in outer membrane and capsular polysaccharide synthesis genes (*bd1677-1702*) and cytochrome biogenesis genes facilitating alternative electron transport (*bd2046, bd2668, bd2597-2602*). These changes are likely due to the terrestrial habitat of *B. bacteriovorus* HD100, compared to the aquatic habitat of *B. bacteriovorus* Tiberius (279).

I have chosen to focus on *B. bacteriovorus* HD100 for my studies, owing to its lifecycle being well studied, and the presence of a complete genome sequence, making it more genetically tractable.

Encoded from the 3.8Mb genome of *B. bacteriovorus* is a wide range of proteins and hydrolytic enzymes that facilitate the predatory lifestyle by enabling the attachment to, invasion and re-modelling, and consumption, of prey macromolecules to produce progeny (280, 281). The genome is atypically large for a small bacterium, due to the array of hydrolytic enzymes and regulatory systems that are required for predation, but this fitness cost is likely outweighed by the exclusive access to the prey cell contents ascribed by the predatory lifecycle (279). Functional categorisation of the genome reveals genes for motility, alongside lipid, amino acid, nucleotide and carbohydrate metabolism and transport, similar to typical Gram-negative bacteria. How *Bdellovibrio* differs is speculatively due to the differential regulation and expression of these genes, rather than the gene content itself.

However, the genome of *B. bacteriovorus* is poorly annotated, with only 55% of the 3584 predicted proteins having a putative homology-assigned function, 11% of proteins having homology to proteins of unknown function and 34% not homologous to any known proteins (281). The function of the majority of the genes that facilitate the predatory lifecycle are unknown, and it is likely these genes that define the largely predatory lifecycle of *Bdellovibrio*, making characterisation of these predation-specific genes exceptionally difficult (281, 282). Lifespan proteomics and transcriptomics to understand further the genomic events that underpin predation are currently ongoing. However, the genes that support the predatory lifecycle of *Bdellovibrio* and how these genes individually contribute to predation are largely known.

Random transposon insertion mutagenesis studies, performed by Tudor and co-workers (283) and Duncan and co-workers (284) revealed that, although non-predatory gene deletion mutants were obtainable, these genes frequently did not code for proteins of known function. The enzymatic toolkit that allows *Bdellovibrio* to prey on other Gram-negative bacteria largely consists of genes that all Gram-negative bacteria possess, mainly for cell wall and membrane homeostasis, but the regulation and expression of these genes differs in *Bdellovibrio*.

The genome of *B. bacteriovorus* has no evidence of recent horizontal gene transfer from prey, based on a comparison of GC content (281). The GC bias within the genome, and the digestion of prey nucleic acids as part of the predatory cycle, suggest that little lateral gene transfer occurs during predation. However, ancient gene transfer has shaped the *Bdellovibrio* genome to a great extent, contributing upwards of 20% of the current genome (285). This is debated by some, with others suggesting that both ancient and recent lateral gene transfer from environmental bacteria (prey and others) into the *B. bacteriovorus* genome is evident (286, 287).

The novel proteins and hydrolytic enzymes that facilitate predation are of great interest to scientists for a different reason; the increasing need for novel antimicrobial therapies to combat Gram-negative mediated multidrug resistant infections. The better understanding of the predation process, and its components, will hopefully be one avenue that provides these novel antimicrobial therapies.

1.6.2. Surface composition

Predation by *B. bacteriovorus* centres around the predator and pathogen cell surface, making the interface between predator and prey surfaces somewhat analogous to that of the host-pathogen interface. Alterations to the pathogen cell surface will impact both recognition and predation by *B. bacteriovorus* and immune action against the pathogen by the host, therefore any pathogen cell surface changes that are induced by the host environment, the immune system or *B. bacteriovorus* predation are important to consider when discussing the use of *B. bacteriovorus* as an antimicrobial therapy and for the resolution of infection.

The surface of *B. bacteriovorus*, like other Gram-negative bacteria, is a patchwork of outer membrane associated components including fimbriae, pili, outer membrane proteins (OMPs), autotransporters and secretion systems, all of which aid in bacterial survival (288).

Bdellovibrio is not known as a pathogenic bacterium to animals and therefore does not have the surface adaptations of animal pathogens which can survive and pathogenically engage with animal hosts (289). Furthermore, the chemical differences between *Bdellovibrio* and its own bacterial prey can be important in it not destroying itself while consuming a bacterium from within (290-292).

1.6.2.1. LPS

The LPS of *B. bacteriovorus* is atypical, yielding an altered lipid conformation and sphingolipid content that aids membrane fluidity and prey invasion (288). The lipid membranes of *B. bacteriovorus* contain phosphatidylethanolamine and phosphatidylglycerol as the predominant glycerophosphatides, with phosphosphingolipids present too, giving an unusual lipid chemistry (293), that increases the fluidity of the outer membrane and aids in the invasion of Gram-negative prey when pulling itself through the tight, enzymatically generated invasion pore. These differences in LPS lipid composition are also important to its predation of other Gram-negative bacteria, who have a “typical” LPS composition, and not targeting or killing itself throughout the predatory process, although, as the ligands that are targeted during predation are unknown, this is poorly characterised.

α-D-pyramannose groups replace the 1' and 4' phosphate groups on *Bdellovibrio* Lipid A, yielding a Lipid A moiety with no negatively charged groups, reducing the endotoxic activity and immunogenicity of *B. bacteriovorus* LPS and reducing cytokine activity also (reduced TNFα and IL-6 c.f. *E. coli* K12) (Schwudke et al., 2003; Schromm et al., 1998). *Bdellovibrio* LPS contains 6 fatty acid chains, all of which are hydroxylated and are approximately 13 or 14 carbon atoms in length (294). The fatty acid chains of Lipid A also play an important role in TLR-4 recognition and binding (295). Fatty acid chain length and hepta-acetylation of Lipid A are comparable to *E. coli* suggesting immunogenicity differences are not due to these components, although they may have a slightly altered conformation due to the alternative head group and interactions between side chains (Schwudke et al., 2003; Schromm et al., 1998).

1.6.2.2. Peptidoglycan

The *B. bacteriovorus* HD100 cell wall is not markedly different in composition to that of other bacteria, but differs in the crosslinking and modifications of the peptidoglycan monomers (296). Bacterial cell walls are comprised of highly crosslinked strands of peptidoglycan monomers, forming a strong structure that is constantly undergoing dynamic remodelling to allow for bacterial growth and division whilst still conferring its primary roles of providing strength and osmotic stability to the cell (297-299). The bacterial cell wall is indispensable and forms one of the key barriers between the bacterial cell and the environment, second only to the bacterial outer membrane (297-299).

Peptidoglycan therefore plays a key role in the predation process and represents a key barrier that *B. bacteriovorus* has evolved to overcome, traverse, modify, utilise and ultimately degrade throughout the predation process (290-292, 300).

As the surface of the *Bdellovibrio* predator and Gram-negative prey are comprised of the same key components, *Bdellovibrio* may alter its outer surface components to target prey without targeting itself. These alterations to the outer surface components may also make *Bdellovibrio* less well recognised by the host immune response. The LPS of *Bdellovibrio* is distinct and differs from the typical LPS of Gram-negative prey (see Section 1.6.2.1) (301). The peptidoglycan of *Bdellovibrio* is of the same composition of Gram-negative prey bacteria, with differences in modification demarcating predator peptidoglycan from prey.

To differentiate between its own peptidoglycan and prey (target) peptidoglycan, *B. bacteriovorus* dynamically alters peptidoglycan acetylation (and therefore lysozyme susceptibility) throughout predation, deacetylating prey peptidoglycan and demarcating it from its own, which remains acetylated, before lysing it to liberate *Bdellovibrio* progeny from the cell (290). *Bdellovibrio* targets 3', 4' crosslinks in prey cell peptidoglycan, cleaving them to form a rounded but osmotically stable bdelloplast. (277)

Bdellovibrio D, D-endopeptidase enzymes do not act on the crosslinks in its own peptidoglycan due to the secretion of regulatory proteins that prevent self-action (277, 291). Also, the D, D-endopeptidase enzymes are not folded into their active state until they cross the *Bdellovibrio* periplasm, therefore they cannot act on the *Bdellovibrio* peptidoglycan. Deacetylation of prey peptidoglycan upon predator entry, and digestion of prey peptidoglycan with a deacetylated-peptidoglycan-specific enzyme at the end of predation are key to the successful completion of predation (290-292).

Acetylation state of peptidoglycan also alters susceptibility to host lysozymes and recognition by host PRRs and accessory proteins, as detailed in Section 1.4.3.2 and 5.5.2.1.2.

1.6.2.4. Pili

Type IV pili are long, retractable surface fibres that play a critical role in predation (302), through attachment to the prey cell wall and forcing of predator through the porthole in the prey cell, without which (via disruption of the pilus fibre gene *pilA,* although pilus extension and retraction ability remained) attachment, entry and predation do not occur (302, 303). Type IV pili have also been shown to be important for the initial recognition and attachment to prey in liquid cultures and in biofilms, where defects in a *pilT* gene lead to an impaired ability to clear biofilms (304, 305).

Upon attachment of *B. bacteriovorus* to a prey cell, Type IV pili retract, bringing the outer membranes of the two bacteria into contact. Pili retraction, through the Host Interaction (HIT) locus, alters the growth state of the *Bdellovibrio* cell, triggering the expression and secretion of peptidoglycan-modifying enzymes that begin the next stage of bacterial predation and predator entry (detailed further in Section 1.6.3). Type IV pili are also implicated in contracting to squeeze the *Bdellovibrio* cell through the enzymatically generated pore, generating a strong physical force to aid predator entry, which increases predation efficiency (302).

1.6.2.5. Flagellum

Flagella are proteinaceous structures associated with cell motility. *B. bacteriovorus* has a single, polar, membrane sheathed flagellum (306) comprised of flagellin monomers, encoded by 6 genes. 1 of these 6 FliC genes is essential for normal flagellar motility and predation, with the other 5 being individually mutated to little effect and so only make a minor contribution to flagellar structure (307, 308).

Flagellar motility is not essential for predation and prey entry but flagellar rotation does drastically improve predation efficiency in planktonic populations, owing to the increased motility of predators increasing the likelihood of predator-prey collision and subsequent attachment and predation (307). The flagellum is internalised upon entry into the prey (309) and resynthesized on progeny attack phase cells at the completion of the predation cycle (306, 310, 311). Flagellar motility is powered by one of three pairs of MotAB proteins that form ion channels near the FliG motor protein and power its rotation and flagellar motility, with each being dispensable for motility (312).

Flagellins, the subunits of flagella, are recognised by the host PRR TLR-5. As mentioned previously, the main recognition site on bacterial flagellins (for TLR-5 recognition) lies between amino acids 89 and 96 (36). This recognition site is also conserved in the 6 *Bdellovibrio* FliC proteins and the FlaA protein (Figure 1.6.2). This is significant as it means that *Bdellovibrio* flagellin is recognised by TLR-5.

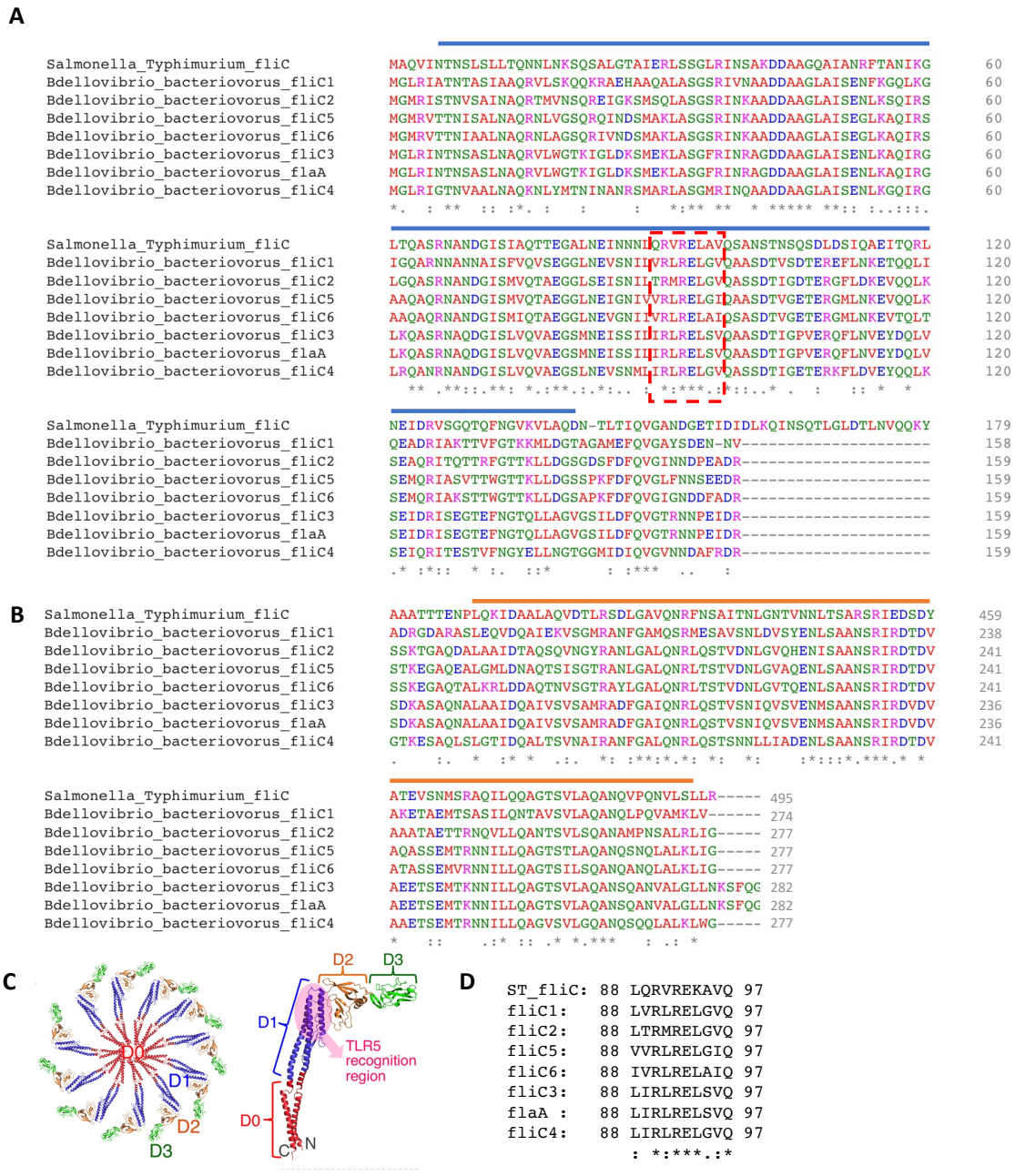

Figure 1.6.2: An alignment of *Bdellovibrio* FliC flagellin proteins (FliC1-6) with *Bdellovibrio* FlaA and *Salmonella* Typhimurium FliC shows a conserved TLR-5 recognition domain. *Bdellovibrio* FliC proteins (FliC1-6; Uniprot ID: Q5W1M9, Q6H8R6, Q6H8R4, Q6H8R2, Q6H8R3, Q6H8R5 respectively) were aligned with *Bdellovibrio* FlaA (Q6MQQ2) and FliC from *Salmonella* Typhimurium (P06179) using Clustal Omega. Blue bar indicates the FliC N-terminal domain (A). Red box indicates the TLR-5 recognition domain, which is conserved within *Bdellovibrio* FliC proteins and with *Bdellovibrio* FlaA and *S.* Typhimurium FliC (A; Zoomed in in D). Orange bar indicates the FliC C-terminal domain (B). FliC monomers (C-Right) assemble into a filament with the N- and C-termini forming a pore down the centre, as represented in the flagellum cross-section (C- Left). Amino acids are coloured by their physicochemical properties. (*) indicates a conserved residue. (:) indicates amino acids sharing strongly similar properties. (.) indicates an amino acid sharing weakly similar properties. Panel C was taken from Lu & Swartz, 2016 .(313).

1.6.3. Lifecycles

B. bacteriovorus exhibits two distinct lifecycles, a host-dependent predatory lifecycle and a host-independent lifecycle (originally named the HI cycle) (Figure 1.6.3) (314, 315). First glimpses of the predation process have been known since 1966, where it was observed that *B. bacteriovorus* attaches (first reversibly then irreversibly) to and forms an enzymatically generated pore, via the action of various endopeptidases (300), through which the predator traverses the Gram-negative cell wall, invades the prey bacterium and grows within the periplasm, consuming the prey cell from within (316).

The predatory lifecycle of *B. bacteriovorus* can be divided into four distinct phases: attachment, invasion, intraperiplasmic growth and cell lysis. Predation of Gram-negative prey by *B. bacteriovorus* typically follows the same progression, with different prey being preyed upon with different efficiency in terms of time taken for completion of predation and the prey population remaining after predation (317, 318).

1.6.3.1. Attachment

Attachment begins when a highly motile, attack phase bacterium navigates itself towards prey using a single, polar flagellum and randomly collides with a prey bacterium via flagellar motility (in liquid) or gliding motility (in biofilms) (319, 320), guided by chemotaxis to regions of high prey abundance (321, 322).

B. bacteriovorus attaches to the prey cell' outer membrane using various pili, which contract to bring the two outer membranes initially into close contact (281, 315). Then, through secreted enzyme action, *B. bacteriovorus* releases a series of peptidoglycan modifying enzymes (277, 296, 323) which de-link and re-link the peptidoglycan and reseal the entry porthole to form an osmotically stable bdelloplast (324, 325).

The ligand required for targeting of *B. bacteriovorus* to prey is still unknown, however a core sugar in the LPS of prey seems to be important (326) and outer membrane porins played no role in targeting (326). Removal of O-antigen seems to increase predation efficiency, perhaps by making core residues more accessible, whereas removing the core decreased predation efficiency/irreversible attachment, but did not abrogate it suggesting that the core oligosaccharide must aid but not be essential for predation (326).

Presence of a thick polysaccharide capsule on the prey bacterium does not prevent predation by *B. bacteriovorus*. The reasons behind this are unknown, although the polysaccharide matrix is not believed to be enzymatically acted upon by *Bdellovibrio* (327).

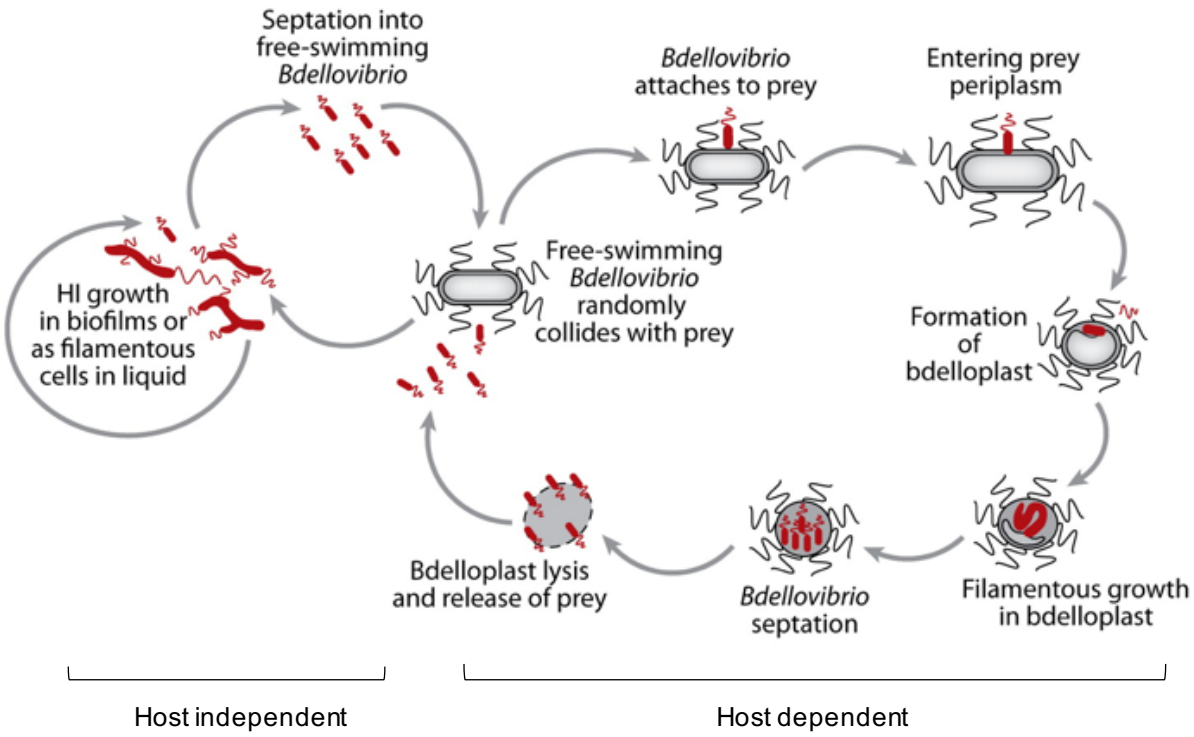

Figure 1.6.3: A schematic of the host dependent and host independent lifestyles of the predatory bacterium *Bdellovibrio bacteriovorus*. Host dependent: Attack phase *B. bacteriovorus* cells randomly collide with Gram-negative prey, attaching and entering the prey via a complex subset of peptidoglycan modification enzymes. Upon entry, *B. bacteriovorus* reseals the entry hole and modifies the prey cell further to form a rounded, osmotically stable bdelloplast. Intraperiplasmic growth proceeds, whereby *B. bacteriovorus* uses and re-purposes prey nutrients and cellular components to form a long filament, which septates upon nutrient exhaustion to form progeny attack phase cells. Upon lysis of the prey bacterium, progeny are released that invade further prey cells and restart the predatory cycle. Host independent: *B. bacteriovorus* undergoes a rare, mutation driven lifestyle whereby it grows in a slower, non-predatory manner. Figure taken from Sockett et al., 2009.

1.6.3.2. Invasion

Upon entry, electron transport across the prey inner membrane ceases and the prey cell is killed (328). The entering *Bdellovibrio* is exposed to the highly oxidising, high proton, low pH environment of the prey periplasm due to a now-dysfunctional electron transport chain (ETC), cytochromes and proton pumps that form part of the bacterial cells aerobic respiratory chain making the periplasm a highly oxidising environment. The oxidative stresses that *Bdellovibrio* experiences throughout predation are largely unknown, but I hypothesise that *Bdellovibrio* will undergo high amounts of oxidative stress when entering the prey cell periplasm, due to the abundance of reactive oxidative species and low pH environment. *Bdellovibrio* must quickly adapt to this hostile microenvironment, upregulating the twin arginine transport (Tat) system and exporting metalloproteinases and other oxidative stress response proteins to soak up the electron radicals (329).

1.6.3.3. Intraperiplasmic growth

Intraperiplasmic growth then begins, whereby *B. bacteriovorus* embeds a wide range of nutrient transporters, porins and outer membrane proteins to transport nutrients from the prey cell cytoplasm and degradative enzymes in to the prey cell (330, 331), using the nutrients and prey cell resources for its own intraperiplasmic growth. The hydrolysis of prey macromolecules by predator enzymes may generate free radicals and reactive oxygen species, leading to *Bdellovibrio* experiencing high levels of oxidative stress.

B. bacteriovorus has evolved to be highly efficient in its use of prey resources for intraperiplasmic growth, using the majority of the prey's nutrients and cellular components in its own growth, with polysaccharides, proteins and lipids all being incorporated into the growing *B. bacteriovorus* filament, often with minimal alteration (332).

Prey DNA and RNA are degraded using nucleases, with the DNA and RNA oligonucleotides and nucleic acids utilised to synthesise its own genome early on in intraperiplasmic growth (331, 333-338). Prey proteins are degraded into amino acids and used as an energy source for predatory growth (332) or as a source of amino acids for predator protein synthesis, owing to *B. bacteriovorus* lacking the biosynthesis pathways for some amino acids (281).

Intraperiplasmic growth results in a large filament growing unidirectionally within the prey periplasm, with chromosome replication, DNA and protein synthesis all occurring simultaneously (339, 340). The septation protein DivIVA controls cell morphology during filamentous cell division, potentially responding to amino acid biosynthesis or redox state cues in the bdelloplast to determine when nutrient exhaustion has occurred and septation and escape is pertinent (341).

Throughout intraperiplasmic growth, the degradation of prey cell molecules and stripping of metal ions from the active sites of prey enzymes, combined with the high rates of metabolism and *Bdellovibrio* growth, will produce an abundance of reactive oxygen species that would prove harmful if left unchecked. I hypothesise that *Bdellovibrio* expresses an arsenal of oxidative stress response proteins to combat this increase in reactive oxygen species.

1.6.3.4. Exit

After intraperiplasmic growth concludes, an unknown signal believed to be triggered by nutrient exhaustion within the prey cell causes further acetylation-sensitive peptidoglycan modification enzymes to be released by the predator, resulting in partial bdelloplast lysis (292, 311). Attack phase *B. bacteriovorus* exit the degraded bdelloplast through discrete pores (342), re-initiating the predatory lifecycle by seeking out new prey.

Exit from the bdelloplast is carefully coordinated with synchronous filament septation (as opposed to binary fission, typical of bacteria) and flagellar synthesis (306, 343), without which a delay in cell motility, bdelloplast exit and subsequent predation are seen (344).

Maintenance of prey cell integrity beyond the cessation of intraperiplasmic growth is possible and is thought to depend upon the availability of susceptible prey cells, via some form of population density sensing mechanism. This mechanism remains uncharacterised, but is believed to be linked to the sensing of prey cell polyamines by *Bdellovibrio* to determine prey cell availability (345). Sustaining bdelloplast integrity until a beneficial, prey rich environment is sensed, may improve predator fitness within the environment as they are protected from other bacteriophage and environmental factors whilst inside the prey cell.

Prey exit requires the hydrolysis of previously pre-modified prey peptidoglycan by predator secreted enzymes (290). Exit from the prey bdelloplasts represents a significant shift in oxygen tension, which may increase the oxidative stresses experienced by *Bdellovibrio* upon prey exit.

To re-cap, the oxidative stresses that are experienced by *Bdellovibrio* when invading a Gram-negative prey cell, and throughout predation are largely unexplored. We can, however, infer where points of high oxidative stress may occur, from other individuals' findings of the oxidative stressors present within the periplasm of "typical" Gram-negative cells (346). *Bdellovibrio* enters the prey cell periplasm, which is dysfunctional owing to it being within a rapidly dying cell and is highly acidic/low pH due to proton pumping into the periplasm by the prey ETC. Disruption of the prey ETC may also lead to free radical release at the terminal cytochrome. During *Bdellovibrio* intraperiplasmic growth, removal of iron from the cytochromes and other metal-containing enzymes/components of the ETC to fuel *Bdellovibrio* growth may lead to oxidative stress.

1.6.4. Host independence

B. bacteriovorus is typically an obligately predatory bacteria that can only grow and survive within Gram-negative prey. However, host independent strains of *B. bacteriovorus* are able to grow on rich lab media, in a state mirroring intraperiplasmic growth inside prey, due to one or several mutations in the host interaction (HIT) locus (347). The HIT locus contains a cluster of Type IVb pilus associated genes, including *bd0108* and *bd0109*, the former of which is unique to *Bdellovibrio* and the latter of which being essential for *Bdellovibrio* viability. A natural 42bp deletion within *bd0108* causes greater Type IVa pilus extrusion than WT or whole gene deletion. Bd0108-Bd0109 interactions regulate pilus production, with the presence and retraction of pili when they contact the prey cell wall, altering the growth state of the *Bdellovibrio* cell (347, 348). Mutation within *bd0108* gives rise to the host independent phenotype of *B. bacteriovorus* (301, 348). This was originally believed to be an artefact of laboratory conditions however isolation of an environmental strain of *B. bacteriovorus* termed *Tiberius* also further supports the point that non-predatory (host independent) growth of *B. bacteriovorus* is also possibly either through mutation, or naturally in high nutrient environments (286). Host independent culturing of mutant *Bdellovibrio* can be a method to test the function of predatorily essential genes.

1.6.5. Unknowns (from 60 years of laboratory experimentation)

There are still many unknowns surrounding the predation process of *B. bacteriovorus,* including:

- What is the molecular signature that facilitates prey recognition and attachment?
- What are the signalling mechanisms that progress each stage of the lifecycle?
- What are the effects of the host environment on predation?

1.6.6. Applications to AMR

1.6.6.1. The need

As detailed in Section 1.2, there is a great an urgent need for novel antimicrobial therapies and approaches to allow for the continued treatment of infectious disease and routine medical interventions, without which healthcare as we know it will rapidly revert to a pre-antibiotic era. Conventional chemical antibiotics have revolutionised healthcare. However, to overcome the problems imposed by the development of resistance to these conventional therapies, new approaches are needed, one of which being the use of the living antibiotic *B. bacteriovorus*.

1.6.6.2. Advantages

There are many advantages to the use of *B. bacteriovorus* as a novel antimicrobial, the largest of which being its potential to not fall foul of conventional antibiotic resistance formation.

1.6.6.2.1. Possible resistance to predation

As with all novel antimicrobial therapies, we need to be mindful about resistance developing. The likelihood of resistance developing to *B. bacteriovorus* predation is thought to be lower to that of conventional antimicrobial drug therapies for a multitude of reasons.

Firstly, *B. bacteriovorus* recognises and targets several components of the prey bacterium during predation, therefore alteration of one component by prey to prevent bacterial death would likely not abrogate predation. The ligand(s) that *B. bacteriovorus* targets are likely to be essential for bacterial cell viability, meaning that they are not readily mutated or lost from the prey cell (349).

An absence of a protective gene response within the early transcriptional response of *E. coli* being preyed upon by *B. bacteriovorus* also suggests that resistance is unlikely, with the majority of gene expression linked to physical stress responses, such as osmotic stress regulation and cell wall and periplasm damage repair, due to cell wall and membrane damage (350).

However, within the predation process, the exact component(s) of the Gram-negative prey cell that *B. bacteriovorus* recognises to attach and begin predation are still unknown. These components must be highly conserved across Gram-negative bacteria, but not recognised and targeted within *B. bacteriovorus* itself. It is well documented that alteration of the bacterial cell surface occurs due to microenvironmental conditions and cellular stresses, including stresses imposed by the host environment and the immune system, and that this alteration of the cell surface may confer protection against recognition by the host immune response. From this, it'll be important to characterise the impact of these cell surface changes on predation by *B. bacteriovorus* within a host environment as this may alter susceptibility of the prey to predation, acting as a form of resistance.

The capsule of Gram-negative bacteria is known to interfere with and protect against bacterial killing by bacteriophage and host immune mechanisms, therefore it might also have the potential to interfere with predation. However, it does not prevent predation of Gram-negative bacteria by *B. bacteriovorus,* where the presence of capsule did not interfere with prey invasion or lysis and did not act as a barrier to predation (21). S-layers did provide protection against predation from *B. bacteriovorus* (24), however any gap in this S-layer allowed predation to proceed, albeit at a slower rate suggesting that predation may still be possible if the S-layer isn't 100% intact, something the host immune response may aid with.

Another important consideration is that prey are never entirely eradicated from the "mix" either due to low probability of predator: prey interaction, or due to a microbial bet-hedging strategy, where prey cells are phenotypically resistant to predation due to random phase variation, but this resistance is not genetically encoded or transferred to progeny. This allows for the survival of a small contingent of prey, which revert back to being phenotypically typical and susceptible to predation when the predator is removed (351).

1.6.6.2.2. Host microbiota

Bdellovibrio is predicted to be less detrimental effect on the host microbiota than broad spectrum chemical antibiotics, owing to it only targeting Gram-negative bacteria. *E. coli* and other Gram-negative bacterial species still form a large component of the gut microbiota and would still be targeted by *B. bacteriovorus* treatment.

However, the detrimental effects associated with conventional antibiotic use are thought to far exceed the impacts of *B. bacteriovorus* treatment, with *B. bacteriovorus* being shown to be non-detrimental to gut microbiota (352-355), and not causing a typical antibiotic-associated dysbiosis response, whilst also being strongly associated with healthy individuals in their gut microbiota and absent in those suffering from gastrointestinal disease such as IBD (inflammatory bowel disease) or Celiac disease. This suggests that *B. bacteriovorus* may aid the control of gut microbiota, keeping it in a healthy state rather than triggering dysbiosis like many conventional antibiotics (356, 357).

1.6.6.2.3. Combination therapy

B. bacteriovorus also shows potential as being able to be used with other treatments such as β-lactam antibiotics, to which it is inherently resistant, or with antibiotics that target Gram-positive pathogens such as *S. aureus* to combat polymicrobial infections (358, 359). A promising study also showed the potential of combined *B. bacteriovorus* and bacteriophage application, where combination therapy led to an increase in bacterial killing due to targeting of pathogens sensitive to both *Bdellovibrio* and bacteriophage, genetically resistant to phage predation or plastically resistant to *Bdellovibrio* predation. Both may co-exist and cause co-incident selective pressure on prey, without falling foul to quick resistance and high specificity setbacks of phage therapy (360).

B. bacteriovorus also does not fall foul to problems associated with bacteriophage therapy, such as impediment by the bacterial capsule, mutation of host recognition sites (the main form of resistance to bacteriophage therapy), and limited host range (*B. bacteriovorus* targets all Gram-negative bacteria).

1.6.6.2.4. Predation on Biofilms

One major drawback of conventional antibiotic therapies and the host immune response that hinders the resolution of infection is the formation of biofilms, polymicrobial communities that exhibit altered gene expression profiles that frequently make them resistance to host immune mechanisms, bacteriophage therapy and conventional antibiotics, making biofilm infections especially hard to treat.

One further advantage of *B. bacteriovorus* is that it preys upon bacteria within biofilms, preventing biofilm formation or eradicating formed biofilms, even targeting senescent cells that are usually immune to antibiotic action (361). Despite being susceptible to predation, biofilms may still allow a greater level of pathogen survival than in preyed upon planktonic populations, possibly due to a "microbial bet-hedging" resistance phenotype or stress response developing (362), but they still represent an improved approach in targeting hard-to-treat biofilm infections, potentially allowing the host immune response or other treatment measures to aid the resolution of infection also. *B. bacteriovorus* releases proteases and nucleases as part of the predation process that on their own may target and degrade biofilm populations, opening them up to targeting by the host immune response (330, 363).

B. bacteriovorus is able to prey on a wide range of clinical Gram-negative pathogens planktonically and in biofilms for mono- and polymicrobial cultures (364), including multidrug resistant clinical isolates (365, 366) and their biofilms, preventing formation or targeting established biofilms (362, 367).

1.6.6.2.5. Low immunogenicity

B. bacteriovorus is only mildly immunogenic in comparison to its bacterial counterparts. This is supported by various studies looking at the cytokines induced by *Bdellovibrio,* of which IL-1β, IL-6, TNFα (proinflammatory) and IL-10 (anti-inflammatory) have been studied (2, 368-370). Whilst *Bdellovibrio* is not immunogenically silent, the amount of cytokine induced compared to other, Gram-negative bacteria is significantly less (discussed below).

1.6.6.2.6. Predicted immunogenicity of *Bdellovibrio*.

Like many Gram-negative bacteria, the first point of contact between the host immune response and the bacterium is the outer surface. *Bdellovibrio* has an LPS outer membrane, which in other Gram-negative bacteria is highly immunogenic. However, the LPS of *Bdellovibrio* is atypical, containing 1' and 4' mannose groups in the Lipid A head group, in place of the typical phosphate groups (301), but a typical fatty acid composition. This reduces the negative charge of the Lipid A molecule, and therefore is predicted to reduce the binding affinity of host TLR-4 (60) to *Bdellovibrio* Lipid A, reducing receptor activation and downstream proinflammatory signalling.

As mentioned previously and like other Gram-negative bacteria, the surface of *B. bacteriovorus* is a patchwork of outer membrane associated components including fimbriae, pili and outer membrane proteins (OMPs) (288). However, as the majority of *Bdellovibrio* gene expression occurs within a bacterial prey cell, with only the outer membrane proteins required for prey sensing and attachment initially expressed, *Bdellovibrio* may express less of these immunogenic surface proteins, compared to other bacteria, potentially reducing its immunogenicity and recognition by the host immune response.

The flagellum of *B. bacteriovorus* is another potentially immunogenic ligand that may be recognised by the host immune response. The flagellum of *Bdellovibrio* is encased in a membranous sheath, shielding the flagellin monomers from recognition by host TLR-5 receptors (307). In other Gram-negative bacteria, the membranous flagellar sheath prevents recognition of flagellin, reducing downstream proinflammatory signalling (371-375), therefore I predict a similar role and consequence for *Bdellovibrio*.

The peptidoglycan cell wall of *Bdellovibrio* is masked from recognition by host TLR-2, NOD1 and NOD2 by the LPS outer membrane, until bacterial lysis occurs. Intracellular components, such as bacterial nucleic acids, are also initially masked from recognition by host PRRs. Within the phagosome, bacteria will be broken down and damaged, exposing peptidoglycan and other immunogenic ligands to recognition.

However, as *B. bacteriovorus* is a proposed novel antibacterial therapy, it will not be present without the presence of Gram-negative pathogenic prey. Recognition of, and activation by, these Gram-negative pathogens may also impact the recognition of *B. bacteriovorus*, which is an important consideration that has so far remained unaddressed when considering how *B. bacteriovorus* is recognised by the innate immune response.

1.6.6.2.7. Limitations and unknowns from *ex-vivo* and laboratory studies

60 years of laboratory research has been very informative about the mechanistic details surrounding the predatory process. However, the findings of these *in vitro* studies in buffer and bacteriological media need to be translated into more physiologically relevant, host-centric conditions. This will inform us of the potential efficacy and limitations to predation in a human or animal host, progressing our knowledge and potential implementation of *Bdellovibrio* as a novel antimicrobial therapy. The interactions between *Bdellovibrio* and the host form the focus of my study. I will document the current knowledge surrounding the use and efficacy of *Bdellovibrio* in a host, highlighting what still needs to be discovered.

Temperature and Oxygen availability. Laboratory studies are typically performed at 29 degrees Celsius, in a well aerated environment whereas most vertebrate hosts have a warmer body temperature (e.g., humans 37°C), and some infection settings e.g., the gut, may be anaerobic. These factors may also impact predation efficacy (376, 377).

Over-simplification. Laboratory studies are also simplified to only contain predator and prey, without the presence of other, non-susceptible cell types such as Gram-positive bacteria and yeast cells. In a host, even if an infection is caused by a single infectious agent, the surrounding environment will contain an array of differing microorganisms, all of which will impact predation efficiency and efficacy.

Modelling of predation in the presence of decoy cells has been carried out by Hobley and co-workers (378) and Wilkinson and co-workers (379), which showed that the presence of live, non-susceptible bacterial “decoy” cells did decrease predation efficiency, although not extensively. However, further investigation is needed.

Host molecules. Other host factors may also impact predation efficacy, including Indole, a bacterial signalling molecule produced by bacteria in the gut, which has been shown to downregulate *B. bacteriovorus* motility through direct effects on flagellar motility genes, inhibiting predation (380). Host sera has also been shown to reduce predation efficacy, with serum albumin and osmolarity limiting predation efficiency (376), although I investigate this further.

Nutrient availability. Most *ex vivo* studies of *Bdellovibrio* have been performed in nutrient depleted Ca/HEPES buffer, which also supplies divalent ions that help predator attachment to prey. The host is a nutrient rich environment by comparison, which will impact the cell surface of potential pathogenic prey and will therefore influence predation dynamics.

Scalability. We must consider whether, if proven safe and effective, *Bdellovibrio* growth could be scaled up to the required amounts to provide a regular and uninterrupted supply, and how *Bdellovibrio* could be stored prior to use (381, 382).

Application. Consideration of the potential infection scenarios, e.g., wound infections and topical treatment, versus gut infection and oral administration and bloodstream infections requiring intravenous treatment, is also important when considering the limits of *Bdellovibrio* treatment.

Serum studies. The few *ex vivo* studies that have been performed in host serum have improved our knowledge of how host factors may affect predation. A combined modelling and experimental approach studying the predation of *K. pneumoniae* in human serum showed that prey regrowth occurred after 24 hours (383), potentially in a similar manner to the phenotypic resistance phenotypes seen previously (351).

Alternatively, the lysis of predator and prey cells upon first exposure to human serum may have liberated nutrients for prey regrowth or decreased predation efficiency through the presence of cellular debris (384). Another interesting observation from this study is the impact of host serum antimicrobials on predation. In both the experimental and modelling approaches, serum antimicrobials initially target both predator and prey, causing a drop in bacterial number.

Serum antimicrobials also slowed predation either through reduced attachment due to the presence of prey fragments, prey rounding or an unknown mechanism. However, after approximately an hour, serum antimicrobials in this closed system are exhausted and no longer play such a defined role.

In a living host, serum antimicrobials would be continually replenished or potentially increased in abundance due to activation of the immune response (in a systemic infection), an important consideration when interpreting the findings of this study. However, the study concluded that in wound infections or peripheral sites, serum antimicrobials may not be replenished as quickly, potentially making the findings of this study more applicable to those scenarios.

Willis and co-workers (detailed further below) showed that synergy between the immune response and *B. bacteriovorus* treatment may also play a key role in the resolution of infection (1). The replenishment of serum antimicrobials and a fully functional immune response may aid resolution of infection, in combination with *B. bacteriovorus* initially lowering prey numbers, eradicating the pathogens before regrowth can occur or to a level where the immune system can control infection (383).

Further details of *in-vivo* and *ex-vivo* studies and their main experimental findings are documented below.

1.6.6.3. Animal models/ in vivo models

Studies of how effective treatment may be within the host is also important, with many factors affecting potential efficacy including host body temperature, host immune response (towards predator and pathogen), oxygen conditions etc. as well as ascertaining the safety and performance of the predator *in vivo* such as dissemination, proinflammatory responses and cytotoxicity. The use of *Bdellovibrio* in animal models has begun to address this.

B. bacteriovorus has been largely successfully used to treat various Gram-negative infections in the eyes of rabbits (385, 386), periodontic, lung, gut and systemic *K. pneumoniae* infections in rats (353, 387-389) and mice (390-392) via various inoculation routes.

Models of dental cavities and periodontal infection against periodontal disease pathogens have also been tested (393), with some successful outcomes and others demonstrating the implications on microbial diversity within the oral microbiome and how increased complexity of these scenarios impacts successful predation and warrants further study (394).

B. bacteriovorus treatment has also been applied to environmental infection sources such as fish ponds (395), or preventing cross contamination in livestock (396) on plants e.g. mushroom spoilage (397, 398) and potato blight (399)

Efficacy, cytotoxicity and immune response of treatment on human corneal cells (368), bovine kidney cells (400, 401), human primary cells (368, 369) and cell lines (386) and murine macrophages (369), all show a lack of cytotoxicity (by cytokine induction studies) and a beneficial impact of predation that is promising for the application of *Bdellovibrio* within a host.

Atterbury et al., 2011. Other flagship studies include the first warm-blooded animal study where *B. bacteriovorus* was administered orally to chicks to combat *Salmonella* infection, with improvements in wellbeing, gut health and inflammation and decreases in *Salmonella* colonisation as some of the studies main findings, alongside no notable effects on gut microbiota diversity (402).

Willlis et al., 2016. The use of *B. bacteriovorus* to treat *Shigella flexneri* infection injected into the hindbrain of zebrafish larvae, where innate immune cells (macrophages and neutrophils) had access to, was the first study where the host immune response to infection and active predation could be observed in real time, have also made great progress in the field. The immune system of zebrafish larvae closely resembles the human innate immune response, as it is predominantly composed of macrophage and neutrophils (403).

This study demonstrated that *B. bacteriovorus* treatment had no impact on zebrafish host survival alone, but strongly improved survival of the host in response to lethal *S. flexneri* infection. It also began to characterise the interactions between *B. bacteriovorus* and the innate immune system *in vivo*, which had not previously been done, where they showed that *B. bacteriovorus* was engulfed and cleared by macrophages and neutrophils, without affecting their viability or causing secondary infection, but had sufficient time to dwell on pathogenic prey within the host. Most importantly they also demonstrated, through studying predation outcomes, alongside depletion of the host innate immune response, reducing leukocyte numbers, that the combination of predation and host immune response gives the best resolution of infection and that they can work synergistically to combat infection within the host (1).

Raghunathan et al., 2019. A study by Raghunathan and co-workers subsequently built on this to further quantify the host innate immune cell-predator interactions at a molecular level by studying the uptake, persistence, cytokine responses and intracellular trafficking of live *B. bacteriovorus* by human phagocytic U937 macrophage-like cultured cells (2). It showed that *B. bacteriovorus* is engulfed by human macrophages and persists within the phagosome for approximately 24 hours without affecting macrophage viability before being trafficked through the phagolysosomal pathway of degradation and being killed.

This study also characterised the cytokine response to *B. bacteriovorus* by looking at expression of IL-1β, TNFα, IL-6, IL-10 and IL-8 in response to *B. bacteriovorus* compared with *K. pneumoniae* and *S. enterica* Typhimurium, concluding that expression levels were always several folds significantly lower in response to *B. bacteriovorus,* supporting its status as being less immunogenic.

Finally, they studied the prevalence of antibodies to *B. bacteriovorus* within the human population and found that antibody levels were low, but present in the majority of the population, suggesting most have previously came into contact with *B. bacteriovorus,* likely through an environmental route, and have not initiated a strong immune response to it.

Animal studies have also thrown up some unexpected results, where it was shown that *B. bacteriovorus* may be able to prey on the Gram-positive bacterium *S. aureus*, although via a different predation mechanism (404), that likely uses the peptidoglycan active enzymes of possible lysed predators. This prompts suggestions that *B. bacteriovorus* treatment could be applied to problematic polymicrobial infections such as those associated with cystic fibrosis (405). The ability of *B. bacteriovorus* to prey on Gram-positive bacteria has been disputed by some (406), but the proteases *B. bacteriovorus* releases during predation also act to degrade Gram-positive biofilms and so some benefit of *B. bacteriovorus* treatment on reducing Gram-positive infection may still be seen (407, 408).

The various published animal studies and their main findings are summarised in Supplementary Table 1.6.1. Briefly, these animal studies show that (i) *Bdellovibrio* is less immunogenic (through ELISA and qtPCR studies of cytokine expression) than other, more typical Gram-negative bacteria. (ii) *Bdellovibrio* is not cytotoxic to host cells. (iii) *Bdellovibrio* is able to prey upon a diverse array of multidrug resistant clinical isolates. (iv) *Bdellovibrio* is successfully able to prey on Gram-negative pathogens *ex-vivo* and within the host, for intraperitoneal (392), ocular (368, 385) intranasal (388, 391) and gastrointestinal (352) infections, but treatment of intravenous infection was less successful (387, 400, 409). However, the zebrafish hindbrain model of infection used by Willis and co-workers (1) is analogous to an intravenous infection but was successful in the resolution of *Shigella flexneri* infection using *B. bacteriovorus*. This suggests that other factors, potentially including interaction with, and uptake by, host immune cells, and the activation state of these immune cells due to the presence of pathogenic prey, impacts predation efficacy and resolution of infection.

1.7. Looking forward

We are currently going from well-established lab experimentation to the discovery of unknown viability of *Bdellovibrio in-vivo* and co-localisation within macrophages, with the subcellular localisation (phagosomal or not) yet to be determined. We need a better understanding of how *Bdellovibrio* interacts with the host immune response to progress.

My contribution in this field is to look at their potential oxidative stress combatting gene products of predators that are silent when in attack phase (not typically expressed in attack phase) and how/if their expression changes during predation. I will then ask how/if their expression changes when the bacterium senses it is in a eukaryotic macrophage cell. This two-pronged experimental approach (testing in bacterial prey and in macrophage) is because entry into/exit from bacterial prey can bring oxidative challenges analogous to those of macrophage engulfment and residency. These oxidative challenges may overlap or be separate to those that occur within the phagosome of host macrophage throughout phagosomal maturation. *Bdellovibrio* is an environmental bacterium that is typically found in soil and water. *Bdellovibrio* may encounter soil amoebae in its natural environment, which have a functional homology to the phagocytes of the host immune response. Such encounters between *Bdellovibrio* and environmental amoebae may select for oxidative stress survival genes that also confer a temporary survival benefit to *Bdellovibrio* within the macrophage phagosome.

From studies of *Bdellovibrio* in zebrafish (1) and macrophage (2) we know that

- *Bdellovibrio* are actively engulfed and cleared by macrophage and neutrophils.
- *Bdellovibrio* have sufficient dwell time to prey on pathogens, therefore they are not immediately phagocytosed and killed.
- *Bdellovibrio* is engulfed and persists for over 24 hours in human macrophage-like cells.
- *Bdellovibrio* is trafficked via the phagolysosomal pathway of degradation and does not appear to perturb uptake or phagosomal maturation.

Therefore, in this thesis, I aim to tell you about the host response to *Bdellovibrio,* putting this in the context of how this may impact the predation of Gram-negative pathogens by *Bdellovibrio* within a human host. I will interrogate how *Bdellovibrio* dwells within macrophage, looking at the differing transcriptional profiles of *Bdellovibrio* and the host throughout *Bdellovibrio* occupation of macrophage.

I used PMA-differentiated U937 cells in this study, which have been demonstrated to be a robust approach for the study of the interactions of various Gram-negative pathogens with host macrophage and were successfully used by Raghunathan and co-workers to characterise the initial interactions of *Bdellovibrio* with human macrophage (2). I use a transcriptional dataset of *Bdellovibrio* within a zebrafish host (Tyson, Moore & Sockett, unpublished) to prime my study and identify candidate genes which may aid survival of *Bdellovibrio* within the host. I test these candidate genes within U937 cells to determine if they assist *Bdellovibrio* in surviving within the macrophage phagosome.

My starting hypothesis is that the host immune response to *Bdellovibrio* is less that than seen for other Gram-negative bacteria and Gram-negative pathogens, and that *Bdellovibrio* persists for longer than most pathogens, by “silent-running” without attacking macrophages and actively modifying/evading phagosomal conditions. This may be due to biochemical surface differences that *B. bacteriovorus* has evolved to be different to the prey bacteria which it recognises and invades (preventing self-killing).

I aim to investigate how *Bdellovibrio* temporarily survives within the phagosome of human macrophage.

1.8. Aims and objectives.

In my PhD, I aimed to understand and further characterise the interactions between *Bdellovibrio bacteriovorus* and the cell-mediated part of the host innate immune response. I wished to apply this knowledge, to further our understanding of how the host environment and host immune response may alter or impede predation dynamics and impact the efficacy of *Bdellovibrio* predation of Gram-negative bacterial pathogens in a host setting.

I also characterised the role of a subset of *Bdellovibrio* genes that I predicted to be involved in the tolerance of oxidative stress and therefore of potential importance in the temporary survival of *Bdellovibrio* within host macrophage. I then characterised the host transcriptional response to *Bdellovibrio,* by host macrophage that had engulfed *Bdellovibrio*, to further characterise the host immune response to *Bdellovibrio*.

I had also aimed to analyse *Bdellovibrio* gene expression within host macrophage, to give the opposing view of how *Bdellovibrio* interacts with the host immune response, from the perspective of the bacterium, however this was limited by low levels of bacterial RNA (versus macrophage RNA).

My PhD aims are laid out as follows:

- **Chapter 3:** Characterise the effects of cell surface adaptation, due to host immune factors, on the dynamics and efficiency of predation by *B. bacteriovorus.*
- **Chapter 4**: Identify and test the roles of novel genes within *B. bacteriovorus* which allow for survival within macrophages, through a greater tolerance to the host immune response and/or host-mediated oxidative stress.
- **Chapter 4**: Elucidate any interface between evolution for oxidative stress tolerance and survival of *B. bacteriovorus* inside bacterial prey versus survival inside the phagosome of macrophages.
- **Chapter 5:** Characterise the transcriptional response of *Bdellovibrio* (Chapter 5a) and host macrophage (Chapter 5b) simultaneously, capturing

the phagocytosis, phagosomal processing and killing of *Bdellovibrio* by host macrophage.

The work associated with these aims allow for a greater insight into how *B. bacteriovorus* can act as a predator of Gram-negative bacteria inside macrophages, targeting pathogens that would normally exploit this protected intracellular niche, or within the wider host environment, asking the question “is predation within a human host possible?”

Chapter 2: Materials and Methods

2.1. Bacterial strains

This thesis focuses on the study of the invasive predatory bacterium *Bdellovibrio bacteriovorus* HD100, a soil isolate that was genome sequenced in 2004 (281) and is the main strain of *B. bacteriovorus* commonly used in our lab. This strain was also used in the work performed by Willis and co-workers, that first visualised active predation *in vivo* within zebrafish (1) and by Raghunathan and co-workers, who characterised the initial uptake and processing of *Bdellovibrio* by macrophage (2).

Bdellovibrio bacteriovorus HD100 is genome sequenced (GenBank Accession: GCA_000196175.1). Predation of Gram-negative bacteria under laboratory conditions is possible in media containing divalent cations, such as Calcium HEPES buffer. *B. bacteriovorus* HD100 is Wildtype, allowing for modified genes to be introduced into the HD100 genome via homologous recombination of donor plasmids.

HD100CFP (2) and HD100mCh (1) are fluorescently tagged strains of *B. bacteriovorus* with cerulean fluorescent protein 3 or cherry fluorescent protein tagged to the C-terminus of the gene product of *bd0064* giving constitutive expression as documented in (1, 2, 341). Bd0064 acts as a cytoplasmic marker to illuminate the cell, which was necessary to act as a background colour to confirm the presence of *B. bacteriovorus* within macrophage-like cells (**Chapter 4 Specific)** when testing for expression of our protein candidates.

Serratia marcescens #42 (**Chapter 3 Specific)** is a multidrug resistant (Tetracycline: 15 µg/ml; Ampicillin 500 µg/ml) clinical isolate that I used in Chapter 3 to test the roles of surface components on predation of *S. marcescens* by *B. bacteriovorus ex vivo* in human serum, to emulate predation in a host environment.

Escherichia coli S17-1 is used as prey for the growth of *B. bacteriovorus* strains, when pre-grown to stationary phase in nutrient rich YT or LB broth.

E. coli S17-1 is also used as a tool for the introduction of gene deletion or fluorescently tagged gene constructs/plasmids into *B. bacteriovorus*, through the mobilisation of RK2 plasmids by rolling circle replication, acting as donors for conjugation of a modified gene construct into *B. bacteriovorus*.

Through the addition of a *pZMR100* plasmid, conferring kanamycin resistance, *E. coli* S17-1 pZMR100 may also be used as prey for growth of *B. bacteriovorus* strains containing a *pk18mobSacB* donor plasmid (also containing a modified *B. bacteriovorus* gene construct for fluorescent tagging and gene knockout studies).

E. coli S17-1 λ-PIR (**Chapter 3 Specific)** is a modified *E. coli* S17-1 strain used for the conjugation of mobilizable plasmids into *S. marcescens* #42. *E. coli* S17-1 λ-PIR contains an additional helper plasmid which increases conjugation efficiency, owing to the *pSC2301* plasmid having a R6K origin of replication and a low copy number, making conjugation of our modified gene constructs into *S. marcescens* by rolling circle replication and conjugation inefficient in the absence of this additional helper plasmid.

Full details of the bacterial strains used in Chapter 3 of this study can be found in Supplementary Table 2.1.1.

Full details of the bacterial strains used in Chapter 4 and 5 of this study can be found in Supplementary Table 2.1.2.

2.2. Bacterial Growth Media

2.2.1. YT broth & agar

YT broth and agar were used for the routine culture of *E. coli* (both for cloning purposes and as prey for *B. bacteriovorus*).

YT broth: 5 g/L Difco yeast extract, 8 g/L Difco tryptone, 5 g/L NaCl, pH 7.5 (adjusted using 2 M sodium hydroxide).

YT Agar: YT broth composition with the addition of 10 g/L select agar (Sigma).

2.2.2. LB broth & agar

LB broth and agar were used for the routine culture and enumeration of *S. marcescens* #42 (Chapter 3) and for enumeration of *E. coli* S17-1 prey in *B. bacteriovorus* predation assays (testing the efficiency of predation by *B. bacteriovorus* gene knockout mutants).

LB broth: 10 g/l tryptone, 10 g/l NaCl, 5 g/l yeast extract (Sigma).

LB agar: LB broth composition, plus 10 g/L select agar (Sigma).

2.2.3. YPSC overlay plates.

YPSC overlay plates were used for the routine culture, genetic modification, and enumeration of *B. bacteriovorus.*

YPSC: 0.25 g/L $MgSO_4 \cdot 7H_2O$, 0.5 g/L sodium acetate, 1 g/L peptone (Sigma), 1 g/L yeast extract, 0.25 g/L $CaCl_2 2H_2O$, adjusted to pH 7.6 using 2 M sodium hydroxide.

For YPSC-Bottom plates, which act as a base for the soft agar overlay, 10 g/L of select agar is added to YPSC media.

For YPSC-Top agar, which acts as a soft overlay within which *E. coli* S17-1 prey is immobilised and plaques of *B. bacteriovorus* grow, 6 g/L of select agar is used.

N.B. For work performed in Chapter 3, broadbean peptone (Sigma) was used in YPSC media, whereas for work performed in Chapter 4 onwards, animal tissue-derived peptone (Sigma) was used in YPSC media. This was due to an issue in obtaining broadbean peptone, and inconsistency in bacterial growth when using broadbean peptone.

2.2.4. Ca/HEPES buffer

Ca/HEPES buffer, a divalent cation-containing medium, was used for the routine sub-culture of liquid predatory cultures of *B. bacteriovorus*.

Ca/HEPES: 5.94 g/L HEPES free acid, 0.294 g/L $CaCl_2 \cdot 2H_2O$, adjusted to pH 7.6 using 2 M sodium hydroxide.

2.2.5. PY broth & agar

PY broth and agar were used for the generation and culture of Host Independent (HI) *B. bacteriovorus*.

PY broth: 10 g/L Difco-Bacto peptone, 3 g/L Difco Yeast extract., adjusted to pH 6.8 using 2 M sodium hydroxide.

PY agar: 10 g/L animal-derived peptone (Sigma), 3 g/L Difco yeast extract, adjusted to pH 6.8 using 2 M sodium Hhdroxide with the addition of 10 g/L select agar (Sigma).

2.3. Chapter 3 specific methods

2.3.1. Bacterial culture

2.3.1.1. *Bdellovibrio bacteriovorus*

B. bacteriovorus wild type strain HD100 was cultured in 10 ml Ca/HEPES containing 600 µl *E. coli* S17-1 prey (cultured as detailed below) and an inoculum of 200 µl of a previous predatory culture, giving a ratio of 3:1 (*E. coli* S17-1: *Bdellovibrio*; Volume: Volume) and incubated at 29°C, 200 rpm. Predatory cultures were routinely sub-cultured every 2 days. Prior to use, *Bdellovibrio* cultures were examined using light microscopy to check for prey lysis and predator release. A 10 ml culture of *B. bacteriovorus*, grown as above, typically contained 2 x 10^8 PFU/ml of bacteria.

Dense predatory cultures required for predation assays (where specified) were comprised of 10 ml of a previous predatory culture, 10 ml of *E. coli* S17-1 prey and 30 ml of Ca/HEPES.

Fresh *B. bacteriovorus* cultures were cultured every 2 weeks by plating 50 µl of a frozen glycerol stock onto a YPSC overlay plate containing 150 µl of *E. coli* S17-1 prey (grown overnight, see below) at 29°C until single plaques appeared on the *E. coli* S17-1 prey lawn, upon which plaques were picked into liquid cultures (2ml Ca/HEPES, 150 µl *E. coli* S17-1 overnight culture) and incubated (29°C, 48 hours) to give liquid predatory cultures containing free-swimming attack phase *Bdellovibrio*.

2.3.1.2. *Escherichia coli*

E. coli S17-1 for *B. bacteriovorus* prey and for gene cloning was cultured in YT broth at 37°C, 200 rpm for 18-24 hours for liquid cultures. For plate cultures and revival of frozen stocks, YT agar was used, with colonies grown at 37°C overnight.

2.3.1.3. *Escherichia coli* λ-Pir (for cloning into *S. marcescens*)

E. coli S17-1 λ-Pir was cultured in YT broth at 37°C, 200 rpm for 18-24 hours for liquid cultures, or on YT agar plates with colonies grown at 37°C (static) overnight.

To provide selection for our suicide plasmid gene knockout constructs, media was supplemented with 25 µg/ml apramycin sulfate (Sigma) where appropriate.

2.3.1.4. *Serratia marcescens*

S. marcescens was cultured in LB broth at 37°C, 200 rpm for 18-24 hours for liquid cultures. For plate cultures, LB agar was used, with colonies grown statically at 37°C overnight.

Bacterial strains (*S. marcescens* #42 and *E. coli* S17-1) were re-streaked weekly from frozen glycerol stocks (comprised of 750 µl of overnight culture and 200 µl of 80 % glycerol; Kept at -80°C) onto YT agar (plus apramycin sulfate selection if appropriate) and incubated overnight at 37°C.

2.3.2. Chapter 3 specific bacterial growth media

2.3.2.1. Minimal media (glucose)

Minimal media (glucose) was used for the generation of *S. marcescens* gene knockout mutants.

Minimal media (Glucose) (per litre): 10 ml 20 % glucose, 0.41 ml 1 M $MgSO_4$, 10 % (w/v) $(NH_4)_2SO_4$, 20 ml 50x phosphate buffer, 16 g select agar.

50x phosphate buffer (per litre): 350 g K_2HPO_4, 100 g KH_2PO_4, pH 7.

2.3.2.2. Minimal media (high sucrose)

Minimal media (high sucrose) was used to cure *S. marcescens* gene knockout mutants of the suicide vector plasmid, causing homologous recombination of the knockout construct.

Minimal media (high sucrose) (per litre): 20 ml 50x phosphate buffer, 0.41 ml 1 M $MgSO_4$, 10 % (w/v) $(NH_4)_2SO_4$, 16 g select agar, 200 ml 50 % sucrose.

2.3.2.3. Brilliance™ *E. coli* Coliform medium (Oxoid)

Chromogenic agar was used to differentiate between *E. coli* S17-1 λ-Pir donors and *S. marcescens* recipients/exconjugants, as both would grow on minimal media and would be apramycin resistant (due to containing the *pSC2301* plasmid containing our gene knockout construct). *E. coli* cleave both chromogenic substrates in the medium, appearing purple, whereas other bacteria only cleave galactosidase and appear pink.

Brilliance™ *E. coli* Coliform medium (per litre): 20.3 g/L chromogenic mix, 3 g/L yeast extract, 5 g/L peptone, 2.5 g/L lactose, 5 g/L sodium chloride, 3.5 g/L di-sodium hydrogen phosphate, 1.5 g/L potassium di-hydrogen phosphate, 0.03 g/L neutral red, 15 g/L agar, pH 7.0.

2.3.3. Construction of *S. marcescens* gene knockout strains

To study the role and importance of gene/protein expression (highlighted by lab RNASeq studies) in the subsequent resistance of *S. marcescens* to predation by *B. bacteriovorus* in human serum, markerless gene deletion mutants of *S. marcescens* were constructed for the genes *arnA, arnT, wza, fim3795-7* and *fim4264-6.*

2.3.3.1. Design and PCR generation of fragments

1 kb of 5' and 1 kb of 3' flanking, upstream and downstream of the gene(s) of interest, were amplified via PCR, using primers designed using NEBuilder (New England BioLabs) and detailed in Supplementary Table 2.3.1.

These fragments also contained remnants of the target gene. If the neighbouring genes are transcribed towards the gene of interest, neighbouring gene expression will not be disrupted by the removal of this gene as the neighbouring genes promoter will not be contained within the section of gene removed in this process. In this case, the upstream fragment was designed to also contain the first 6 bp of the target gene, and the downstream fragment was designed to contain the last 9bp of the target gene.

If the neighbouring genes are transcribed away from the target gene, it is likely that the promoter for these neighbouring genes is contained within the gene that we are aiming to knock out, therefore removal of the target gene will also impact neighbouring gene expression. To avoid this, 50 bp of the start or end of the target gene was included in the 5' or 3' fragments respectively and where appropriate, to avoid disruption of neighbouring gene expression.

For constructs where multiple genes are removed in one go, the 5' fragment is located upstream of the first gene, and the 3' fragment is located downstream of the last gene in the operon to be removed.

Each 100 μl PCR reaction contained:

- 66 μl analar water
- 20 μl 5x Phusion High Fidelity (HF) Buffer
- 2 μl 10 mM dNTPs
- 1 μl Phusion DNA Polymerase
- 5 μl forward and reverse primers (10 mM)
- 1 μl *S. marcescens* genomic DNA template

The thermocycling conditions used to generate these fragments were as follows:

- Initial denaturation: 98°C, 5 minutes
- 30 cycles of:
    - Denaturation: 98°C, 30 seconds
    - Annealing: 70°C, 30 seconds
    - Extension: 72°C, 1 minute per kb of product
- Final extension: 72°C, 5 minutes

PCR products were mixed with 6x purple loading dye and ran on a 0.8 % agarose TBE gel (1 hour, 100 volts), against a 1 kb ladder (New England BioLabs), prior to excision and DNA extraction using the GenElute gel extraction kit (Sigma), following the manufacturer's instructions.

2.3.3.2. Ligation of fragments into *pSC2301*

The two fragments generated above form the gene knockout construct, but they must first be ligated to one another and into *pSC2301*, a mobilizable suicide vector containing an apramycin resistance cassette (see Supplementary Table 2.3.2**)** via Gibson assembly.

After extraction, PCR fragments were ligated to each other and into a *pSC2301* vector via Gibson assembly (410). PCR products were added at a ratio of 7:1, relative to digested *pSC2301* plasmid vector, and combined with 10 μl of 2x Gibson assembly master mix (from the NEBuilder HiFi DNA assembly cloning kit; New England BioLabs). These reactions were incubated at 50°C for 1 hour to ligate the individual fragments into one circularised vector (*pSC2301* plus our gene knockout construct fragments).

2.3.3.3. Generation of chemically competent *E. coli* S17-1 λ-Pir donor cells

Chemically competent *E. coli* S17-1 λ-Pir cells were required for the conjugation of gene knockout constructs into *S. marcescens*.

An overnight liquid culture of *E. coli* S17-1 λ-Pir, grown in YT broth (37°C, 200 rpm, 18 hours) that had reached stationary phase (Typical OD_{600} of 4.0 approximately) was back-diluted and grown to an OD_{600} of 0.4, prior to centrifugation (4000 rpm, 10 minutes) and re-suspension in 20 ml of TFB-1. After 5 minutes of incubation (on ice), cells were pelleted (4000 rpm, 10 minutes) and re-suspended in 2 ml of TFB-2, prior to incubation (on ice) for 1 hour. Cells were then aliquoted and snap-frozen, upon which they were stored at – 80°C until required.

The same method was used to generate the chemically competent *E. coli* S17-1 cells required in Chapter 4.

2.3.3.4. Transformation into *E. coli* S17-1 λ-Pir donor cells

Circularised vectors were transformed into chemically competent *E. coli* S17-1 λ-Pir cells according to the NEBuilder HiFi DNA assembly cloning kit manufacturers protocol, before plating on YT agar plates with apramycin sulfate (50 μg/ml) to select for successful transformants.

Apramycin selection ensures that only *E. coli* containing the *pSC2301* plasmid will be apramycin resistant and able to grow. This does not guarantee that these recipients contain the plasmid containing our PCR fragments, as the digested *pSC2301* plasmid may have re-ligated with itself, without the PCR fragments.

2.3.3.5. Validation of *E. coli* S17-1 λ-Pir Plasmids

To check that the individual PCR fragments had ligated into the *pSC2301* vector in the correct order (although construct design should ensure that the fragments can only combine in one conformation), validation of potential transformants (and their plasmids) was performed by plasmid extraction and restriction digest.

E. coli S17-1 λ-Pir transformants were inoculated into YT broth (as above) and grown overnight (37°C, 200 rpm). Plasmids were extracted using the GenElute plasmid miniprep kit (Sigma), according to the manufacturer's instructions.

Plasmids were then validated by restriction digest, with (actual) band sizes being compared to expected band sizes to identify transformants containing a plasmid with the correct PCR fragment conformation.

Restriction digest reactions (10 μl) consisted of:

- 1 μl plasmid (Extracted as above or WT *pSC2301* as a positive control)
- 1 μl FastDigest restriction enzyme (ThermoScientific)
- 1 μl FastDigest restriction digest (10x) Buffer
- 7 μl analar water

Reactions were subsequently incubated (37°C, 1 hour), prior to being ran on a 0.8 % agarose gel (1 hour, 100 volts), against a 1 kb Ladder (New England BioLabs).

Plasmids from the "correct" transformants were then verified further by Sanger sequencing.

2.3.3.6. Conjugation into *S. marcescens* #42

E. coli S17-1 λ-Pir strains containing our desired gene knockout constructs act as donors for transmission of the plasmid construct into *S. marcescens* by conjugation and rolling circle replication.

E. coli S17-1 λ-Pir donors (containing our constructs of interest) and *S. marcescens* #42 recipients were grown as detailed in Section 2.3.1. *S. marcescens* and *E. coli* S17-1 λ-Pir cultures were pelleted (4000 rpm, 20 minutes), prior to resuspending each (individually) in 100 µl of LB broth. *S. marcescens* cell suspension was pipetted onto a nylon membrane, suspended on a LB agar plate, and allowed to dry. Once dry, the *E. coli* S17-1 λ-Pir cell suspension was then added on top of the *S. marcescens* cell residue. This plate was then incubated overnight (18 hours) at 29°C.

Cells were then washed off the membrane and re-suspended in LB broth. This cell suspension was then serially diluted and plated onto minimal media + glucose (MM-G) agar plates (containing 50 µg/ml apramycin sulfate). These plates were incubated for 24 hours (37°C) until single colonies appeared.

E. coli S17-1 λ-Pir donor cells with the construct should not be able to grow on minimal media due to the carbon auxotrophy present meaning it has no available carbon source to grow on. Some *E. coli* may still grow due to the dead *S. marcescens* and *E. coli* cells acting as an alternative carbon source, therefore 15 µg/ml of tetracycline, of which our clinical *S. marcescens* isolate is resistant to, was used to select against *E. coli* growth also.

2.3.3.7. Further validation of *S. marcescens* exconjugants

Potential exconjugants were patched in parallel onto fresh MM-G plates containing 50 µg/ml apramycin and 15 µg/ml tetracycline, and onto Brilliance Chromogenic agar before being grown for a further 24 hours (37°C). Cross-referencing of these plates allowed me to determine which colonies were *S. marcescens* exconjugants containing the desired gene knockout constructs and which were *E. coli* donor cells. Exconjugants were tested by colony PCR to test for gene knockout construct integration (primers detailed in Supplementary Table 2.3.1).

Colony PCR (per 25 μl reaction)

- 5 μl bacterial culture (potential KO or WT *S. marcescens* as a positive control)
- 3 μl forward and reverse primer (10 mM)
- 2 μl dNTPs (10 mM)
- 2 μl 10x DreamTaq buffer
- 0.3 μl DreamTaq Polymerase enzyme
- 9.7 μl analar water

Thermocycling conditions (DreamTaq PCR)

- Initial denaturation: 98°C, 8 minutes
- 35 cycles of:
    - Denaturation: 98°C, 30 seconds
    - Annealing: 60°C, 30 seconds
    - Extension: 72°C, 1 minute per kb of product
- Final extension: 72°C, 5 minutes

PCR products were run on a 0.8 % agarose TBE gel (1 hour, 100 volts), against a 1 kb ladder (New England BioLabs).

Successful exconjugant candidates were grown in larger overnight cultures (37°C, 24 hours, 200 rpm), prior to genomic DNA being extracted (using the GenElute bacterial genomic DNA extraction kit (Sigma), as per the manufacturer's instructions), the knockout region amplified by PCR (primers detailed in Supplementary Table 2.3.1) and then sequenced by Sanger sequencing.

2.3.3.8. Generation of double-crossover gene knockout mutants via homologous recombination

Exconjugant *S. marcescens* cells contain our gene knockout construct on one strand of their chromosome (that has integrated via homologous recombination), and a WT copy of the gene on the other strand. To form a complete gene deletion strain, we need to encourage the homologous recombination of our gene knockout construct into the other strand of the chromosome also, via a second genetic recombination event, and cure the exconjugants of the plasmid, removing it to create a markerless gene deletion that will no longer contain the target gene and will not be apramycin resistant.

To do this, the strain undergoes a sucrose-mediated counter-selection (detailed in (411)). The addition of sucrose to culture media, combined with the omission of apramycin selection, encourages the excision of the *pSC2301* plasmid backbone from the genome, as the *sacB* gene contained within the plasmid encodes a levansucrase enzyme that converts sucrose to a toxic product. This selects against plasmid retention, resulting in the generation of two sub-populations. One loses the plasmid and recombines to restore the WT copy of the gene on both strands of the bacterial chromosome, resulting in a “WT revertant” bacterium. The second population recombines immediately before the gene knockout construct, integrating the gene knockout construct into both strands of the bacterial chromosome and forming a “gene knockout” bacterium.

Successful exconjugants were serially diluted onto minimal media + 50 % sucrose plates (with no antibiotic selection) and incubated at 37°C for 24 hours. Individual colonies were inoculated into LB broth, grown overnight (37°C, 24 hours, 200 rpm) and then tested for gene knockout integration by colony PCR (as detailed above). Gene knockout mutants were identified due to the PCR band being smaller than WT controls, by approximately the same size as the removed gene.

2.3.3.8.1. Validation of gene deletion mutants

Candidates for successful gene knockout candidates of *S. marcescens* were grown in larger overnight cultures (37°C, 24 hours, 200 rpm), prior to genomic DNA being extracted. Genomic DNA was extracted using the GenElute bacterial genomic DNA extraction kit (Sigma), as per the manufacturer’s instructions.

The knockout region, consisting of the 5’ (upstream) and 3’ (downstream) flanking regions, either side of the deleted gene, that made up the knockout construct, plus an additional 1kb of 5’ and 3’ flanking, from the genome of *S. marcescens,* was amplified by PCR using primers detailed in Supplementary Table 2.3.1, and subsequently sequenced by Sanger sequencing by Source Bioscience (services available at https://www.sourcebioscience.com/genomics/sanger-sequencing). These sequencing reads were compared to the *S. marcescens* genome to confirm that the target gene had been deleted, and that no other mutations had occurred within the 5’ and 3’ flanking regions surrounding the target gene.

2.3.4. Human serum

Human serum (Sigma; Batch numbers: SLBN8826V and SLBN9196V) from pools of Male AB humans was used in these experiments. Upon arrival, serum was thawed once and aliquoted to avoid repeated freeze-thaw cycles, and then stored at -20°C until needed.

2.3.5. *S. marcescens* mutant viability in human serum

To determine whether the removal of surface genes from *S. marcescens* alters the dynamics of in-serum predation by *B. bacteriovorus*, we had to first check that our bacterial clones were still viable in human serum.

S. marcescens WT and mutant strains were grown overnight (10 ml LB broth, 37°C, 200 rpm, 18 hours) and suspended in human serum at an OD_{600} of 0.01. Viability was then measured via serial dilution and Miles and Misra plating (20 µl, in triplicate) onto LB agar for a 48-hour period, with plates being incubated at 29°C overnight and individual bacterial colonies counted the next day.

2.3.6. Predation of *S. marcescens* gene deletion strains by *B. bacteriovorus* in human serum

To determine whether the removal of surface gene products would affect the susceptibility of *S. marcescens* to predation by *B. bacteriovorus*, *S. marcescens* WT and mutant strains were incubated with *B. bacteriovorus* HD100 in human serum.

S. marcescens WT and mutant strains were grown overnight (10 ml LB broth, 37°C, 200 rpm, 18 hours) and suspended in human serum at an OD_{600} of 0.01. Dense predatory cultures of *B. bacteriovorus* were prepared as detailed previously, prior to centrifugation (4000 rpm, 20 minutes) and resuspension in 500 µl of Ca/HEPES buffer to give a 100x cell suspension. *B. bacteriovorus* cell suspension was added to the *S. marcescens* (in human serum) to give an MOI of 10:1 (*Bdellovibrio: Serratia*) respectively and incubated at 29°C, 200 rpm.

Predator numbers were enumerated at 0 hours, 1 hour, 4 hours, 24 hours, 48 hours, and 72 hours by plating onto YPSC overlay plates (as above).

Prey numbers were enumerated every hour at 0-10 hours, and subsequently at 24 hours, 48 hours and 72 hours via Miles and Misra technique onto LB agar.

2.3.7. Statistical analysis

Statistical analysis of the results generated in the “predation of *S. marcescens* knockout strains by *B. bacteriovorus* in human serum” experiments was not carried out for *S. marcescens* ΔarnT, *S. marcescens* ΔFim3795-7 and *S. marcescens* ΔFim4264-6 experiments as it was deemed to be inappropriate, considering that only one biological replicate was obtained for these experiments. Further repeats would be required before considering statistical analysis of these data.

Statistical analysis on *S. marcescens* ΔarnA and Δwza data sets was performed using GraphPad Prism 8.0. First, data were analysed for normality using a D’Agostino-Pearson test, which deemed our data to not be normally distributed. Data were then analysed using the non-parametric, Two-way ANOVA multiple comparisons T test function. N.S indicates non-significance ($P>0.05$), * indicates significance ($P<0.05$), ** indicates significance ($P<0.01$).

2.4. Chapter 4 Specific Methods

2.4.1. Bacterial culture

2.4.1.1. *Bdellovibrio bacteriovorus*

B. bacteriovorus wild type strain HD100 was cultured as detailed above (Chapter 3 Specific Methods).

B. bacteriovorus strains containing fluorescent tag constructs were kanamycin resistant, and so they were cultured/grown on *E. coli* S17-1 containing a *pZMR100* plasmid that conferred kanamycin resistance, with the addition of 50 μg/ml of kanamycin sulphate to the culture media.

2.4.1.2. *Escherichia coli*

As detailed above, *E. coli* S17-1 for *B. bacteriovorus* prey and for gene cloning was cultured in YT broth at 37°C, 200 rpm for 18-24 hours for liquid cultures. For plate cultures and revival of frozen stocks, YT agar was used, with colonies grown at 37°C overnight.

E. coli S17-1 was used for cloning *mCerulean3*-tagged or *mCherry*-tagged gene constructs and gene knockout constructs into *B. bacteriovorus,* and as prey for *B. bacteriovorus* culture.

To provide selection for our *mCerulean3*-tagged, *mCherry*-tagged and gene knockout constructs, media was supplemented with 50 μg/ml kanamycin sulphate where appropriate.

Full details of the bacterial strains used in this study can be found in Supplementary Table 2.1.2.

2.4.2. Construction of *B. bacteriovorus* mCerulean3- and mCherry-tagged strains.

To investigate the role of a subset of genes in survival within macrophages, a subset of gene products (detailed in Chapter 4: Table 4.2.1) were tagged with an mCerulean3 or mCherry protein fluorescent tag and subsequently visualised via microscopy. The process behind the construction of mCerulean/mCherry tagged strains is detailed in Figure 2.4.1.

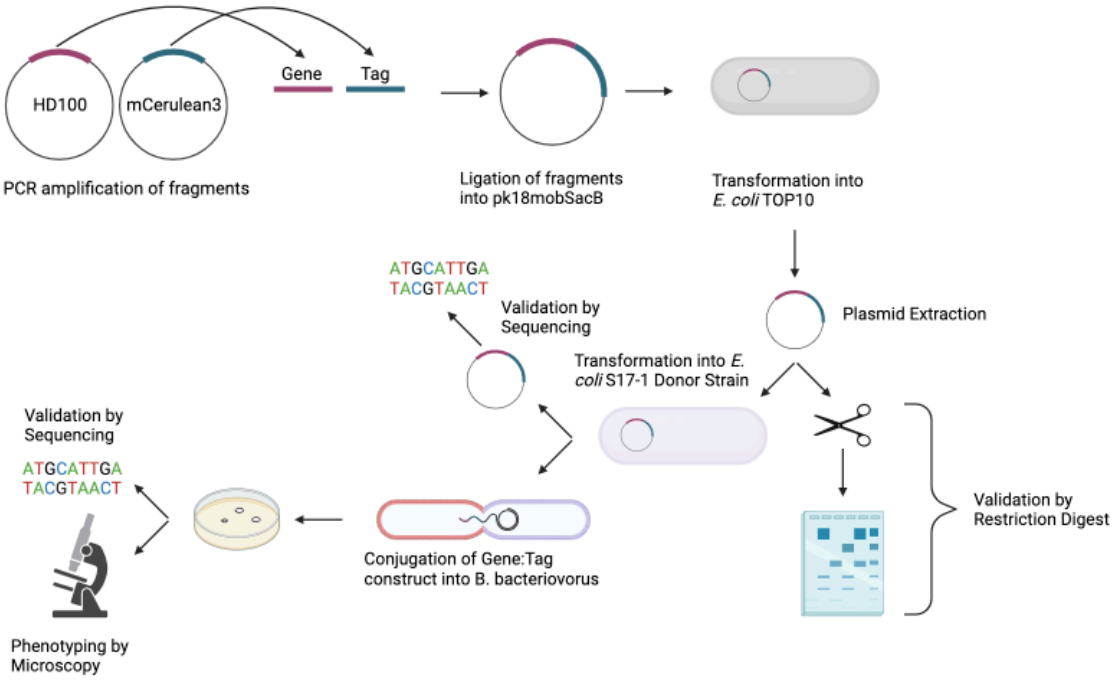

Figure 2.4.1: A schematic summarising the construction of fluorescently tagged *B. bacteriovorus* strains.

2.4.2.1. Design and PCR generation of fragments

For *mCerulean3* and *mCherry* tagged genes, gene and *mCerulean3/mCherry* tag fragments were constructed using primers (detailed in Supplementary Table 2.4.1) that amplified the gene and *mCerulean3/mCherry* tag fragments (from *B. bacteriovorus* HD100 genomic DNA and *pmCerulean3-N1/pAFK56* plasmid backbone respectively) via PCR (using the same reagents and thermocycling conditions used in Section 2.3.4.1 but a different DNA template), producing two overlapping fragments with complimentary sticky ends to one another.

2.4.2.2. Ligation of fragments into *pk18mobSacB*

After extraction, PCR fragments were ligated to each other and into a *pk18mobSacB* vector via Gibson assembly (410) (Figure 2.4.2), using the same reaction parameters as detailed in Section 2.3.4.2. This ligates the individual fragments into one circularised vector (*pk18mobSacB* plus our gene and fluorescent tag fragments).

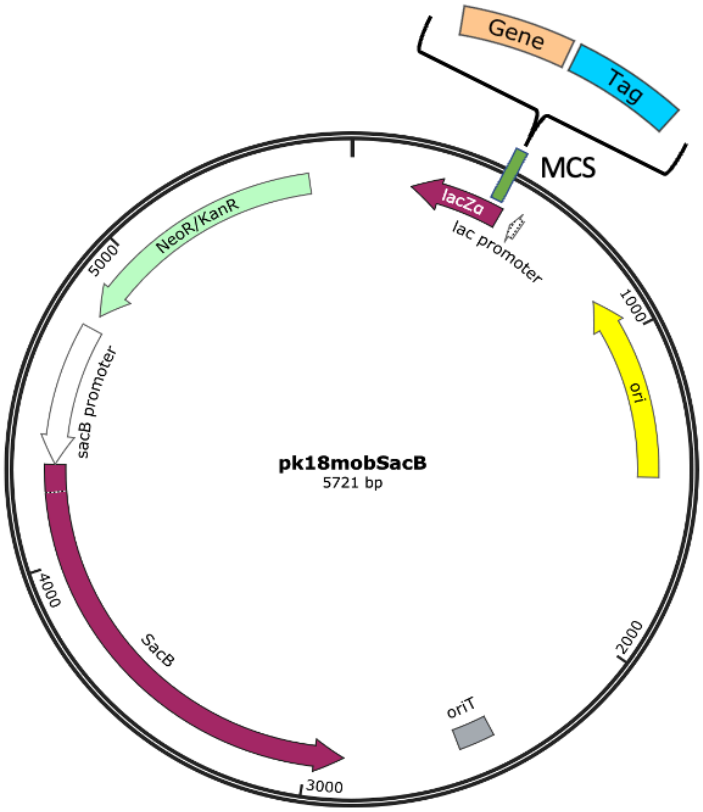

Figure 2.4.2: A plasmid map of the *pk18mobSacB* plasmid used for gene deletion and fluorescent tagging studies. *Ori:* Origin of Replication; MCS: Multiple Cloning Site (Site of insertion for gene-tag and gene knockout constructs); lacZα: *lacZ* gene (used for blue-white selection); NeoR/KanR: Neomycin Phosphotransferase gene (confers Kanamycin and Neomycin resistance); SacB Promoter/SacB: Encodes a Levansucrase enzyme that renders bacteria susceptible to sucrose (Used for Sucrose counter-selection); oriT: Origin of Transfer.

2.4.2.3. Transformation into *E. coli* DH5α

Circularised vectors were transformed into chemically competent *E. coli* NEB5α (*E. coli* DH5α cells sourced from New England BioLabs as a component of their NEBuilder HiFi DNA Assembly Cloning Kit) according to the manufacturers protocol, before plating on YT agar plates with kanamycin sulphate (50 μg/ml), X-Gal (40 μg/ml) and IPTG (40 μg/ml) to select for successful transformants and screening by blue-white selection.

Kanamycin selection ensures that only *E. coli* containing the *pk18mobSacB* plasmid will be kanamycin resistant and able to grow. This does not guarantee that these recipients contain the plasmid containing our PCR fragments, as the digested *pk18mobSacB* plasmid may have re-ligated with itself, without the PCR fragments.

Blue-white selection acts as a secondary selection measure for this. Successful and correct transformants will appear white on agar plates containing X-Gal and IPTG, as ligation of PCR fragments into the digested vector disrupts the *lacZα* gene contained within the *pk18mobSacB* vector backbone, subsequently preventing *E. coli* transformants from utilising X-Gal and IPTG in the media, and therefore colonies appear white. Digested plasmid that self-ligates to reform the *pk18mobSacB* backbone without our PCR fragments will appear blue on YT agar plates containing IPTG and X-Gal.

2.4.2.4. Validation of plasmids in *E. coli* DH5α

Constructs were validated by restriction digest, as detailed in Section 2.3.4.5, using WT *pk18mobSacB* DNA as a positive control.

2.4.2.5. Transformation into *E. coli* S17-1 donor cells

Plasmids that had been confirmed to be correct (via restriction digest) were transformed into chemically competent *E. coli* S17-1 cells (as detailed in Section 2.4.2.4), prior to being plated onto YT agar containing 50 μg/ml kanamycin sulfate and incubated for 18 hours at 37°C.

Plasmids from the “correct” *E. coli* S17-1 transformants were then verified further by Sanger sequencing. These plasmids are summarised in Supplementary Table 2.4.2.

2.4.2.6. Conjugation into *B. bacteriovorus*

E. coli S17-1 containing our desired fluorescently tagged gene constructs act as donors for transmission of the plasmid construct into *B. bacteriovorus* by conjugation and rolling circle replication.

E. coli S17-1 donors (containing our constructs of interest) and *B. bacteriovorus* HD100 recipients were grown as detailed in Section 2.3.1. *B. bacteriovorus* and *E. coli* S17-1 cultures were pelleted (4000 rpm, 20 minutes), prior to resuspending each (individually) in 200 µl of YT broth. *B. bacteriovorus* cell suspension was pipetted onto a nylon membrane, suspended on a PY agar plate, and allowed to dry. Once dry, the *E. coli* S17-1 cell suspension was then added on top of the *B. bacteriovorus* cell residue. This plate was then incubated overnight (18 hours) at 29°C.

Cells were then washed off the membrane and re-suspended in Ca/HEPES. This cell suspension was then serially diluted and plated onto YPSC overlay plates with 50 μg/ml kanamycin sulfate selection and YPSC-Top overlays containing Kanamycin-resistant *E. coli* S17-1 pZMR100 prey. These plates were incubated for 5 days (29°C) until single plaques (clearings in the *E. coli* S17-1 pZMR100 prey lawn) appeared. These plaques were picked into Ca/HEPES containing Kanamycin-resistant *E. coli* S17-1 pZMR100 prey and incubated (29°C, 200 rpm, 48 hours) to give predatory cultures of *B. bacteriovorus.*

Exconjugant *B. bacteriovorus* cells contain a fluorescently tagged gene construct on one strand of their chromosome (that has integrated via homologous recombination), and an untagged, WT copy of the gene of interest on the other strand.

Fluorescently tagged gene constructs were also conjugated into Bd0064mCherry/Bd0064mCerulean3-containing *B. bacteriovorus,* to allow for fluorescent visualisation of predators inside bacterial prey or host macrophage.

2.4.2.7. Further validation of fluorescently tagged *B. bacteriovorus* exconjugants.

Genomic DNA was extracted from liquid cultures of *B. bacteriovorus* exconjugants to determine whether target genes had been successfully fluorescently tagged, without any deleterious mutations occurring.

Genomic DNA was extracted using the GenElute bacterial genomic DNA extraction kit (Sigma), as per the manufacturer's instructions.

Genomic DNA was then used as a template to amplify the region containing the gene-fluorescent tag fusion via PCR, using primers (detailed in Supplementary Table 2.4.1) that bind approximately 200bp upstream and downstream of the gene, encompassing the whole gene, whole fluorescent tag and the gene-tag fusion junction. This PCR product was sequenced, via Sanger sequencing. These sequencing reads were compared to the *B. bacteriovorus* HD100 genome and the fluorescent tag plasmid reference sequence to confirm that the target gene and fluorescent tag were correct i.e., no deleterious mutations had occurred.

2.4.3. Construction of *B. bacteriovorus* single gene knockout mutants

To study the role and importance of gene/protein expression in the survival of *B. bacteriovorus* within macrophage, markerless, single gene deletion strains of *B. bacteriovorus* were generated. This process is summarised in Figure 2.4.3.

2.4.3.1. Design and PCR generation of fragments

For gene knockout constructs, 1 kb of 5' and 1 kb of 3' flanking, upstream and downstream of the gene of interest, were amplified via PCR, using primers designed using NEBuilder (New England BioLabs) and detailed in Supplementary Table 2.4.3, with the same stipulations as documented in Section 2.3.3.1.

2.4.3.2. Synthesis, transformation and conjugation of gene knockout constructs.

PCR fragments were then synthesised, ligated into *pk18mobSacB*, transformed into *E. coli* DH5α, validated by restriction digest, transformed into *E. coli* S17-1 and conjugated in *B. bacteriovorus* HD100, as detailed in Sections 2.4.2.1-2.4.2.6 inclusive.

Gene knockout constructs were also conjugated into Bd0064mCherry/ Bd0064mCerulean3-containing *B. bacteriovorus,* to allow for fluorescent visualisation of predators.

Exconjugant *B. bacteriovorus* cells contain a gene knockout construct on one strand of their chromosome (that has integrated via homologous recombination), and a WT copy of the gene of interest on the other strand. To form a complete gene deletion strain, we need to encourage the homologous recombination of our gene knockout construct into the other strand of the chromosome also, via a second genetic recombination event, and cure the exconjugants of the plasmid, removing it to create a markerless gene deletion that will no longer contain the target gene and will not be kanamycin resistant.

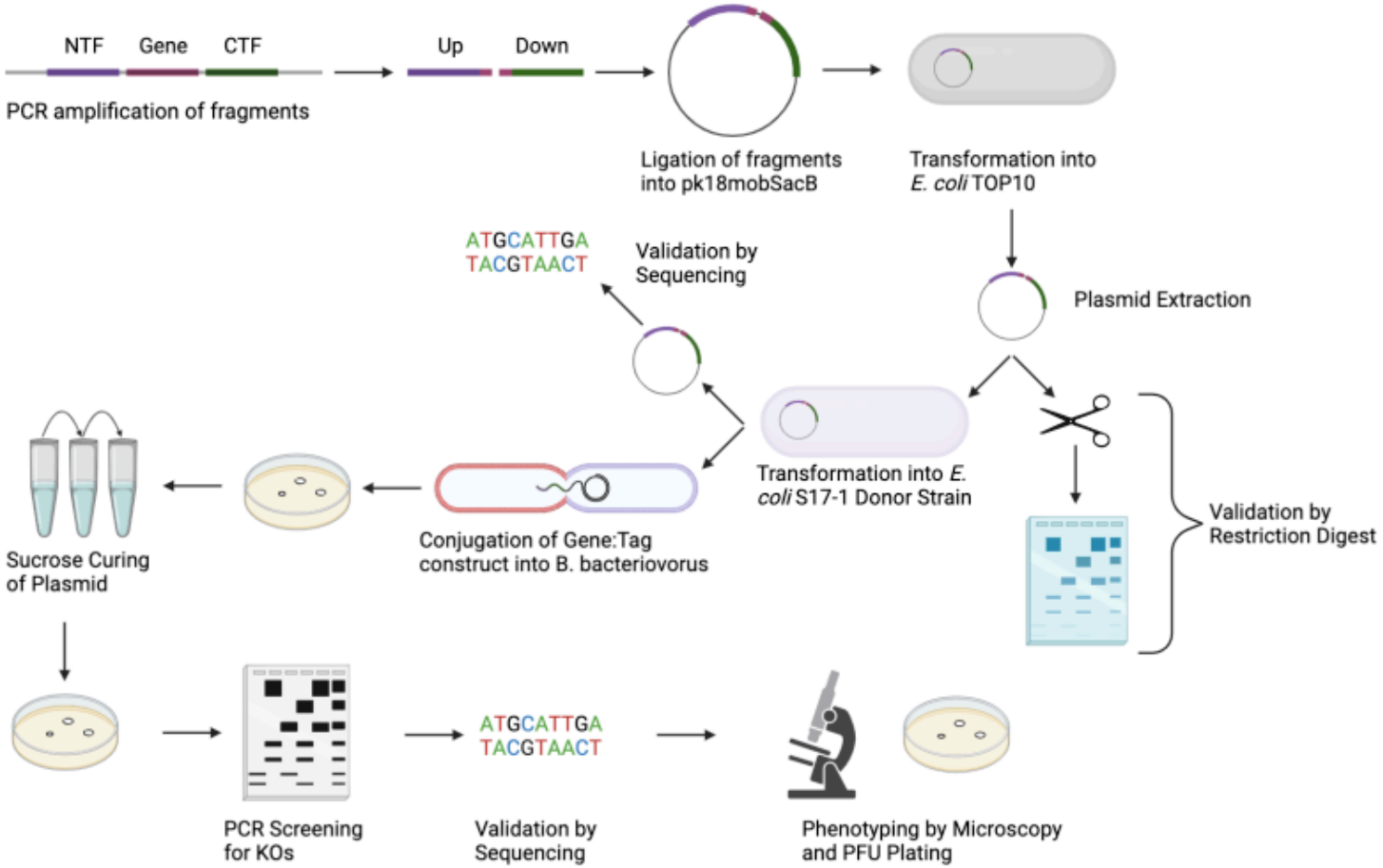

Figure 2.4.3: A schematic summarising the construction of single gene deletion mutants in *B. bacteriovorus*.

2.4.3.3. Generation of double-crossover Gene Knockout mutants via homologous recombination

To cure merodiploid *B. bacteriovorus* exconjugants of the *pk18mobSacB* plasmid and encourage the second genetic event that incorporates the gene knockout construct fully (or reversion to WT), sucrose counter selection is used. The addition of sucrose to culture media, combined with the omission of kanamycin selection, encourages the excision of the *pk18mobSacB* plasmid backbone from the genome, as the *sacB* gene contained within the plasmid encodes a levansucrase enzyme that converts sucrose to a toxic product. This selects against plasmid retention, resulting in the generation of two sub-populations. One loses the plasmid and recombines to restore the WT copy of the gene on both strands of the bacterial chromosome, resulting in a “WT revertant” bacterium. The second population recombines immediately before the gene knockout construct, integrating the gene knockout construct into both strands of the bacterial chromosome and forming a “gene knockout” bacterium (Figure 2.4.4).

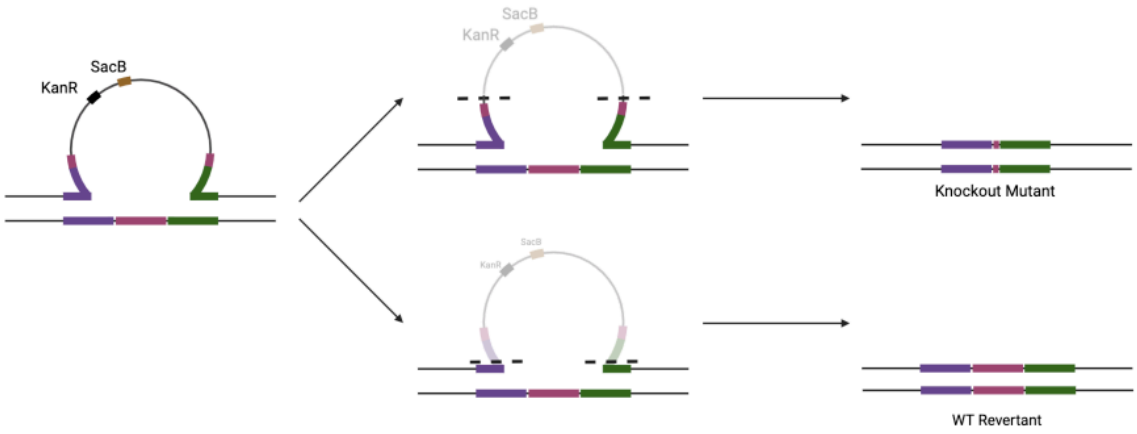

Figure 2.4.4: A schematic summarising the two outcomes of a second genetic crossover event in merodiploid *B. bacteriovorus* containing a gene knockout construct.

Predatory cultures of *B. bacteriovorus* were serially passage through Ca/HEPES buffer containing 5 % sucrose, 150 μl of *E. coli* S17-1 prey (heat killed at 105°C for 3 minutes) and 50 μl of *B. bacteriovorus* predatory culture. After 9 rounds of passaging, predatory cultures were serially diluted and plated onto YPSC overlay plates to yield single plaques. After incubation for 5 days (29°C), single plaques were picked into Ca/HEPES buffer (containing *E. coli* S17-1 prey) into 96-well plates.

After lysis of prey and growth of *B. bacteriovorus* to form predatory cultures (after 48 hours, 29°C), each of which has originated from a single plaque, each well was screened for kanamycin resistance by subbing into 96-well plates containing Ca/HEPES and *E. coli* S17-1 or Ca/HEPES, *E. coli* S17-1 pZMR100 and 50 μg/ml kanamycin.

Kanamycin resistant isolates still contain the *pk18mobSacB* plasmid and were therefore discarded. Kanamycin sensitive isolates were screened by colony PCR to identify potential gene deletion mutants (using the same reagent and thermocycling parameters as stated in Section 2.4.3.7). A gene knockout mutant was identifiable by a difference in band size, compared to WT controls.

2.4.3.4. Further validation of *B. bacteriovorus* gene knockout exconjugants

Gene knockout mutants confirmed by colony PCR were then further tested by Sanger sequencing to determine whether target genes had been successfully deleted.

Genomic DNA was extracted from liquid predatory cultures of *B. bacteriovorus* using the GenElute bacterial genomic DNA extraction kit (Sigma), as per the manufacturer's instructions.

The knockout region, consisting of the 5' (upstream) and 3' (downstream) flanking regions, either side of the deleted gene, that made up the knockout construct, plus an additional 1kb of 5' and 3' flanking DNA, outside of the construct region, was amplified from the candidate genomes, by PCR using primers detailed in Supplementary Table 2.4.2, and subsequently sequenced by Sanger sequencing by Source Bioscience. These sequencing reads were compared to the *B. bacteriovorus* HD100 genome to confirm that the target gene had been deleted, and that no other mutations had occurred within the 5' and 3' flanking regions surrounding the target gene.

2.4.4. Host-independent Gene Knockout strain generation

2.4.4.1. Generation of host independent strains from merodiploid

If removal of individual genes from host dependent *B. bacteriovorus* was deemed unlikely, due to the target gene(s) being essential for predation, therefore making gene knockout clones non-viable, a host-independent gene knockout clone, that doesn't carry out a predatory lifecycle that is dependent on Gram-negative prey cells, was sought. These bacteria grow by binary fission and are further explained in (348).

To generate host-independent gene knockout mutants, gene knockout constructs were conjugated from *E. coli* S17-1 (containing the gene knockout construct) into *B. bacteriovorus* HD100 (as before). Merodiploid exconjugants, containing one WT gene copy on one DNA strand and the gene knockout construct integrated into the other DNA strand, were selected, and picked into predatory cultures as before (containing 150 μl *E. coli* S17-1 overnight liquid culture, grown as before, and 2ml Ca/HEPES). Predatory cultures were filtered to remove any remaining Gram-negative prey and plated onto PY agar plates to select for host-independent *B. bacteriovorus* that will grow on the nutrient rich media in the absence of Gram-negative prey.

After incubation for 2 weeks, due to the slow-growing nature of these bacteria, individual colonies were selected and serially passaged on PY agar plates +/- 5 % Sucrose to counter-select against the *sacB* containing *pk18mobSacB* containing plasmid, to cure exconjugants of the plasmid and encourage homologous recombination of the gene knockout construct into the genome of *B. bacteriovorus* (by the same process as detailed in host-dependent gene knockout clone generation). Potential gene knockout clones were then tested by PCR and sequenced.

2.4.4.2. Conjugation of gene knockout constructs direct into host-independent *B. bacteriovorus*

If generation of gene knockout clones in host-dependent *B. bacteriovorus* or by conversion and sucrose-curing of merodiploid gene knockout exconjugants was unsuccessful, conjugation of the gene knockout construct from *E. coli* S17-1 (containing the gene knockout construct) directly into host-independent *B. bacteriovorus* is a strategy of last resort due to its difficult nature. This is necessary due to the genetic event involving the integration of the gene knockout construct may be immediately selected against in merodiploid (host-dependent) *B. bacteriovorus* if the target gene is essential, therefore conversion of merodiploid *B. bacteriovorus* into host-independent strains may only yield WT *B. bacteriovorus* as the genetic event is quickly selected against and the gene knockout construct lost from the bacterial genome. Conjugation of the gene knockout construct directly into host-independent *B. bacteriovorus* strains may bypass this issue.

To conjugate gene knockout constructs directly into a host-independent *B. bacteriovorus*, dense cultures of HID13 or HID22, two separate host-independent *B. bacteriovorus* strains containing two separate groups of mutations, were prepared by spreading liquid cultures of HID13 or HID22 onto PY agar plates, growing at 29°C for a week, and suspending the entire plate of bacterial growth in a small volume of PY broth.

This is because HID13 and HID22 grow very poorly at low population densities in liquid culture. The thick bacterial suspension of HID13 or HID22 was suspended on a nylon filter, on a PY agar plate, and allowed to dry. A liquid culture of *E. coli* S17-1, containing the gene knockout construct, was grown overnight (37°C, 200 rpm, 18 hours), centrifuged (4000 rpm, 10 minutes) and resuspended to give a 100x concentrated bacterial cell suspension. This bacterial cell suspension was added onto the membrane containing HID13/HID22 and allowed to dry. Plates were then incubated overnight at 29°C to allow for conjugation of the gene knockout construct into HID13/HID22. The dried cell mass was recovered, resuspended in PY broth, and filtered (0.45 nm) to remove any remaining *E. coli* S17-1 donor cells, before being serially diluted and plated onto PY agar. After 7 days of incubation (29°C), individual colonies were selected and patched onto PY agar plates +/- 5 % sucrose and passaged and screened for knockout construct integration as detailed above.

2.4.5. Macrophage culture

U937s are a monocyte derived cell line that when stimulated can assume the morphological and physiological characteristics of mature macrophages.

U937 cells (ATCC CRL-1593.2), a human monocyte-like cell line, were grown in RPMI medium containing 12 mM sodium bicarbonate, 2 mM L-glutamine, 10 mM HEPES, 1 mM sodium pyruvate, 25 mM D-glucose, 10 % foetal bovine serum (FBS) and 1 U/ml penicillin and 100 µg/ml streptomycin at 37°C, 5 % CO_2.

U937 cells were routinely passaged every 72 hours, during which the cells were dislodged via gentle scraping, washed in Dulbecco's phosphate buffered saline (D- PBS) (2.7 mM KCl, 1.5 mM KH_2PO_4, 137 mM NaCl and 8.8 mM $Na_2HPO_4 \cdot 7H_2O$, pH 7.4), and seeded into fresh media at 5 x10^4 cells/ml.

For experimental use, U937 cells were seeded at 5 x10^5 cells/ml in T-75 flasks (Corning) and differentiated into macrophage-like cells via the addition of 100 nM PMA (phorbol 12- myristate 13-acetate), then incubated for 48 hours, 37°C, 5 % CO_2. Cells were then harvested via gentle scraping, washed in D-PBS, pelleted via centrifugation (300 xg, 5 minutes) counted and then seeded at the desired concentration in fresh media, allowing them to adhere overnight (18 hours, 37°C, 5 % CO_2).

2.4.6. Visualisation of fluorescently tagged attack phase *B. bacteriovorus* via microscopy.

To determine the expression and localisation of our candidate genes in attack phase *B. bacteriovorus*, bacteria from predatory cultures (routinely cultured as detailed above) were immobilised on a bed of Ca/HEPES containing 1 % agarose and imaged using a Nikon Eclipse Ti-E inverted fluorescence microscope equipped with a Plan Apo 100x Ph3 oil objective lens. Images were taken using phase contrast (Exposure: 250 ms; Gain 1) mCherry (Exposure: 10 s; Excitation: 550-600 nm; Emission: 610-665 nm) and mCerulean3 (Exposure: 10 s; Excitation: 420-450 nm; Emission: 460-500 nm) filters. Images were acquired using Nikon NIS Elements software and an Andor Neo sCMOS camera.

2.4.7. Image analysis

Images taken on the Nikon TiE microscope (.nd2 format) were opened and analysed using Fiji image analysis software, a subsidiary of ImageJ (412). From raw image files, regions of interest (ROIs) were selected and adjusted using the brightness and contrast toggles. Scale bars were added, and ROIs were saved as .tiff files.

2.4.8. Visualisation of fluorescently tagged *B. bacteriovorus* strains throughout the predatory lifecycle via microscopy.

This assay aimed to characterise the expression of our proteins of interest throughout the predatory lifecycle of *B. bacteriovorus,* using fluorescence as a proxy for protein expression.

B. bacteriovorus strains containing a fluorescently (*mCerulean3* or *mCherry*)-tagged candidate gene were grown as detailed previously (10 ml Ca/HEPES, 600 μl *E. coli* S17-1 pZMR100, 200 μl of a previous predatory culture, 50 μg/ml kanamycin sulfate) for 24 hours, 200 rpm, prior to being checked via light microscopy to ensure total *E. coli* prey lysis. *B. bacteriovorus* liquid cultures were concentrated (10x) by centrifuging 5 ml of liquid predatory culture (4000 rpm, 20 minutes) and re-suspending in 500 μl of Ca/HEPES buffer.

To synchronise the invasion and predatory process so that all *E. coli* prey are invaded by *B. bacteriovorus* simultaneously, an excess of *B. bacteriovorus* predators was used. Approximately 1 x 10^9 PFU of *B. bacteriovorus* (suspended in 500 μl of Ca/HEPES buffer) were combined with 1x10^8 CFU/ml of *E. coli* prey (grown for 18 hours, 37°C, 200 rpm in YT-broth) in 1200 μl of Ca/HEPES buffer. This ratio of Predator:Prey:Buffer ensures synchronous predation. Samples were taken at 0 hours (post-mixing of *B. bacteriovorus* and *E. coli*), 15 minutes, 30 minutes, 45 minutes, 1 hour, 2 hours, 3 hours, and 4 hours to capture each characteristic/landmark stage of predation and characterise fluorescent protein expression at these points. Samples were immobilised on a bed of Ca/HEPES containing 1 % agarose and imaged using a Nikon Eclipse Ti-E inverted fluorescence microscope as before. The process used to visualise fluorescently tagged *B. bacteriovorus* strains throughout the predatory lifecycle via microscopy is summarised in Figure 2.4.5.

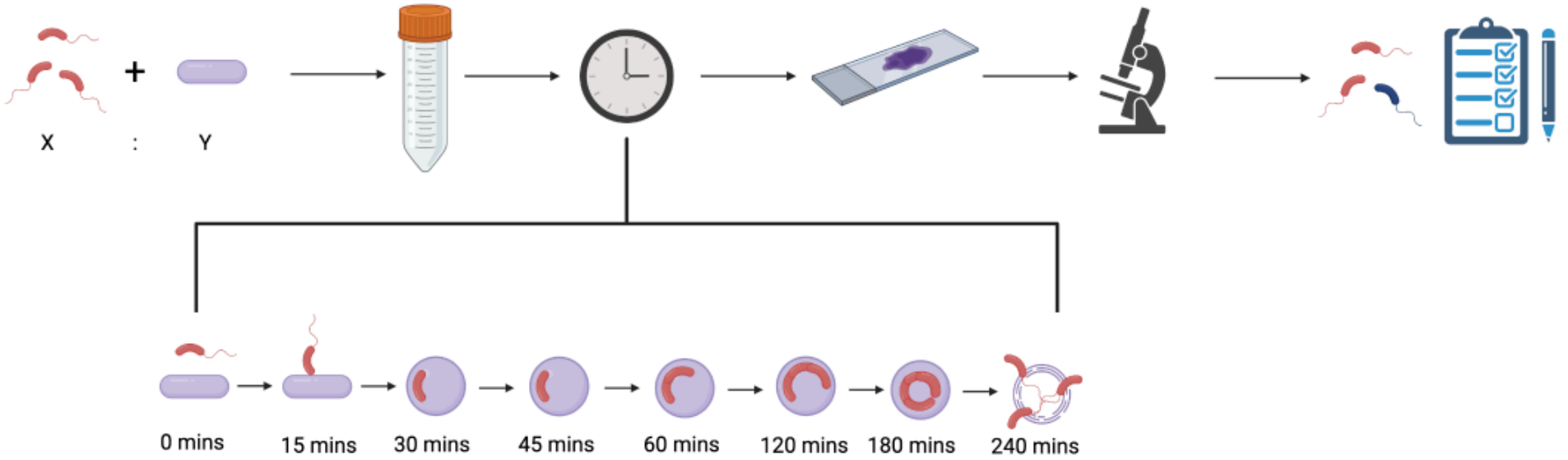

Figure 2.4.5: A schematic summarising how the expression of fluorescently tagged proteins in *B. bacteriovorus* is visualised throughout the predatory cycle.

2.4.9. Visualisation of fluorescently tagged *B. bacteriovorus* strains inside U937 macrophage-like cells via microscopy.

U937 cells (grown and differentiated as described above) were seeded onto glass cover slips within 24-well plates at 2 x 10^5 cells per ml and left to adhere overnight at 37°C, 5 % CO_2. Cells were then washed with D-PBS (Dulbecco PBS: phosphate buffered saline with Mg^{2+} and Ca^{2+}) and the media replaced with growth media containing 1 x 10^7 PFU/ml of our fluorescently tagged *B. bacteriovorus* strains (grown as previously described), giving an MOI of 1:50 (macrophage: bacteria). After 2 hours of incubation (37°C, 5 % CO_2), the media containing *B. bacteriovorus* was removed and cells were washed with D-PBS. For the 2-hour timepoint, infected cells were immediately imaged via fluorescence microscopy (as above) to determine whether expression of the *mCerulean3/mCherry* tagged genes was altered within macrophages. For 4 and 24-hour timepoints, infected cells were incubated with fresh, bacteria-free growth media (37°C, 5 % CO_2) until 4 or 24 hours post-bacterial addition, after which they were washed with D-PBS. Cells were then imaged as above. This is summarised in Figure 2.4.6.

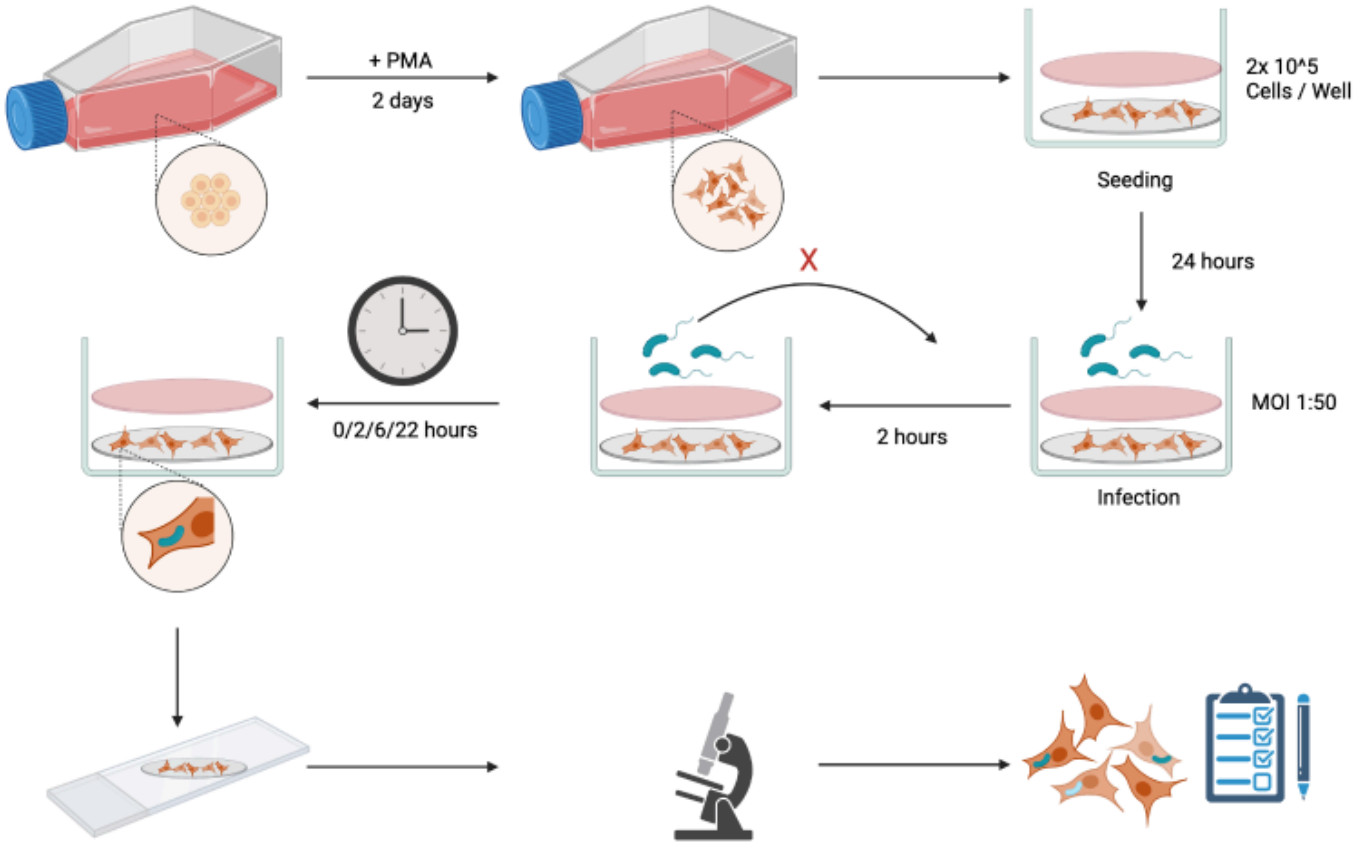

Figure 2.4.6: A schematic detailing how the expression of fluorescently tagged proteins by *B. bacteriovorus* is investigated inside U937 macrophage-like cells via microscopy.

2.4.10. Viability of gene knockout mutants of *B. bacteriovorus* inside U937 macrophage-like cells, via enumeration.

Plaque counts were used as a proxy for *B. bacteriovorus* quantification, as these bacteria are too small to be quantified via typical optical density-based methods. These plaque counts are expressed as PFU/ml (Plaque Forming Units per ml), analogous to the CFU/ml (Colony Forming Units/ml) used for "typical" colony-forming bacteria such as *E. coli.*

PMA-differentiated U937 cells (grown as detailed in Section 2.4.5) were seeded into 24-well plates at 2 x 10^5 cells per well for 24 hours (37°C, 5 % CO_2) prior to being washed with D-PBS. Cells were then exposed to *B. bacteriovorus* HD100 (or single gene deletion strains of *B. bacteriovorus*) at an MOI of 1:50 (Macrophage: *B. bacteriovorus*) for 2 hours, after which the *B. bacteriovorus* containing medium was removed and cells were washed with D-PBS+ 5 % FBS. RPMI was then added to the wells, whereby they were then incubated at 37°C, 5 % CO_2 until the designated timepoints, except for the 2-hour timepoint where cells were lysed immediately.

To measure the viability of the single gene deletion strains, *Bdellovibrio*-containing macrophage were lysed through the addition of ice cold, sterile, distilled water and incubated (on ice) for 10 minutes. Cell suspensions were pipetted vigorously to ensure a homogenous mixture, prior to being serially diluted and enumerated on YPSC plates. Briefly, 100 μl of the appropriate dilution of cell suspension was added to 150 μl of *E. coli* S17-1 bacterial culture (grown as previously described) and 5 ml of YPSC-Top agar (molten but cooled), before being poured onto a set YPSC-bottom agar plate to form a layer of soft-set agar with *Bdellovibrio* and *E. coli* suspended within. These plates were incubated for 5 days (29°C), until plaques (clearings in the *E. coli* prey lawn) appeared after which they were counted and compared to wildtype *B. bacteriovorus* HD100. This process is summarised in Figure 2.4.7.

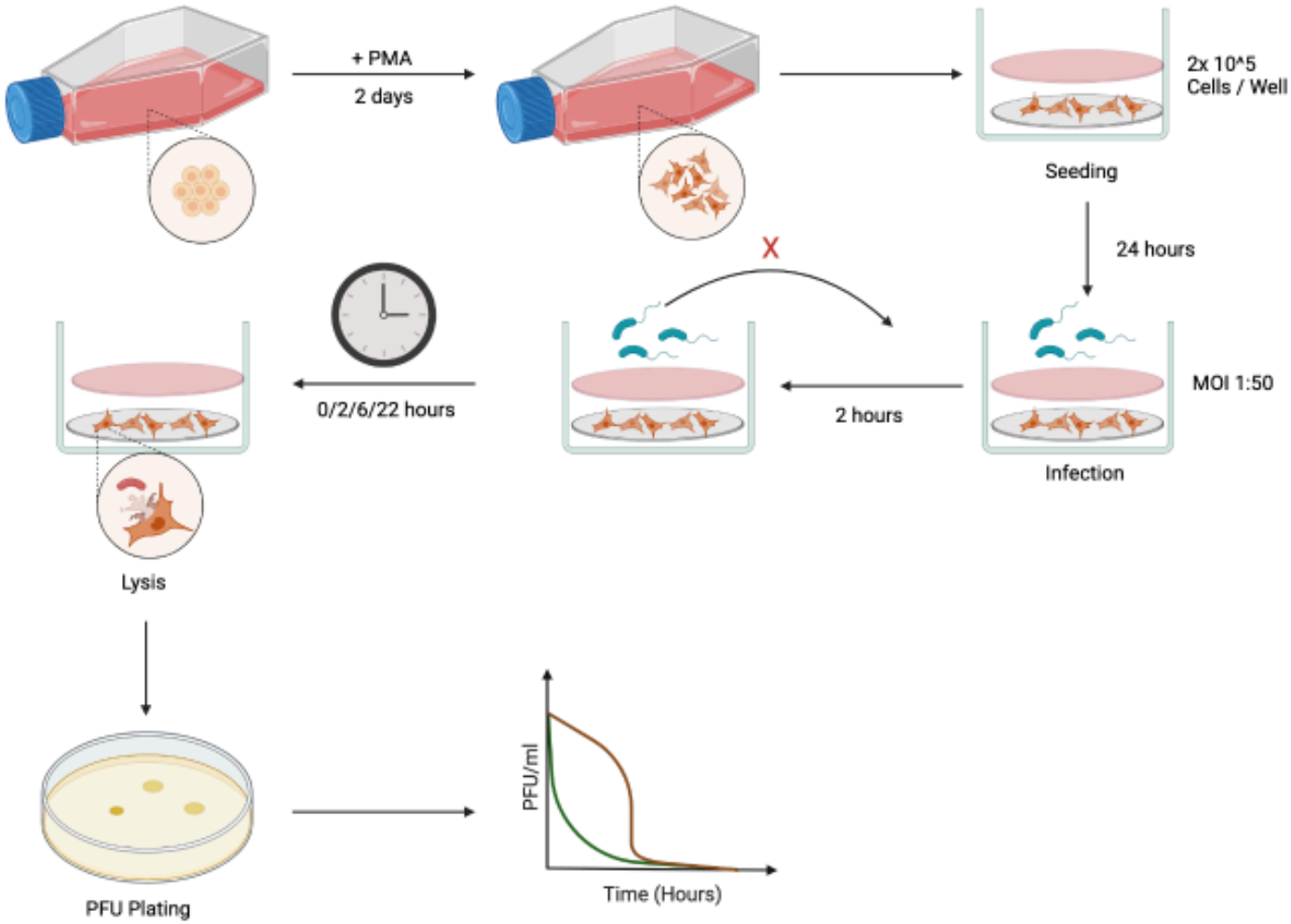

Figure 2.4.7: A schematic detailing how the viability of gene knockout mutants of *B. bacteriovorus* is investigated inside U937 macrophage-like cells via enumeration.

2.4.11. Testing the efficiency of *B. bacteriovorus* gene deletion mutants throughout predation

This experimental approach was adapted from the protocol documented in Remy et al., 2022 (413), by Dr Carey Lambert in our lab. Dr Carey Lambert aided and supervised me for this set of experiments, for which I am extremely grateful.

To determine whether the removal of our candidate gene products would affect the efficiency of predation by *B. bacteriovorus,* our gene deletion strains were incubated with *E. coli* S17-1 prey, and the OD_{600} of the predation culture measured over time. As *B. bacteriovorus* are too small to be measured accurately by optical density, the growth of *E. coli* S17-1/optical density of the predatory culture containing *E. coli* S17-1 was used as a proxy for successful predation (indicated by prey cell lysis and a drop in optical density).

B. bacteriovorus gene deletion mutants were grown overnight as documented previously (Section 2.3.1). Plaque forming units (PFU) inputs for each strain were then matched using SYBR Green DNA stain, to ensure that equal titres of *Bdellovibrio* for each strain were used as starting inputs in our predatory cultures. This approach is documented in Remy et al., 2022 (413). Briefly, samples of *Bdellovibrio* were incubated with SYBR Green dye for 90 minutes (300 rpm double orbital, in darkness, in triplicate), before fluorescence was measured using a FLUOStar Omega Plate Reader (BMG Labtech) (excitation: 485 nm, emission: 520 nm, Gain: 800), with fluorescence values being interpolated into relative PFU/ml counts using a PFU:SYBR Green Fluorescence correlation curve (provided by Dr Carey Lambert).

PFU inputs were matched for each single gene deletion strain, giving an input of 1 x 10^8 PFU/ml of *Bdellovibrio* with a starting OD_{600} of *E. coli* prey of 1.0, corresponding to 1x 10^9 CFU/ml of *E. coli* S17-1, giving a predator: prey ratio of approximately 1:10. Predatory cultures (containing *E. coli* prey and *Bdellovibrio bacteriovorus* WT or mutant) were inoculated in triplicate into a black OptiPlate (Corning), along with media only, *Bdellovibrio* only (no prey) and Prey only (no *Bdellovibrio*) controls. The optical density (OD_{600}) of the predatory culture was measured every 20 minutes, for 18 hours (200 rpm, double orbital, in triplicate) to give a prey survival curve, where a drop in OD_{600} is indicative of successful predation and prey lysis.

OD_{600} values were exported using MARS OMEGA data analysis software and plotted compared to WT *B. bacteriovorus* HD100 to analyse any differences in predation efficiency caused by gene deletion.

In addition to this, OD_{600} data was analysed using CurveR, according to the method documented in Remi et al., 2022, to analyse prey cell lysis and predation dynamics. This generates a table of values showing the quality of analysis and key criteria of the modelled curve. VEcv represents the fit of the curve (where 100 represents a perfect match). R_{max} indicates the maximum rate of prey cell lysis. S indicates the inflection point, the time at which the maximum rate of prey cell lysis (R_{max}) occurs i.e., the steepest point on the curve.

2.4.12. Bioinformatic analyses

Features of the candidate genes/proteins in this study were investigated using various bioinformatic tools and servers to tell us more about the structure and function of the proteins in this study. These tools are listed below and detailed in Table 2.4.1.

xBASE: https://hactar.shef.ac.uk/xbase/viewregion.cgi (414)
UniProt: https://www.uniprot.org/ (415)
NCBI BLAST: https://blast.ncbi.nlm.nih.gov/Blast.cgi (416)
SignalP 6.0: https://services.healthtech.dtu.dk/service.php?SignalP-6.0 (417)
PredTAT: http://www.compgen.org/tools/PRED-TAT/ (418)
PFAM: http://pfam.xfam.org/ (419)
EMBOSS Needle: https://www.ebi.ac.uk/Tools/psa/emboss_needle/ (420)
Clustal Omega: https://www.ebi.ac.uk/Tools/msa/clustalo/ (420)
STRING: https://string-db.org/cgi/ (421-423)
KEGG: https://www.genome.jp/kegg/ (424, 425)

Analysis of RNASeq data, and the tools used in this process, will be detailed separately.

Table 2.4.1: Bioinformatic tools used in this study.

Server/Tool	Function	Reference
xBASE	Used to retrieve DNA sequences for each of the *B. bacteriovorus* genes in this study	Chaudhari et al., 2008
UniProt	Used to retrieve Protein sequences encoded by each of the *B. bacteriovorus* genes in this study	The Uniprot Consortium, 2021
NCBI BLAST	Used to compare DNA/Protein sequences of interest with homologues in *B. bacteriovorus* or other Gram-negative bacteria	Altschul et al., 1990
Signal P 6.0	Identification/Prediction of signal peptides and secretion signals in protein sequences	Teufel et al., 2022
PredTAT	Identification/Prediction of Sec/Tat signal peptides and secretion signals in protein sequences	Bagos et al., 2010
PFAM	Identification/Prediction of well-characterised domains	Mistry et al., 2020
EMBOSS Needle	Pairwise alignment of DNA/Protein sequences to investigate homology between gene/protein homologues	Madeira et al., 2022
Clustal Omega	Pairwise alignment of DNA/Protein sequences to investigate homology between gene/protein homologues	
STRING	Gene neighbourhood and association studies to highlight other genes with similar functions within the genome of *B. bacteriovorus.* Magenta threads represent experimentally determined interactions; Green threads represent gene neighbourhood interactions; Dark blue threads represent gene co-occurrence; Black threads represent co-expression; Lilac threads represent protein homology; Yellow threads represent textmining (i.e. associations in literature).	Szklarczyk et al., 2021
KEGG	Identify related genes and pathways, interacting with the proteins in our study	Kanehisa et al., 2016

2.4.12.1. Statistical analysis

Statistical analysis on each dataset was performed using GraphPad Prism 9.0. Data was analysed for normality using a Shapiro-Wilk normality test. If the data fitted a parametric/normal distribution, a One-Way ANOVA test was used to assess statistical significance (testing if each condition was statistically different from a control group). If the data fitted a non-parametric/non-normal distribution more closely, a Two-Way Repeated Measure ANOVA with a Sidak's multiple-comparison test was used to assess statistical significance. Statistical analysis of the data generated in "Determining the importance of our candidate proteins in the predation of *E. coli* by *B. bacteriovorus*." and "Determining the Viability of *B. bacteriovorus* gene deletion mutants in macrophage" was performed using a Two-Way Repeated Measure ANOVA with a Sidak's multiple-comparison test. The number of biological replicates is indicated in the appropriate result figure legends.

2.5. Chapter 5 Specific Methods: RNASeq analysis

The aim of this work was to see the gene expression by *Bdellovibrio bacteriovorus* engulfed by U937 macrophage-like cells (PMA-differentiated from a U937 monocytic cell line and hereafter described as macrophages) and persisting for up to 24 hours, alongside gene expression induced in macrophage by *Bdellovibrio* persistence. I was able to make use of pre-existing frozen samples of *Bdellovibrio* inside macrophages from 2-, 4-, 8- and 24- hours, that were prepared by Dhaarini Raghunathan during her study on *Bdellovibrio* persistence (2).

2.5.1. Sample preparation

2.5.1.1. Cell culture and infection

PMA-differentiated U937 cells (grown as detailed in Section 2.4.5) were seeded into 24-well plates at 2 x 10^5 cells per well for 24 hours (37°C, 5 % CO_2) prior to being washed with D-PBS. Cells were then exposed to *B. bacteriovorus* HD100 at an MOI of 1:50 (Macrophage: *B. bacteriovorus*) for 2 hours, after which the *B. bacteriovorus* containing medium was removed and cells were washed with D-PBS+ 5 % FBS. RPMI was then added to the wells, whereby they were then incubated at 37°C, 5 % CO_2 until the designated timepoints.

At 2 hours post-bacterial addition, all media was removed from the wells and 1ml of TRI Reagent (a monophasic solution containing phenol and guanidine isothiocyanate; Invitrogen) was added to each well, homogenising and lysing the sample. The sample was then transferred to a sterile 1.5ml Eppendorf and flash frozen at -80°C to preserve total nucleic acids in the sample.

The same approach was performed at 4 hours, 8 hours, 24 hours, and 48 hours post-addition for both *Bdellovibrio*-containing and macrophage-only wells.

The above steps were performed by Dr Dhaarini Raghunathan, a previous postdoctoral researcher in the lab.

2.5.1.2. RNA isolation and preparation

To isolate both the host and bacterial RNA, homogenised samples were defrosted on ice and mixed thoroughly. Total nucleic acids were then extracted from the sample through the addition of 200 μl of chloroform (Sigma) to suspend the nucleic acids in the aqueous phase of our sample (DNA is held at the interface between the organic and aqueous phases due to its association with histones/other host proteins), followed by ethanol precipitation. The samples were then purified for total RNA using the Qiagen RNEasy kit (with on-column DNase digestion) as per the protocol suggested (Figure 2.5.1).

RNA samples were analysed using an Agilent 2100 Bioanalyser and Agilent RNA 6000 Nano kit, according to manufacturer's instructions by Dr Carey Lambert. This was performed to check electrophoretically for RNA quality and quantity (including examining ribosomal RNA bands as a measure of total, undegraded RNA), DNA contamination and RNA degradation (Table 2.5.1) and then checked for the presence of bacterial RNA by RT-PCR (Qiagen one-step RT- PCR kit; reaction details in Section 2.5.1.3), probing for *dnaK* using primers (dnaK_F: TGAGGACGAGATCAAACGTG; dnaK_R: AAACCAGGTTGTCGAGGTTG) to amplify a 100bp product within the *dnaK* gene. *dnaK* was used as a control for the presence of *B. bacteriovorus* DNA as it is constitutively expressed by the bacterium. RT-PCR products were visualised on a 2 % agarose gel (1 hour, 100 volts) against a 100bp ladder (New England Biolabs) to check for the presence of DNA in our RNA samples.

2.5.1.3. RT-PCR (To test for the presence of bacterial DNA)

Per 25 μl reaction

- 5 μl of 5X buffer
- 5 μl of Q solution
- 1 μl dNTPs
- 1.5 μl *dnaK_F* primer (10mM)
- 1.5 μl *dnaK_R* primer (10mM)
- 1 μl of Enzyme MasterMix
- 0.5 μl of template*
- 9.5 μl Nuclease-free water

*Test: RNA sample
Positive Control: *B. bacteriovorus* genomic DNA
Negative Control: Nuclease-free water

Using the thermocycling conditions:

- Reverse transcription (conversion of RNA to cDNA): 50°C, 30 minutes
- Initial denaturation: 94°C, 15 minutes
- 35 cycles of:
    - Denaturation: 94°C, 1 minute
    - Annealing: 50°C, 1 minute
    - Extension: 72°C, 1 minute
- Final extension: 72°C, 10 minutes

2.5.1.4. Quality control (prior to RNA sequencing)

Samples from 48 hours post-uptake were excluded from RNA sequencing and further analysis as they were of poor quality, with low quantity and poor RIN (RNA Integrity Number: Calculated by the ratio of 28s to 18s rRNA) quality values. Electropherograms also indicated RNA degradation in one of the two samples from 48-hour Cell only controls and U937 + *Bdellovibrio* test samples (See Supplementary Table 2.5.1), therefore the 48-hour timepoint was excluded from further studies due to a lack of (high quality) RNA.

Technical replicates for each of the 8 remaining conditions (U937 Cell only control and U937 + *Bdellovibrio* test samples, for each of 4 timepoints (2-, 4-, 8- and 24-hours after *Bdellovibrio* engulfment) were pooled and sent for Dual RNA Sequencing to Vertis Biotechnologie, Germany.

The samples were named as follows:

T2C: PMA-differentiated U937 cells only; 2 hours

T2CBd: PMA-differentiated U937 cells with *Bdellovibrio*; 2 hours post-uptake

T4C: PMA-differentiated U937 cells only; 4 hours

T4CBd: PMA-differentiated U937 cells with *Bdellovibrio*; 4 hours post-uptake

T8C: PMA-differentiated U937 cells only; 8 hours

T8CBd: PMA-differentiated U937 cells with *Bdellovibrio*; 8 hours post-uptake

T24C: PMA-differentiated U937 cells only; 24 hours

T24CBd: PMA-differentiated U937 cells with *Bdellovibrio*; 24 hours post-uptake

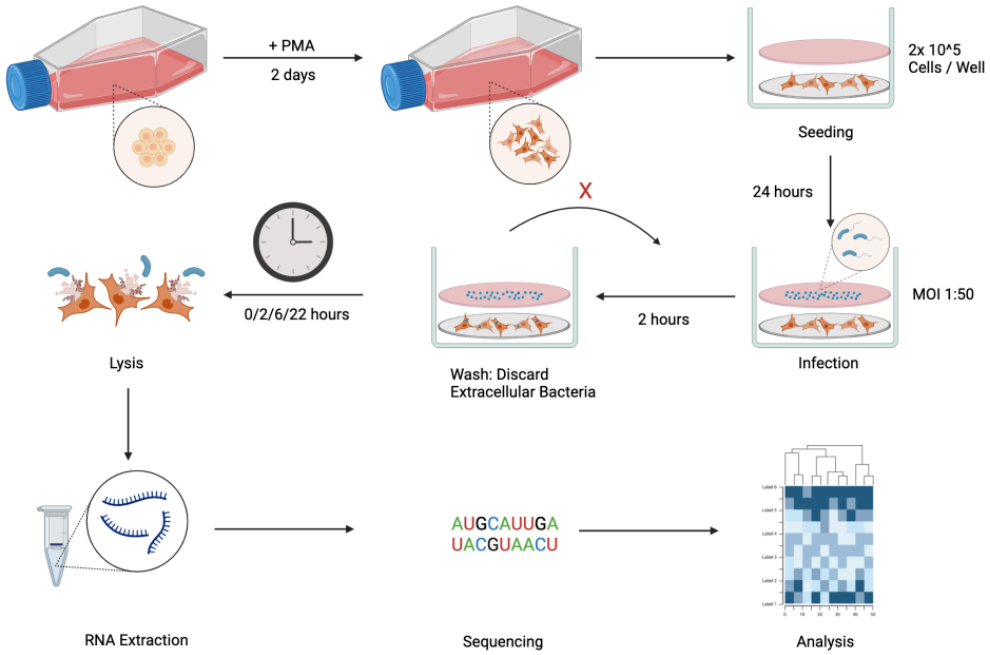

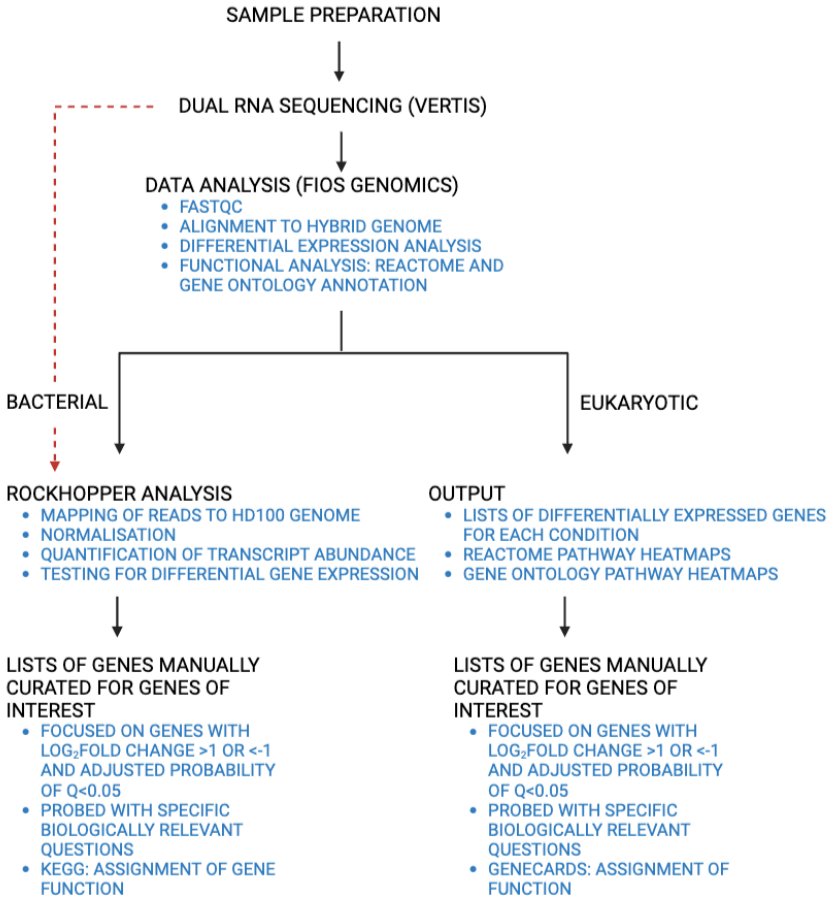

Figure 2.5.1: A schematic showing the approach used for Sample Preparation, RNA isolation, Dual RNA Sequencing and Analysis in this study. PMA-differentiated U937 cells were exposed to *B. bacteriovorus* at a Multiplicity of Infection (MOI) of 1:50 (U937: *Bdellovibrio*) for two hours, prior to removing the *Bdellovibrio*-containing media and periodically lysing the U937 cells at 2-, 4-, 8- and 24-hours post-uptake to isolate total RNA (Bacterial and Eukaryotic) at each timepoint. RNA was extracted and sent for Dual RNA sequencing, prior to RNASeq analysis.

2.5.2. Dual RNA sequencing (performed by Vertis Biotechnologie, Germany)

Total RNA samples were examined by capillary electrophoresis. Ribosomal RNA was then depleted from the total RNA samples (Vertis Biotechnologie, in-house protocol). Ribosomal RNA depleted samples were fragmented by ultrasound (30s, 4°C), prior to 3' oligonucleotide adaptor ligation. cDNA synthesis was performed using M-MLV reverse transcriptase, with the 3' adaptor acting as a primer. cDNA was purified, after which a 5' Illumina TruSeq sequencing adaptor was ligated to the 3' end of the antisense cDNA. The resulting cDNA was amplified to 10-20 ng/μl by PCR, using a high-fidelity DNA polymerase. cDNA was purified using an Agencourt AMPure XP Kit (Beckman Coulter Genomics) and analysed by capillary electrophoresis.

cDNA samples were pooled in approximately equimolar amounts, prior to size fractionation (200 – 500bp) using a preparative agarose gel, a sample of which was analysed by capillary electrophoresis. The cDNA pool was sequenced on an Illumina NextSeq 500 system using a 75bp read length. Sample details, including the number of reads obtained from each sample, are documented in Supplementary Table 2.5.2.

Fastq files were sent to FIOS Genomics, Edinburgh for analysis.

2.5.3. Fios Genomics RNASeq analysis

2.5.3.1. Eukaryotic analysis

2.5.3.1.1. Quality control

FastQC was used to calculate several metrics assessing the quality of the cDNA reads (derived from the RNA) in each sample was sufficient for further analysis, including per-base sequence quality, per tile sequence quality, per sequence quality scores, per sequence GC content, sequence length distribution, overrepresented sequences, and adapter content. Per-base sequence quality was high and stable in all samples. Other metrics tested also showed that the samples met the required quality conditions for further analysis.

2.5.3.1.2. Alignment

Reads (for the *Bdellovibrio* and macrophage DualSeq) were aligned to a hybrid genome, created by combining the human reference genome (GRCh38.p13) with the *B. bacteriovorus* HD100 genome. 75-85 % of the reads were successfully mapped to the hybrid genome using the STAR aligner (426). The first 4 samples (T2C, T2CBd, T4C and T4CBd) relating to 2- and 4-hour timepoints for both cell only and cell + *Bdellovibrio* samples contained 20 % unmapped reads whereas the latter 4 samples (T8C, T8CBd, T24C and T24CBd) contained less than 20 % unmapped reads. This may be down to a batch effect introduced during RNA sample harvesting or prior to RNA sequencing, but this is unlikely to affect further analysis. 5-11 % of the successfully mapped reads did not map to known features within the hybrid genome. This may be due to them mapping to prophage sequences that are not part of the reference genomes (human or *Bdellovibrio bacteriovorus* HD100). The U937 cell line has been certified to be free of viruses and other microbial contaminants (ATCC), however running the reads through readily available software e.g. Kraken (427), would test for contamination and determine whether these unmapped reads belong to another characterised organism.

The (eukaryotic) raw data was then assessed by a further 6 quality control tests, with PCA (Principal Component Analysis) plots revealing no apparent major batch effects in the samples. PCA highlighted that introducing *B. bacteriovorus* to cells caused a significant shift in the expression profiles (as expected). Unexpectedly, incubation time did not lead to noticeable stratification of the samples. Despite this, I looked at later timepoints (24 hours) compared to earlier timepoints (2, 4 and 8 hours) of *Bdellovibrio* occupation to investigate any differentially expressed genes. Human genes outnumber *Bdellovibrio* genes 63,494 to 3619 and so the expression data would have been stratified mainly by changes in macrophage gene expression.

2.5.3.1.3. Eukaryotic association analysis

As no replicates were prepared for this experiment, it was not possible to employ any statistical tool to find differentially expressed genes. Therefore, only fold changes in expression between control and *Bdellovibrio*-containing samples were calculated and used for further analyses. This was due to the financial cost of further replicates totalling £60,000 for 3 biological repeats, making this unfeasible. As we originally envisaged using this experiment as a general look at the two transcriptional responses (macrophage and bacteria), prior to experimentally validating and following up our findings, one biological repeat was deemed feasible.

Tables of differentially expressed genes (fold change >2 or < 0.5, comparing cell only controls to *Bdellovibrio*-containing samples) were provided for each timepoint, highlighting differences in gene expression induced by *Bdellovibrio*, by comparing cell only controls to *Bdellovibrio*-containing samples. Each timepoint gave approximately 5000 differentially expressed genes.

Differences in gene expression at certain timepoints, relative to other timepoints, was also calculated. Genes of interest were then manually curated from this data by asking certain biologically and contextually relevant questions, probing gene expression profiles in our data to support this.

2.5.3.1.4. Eukaryotic functional analysis

The approximately 5000 genes differentially expressed at each timepoint (*Bdellovibrio*-containing samples relative to cell only controls), were mapped (by Fios Genomics) to Reactome pathways and Gene Ontology terms, correcting for the number of genes in each pathway/term that may be expected by chance.

2.5.3.2. Analysis of bacterial gene expression using the Rockhopper pipeline

2.5.3.2.1. Rockhopper analysis

Rockhopper is a purpose-built interface designed for the analysis of bacterial RNASeq data. The underlying process Rockhopper uses is documented fully by McClure, Tjaden and co-workers (428-430). Essentially, Rockhopper aligns the bacterial reads to the *B. bacteriovorus* HD100 genome, constructing a transcriptome map to which it quantified transcript abundance and tested for differential gene expression using a negative binomial distribution. In this study, Rockhopper was used to map our reads to the *B. bacteriovorus* HD100 genome, quantify transcript abundance and test for differential gene expression. I then manually curated the dataset to examine which genes were present and highly differentially expressed by *Bdellovibrio*, within macrophage, at each timepoint.

2.5.4. Comparison to *Bdellovibrio* gene expression throughout predation

Comparison of the differential regulation of *B. bacteriovorus* genes throughout the predatory lifecycle of *B. bacteriovorus* was made possible by the work of (and kind gift of this work by) Dr Simona Huwiler, a former post-doctoral researcher in the Sockett Laboratory. Dr Huwiler isolated RNA from *B. bacteriovorus* from each characteristic stage of the predatory lifecycle, whilst it preyed upon *E. coli* K12, subsequently sequencing this RNA to form a (yet unpublished) RNASeq profile of the transcriptional regulation of every gene within the *B. bacteriovorus* genome, at each stage of predation. Read per kb per million reads (RPKM) were used as a proxy for gene expression and compared to attack phase transcription values to determine the differential expression of individual genes throughout predation.

Chapter 3: Exploring the function and regulation of surface proteins on the resistance of *Serratia marcescens* during predation by *Bdellovibrio bacteriovorus* in human serum.

3.1. Introduction

3.1.1. Rationale behind Chapter 3

Before any potential use of *Bdellovibrio bacteriovorus* as a novel antimicrobial therapy, the interplay between the host immune response, the pathogen and *Bdellovibrio bacteriovorus* must firstly be understood.

It is well documented (431, 432) that alteration of the bacterial cell surface occurs due to microenvironmental conditions and cellular stresses, including stresses imposed by the host environment and the immune system, and that this alteration of the cell surface may confer protection against recognition by the host immune response. From this, it'll be important to characterise the impact of these cell surface changes on predation by *B. bacteriovorus* within a host environment as this may alter susceptibility of the prey to predation, acting as a form of resistance.

Building on pilot work from the lab, this chapter will elaborate the mechanisms that interface with predation of pathogenic prey within the host, aiding the future application of *B. bacteriovorus* as a novel antimicrobial therapy.

As bacterial surfaces are central to the first interactions between predator and prey, and as the subset of differentially expressed genes that I investigated further in this chapter all encode surface proteins (or modifications thereof), I aimed to test how bacterial surface alterations affect the dynamics of predation in a host setting. In this study, I characterise the host factor-induced alterations that occur on the pathogen cell surface during predation by *B. bacteriovorus* in human serum, asking if such alterations confer a decreased susceptibility to predation.

As mentioned previously, multidrug resistant Gram-negative bacterial pathogens are of great concern for the continued treatment of bacterial infection. One such multidrug resistant pathogen is *Serratia marcescens*.

The strain of *S. marcescens* used in this study, *S. marcescens* #42, is a clinical respiratory isolate of *S. marcescens* (detailed in Supplementary Table 2.1.1) that was sequenced by Dr Dhaarini Raghunathan. The genome of *S. marcescens* #42 was then annotated by Dr Dhaarini Raghunathan, through comparison to the genome-sequenced Type strain *S. marcescens* DB11 (NCBI Taxonomy ID: 273526). This strain was chosen as it represents a clinically relevant pathogen, similar to which we would aim to treat with *B. bacteriovorus* in future, and was selected from a panel of bacterial pathogenic isolates that were seen to cause infections within the Nottingham University hospital trust. *S. marcescens* #42 is of the same lineage as the *S. marcescens* Type strain DB11.

As detailed in Section 1.4.4, plasma is where the majority of immunological and bactericidal exchanges occur and where therapeutic *Bdellovibrio* would encounter bacterial pathogens during treatment. Experimentally, or *ex vivo*, we are able to investigate the effects of plasma on predation using human serum. This is derived from whole blood which has been clotted to remove all cells (red blood cells, lymphocytes etc.) and just contains the soluble components of blood plasma, such as, but not limited to, antibodies, complement proteins and antimicrobial proteins. Serum contains two predominant microbicidal mechanisms which target bacterial surfaces, as the key component of the host-pathogen interface, complement deposition and antimicrobial proteins, both of which mediated killing through bacterial cell lysis (discussed in Section 1.4.4).

Previous work ((383)), showed that *Bdellovibrio* predation was possible in serum, but I wanted to investigate this further, by studying whether predation of a clinical isolate of *S. marcescens* was possible in human serum, and how surface modifications impact predation efficacy.

3.1.2. *Serratia marcescens*

3.1.2.1. Virulence

Serratia marcescens infection is typically associated with intravenous or urinary catheter use and is a common nosocomial infection, potentially resulting in sepsis, pneumonia and urinary tract infections are common (433, 434).

The components of the bacterial cell surface of *S. marcescens* are largely typical (documented in Section 1.3). Modifications to the bacterial cell surface assist in resisting the actions of the host immune response, contributing to bacterial virulence. These include the upregulation of capsule production, where capsulation is associated with bacteraemia, to resist the actions of host complement (435-437), as detailed in Section 1.4.4.3, and extension of O-antigen regions, decreasing C3 (complement protein 3) deposition and causing MACs to form away from the bacterial outer membrane (169, 435).

3.1.2.2. *S. marcescens* complement resistance.

Studies of complement activation by *S. marcescens* show that all three complement pathways are activated in human serum, resulting in MAC formation on the bacterial cell surface, suggesting that complement pathway activation is not perturbed in these isolates (438). Instead, complement-resistance is suggested to be conferred by an increase in LPS synthesis and potential degradation of C3b on the surface into its subunits, minimising MAC formation, whereby an alternative unknown mechanism may subsequently prevent phagocytosis (438).

S. marcescens expresses fimbriae, otherwise known as Type I pili, on its outer surface (439, 440). The structure and function of pili, and other outer membrane proteins such as OmpC and OmpF (441, 442), may vary based on different stresses reflecting adaptation to differing microenvironmental conditions (31).

Fimbriae have not been extensively studied in *Serratia,* but our sequencing detected two fimbrial gene clusters within our isolate, based on homology to *S. marcescens* DB11 fimbrial clusters. As the fimbrial clusters of *S. marcescens* have not been extensively studied, they do not have annotated names.

Capsular export and synthesis in *S. marcescens* are summarised below (Figure 3.1.2) (19, 437, 443-451).

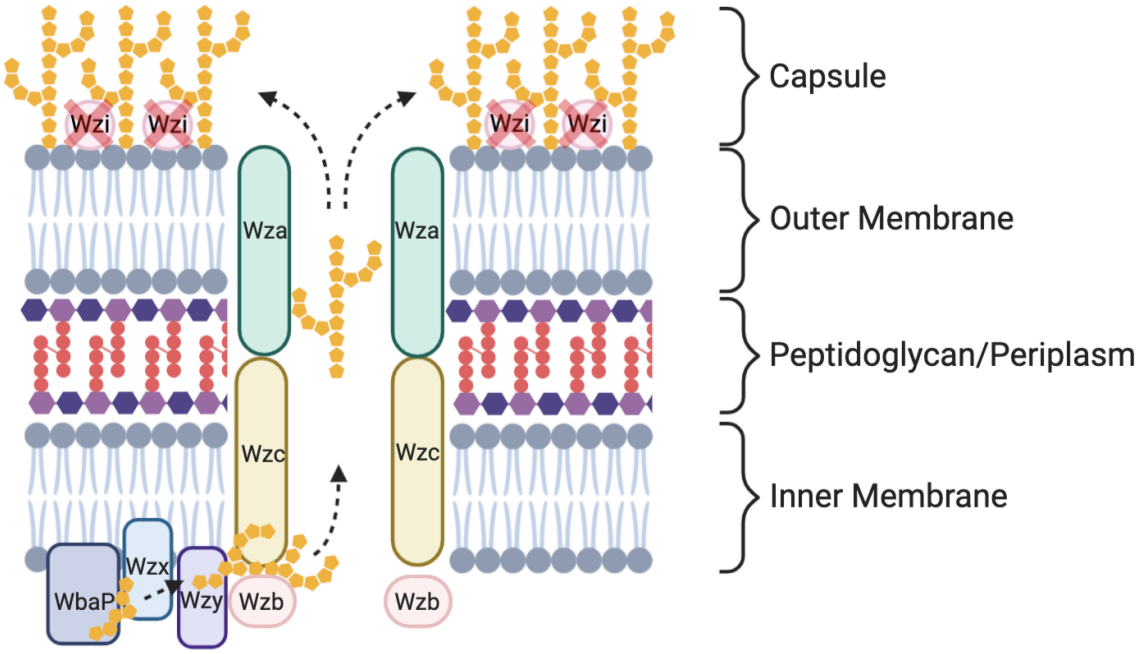

Figure 3.1.1: A schematic of the machinery involved in capsular synthesis and export in *Serratia marcescens.* Capsular biosynthesis is initiated by WbaP, which catalyses the transfer of galactose-1-phosphate from UDP-galactose to an undecaprenyl phosphate carrier lipid at the cytoplasmic face of the inner membrane. Further hexose sugar moieties are then added by other glycosyltransferases to build the polysaccharide region, upon which this complex is then flipped to the periplasmic face of the inner membrane by Wzx. This repeating unit is then polymerised to form the capsular polysaccharide, through the polymerase-mediated addition of units to the chain, controlled by the actions of Wzc, a tyrosine kinase, and Wzb, a phosphatase, which both regulate capsular polymerisation and export. This then cues Wza to export the large capsular polysaccharide across the outer membrane. In *S. marcescens* strains the capsule tethering protein Wzi is absent. Figure designed by C.C., originally based on (Haas, E., 2012).

3.1.2.3. *S. marcescens* antimicrobial peptide resistance

S. marcescens also modifies the Lipid A core of its LPS outer membrane with a L-Ara(4)N sugar, encoded by the *arnBCADTEF* operon. This subset of genes encodes the addition of 4-amino-4-deoxy-L-arabinose (L-Ara(4)N) to the 1' and 4' phosphate groups of Lipid A, and the Kdo_2 residues of the core oligosaccharide, altering the overall negative charge of the region and negating the binding of cationic antimicrobial peptides, conferring polymyxin and CAMP resistance (129-131). This is further discussed in Section 1.4.4.1.2 and summarised in Figure 3.1.2.

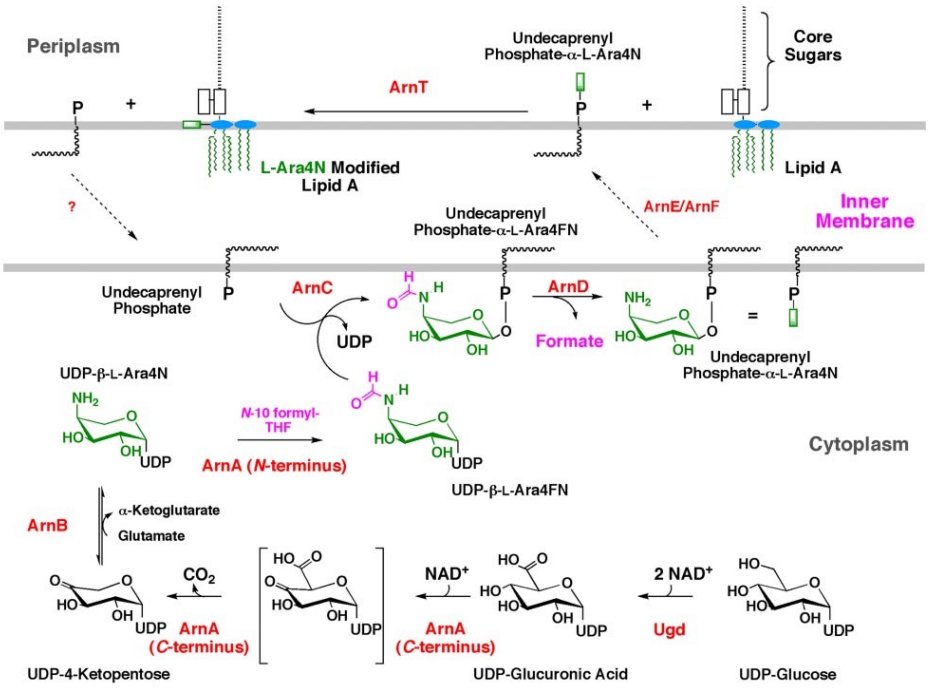

Figure 3.1.2: Arn-mediated modification of Gram-negative LPS Lipid A with an L-Ara(4)N sugar. The synthesis of L-Ara(4)N, before it is attached to Lipid A 1' and 4' phosphate groups, is initiated by the conversion of UDP-Glucose to UDP-Glucuronic acid via UDP-glucose dehydrogenase (Ugd). UDP-Glucuronic acid is converted to UDP-4'-Ketopentose by ArnA. ArnB converts UDP-4'-Ketopentose to UDP-β-L-Ara(4)N after which ArnA further modifies UDP-β-L-Ara(4)N to UDP-β-L-Ara4FormylN. UDP is switched out for an undecaprenyl phosphate carrier to form undecaprenyl phosphate-L-Ara4FN, catalysed by ArnC, before undergoing deformylation by ArnD. ArnE/F flippases transport undecaprenyl phosphate-L-Ara(4)N across the bacterial inner membrane, into the periplasm, where it is attached to Lipid A by ArnT forming (Lipid A)-1', 4'-L-Ara(4)N. Figure taken from Yan et al, 2007, using information from Williams et al., 2005.

3.1.3. Preliminary results that primed my work

3.1.3.1. *S. marcescens* becomes resistant to predation by *B. bacteriovorus* in human serum after an initial period of successful predation.

Predation of various multidrug resistant clinical isolates and pathogens by *B. bacteriovorus* has been tested within our lab in a Ca/HEPES buffer medium.

Our lab (Dr Dhaarini Raghunathan & Dr Dave Negus) then sought (383) to determine how predation may proceed within pooled male AB human serum, a medium with multiple host microbicidal mechanisms, and whose findings may be more applicable to the host than predation in buffer. How *Bdellovibrio* and *S. marcescens* change when they are grown in human serum is unknown, therefore this study also aimed to qualify this. To achieve this, *S. marcescens* #42 was incubated in human serum with *B. bacteriovorus* at an MOI of 1:10 (*Serratia*: *Bdellovibrio*), and the viability of both predator and prey measured over a 72-hour period. *S. marcescens* was shown to initially be preyed upon by *B. bacteriovorus*, represented by the initial drop in recoverable CFU at 1 hour, but subsequently became resistant to predation by *B. bacteriovorus*, at approximately 8 hours, after which *S. marcescens* appeared to be resistant to predation and grew unaffected within human serum. No effect on predator numbers was observed, suggesting that this resistance to predation was not due to predator death, and that *S. marcescens* was adapting during predation to become less susceptible (Figure 3.1.3). Addition of further *Bdellovibrio* at 8 hours did not result in any further predation (indicated by a drop in *S. marcescens* CFU count) (data not shown), which also suggests that resistance to predation is due to a host-mediated effect on *S. marcescens*, that impacts predation susceptibility, rather than resistance to predation being due to an absence of viable and/or functional predators.

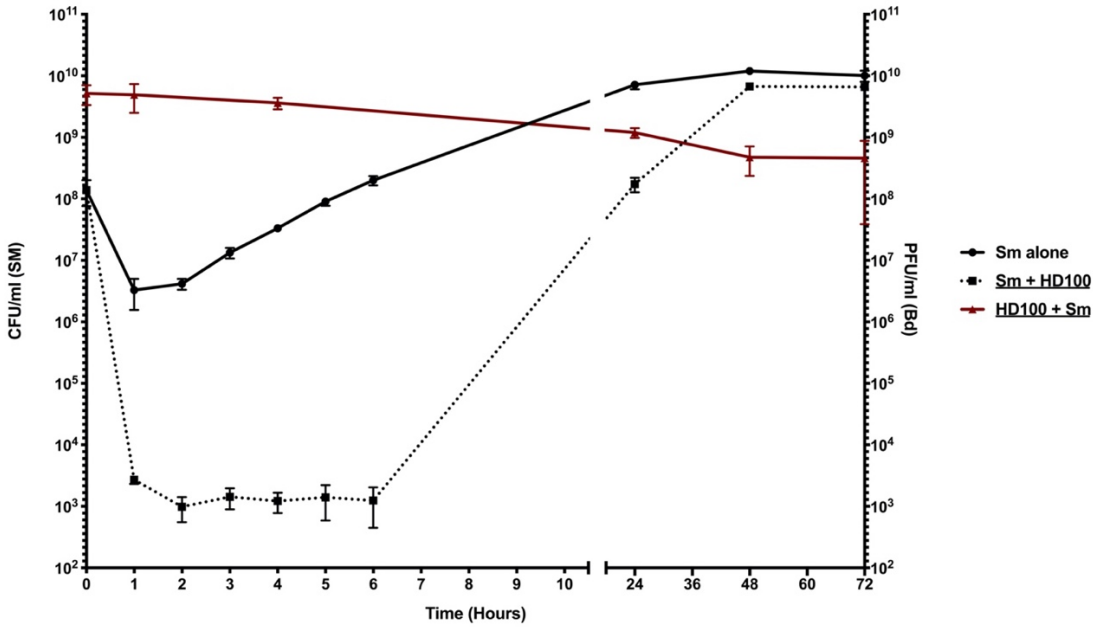

Figure 3.1.3: *S. marcescens* becomes resistant to predation by *B. bacteriovorus* in human serum, after an initial period of successful predation (Sockett Lab, unpublished). WT *S. marcescens* is initially preyed upon by *B. bacteriovorus* in human serum, resulting in a drop in recoverable CFU. After a period of approximately 8 hours, *S. marcescens* becomes resistant to predation by *B. bacteriovorus*, resulting in growth of *S. marcescens* in human serum. Sm alone refers to the viability (CFU) of *S. marcescens* incubated in human serum. Sm + HD100 refers to the viability (CFU) of *S. marcescens* incubated (in human serum) with WT *B. bacteriovorus* HD100 at an MOI of 1:10 (*Serratia: Bdellovibrio*). HD100 + Sm refers to the viability (PFU) of *B. bacteriovorus* HD100, incubated (in human serum) with *S. marcescens*. Data was analysed with a two-way ANOVA multiple comparisons test. Data points represent the mean of each of three biological replicates. N=3, where n represents the number of independent biological replicates obtained for this experiment. Error bars represent the standard error of the mean of the data set.

3.1.3.2. Cell surface factors are responsible for resistance of *S. marcescens* to predation by *B. bacteriovorus* in human serum.

To determine the mechanism through which *S. marcescens* becomes resistant to predation by *B. bacteriovorus* in human serum, RNASeq analysis of *S. marcescens* differential gene expression during the period of resistance to predation (at 12 hours) was performed, comparing *S. marcescens* gene expression at 12 hours of predation by *B. bacteriovorus* in human serum, with *S. marcescens* in human serum alone.

Dr Dhaarini Raghunathan interrogated the genes that are differentially expressed by *S. marcescens* #42 in a period of resistance to predation by *B. bacteriovorus*, in human serum and identified 5 main gene targets that were to be investigated further, which form the basis of this study (Table 3.3.1). Of the larger list of differentially upregulated and downregulated genes, these genes were picked as they were highly upregulated by *S. marcescens* during resistance to predation, and, as predation initially focuses on the bacterial cell surface, each of these genes were potentially related to a change in bacterial surface composition.

ArnA catalyses the conversion of UDP-Glucuronic acid to UDP-4'-Ketopentose and later UDP-β-L-Ara(4)N to UDP-β-L-Ara4FormylN in the L-Ara(4)N Lipid A modification pathway and is also the most highly upregulated gene in the arn operon. ArnT transfers the L-Ara(4)N sugar onto Lipid A as the final step in the arn-modification pathway. Individual deletion of the genes encoding these two proteins gives Δ*arnA* and Δ*arnT* mutants respectively. Wza is a capsular polysaccharide exporter which is essential for capsule production. Deletion of *wza* gives an acapsular mutant (Δ*wza*). Fimbriae are composed of a chaperone protein (FimC), an usher protein (FimD) and pilin proteins (major pilin: FimA; Minor pilins: FimF, FimG and FimH)(Figure 3.2.6). Deletion of the major fimbrial subunit (*fimA; fim3795* or *fim4264* in each of the two fimbrial operons), chaperone protein (*fimC; fim3796* or *fim4265*) and usher protein (*fimD; fim3797* or *fim4266*) disrupts fimbrial synthesis and produces bacterial mutants where fimbriae are absent from the bacterial surface (Δ*fim3795-7* or Δ*fim4264-6*).

Table 3.1.1: *S. marcescens* genes associated with resistance to predation by *B. bacteriovorus* in human serum. Relative expression of 5 genes/gene clusters of interest in this study that are upregulated by *S. marcescens*, according to RNASeq analysis at the 12-hour timepoint, in a period of resistance during predation by *B. bacteriovorus* in human serum. Fold change represents the (positive) fold change in expression of the gene in human serum with *B. bacteriovorus* compared to human serum alone (*B. bacteriovorus* absent). Log_2FC represents the Log_2 function of the fold change. Corrected P value indicates the probability value of each gene being differentially regulated by chance, adjusted for multiple comparisons using a Benjamini-Hochberg correction.

Gene		Function	Fold Change	Log_2FC	Corrected P Value
arnA		Lipid A modification; Initial L-Ara(4)N synthesis	10.20	3.35	2.5×10^{-8}
arnT		Lipid A modification; Addition of L-Ara(4)N to Lipid A	6.56	2.71	6.2×10^{-6}
wza		Capsular polysaccharide exporter	3.93	1.98	1.3×10^{-1}
Fimbrial Cluster 1	***fim3795***	Major fimbrial subunit (*fimA*)	12.30	3.62	4.6×10^{-3}
	fim3796	Chaperone protein (*fimC*)	8.68	3.12	4.0×10^{-2}
	fim3797	Usher protein (*fimD*)	7.98	3.00	5.6×10^{-3}
Fimbrial Cluster 2	***fim4264***	Major fimbrial subunit (*fimA*)	105.41	6.72	3.2×10^{-5}
	fim4265	Chaperone protein (*fimC*)	37.06	5.21	3.4×10^{-4}
	fim4266	Usher protein (*fimD*)	11.29	3.50	1.5×10^{-3}

3.1.4. Research aims.

Although resistance to *B. bacteriovorus* has not yet been observed in pathogenic prey, the effect of cell surface changes (in response to the hostile serum environment) on predation has not been characterised and may alter predation susceptibility. Additionally, the specific components that *B. bacteriovorus* targets to initiate attachment to Gram-negative prey also remain unknown and needs further investigation.

To investigate the roles of the aforementioned genes further, Dr Raghunathan began the construction of suicide plasmid vectors containing knockout constructs for these genes. In this study, I continued her work by sequencing and validating the knockout construct plasmids and conjugating them into *S. marcescens*. I removed *arnA*, *arnT* and *wza* individually via markerless gene deletion, giving mutants disrupted in Lipid A modification (Δ*arnA* & Δ*arnT*) or capsule expression (Δ*wza*). I also removed, as a trio, the *fimA* (major pilin subunit)*, fimC* (chaperone) and *fimD* (usher) genes for each of the two fimbrial gene clusters in *S. marcescens*, giving mutants defective in fimbriae synthesis (Δ*fim3795-7* and Δ*fim4264-6*). I then tested the susceptibility of *S. marcescens* to predation by *B. bacteriovorus*, hypothesising that removal of these genes would restore susceptibility to predation and disrupt the development of resistance.

These 5 genes/subsets encode some potentially important roles, but they are a small number of genes within the large transcriptional response of *S. marcescens* to host serum and predation by *B. bacteriovorus*. Therefore, even though we have chosen to investigate the most important candidates, it is important to consider that we are only looking at a small snapshot of a much larger transcriptional response.

The further understanding of the roles of these genes in susceptibility to predation, and the impact of cell surface adaptation due to host immune factors on the dynamics of predation will aid our understanding of how predation may unfold within the host, aiding the potential application of *B. bacteriovorus* as a novel antimicrobial therapy.

3.2. Results

In this chapter, I aimed to characterise the effects of cell surface adaptation, due to host immune factors, on the dynamics and efficiency of predation by *B. bacteriovorus*. I removed genes that encode major surface components from *S. marcescens*, each of which were significantly upregulated by *S. marcescens* in transcriptional studies during a period of resistance to predation by *B. bacteriovorus* within human serum. This phase of resistance to predation was more extensive in human serum, compared to Ca/HEPES buffer, suggesting that host environment-induced alterations to the bacterial surface were responsible for this resistance phenotype.

First, I tested the viability of my gene deletion mutants, each of which has a significantly altered bacterial surface, in human serum. This was necessary as large surface changes may alter the viability of *S. marcescens*, and as these surface components are closely associated with serum resistance and survival, mutants in these surface components may not be viable in human serum. Next, I tested the efficacy of predation of *S. marcescens* surface mutants by *B. bacteriovorus*, in human serum.

3.2.1. *S. marcescens* gene knockout mutants remain viable in human serum.

During predation of *S. marcescens* WT by *B. bacteriovorus* in human serum, genes encoding lipid A modification (*arnA* and *arnT*), fimbriae biosynthesis (*fim3795, fim3796, fim3797, fim4264, fim4265* and *fim4266*) and capsule biosynthesis (*wza*) are upregulated in a phase of resistance to predation. The removal of these genes confers large surface changes to *S. marcescens*, some of which I and Dr Raghunathan postulated may be essential for viability in human serum. To determine whether *S. marcescens* gene knockout mutants remain viable in human serum, *S. marcescens* WT and gene mutants were inoculated into human serum and their viability measured over a 48-hour period. Despite an initial 20x drop in viable CFU within the first 90 minutes of serum incubation, *S. marcescens* gene knockout mutants remain viable in human serum (Figure 3.2.1), allowing the testing of susceptibility to *B. bacteriovorus* predation in mutant strains to go ahead.

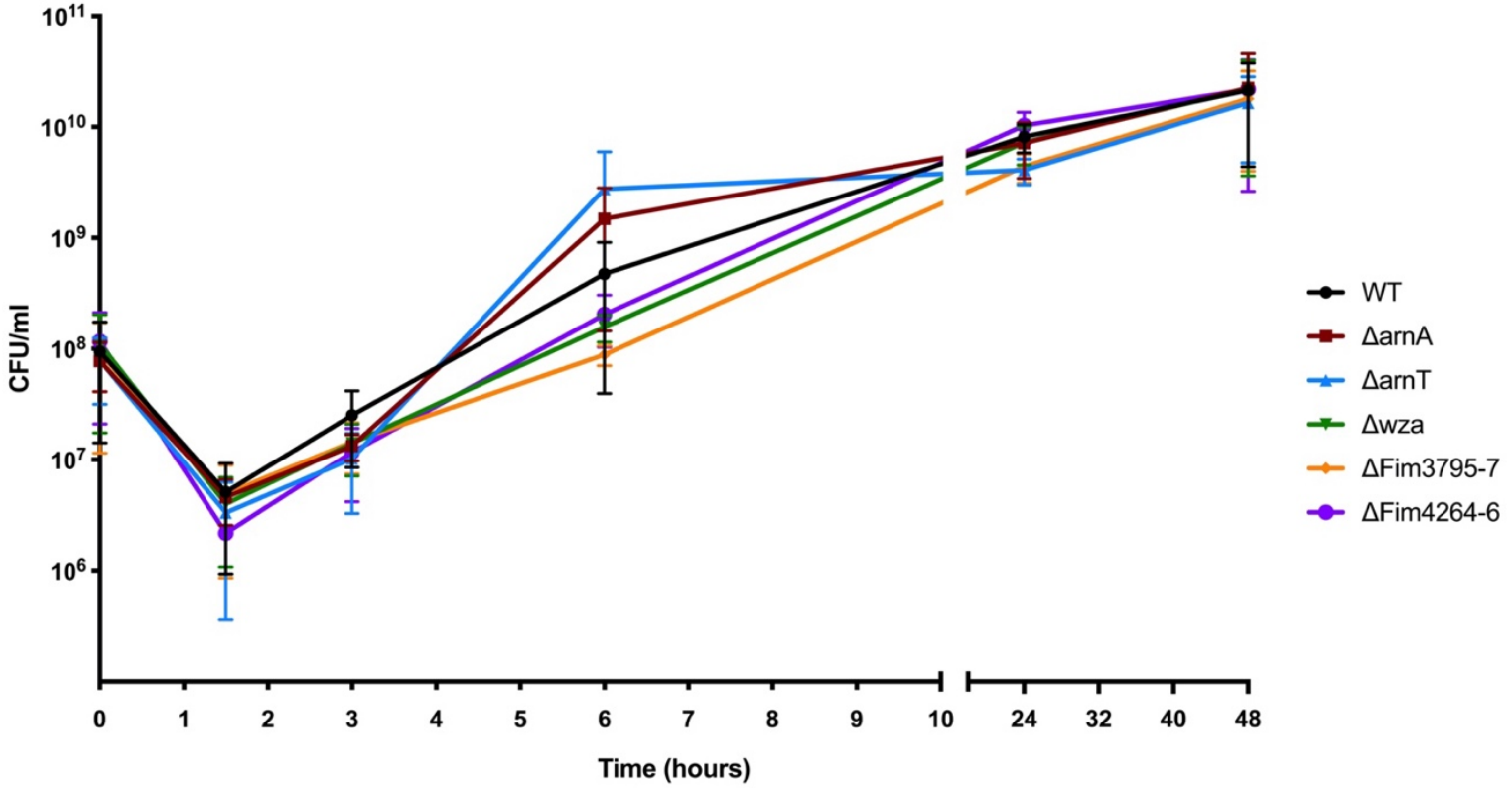

Figure 3.2.1: *S. marcescens* gene knockout mutants remain viable in human serum. Single gene knockout mutants of *S. marcescens* are viable in human serum over a period of 48 hours. *S. marcescens* mutants with single gene knockouts in *arnA*, *arnT* and *wza* or triple gene knockouts in *fim3795-7* and *fim4264-6* were incubated in human serum over a period of 48 hours and their viability monitored. After an initial drop in viability after approximately 1.5 hours, *S. marcescens* mutants recovered and grew in human serum, remaining viable for beyond 48 hours. Data was analysed with a two-way ANOVA multiple comparisons test. No significant differences were found (WT vs mutant) throughout the data set ($P>0.05$). Data points represent the mean of each of three technical replicates. N=2 where n represents the number of independent biological replicates obtained for this experiment. Error bars represent the standard error of the mean of the data set.

3.2.2. Removal of ArnA-mediated Lipid A modification, but not ArnT-mediated modification, from *S. marcescens* delays resistance to predation in human serum

To determine whether Lipid A modification alters the susceptibility of *S. marcescens* to predation by *B. bacteriovorus* in human serum, single gene knockout mutants in *arnA* and *arnT*, genes encoding the most highly upregulated and the most important genes in the arn lipid A modification operon respectively, were constructed (Figure 3.1.1; Figure 3.2.2). Susceptibility to predation by *B. bacteriovorus* in human serum was then tested. Removal of *arnA* from *S. marcescens* did not prevent resistance to predation but did delay it by approximately 2-3 hours (Figure 3.2.3). Removal of *arnT* did not alter susceptibility to predation by *B. bacteriovorus* in human serum (Figure 3.2.3).

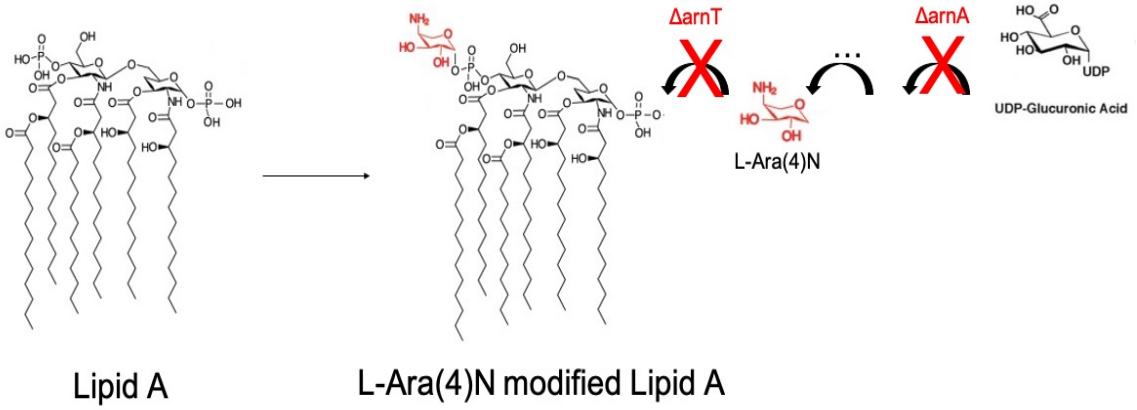

Figure 3.2.2: Lipid A phosphate groups are modified with a L-Ara(4)N sugar by enzymes of the arn operon. The 1' and 4' phosphate groups of Lipid A molecules are modified through the addition of an L-Ara(4)N sugar, reducing the negative charge of the Lipid A moiety and conferring polymyxin and antimicrobial peptide resistance. arnA catalyses the conversion of UDP-Glucuronic acid to UDP-4'-Ketopentose and later UDP-β-L-Ara(4)N to UDP-β-L-Ara(4)FormylN. arnT transfers the L-Ara(4)N sugar onto Lipid A as the final step in the arn-modification pathway. Figure modified from Yan et al., 2007.

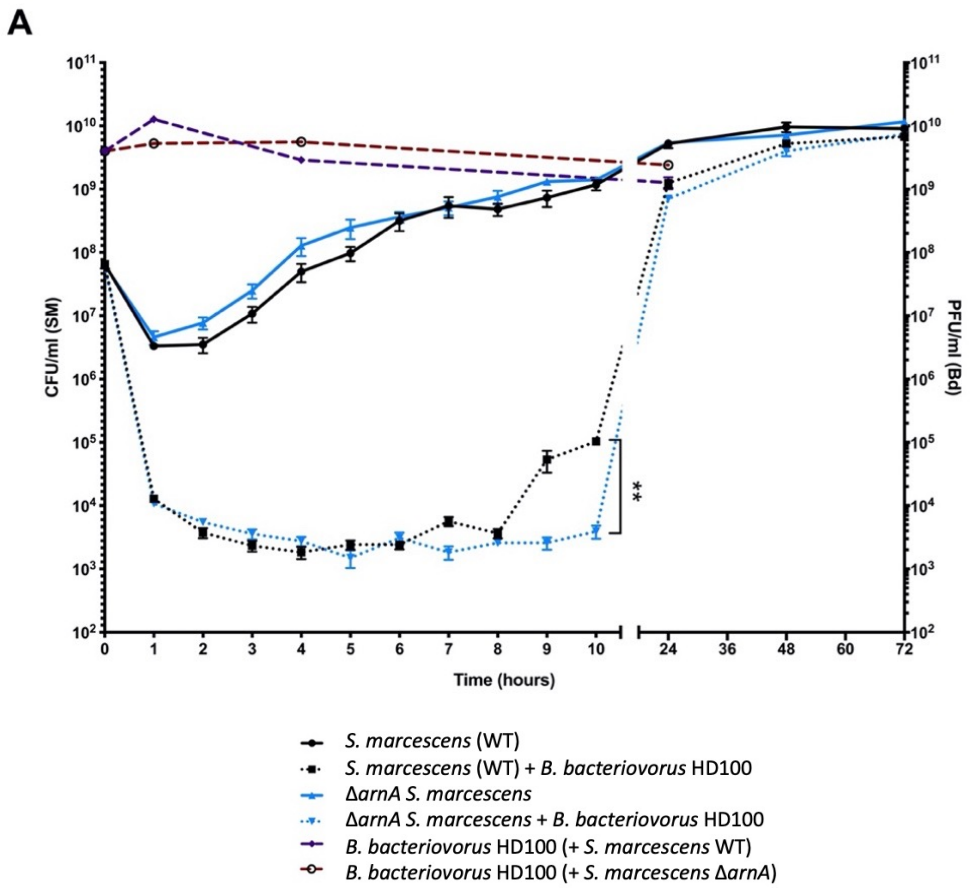
A
CFU/ml (SM)
PFU/ml (Bd)
Time (hours)
**
S. marcescens (WT)
S. marcescens (WT) + B. bacteriovorus HD100
ΔarnA S. marcescens
ΔarnA S. marcescens + B. bacteriovorus HD100
B. bacteriovorus HD100 (+ S. marcescens WT)
B. bacteriovorus HD100 (+ S. marcescens ΔarnA)

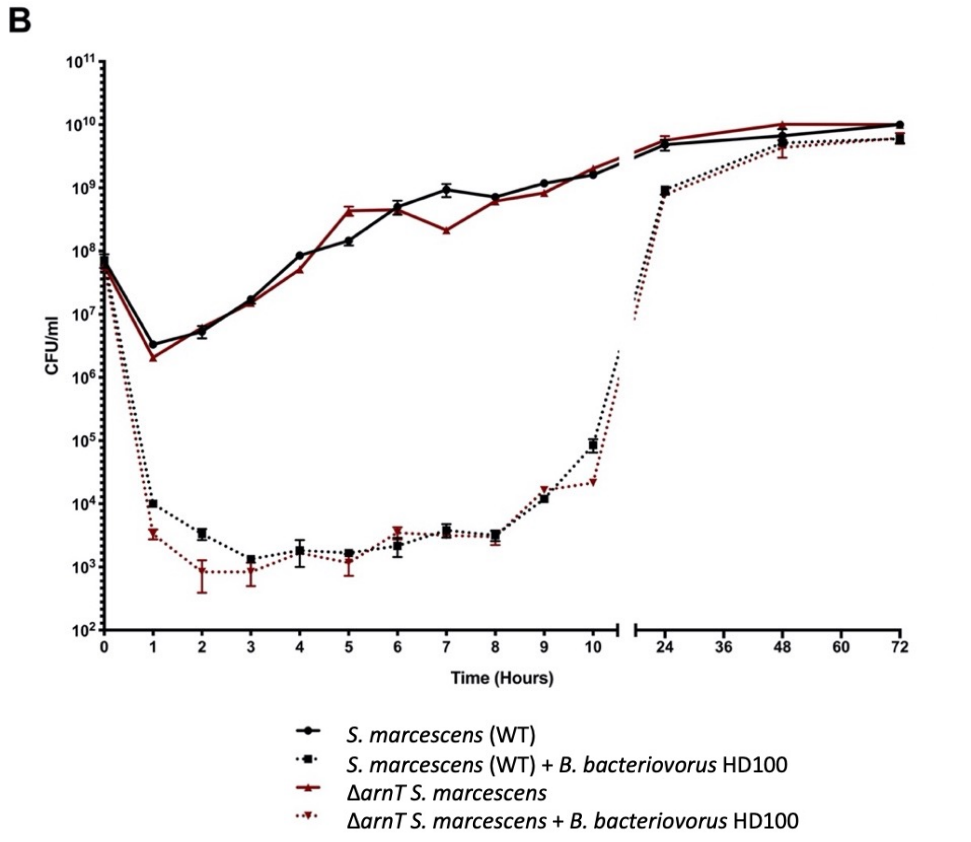
B
CFU/ml
Time (Hours)
S. marcescens (WT)
S. marcescens (WT) + B. bacteriovorus HD100
ΔarnT S. marcescens
ΔarnT S. marcescens + B. bacteriovorus HD100

Figure 3.2.3: Lipid A modification alters the susceptibility of *S. marcescens* to predation by *B. bacteriovorus* in human serum but does not prevent resistance. Removal of the Lipid A modification gene *arnA* from *S. marcescens* delays resistance to predation (A), whereas removal of *arnT*, another Lipid A modification gene, does not alter susceptibility to predation (B). Single gene knockout *S. marcescens* mutants of Lipid A modification genes *arnA* and *arnT* were incubated with *B. bacteriovorus* at an MOI of 1:10 in human serum over a period of 72 hours to determine whether removal of the aforementioned genes affects susceptibility to predation. Viability of all three *S. marcescens* strains (WT and two mutants) drops initially with predation. After 8 hours, WT and Δ*arnT S. marcescens* become resistant to predation and CFU levels recover (B). Δ*arnA S. marcescens* exhibits a delay in predation resistance formation, suggesting removal of ArnA has altered the susceptibility of *S. marcescens* to continued predation (A). Data was analysed with a two-way ANOVA multiple comparisons test. N.S. indicates non significance ($P>0.05$). ** indicates significance ($P<0.01$) (A). Statistical analysis was not carried out on this data set owing to a lack of biological replicates (B). Data points represent the mean of each of six technical replicates (A) or 3 technical replicates (B). N=2 (A), N=1 (B), where n represents the number of independent biological replicates obtained for this experiment. Error bars represent the standard error of the mean of the data set.

3.2.3. Removal of the capsule from *S. marcescens* does not alter susceptibility to predation by *B. bacteriovorus.*

Capsule production is a major component of the surface of *S. marcescens*, whose production is upregulated during the period of predation resistance during *S. marcescens* predation, likely altering how *S. marcescens* is perceived by *B. bacteriovorus* during attachment and predation. To determine whether capsule biogenesis alters the susceptibility of *S. marcescens* to predation by *B. bacteriovorus*, a single gene knockout of *wza*, the capsule exporter protein (Figure 3.1.2), was generated. Susceptibility to predation by *B. bacteriovorus* in human serum was then tested. Removal of capsule export did not prevent resistance or alter susceptibility to predation by *B. bacteriovorus* (Figure 3.2.4).

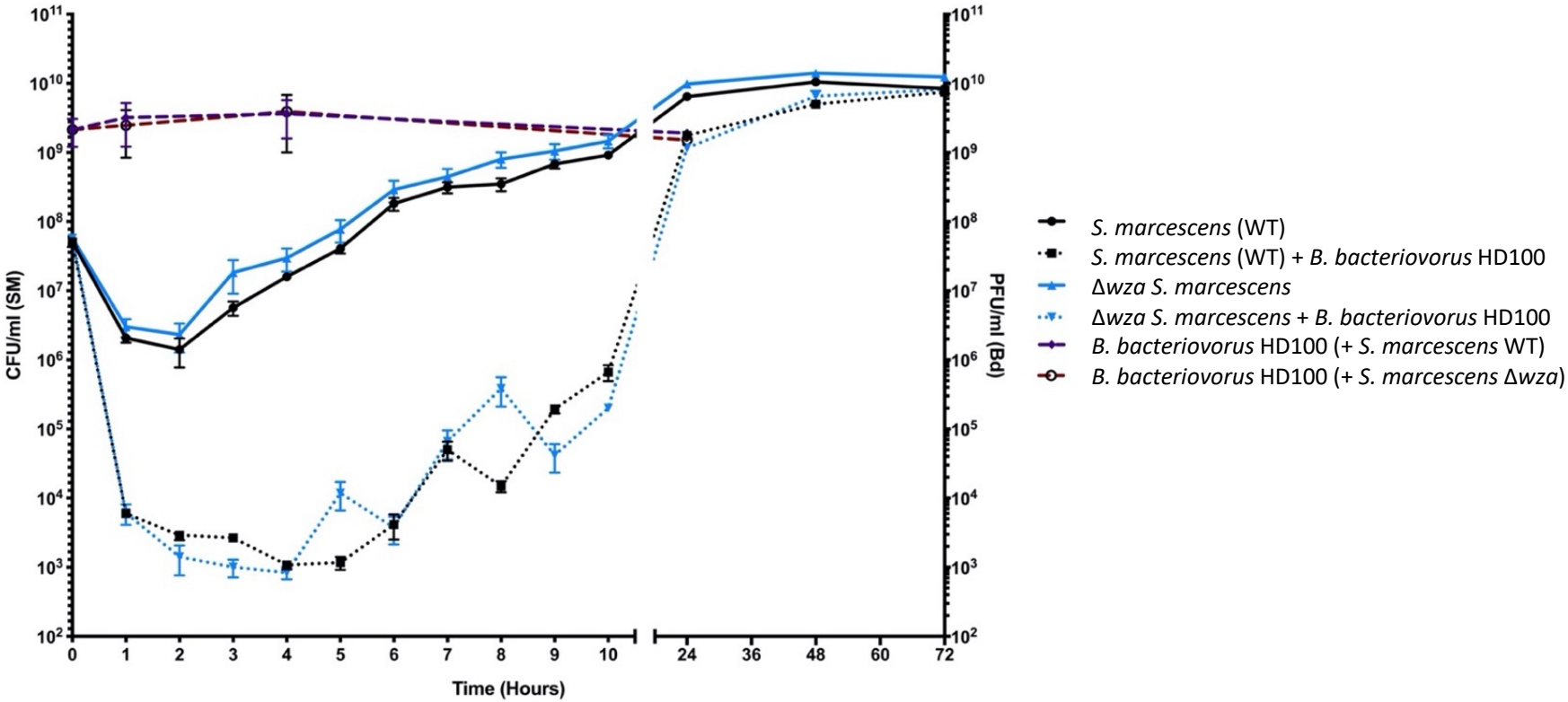

Figure 3.2.4: Deletion of capsule production does not alter the susceptibility of *S. marcescens* to predation by *B. bacteriovorus* in human serum. Removal of the capsule exporter gene *wza* from *S. marcescens* does not affect susceptibility to predation. A single gene knockout mutant of the capsule exporter protein Wza was incubated with *B. bacteriovorus* at an MOI of 1:10 in human serum over a period of 72 hours to determine whether removal of Wza affected susceptibility to predation. Viability of both *S. marcescens* strains (WT and Δ*wza* mutant) drops initially with predation. After 8 hours, WT and Δ*wza S. marcescens* become resistant to predation and CFU levels recover. Data was analysed with a two-way ANOVA multiple comparisons test. Statistical significance ($P<0.05$) was seen at 3 hours and 9 hours between WTBd and WzaBd, however this was deemed to not be biologically relevant due to the variation within the data throughout the assay. Data points represent the mean of each of six technical replicates. N=2, where n represents the number of independent biological replicates obtained for this experiment. Error bars represent the standard error of the mean of the data set.

3.2.4. Removal of fimbriae from *S. marcescens* does not alter susceptibility to predation by *B. bacteriovorus*.

Fimbriae biogenesis plays a multitude of roles in *S. marcescens*, including how the surface of the bacterium is perceived by elements of the host immune response, and by *B. bacteriovorus*. Fimbriae synthesis genes (*fim3795, fim3796, fim3797, fim4264, fim4265* and *fim4266*) were majorly upregulated during the resistance period of *S. marcescens* suggesting their potential importance in resistance to predation. To determine whether fimbriae synthesis and expression alters the susceptibility of *S. marcescens* to predation by *B. bacteriovorus* in human serum, genes encoding the chaperone (FimC; Fim3796; Fim4265), usher (FimD; Fim3797; Fim4266), and major subunit (FimA; Fim3795; Fim4264) proteins from both fimbrial clusters of *S. marcescens* were removed (Δ*fim3795-7* or Δ*fim4264-6*) (Figures 3.2.5 and 3.2.6) and susceptibility to predation by *B. bacteriovorus* tested. Removal of fimbriae from the surface of *S. marcescens* does not alter susceptibility to predation and resistance (Figure 3.2.7).

Sm_3802; prsF; Pilus assembly protein; Pilus-like adhesion protein; 498bp
Sm_3801; mrfF; Minor fimbrial protein mrrF; 936bp
Sm_3800; Hypothetical protein; 333bp
Sm_3799; smfA; Fimbrial A protein; 522bp
Sm_3798; mrpA_2; Pilin; 537bp
Sm_3797; bioD1/papC; Fimbrial assembly protein; 2535bp
Sm_3796; papD; Molecular chaperone; 765bp
Sm_3795; fimA; Fimbrial protein; 639bp
Sm_3794; mrpA_1; exotoxin; 555bp

Sm_4263; yhjH; diguanylate phosphodiesterase; 717bp
Sm_4264; fimA; ferrous iron transporter B; 558bp
Sm_4265; papD/fimC/ecpD; Pilus assembly protein; 729bp
Sm_4266; fimD; fimbrial outer membrane usher protein; 2562bp
Sm_4267; fimA; Major Type I fimbrial protein; 1038bp

Figure 3.2.5: Schematics representing the genes surrounding the *fim3795-fim3796-fim3797* (Top) and *fim4264-fim4265-fim4266* (Bottom) gene clusters. Gene colours match proteins on Figure 3.2.6.

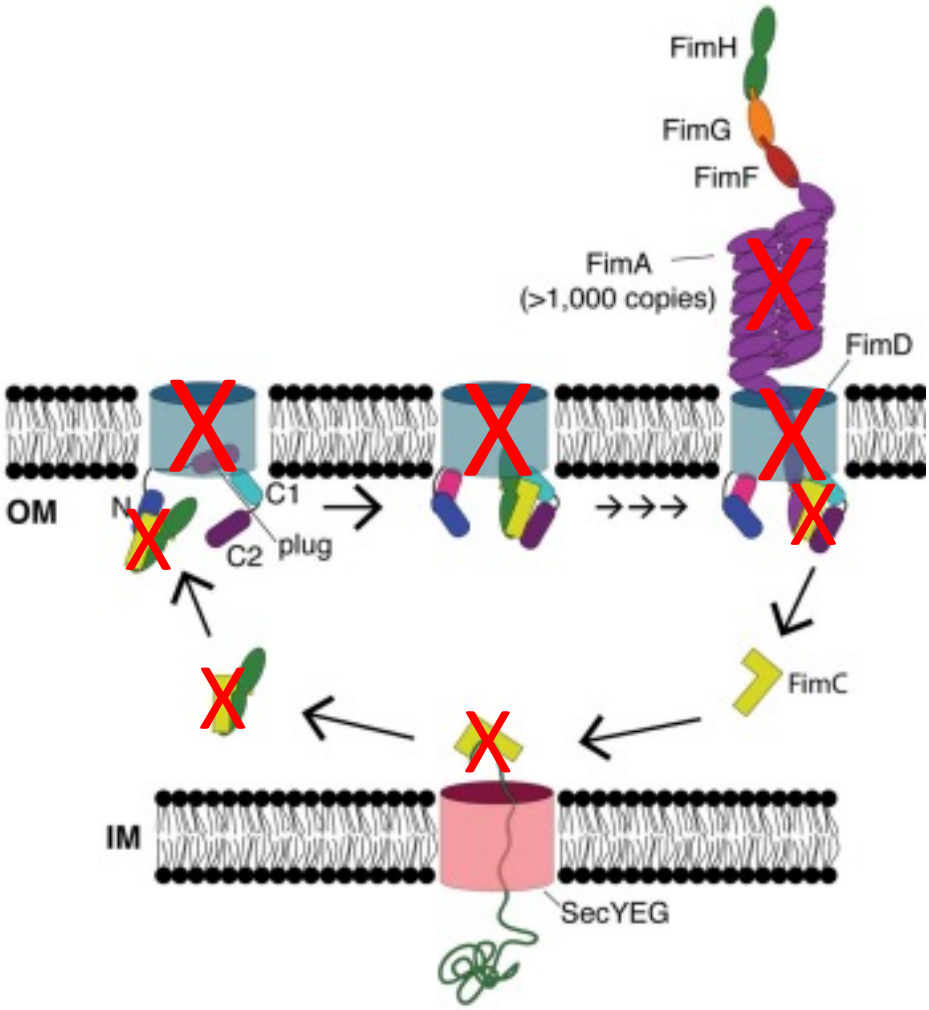

Figure 3.2.6: A schematic showing Type I Pilus/Fimbriae biogenesis. Figure adapted from Werneburg & Thanassi, 2018. FimA Pilin subunits are translocated across the inner membrane, into the periplasm, via the SecYEG translocon. Pilin subunits bind with FimC chaperone, and fold into their active state. FimA-FimC complexes interact with the FimD usher protein (situated in the outer membrane), enabling FimA secretion across the outer membrane, FimA integration into the pilus fibre and release of the FimC chaperone. In my Δ*fim3795-7* and Δ*fim4264-6* mutants, FimA, FimC and FimD are absent, as indicated by the red crosses on this diagram.

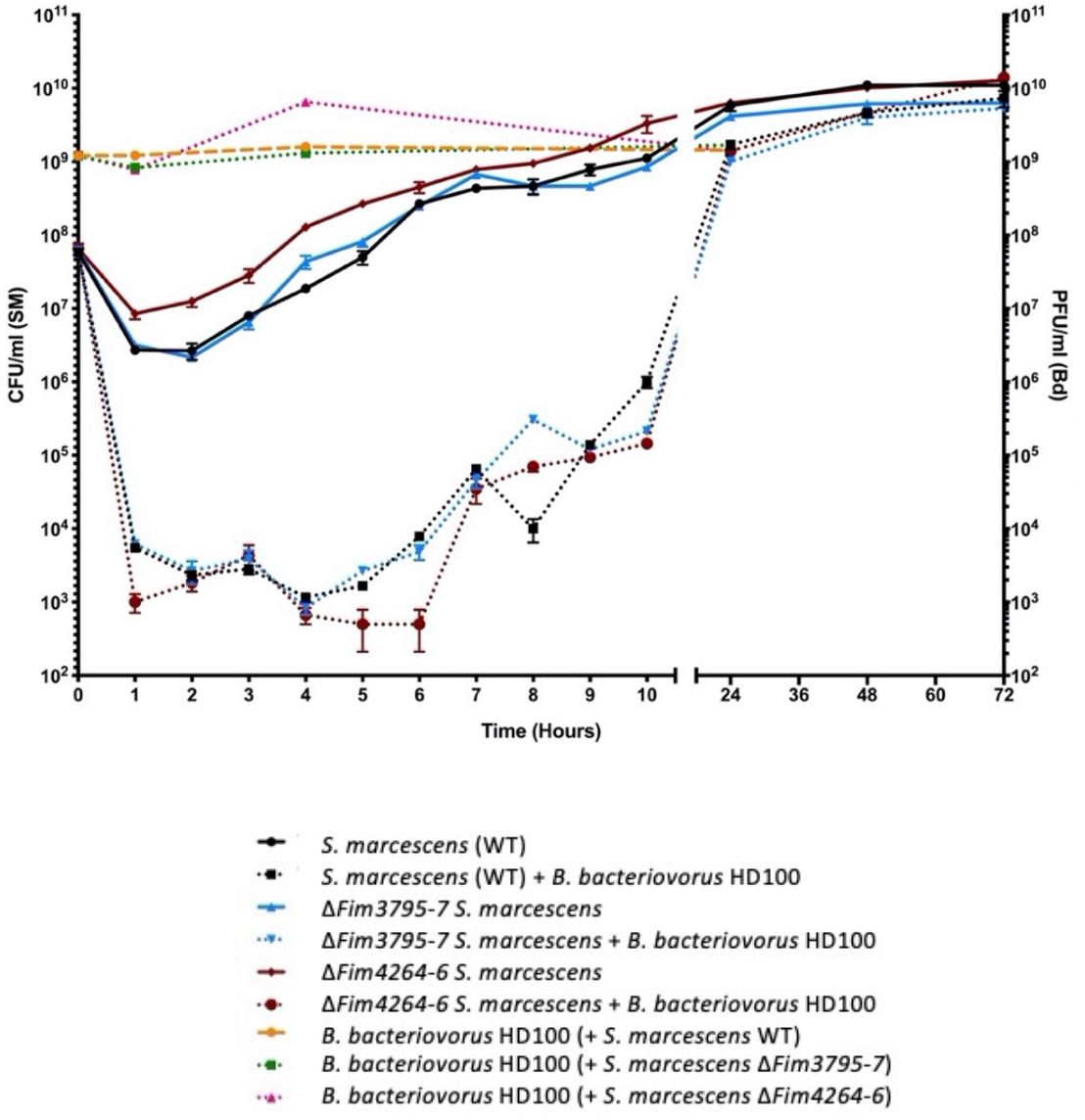

Figure 3.2.7: Removal of fimbriae from *S. marcescens* does not alter susceptibility to predation by *B. bacteriovorus* in human serum. Removal of genes encoding fimbriae biosynthesis the chaperone protein, usher protein and major subunit protein within each of two fimbrial clusters from *S. marcescens* does not affect susceptibility to predation. A triple gene knockout mutant of the fimbrial biosynthesis genes (Δ*fim3795-7* or Δ*fim4264-6*) was incubated with *B. bacteriovorus* at a MOI of 1:10 in human serum over a period of 72 hours to determine whether removal of fimbriae affected susceptibility to predation. Viability of all three *S. marcescens* strains (WT and the two mutants) drops initially with predation. After 4 hours, WT, Δ*fim3795-7* and Δ*fim4264-6 S. marcescens* become resistant to predation and CFU levels recover. Statistical analysis was not carried out on this data set owing to a lack of biological replicates. Data points represent the mean of each of three technical replicates. N=1, where n represents the number of independent biological replicates obtained for this experiment. Error bars represent the standard error of the mean of the data set.

3.2.5. Different serum compositions alter Δ*arnA S. marcescens* survival and susceptibility to predation by *B. bacteriovorus* in human serum.

In a clinical setting, individual patients, and the immune response they mount to infection will differ. Despite using pooled human sera from multiple individuals, I decided that it was important to test how widespread the effect I had found was within the wider population by changing the batch number and thus the source of the human serum, incorporating potential differences in serum diversity and complexity into this study.

To widen the applicability of our findings with regards to Δ*arnA S. marcescens* being delayed in resistance development when being preyed upon by *B. bacteriovorus* in human serum, I used serum from a different batch, although still pooled human sera from AB Human males, as the medium for another predation assay with the same experimental set up. Despite both *S. marcescens* WT and Δ*arnA S. marcescens* being initially preyed upon by *B. bacteriovorus* (as before), both *S. marcescens* strains entered the phase of resistance to predation earlier (4 hours c.f. 8 hours previously). Δ*arnA S. marcescens* also grew back at a faster rate than WT *S. marcescens* in this serum (Figure 3.2.8), in direct contradiction to our previous findings (Figure 3.2.3).

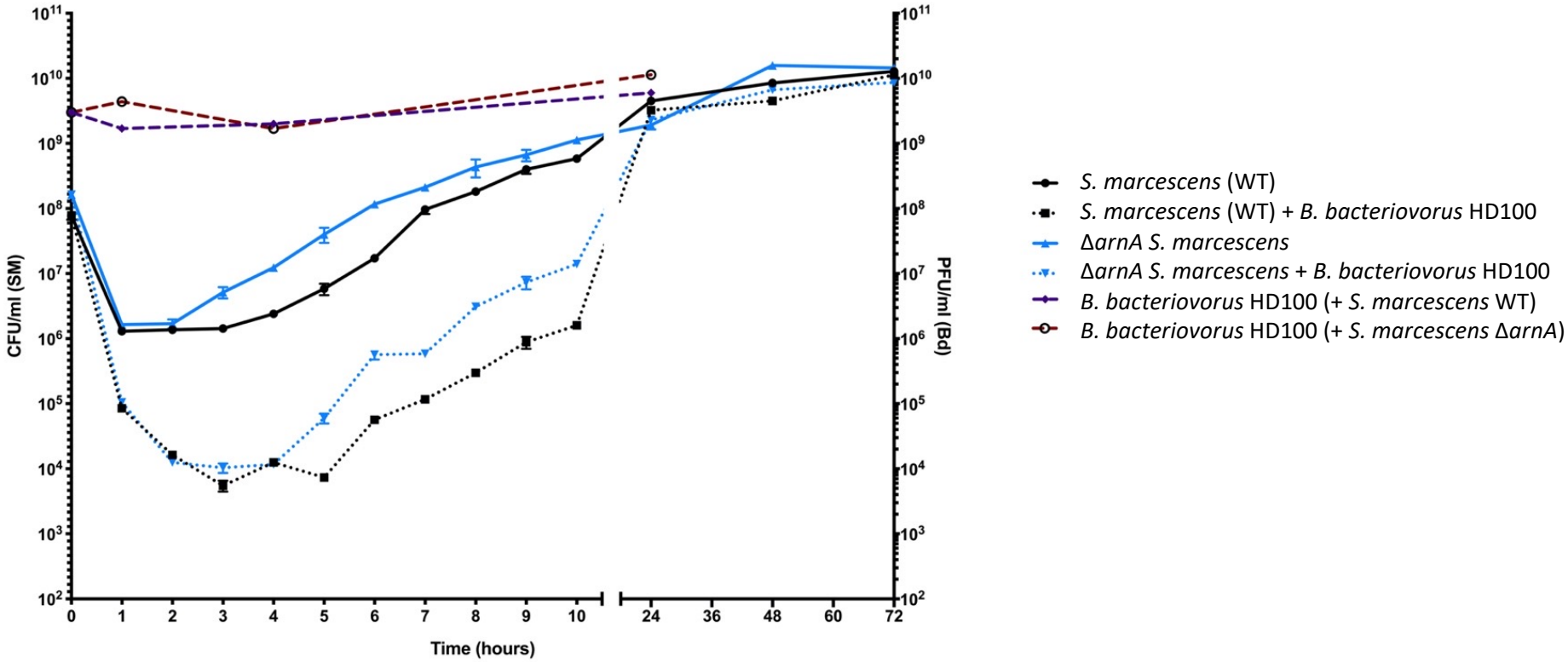

Figure 3.2.8: Serum composition changes alter Δ*arnA S. marcescens* survival and susceptibility to predation by *B. bacteriovorus* in human serum. Predation of Δ*arnA S. marcescens* by *B. bacteriovorus* in human serum of a different batch (with unknown variation in composition) was less successful, with both WT and Δ*arnA S. marcescens* being preyed upon initially, but entering the phase of resistance to predation faster (c.f. previous serum). Δ*arnA S. marcescens* also grew at a faster rate in the presence of *B. bacteriovorus* in human serum compared to WT *S. marcescens* in direct contradiction to our previous findings (Figure 3.2.2). Statistical analysis was not carried out on this data set owing to a lack of biological replicates. Data points represent the mean of each of three technical replicates. N=1, where n represents the number of independent biological replicates obtained for this experiment. Error bars represent the standard error of the mean of the data set.

3.3. Discussion

The intricacies of how predation may occur within the diverse immunological environments of different human hosts are not fully understood, preventing the development of a safe application of *B. bacteriovorus* as an antimicrobial therapy. Characterisation of the bacterial cell surface, which is known to act as the main trigger of the host immune response and is key to the initiation of the predation process (although the specific target remains unknown), and how the surface and thus detection is altered within a host environment will provide further understanding of the predation process in a host setting and will facilitate the development of *B. bacteriovorus* as a novel antimicrobial therapy.

Some studies (376) suggest that predation by *B. bacteriovorus* in human serum is not possible, due to serum albumin coating the predator and preventing predation. I, however, demonstrate that in this study, predation was possible. This is likely due to several factors, including serum composition and the number of *Bdellovibrio* used. This contrast in findings warrants further investigation.

In this study, I focused on 4 cell surface components, the genes encoding which were differentially expressed by *S. marcescens* during a period of resistance to predation by *B. bacteriovorus*, within human serum (Figure 3.2.1 & Table 3.2.1). This differential gene expression and resistance to predation occurred to a much lesser extent during predation in Ca/HEPES buffer (data not shown) suggesting that this differential gene expression is a host-mediated as well as a predation-mediated response. Removal of single genes (Δ*arnA*, Δ*arnT* & Δ*wza*), or gene clusters (Δ*fim3795-7* & Δ*fim4264-6*) via markerless gene deletion through homologous recombination was followed by testing of predation susceptibility to establish whether expression, and thus removal, of these genes altered susceptibility to predation and was responsible for the observed resistance to predation.

A summation of the results presented in Chapter 3 is shown below.

Table 3.3.1: A summary of the findings presented in Chapter 3. CFU refers to colony forming units, which were used as a proxy for *S. marcescens* viability. WT refers to wildtype.

***S. marcescens* mutant**	**Genotype**	**Proposed phenotypic effect**	**Growth in serum**	**Predation in serum**
Wildtype	N/A / WT	N/A	Approximate 12-fold drop in viability initially (1.5 hours), followed by regrowth (2-48 hours)	Approximate 10^4 drop in viable CFU at 1 hour, with CFU remaining constant until 8 hours, upon which *S. marcescens* grew and was considered resistant to predation, reaching levels similar to non-preyed upon cultures at 24 hours
Arn-mediated Lipid A mutant	Δ*arnA*	Deletion of a L-Ara(4)N synthesis protein	Initial drop in viability comparable to WT, followed by stronger regrowth than WT at 6 hours (represented by higher viable CFU), then comparable growth to WT at 24 and 48 hours	Initial drop in CFU comparable to WT, due to predation, at 1 hour. Growth of *S. marcescens* did not recommence until 10 hours (significantly later than WT), reaching levels similar to non-preyed upon cultures and WT cultures at 24 hours
	Δ*arnT*	Deletion of the export protein that incorporates L-Ara(4)N into the 1' and 4' positions on Lipid A		Initial drop in CFU, due to predation, lower than WT at 1-3 hours, followed by growth mirroring that of WT from 3 hours onwards
Capsule biosynthesis mutant	Δ*wza*	Deletion of the capsular export protein Wza, giving an acapsular mutant	Initial drop in viability comparable to WT, followed by slower regrowth than WT at 6 hours (represented by lower viable CFU), then comparable growth to WT at 24 and 48 hours	Initial drop in CFU, due to predation, comparable to WT at 1 hour, followed by growth mirroring that of WT from 1 hours onwards
Fimbriae deletion mutant	Δ*fim3795* Δ*fim3796* Δ*fim3797*	Deletion of the first (of two) fimbriae clusters		Initial drop in CFU, due to predation, comparable to WT at 1 hour, followed by growth mirroring that of WT from 1 hours onwards
	Δ*fim4264* Δ*fim4265* Δ*fim4266*	Deletion of the second (of two) fimbriae clusters		

As seen in Figure 3.1.3, *S. marcescens* is initially preyed upon by *B. bacteriovorus*, before becoming resistant to predation at approximately 8 hours onwards. RNASeq studies at 12 hours show that a subset of surface modification genes are upregulated, corresponding with the time where *S. marcescens* is growing well in human serum and there is limited to no predation. Either these genes are expressed as a protective mechanism against *Bdellovibrio* predation or a protective mechanism against growth in serum. As our RNASeq study compared growth of *S. marcescens* in human serum with *Bdellovibrio*, to *S. marcescens* grown in human serum without *Bdellovibrio*, I suggest that these changes in gene expression are indicative of a protective response against *Bdellovibrio* predation. Removal of *arnA* likely impacts predation by *Bdellovibrio* or growth in human serum. The improved growth of an *arnA* mutant in human serum suggests that *arnA* expression incurs a fitness cost (deletion improves bacterial growth; see Figure 3.2.1) and that expression is due to *Bdellovibrio* predation. Loss of *arnA* should increase the susceptibility of *S. marcescens* to predation. We see a slight delay in resistance to predation and subsequent *S. marcescens* growth in the Δ*arnA* mutant (Figure 3.2.3), but resistance to predation does still ensue, suggesting that other resistance mechanisms against predation are present.

This effect is likely only seen at later timepoints (between 7 and 12 hours) because *arnA* expression is only induced and ArnA functionally expressed, thus modifying the Lipid A of *S. marcescens* at these timepoints. Serum complement proteins and AMPs are quickly depleted from the medium, owing to it being a closed system. Within a live host, serum antimicrobials would be continually replenished, adding another dimension of complexity to this interaction. This time-dependent effect, which applies to all of the genes of interest in this study, is likely a combination of the initial assault of antimicrobial peptides and complement proteins, followed by a response to predation by *B. bacteriovorus*, which culminates in a delayed transcriptional response to both predation and human serum, owing to a lack of nutrients, until translation of this gene expression provides a discernible fitness benefit.

Quantification of *arnA* expression throughout the earlier timepoints of *S. marcescens* growth in human serum, both with and without *Bdellovibrio,* through qtPCR would be very informative. I would hypothesise that significant *arnA* expression would not occur until 7 hours onwards, although a delay between *arnA* transcription and ArnA translation and functional modification of Lipid A must be taken into account.

In the case of *arnA* deletion, wildtype *S. marcescens* is preyed upon and subsequently grows in human serum from 8 hours onwards, after the initial depletion in viable CFU (by predation) between 0 and 8 hours, whereas Δ*arnA S. marcescens* does not recover until 10 hours. As this difference in time-dependent growth does not occur in the *S. marcescens* without *Bdellovibrio*, this suggests that this delay is a predation specific effect and that *arnA* deletion alters the susceptibility of *S. marcescens* to predation.

3.3.1. Resistance to Predation by *B. bacteriovorus* is more prominent in human serum, than in laboratory buffer

Human serum contains an array of antimicrobial peptides that non-specifically kill bacteria. The L-Ara(4)N pathway is typically activated in *Salmonella enterica* and *Salmonella* Typhimurium due to iron excess (452), magnesium limitation (453, 454) and the detection of CAMPs (455), but not typically activated under lab conditions (456). As antimicrobial proteins are not present in buffer but are in human serum, this suggests that induced Arn-mediated surface modification, alongside other host induced surface changes, which are largely uncharacterised, has a strong role in the differential gene expression and remodelling of the surface of *S. marcescens* that ultimately results in this decrease in susceptibility to predation. If a host-induced change is responsible for this altered susceptibility to predation, I would hypothesise that predation of Δ*arnA S. marcescens* should mirror WT *S. marcescens*, as the Arn-mediated modification system should not be active in Ca/HEPES buffer. This would be interesting to test.

3.3.2. Removal of *arnA* altered the resistance of *S. marcescens* to predation, whilst removal of *arnT* did not.

Surprisingly, removal of the *arnT* gene, another component of the arn operon, from *S. marcescens* did not affect resistance to predation by *B. bacteriovorus* (Figure 3.2.3). ArnT is responsible for the export of L-Ara(4)N and substitution of the 1' and 4' phosphates of Lipid A, making it a key gene within the operon and therefore it was hypothesised to have played more of a role in this phenotype. ArnA is responsible for catalysing two of the initial steps of L-Ara(4)N synthesis and was the most upregulated gene in the operon, suggesting it plays an important role also (Figure 3.2.2). The steps catalysed by ArnA do not represent commitment to the Arn-mediated Lipid A modification pathway, suggesting that their upregulation may play a role in a different, and yet unknown, process instead, potentially explaining the lack of impact of ArnT removal also.

In other studies, individual removal of the *arnA, arnT*, *arnB* and *arnC* has abrogated polymyxin and AMP resistance, suggesting it is integral for the functioning of the Arn operon (457-459). No assays like ours have been carried out for direct comparison, so we must take polymyxin resistance as an indication of Arn-modification function. No visible changes in colony morphology were seen for *S. marcescens* Δ*arnA* and Δ*arnT* mutants. Testing the resistance of Δ*arnT* and Δ*arnA* mutants to polymyxins would confirm whether deletion fully disrupts Arn-mediated LPS modification.

One explanation may be that the synthesis of the L-Ara(4)N sugar is sufficient to alter the surface and appearance of *S. marcescens* sufficiently to perturb predation and that its export and integration into Lipid A is not required, however this seems unlikely. Alternatively, there may be an alternative L-Ara(4)N export mechanism that is replacing the function of ArnT in this scenario, or some other mechanism may be compensating for the effect of inactivation of the Arn operon and conferring resistance to predation instead, potentially through a similar Lipid A modification pathway. Unfortunately, the only assays conducted around the Arn operon have focused on AMP resistance where removal of ArnT has restored susceptibility, making the comparison of our study to theirs more difficult.

However, this was only investigated in a single experiment and would therefore require further investigation and repeats before any firm conclusions regarding the role of ArnT can be drawn.

3.3.3. Removal of major surface components of *S. marcescens* does not affect bacterial viability in human serum.

All of our *S. marcescens* mutants were significantly killed but remained viable in human serum. There is an initial drop in *S. marcescens* mutant viability that represents initial bactericidal killing, as seen in Figure 3.2.1, between 0 and 2 hours, after which all *S. marcescens* strains grow and recover. Deletion of any of the surface components in this study did not impact the ability of *S. marcescens* to survive in human serum, compared to Wildtype *S. marcescens*.

This was surprising in the case of the ArnA and ArnT mutants, and the capsular export Wza mutant as the role of the Arn operon in conferring antimicrobial protein resistance (113, 127, 177, 457, 460-462) and the capsule in protection against complement mediated killing (18-20, 170, 171) are well documented. Deletion of *arnA* and *arnT* also appeared to improve the growth of *S. marcescens* within human serum, between 4 and 6 hours. The reasons behind this are unknown and would need to be further invesitigated. Alterations to the cell surface are known to cause changes in cell aggregation, which could affect how bacterial growth is calculated (from CFU plating counts), leading to experimental error. However, no discernible changes in aggregation were seen in these experiments. It is possible that deletion of one cell surface modification mechanism induces or impacts the expression of another, conferring a previously unseen fitness benefit. However, this is purely speculative.

Alternatively, the presence of other mechanisms that confer protection against AMP- and complement-mediated killing, and are upregulated in response to serum exposure, could contribute to the lack of growth defect in human serum. However, the mechanisms behind this are purely speculative such as alternative residues and extended O-antigen polysaccharide chains conferring complement resistance (128, 172-176). Viability of *S. marcescens* mutants has only been characterised in one batch of human serum, something that is easily rectified and could be tested further in future; however, all human sera will contain varying degrees of AMP and complement-mediated killing effects, but neither will ever be entirely absent. Characterisation of the different compositions of Human sera batches would aid these investigations (see future work).

3.3.4. The viability of *B. bacteriovorus* was not discernibly impacted by human serum.

The viability of *B. bacteriovorus* was not affected by human serum in our assays. Considering human serum contains an array of antimicrobial mechanisms, the absence of a significant drop in bacterial viability is surprising. However, *B. bacteriovorus*, and its cell surface, are highly atypical. A significant proportion of the immunogenic activity directed towards Gram-negative LPS is centred around the presence of phosphate groups in the Lipid A region, which as I have mentioned, can be modified to reduce AMP binding, antibody binding and host pattern recognition receptor binding (463). In *B. bacteriovorus*, the modified Lipid A moiety, where the phosphate residues are substituted for mannose (294), has a reduced negative charge, resulting in decreased AMP attraction and binding and less antibody deposition, potentially leading to less activation of the classical complement deposition pathway also. These effects culminate in *B. bacteriovorus* being resistant to some of the bactericidal mechanisms present in human serum, explaining its sustained viability in human serum.

3.3.5. Removal of fimbriae did not impact the susceptibility of *S. marcescens* to predation by *B. bacteriovorus.*

Despite fimbrial synthesis being highly upregulated during the resistance period of *S. marcescens* predation (Table 3.1.1), abrogation of fimbrial synthesis in each of the two fimbrial clusters by deleting genes encoding the major subunit, chaperone protein and usher protein for each, did not alter susceptibility of *S. marcescens* to predation or abrogate resistance formation (Figure 3.2.7). One possible explanation for this is that the two fimbrial clusters are compensating for one another and therefore the removal of both fimbrial clusters is required for abrogation of resistance. Alternatively, fimbrial biosynthesis may be a stress response to predation, triggering adhesion and biofilm formation and may not play a role in protection against predation at all. Future work would consist of the construction of a double fimbriae mutant to confirm the role of fimbrial synthesis on decreased susceptibility to predation more definitively. Electron microscopy would also be performed to visually check if alternative fimbriae have replaced the previously deleted fimbriae (mutated in this study), encoded by other genes of yet unknown function within the *S. marcescens* genome, and to check if fimbriae are diminished in our mutants by negative staining.

3.3.6. Removal of the polysaccharide capsule did not impact the susceptibility of *S. marcescens* to predation by *B. bacteriovorus.*

Removal of the capsule exporter gene *wza*, thus producing an acapsular strain of *S. marcescens* appeared to not alter the susceptibility of *S. marcescens* to predation as it was still preyed upon and grew comparably to wildtype *S. marcescens*.

Predation of capsular Gram-negative bacteria by *B. bacteriovorus* has previously been demonstrated (327), therefore increased susceptibility to predation through the removal of the capsule is not expected. RNASeq analysis between *S. marcescens* in human serum and *S. marcescens* with *B. bacteriovorus* in human serum should remove the possibility that upregulation of capsule biosynthesis is due to the effects of human serum on *S. marcescens* alone, therefore an absence in alteration of predation susceptibility when Wza is removed is surprising. It is possible that capsule synthesis may act as a signal to other surface-modification processes that ultimately confer a decreased susceptibility to predation, hence the upregulation of capsule synthesis genes but the absence in alteration of predation susceptibility with their removal, however this would require a multitude of further experiments to determine this.

3.3.7. Serum composition alters the susceptibility of *S. marcescens* to predation by *B. bacteriovorus.*

Human serum is composed of various immune surveillance and bactericidal proteins such as antibodies, complement proteins and antimicrobial proteins, all in varying concentrations. The use of a different batch of human serum in these experiments yielded a different phenotype whereby *S. marcescens* (both WT and Δ*arnA* mutant) grew back faster than previously, and grew back at the same time and rate (i.e. deletion of Δ*arnA* did not delay resistance formation or increase susceptibility to predation as seen previously). This is likely due to a difference in serum composition but without metabolomic analysis of each it is hard to conclude which component(s) vary and are having this effect. One suggestion is that the latter batch of serum contained less AMPs and therefore would not induce the Arn operon and incur a viability cost on the Δ*arnA* mutant, making both the WT and mutant comparably fit and susceptible to predation. One approach to quantifying the differences between human sera batches without full metabolomic analysis would be to heat-treat and thus complement deplete samples of sera, enabling the role of complement proteins in this varying phenotype to be determined.

Alternatively, host antibody binding to O-antigen side chains has been demonstrated to provide serum resistance in *Pseudomonas aeruginosa*, Enteropathogenic *E. coli* and *S. typhimurium* infection by sterically hindering complement protein binding. One possibility is that serum antibody composition may vary between batches and thus different levels of steric hindrance to complement killing is seen (113, 464, 465). There is, however, no evidence currently to suggest that antibody-mediated steric hindrance of complement killing is occurring in this scenario. Further studies of predation with other batches of human sera may aid the elucidation of the cause of this difference in response, and the scale to which it may affect predation (see future work).

3.3.8. Limitations

Many of the experiments require further biological repeats before any firm conclusions can be drawn. This has also led to the conclusions that have been drawn being highly likely to be oversimplified of the actual situation, where a multitude of factors are likely to participate towards our phenotype of resistance to predation.

What this study has achieved is the demonstration that host factors do alter the dynamics of the predation process and therefore must be considered and their implications studied in further detail before *B. bacteriovorus* can be used as a novel antimicrobial therapy.

3.3.9. Future work

How do immune-mediated bacterial surface changes alter predation?

As deletion of any single surface modification gene did not abrogate the resistance phenotype investigated in this study, I propose that further serum-induced changes conferred on *S. marcescens* through growth in human serum, are responsible for its resistance to predation by *B.* bacteriovorus. Future work would aim to test the predation susceptibility of more complex *S. marcescens* mutants including a double ∆*arnA*∆*arnT* mutant to determine whether this further amplifies the delay in resistance seen with the single ∆*arnA S. marcescens* predation. The capsule exporter protein Wza is a polysaccharide transporter protein whose role likely extends beyond capsular polysaccharide export, i.e., in signalling further surface changes across the bacterium. Although a single ∆*wza* *S. marcescens* mutant did not reveal any discernible difference in their susceptibility to predation, the construction of other surface mutants in combination with removal of Wza such as a ∆*arnA*∆*wza* double *S. marcescens* mutant is likely to induce further surface changes that may alter susceptibility to predation. Determining the effect of these proposed surface changes on predation will provide further details on the factors that aid or impede predation within the host environment, taking us one step closer to the application of *B. bacteriovorus* as a novel antimicrobial therapy.

How does Serum Composition impact the susceptibility of *S. marcescens* to predation by *B. bacteriovorus*?

Serum composition, much like the immune response of individuals, can vary dramatically and therefore the impact of host factors on the dynamics of predation is also likely to vary. One experiment that I hoped to perform was the assaying of predation efficacy across a panel of human sera samples. By measuring the optical density (OD_{600}) of *S. marcescens* as a proxy for predation, I would incubate *S. marcescens* with/without *Bdellovibrio* to determine the viability and susceptibility of *S. marcescens* (Wildtype and surface mutants) within over 100 different batches of sera. This would significantly widen the scope of my findings and would more conclusively inform me if the removal of certain structural components from the surface of *S. marcescens* impacted bacterial survival and predation susceptibility. This would also help to abrogate the effects of batch-to-batch variation in human sera composition and determine if my preliminary findings are biologically relevant.

Further characterisation of the differences between different batches of human sera would also be useful in assisting our understanding as to why the susceptibility of *S. marcescens* to predation by *B. bacteriovorus* varies between batches. Quantification of complement protein titres and antibody titres (to both *S. marcescens* and *B. bacteriovorus*), through a combination of Western blot and ELISA analyses would be beneficial. Depletion of complement by heat-treatment of serum, and then repetition of these assays would also help to determine the possible effects of complement within this assay.

Pre-incubation of *S. marcescens* in human serum, prior to exposure and attempted predation by *B. bacteriovorus* would be a useful approach to further characterising these interactions. I would hypothesise that, if host factors were inducing changes on the *S. marcescens* bacterial surface that reduced its susceptibility to predation by *B. bacteriovorus*, *B. bacteriovorus* would not be able to prey upon *S. marcescens*, or to a much lesser extent, signified by a smaller reduction in viable CFU upon *Bdellovibrio* exposure.

Alternative ways of establishing which bacterial factors which facilitate or resist predation.

In place of RNASeq studies, other labs have aimed to characterise which bacterial factors facilitate or resist predation through taking libraries of mutants with deletions in known phage receptor genes, such as those highlighted in Mun et al., 2022 (466), and testing them for predation susceptibility, based on the assumption that there will be some overlap between the surface receptors targeted by bacteriophage and Bdellovibrio. Mun and co-workers found that deletion of OmpF in *E. coli* significantly reduced predation susceptibility although, by their own admission, predation still occurred but at a much slower rate, and this effect was specific to this single bacterial strain (466). This highlights that there are clearly multiple surface factors targeted by *Bdellovibrio* during prey recognition. I could also aim to characterise factors that resist or enable predation in human serum, via a similar approach.

3.3.10. Final remarks

In this Chapter, I aimed to test how bacterial surface alterations affect the dynamics of predation in a host setting. I characterised the host factor-induced alterations that occur on the pathogen cell surface during predation by *B. bacteriovorus* in human serum, asking if such alterations confer a decreased susceptibility to predation. Prey cell surface modifications involving the bacterial capsule, LPS and fimbriae are most prominent in this resistance period. Deleting cell surface modifying genes and testing serum survival and predation reveals that LPS modification in response to human serum antimicrobial proteins is likely an important mechanism, although a combination of mechanisms and cell surface changes likely contributes to this resistance phenotype. Collectively, my results suggest that bacterial cell surface LPS alteration, in response to bacterial predation, is a key consideration when considering the application of *B. bacteriovorus* as a novel antimicrobial therapy. Future work will elaborate further the combination of cell surface changes that contribute to predation resistance phenotypes. This improves our understanding of how predation would occur, and the potential barriers to predation, within a human host, in collaboration with the host immune system. Overall, this aids the potential application of *B. bacteriovorus* as a novel antimicrobial therapy through this improved understanding.

Chapter 4: Exploring the roles of novel genes that allow for temporary *Bdellovibrio* intramacrophage survival.

4.1. Rationale for Chapter 4

In this Chapter, I identify and test the roles of a subset of novel genes in *B. bacteriovorus* which, I propose, allow for prolonged survival of *Bdellovibrio* within macrophage, through a greater tolerance to host-mediated oxidative stresses and the immune response. I also explore the roles of these genes in predation of Gram-negative bacteria by *B. bacteriovorus*, positing that if these genes aid the tolerance of oxidative stress throughout predation, they may also aid the survival of *Bdellovibrio* in the macrophage phagosome. Further characterisation of the immune response to *Bdellovibrio*, and the interactions between the host immune response, Gram-negative prey and *Bdellovibrio bacteriovorus* will aid the potential development of *B. bacteriovorus* as a novel antimicrobial therapy.

I will first outline how I have selected the subset of gene/protein candidates in this study, followed by what is currently known/can be inferred through bioinformatic analyses about these proteins. I then characterise the roles of these proteins in predation and intramacrophage survival through fluorescent microscopy, gene deletion and transcriptional studies.

4.2. Selection of gene candidates

The innate immune system of zebrafish embryos is highly similar to that of humans, with the primary response being mediated by macrophages and neutrophils (403). This suggests that genes that are upregulated in response to survival within a zebrafish hindbrain model of infection may also play a role in survival within human macrophage. Previous studies have shown that *B. bacteriovorus* doesn't perturb phagosomal maturation or resist phagocytic uptake and that once it is passively taken up, it resides within the phagocyte until it is killed, predominantly between 8- and 24-hours post-uptake (2). My study aims both to address what expression is induced in the macrophage by *B. bacteriovorus*, and, in this section, whether its macrophage-induced transcription explains how it survives and tolerates the actions of the phagolysosome for that long, before eventually being degraded and killed.

Previous, unpublished RNASeq studies have profiled the transcriptional response of *B. bacteriovorus* injected into the hindbrain and thus circulation of a zebrafish larvae model (Tyson, Moore, Sockett et al., manuscript in prep.). It is known that *B. bacteriovorus* survives live within zebrafish larvae for over 24 hours and encounters macrophages and neutrophils (1). To determine whether changed expression levels of any genes may confer a temporary survival advantage to *B. bacteriovorus* whilst inside a zebrafish host, differentially up- or downregulated genes were studied by those authors. The levels of bacterial expression were low due to *B. bacteriovorus* not being a replicating pathogen. However, a (limited) differentially expressed list of genes was prepared.

I then interrogated these differentially expressed *B. bacteriovorus* genes and found a subset of genes that I believed would assist in tolerance to phagosomal conditions and temporary survival in macrophage, due to their known functional annotations in oxidative stress tolerance. These genes are listed in Table 4.2.1**.** I then interrogated the literature surrounding survival of bacterial pathogens in macrophage and interrogated the *B. bacteriovorus* HD100 genome for other homologues of my candidate proteins to give 7 further proteins of interest (*bd0017/surA, bd0799/ankB, bd1154/katA*, *bd1155/ankB* and *bd1401/sodC*). I explored the predicted functions of these encoded proteins, using freely available bioinformatic tools, to gather more information about their function before exploring their importance experimentally.

Table 4.2.1: Differentially expressed genes predicted to confer a survival advantage in a zebrafish larvae model of infection. *Confidential: Tyson, Moore, Sockett et al., manuscript in prep*. 7 genes, 5 of which are related to the oxidative stress defence response and 2 of which are hypothetical, were chosen for further investigation in my study to determine if they aid tolerance and prolong survival within human macrophage. p.i.: post-inoculation into zebrafish larvae; buffer: Ca/HEPES buffer; N.D. indicates not detected.

Gene	**Function**	**Expression (Fold change)**		
		1hr post zebrafish hindbrain injection cf. buffer	**6hrs post zebrafish hindbrain injection cf. buffer**	**6hrs post zebrafish hindbrain injection cf. 1hr p.i.**
bd0295	SodC*;* Cu/Zn Superoxide dismutase	-4.39	-3.05	**1.34**
bd0798	CatA*:* catalase	N.D.	**3.75**	N.D.
bd1815	Hypothetical protein	**2.62**	**3.54**	N.D.
bd2517	AhpC*;* alkylhydroperoxide reductase	N.D.	**3.27**	N.D.
bd2518	AhpF*;* alkylhydroperoxide reductase	-1.68	N.D.	**3.34**
bd2620	Dps*;* DNA protection protein during starvation and oxidative stress transcription regulator protein	-5.26	-2.88	**2.38**
bd3203	Hypothetical protein	-2.78	N.D.	**3.19**

4.3. Bioinformatic analyses and informatic predictions for each gene product of interest

Firstly, I sought to analyse each of the highlighted genes using publicly available bioinformatics tools to confirm that their functional annotation was in-line with literature of other characterised proteins or to determine whether any additional homologues of these proteins existed within the *Bdellovibrio* genome or within other well-characterised bacteria, to help ascribe (or confirm) a functional annotation to the proteins in this study.

4.3.1. Predicted Copper-Zinc superoxide dismutases.

4.3.1.1. Bd0295/SodC

Bd0295 is predicted to be a Copper-Zinc superoxide dismutase, 189 amino acids in length and 19.5 kDa in size (UniProt). Superoxide dismutases convert superoxide (O_2^-) molecules into hydrogen peroxide (H_2O_2) and diatomic oxygen (Figure 1.4.6), preventing DNA and protein mutation and oxidative damage to the cell. Bd0295 is a periplasmic superoxide dismutase meaning that, as superoxide radicals cannot naturally cross the cytoplasmic membrane, SodC can protect Gram negative bacterial cell from superoxide radicals that are generated in the periplasm or exogenously (467, 468).

Analysis of predicted domain structure

Analysis of the predicted domain structures within Bd0295, using PFam, shows a signal peptide at the N-terminus of Bd0295 (Amino acids 1-19) and a Cu/Zn Superoxide dismutase domain. Bd0295 has a lipobox signature/attachment site (a Cysteine residue at the C-terminus of the N-terminal signal peptide), indicating that Bd0295 is secreted across the cytoplasmic membrane, into the periplasm, and processed by lipid attachment using the Cys signal and then likely anchored to the outer leaflet of the cytoplasmic membrane (469).

Analysis of Bd0295 with SignalP 6.0, a programme that predicts the presence of signal peptides, confirms the presence of a lipoprotein signal peptide at the N-terminus of Bd0295 (Figure 4.3.1), with a predicted cleavage site between amino acids 16 and 17.

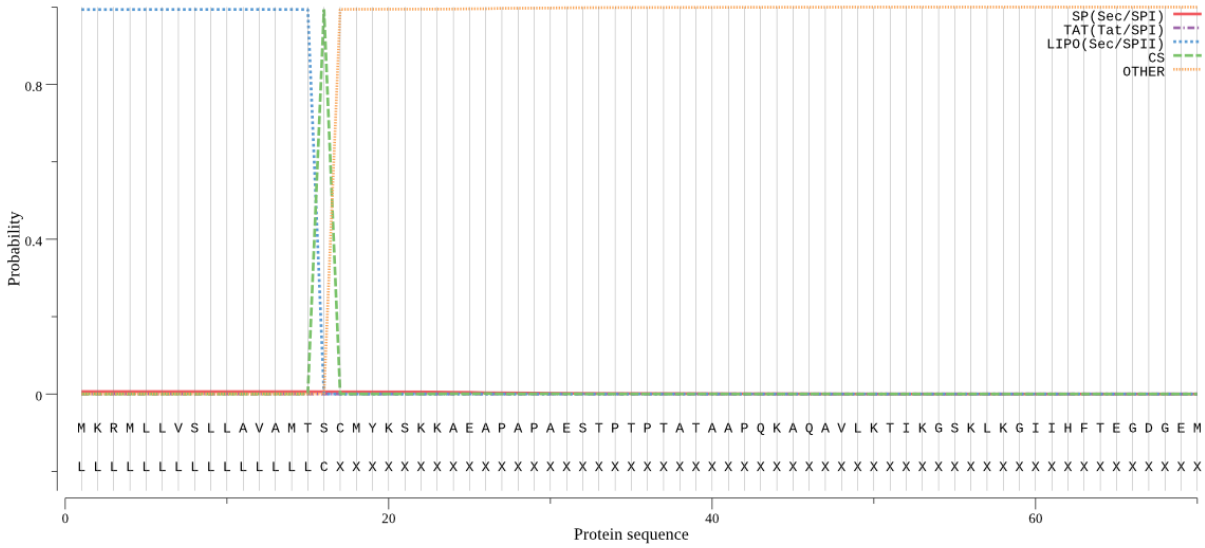

Figure 4.3.1: Prediction of a lipoprotein signal peptide at the N-terminus of Bd0295. Figure generated using SignalP 6.0.

Gene neighbourhood and association analyses

bd0295 is monocistronic, bordered by a fumarylacetoacetate hydrolase family protein (gene: *bd0294*), responsible for tyrosine and phenylalanine metabolism, and a large lipoprotein (gene: *bd0296*) of unknown function (Figure 4.3.2) (xBase).

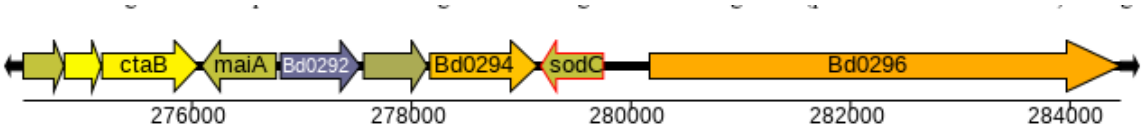

Figure 4.3.2: A schematic showing the gene neighbourhood of *bd0295*. Diagram taken from xBase.

Using STRING to analyse the predicted protein-protein interactions and functional enrichment, Bd0295 is predicted to interact with other oxidative stress defence proteins, including CatA (Bd0798) and KatA (Bd1154), both of which are catalase proteins that detoxify hydrogen peroxide within the cell, and $SodB_{Bd2407}$ and $SodB_{Bd3617}$, which are both Manganese-Iron superoxide dismutases that detoxify superoxide radicals within the cytoplasm of the cell, that originate from the electron transport chain of aerobically respiring cells (467, 468). Bd0295 is also predicted to be associated with Bd2609 and Bd1348, both of which have predicted roles in cation transport, and $ResA_{Bd1980}$ and $ResA_{Bd2208}$, both of which are thioredoxins associated with cytochrome c biogenesis. Bd1341 is a putative disulphide-isomerase also associated with thioredoxin function (Figure 4.3.3).

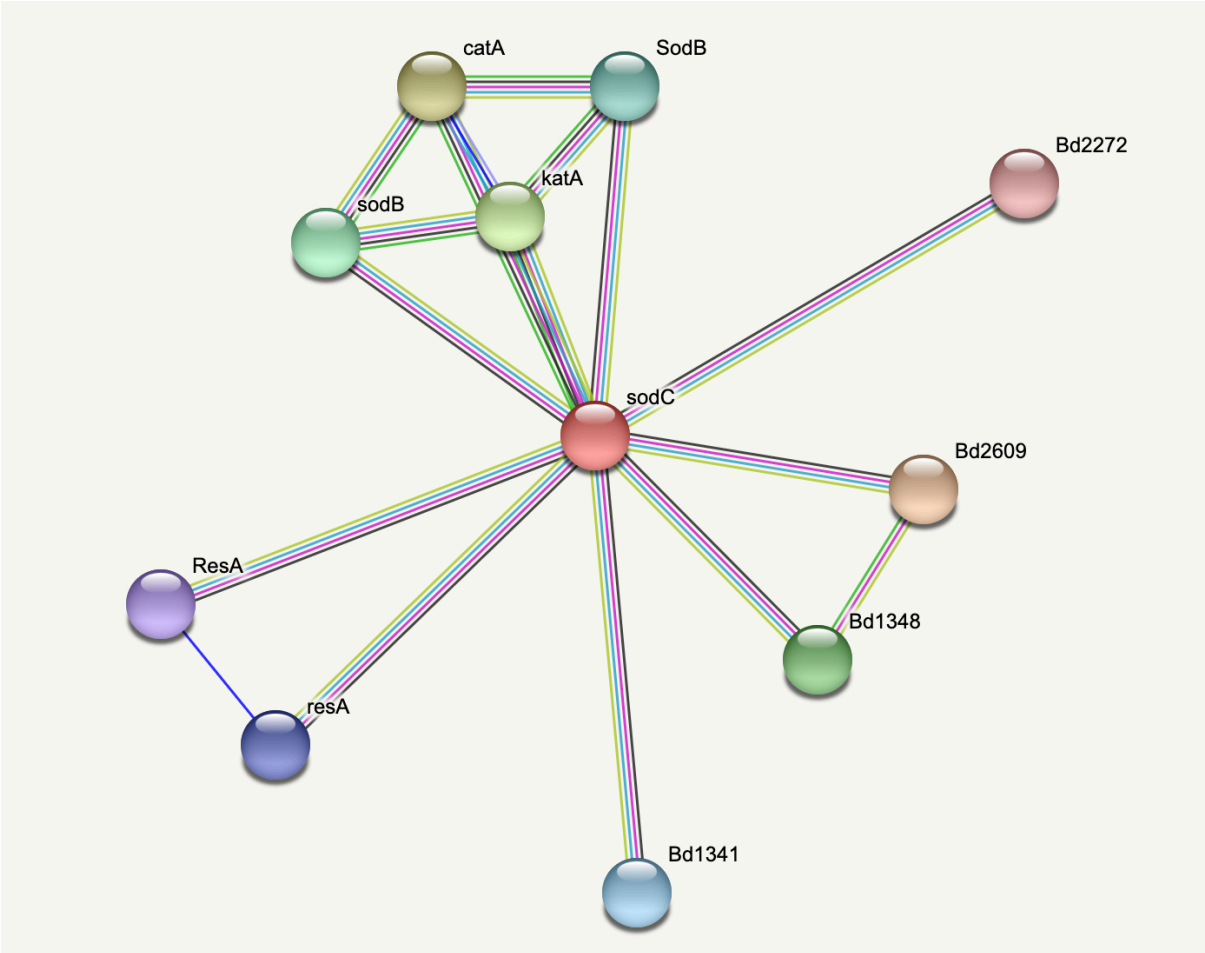

Figure 4.3.3: A schematic showing the predicted protein-protein interactions of $SodC_{Bd0295}$. Figure generated using STRING. Magenta threads represent experimentally determined interactions; Green threads represent gene neighbourhood interactions; Dark blue threads represent gene co-occurrence; Black threads represent co-expression; Lilac threads represent protein homology; Yellow threads represent text mining (i.e., associations in literature) (STRING).

Searches for homologues in *Bdellovibrio* and other bacterial species

Searches of the *B. bacteriovorus* HD100 genome, using BlastP to check for proteins with a high sequence similarity at the amino acid level, reveals a second Cu/Zn SodC superoxide dismutase, Bd1401, which shows a 42% sequence similarity (Figure 4.3.5). SodC homologues are also present in the closely related environmental strain *B. bacteriovorus* str. Tiberius.

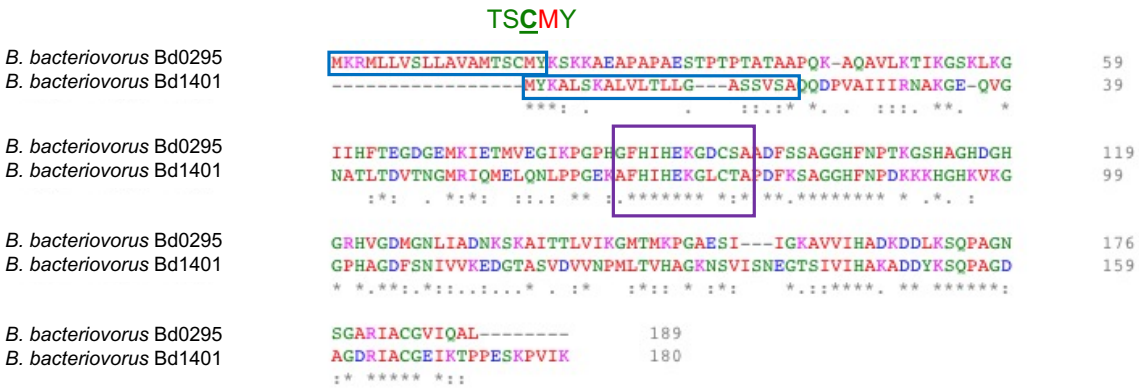

Figure 4.3.4: An alignment of Bd0295 to the other SodC protein, Bd1401, in the *B. bacteriovorus* HD100 genome. Purple box indicates the Copper/Zinc binding site, that is highly conserved amongst Cu/Zn Superoxide dismutase/SodC proteins. Blue boxes indicate the signal peptide for each protein. **Bold** and underlined is the cysteine residue for the Bd0295 lipobox. Bd0295/sodC of *B. bacteriovorus* (Uniprot accession: Q6MR06) was aligned to the SodC protein Bd1401 (Q6MN60) using Clustal Omega. Complete amino acid sequences are shown for both proteins. Amino acids are coloured by their physicochemical properties. (*) indicates a conserved residue. (:) indicates amino acids sharing strongly similar properties. (.) indicates an amino acid sharing weakly similar properties.

Like Bd0295, Bd1401 is predicted to be a Copper-Zinc Superoxide dismutase protein. The gene *bd1401* is monocistronic. Bd1401 is an 18.9 kDa protein, 180 amino acids in length (UniProt). The gene *bd1401* is bordered by a DUF3747 domain containing protein (Gene: *bd1400*) and a Murein L, D-transpeptidase catalytic domain family protein (Gene: *bd1402*) (Figure 4.3.5) (xBase).

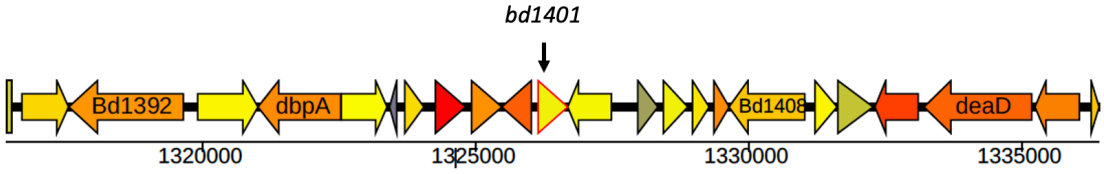

Figure 4.3.5: A schematic showing the gene neighbourhood of *bd1401*. Diagram taken from xBase.

Analysis of predicted domain structure

Analysis of the predicted domain structures within Bd1401, using PFam, shows a signal peptide at the N-terminus of Bd1401 (Amino acids 1-20) and a Cu/Zn Superoxide Dismutase domain. Unlike Bd0295, Bd1401 does not have a lipobox signature/attachment site at the C-terminus of the N-terminal signal peptide, indicating that Bd1401 is secreted across the cytoplasmic membrane, into the periplasm, but is not anchored to the cytoplasmic membrane.

Analysis of Bd1401 with SignalP 6.0, a programme that predicts the presence of signal peptides, confirms the presence of a lipoprotein signal peptide at the N-terminus of Bd1401 (Figure 4.3.6).

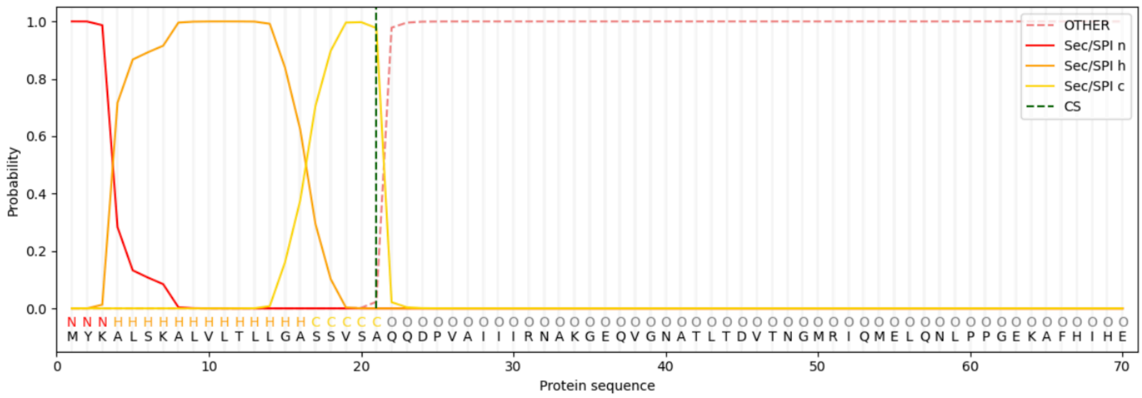

Figure 4.3.6: Prediction of a signal peptide at the N-terminus of Bd1401. Figure generated using SignalP 6.0.

Gene neighbourhood and association analyses

Using STRING to analyse the predicted protein-protein interactions and functional enrichment, Bd1401 is predicted to interact with a similar network of proteins to Bd0295. Bd1401 is predicted to interact with CatA (Bd0798), KatA (Bd1154), SodB$_{Bd2407}$, SodB$_{Bd3617}$, Bd2609, Bd1348, Bd1980, Bd2208 and Bd1341 (Figure 4.3.7).

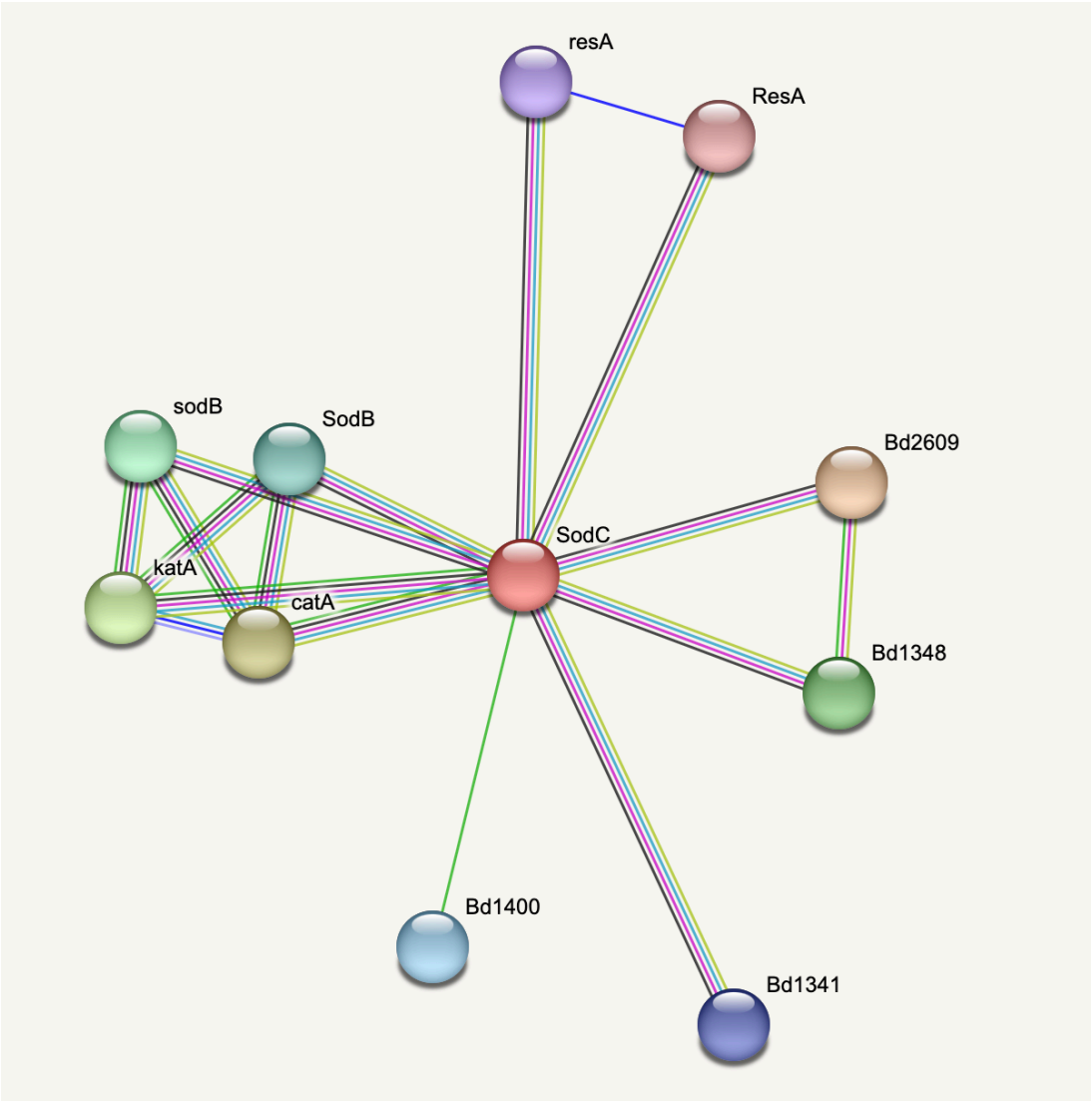

Figure 4.3.7: A schematic showing the predicted protein-protein interactions of Bd1401. Figure generated using STRING. Magenta threads represent experimentally determined interactions; Green threads represent gene neighbourhood interactions; Dark blue threads represent gene co-occurrence; Black threads represent co-expression; Lilac threads represent protein homology; Yellow threads represent textmining (i.e. associations in literature) (STRING).

Predicted structure analyses

To compare the (predicted) structures of these two SodC homologues, I downloaded the PDB (Protein Data Bank) structural prediction files for both proteins from AlphaFold (470) and aligned them using TMalign (471) to compare their structures. Comparing the structures of Bd0295 and Bd1401, although they have a highly similar amino acid sequence in their core region (Figure 4.3.8), structurally, the N- and C- termini differ.

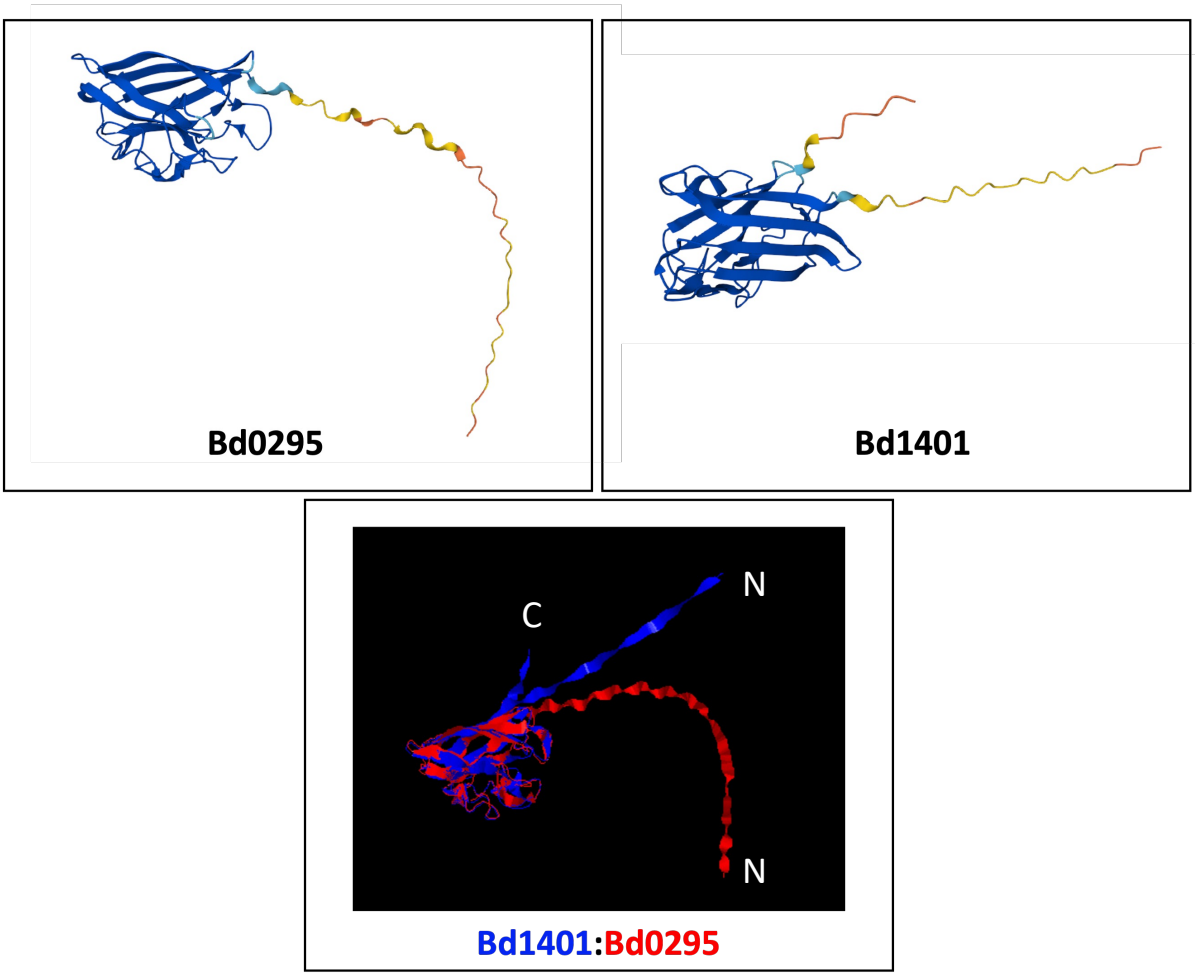

Figure 4.3.8: Predicted structures of the two SodC proteins, Bd0295 and Bd1401. Structural predictions and Protein Data Bank (.pdb) files were obtained from AlphaFold for Bd0295 (UniProt accession: Q6MR06; Top, Left) and Bd1401 (Q6MN60; Top, Right). PDB files were aligned using TMPred to generate the structural overlay depicted (lower, centre). Despite having a similar structure at their centre, the N and C termini of Bd0295 and Bd1401 differ significantly (labelled).

Searches for structural homologues in known bacterial pathogens also revealed a low similarity (at the consensus amino acid level) with the SodC proteins of other bacteria. $SodC_{Bd0295}$ (Uniprot accession: Q6MR06) and $SodC_{Bd1401}$ (Uniprot accession: Q6MN60) of *B. bacteriovorus* were aligned to the SodC proteins of *Legionella pneumophila* (P69049), *Salmonella* Typhimurium (P0CW86 & O68901), *Neisseria meningitidis* (EON866), *Brucella abortus* (D9YMC5) and *Salmonella enterica* (A0A0M0QRP9 & A0A242UPN8) using Clustal Omega.

Consensus amino acid structure appears dissimilar between $SodC_{Bd0295}$ and the SodC proteins tested (P69049: 36.6%, P0CW86: 33.6%, O68901: 34.4%, EON866: 31.4%, D9YMC5: 33.8%, A0A0M0QRP9: 35.6% and A0A242UPN8: 35.0% percentage identity) (Figure 4.3.9). Aligned regions begin at Ala28 and cover the whole of the remainder of the amino acid sequence, including the conserved Copper-Zinc superoxide domain. This demonstrates that $SodC_{Bd0295}$ is a homolog of other bacterial SodC proteins and shares a conserved CuZn binding site that is indicative of this protein.

Consensus amino acid structure appears dissimilar between $SodC_{Bd1401}$ and the SodC proteins tested (P69049: 32.5%, P0CW86: 33.1%, O68901: 34.8%, EON866: 37.3%, D9YMC5: 29.8%, A0A0M0QRP9: 34.8% and A0A242UPN8: 34.3% percentage identity) (Figure 4.3.9). Aligned regions begin at Tyr2 and cover the whole of the remainder of the amino acid sequence, including the conserved Copper-Zinc superoxide domain. This is in contrast with $SodC_{Bd0295}$, where homology only begins after 28 amino acids. Although the consensus amino acid percentage identities are of similar values, this highlights that the first 28 amino acids at the Bd0295 N-terminus are atypical of SodC proteins found in other bacteria, whereas the structure of Bd1401 much more closely resembles “typical” SodC protein structure.

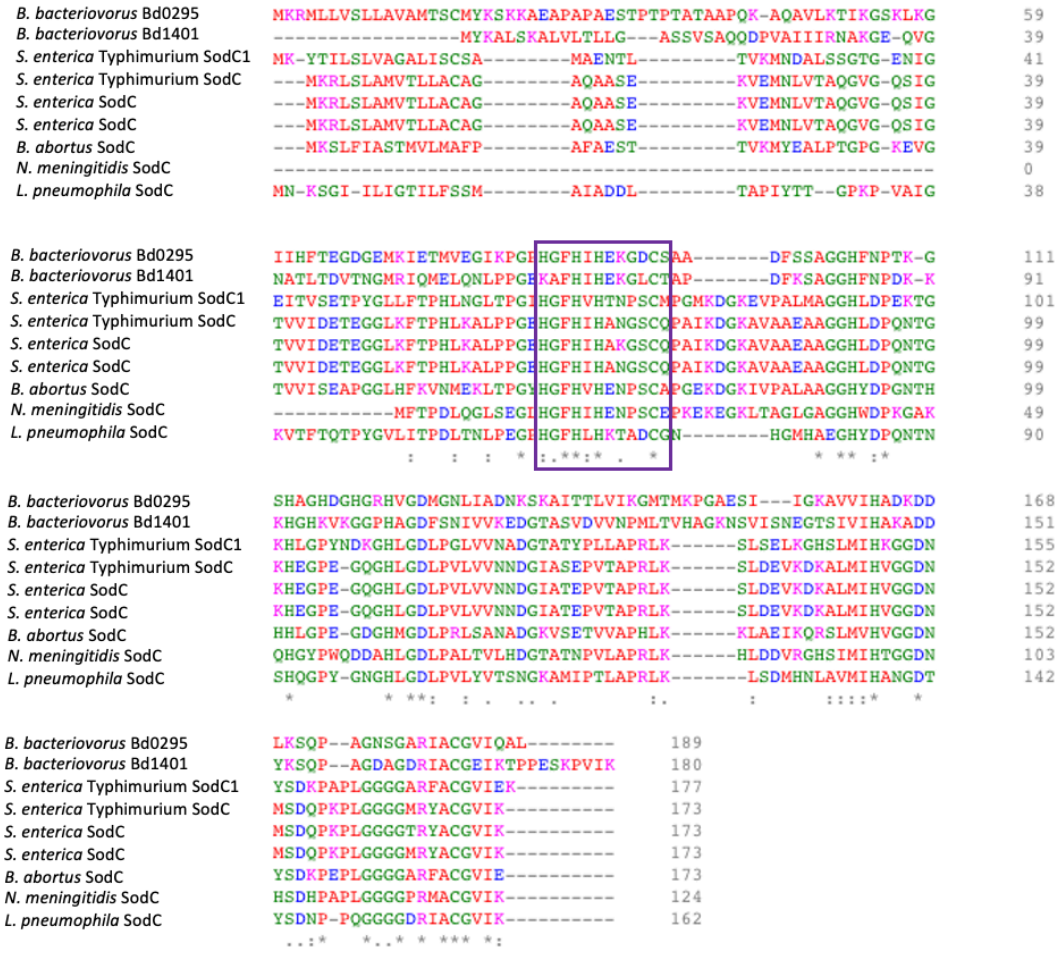

Figure 4.3.9: An alignment of SodC$_{Bd0295}$ and SodC$_{Bd1401}$ to the SodC proteins of other bacterial pathogens. Purple box indicates the Copper/Zinc binding site, that is highly conserved amongst Cu/Zn Superoxide dismutase/ SodC proteins. SodC$_{Bd0295}$ and SodC$_{Bd1401}$ of *B. bacteriovorus* (Uniprot accessions: Q6MR06 and Q6MN60) were aligned to the SodC proteins of *Legionella pneumophila* (P69049), *Salmonella* Typhimurium (P0CW86 & O68901), *Neisseria meningitidis* (EON866), *Brucella abortus* (D9YMC5) and *Salmonella enterica* (A0A0M0QRP9 & A0A242UPN8) using Clustal Omega. Complete amino acid sequences are shown for each protein. Amino acids are coloured by their physicochemical properties. (*) indicates a conserved residue. (:) indicates amino acids sharing strongly similar properties. (.) indicates an amino acid sharing weakly similar properties.

4.3.2. Hydrogen peroxide detoxification

4.3.2.1. Bd0798/CatA

Bd0798 (CatA) is a predicted catalase protein, 54.4 kDa in size and 477 amino acids in length. Catalases are enzymes that detoxify hydrogen peroxide, which is produced within cells when superoxide radicals are broken down or by NADPH in the membrane of macrophage during phagosomal maturation, into water and oxygen (Figure 1.4.7). Hydrogen peroxide reacts with histidine and asparagine residues within the catalase protein, reducing H_2O_2 and breaking the O-H bond to form H_2O. O^+ reacts with the Fe(III) haem group within the catalase protein, displacing the water molecule. Fe(IV)=O reacts with a further H_2O_2 molecule, oxidizing the haem group and forming H_2O and diatomic oxygen (O_2).

Analysis of predicted domain structure

Analysis of the predicted domains present within Bd0798, using PFam, highlighted the presence of a catalase domain (Amino acids 5-388), containing the active site (containing the relevant histidine and asparagine residues) (Amino acids 42-58) and an iron metal binding site (Amino acids 332- 341), and a catalase-related immune-responsive domain (Amino acids 411- 474). Analysis using PFam and SignalP 6.0 confirms that no signal peptide is present within Bd0798, suggesting that it detoxifies hydrogen peroxide within the cytoplasm of the cell (Figure 4.3.10). Hydrogen peroxide can diffuse across the cytoplasmic membrane therefore hydrogen peroxide may be generated within the cell or externally.

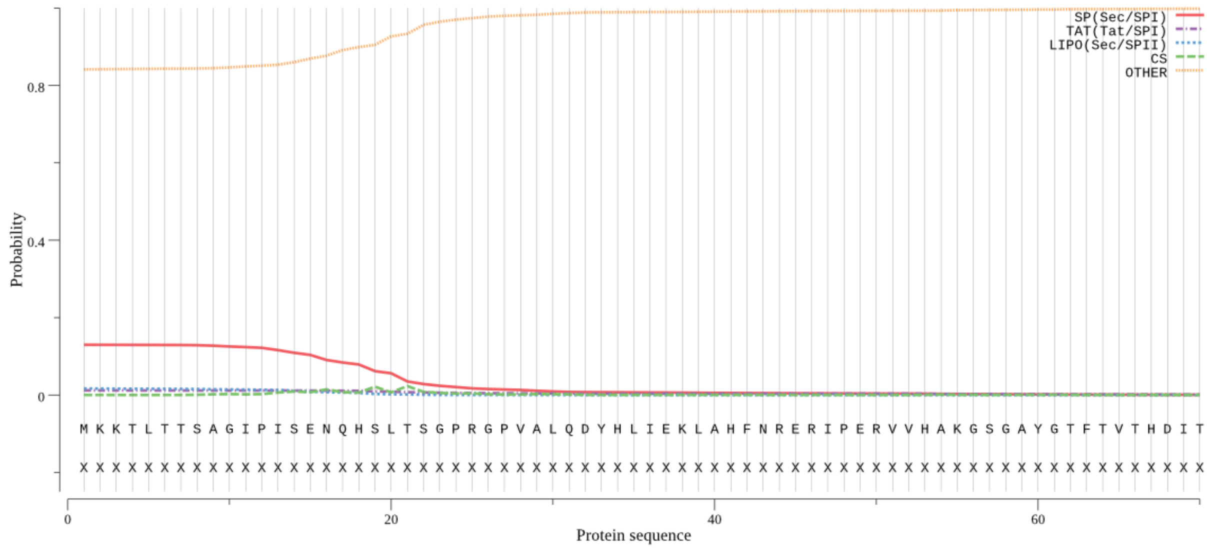

Figure 4.3.10: Prediction Test for a signal peptide at the N-terminus of Bd0798. Figure generated using SignalP 6.0.

Gene neighbourhood and association analyses

bd0798 is in a two gene operon with *bd0799*, which encodes an AnkB protein that we (I and an MSci student that I co-supervised, Syawal Hazanan) hypothesised could regulate the function of the catalase enzyme. Gene *bd0798* is also located near a cluster of genes encoding several hypothetical proteins of unknown function (genes: *bd0800* and *bd0801*), a polyketide synthase (*bd0797/curC*) and an enolase protein (gene*: bd0796*) (Figure 4.3.11) (xBase).

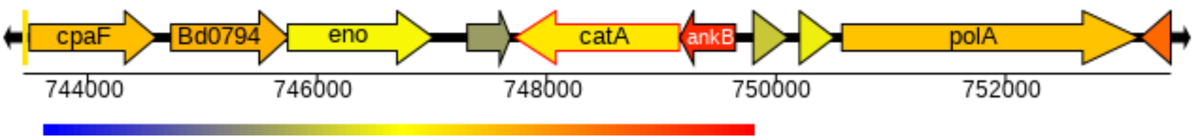

Figure 4.3.11: A schematic showing the gene neighbourhood of *bd0798*. Diagram taken from xBase.

Using STRING to analyse the predicted protein-protein interactions and functional enrichment, Bd0798 is predicted to interact or interact with other oxidative stress related genes (Bd0295/SodC, Bd1401/SodC, Bd2407/SodB and Bd3617/SodB), its proposed regulatory ankyrin partner Bd0799/AnkB. Bd0798 is also associated with another catalase present within the genome of *B. bacteriovorus* HD100, Bd1154/KatA, an alkylhydroperoxide reductase (Bd2517/AhpC) and a Tryparedoxin peroxidase (Bd3525), all of which also detoxify hydrogen peroxide into water (Figure 4.3.12).

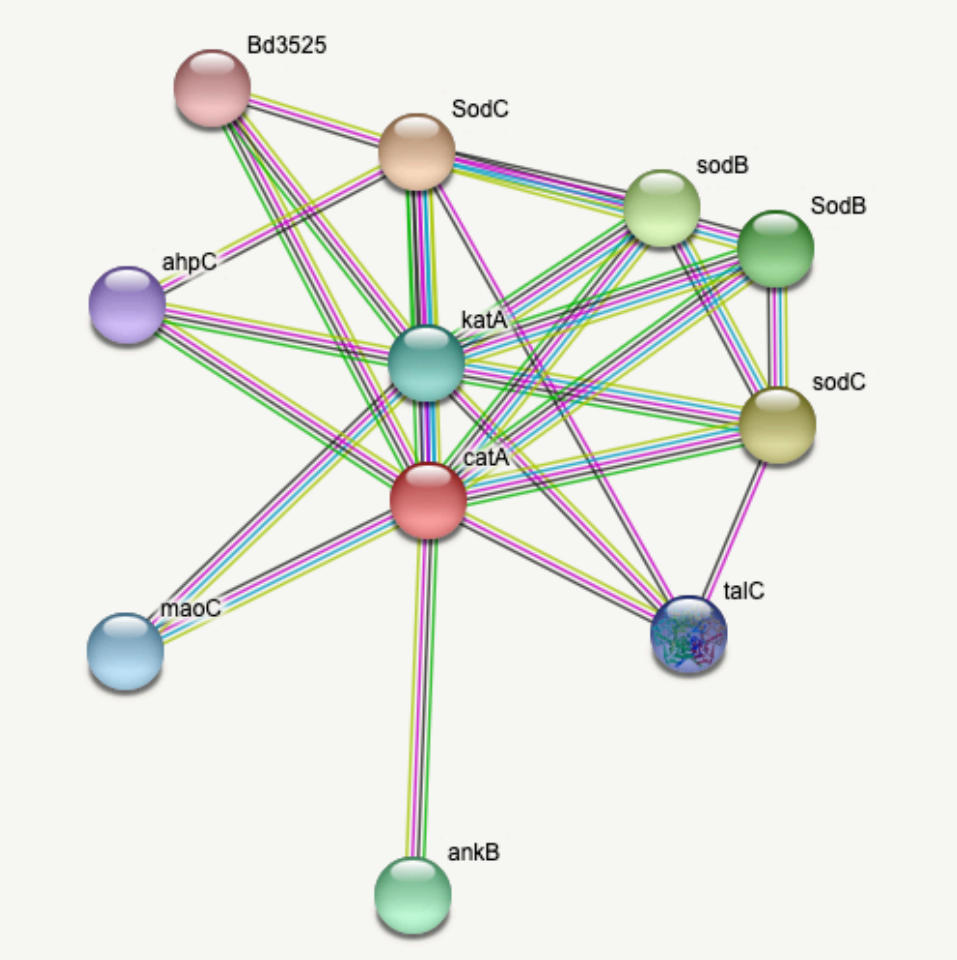

Figure 4.3.12: A schematic showing the predicted protein-protein interactions of Bd0798. Figure generated using STRING. Magenta threads represent experimentally determined interactions; Green threads represent gene neighbourhood interactions; Dark blue threads represent gene co-occurrence; Black threads represent co-expression; Lilac threads represent protein homology; Yellow threads represent textmining (i.e., associations in literature) (STRING).

Searches for homologues in *Bdellovibrio* and other bacterial species

Searches of the *B. bacteriovorus* HD100 genome, using BlastP to check for proteins with a high sequence similarity at the amino acid level, reveals a second catalase enzyme, Bd1154/KatA, which shows a 59.8% sequence similarity (Figure 4.3.13).

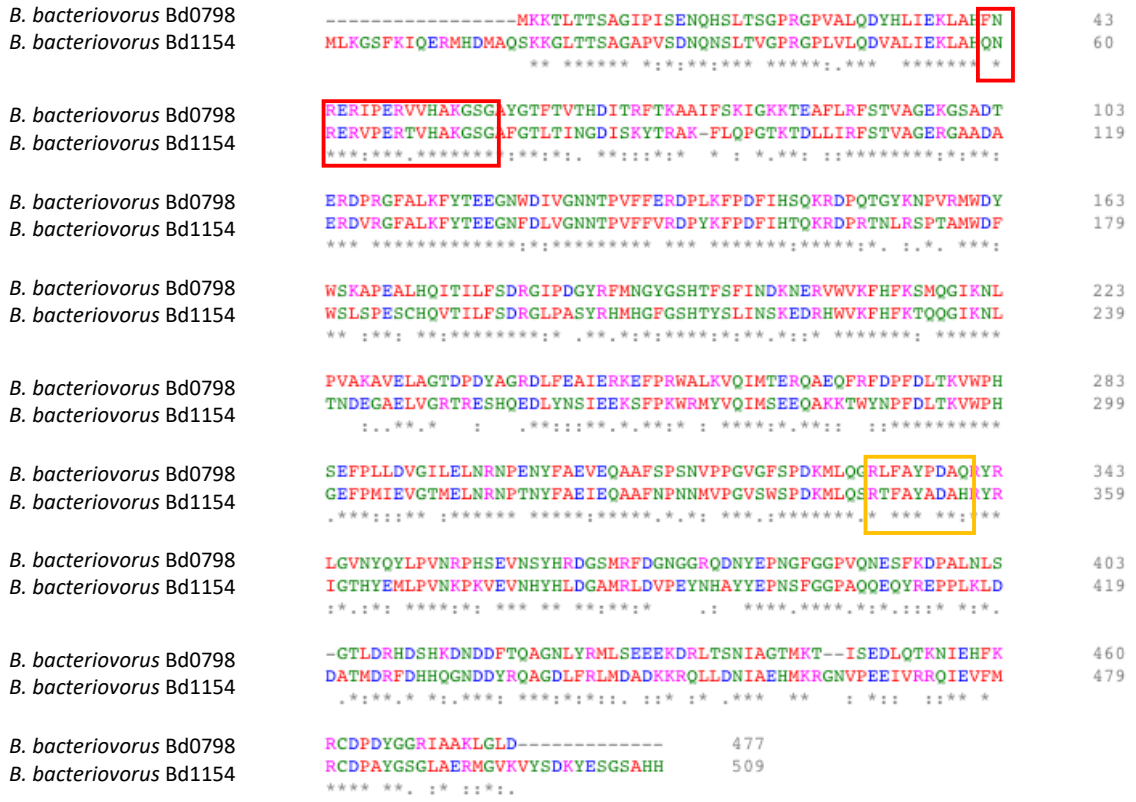

Figure 4.3.13: An alignment of Bd0798 to the other catalase protein in the *B. bacteriovorus* HD100 genome. Red box indicates the active site, to which hydrogen peroxide molecules bind, that is highly conserved amongst catalase proteins. Yellow box indicates the Iron binding site. Bd0798/CatA of *B. bacteriovorus* (Uniprot accession: Q6MPQ0) was aligned to the CatA protein Bd1154 (Q6MNT2) using Clustal Omega. Complete amino acid sequences are shown for each protein. Amino acids are coloured by their physicochemical properties. (*) indicates a conserved residue. (:) indicates amino acids sharing strongly similar properties. (.) indicates an amino acid sharing weakly similar properties.

Searches for structural homologues in known bacterial pathogens also revealed a high similarity (at the consensus amino acid level) with the catalase proteins of other bacteria. Catalase proteins CatA/Bd0798 (Uniprot accession: Q6MPQ0) and KatA/Bd1154 (Q6MNT2) of *B. bacteriovorus* were aligned to the CatA/KatA proteins of *Campylobacter jejuni* (Q59296), *Staphylococcus aureus* (Q2FYU7), *Pseudomonas aeruginosa* (O52762) and *Bordetella pertussis* (P0A323) using Clustal Omega. Consensus amino acid structure appears highly similar between CatA/Bd0798 and the catalase proteins tested (Q59296: 57.2%, Q2FYU7: 54.2%, O52762: 58.2%, P0A323: 60.4% and Q6MNT2: 59.8% percentage identity) (Figure 4.3.14). These alignments cover the entire length of the catalase proteins in each instance. Alignment with *Acinetobacter baumannii, Legionella pneumophila* and *Burkholderia cenopacea* were also considered but were excluded due to a high dissimilarity. This is potentially due to their annotation of catalase peroxidase, instead of catalase, meaning they belong to a different class of catalase.

Alignment of the catalase domains for each of the above proteins shows a marginally higher percentage identity (Q59296: 63.25%, Q2FYU7: 59.8%, O52762: 64.4%, P0A323: 66.5% and Q6MNT2: 64.0% percentage identity) (Figure 4.3.15). Alignments of the catalase immune responsive domains shows a lower percentage identity (Q59296: 32.6%, Q2FYU7: 33.3%, O52762: 35.4%, P0A323: 37.0% and Q6MNT2: 41.8% percentage identity) (Figure 4.3.16).

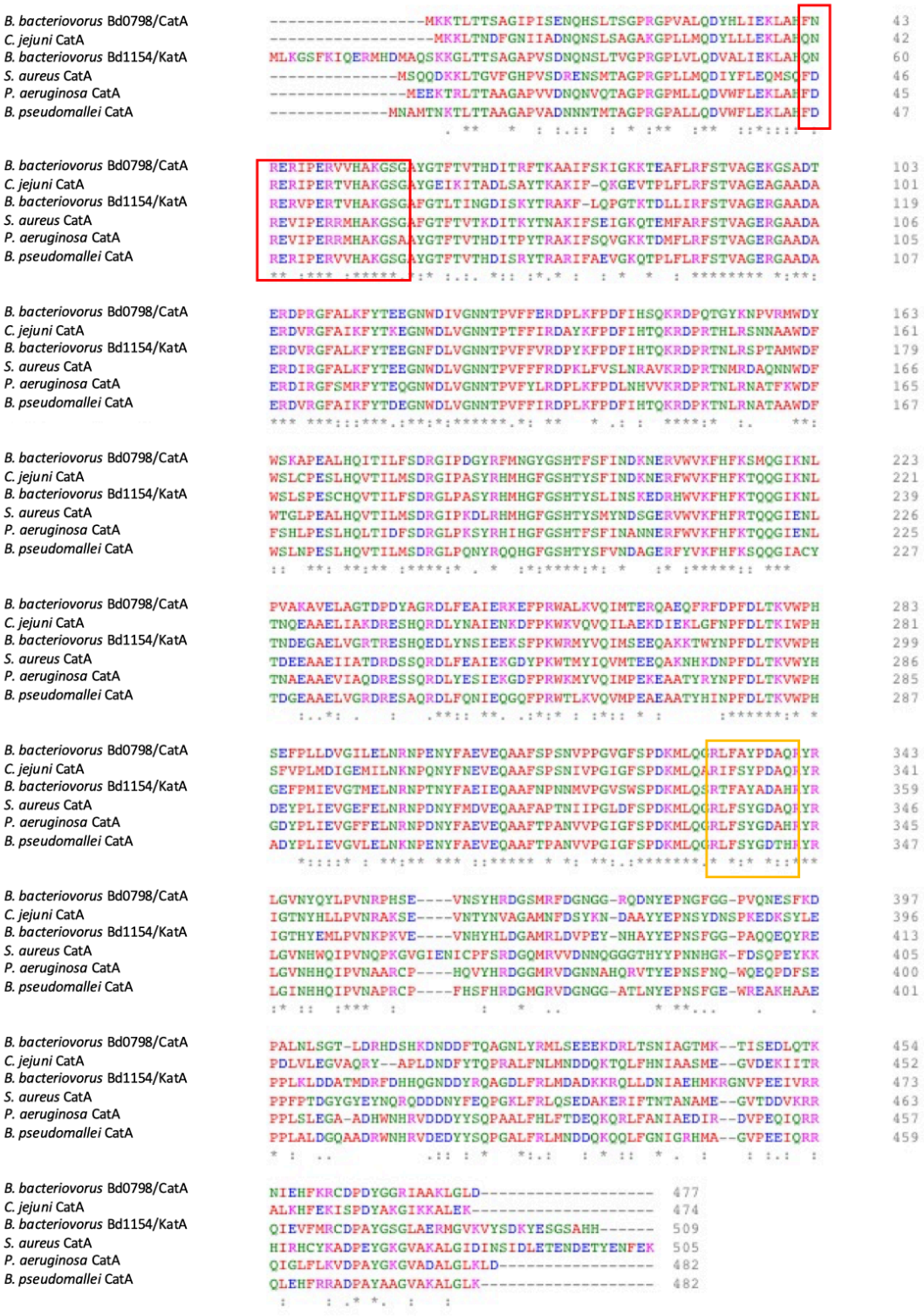

Figure 4.3.14: An alignment of Bd0798(CatA) to Bd1154(KatA) and CatA/KatA proteins of other bacterial pathogens. Red box indicates the hydrogen peroxide binding site/active site, that is highly conserved amongst catalases. The Catalase protein CatA/Bd0798 (Uniprot accession: Q6MPQ0) was aligned to KatA/Bd1154 (Q6MNT2) of *B. bacteriovorus* and the catA/katA proteins of *Campylobacter jejuni* (Q59296), *Staphylococcus aureus* (Q2FYU7), *Pseudomonas aeruginosa* (O52762) and *Bordetella pertussis* (P0A323) using Clustal Omega. Complete amino acid sequences are shown for each protein. Amino acids are coloured by their physicochemical properties. (*) indicates a conserved residue. (:) indicates amino acids sharing strongly similar properties. (.) indicates an amino acid sharing weakly similar properties.

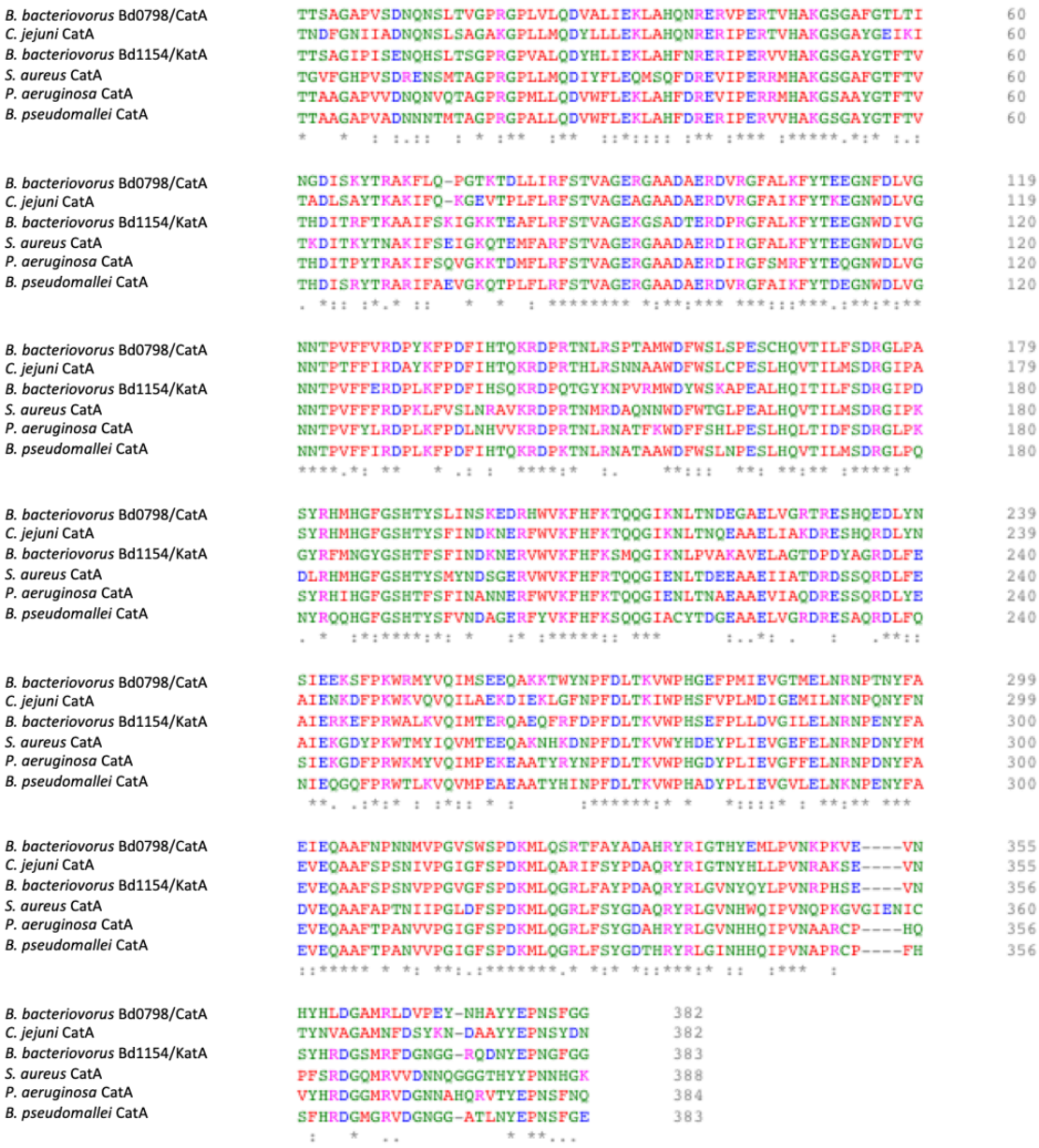

Figure 4.3.15: An alignment of the catalase domain of Bd0798 to Bd1154 and the catalase domains of CatA/KatA proteins of other bacterial pathogens. The catalase domain of the catalase protein CatA/Bd0798 (Uniprot accession: Q6MPQ0) was aligned to the catalase domain of *B. bacteriovorus* KatA/Bd1154 (Q6MNT2)*, Campylobacter jejuni* (Q59296), *Staphylococcus aureus* (Q2FYU7), *Pseudomonas aeruginosa* (O52762) and *Bordetella pertussis* (P0A323) using Clustal Omega. Complete amino acid sequences are shown for each domain. Amino acids are coloured by their physicochemical properties. (*) indicates a conserved residue. (:) indicates amino acids sharing strongly similar properties. (.) indicates an amino acid sharing weakly similar properties.

Figure 4.3.16: An alignment of the catalase immune responsive domain of Bd0798 to Bd1154 and the catalase immune responsive domain of CatA/KatA proteins of other bacterial pathogens. The catalase immune responsive domain of the catalase protein CatA/Bd0798 (Uniprot accession: Q6MPQ0) was aligned to the catalase domain of *B. bacteriovorus* KatA/Bd1154 (Q6MNT2)*, Campylobacter jejuni* (Q59296), *Staphylococcus aureus* (Q2FYU7), *Pseudomonas aeruginosa* (O52762) and *Bordetella pertussis* (P0A323) using Clustal Omega. Complete amino acid sequences are shown for each domain. Amino acids are coloured by their physicochemical properties. (*) indicates a conserved residue. (:) indicates amino acids sharing strongly similar properties. (.) indicates an amino acid sharing weakly similar properties.

Predicted structure analyses

To compare the (predicted) structures of these two catalase homologues, I downloaded the PDB (Protein Data Bank) structural prediction files for both proteins from AlphaFold (470) and aligned them using TMalign (471) to compare their structures. Comparing the structures of Bd0798 and Bd1154, both have a highly similar predicted structure (Figure 4.3.17).

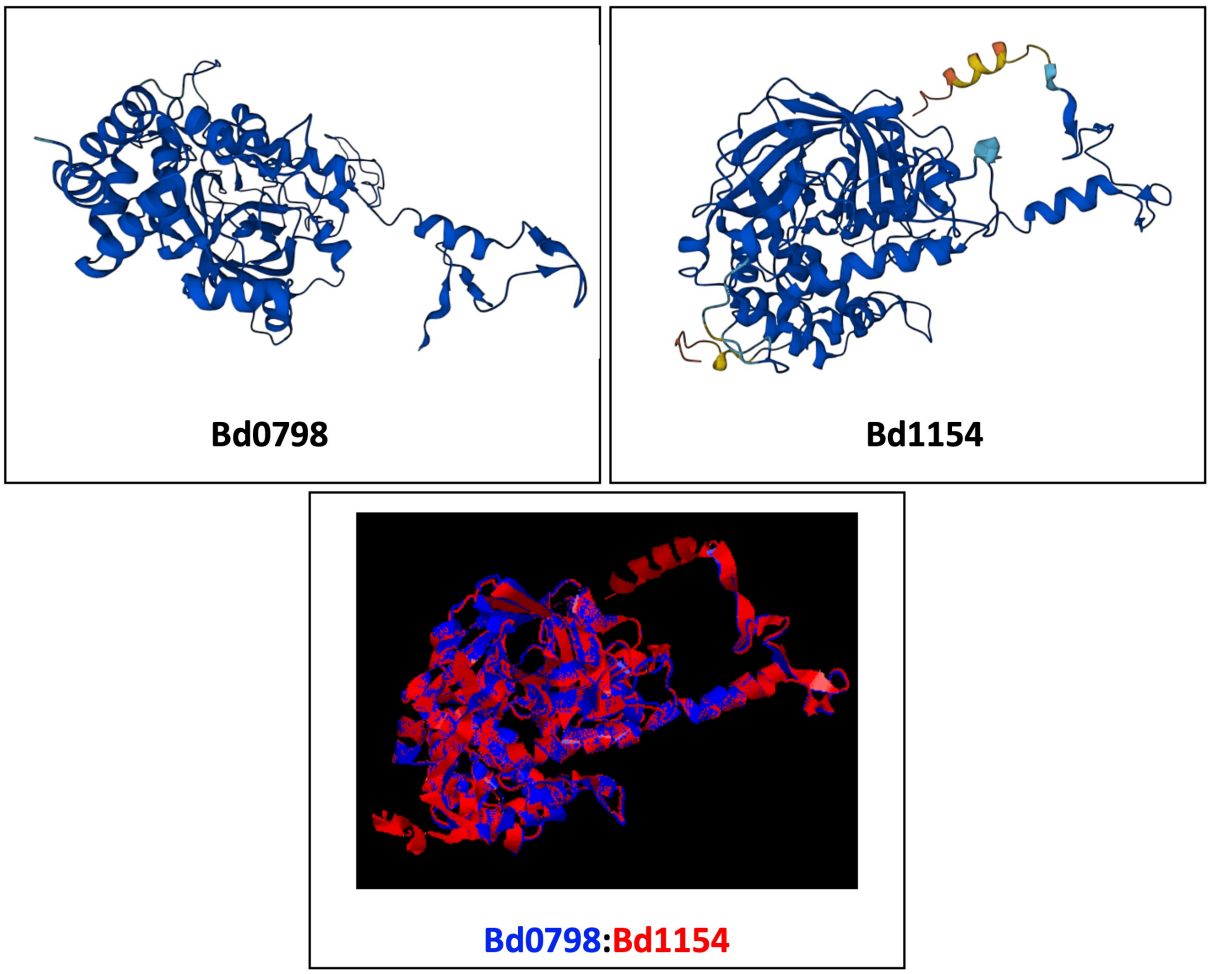

Figure 4.3.17: Predicted structures of the two catalase proteins, Bd0798 and Bd1154. Structural predictions and Protein Data Bank (.pdb) files were obtained from AlphaFold for Bd0798 (UniProt accession: Q6MPQ0; Top, Left) and Bd1154 (Q6MNT2; Top, Right). PDB files were aligned using TMPred to generate the structural overlay depicted (lower, centre). Bd0798 and Bd1154 have a highly similar structure.

4.3.2.2. Bd0799

Bd0799/AnkB is predicted to be an ankyrin domain protein, 18kDa in size and 161 amino acids in length (UniProt).

Analysis of predicted domain structures

Analysis of the predicted domains present within Bd0799, using PFam, highlighted the presence of two ankyrin repeat domains (Amino acids 45-77 and 78-110). Analysis using PFam and SignalP 6.0 confirms that no signal peptide is present within Bd0799, suggesting that it localises within the cytoplasm of the cell (Figure 4.3.18).

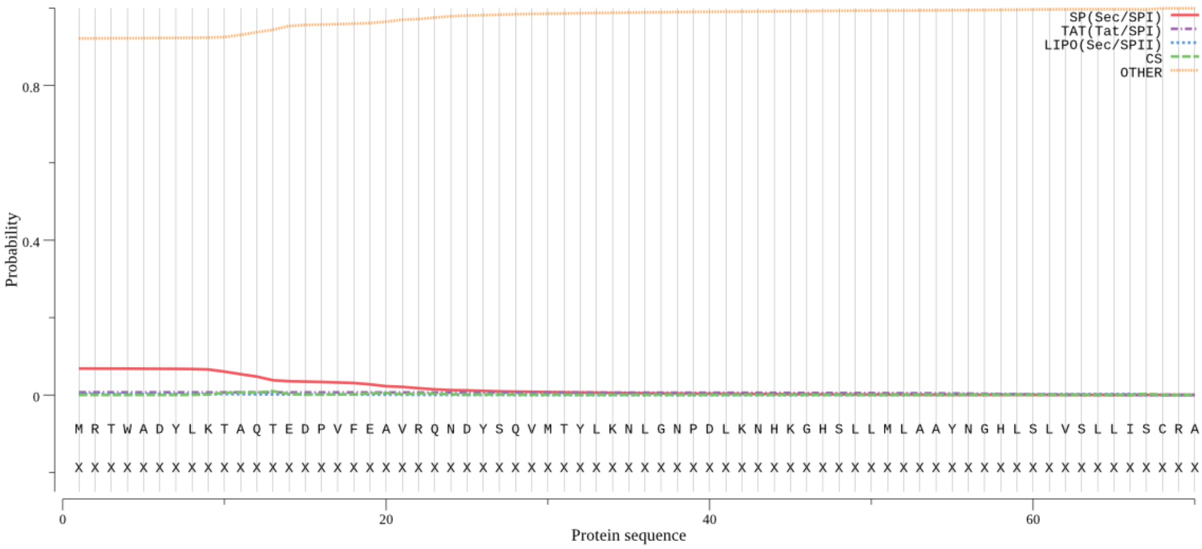

Figure 4.3.18: Prediction test for a signal peptide at the N-terminus of Bd0799. Figure generated using SignalP 6.0.

Gene neighbourhood and association analyses

Using STRING to analyse the predicted protein-protein interactions and functional enrichment, Bd0799 is predicted to interact with a different network of proteins to Bd0798/CatA.

Bd0799 is predicted to interact with its proposed catalase partner Bd0798/CatA, Bd0800, a putative septum formation protein, Bd0633/Pal, a peptidoglycan associated lipoprotein involved in cell division, and Bd3734/MglA, a gliding motility protein. Bd0799 is also predicted to interact with Bd1360, another membrane associated lipoprotein, Bd2718, a regulator of glycerol uptake and metabolism, Bd3148, a Serine/Threonine protein kinase and Bd0397, a Ppm family protein phosphatase (Figure 4.3.19).

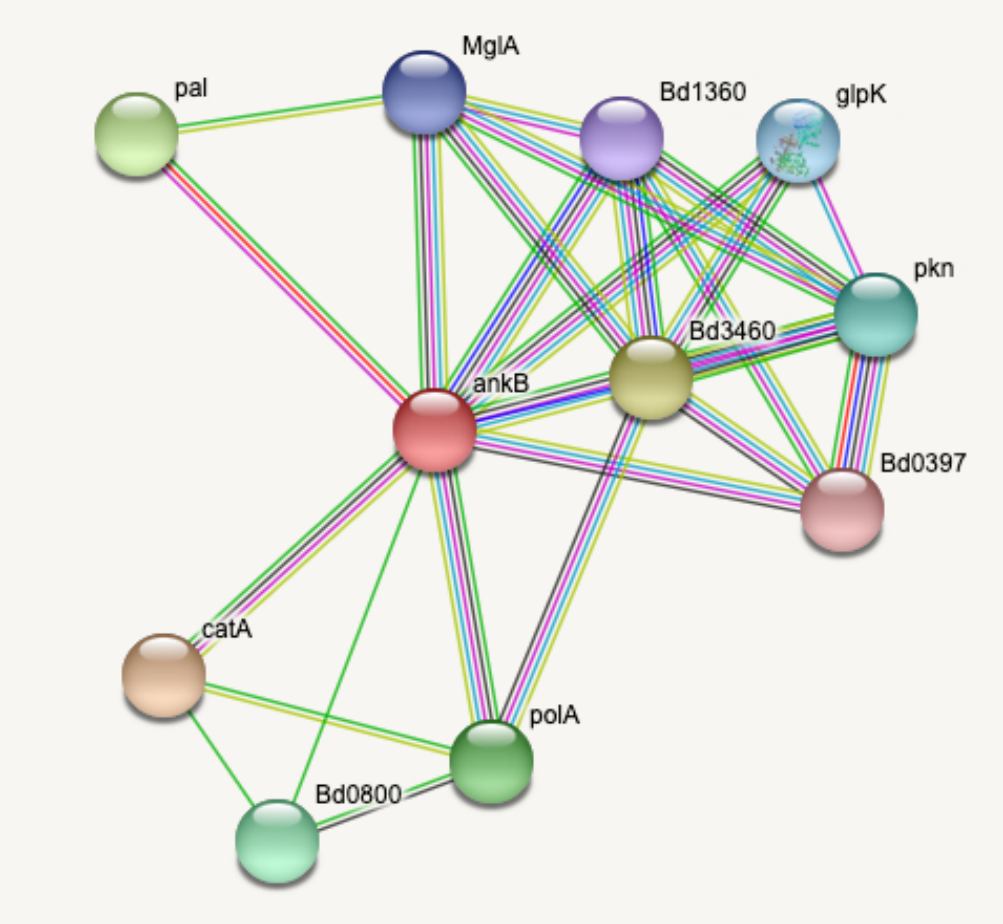

Figure 4.3.19: A schematic showing the predicted protein-protein interactions of Bd0799. Figure generated using STRING. Magenta threads represent experimentally determined interactions; Green threads represent gene neighbourhood interactions; Dark blue threads represent gene co-occurrence; Black threads represent co-expression; Lilac threads represent protein homology; Yellow threads represent textmining (i.e., associations in literature) (STRING).

Searches for homologues in *Bdellovibrio* and other bacterial species

Searches of the *B. bacteriovorus* HD100 genome, using BlastP to check for proteins with a high sequence similarity at the amino acid level to Bd0799 (Q6MPP9), reveals a second ankyrin AnkB protein, Bd1155 (Q6MNT1), which shows a 43.9% sequence similarity (Figure 4.3.20).

Excluding *Bdellovibrio* from our search, the closest structural homologue to Bd0799 was an ankyrin repeat protein from *Leptospira* alstonii. Alignment of Bd0799 to an ankyrin repeat protein of *Leptospira alstonii* (NCBI reference: WP_061249064.1) shows a 52% sequence similarity (Figure 4.3.21). Alignment of Bd0799 to ankyrin repeat protein of *Pseudomonas aeruginosa* (NCBI reference: WP_079384021.1) shows a 38% sequence similarity (Figure 4.3.21).

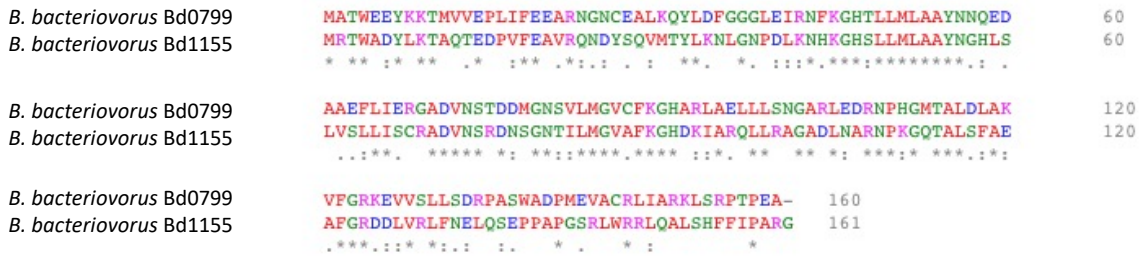

Figure 4.3.20: An alignment of Bd0799 to the other AnkB protein, Bd1155, in the *B. bacteriovorus* HD100 genome. Bd0799/AnkB of *B. bacteriovorus* (Uniprot accession: Q6MPP9) was aligned to Bd1155 (Q6MNT1) using Clustal Omega. Complete amino acid sequences are shown for each protein. Amino acids are coloured by their physicochemical properties. (*) indicates a conserved residue. (:) indicates amino acids sharing strongly similar properties. (.) indicates an amino acid sharing weakly similar properties.

Figure 4.3.21: An alignment of Bd0799 to the ankyrin proteins of *Leptospira alstonii* and *Pseudomonas aeruginosa*. Bd0799/AnkB of *B. bacteriovorus* (Uniprot accession: Q6MPP9) was aligned to the ankyrin proteins of *Leptospira alstonii* (NCBI reference: WP_061249064.1) and *Pseudomonas aeruginosa* (NCBI reference: WP_079384021.1) using Clustal Omega. Complete amino acid sequences are shown for each protein. Amino acids are coloured by their physicochemical properties. (*) indicates a conserved residue. (:) indicates amino acids sharing strongly similar properties. (.) indicates an amino acid sharing weakly similar properties.

Predicted structure analyses

To compare the (predicted) structures of these two ankyrin homologues, I downloaded the PDB (Protein Data Bank) structural prediction files for both proteins from AlphaFold (470) and aligned them using TMalign (471) to compare their structures. Comparing the structures of Bd0799 and Bd1155, both have a highly similar predicted structure in their core region (Figure 4.3.22), structurally, the N- and C- termini differ.

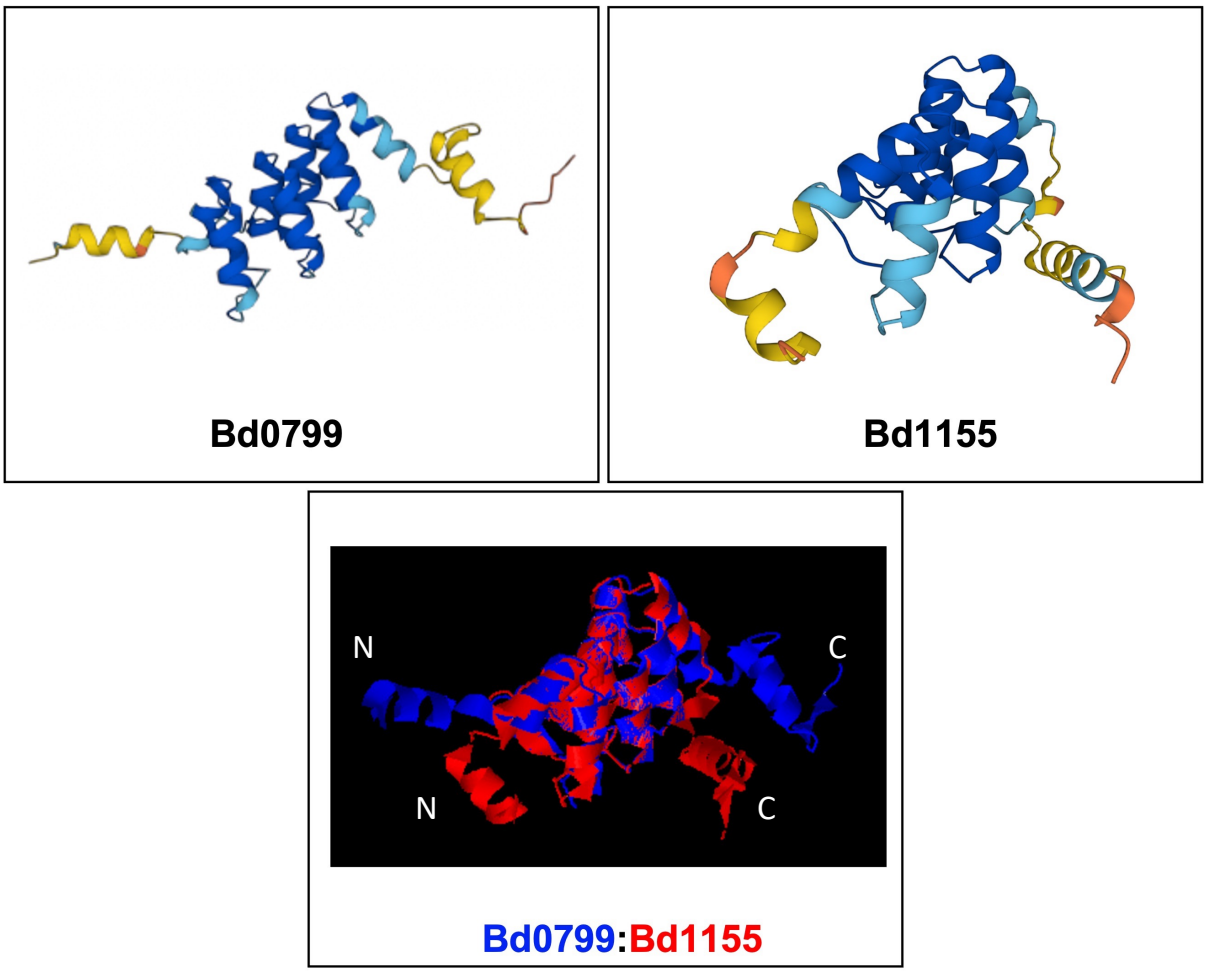

Figure 4.3.22: Predicted structures of the two ankyrin proteins, Bd0799 and Bd1155. Structural predictions and Protein Data Bank (.pdb) files were obtained from AlphaFold for Bd0799 (UniProt accession: Q6MPQ0; Top, Left) and Bd1155 (Q6MNT2; Top, Right). PDB files were aligned using TMPred to generate the structural overlay depicted (lower, centre). Bd0799 and Bd1155 have a highly similar structure at their core, but their N and C termini appear to differ (labelled).

4.3.2.3. Bd1154/KatA

Bd1154 (KatA) is predicted to be a catalase protein 58.5 kDa in size and 509 amino acids in length. Like Bd0798, Bd1154 is predicted to detoxify hydrogen peroxide into water and oxygen, assisting in oxidative stress tolerance. The gene *bd1154* is in a large, seven gene operon with *bd1155*, an AnkB protein that we hypothesised regulates the function of the catalase enzyme, and a cluster of hypothetical proteins (Figure 4.3.23) (xBase).

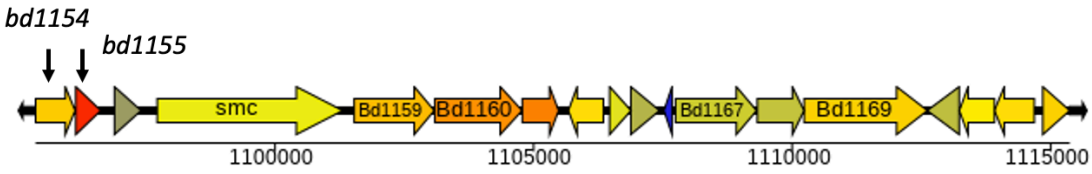

Figure 4.3.23: A schematic showing the gene neighbourhood of *bd1154*. Diagram taken from xBase.

Analysis of predicted domain structure

Analysis of the predicted domains present within Bd1154, using PFam, highlighted the presence of a catalase domain (Amino acids 23-406), containing the histidine and aparagine residue active sites (amino acids 70 and 142) and an Iron metal binding site (Amino acid 352), and a catalase-related immune-responsive domain (Amino acids 429-492). Analysis using PFam and SignalP 6.0 confirms that no signal peptide is present within Bd1154, suggesting that it detoxifies hydrogen peroxide within the cytoplasm of the cell (Figure 4.3.24).

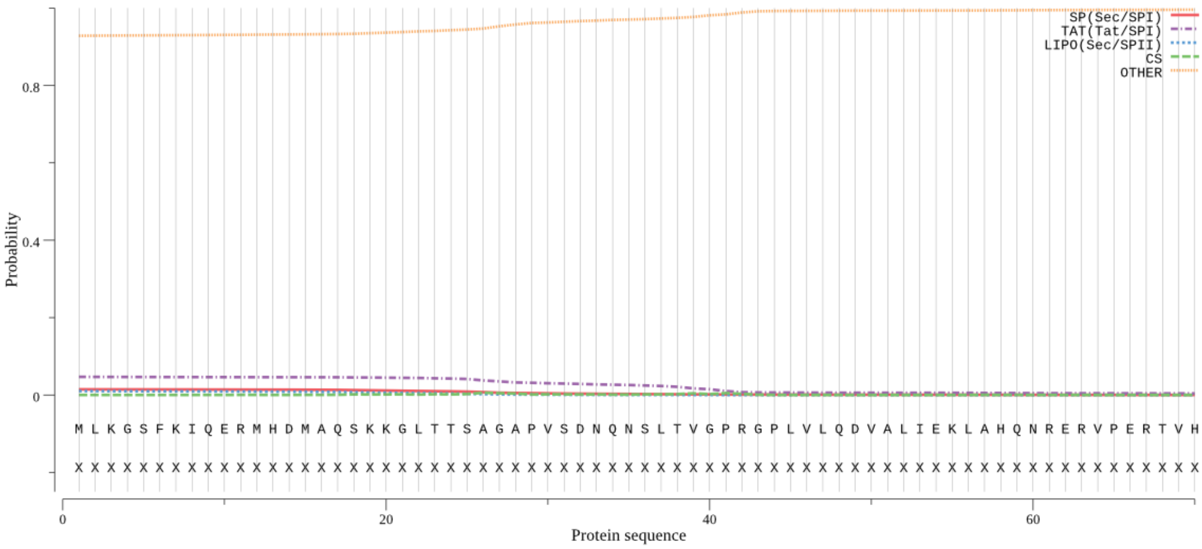

Figure 4.3.24: Prediction test for a signal peptide at the N-terminus of Bd1154. Figure generated using SignalP 6.0.

Gene neighbourhood and association analyses

Using STRING to analyse the predicted protein-protein interactions and functional enrichment, like Bd0798, Bd1154 is predicted to interact or interact with other oxidative stress related genes (Bd0295/SodC, Bd1401/SodC, Bd2407/SodB and Bd3617/SodB), its proposed regulatory ankyrin partner Bd1155/AnkB. Like Bd0798, Bd1154 is also associated with Bd2517/AhpC and a Tryparedoxin peroxidase (Bd3525), all of which also detoxify/metabolise hydrogen peroxide into water (Figure 4.3.25).

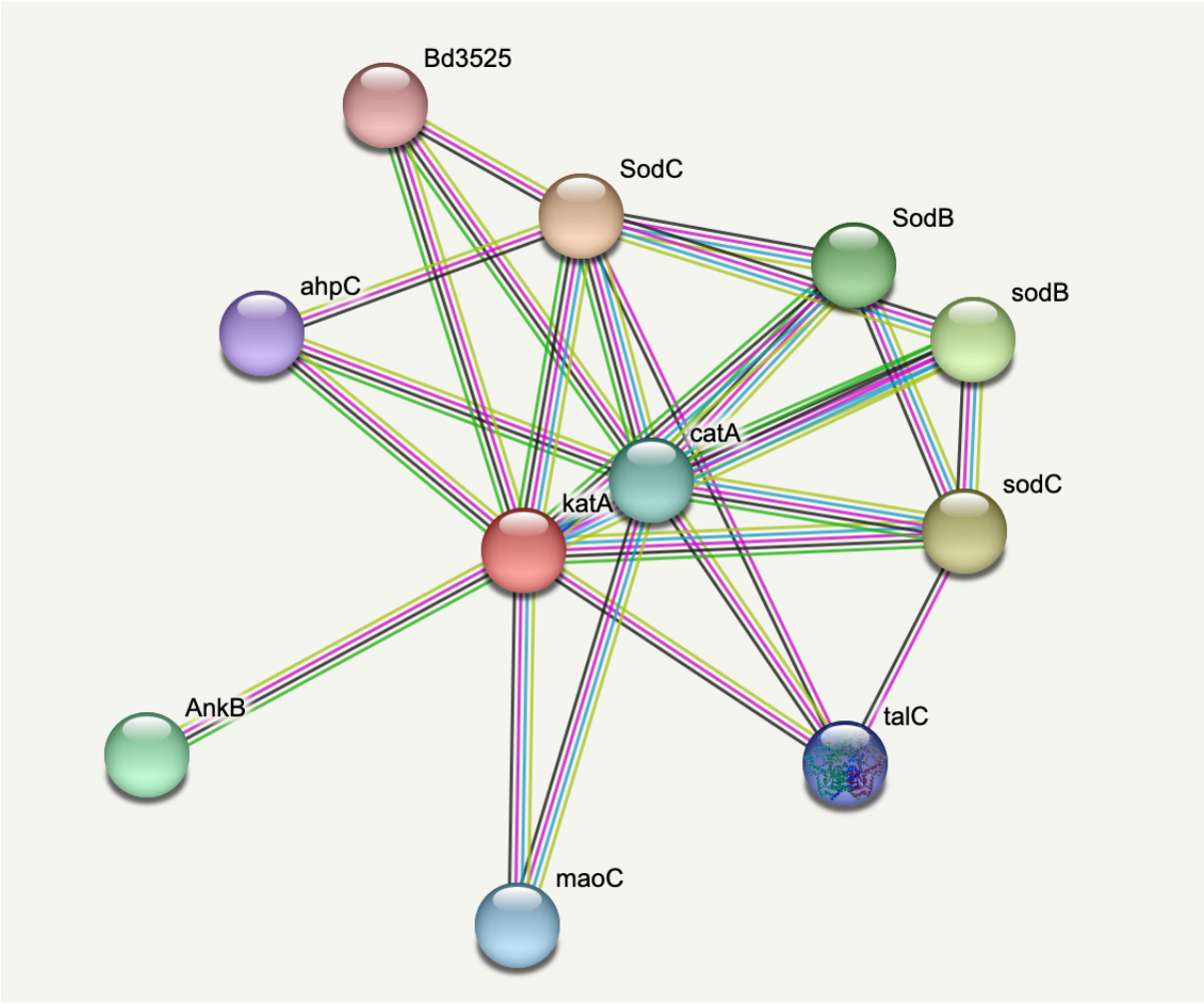

Figure 4.3.25: A schematic showing the predicted protein-protein interactions of Bd1154. Figure generated using STRING. Magenta threads represent experimentally determined interactions; Green threads represent gene neighbourhood interactions; Dark blue threads represent gene co-occurrence; Black threads represent co-expression; Lilac threads represent protein homology; Yellow threads represent textmining (i.e. associations in literature) (STRING).

4.3.2.4. Bd1155/ankB

Bd1155/AnkB is predicted to be an ankyrin domain protein, 17.7 kDa in size and 160 amino acids in length (UniProt).

Analysis of predicted domain structure

Like Bd0799, Analysis of the predicted domains present within Bd1155, using PFam, highlighted the presence of three ankyrin repeat domains (Amino acids 21-76). Analysis using PFam and SignalP 6.0 confirms that no signal peptide is present within Bd1155, suggesting that it localises within the cytoplasm of the cell (Figure 4.3.26).

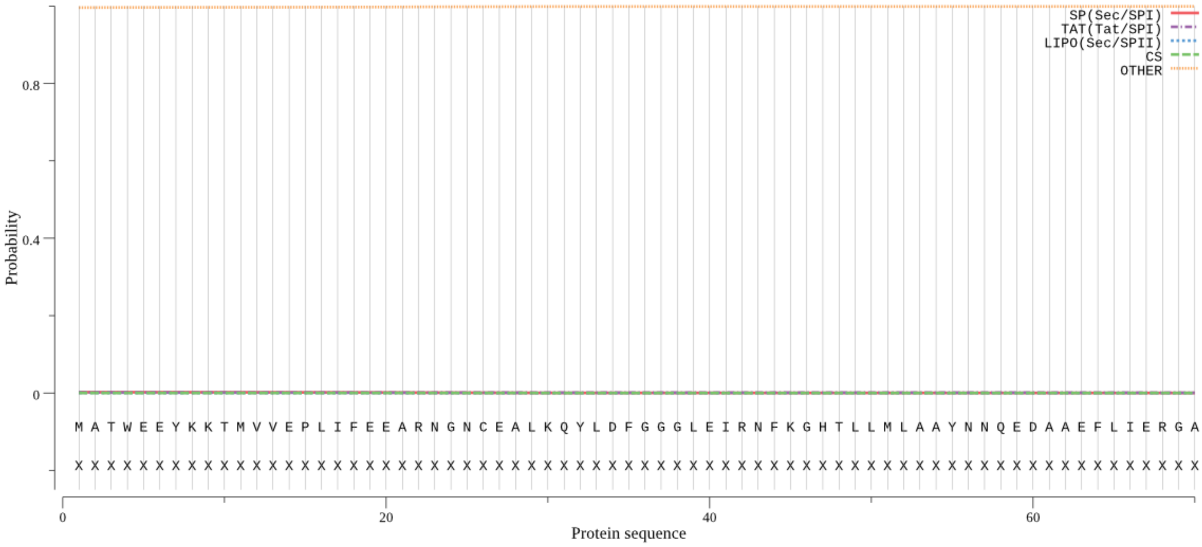

Figure 4.3.26: Prediction test for a signal peptide for Bd1155. Figure generated using SignalP 6.0.

Gene neighborhood and association analyses

Using STRING to analyse the predicted protein-protein interactions and functional enrichment, Bd1155 is predicted to interact with a different network of proteins to Bd1154/KatA, and a similar network of proteins to Bd0799.

Bd1155 is predicted to interact with its proposed catalase partner Bd1154/KatA. Like Bd0799, Bd1155 is predicted to interact with Bd3734/MglA, Bd1360, Bd2718, Bd3148 and Bd0397. Unlike Bd0799, Bd1155 is also predicted to be associated with Bd1152/PqiB and Bd1153/PqiA, both paraquat inducible proteins, although this is likely a gene neighbourhood association (Figure 4.3.27).

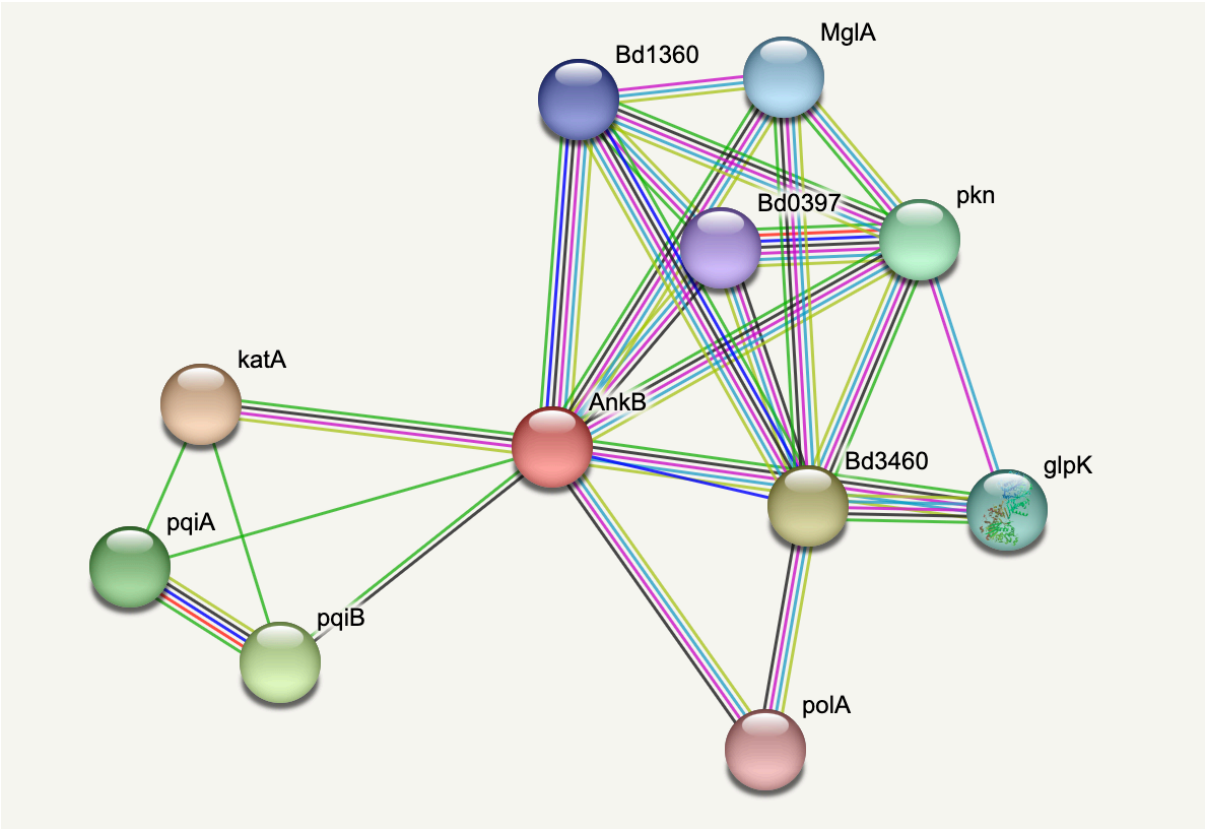

Figure 4.3.27: A schematic showing the predicted protein-protein interactions of Bd1155. Figure generated using STRING. Magenta threads represent experimentally determined interactions; Green threads represent gene neighbourhood interactions; Dark blue threads represent gene co-occurrence; Black threads represent co-expression; Lilac threads represent protein homology; Yellow threads represent textmining (i.e. associations in literature) (STRING).

Searches for homologues in *Bdellovibrio* and other bacterial species

Excluding *Bdellovibrio* from our search, the closest structural homologue to Bd1155 was an ankyrin repeat protein from *Leptospira interrogans*. Alignment of Bd1155 to an ankyrin repeat protein of *Leptospira interrogans* (NCBI reference: WP_017851344.1) shows a 52% sequence similarity (Figure 4.3.28). Alignment of Bd1155 to ankyrin repeat protein of *Pseudomonas aeruginosa* (NCBI reference: WP_079385475.1) shows a 38% sequence similarity (Figure 4.3.28).

Figure 4.3.28: An alignment of Bd1155 to the ankyrin proteins of *Leptospira interrogans* and *Pseudomonas aeruginosa*. Bd1155/AnkB of *B. bacteriovorus* (Uniprot accession: Q6MNT1) was aligned to the ankyrin proteins of *Leptospira interrogans* (NCBI reference: WP_017851344.1) and *Pseudomonas aeruginosa* (NCBI reference: WP_079385475.1) using Clustal Omega. Complete amino acid sequences are shown for each protein. Amino acids are coloured by their physicochemical properties. (*) indicates a conserved residue. (:) indicates amino acids sharing strongly similar properties. (.) indicates an amino acid sharing weakly similar properties.

4.3.2.1. Bd2517/AhpC

Bd2517/AhpC is predicted to be an alkyl hydroperoxide reductase C enzyme 21 kDa in size and 188 amino acids in length. AhpC detoxifies hydrogen peroxide into alcohol and water, using NADH as a co-factor (Figure 4.3.29).

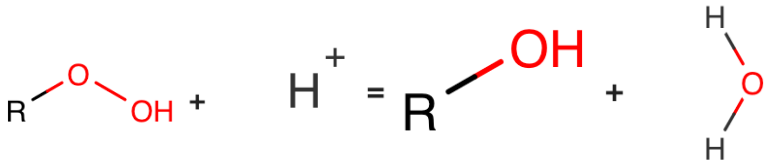

Figure 4.3.29: A schematic showing the chemical reaction of the detoxification of hydrogen peroxide into alcohol and water, which is catalysed by AhpC. Figure adapted from Uniprot.

Analysis of predicted domain structure

Analysis of the domain structures of Bd2517 shows that a Thioredoxin domain is present at the N-terminus of Bd2517 (Amino acids 3-158), with the active site at amino acid 48, followed by a C-terminal domain (of 1-Cys peroxiredoxin) (amino acids 157-179) (PFam). Analysis of the amino acid sequence using SignalP 6.0 also confirms the absence of a signal peptide (Figure 4.3.30), suggesting that Bd2517 acts within the cytoplasm of the cell.

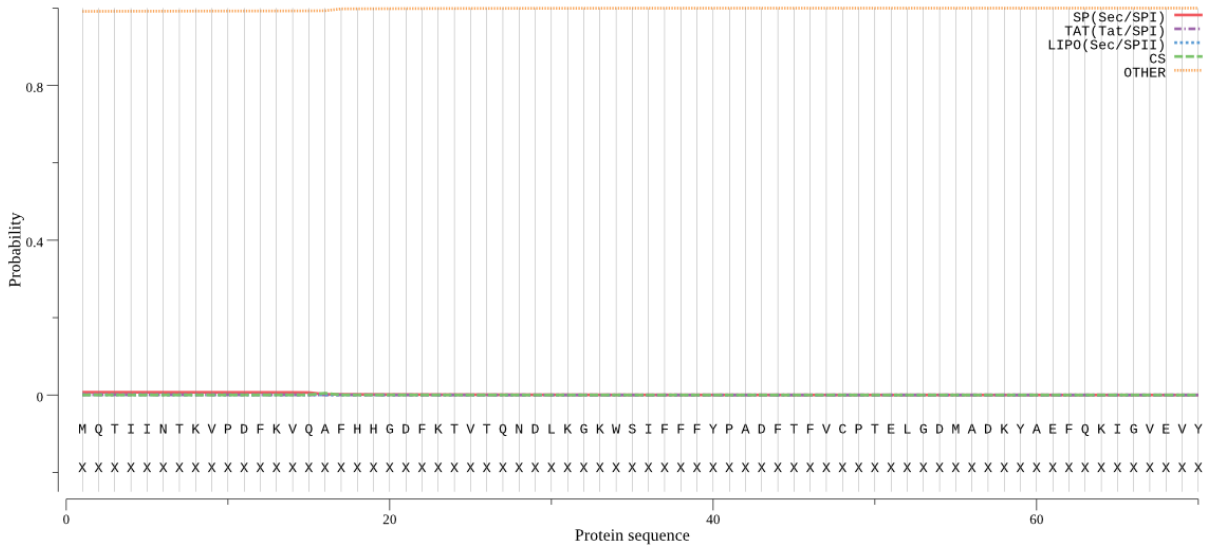

Figure 4.3.30: Prediction test for a signal peptide for the protein Bd2517/AhpC. Figure generated using SignalP 6.0.

Gene neighborhood and association analyses

The gene *bd2517* is part of a three gene operon with *ahpF/bd2518*, another alkyl hydroperoxide reductase that acts as a co-factor to increase the efficiency of AhpC-mediated hydrogen peroxide detoxification. The gene *bd2517* is also in an operon with *bd2519*, a dipeptidyl aminopeptidase. AhpC expression is typically under the control of an OxyR regulon, a redox sensitive transcriptional activator, such as Bd2516, although *bd2516* is in the opposing orientation to *bd2517*. *bd2517* is also in the same neighbourhood as two hypothetical genes (*bd2512* and *bd2514*), a citrate synthase (*bd2511*), a phosphodiesterase/alkaline phosphatase D gene (*bd2513*/*phoD*), a Sec-independent translocase gene (*bd2515*), a putative lactoylglutathione lyase (*bd2520*) and another aminopeptidase (*bd2521*/*pepN*) (Figure 4.3.31).

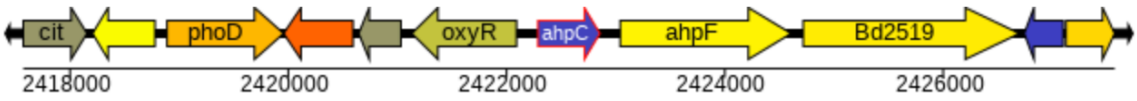

Figure 4.3.31: A schematic showing the gene neighbourhood of *bd2517*. Diagram taken from xBase.

Using STRING to analyse the predicted protein-protein interactions of Bd2517, it is predicted to associate/interact with a similar network of proteins to CatA/Bd0798, KatA/Bd1154 and Bd0295/SodC, to which Bd2517 associates with the first two. Bd2517 associates with ResA/Bd2208, ResA/Bd1980 and Bd1341, a putative disulphide isomerase associated with thioredoxin function, like Bd0295. Bd2517 also associates with its neighbouring AhpF protein (Bd2518), a thioredoxin reductase (Bd0373), a FAD binding protein (Bd2839) and a Spb1 foreserine protease (Figure 4.3.32). This further supports the role of Bd2517 in hydrogen peroxide detoxification.

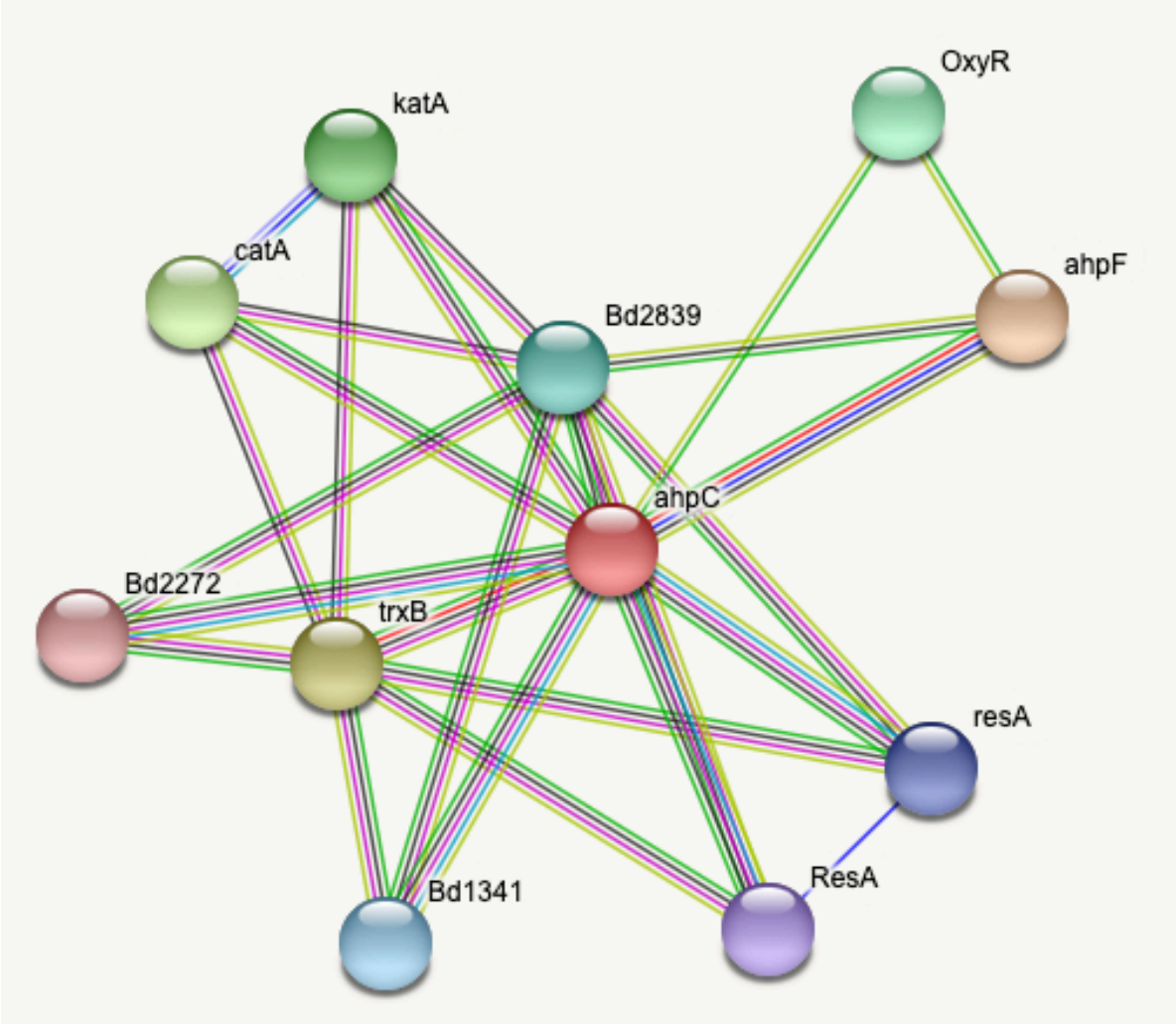

Figure 4.3.32: A schematic showing the predicted protein-protein interactions of Bd2517. Figure generated using STRING. Magenta threads represent experimentally determined interactions; Green threads represent gene neighbourhood interactions; Dark blue threads represent gene co-occurrence; Black threads represent co-expression; Lilac threads represent protein homology; Yellow threads represent textmining (i.e. associations in literature) (STRING).

Searches of the *B. bacteriovorus* HD100 genome, using BlastP, for homologues to Bd2517 highlights two peroxiredoxins/thioredoxin peroxidases of low sequence similarity, Bd3525 and Bd1805 with sequence similarities of 40.5% and 30.2% respectively (Alignments: Figure 4.3.33).

Figure 4.3.33: An alignment of Bd2517 to the other peroxidase proteins in the *B. bacteriovorus* HD100 genome. Bd2517/AhpC of *B. bacteriovorus* (Uniprot accession: Q6MK92) was aligned to the thioredoxin proteins Bd1805 (Q6MM40) and Bd3525 (Q6MHL7) using Clustal Omega. Complete amino acid sequences are shown for each protein. Amino acids are coloured by their physicochemical properties. (*) indicates a conserved residue. (:) indicates amino acids sharing strongly similar properties. (.) indicates an amino acid sharing weakly similar properties.

Searches for Homologues in *Bdellovibrio* and other bacterial species

Searches for structural homologues in known bacterial pathogens also revealed a high similarity (at the consensus amino acid level) of Bd2517/AhpC with the AhpC proteins of other bacteria. Bd2517/AhpC (Uniprot accession: Q6MK92) of *B. bacteriovorus* was aligned to the AhpC proteins of *Salmonella* Typhimurium (P0A251), *Shigella flexneri* (P0AE11), *E. coli* (POAE08), *Pseudomonas aeruginosa* (Q02UU0), *Staphylococcus aureus* (P0A0B7), *Francisella tularensis* (A0A6I4RTP5), *Mycobacterium tuberculosis* (P9WQB7) and *Helicobacter pylori* (P56876) using Clustal Omega. Consensus amino acid structure appears similar between Bd2517/AhpC and the AhpC proteins of *S. typhimurium* (65.6% sequence identity), *S. flexneri* (64.5%), *E. coli* (64.5%), *P. aeruginosa* (60.75%) and *S. aureus* (56.9%). The consensus amino acid sequence was less similar for *F. tularensis* (38.0%), *M. tuberculosis* (37.7%) and *H. pylori* (35.7%) (Figure 4.3.34).

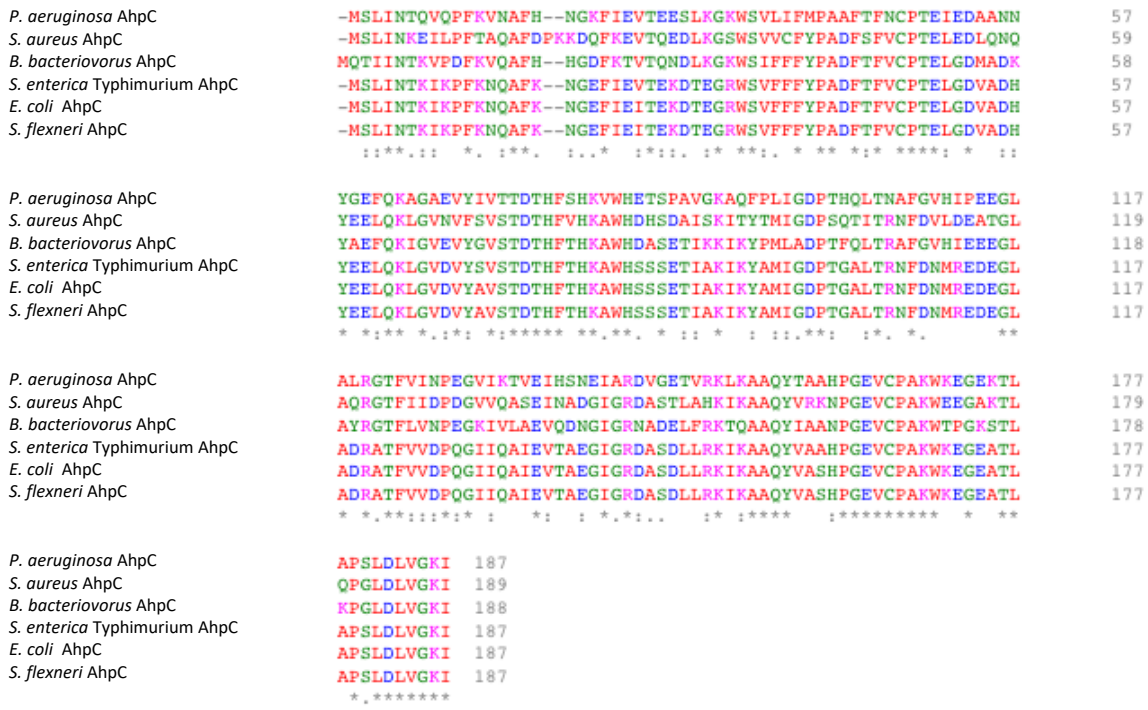

Figure 4.3.34: An alignment of Bd2517 to the AhpC proteins in bacterial pathogens. Bd2517/AhpC of *B. bacteriovorus* (Uniprot accession: Q6MK92) was aligned to the AhpC proteins of *Salmonella* Typhimurium (P0A251), *Shigella flexneri* (P0AE11), *E. coli* (POAE08), *Pseudomonas aeruginosa* (Q02UU0) and *Staphylococcus aureus* (P0A0B7) using Clustal Omega. Complete amino acid sequences are shown for each protein. Amino acids are coloured by their physicochemical properties. (*) indicates a conserved residue. (:) indicates amino acids sharing strongly similar properties. (.) indicates an amino acid sharing weakly similar properties.

4.3.2.2. Bd2518/AhpF

Like Bd2517/AhpC, Bd2518/AhpF is an alkyl hydroperoxide reductase protein (F subunit) that detoxifies hydrogen peroxide into alcohol and water within the cell. Bd2518/AhpF is 56.4 kDa in size and 521 amino acids in length.

Analysis of predicted domain structure

Analysis of the domain structures present within Bd2518 (PFam) shows a thioredoxin-like fold (amino acids 125-194) and a pyridine nucleotide-disulphide oxidoreductase domain (amino acids 218-506). There are also two FAD binding sites (amino acids 219-234 and 480-490) and a NAD^+ binding site (amino acids 359-373). Analysis of the amino acid sequence using SignalP 6.0 also confirms the absence of a signal peptide (Figure 4.3.35), suggesting that Bd2518 acts within the cytoplasm of the cell.

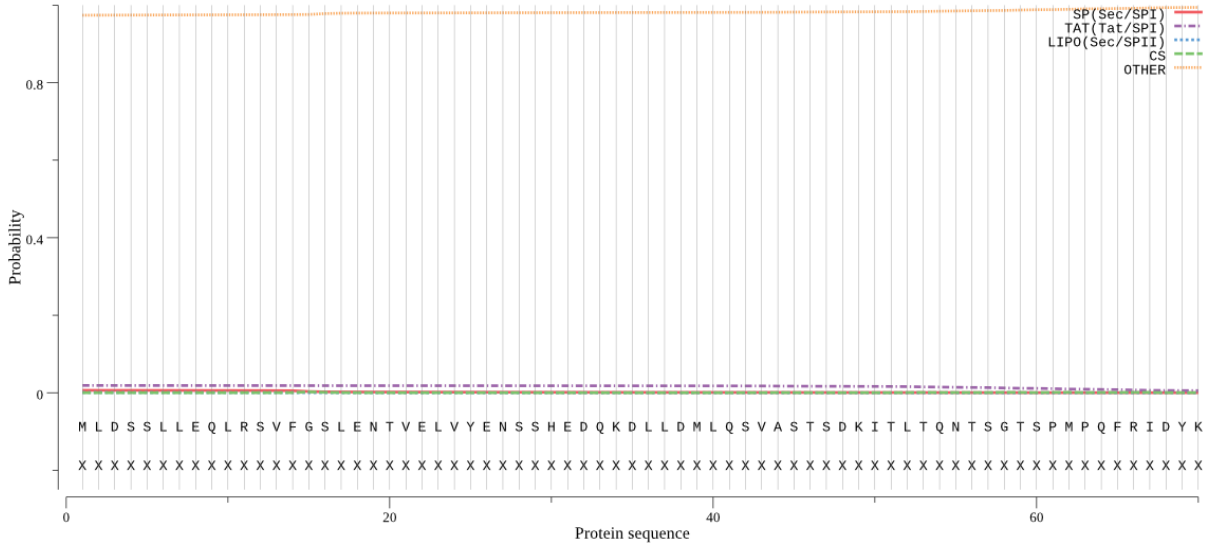

Figure 4.3.35: Prediction Test for a Signal Peptide for the protein Bd2518/AhpF. Figure generated using SignalP 6.0.

Gene neighbourhood and association analyses

Like Bd2517/AhpC, Bd2518/AhpF is predicted (STRING) to interact with Bd2516/OxyR, Bd2517/AhpC (it's subunit partner) and Bd2839, a FAD binding protein. In addition to this, Bd2518 is predicted to interact with Bd2519, likely because it is adjacent to Bd2518, and Bd3525, a Tryparedoxin peroxidase which I highlighted earlier as having a small amino acid sequence homology to Bd2517 (Figure 4.3.36).

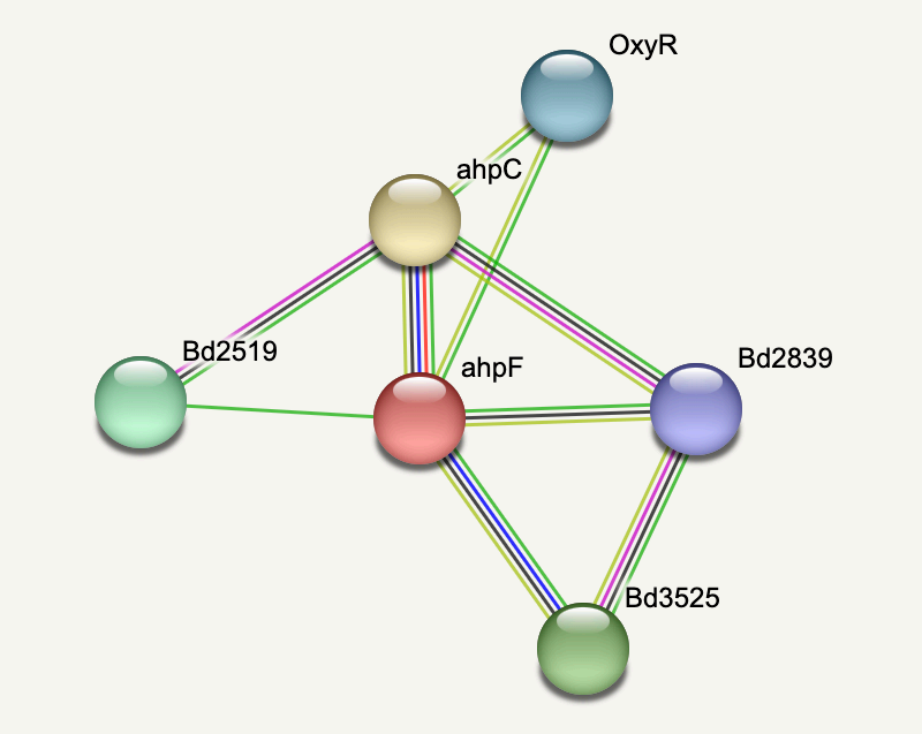

Figure 4.3.36: A schematic showing the predicted protein-protein interactions of Bd2518. Figure generated using STRING. Magenta threads represent experimentally determined interactions; Green threads represent gene neighbourhood interactions; Dark blue threads represent gene co-occurrence; Black threads represent co-expression; Lilac threads represent protein homology; Yellow threads represent textmining (i.e. associations in literature) (STRING).

Searches for homologues in *Bdellovibrio* and other bacterial species

Searches of the *B. bacteriovorus* HD100 genome, using BlastP, for homologues to Bd2518 suggest no homologues of AhpF are present. Searches for structural homologues in known bacterial pathogens reveal a single homologue in *P. aeruginosa* (Uniprot ID: Q9I6Z2), to which Bd2518 has a sequence similarity of 47.1% (Figure 4.3.37), across the entire length of both proteins.

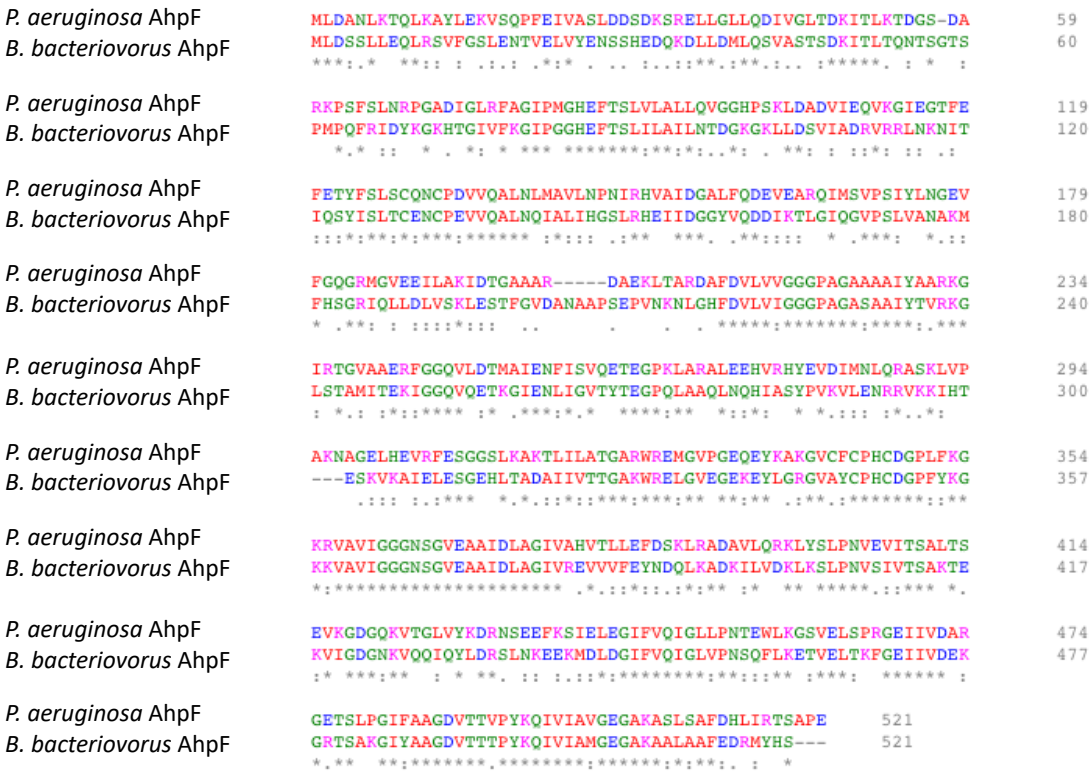

Figure 4.3.37: An alignment of Bd2518 to the AhpF protein of *P. aeruginosa*. Bd2518/AhpF of *B. bacteriovorus* (Uniprot accession: Q6MK91) was aligned to the AhpF protein of *P. aeruginosa* (Q9I6Z2) using Clustal Omega. Complete amino acid sequences are shown for each protein. Amino acids are coloured by their physicochemical properties. (*) indicates a conserved residue. (:) indicates amino acids sharing strongly similar properties. (.) indicates an amino acid sharing weakly similar properties.

4.3.3. Proteins with predicted roles in macrophage in other bacteria, outside of oxidative stress tolerance

4.3.3.1. Bd0017/SurA

Bd0017/SurA is predicted to be a survival protein 34.8 kDa in size and 307 amino acids in length (UniProt). SurA is a periplasmic chaperone protein that facilitates the correct folding of outer membrane proteins and porins in Gram-negative bacteria (472), and therefore has an important effect on outer membrane permeability and LPS composition.

Analysis of predicted domain structure

Analysis of the predicted domains present within Bd0017, using PFam, highlighted a SurA N-terminal domain, a helical domain of unknown function (amino acids 12-128), and a rotamase PPIase domain (Amino acids 171-260). *E. coli* SurA contains two PpiC-like domains/PPIase (peptidyl-prolyl cis-trans isomerase) domains which accelerate protein folding. Bd0017 only has one PPIase domain. Initial investigations using PFam and SignalP 6.0 suggested that Bd0017 did not have a signal peptide and therefore was not secreted and would localize in the cytoplasm of the bacterial cell (Figure 4.3.38). This was unusual, compared to other bacterial SurA proteins which contain a signal peptide.

However, SurA proteins in other bacteria are well documented as periplasmic proteins, therefore it was unusual that Bd0017 was lacking a signal peptide for secretion across the cytoplasmic membrane. Comparison of Bd0017, to SurA in other *Bdellovibrio* species (Predatorily invasive *B. bacteriovorus* str. Tiberius and epibiotic strain *Pseudobdellovibrio exovorus* which does not invade prey and attaches to the outside), revealed that *P. exovorus* SurA contained a signal peptide (Figure 4.3.39).

I retrieved the nucleotide sequence for *bd0017* and the SurA proteins from *B. bacteriovorus* str. Tiberius (*bdt*_0016) and *P. exovorus* (*A11Q_13*), plus 100bp of N-terminal flanking and aligned these DNA sequences using BLAST (Figure 4.3.40).

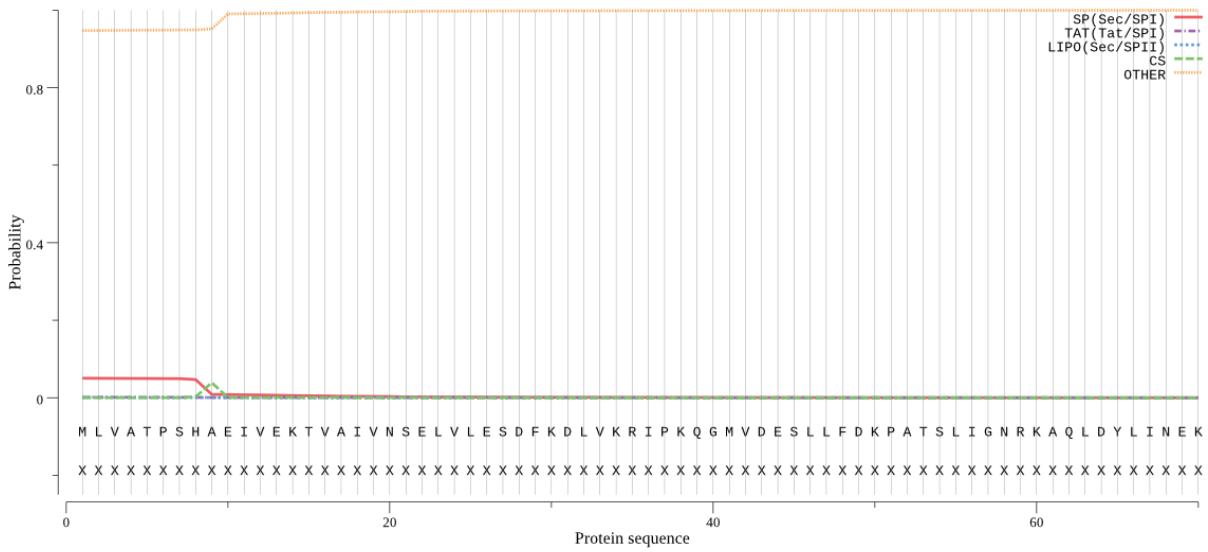

Figure 4.3.38: Prediction test for a signal peptide for Bd0017. Figure generated using SignalP 6.0.

```
P. exovorus SurA                    MKMLFVKLFAISFLFFSSLVASSQAHAKEVVNKIITIVNEEIILQSDLADMDKRIDRIGS   60
B. bacteriovorus SurA               ------------------MLVATPSHAEIVEKTVAIVNSELVLESDFKDLVKRIPKQGM   41
B. bacteriovorus str. Tiberius SurA ------------------------------MEKTVAIVNSELVLESDFKDLVKRIPKQGM   30
                                                        ::* ::***.*::*:**: *: *** : *

P. exovorus SurA                    VDETLLLGNKVESLKGNKKAQLEFLIREKLVDSEIKRQNMTVADEQVTAEISQMAKKNQM   120
B. bacteriovorus SurA               VDESLLFDKPATSLIGNRKAQLDYLINEKILQSEIKRLNLAVTNDRVESELKEMARKNQV   101
B. bacteriovorus str. Tiberius SurA VDESLLFDKPATSLVGNRKAQLDYLINEKILQSEIKRLNLAVTNDRVESELKEMARKNQV   90
                                    ***:**:.: . ** **:****::**.**:::***** *::*::::* :*:.:**:***:

P. exovorus SurA                    SSAEFASYMKSQGYTVDQYKVVLKTRMERQTFFERDIISKLRITDEDAYSVYRANAPNYR   180
B. bacteriovorus SurA               SEAELAKVIQQQGVSMDDYRRFLKDSIEKRSLMDAEIISKLRISDEDALNEYLKTNPNNR   161
B. bacteriovorus str. Tiberius SurA SETELAKVIQQQGVSMDDYRRFLKDSIEKRSLMDAEIISKLRISDEDALNEYLKTNPNNR   150
                                    *.:*:*. ::.** ::*:*: .**  :*::::::: :*******:**** . *  . ** *

P. exovorus SurA                    PSVSEYRIAQIFFSTRKGGDEAALTRARAASERLRAGESFESLANQVDETPGANKDGVLG   240
B. bacteriovorus SurA               PSIDEFSVSHIFFNPKKGGAEASIKRAETVLGKLRSGENFENLAQQFSEDPNFSTGGALG   221
B. bacteriovorus str. Tiberius SurA PSIDEFSVSHIFFNPKKGGAEASIKRAETVLGKLRSGENFENLAQQFSEDPNFSTGGALG   210
                                    **:.*: :::***. :*** **::.**.:.  :**:**.**.**:*..* *. ...*.**

P. exovorus SurA                    TFKSGEFAPALERGVESLSVGETSGIIEGSTGYHIIKLLSKNTILDPNFVRVKEQIKAGL   300
B. bacteriovorus SurA               TFKSGEFLPEIEEAISSLKVNETTPIVKSRMGFHIVKLTGKKLTTDPKFERAKDKIKAQL   281
B. bacteriovorus str. Tiberius SurA TFKSGDFLPEIEEAISSLKVNETTPIVKSRMGFHIVKLTGKKLTTDPKFERAKDKIKAQL   270
                                    *****:* * :*..:.**.*.**: *::.  *:**:** .*:   **:* *.*::*** *

P. exovorus SurA                    VQQNFERQLKNWFEIKKSQAHIENLNNETP  330
B. bacteriovorus SurA               LENSFKRQLKNWLQTKRDESFIRINE----  307
B. bacteriovorus str. Tiberius SurA LENSFKRQLKNWLQSKRDESFIRINE----  296
                                    :::.*:******:: *:.::.*.  :
```

Figure 4.3.39: An alignment of Bd0017 to the other SurA proteins in *B. bacteriovorus* str. Tiberius and *Pseudobdellovibrio exovorus.* Bd0017/SurA of *B. bacteriovorus* (Uniprot accession: Q6MRQ7) was aligned to *B. bacteriovorus* str. Tiberius Bdt_0016 (K7YT10) and *P. exovorus* A11Q_13 (M4V4X8) using Clustal Omega. Green text indicates a signal peptide. Red text indicates the SurA N-terminal domain. Purple text indicates the rotamase domain. Complete amino acid sequences are shown for each protein. (*) indicates a conserved residue. (:) indicates amino acids sharing strongly similar properties. (.) indicates an amino acid sharing weakly similar properties.

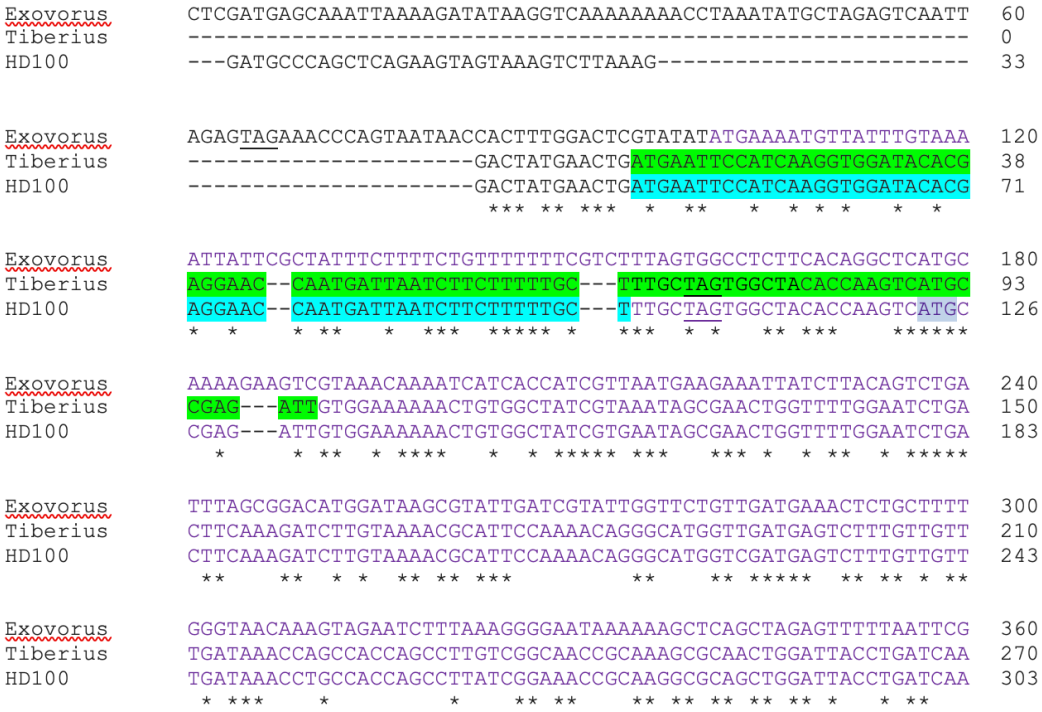

Figure 4.3.40: An alignment of *bd0017* to the other SurA nucleotide sequences in *B. bacteriovorus* str. Tiberius and *Pseudobdellovibrio exovorus*. The nucleotide sequence encoding Bd0017/SurA of *B. bacteriovorus* (Uniprot accession: Q6MRQ7) was aligned to nucleotide sequences encoding *B. bacteriovorus* str. Tiberius Bdt_0016 (K7YT10) and *P. exovorus* A11Q_13 (M4V4X8) using Clustal Omega. Green highlight indicates the N-terminal upstream nucleotide sequence from *B. bacteriovorus* str. Tiberus that aligned to *surA* of *P. exovorus*. Blue highlight indicates the N-terminal upstream nucleotide sequence from *B. bacteriovorus* HD100 that aligned to *surA* of *P. exovorus*. Grey highlight indicates the original start site of *bd0017*. (*) indicates a conserved nucleotide.

The nucleotide sequence upstream of *bd0017*, that was homologous and aligned to the nucleotide sequence encoding the signal peptide of A11Q_13 (ATG-AAT-TCC-ATC-AAG-GTG-GAT-ACA-CGA-GGA-ACC-AAT-GAT-TAA-TCT-TCT-TTT-TGCT) was converted to an amino acid sequence, using ExPASY, (MNPSRWIHEEPMINLLFA) and then pasted upstream of the amino acid sequence of Bd0017. After checking that the additional N-terminal sequence was in-frame with the start of Bd0017, I checked for a signal peptide using SignalP 6.0. Further investigation revealed that the initial annotation of the *B. bacteriovorus* HD100 genome had misannotated the start site of *bd0017*, and by traversing upstream of *bd0017*, a signal peptide was encoded upstream of the predicted start site of *bd0017*. Analysis using SignalP 6.0 confirms that a signal peptide is present within Bd0017, suggesting that it localises within the periplasm of the cell (Figure 4.3.41).

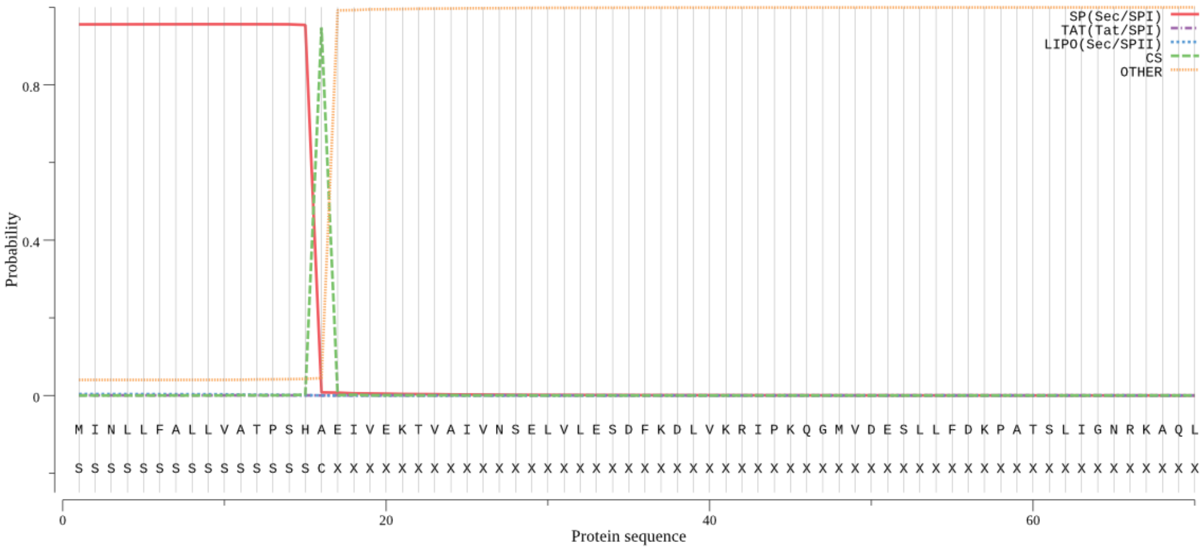

Figure 4.3.41: Prediction test for a signal peptide for modified Bd0017. Figure generated using SignalP 6.0.

Other predatory bacteria do not have a SurA protein. Instead, they encode a trigger factor protein, homologous to Bd3764/tig of *B. bacteriovorus* HD100. The C-terminus of tig is highly similar to the peptide binding domain of SurA and perform similar functions in protein export, acting as chaperones to maintain proteins in the correct conformation.

Gene neighborhood and association analyses

The gene *bd0017* is part of a large, eight gene operon, consisting of genes encoding electron transport flavoprotein alpha and beta proteins (EtfB/Bd0022 and EtfA/Bd0021 respectively), Bd0020, a putative lipoprotein, Bd0019, a PpiD/Peptidyl prolyl isomerase, Bd0018/PpiC, a parvulin-like peptidyl prolyl isomerase, Bd0015/PdxA, a pyridoxal phosphate biosynthetic protein, and Bd0014/Pmm, a phosphomannomutase (Figure 4.3.42)(xBase).

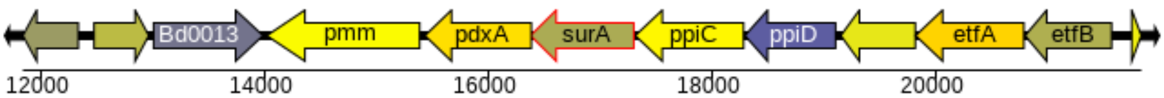

Figure 4.3.42: A schematic showing the gene neighbourhood of *bd0017*. Diagram taken from xBase**.**

Using STRING to analyse the predicted protein-protein interactions and functional enrichment, Bd0017 is predicted to interact with many other PPIase-like proteins, including Bd0336/SlyD, Bd2569/FkpA, Bd1903/FkpA, Bd0018 and Bd0019. Bd0017 is also predicted to interact with Bd3764/Tig, a chaperone protein trigger factor involved in protein export, Bd0125/ComL and Bd2031, two outer membrane protein assembly complex proteins, and Bd2113/OstA, an organic tolerance solvent protein involved in LPS assembly (Figure 4.3.43).

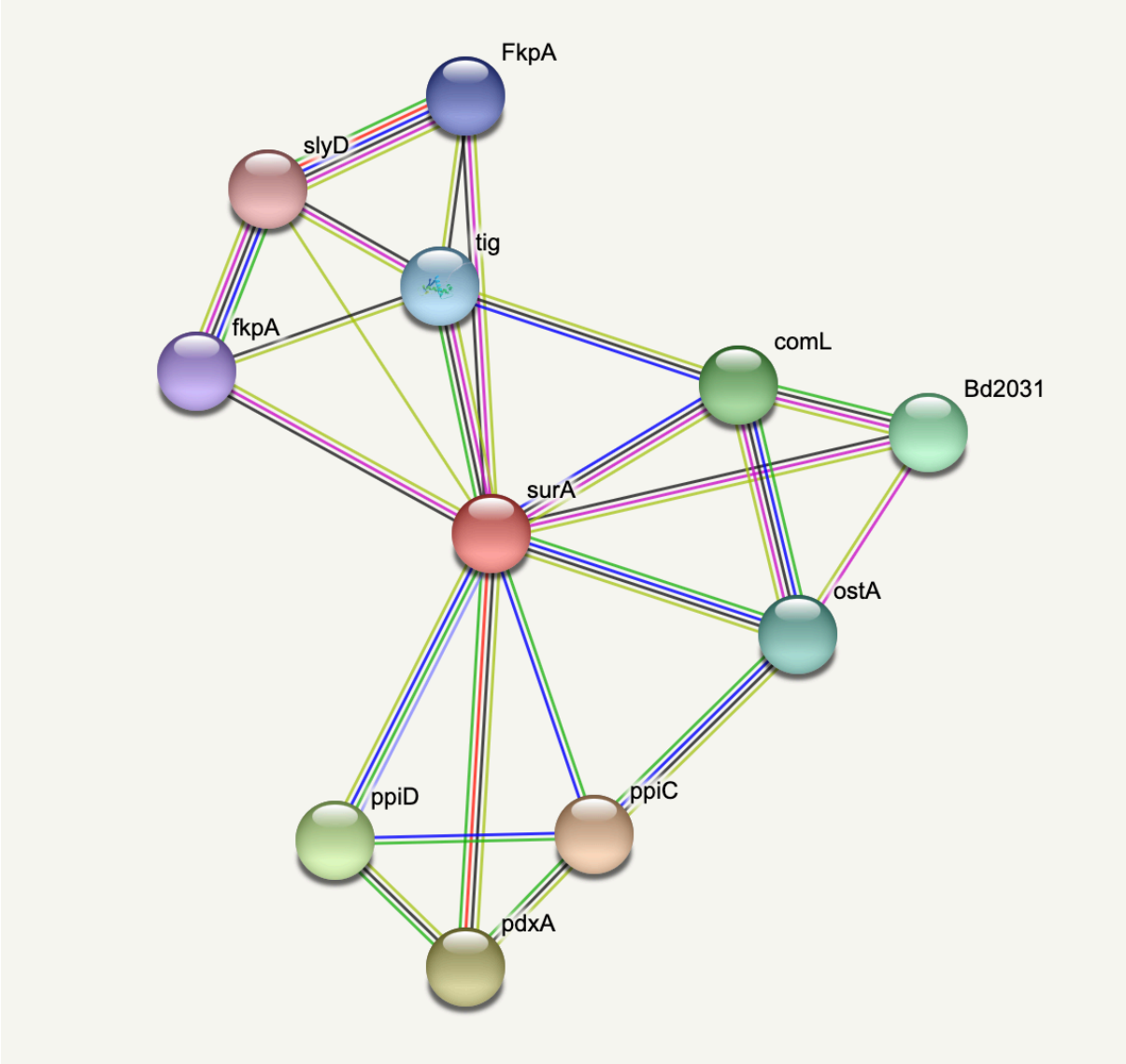

Figure 4.3.43: A schematic showing the predicted protein-protein interactions of Bd0017. Figure generated using STRING. Magenta threads represent experimentally determined interactions; Green threads represent gene neighbourhood interactions; Dark blue threads represent gene co-occurrence; Black threads represent co-expression; Lilac threads represent protein homology; Yellow threads represent textmining (i.e. associations in literature) (STRING).

Searches for homologues in other bacterial pathogens

I then compared Bd0017 to structural homologues in known bacterial pathogens. Initial observations showed that Bd0017 was significantly smaller than homologues in other bacteria, so I chose to align each domain individually, rather than aligning the entire protein sequence.

The SurA N-terminal domain of Bd0017 from *B. bacteriovorus* HD100 (Q6MRQ7) was aligned to the SurA proteins of *P. aeruginosa* (Q9I5U3), *E. coli K12* (P0ABZ6), *L. pneumophila (*Q5ZYR3), *S. dysenteriae (*Q32K41), *S. typhimurium (*Q7CR87), *Y. pestis (*Q7CG87), *B. pseudomallei (*Q63X78) and *V. cholerae (*Q9KUS0) using Clustal Omega. Consensus amino acid structure appears dissimilar between Bd0017 SurA N-terminal domain and the SurA N-terminal domains tested (Q9I5U3: No significant similarity found, P0ABZ6: 17%, Q5ZYR3: 25.0%, Q32K41: 19.8%, Q7CR87: 20.2%, Q7CG87: 23.5%, Q63X78: No significant similarity found and Q9KUS0: 26.9% percentage identity), even though they align well across the entirety of their respective lengths (Figure 4.3.44).

The rotamase domain of Bd0017 from *B. bacteriovorus* HD100 (Q6MRQ7) was aligned to the SurA rotamase domains of *P. aeruginosa* (Q9I5U3), *E. coli K12* (P0ABZ6), *L. pneumophila* (Q5ZYR3), *S. dysenteriae* (Q32K41), *S. typhimurium* (Q7CR87), *Y. pestis* (Q7CG87), *B. pseudomallei* (Q63X78) and *V. cholerae* (Q9KUS0) using Clustal Omega. Consensus amino acid structure appears dissimilar between Bd0017 SurA N-terminal domain and the SurA N-terminal domains tested (Q9I5U3: 30.1%, P0ABZ6: 27.2%, Q5ZYR3: 29.0%, Q32K41: 27.2%, Q7CR87: 28.2%, Q7CG87: 30.4%, Q63X78: 29.4% and Q9KUS0: 29.3% percentage identity). The alignment (Figure 4.3.45) suggests that Bd0017 only has one rotamase domain, compared to the two rotamase domains that other bacteria have, perhaps accounting for the difference in size between these proteins. I aligned the Bd0017 rotamase domain to the matching rotamase domain in the bacterial pathogens (Figure 4.3.46), with identical similarity scores being found.

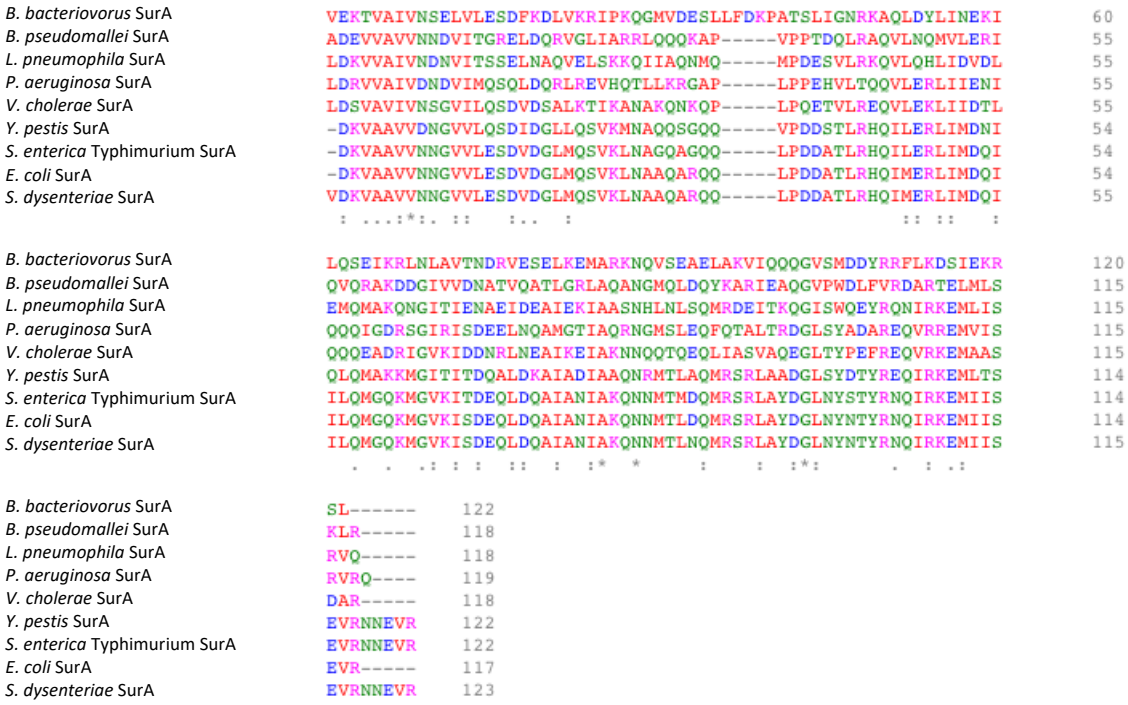

Figure 4.3.44: An alignment of Bd0017 SurA N-terminal domain to the SurA N-terminal domain of other bacterial pathogens. The SurA N-terminal domain of Bd0017 from *B. bacteriovorus* HD100 (Q6MRQ7) was aligned to the SurA N-terminal domains of *P. aeruginosa* (Q9I5U3), *E. coli K12* (P0ABZ6), *L. pneumophila* (Q5ZYR3), *S. dysenteriae* (Q32K41), *S. typhimurium* (Q7CR87), *Y. pestis* (Q7CG87), *B. pseudomallei* (Q63X78) and *V. cholerae* (Q9KUS0) using Clustal Omega. Complete amino acid sequences are shown for each domain. Amino acids are coloured by their physicochemical properties. (*) indicates a conserved residue. (:) indicates amino acids sharing strongly similar properties. (.) indicates an amino acid sharing weakly similar properties.

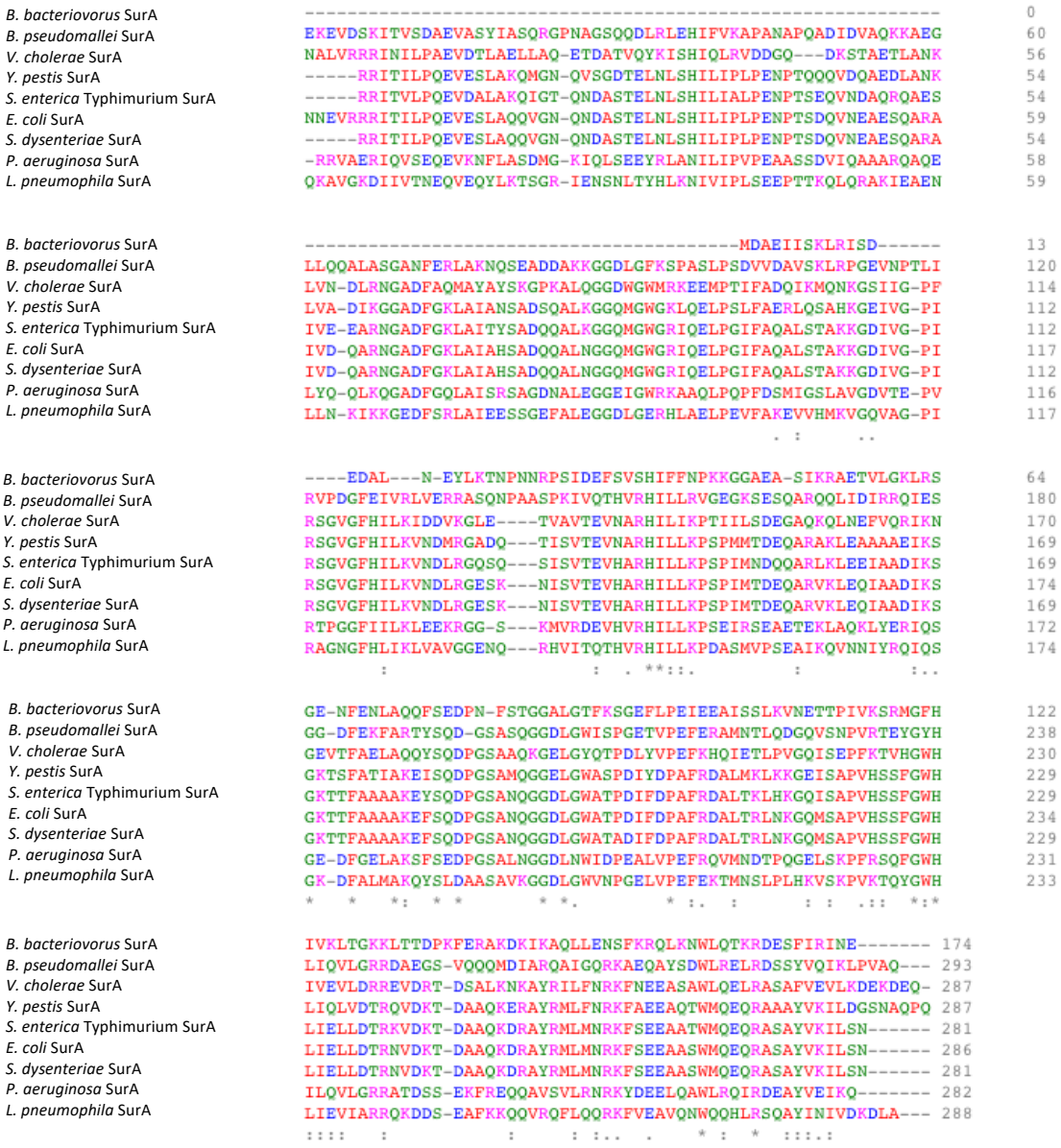

Figure 4.3.45: An alignment of Bd0017 rotamase domain to the rotamase domains of other bacterial pathogens. The SurA rotamase domain of Bd0017 from *B. bacteriovorus* HD100 (Q6MRQ7) was aligned to the SurA rotamase domains of *P. aeruginosa* (Q9I5U3), *E. coli K12* (P0ABZ6), *L. pneumophila* (Q5ZYR3), *S. dysenteriae* (Q32K41), *S. typhimurium* (Q7CR87), *Y. pestis* (Q7CG87), *B. pseudomallei* (Q63X78) and *V. cholerae* (Q9KUS0) using Clustal Omega. Complete amino acid sequences are shown for each protein. Amino acids are coloured by their physicochemical properties. (*) indicates a conserved residue. (:) indicates amino acids sharing strongly similar properties. (.) indicates an amino acid sharing weakly similar properties.

Figure 4.3.46: An alignment of Bd0017 rotamase domain to a single rotamase domain of other bacterial pathogens. The SurA rotamase domain of Bd0017 from *B. bacteriovorus* HD100 (Q6MRQ7) was aligned to the most homologous of the two SurA rotamase domains of *P. aeruginosa* (Q9I5U3), *E. coli K12* (P0ABZ6), *L. pneumophila* (Q5ZYR3), *S. dysenteriae* (Q32K41), *S. typhimurium* (Q7CR87), *Y. pestis* (Q7CG87), *B. pseudomallei* (Q63X78) and *V. cholerae* (Q9KUS0) using Clustal Omega. Complete amino acid sequences are shown for each protein. Amino acids are coloured by their physicochemical properties. (*) indicates a conserved residue. (:) indicates amino acids sharing strongly similar properties. (.) indicates an amino acid sharing weakly similar properties.

4.3.3.2. Bd1815

Bd1815 is a hypothetical protein of unknown function, 19 kDa in size and 179 amino acids in length (UniProt). The gene *bd1815* is in a two gene operon with *bd1814*, another hypothetical protein of unknown function (xBase), and in the same gene neighbourhood as multiple other hypothetical proteins (genes: *bd1813*, *bd1817*, and *bd1818*), a chloride channel protein (gene: *bd1816/eriC*) and an iron sulfur cluster binding protein (gene: *bd1819/yjeS*) (Figure 4.3.47) (xBase).

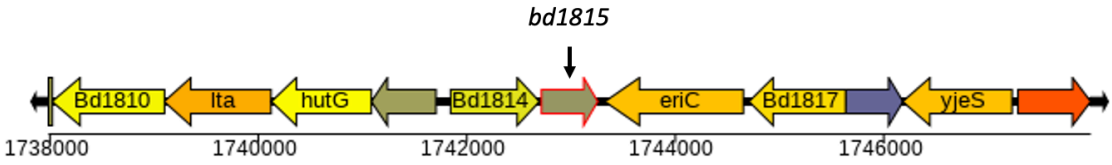

Figure 4.3.47: A schematic showing the gene neighbourhood of *bd1815*. Diagram taken from xBase.

Analysis of predicted domain structure

Analysis of the predicted domains present within Bd1815, using PFam, reveals a signal peptide at the N-terminus of Bd1815 (amino acids 1-23), followed by a chain (amino acids 24-179). The presence of a signal peptide at the beginning of Bd1815 is also confirmed by SignalP 6.0 analysis. (Figure 4.3.48).

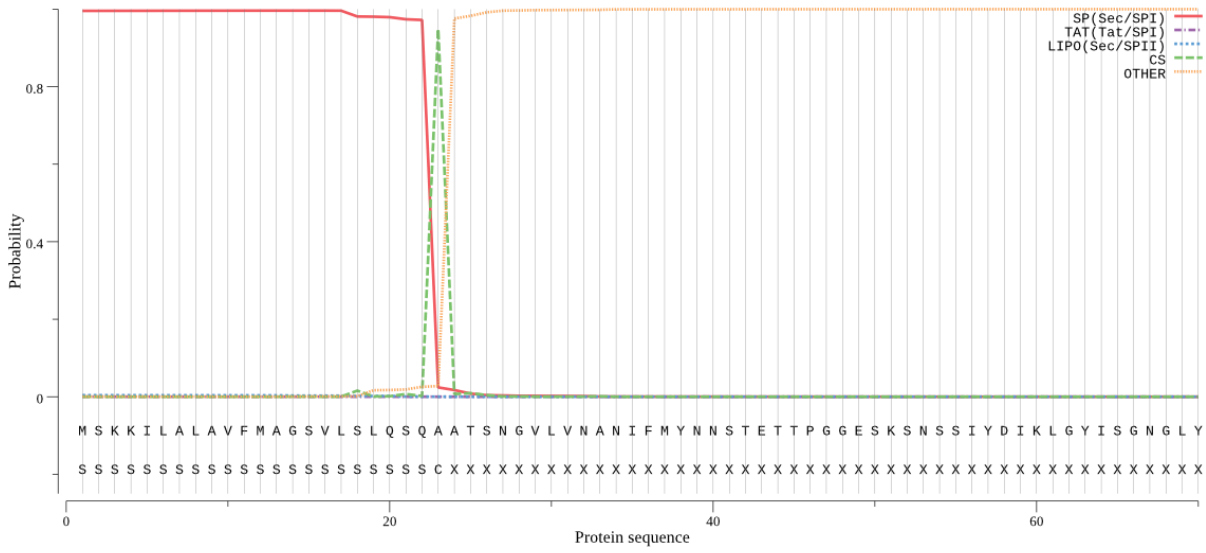

Figure 4.3.48: Prediction test for a signal peptide for Bd1815. Figure generated using SignalP 6.0.

Gene neighbourhood and association analyses

Using STRING to analyse the predicted protein-protein interactions of Bd1815, places Bd1815 in a network with the proteins in its immediate vicinity within the genome, including Bd1813 and Bd1814, whose functions are uncharacterised, Bd1810/KynA, a haem-dependent dioxygenase, Bd1811/Ita, a threonine aldolase, and Bd1812/HutG, a formimidoylglutamase (Figure 4.3.49). Protein network interactions do not help us infer a function for Bd1815.

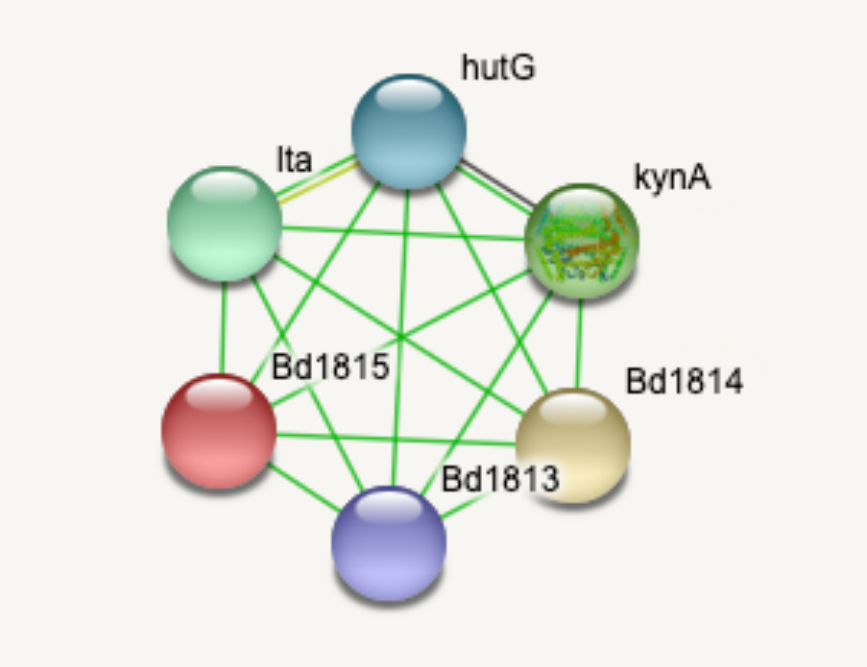

Figure 4.3.49 A schematic showing the predicted protein-protein interactions of Bd1815. Figure generated using STRING. Magenta threads represent experimentally determined interactions; Green threads represent gene neighbourhood interactions; Dark blue threads represent gene co-occurrence; Black threads represent co-expression; Lilac threads represent protein homology; Yellow threads represent textmining (i.e. associations in literature) (STRING).

Predicted structure analyses

Aligning Bd1815 to its closest structural homologues, by aligning the 3D model of the predicted protein structure to a database of other proteins, does aid in inferring a function. I used ITASSER, an online protein modelling database, to search for similar structural homologues to Bd1815.

This showed a close match to the *E. coli* outer membrane protein OmpA (PDB:1bxwA) (template modelling score 0.681, where 1 indicates an identical match), which has annotated roles in outer membrane functionality and peptidoglycan positioning. Alignment of Bd1815 and OmpA using TMalign shows that their structures do differ slightly at the N and C termini, however. This difference may be attributable to the size difference between these two proteins. These alignments are depicted in Figure 4.3.50. The amino acid sequences of Bd1815 and *E. coli* OmpA are highly dissimilar (Figure 4.3.51). Bd1815 also gave close structural matches to *Neisseria* NspA (PDB: 1P4T), *E. coli* OmpW and *P. aeruginosa* OprH, OprF, OprG, further supporting its role as an outer membrane protein (ITASSER; Data not shown). Even though the amino acid sequences of Bd1815 and OmpA are dissimilar, structure dictates function and therefore as these proteins have a similar structure, I suggest that they have a similar function.

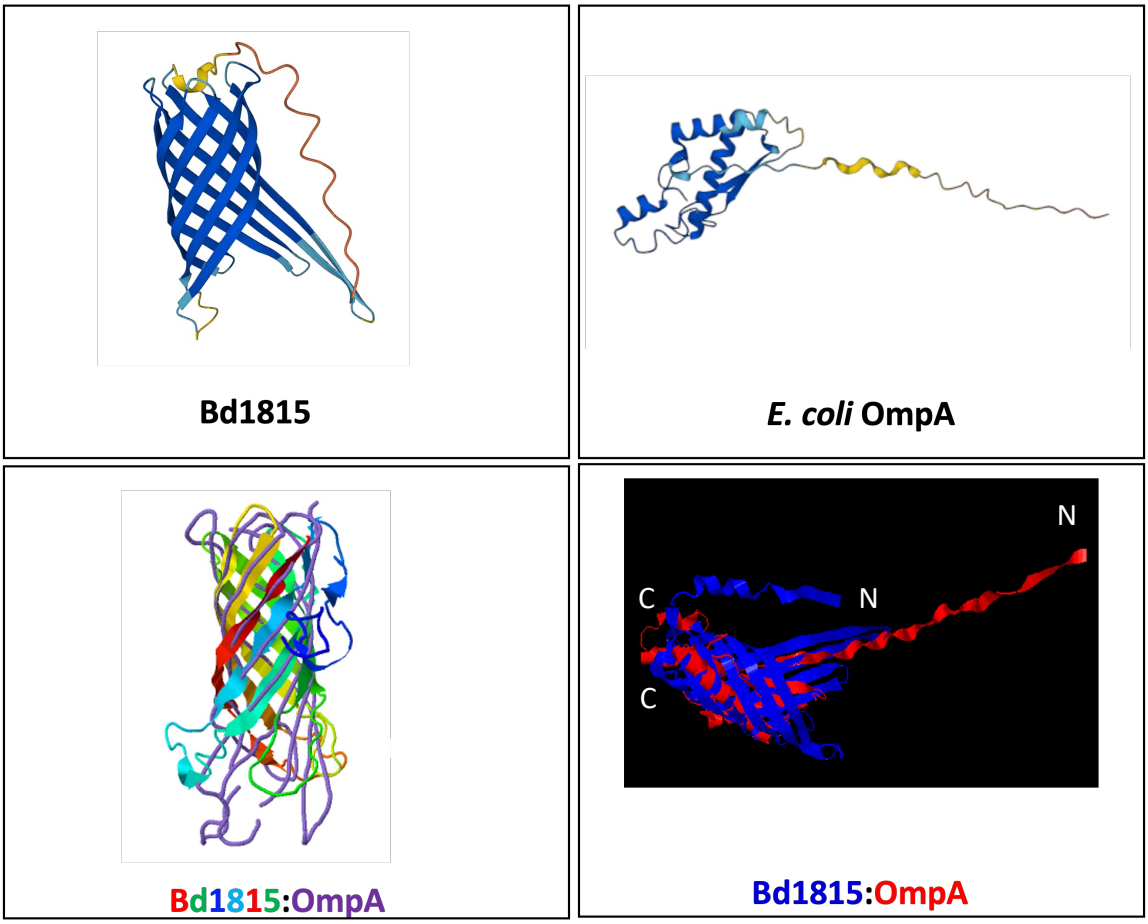

Figure 4.3.50: Predicted structures of Bd1815 and OmpA. Structural predictions and Protein Data Bank (.pdb) files were obtained from AlphaFold for Bd1815 (UniProt accession: Q6MM32; Top, Left) and OmpA (P0A910; Top, Right). The amino acid sequence was 3D modelled and screened against other bacterial proteins for homology using ITASSER (Bottom, Left). PDB files were aligned using TMalign to generate the structural overlay depicted (Bottom, Right). Bd1815 and OmpA have a highly similar Beta barrel structure at their core, but their N termini appear to differ (labelled).

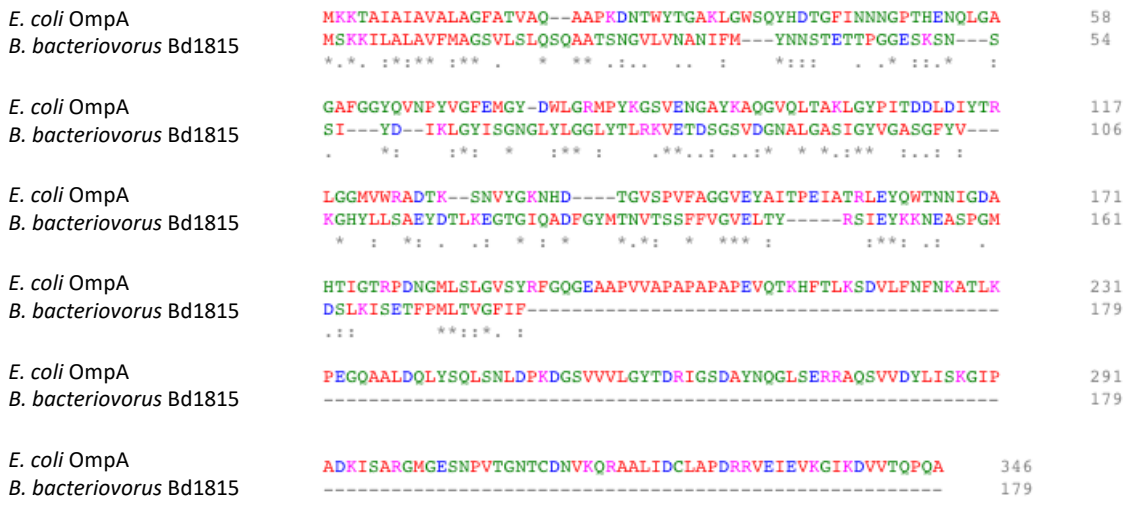

Figure 4.3.51: An alignment of Bd1815 to the *E. coli* OmpA protein. Bd1815 of *B. bacteriovorus* (Uniprot accession: Q6MM32) was aligned to *E. coli* OmpA (P0A910) using Clustal Omega. Complete amino acid sequences are shown for each protein. Amino acids are coloured by their physicochemical properties. (*) indicates a conserved residue. (:) indicates amino acids sharing strongly similar properties. (.) indicates an amino acid sharing weakly similar properties.

Searching the *Bdellovibrio* genome for other, known porins, I decided to compare the structure and amino acid sequence of Bd1815 with the *Bdellovibrio* porin CAE47737.1. I aligned the amino acid sequences (Clustal Omega) and predicted 3D structures (AlphaFold (470); TMalign (471)) of both proteins. Bd1815 gives a poor alignment to a known *Bdellovibrio* porin CAE47737.1, with no significant similarities in amino acid sequence or structure found (Figure 4.3.52 & 4.3.53). Searching the *B. bacteriovorus* HD100 genome for homologues with a similar amino acid sequence revealed no homologues in the genome (BlastP).

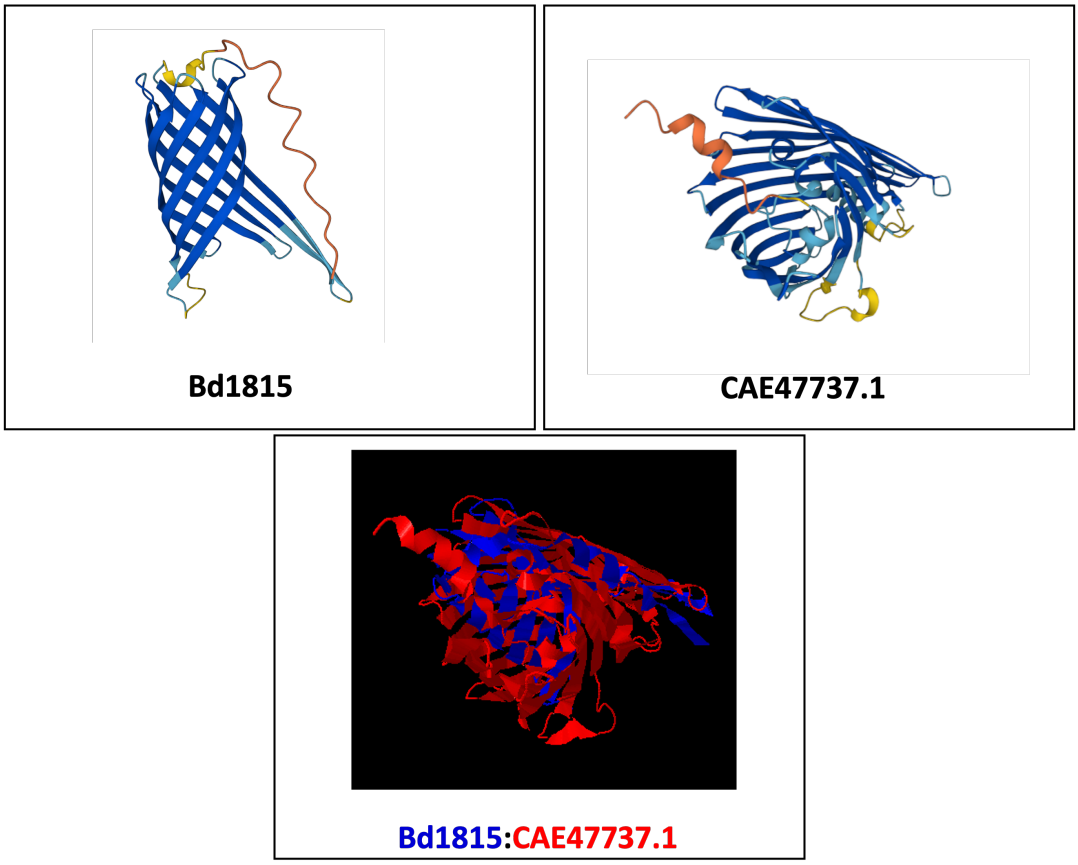

Figure 4.3.52: Predicted structures of Bd1815 and *Bdellovibrio* OMP CAE47737.1. Structural predictions and Protein Data Bank (.pdb) files were obtained from AlphaFold for Bd1815 (UniProt accession: Q6MM32; Top, Left) and CAE47737.1 (Q70EK1; Top, Right). PDB files were aligned using TMPred to generate the structural overlay depicted (Bottom, Centre). Bd1815 and CAE47737.1 have a highly dissimilar structure.

```
B. bacteriovorus OMP      -MKKILVVAALTMAAAPAAMASKARVEALANSRHVLDFQTAFDRPYQFMALSEQATIEWG   59
B. bacteriovorus Bd1815   MSKKILALA-VFMAGSVLSLQSQAA-----TSNGVLV------NANIFM---------YN   39
                            ****.:* : **.:  :: *:*      .*. **       .   **         :.

B. bacteriovorus OMP      ATGEGAPHAE-----GGFVKRHGDDSAFGIYFGRRSADFSEAVDTANAAIPAPDLLKEQN  114
B. bacteriovorus Bd1815   NSTETTPGGESKSNSSIYDIKLGYISGNGLYLGGLYT----------------------   76
                           : * :* .*      . :  : *  *. *:*:*   :

B. bacteriovorus OMP      GLNLFYASKMGEWTWGATVKYSNGKNDTDDAKVSSMGVAVAASNGTWDFELVQGFTGKSE  174
B. bacteriovorus Bd1815   ----------------------LRKVETDSGSVD--GNALGASIG---YVGASGFYVK--  107
                                               * :**...*.  * *:.** *   :  ..**  *

B. bacteriovorus OMP      NVNAEVESKGLTNLTVGYHMSPEMEVYANAKMSKVEGGGALAGVEVETNTYKVGMVNTLV  234
B. bacteriovorus Bd1815   ---------G------HYLLSAEYDTL-------KEGTGIQADF-----------GYM  132
                                    *       * :* * :.         ** *  *..            :

B. bacteriovorus OMP      KSEEGNFFYGVEVASTKVKDDSESLLMPVYMGVEHNAASWLVLRASVSQNVILNETKDDA  294
B. bacteriovorus Bd1815   TNVTSSFFVGVELTYRSIEYKK-----------------------------------NEA  157
                          ..  ..** ***::  .:: ..                                    ::*

B. bacteriovorus OMP      SGDKTDLDSTAMAAGAGIKFGKSMIDATFTQTAAGTINSDNLFSNVAYTYTF        346
B. bacteriovorus Bd1815   SP---GMDSL-------------KISETFP-------------MLTVGFIF        179
                          *    .:**               *. **                ::  : *
```

Figure 4.3.53: An alignment of Bd1815 to the *Bdellovibrio* OMP CAE47737.1. Bd1815 of *B. bacteriovorus* (Uniprot accession: Q6MM32) was aligned to *Bdellovibrio* CAE47737.1 (Q70EK1) using Clustal Omega. Complete amino acid sequences are shown for each protein. Amino acids are coloured by their physicochemical properties. (*) indicates a conserved residue. (:) indicates amino acids sharing strongly similar properties. (.) indicates an amino acid sharing weakly similar properties.

4.3.3.3. Bd2620

Bd2620/Dps is annotated as a Putative DNA protection from starvation or oxidative stress transcriptional regulator protein (UniProt). Bd2620 is 19.1 kDa in size and 168 amino acids in length.

Analysis of predicted domain structure

Analysis of the amino acid sequence of Bd2620 shows a large ferritin-like domain between amino acids 29 and 166 (PFam). Analysis of Bd2620 using SignalP 6.0 confirms that no signal peptide is present, supporting the role of Bd2620 of a DNA associated protein that exists within the cytoplasm of the cell (Figure 4.3.54).

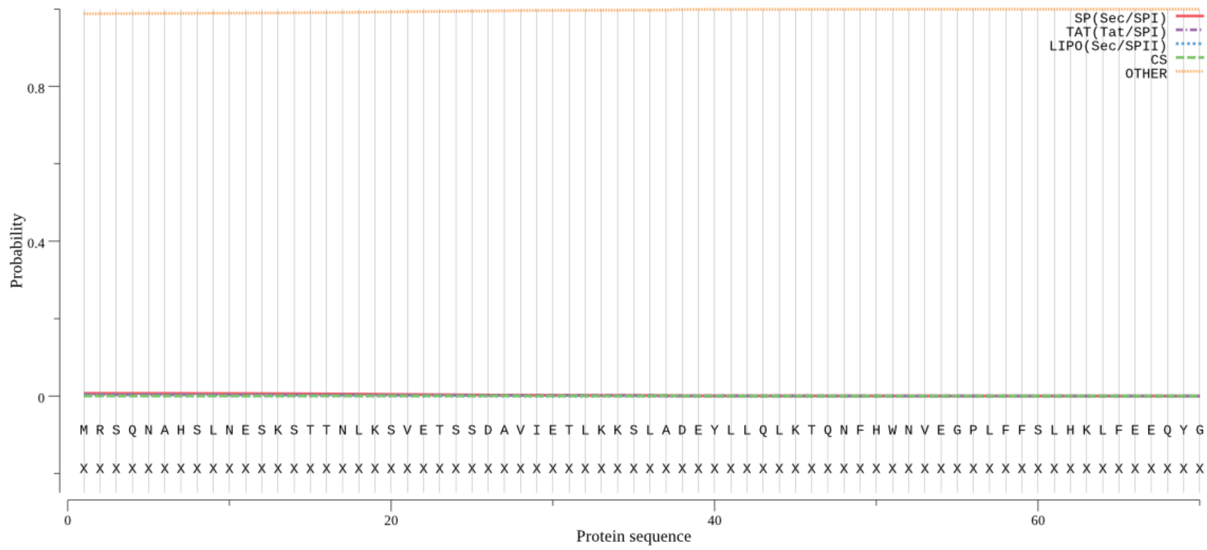

Figure 4.3.54: Prediction test for a signal peptide for the protein Bd2620/Dps. Figure generated using SignalP 6.0.

Gene neighbourhood and association analyses

The gene *bd2620* is part of a five gene operon with *bd2619*/*oxyR* regulon transcriptional regulator, supporting its role in tolerance against oxidative stress, *bd2621/gufA, bd2622/trg,* a methyl accepting chemotaxis protein, and *bd2623/gltS,* a sodium glutamate carrier protein (Figure 4.3.55). Using STRING to analyse the predicted protein-protein interactions, it is suggested that Bd2620 may interact with Bd1298/DnaK, a molecular chaperone protein, Bd0026/SdhB, a succinate dehydrogenase/fumarate reductase/ferredoxin protein, Bd1436, a lipoyl-dependent peroxiredoxin and osmotic stress induced protein, Bd2621/GufA, a Zinc transporter, Bd2628, a NAD/FAD dependent dehydrogenase, Bd1289/ClpS, an ATP-dependent clp protease and Bd2619/OxyR, a LysR family transcriptional regulator and hydrogen peroxide inducible gene activator (Figure 4.3.61). Bd2620 may also associate/interact with two hypothetical proteins (Bd1168 and Bd0659) (Figure 4.3.56).

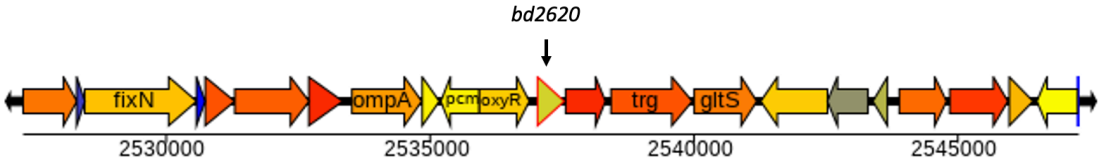

Figure 4.3.55: A schematic showing the gene neighbourhood of *bd2620*. Diagram taken from xBase.

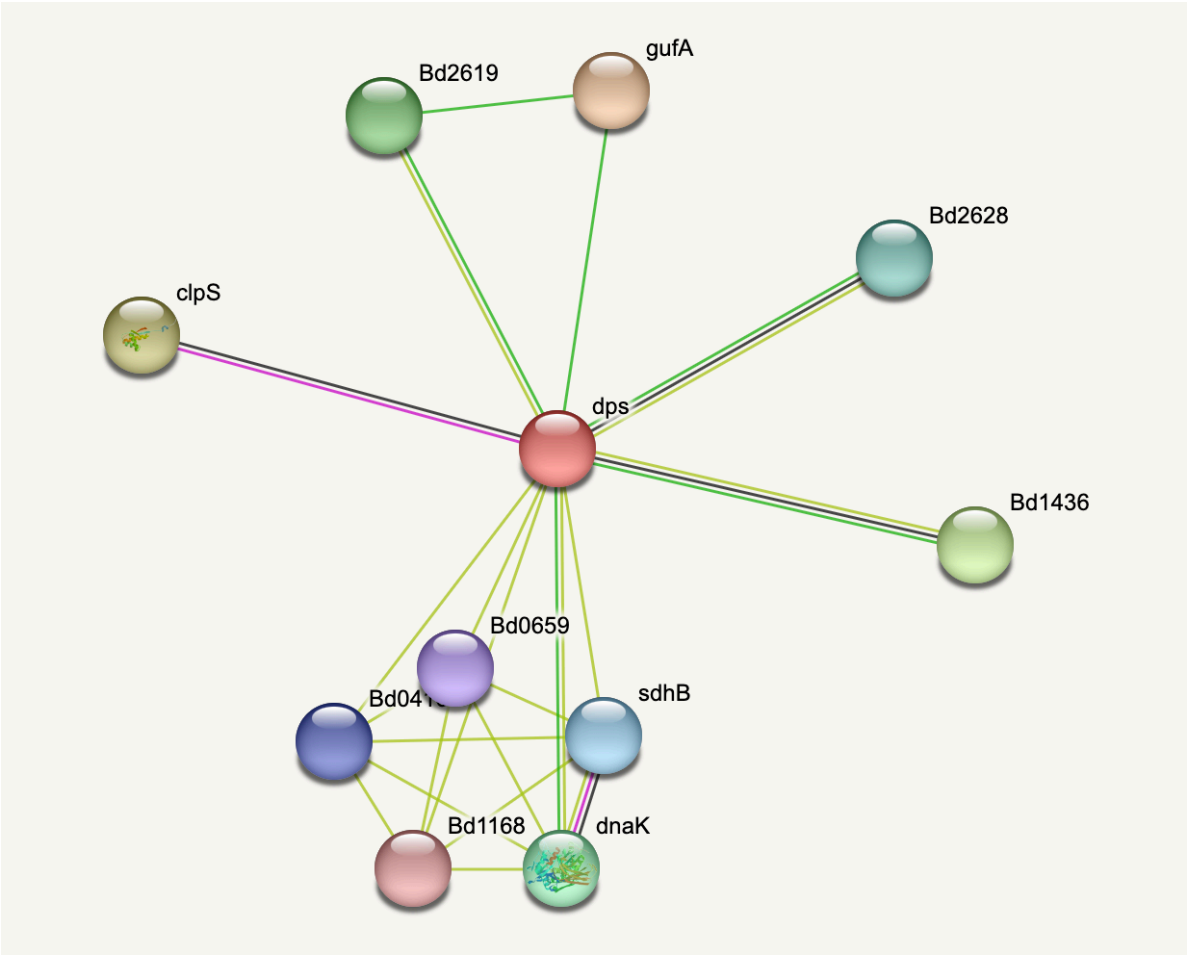

Figure 4.3.56: A schematic showing the predicted protein-protein interactions of Bd2620. Figure generated using STRING. Magenta threads represent experimentally determined interactions; Green threads represent gene neighbourhood interactions; Dark blue threads represent gene co-occurrence; Black threads represent co-expression; Lilac threads represent protein homology; Yellow threads represent textmining (i.e. associations in literature) (STRING).

Searches for homologues in *Bdellovibrio* and other bacterial species

Searches of the *B. bacteriovorus* HD100 genome, using BlastP, for homologues to Bd2620 shows no homologues with significant sequence similarity. Searches for homologues of Bd2620 in well-known bacterial pathogens reveals Dps protein homologues of similar size and consensus amino acid sequence. Bd2620/Dps (Q6MJZ6) was aligned to the Dps proteins of *Acinetobacter junii* (A0A2R4UN04), *Klebsiella pneumoniae* (Q84FI0), *Escherichia coli* (P0ABT2), *Salmonella enterica* (A0A628UWD2) and *Legionella pneumophila* (A0A129F132) using Clustal Omega. These analyses show that Bd2620/Dps is of similar size and consensus amino acid structure to the Dps proteins of other bacteria, despite having low amino acid sequence similarity (A0A2R4UN04: 24.3% similarity, 49% coverage, Q84FI0: 28% similarity, 57% coverage, P0ABT2: 29.2% similarity, 50% coverage and A0A628UWD2: 27.8% similarity, 42% coverage). Bd2620/Dps was most similar to the Dps protein of *Legionella pneumophila,* of the bacterial proteins tested, with a 44.3% similarity, and 83% coverage (BlastP) (Figure 4.3.57).

Figure 4.3.57: An alignment of Bd2620/Dps to the Dps proteins of *A. junii*, *K. pneumoniae*, *E. coli, S. enterica* and *L. pneumophila*. Bd2620/Dps of *B. bacteriovorus* (Uniprot accession: Q6MJZ6) was aligned to the Dps proteins of *Acinetobacter junii* (A0A2R4UN04), *Klebsiella pneumoniae* (Q84FI0), *Escherichia coli* (P0ABT2), *Salmonella enterica* (A0A628UWD2) and *Legionella pneumophila* (A0A129F132) using Clustal Omega. Complete amino acid sequences are shown for each protein. Amino acids are coloured by their physicochemical properties. (*) indicates a conserved residue. (:) indicates amino acids sharing strongly similar properties. (.) indicates an amino acid sharing weakly similar properties.

4.3.3.4. Bd3203

Bd3203 is a hypothetical protein of unknown and uncharacterised function. Bd3203 is 17.5 kDa in size and 156 amino acids in length. The gene *bd3203* is monocistronic (Figure 4.3.58) (xBase)

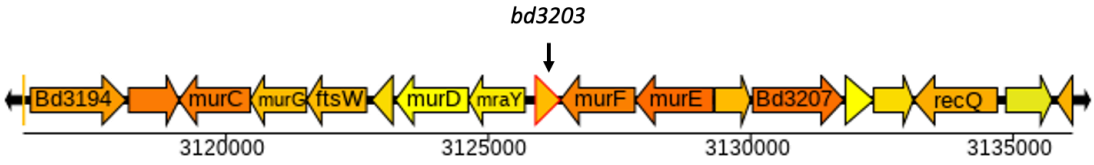

Figure 4.3.58: A schematic showing the gene neighbourhood of *bd3203*. Diagram taken from xBase.

Analysis of predicted domain structure

Analysis of the domain structure revealed that Bd3203 contains a CBS (Cystathionine Beta Synthase) domain (PFam), which are known to be involved in the regulation of protein dimerisation and sensitivity to adenosyl carrying ligands, suggesting that they may function as intracellular sensors of metabolites (473, 474). Analysis of Bd3203 using SignalP 6.0 confirms that no signal peptide is present, suggesting that Bd3203 acts within the cytoplasm of the cell (Figure 4.3.59).

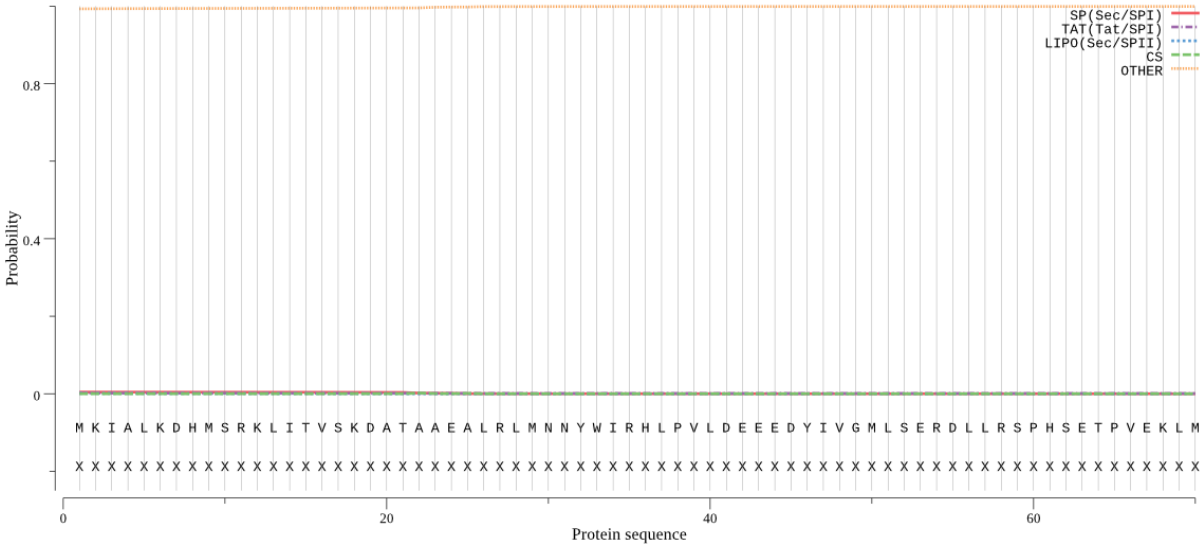

Figure 4.3.59: Prediction Test for a Signal Peptide for the protein Bd3203. Figure generated using SignalP 6.0.

Gene neighbourhood and association analyses

The gene *bd3203* is neighbouring *bd3200*/*murD* and *bd3201*/*mraY*, a UDP-N-acetylmuramoylalanine-d-glutamate ligase involved in cell wall formation and a peptidoglycan biosynthesis protein respectively, suggesting that Bd3203 may regulate proteins involved in cell wall synthesis or modification. Using STRING to analyse the predicted protein-protein interactions, it is suggested that Bd3203 is associated with Bd3200 and Bd3201, along with various other metabolic enzymes including Bd2647/Tyrdc (tyrosine decarboxylase), Bd2921 (glutamine amidotransferase), Bd2080/GuaA (Gmp synthase) and Bd1049/Gapdh (Glyceraldehyde-3- phosphate). Bd3203 may also be associated with Bd2084, a monovalent cation proton antiporter, Bd3734/MglA, a gliding motility protein and Bd3199, a hypothetical protein (Figure 4.3.60).

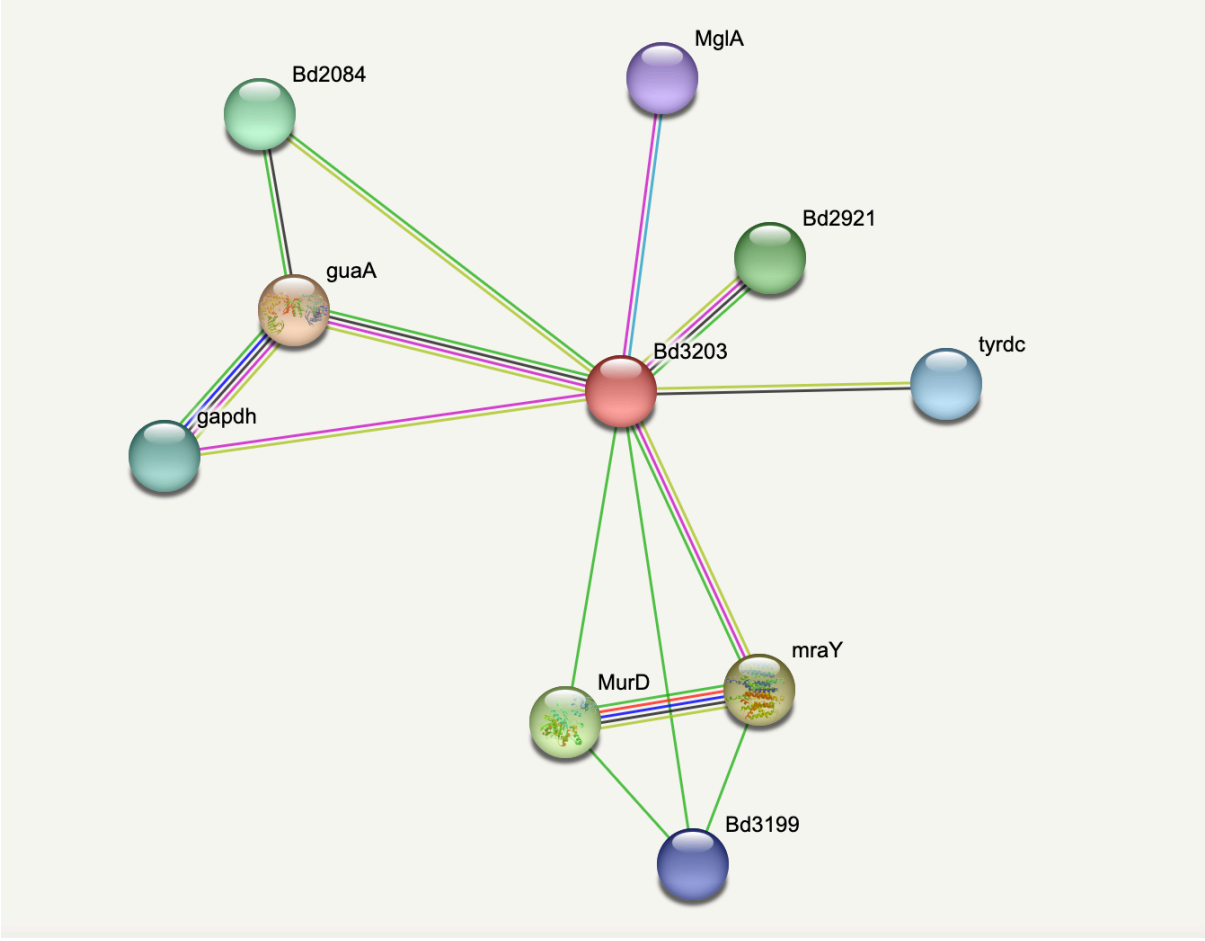

Figure 4.3.60: A schematic showing the predicted protein-protein interactions of Bd3203. Figure generated using STRING. Magenta threads represent experimentally determined interactions; Green threads represent gene neighbourhood interactions; Dark blue threads represent gene co-occurrence; Black threads represent co-expression; Lilac threads represent protein homology; Yellow threads represent textmining (i.e. associations in literature) (STRING).

Searches for homologues in *Bdellovibrio* and other bacterial species

Searches for homologues in *Bdellovibrio* revealed no known homologues of significant similarity (BlastP). Searches for homologues in other bacterial species revealed a low homology with short part of an *E. coli* CBS-domain containing protein, but no further matches beyond this (BlastP).

4.3.4. Summary

The purpose of these analyses were to firstly confirm that the functional annotations ascribed to these proteins were correct, owing to the genome and proteome of *B. bacteriovorus* being less well-characterised, compared to other Gram-negative bacteria. Secondly, these analyses helped me to identify where these proteins would localise within the bacterial cell, aiding my understanding of their biological function and importance. Thirdly, these analyses identified other homologues within the *B. bacteriovorus* genome that may also be of interest to my studies. The genes (and proteins) that I will investigate further, and the initial sources that highlighted them are summarised in Table 4.3.1, below.

Table 4.3.1: A summary of the genes taken forward for further study and how they were highlighted. Zebrafish transcriptional study refers to the transcriptomic dataset mentioned in Section 4.2.

Gene	Source/Highlighted by…
surA (*bd0017*)	*Bdellovibrio* Macrophage transcriptional study
sodC (*bd0295*)	Zebrafish transcriptional study
sodC (*bd1401*)	Homology with *bd0295*
catA (*bd0798*)	Zebrafish transcriptional study
ankB (*bd0799*)	Literature searches
katA (*bd1154*)	Homology with *bd0798*
ankB (*bd1155*)	Literature searches
ahpC (*bd2517*)	Zebrafish transcriptional study
ahpF (*bd2518*)	Zebrafish transcriptional study
dps (*bd2620*)	Zebrafish transcriptional study
bd3203	Zebrafish transcriptional study
bd1815	Zebrafish transcriptional study

4.4. Transcriptional expression of our candidate genes throughout predation of *E. coli* by *Bdellovibrio* and throughout macrophage occupation

4.4.1. Transcriptional expression of our candidate genes within macrophage

To test whether these genes also play a role in survival within human macrophage, I interrogated my bacterial transcriptome (generated from a dual RNA sequencing study of the host and bacterial transcriptional response to *Bdellovibrio* occupation of macrophage) for the expression of each candidate genes (Figure 4.4.1).

- ***bd0017/surA*** expression was upregulated at 24 hours post-uptake during *Bdellovibrio* occupation of macrophage, but was not detected at 2-, 4- and 8-hours post-uptake.
- ***bd0295/sodC*** was highly expressed at 2 hours post-uptake but downregulated throughout *Bdellovibrio* occupation of macrophage.
- The expression of ***bd0798/catA*** and its (proposed) regulatory ankyrin partner ***bd0799/ankB*** were not significantly changed throughout *Bdellovibrio* occupation of macrophage.
- Expression of ***bd1154/katA*** and its (proposed) regulatory ankyrin partner ***bd1155/ankB*** were not captured, due to the potential mapping of sequencing reads to *bd0798* and *bd0799* respectively, due to their highly similar DNA sequence.
- ***bd1401/sodC*** was upregulated at 24 hours post-uptake during *Bdellovibrio* occupation of macrophage, but was not detected at 2-, 4- and 8- hours post-uptake.

- ***bd1815*** was expressed at earlier timepoints of *Bdellovibrio* occupation of macrophage (2- and 4-hours post-uptake) but was downregulated at later timepoints (8- and 24-hours post-uptake).
- Expression of ***bd2517/ahpC*** was high at 2 hours post-uptake, prior to being downregulated at 4- and 8-hours post-uptake, and significantly upregulated at 24 hours post-uptake, during *Bdellovibrio* occupation of macrophage.
- The expression of ***bd2518/ahpF*** was not significantly changed throughout *Bdellovibrio* occupation of macrophage.
- Expression of ***bd2620/dps*** was high throughout *Bdellovibrio* occupation of macrophage but was not significantly altered throughout.
- Expression of ***bd3203*** was high throughout *Bdellovibrio* occupation of macrophage but was largely unchanged throughout.

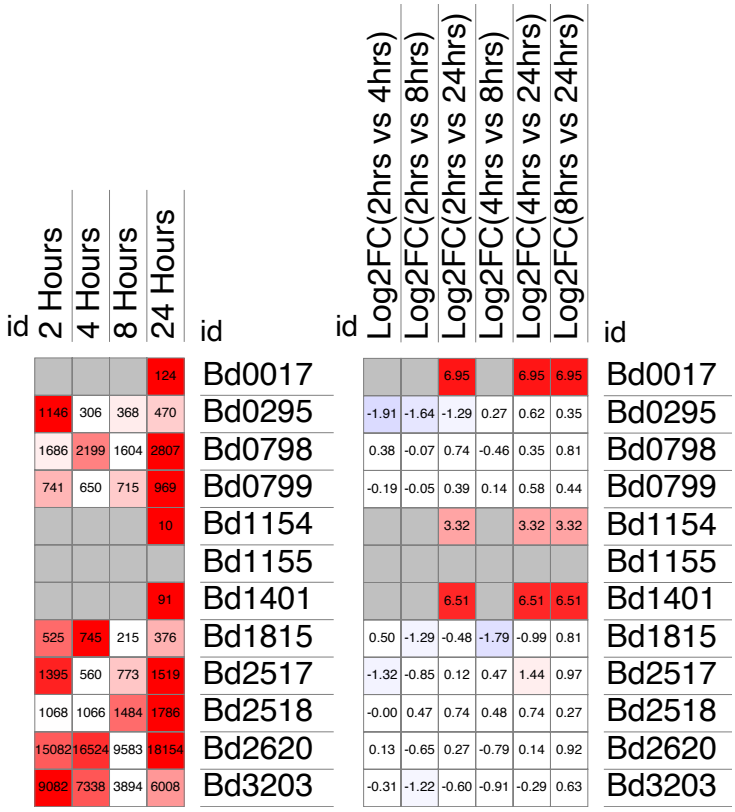

Figure 4.4.1: Heatmaps showing the expression of our candidate genes throughout *Bdellovibrio* occupation of macrophage. The bacterial transcriptome, obtained from my Dual RNA Sequencing study of the host and bacterial transcriptional response, was interrogated for the candidate genes in my study. Raw number of reads are shown (Left), compared with the Log_2 fold change for each of my candidate genes (Right). For calculation of fold change values, where no reads/expression was detected, expression values were set to 1. Heatmaps were generated using Morpheus.

4.4.2. Transcriptional Expression of our Candidate Genes throughout Predation

To interrogate whether my candidate genes may also play an important role in predation, I interrogated the bacterial transcriptome of *B. bacteriovorus* throughout its predation of *E. coli* (data generated by Dr Simona Huwiler), for my candidate genes (Figure 4.4.2).

- The expression of ***bd0017/surA*** was significantly downregulated during the first hour of predation (T_{15min}- T_{1H}), compared to attack phase *Bdellovibrio* expression.
- The expression of ***bd0295/sodC*** was significantly downregulated throughout predation, compared to attack phase (T_0) *Bdellovibrio*, including in the newly released *Bdellovibrio* progeny at 4 and 5 hours.
- The expression of ***bd0798/catA*** and its (proposed) regulatory ankyrin partner *bd0799/ankB* were significantly downregulated throughout predation.
- Expression of ***bd1154/katA*** and its (proposed) regulatory ankyrin partner ***bd1155/ankB*** were not captured. I believe that the mapping of reads is biased towards *bd0798* and *bd0799*, due to their highly similar DNA sequences, falsely mapping a proportion of the reads to these two genes and underrepresenting the expression of *bd1154* and *bd1155*.
- The expression of ***bd1401/sodC*** was upregulated from T_{45min} onwards until $T_{3H,}$ corresponding with the intraperiplasmic growth phase of *Bdellovibrio* within prey.
- The expression of ***bd1815*** was significantly downregulated throughout predation, compared to attack phase *Bdellovibrio*.
- The genes encoding the alkyl hydroperoxide reductase proteins **Bd2517/ahpC** and **Bd2518/ahpF** were significantly downregulated within the first hour of predation, with *bd2518* expression remaining significantly downregulated for the remainder of predation also, compared to attack phase *Bdellovibrio*.
- The expression of ***bd2620/dps*** was highly significantly downregulated throughout predation, compared to attack phase *Bdellovibrio*.
- The expression of ***bd3203*** was significantly downregulated throughout predation, compared to attack phase *Bdellovibrio*.

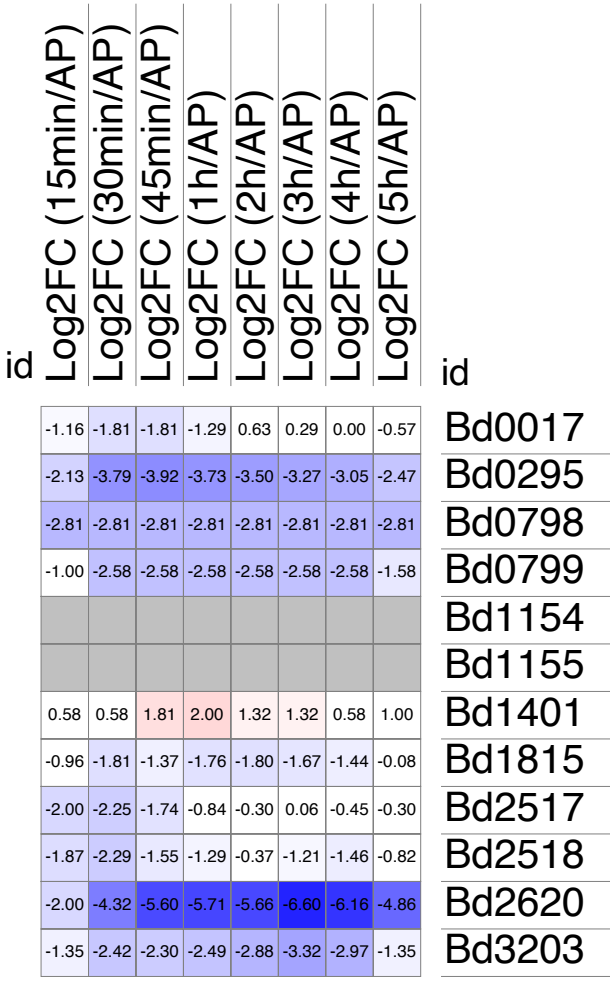

Figure 4.4.2: A heatmap showing the expression of our candidate genes throughout predation of *E. coli* by *B. bacteriovorus*. The bacterial transcriptome (generated by Dr Simona Huwiler; Huwiler & Sockett, unpublished) of *B. bacteriovorus* throughout predation of *E. coli* was interrogated for the candidate genes in my study. Shown are the Log_2 fold change values for each of my candidate genes. Heatmaps were generated using Morpheus.

4.4.3. Summary

The majority of these genes are downregulated throughout predation and are highly expressed at 24 hours, within macrophage. A summary of the expression of these genes can be found in Table 4.4.1 below.

Table 4.4.1: A summary of the transcriptional expression of candidate genes by *B. bacteriovorus* throughout predation and within macrophage.

Gene	Expression throughout predation	Expression within macrophage
bd0017	Downregulated throughout predation, most significantly at 30 and 45 minutes.	Most highly upregulated (and only detected) at 24 hours.
bd0295	Highly downregulated throughout predation.	Most highly expressed at 2 hours.
bd0798	Highly downregulated throughout predation.	Highly expressed throughout. Highest at 24 hours.
bd0799	Highly downregulated throughout predation.	Highly expressed throughout. Highest at 24 hours.
bd1154	Not detected.	Only detected at 24 hours, at a low level
bd1155	Not detected.	Not detected
bd1401	Upregulated during intraperiplasmic growth (45 minutes to 180 minutes)	Only detected at 24 hours
bd1815	Highly downregulated throughout predation.	Expressed throughout. Highest at 2 and 4 hours.
bd2517	Downregulated at the beginning of predation, especially between 15 and 45 minutes.	Expressed throughout. Highest at 2 and 24 hours.
bd2518	Downregulated at the beginning of predation, especially between 15 and 45 minutes and at 4 hours.	Highly expressed throughout. Highest at 8 and 24 hours.
bd2620	Highly downregulated throughout predation.	Highly expressed throughout.
bd3203	Highly downregulated throughout predation.	Highly expressed throughout.

bd0017 expression is downregulated throughout predation, suggesting it is not involved in predation, or is more prominently involved in attack phase *Bdellovibrio*. It is expressed at 24 hours post-uptake, within macrophage, suggesting it may be involved in responding to phagosomal conditions.

Transcriptional expression of the *sodC* genes, *bd0295* and *bd1401*, suggests contrasting roles within predation and macrophage survival. *bd0295* expression is downregulated throughout predation, suggesting it is not involved in predation, or is more prominently involved in attack phase *Bdellovibrio.* Conversely, *bd1401* expression is upregulated throughout intraperiplasmic growth, suggesting that Bd1401 is involved in predation, potentially in tolerating oxygen radical stress generated through the degradation of prey macromolecules during the intraperiplasmic growth of *Bdellovibrio*. *bd0295* expression is highest at 2 hours, within macrophage, suggesting that it may aid in the tolerance of superoxide radicals when *Bdellovibrio* is first phagocytosed by macrophage. *bd1401* expression is only detected at 24 hours, when the majority of oxidative stress and bacterial killing is occurring, suggesting it may be involved in tolerating superoxide stress at this timepoint, to resist bactericidal killing.

Catalases (Bd0798/CatA) and alkylhydroperoxide reductases (Bd2517/AhpC and Bd2518/AhpF) detoxify hydrogen peroxide within the cell. The downregulation of *bd0798, bd0799, bd2517* and *bd2518* throughout predation suggest that peroxide stress is not evident throughout predation and intraperiplasmic growth, or that peroxide stress is significantly higher in attack phase *Bdellovibrio*, which is unlikely. Conversely*, bd0798* and *bd0799* expression is high at 24 hours within macrophage. *bd2517* and *bd2518* are also highly expressed at 24 hours, in line with significant oxidative stress and bacterial killing, indicating that high levels of peroxide-mediated stress are present within macrophage at this timepoint, in line with current literature (475), and that Bd0798, Bd0799, Bd2517 and Bd2518 are involved in the peroxide tolerance response.

bd1815 is highly downregulated throughout predation, suggesting that it is not involved in predation, or is more prominently involved in attack phase *Bdellovibrio*. If it adopts a nutrient transport role, similar to the role of OmpF to which it is structurally similar, downregulation throughout predation may indicate the absence of nutrient starvation whilst within a prey cell environment. This may also suggest that during macrophage occupation, where nutrients are restricted, upregulation of *bd1815* at 2 and 4 hours may indicate nutrient starvation.

bd2620 is highly downregulated throughout predation. Bd2620/Dps has a role in DNA packaging and protection against oxidative stress and nutrient starvation. The prey cell is a nutrient rich environment. Throughout intraperiplasmic growth, DNA needs to remain accessible to transcriptional machinery due to the high levels of transcription that are occurring as part of the intraperiplasmic growth phase of *Bdellovibrio.* This may explain why *bd2620* is downregulated throughout predation. Conversely, in macrophage, *Bdellovibrio* are facing nutrient starvation and high levels of oxidative stress and are not actively growing, therefore the packaging of DNA to protect against oxidative and nutrient stress would be beneficial. This may explain why *bd2620* is highly expressed throughout macrophage residency.

bd3203 is also highly downregulated throughout predation. The lack of an annotated function makes it difficult to speculate on the role of Bd3203. If we ascribe a cell wall homeostasis function, based on its association with the surrounding cell wall modification enzymes in its gene neighbourhood, we can speculate that Bd3203 may preserve the cell wall during attack phase, but when the cell wall is undergoing extensive modification during intraperiplasmic growth, this function is not required. Equally, ascribing the same speculative function, Bd3203 may act to protect and preserve the cell wall when *Bdellovibrio* are residing within macrophage and are not actively growing, hence why *bd3203* transcription is upregulated throughout macrophage residency.

4.5. Visualisation of fluorescently tagged protein expression throughout predation of *E. coli* by *B. bacteriovorus.*

Transcriptional analyses depicting the expression for my subset of genes suggested that the majority of these proteins would not be expressed, or their expression would be downregulated, throughout predation. Within this experiment, I aimed to characterise whether any of the subset of proteins that I had highlighted previously were expressed at the protein level, throughout predation, via the characterisation of fluorescent protein expression.

To determine whether our proteins of interest are expressed and therefore play a role in predation, *B. bacteriovorus* containing our fluorescently tagged proteins of interest and a fluorescently tagged Bd0064 protein, a constitutively expressed cytoplasmic protein that, when fluorescently tagged with an mCerulean3 or mCherry protein, illuminates the cytoplasm and cell body of *Bdellovibrio*, were visualised throughout predation of *E. coli* by *B. bacteriovorus*. Bd0064mCerulean or Bd0064mCherry expression acts as a background cytoplasmic marker in this assay, to be used in combination with our fluorescently tagged proteins of interest to associate fluorescent protein expression with individual *Bdellovibrio* cells within *E. coli* prey. Cells were imaged during attack phase (T_0), attachment (T_{15}), invasion (T_{30}), establishment (T_{45}), intraperiplasmic growth (T_{60}, T_{120}, T_{180}) and *Bdellovibrio* progeny release (T_{240}).

4.5.1. Bd0017/SurAmCherry is expressed throughout predation of *E. coli* by *B. bacteriovorus.*

To determine whether Bd0017, a SurA survival associated protein highlighted by my dual transcriptional study of *Bdellovibrio* transcription within macrophage, and by literature searches of bacterial pathogens, was expressed by *Bdellovibrio* during predation of *E. coli*, I fluorescently tagged SurA with an mCherry fluorescent tag at the C-terminus. Bd0017mCherry-tagged *B. bacteriovorus* were visualised throughout predation. Bd0017mCherry was expressed diffusely in attack phase *Bdellovibrio* (T_0 and T_{240}) and throughout predation, with some Bd0017mCherry expression forming foci at T_{120} in 18.5% of *Bdellovibrio* (Figure 4.5.1).

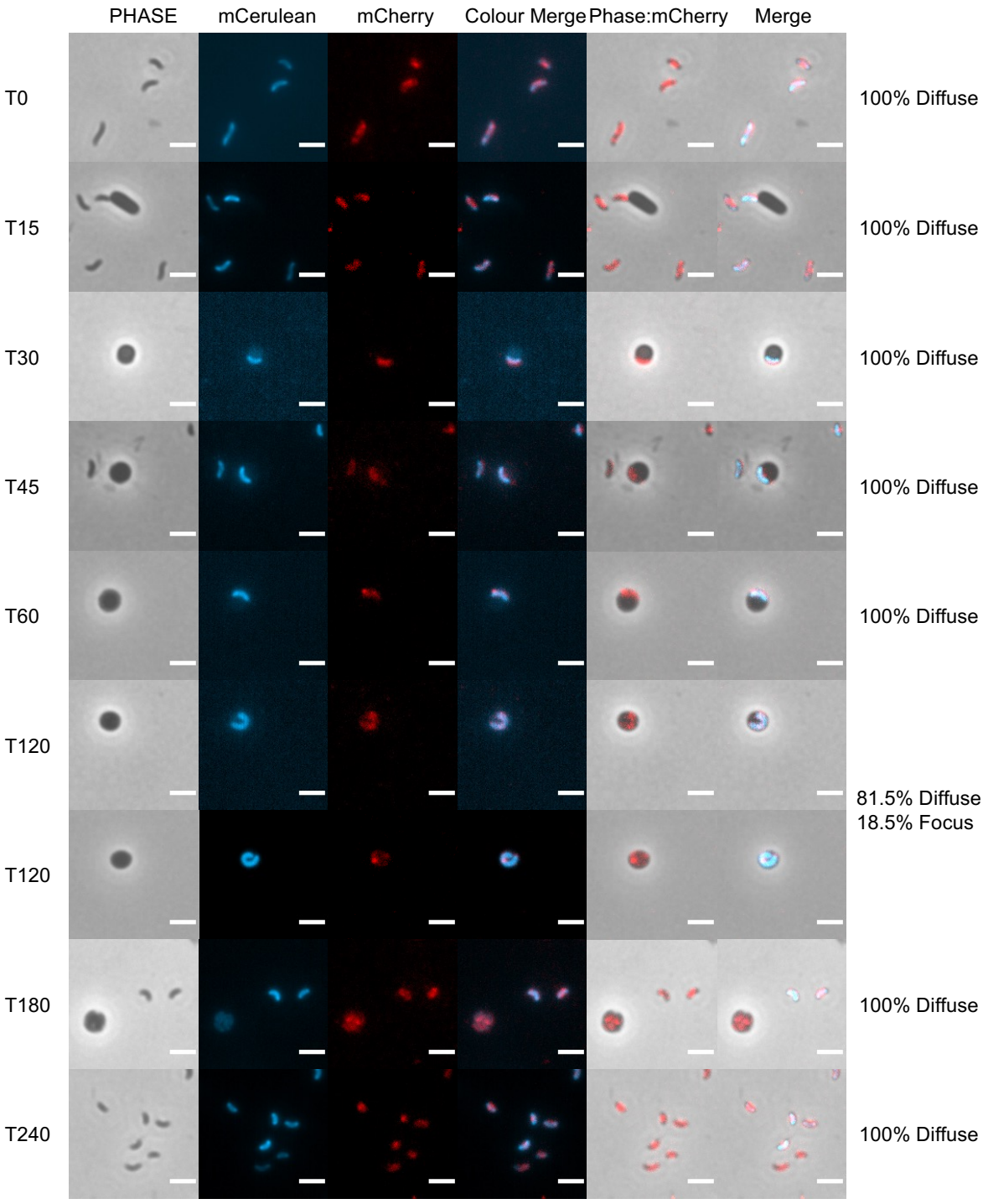

Figure 4.5.1: Bd0017mCherry is expressed by *B. bacteriovorus* throughout predation. *B. bacteriovorus* containing a C-terminally tagged mCherry-tagged Bd0017 protein and a constitutively expressed mCerulean-tagged Bd0064 protein (illuminating the cell body of the *Bdellovibrio*) were visualised via fluorescence microscopy, throughout predation of *E. coli*. Bd0017mCherry was diffusely expressed throughout predation. Foci of Bd0017mCherry expression are seen in some instances at 2 hours of predation. At least 5 fields of view were imaged from each of 2 biological replicates. Phase: Exposure 50 ms; mCerulean: Exposure 10 s, Excitation: 420-450 nm, Emission: 460-500 nm; mCherry: Exposure 10s, Excitation: 550-600 nm Emission: 610-665 nm. White scale bars represent 2 μM.

4.5.2. Fluorescently tagged SodC proteins, $SodC_{Bd0295}$ and $SodC_{Bd1401}$, are not discernibly expressed throughout predation of *E. coli* by *B. bacteriovorus.*

4.5.2.1. Bd0295

To determine whether Bd0295, a SodC Copper-Zinc Superoxide Dismutase protein, highlighted by the initial bacterial transcriptome study in zebrafish, was expressed by *Bdellovibrio* during predation, I fluorescently tagged Bd0295 with an mCherry and an mCerulean fluorescent tag at the C-terminus. Bd0295mCherry-tagged or Bd0295mCerulean-tagged *B. bacteriovorus* were visualised throughout predation. Bd0295mCherry and Bd0295mCerulean were not discernibly expressed throughout predation of *E. coli* by *B. bacteriovorus* (Figures 4.5.2 and 4.5.3).

4.5.2.2. Bd1401/SodC

To determine whether Bd1401, the other SodC Copper-Zinc Superoxide Dismutase protein in the *Bdellovibrio* genome, highlighted by literature searches and searches for sodC homologues within the *Bdellovibrio* genome, was expressed by *Bdellovibrio* during predation, I fluorescently tagged Bd1401 with an mCherry fluorescent tag at the C-terminus. Bd1401mCherry-tagged *B. bacteriovorus* were visualised throughout predation.

Bd1401mCherry was not discernibly expressed throughout predation of *E. coli* by *B. bacteriovorus* (Figure 4.5.4), except in a few rare instances (Figure 4.5.4, lower panel). However, tagging of Bd1401 with an mCherry tag appears to slow and impact predation, demonstrated through the presence of bdelloplasts at 4 hours, which would usually have lysed at this point. To conclusively prove that mCherry tagging of Bd1401 was impacting predation, I would need to repeat this timecourse in parallel with a Bd0064mCherry control, with matched *Bdellovibrio* PFU inputs, to rule out other experimental factors that may have slowed predation.

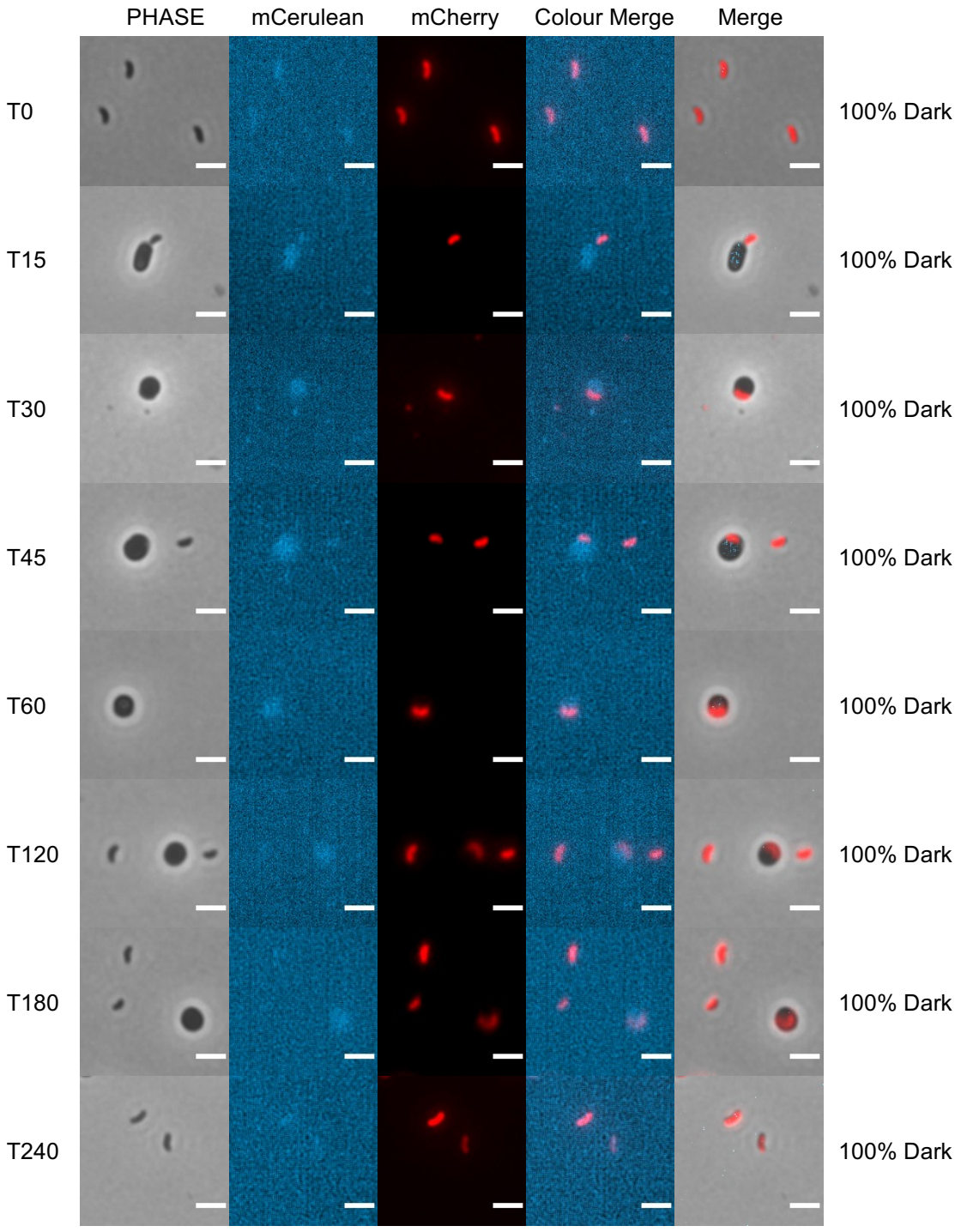

Figure 4.5.2: Bd0295mCerulean is not discernibly expressed by *B. bacteriovorus* throughout predation. *B. bacteriovorus* containing a C-terminally tagged mCerulean-tagged Bd0295 protein and a constitutively expressed mCherry-tagged Bd0064 protein (illuminating the cell body of the *Bdellovibrio*) were visualised via fluorescence microscopy, throughout predation of *E. coli*. Bd0295mCerulean was not discernibly expressed throughout predation. At least 5 fields of view were imaged from each of 2 biological replicates. Phase: Exposure 50 ms; mCerulean: Exposure 10 s, Excitation: 420-450 nm, Emission: 460-500 nm; mCherry: Exposure 10s, Excitation: 550-600 nm Emission: 610-665 nm. White scale bars represent 2 μM.

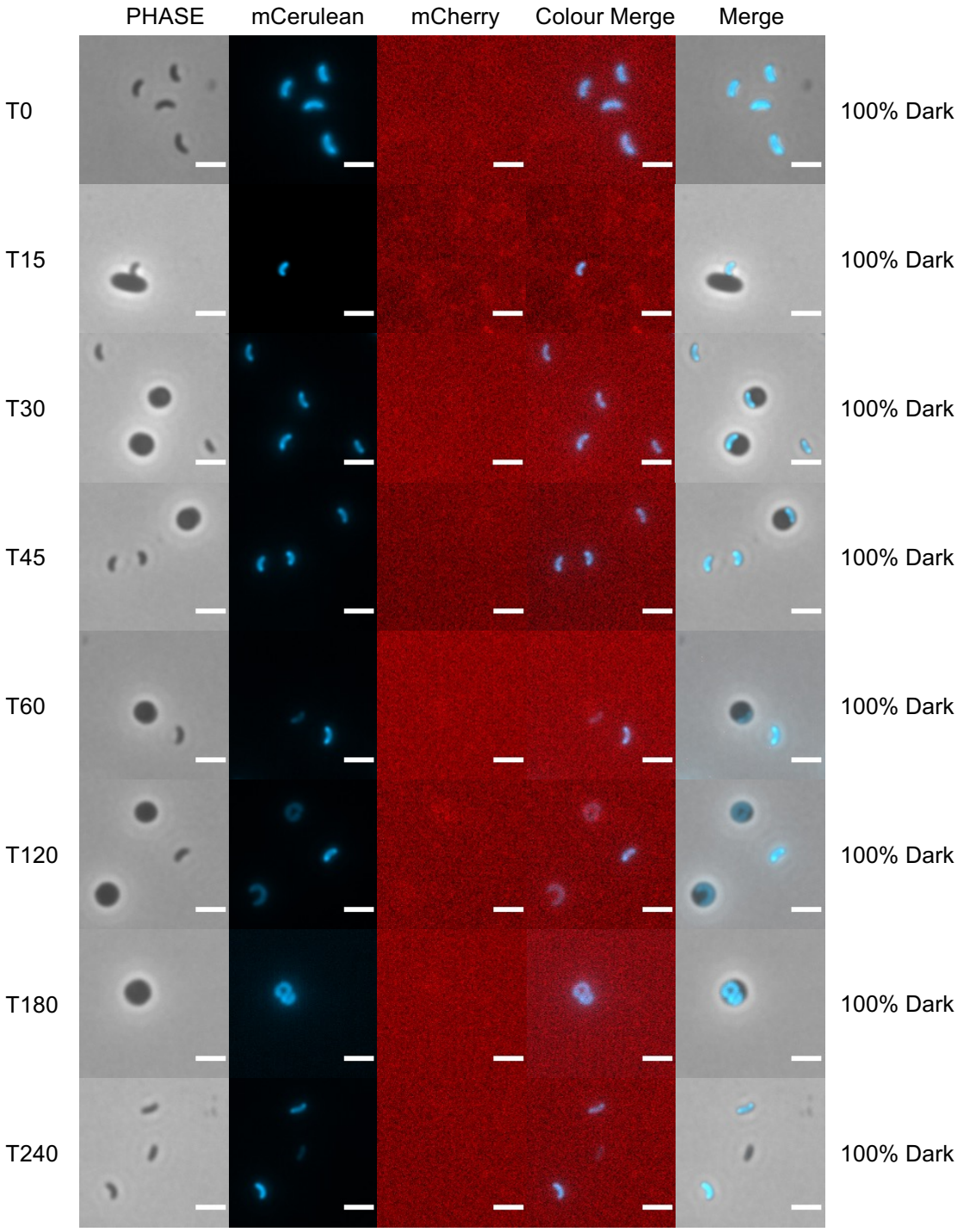

Figure 4.5.3: Bd0295mCherry is not discernibly expressed by *B. bacteriovorus* throughout predation. *B. bacteriovorus* containing a C-terminally tagged mCherry-tagged Bd0295 protein and a constitutively expressed mCerulean-tagged Bd0064 protein (illuminating the cell body of the *Bdellovibrio*) were visualised via fluorescence microscopy, throughout predation of *E. coli*. Bd0295mCherry was not discernibly expressed throughout predation. At least 5 fields of view were imaged from each of 2 biological replicates. Phase: Exposure 50 ms; mCerulean: Exposure 10 s, Excitation: 420-450 nm, Emission: 460-500 nm; mCherry: Exposure 10s, Excitation: 550-600 nm Emission: 610-665 nm. White scale bars represent 2 μM.

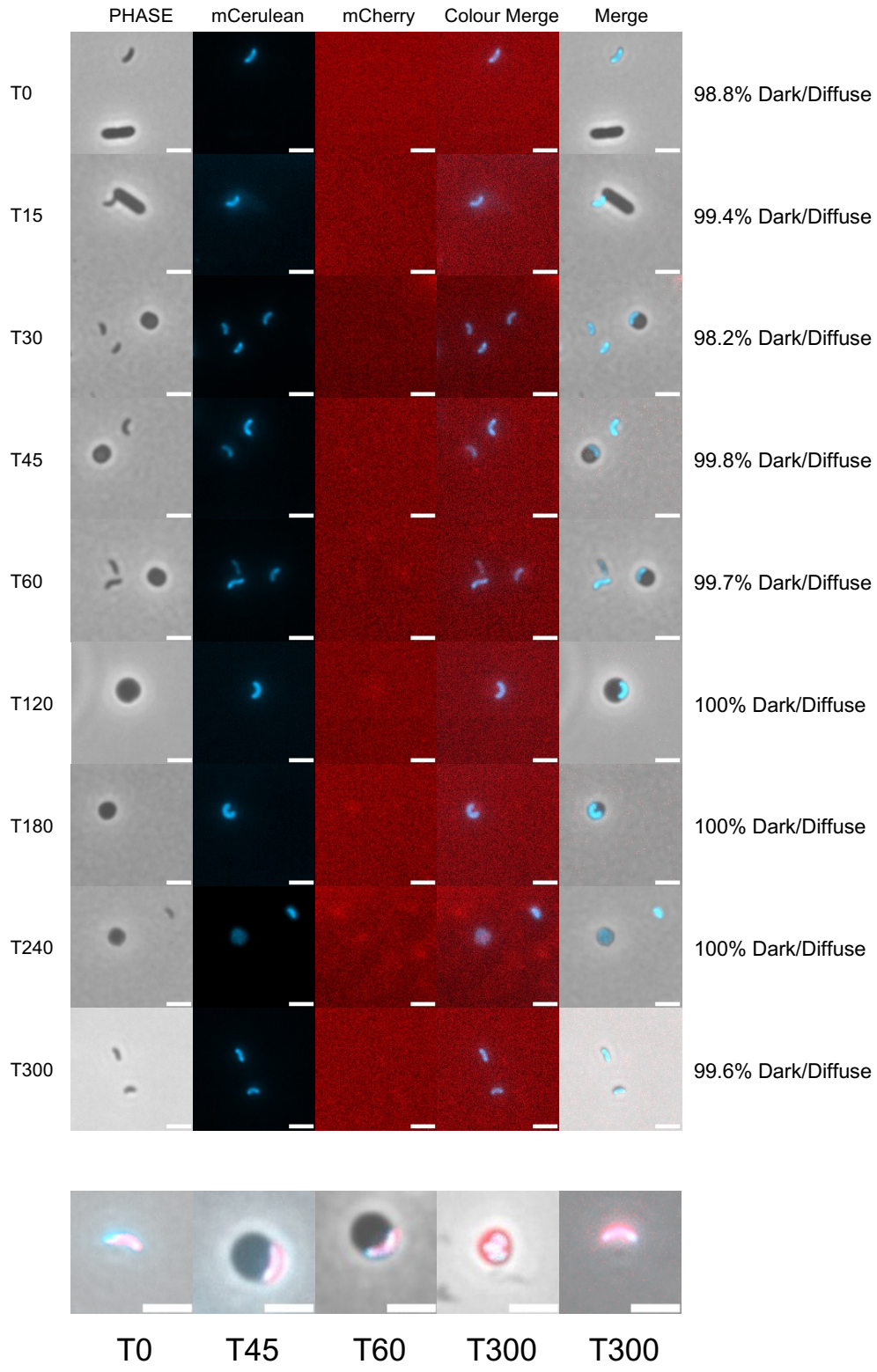

Figure 4.5.4: Bd1401mCherry is not discernibly expressed by *B. bacteriovorus* throughout predation. *B. bacteriovorus* containing a C-terminally tagged mCherry-tagged Bd1401 protein and a constitutively expressed mCerulean-tagged Bd0064 protein (illuminating the cell body of the *Bdellovibrio*) were visualised via fluorescence microscopy, throughout predation of *E. coli*. Bd1401mCherry was not discernibly expressed throughout predation. Some instances of Bd1401mCherry expression were seen throughout predation (lower panel) but these instances were very rare. At least 5 fields of view were imaged from each of 2 biological replicates. Phase: Exposure 50 ms; mCerulean: Exposure 10 s, Excitation: 420-450 nm, Emission: 460-500 nm; mCherry: Exposure 10s, Excitation: 550-600 nm Emission: 610-665 nm. White scale bars represent 2 μM.

4.5.3. Fluorescently tagged catalase proteins, Bd0798/CatA and Bd1154/KatA, and their neighbouring regulatory ankyrin proteins, Bd0799/AnkB and Bd1155/AnkB, are not discernibly expressed throughout predation of *E. coli* by *B. bacteriovorus.*

4.5.3.1. Bd0798/CatA

To determine whether Bd0798, a catalase protein highlighted by the initial bacterial transcriptome study in zebrafish, was expressed by *Bdellovibrio* during predation, I fluorescently tagged Bd0798 with an mCherry and an mCerulean fluorescent tag at the C-terminus. Bd0798mCherry-tagged or Bd0798mCerulean-tagged *B. bacteriovorus* were visualised throughout predation. Bd0798mCherry and Bd0798mCerulean were not discernibly expressed throughout predation (Figure 4.5.5 and 4.5.6).

4.5.3.2. Bd0799/ankB

To determine whether Bd0799, a regulatory ankyrin protein, was expressed by *Bdellovibrio* during predation, I fluorescently tagged Bd0799 with an mCherry fluorescent tag at the C-terminus.

Bd0799mCherry-tagged *B. bacteriovorus* were visualised throughout predation. Fluorescent tagging of Bd0799 with an mCherry protein required the incorporation of a flexible peptide linker, as repeated attempts to tag Bd0799 directly with the mCherry tag caused mutations in the fluorescent tag and gene (Rob Till, Personal Communication), suggesting that the mCherry tag was interfering with the expression of Bd0799 in some way. Bd0799mCherry was not discernibly expressed throughout predation (Figure 4.5.7).

4.5.3.3. Bd1154/KatA

To determine whether Bd1154, a catalase protein homologous to Bd0798 and highlighted by searches of the *Bdellovibrio* genome for potential homologues, was expressed by *Bdellovibrio* during predation, I fluorescently tagged Bd1154 with an mCherry fluorescent tag at the C-terminus. Bd1154mCherry-tagged *B. bacteriovorus* were visualised throughout predation. Bd1154mCherry was not discernibly expressed throughout predation of *E. coli* by *B. bacteriovorus* (Figure 4.5.8).

4.5.3.4. Bd1155/AnkB

To determine whether Bd1155 was expressed by *Bdellovibrio* during predation, I fluorescently tagged Bd1155 with an mCerulean fluorescent tag at the C-terminus. Bd1155mCerulean-tagged *B. bacteriovorus* were visualised throughout predation. Bd1155mCerulean was not discernibly expressed by the majority of *Bdellovibrio* throughout predation of *E. coli* by *B. bacteriovorus* (Figure 4.5.9). The expression of Bd1155mCerulean in attack phase *Bdellovibrio*, and the conditions under which this occurs, would require further investigation.

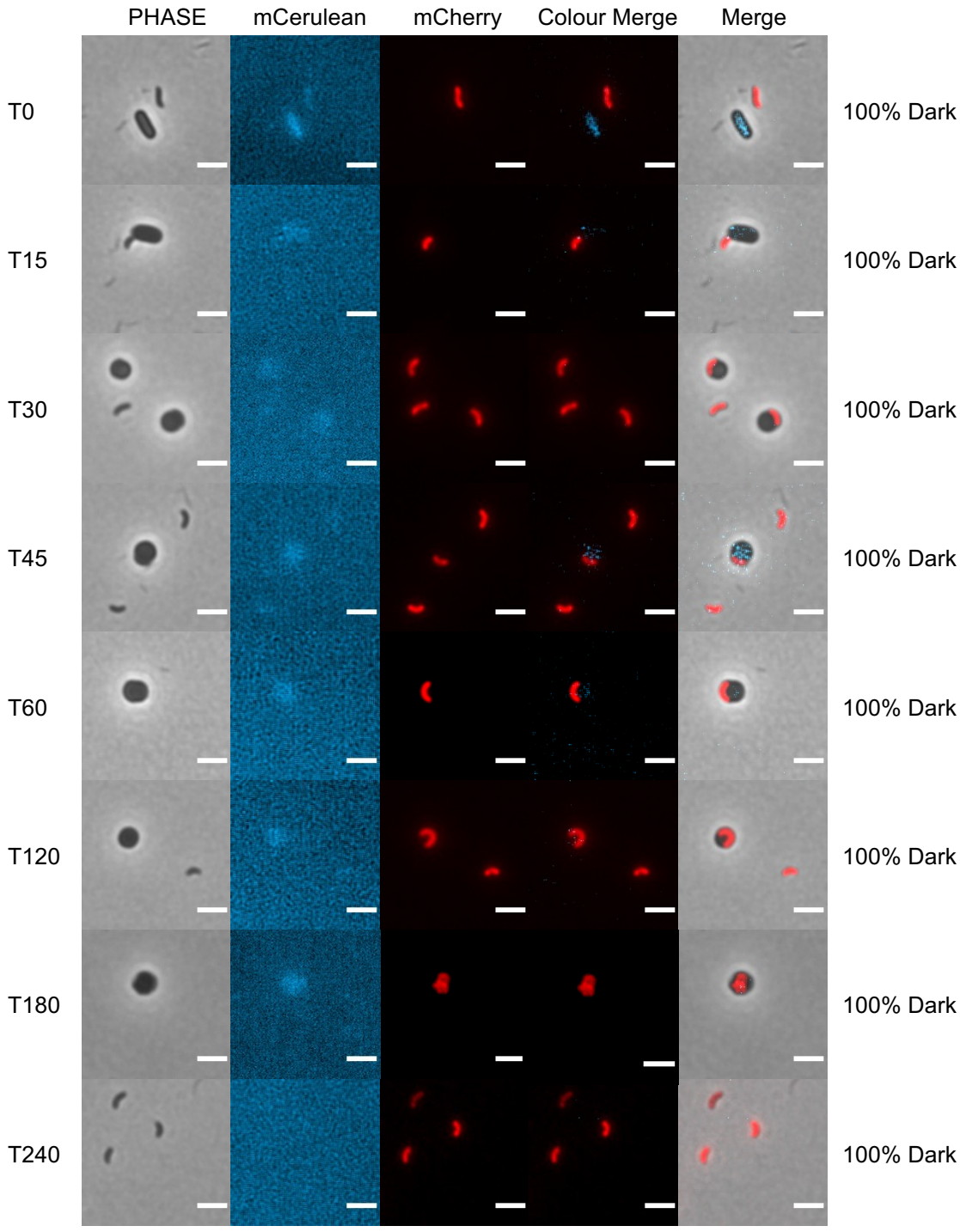

Figure 4.5.5: Bd0798mCerulean is not discernibly expressed by *B. bacteriovorus* throughout predation. *B. bacteriovorus* containing a C-terminally tagged mCerulean-tagged Bd0798 protein and a constitutively expressed mCherry-tagged Bd0064 protein (illuminating the cell body of the *Bdellovibrio*) were visualised via fluorescence microscopy, throughout predation of *E. coli*. Bd0798mCerulean was not discernibly expressed throughout predation. At least 5 fields of view were imaged from each of 2 biological replicates. Phase: Exposure 50 ms; mCerulean: Exposure 10 s, Excitation: 420-450 nm, Emission: 460-500 nm; mCherry: Exposure 10s, Excitation: 550-600 nm Emission: 610-665 nm. White scale bars represent 2 μM.

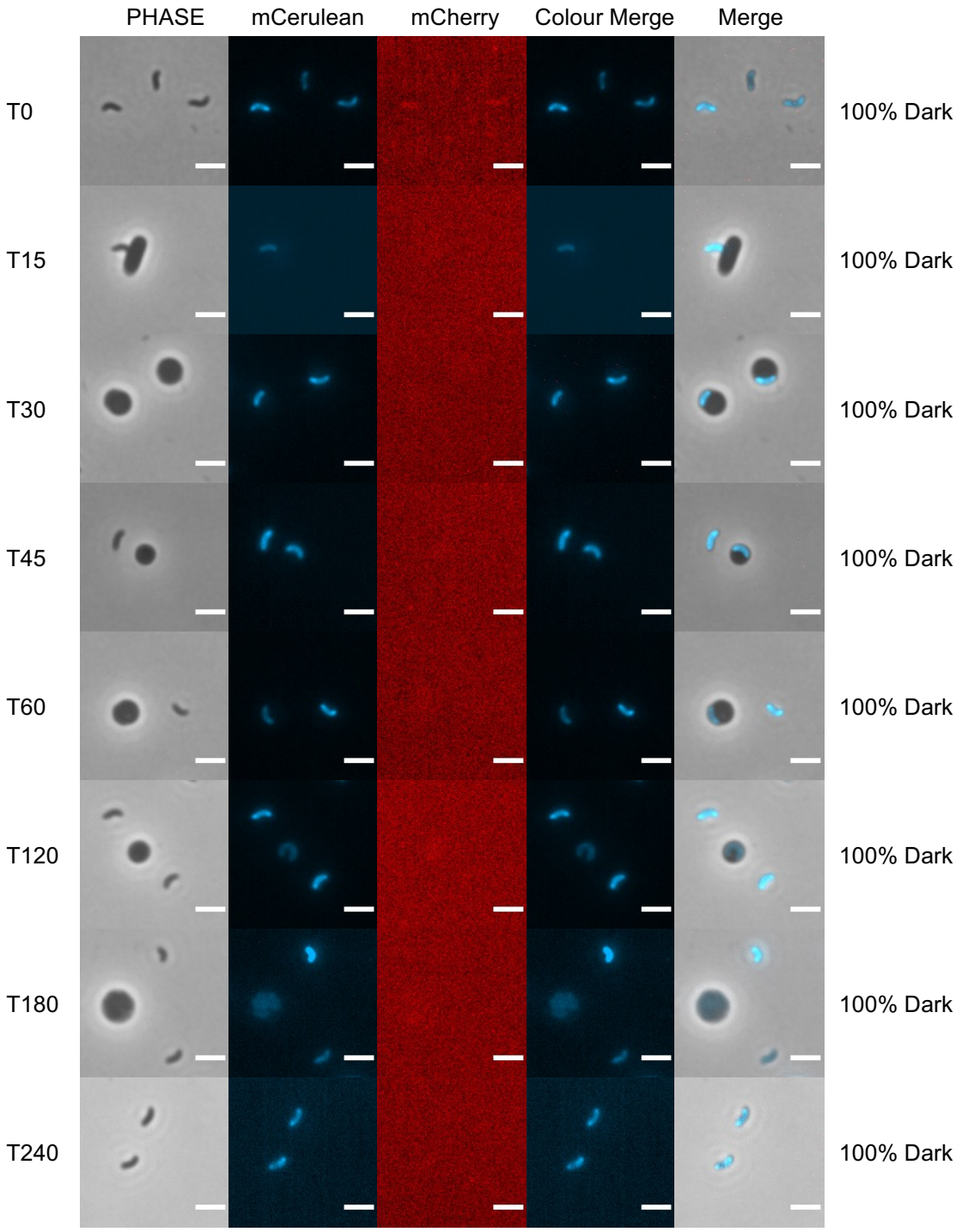

Figure 4.5.6: Bd0798mCherry is not discernibly expressed by *B. bacteriovorus* throughout predation. *B. bacteriovorus* containing a C-terminally tagged mCherry-tagged Bd0798 protein and a constitutively expressed mCerulean-tagged Bd0064 protein (illuminating the cell body of the *Bdellovibrio*) were visualised via fluorescence microscopy, throughout predation of *E. coli*. Bd0798mCherry was not discernibly expressed throughout predation. At least 5 fields of view were imaged from each of 2 biological replicates. Phase: Exposure 50 ms; mCerulean: Exposure 10 s, Excitation: 420-450 nm, Emission: 460-500 nm; mCherry: Exposure 10s, Excitation: 550-600 nm Emission: 610-665 nm. White scale bars represent 2 μM.

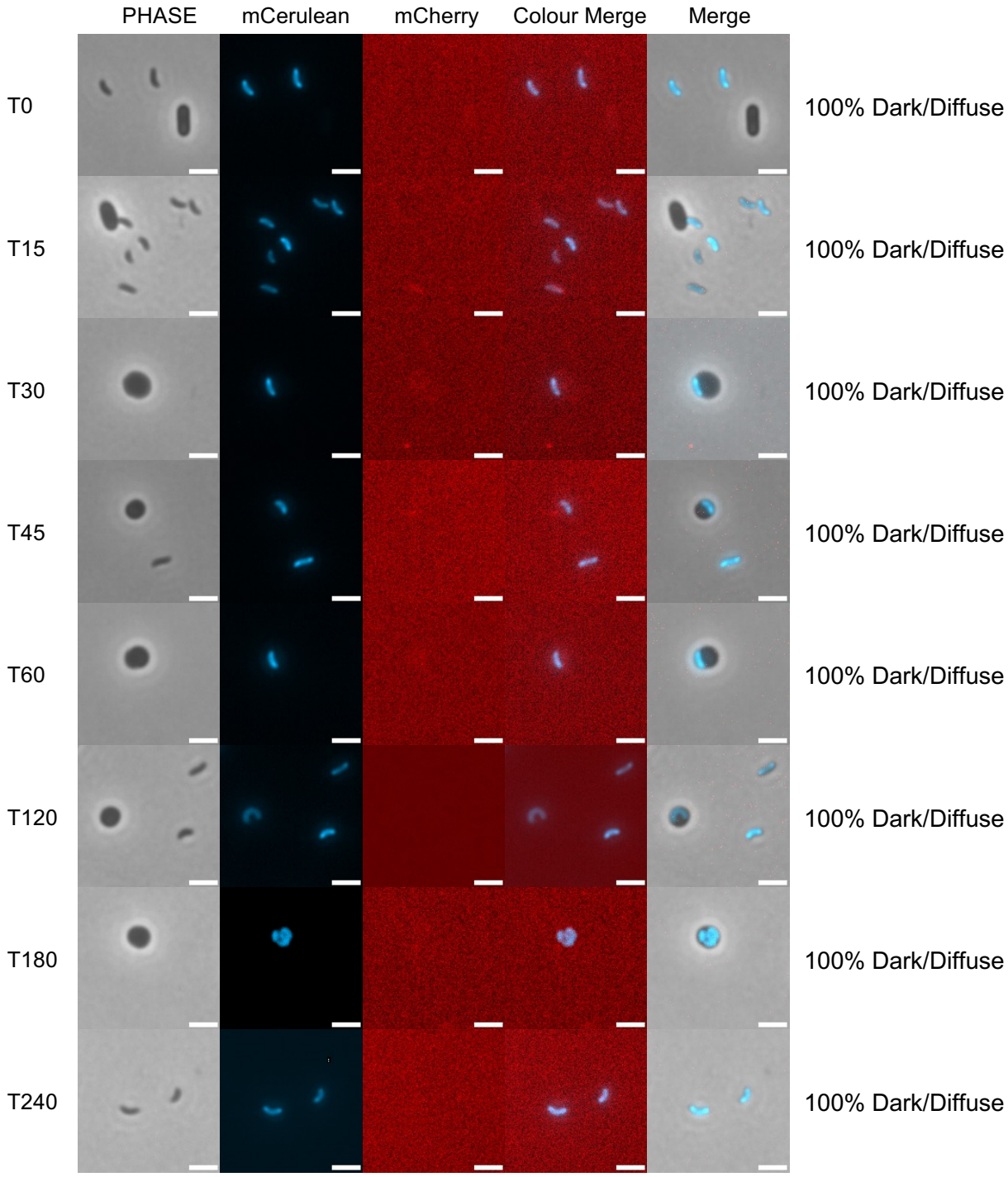

Figure 4.5.7: Bd0799mCherry is not discernibly expressed by *B. bacteriovorus* throughout predation. *B. bacteriovorus* containing a C-terminally tagged mCherry-tagged Bd0799 protein and a constitutively expressed mCerulean-tagged Bd0064 protein (illuminating the cell body of the *Bdellovibrio*) were visualised via fluorescence microscopy, throughout predation of *E. coli*. Bd0799mCherry was not discernibly expressed throughout predation. At least 5 fields of view were imaged from each of 2 biological replicates. Phase: Exposure 50 ms; mCerulean: Exposure 10 s, Excitation: 420-450 nm, Emission: 460-500 nm; mCherry: Exposure 10s, Excitation: 550-600 nm Emission: 610-665 nm. White scale bars represent 2 μM.

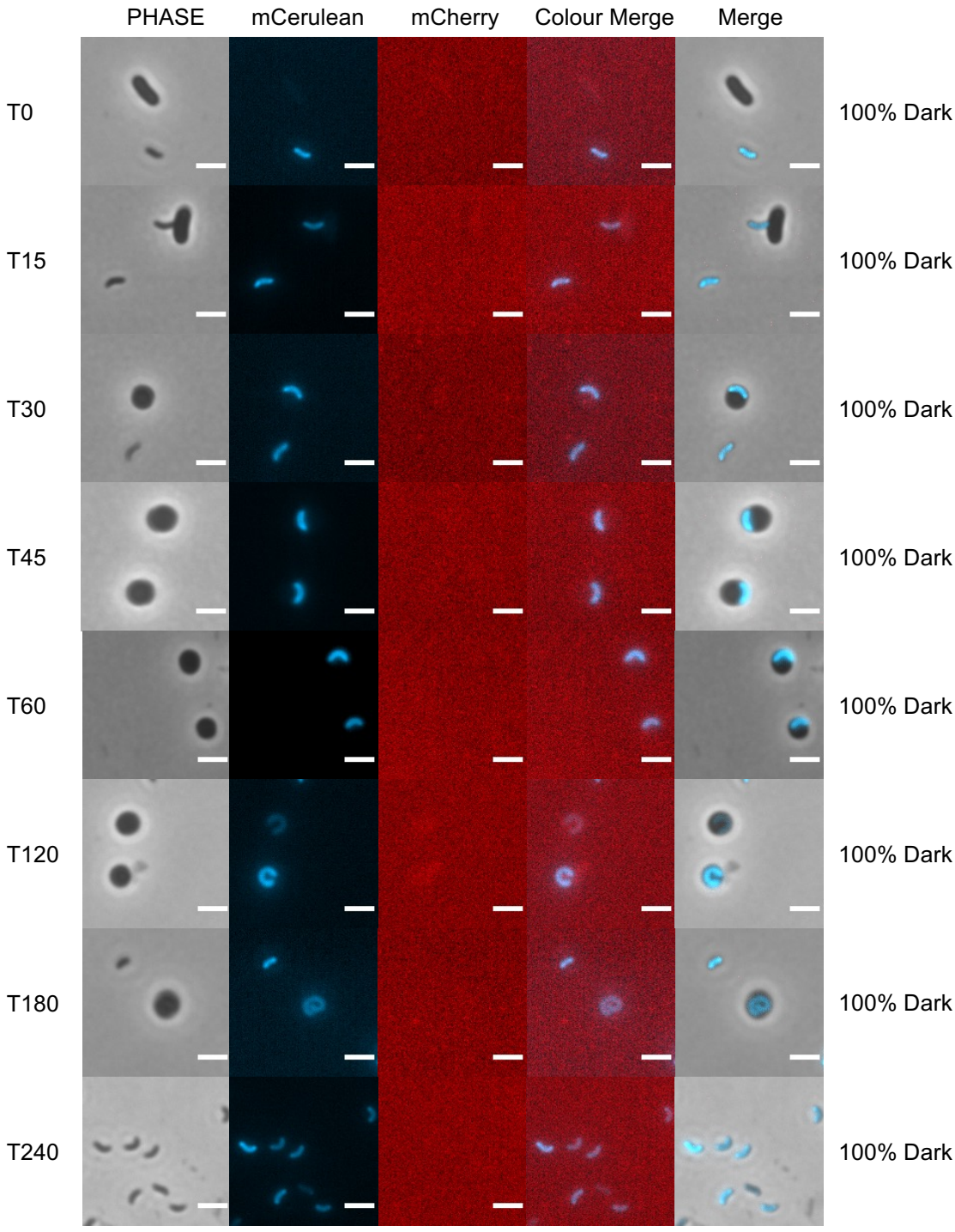

Figure 4.5.8: Bd1154mCherry is not discernibly expressed by *B. bacteriovorus* throughout predation. *B. bacteriovorus* containing a C-terminally tagged mCherry-tagged Bd1154 protein and a constitutively expressed mCerulean-tagged Bd0064 protein (illuminating the cell body of the *Bdellovibrio*) were visualised via fluorescence microscopy, throughout predation of *E. coli*. Bd1154mCherry was not discernibly expressed throughout predation. At least 5 fields of view were imaged from each of 2 biological replicates. Phase: Exposure 50 ms; mCerulean: Exposure 10 s, Excitation: 420-450 nm, Emission: 460-500 nm; mCherry: Exposure 10s, Excitation: 550-600 nm Emission: 610-665 nm. White scale bars represent 2 μM.

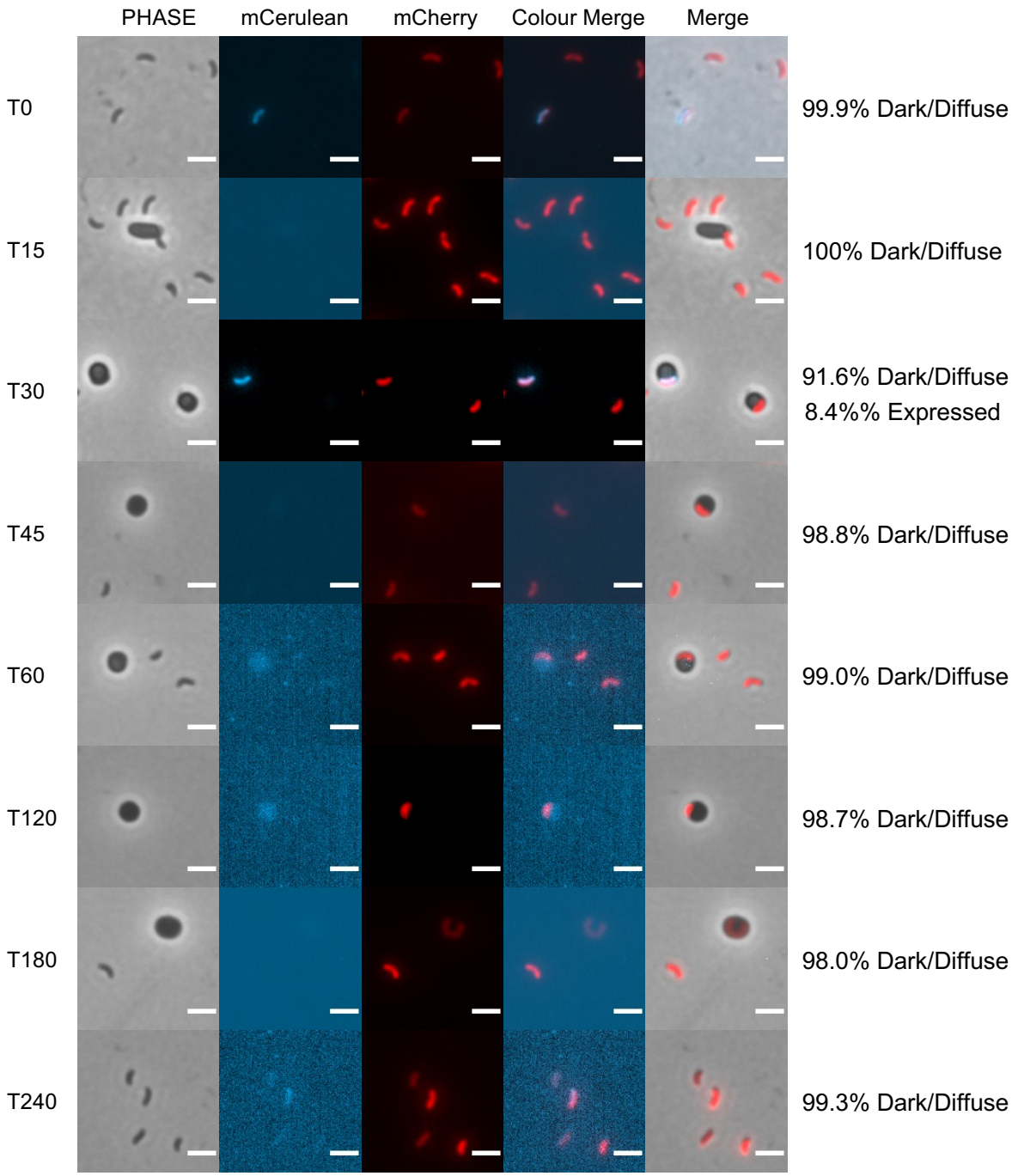

Figure 4.5.9: Bd1155mCerulean is not discernibly expressed by the majority of *B. bacteriovorus* cells throughout predation. *B. bacteriovorus* containing a C-terminally tagged mCerulean-tagged Bd1155 protein and a constitutively expressed mCherry-tagged Bd0064 protein (illuminating the cell body of the *Bdellovibrio*) were visualised via fluorescence microscopy, throughout predation of *E. coli*. Bd1155mCerulean was not discernibly expressed by the majority of *Bdellovibrio* throughout predation. In some instances, Bd1155mCerulean is diffusely expressed in attack phase cells at 0 and 15 minutes of predation At least 5 fields of view were imaged from each of 2 biological replicates. Phase: Exposure 50 ms; mCerulean: Exposure 10 s, Excitation: 420-450 nm, Emission: 460-500 nm; mCherry: Exposure 10s, Excitation: 550-600 nm Emission: 610-665 nm. White scale bars represent 2 μM.

4.5.4. Fluorescently tagged Bd1815 is expressed throughout predation of *E. coli* by *B. bacteriovorus.*

To determine whether Bd1815, a hypothetical protein that I hypothesise to resemble an Outer Membrane Protein or porin and highlighted by the initial bacterial transcriptome study in zebrafish, was expressed by *Bdellovibrio* during predation, I fluorescently tagged Bd1815 with an mCherry and an mCerulean fluorescent tag at the C-terminus. Bd1815mCherry-tagged or Bd1815mCerulean-tagged *B. bacteriovorus* were visualised throughout predation. Both fluorescent tags were assessed as I did not know which would be more visible within the macrophage, with macrophage showing autofluorescence in both the mCherry and mCerulean channels, and whether the location of the protein would influence fluorescent tag expression, as Bd1815 has a signal peptide and will localise to the periplasm. Bd1815mCherry and Bd1815mCerulean were expressed throughout predation of *E. coli* by *B. bacteriovorus,* forming single foci in approximately 14% of attack phase cells at T_0 and T_{240} (Figures 4.5.10 and 4.5.11). The expression of Bd1815mCherry suggests that Bd1815 is expressed in single foci in a small proportion of *Bdellovibrio* throughout predation, rather than just in attack phase. This may be due to the mCherry signal being clearer throughout predation than the mCerulean signal, which is sometimes indiscernible from the blue autofluorescence of *E. coli* prey.

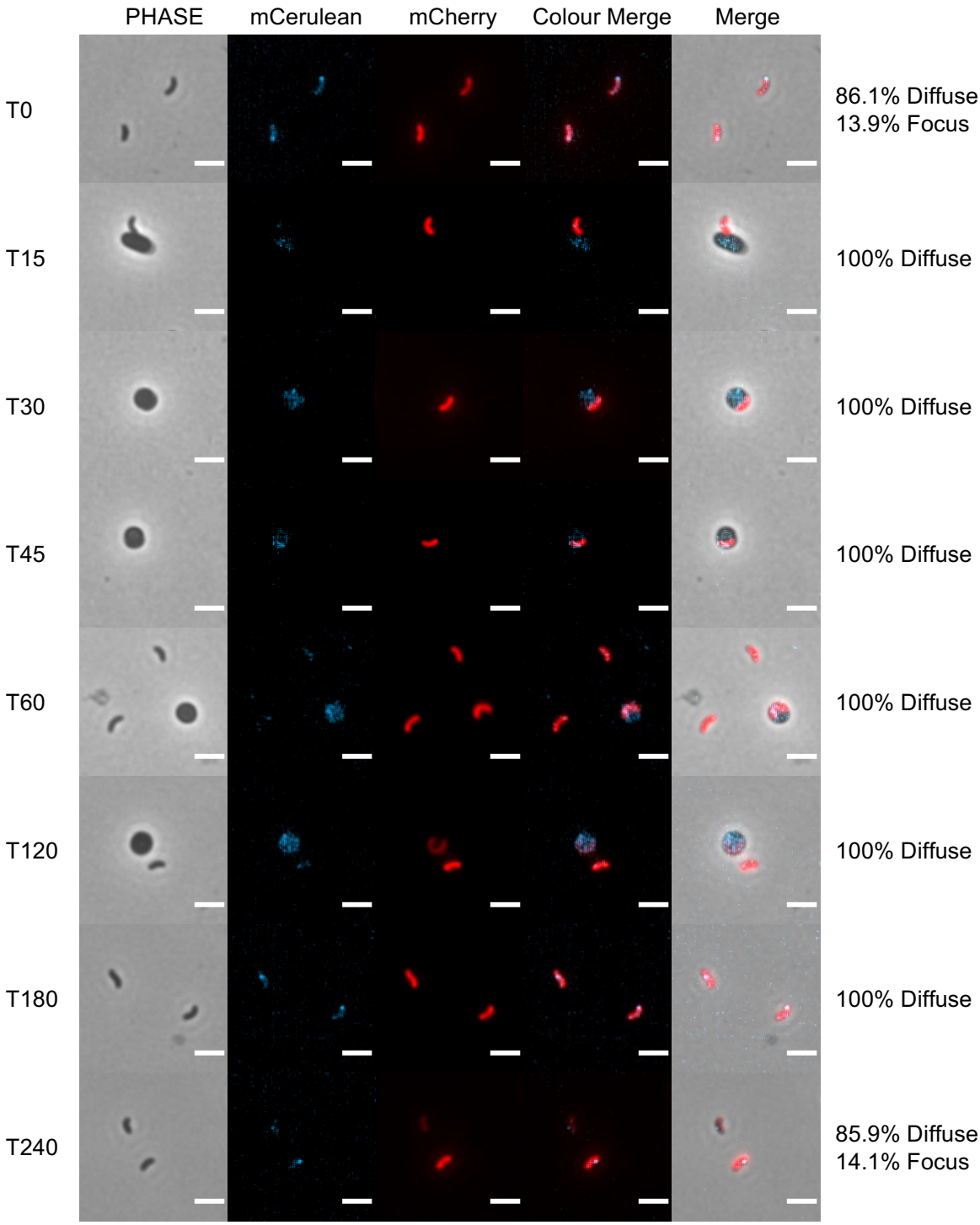

Figure 4.5.10: Bd1815mCerulean is expressed by *B. bacteriovorus* throughout predation. *B. bacteriovorus* containing a C-terminally tagged mCerulean-tagged Bd1815 protein and a constitutively expressed mCherry-tagged Bd0064 protein (illuminating the cell body of the *Bdellovibrio*) were visualised via fluorescence microscopy, throughout predation of *E. coli*. Bd1815mCerulean was expressed throughout predation, forming foci in some instances in attack phase cells, and expressed diffusely throughout the remainder of predation. At least 5 fields of view were imaged from each of 2 biological replicates. Phase: Exposure 50 ms; mCerulean: Exposure 10 s, Excitation: 420-450 nm, Emission: 460-500 nm; mCherry: Exposure 10s, Excitation: 550-600 nm Emission: 610-665 nm. White scale bars represent 2 μM.

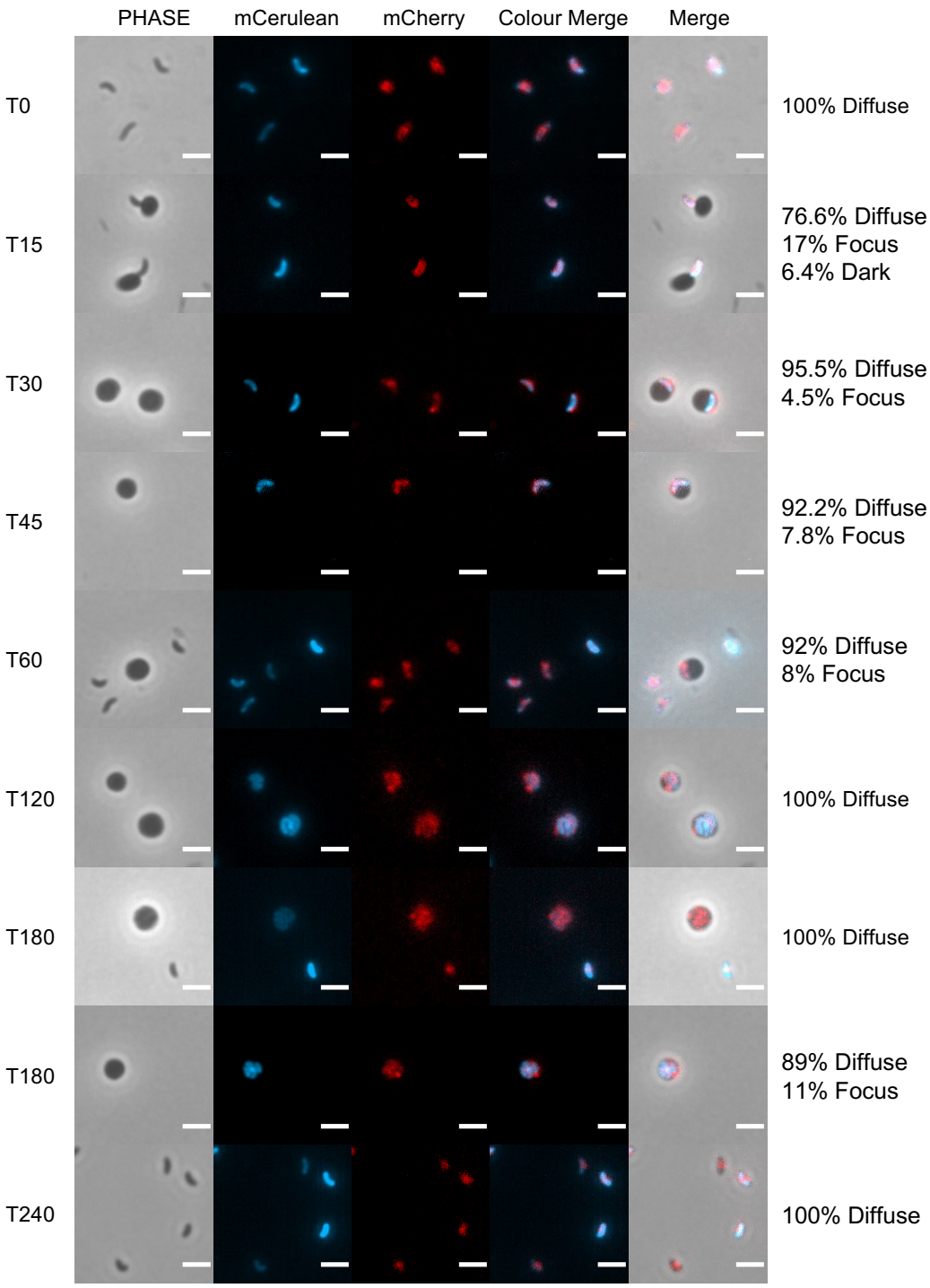

Figure 4.5.11: Bd1815mCherry is expressed by *B. bacteriovorus* throughout predation. *B. bacteriovorus* containing a C-terminally tagged mCherry-tagged Bd1815 protein and a constitutively expressed mCerulean-tagged Bd0064 protein (illuminating the cell body of the *Bdellovibrio*) were visualised via fluorescence microscopy, throughout predation of *E. coli*. Bd1815mCherry was expressed throughout predation, forming a central distribution in attack phase cells, and expressed diffusely throughout the remainder of predation. At least 5 fields of view were imaged from each of 2 biological replicates. Phase: Exposure 50 ms; mCerulean: Exposure 10 s, Excitation: 420-450 nm, Emission: 460-500 nm; mCherry: Exposure 10s, Excitation: 550-600 nm Emission: 610-665 nm. White scale bars represent 2 μM.

4.5.5. Fluorescently tagged alkyl hydroperoxide reductase proteins, Bd2517/AhpC and Bd2518/AhpF, are expressed throughout predation of *E. coli* by *B. bacteriovorus*.

To determine whether Bd2517 and Bd2518, two alkyl hydroperoxide reductase proteins involved in hydrogen peroxide detoxification and highlighted by initial transcriptional studies in zebrafish, were expressed by *Bdellovibrio* during predation, I fluorescently tagged Bd2517 and Bd2518 with an mCerulean fluorescent tag at the C-terminus. Bd2517mCerulean-tagged or Bd2518mCerulean-tagged *B. bacteriovorus* were visualised throughout predation. Bd2517mCerulean was expressed as two foci in the majority of attack phase cells at T_0, after which Bd2517mCerulean expression shifts, towards a diffuse expression throughout intraperiplasmic growth (T45 onwards), resuming its bipolar foci expression in newly released attack phase progeny at 4 hours (Figure 4.5.12). Bd2518mCerulean was expressed diffusely throughout predation of *E. coli* by *B. bacteriovorus* (Figure 4.5.13).

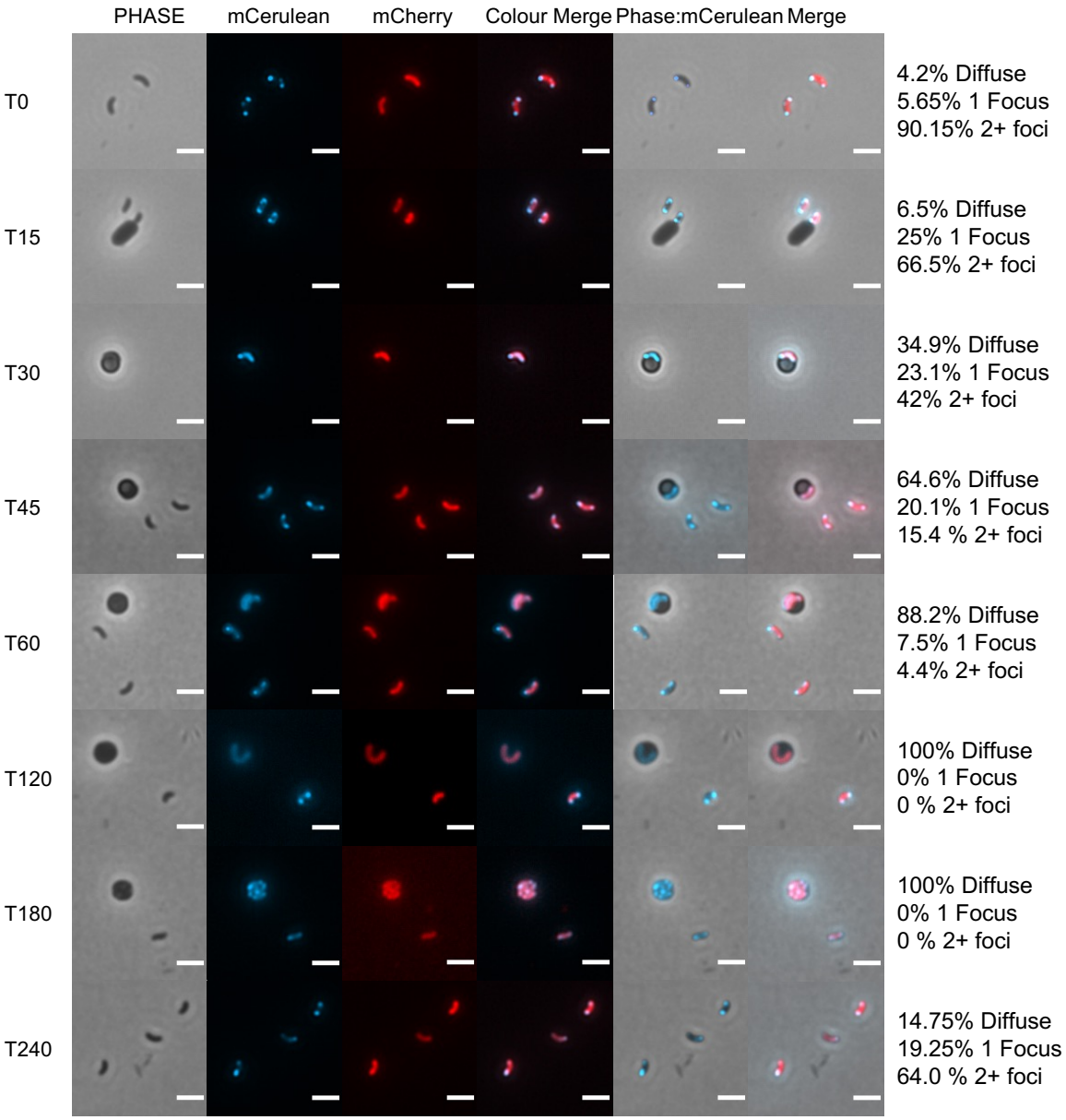

Figure 4.5.12: Bd2517mCerulean is expressed by *B. bacteriovorus* throughout predation. *B. bacteriovorus* containing a C-terminally tagged mCerulean-tagged Bd2517 protein and a constitutively expressed mCherry-tagged Bd0064 protein (illuminating the cell body of the *Bdellovibrio*) were visualised via fluorescence microscopy, throughout predation of *E. coli*. Bd2517mCerulean was expressed in a bipolar foci distribution in the majority of *Bdellovibrio* during attack phase. Throughout predation, Bd2517mCerulean shifts from a bipolar foci distribution, towards a diffuse expression throughout intraperiplasmic growth (T45 onwards), resuming its bipolar foci expression in newly released attack phase progeny at 4 hours. At least 5 fields of view were imaged from each of 2 biological replicates. Phase: Exposure 50 ms; mCerulean: Exposure 10 s, Excitation: 420-450 nm, Emission: 460-500 nm; mCherry: Exposure 10s, Excitation: 550-600 nm Emission: 610-665 nm. White scale bars represent 2 μM.

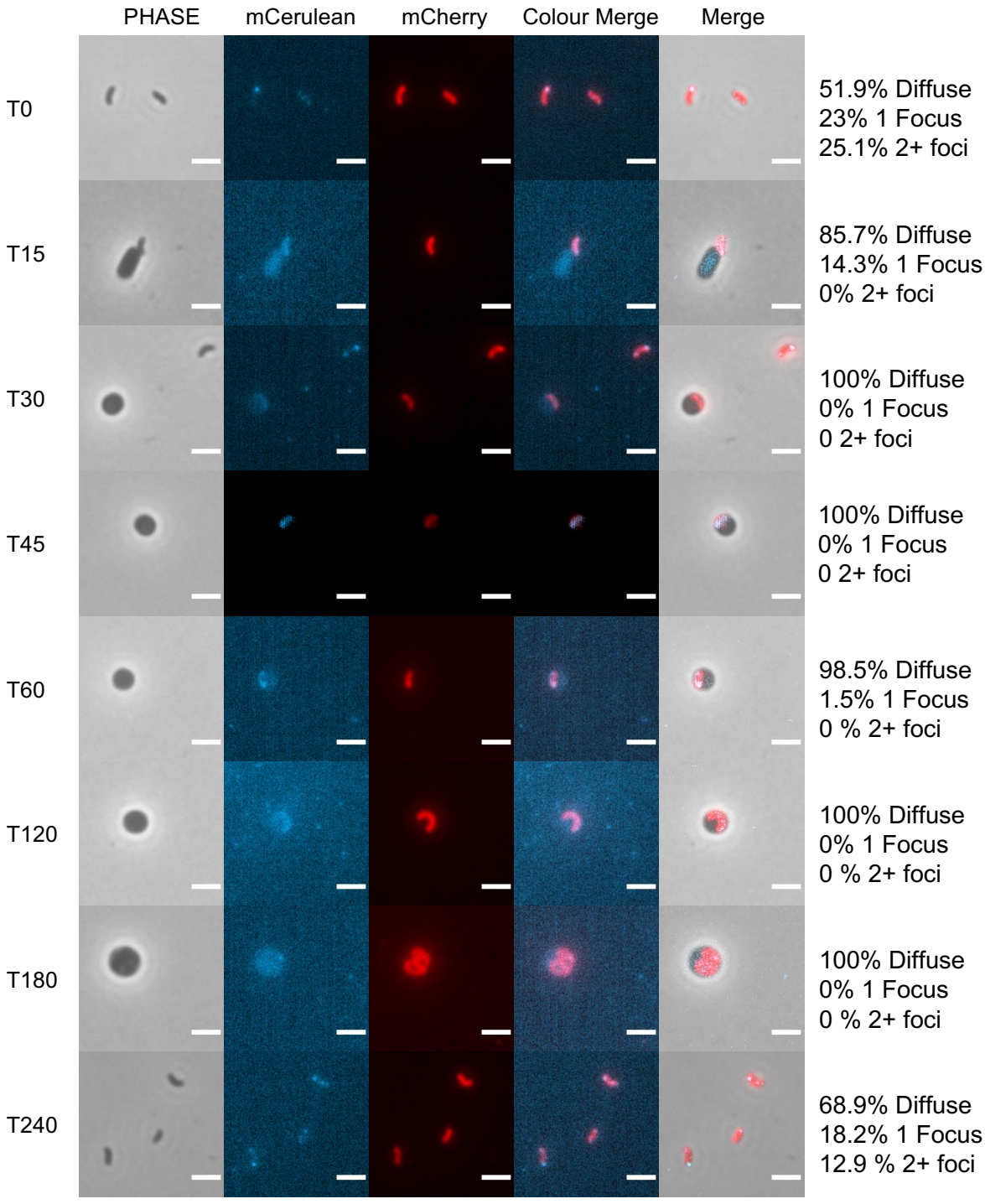

Figure 4.5.13: Bd2518mCerulean is expressed by *B. bacteriovorus* throughout predation. *B. bacteriovorus* containing a C-terminally tagged mCerulean-tagged Bd2518 protein and a constitutively expressed mCherry-tagged Bd0064 protein (illuminating the cell body of the *Bdellovibrio*) were visualised via fluorescence microscopy, throughout predation of *E. coli*. Bd2518mCerulean was expressed diffusely in the majority of *Bdellovibrio* during attack phase and throughout predation. At least 5 fields of view were imaged from each of 2 biological replicates. Phase: Exposure 50 ms; mCerulean: Exposure 10 s, Excitation: 420-450 nm, Emission: 460-500 nm; mCherry: Exposure 10s, Excitation: 550-600 nm Emission: 610-665 nm. White scale bars represent 2 μM.

4.5.6. Bd2620/Dps is expressed throughout predation of *E. coli* by *B. bacteriovorus.*

To determine whether Bd2620, a Dps DNA protection from starvation protein highlighted by initial transcriptional studies in zebrafish, was expressed by *Bdellovibrio* during predation, I fluorescently tagged Bd2620 with an mCerulean fluorescent tag at the C-terminus. Bd2620mCerulean-tagged *B. bacteriovorus* were visualised throughout predation. Bd2620mCerulean was expressed throughout predation of *E. coli* by *B. bacteriovorus* (Figure 4.5.14).

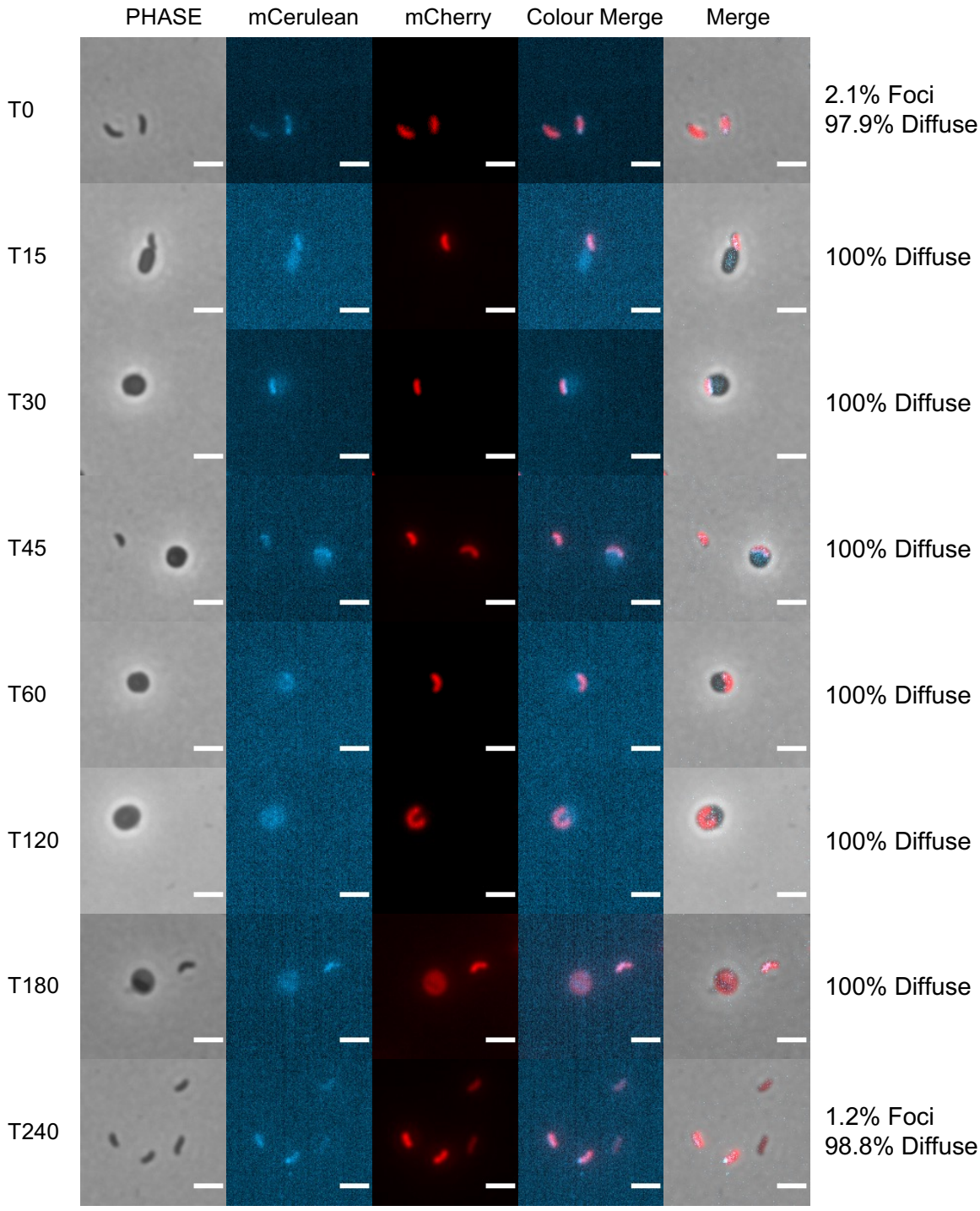

Figure 4.5.14: Bd2620mCerulean is expressed by *B. bacteriovorus* throughout predation. *B. bacteriovorus* containing a C-terminally tagged mCerulean-tagged Bd2620 protein and a constitutively expressed mCherry-tagged Bd0064 protein (illuminating the cell body of the *Bdellovibrio*) were visualised via fluorescence microscopy, throughout predation of *E. coli*. Bd2620mCerulean was expressed throughout predation, although expression appears fainter throughout intraperiplasmic growth (T60-T180) and is not discernible above prey autofluorescence. At least 5 fields of view were imaged from each of 2 biological replicates. Phase: Exposure 50 ms; mCerulean: Exposure 10 s, Excitation: 420-450 nm, Emission: 460-500 nm; mCherry: Exposure 10s, Excitation: 550-600 nm Emission: 610-665 nm. White scale bars represent 2 μM.

4.5.7. Bd3203 is expressed throughout predation of *E. coli* by *B. bacteriovorus.*

To determine whether Bd3203, a hypothetical protein highlighted by initial transcriptional studies in zebrafish, was expressed by *Bdellovibrio* during predation, I fluorescently tagged Bd3203 with an mCerulean fluorescent tag at the C-terminus. Bd3203mCerulean-tagged *B. bacteriovorus* were visualised throughout predation. Bd3203mCerulean was expressed throughout predation of *E. coli* by *B. bacteriovorus* (Figure 4.5.15).

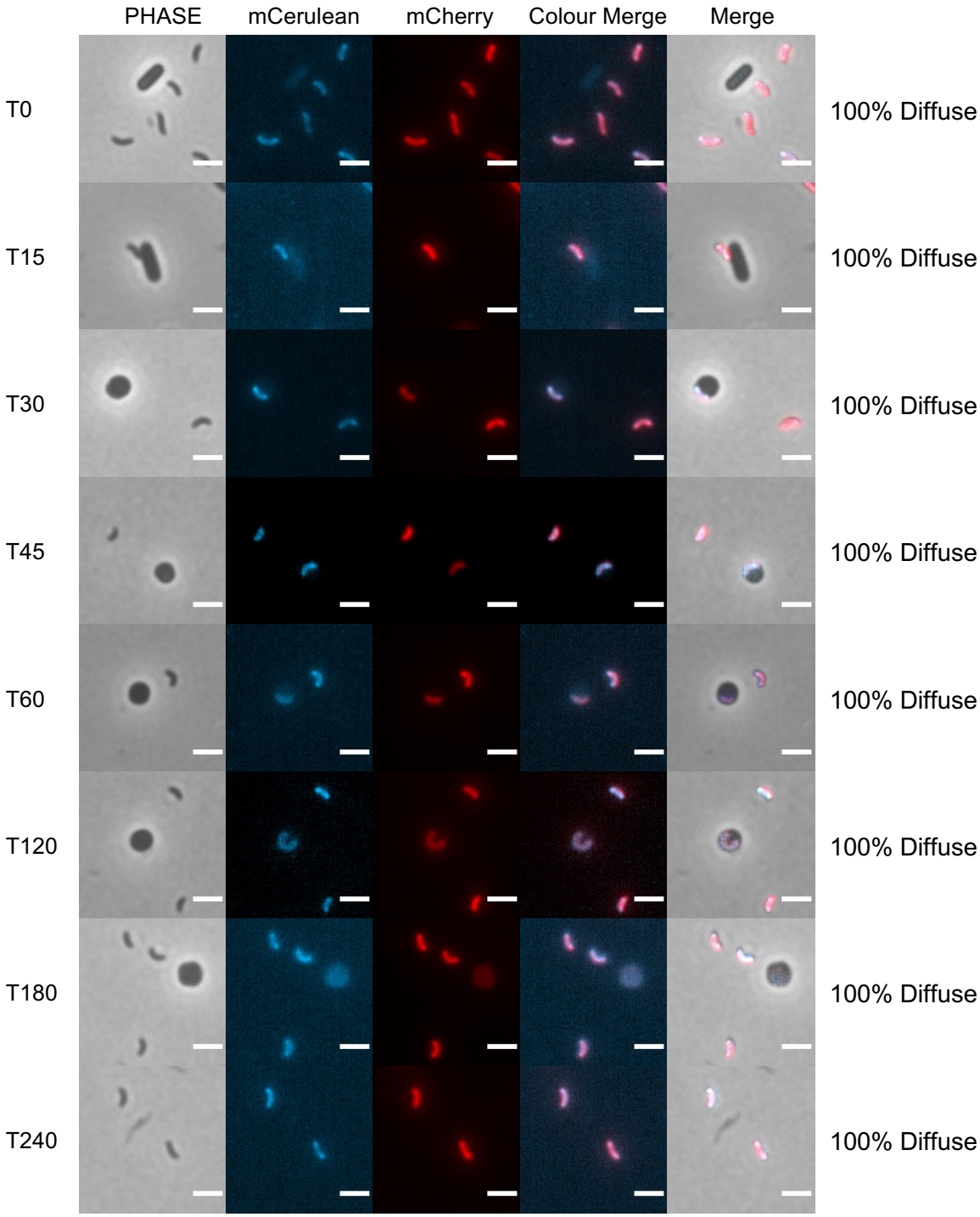

Figure 4.5.15: Bd3203mCerulean is expressed by *B. bacteriovorus* throughout predation. *B. bacteriovorus* containing a C-terminally tagged mCerulean-tagged Bd3203 protein and a constitutively expressed mCherry-tagged Bd0064 protein (illuminating the cell body of the *Bdellovibrio*) were visualised via fluorescence microscopy, throughout predation of *E. coli*. Bd3203mCerulean was expressed throughout predation. At least 5 fields of view were imaged from each of 2 biological replicates. Phase: Exposure 50 ms; mCerulean: Exposure 10 s, Excitation: 420-450 nm, Emission: 460-500 nm; mCherry: Exposure 10s, Excitation: 550-600 nm Emission: 610-665 nm. White scale bars represent 2 μM.

4.6. Visualisation of fluorescently tagged protein expression throughout *Bdellovibrio* occupation of macrophage.

To determine whether the expression of our proteins of interest could be visualised and therefore their expression characterised, whilst *Bdellovibrio* resides within the phagosome of macrophage (see Raghunathan et al., 2018; (2)), *B. bacteriovorus* containing a fluorescently tagged Bd0064 protein, a constitutively expressed cytoplasmic protein that, when fluorescently tagged with an mCerulean3 or mCherry protein, illuminates the cytoplasm and cell body of *Bdellovibrio*, was visualised following uptake by macrophage at 2-, 4- and 24-hours post-uptake. Bd0064mCerulean was expressed throughout *Bdellovibrio* occupation of macrophage (Figure 4.6.1), demonstrating its suitability as a background cytoplasmic marker in this assay, to be used in combination with our fluorescently tagged proteins of interest to associate fluorescent protein expression with individual *Bdellovibrio* cells within the phagosomal compartment, within macrophage.

I initially intended to characterise (fluorescently tagged) protein expression to further ascertain the expression and relative importance of these proteins within macrophage. However, due to the autofluorescence of macrophage, the results of this microscopy are largely inconclusive. In future, I would tag these proteins with a small avidin tag, which I would clone into their protein sequence through a process analogous to the one I used to fluorescently tag these proteins initially. I would then use a biotinylated antibody to bind the avidin tag, which would then be quantified using an anti-biotin secondary antibody conjugated to a luminescent marker (e.g. horseradish peroxidase) to quantify protein expression by Western blot. I would quantify protein expression by *Bdellovibrio*, within macrophage, at these timepoints, and in response to exogenous oxidative stresses such as hydrogen peroxide or superoxide radicals. This would give a much more accurate picture of protein expression throughout macrophage occupation. Nevertheless, I present the fluorescent protein expression data below, for some proteins of which visible and discernible expression is present.

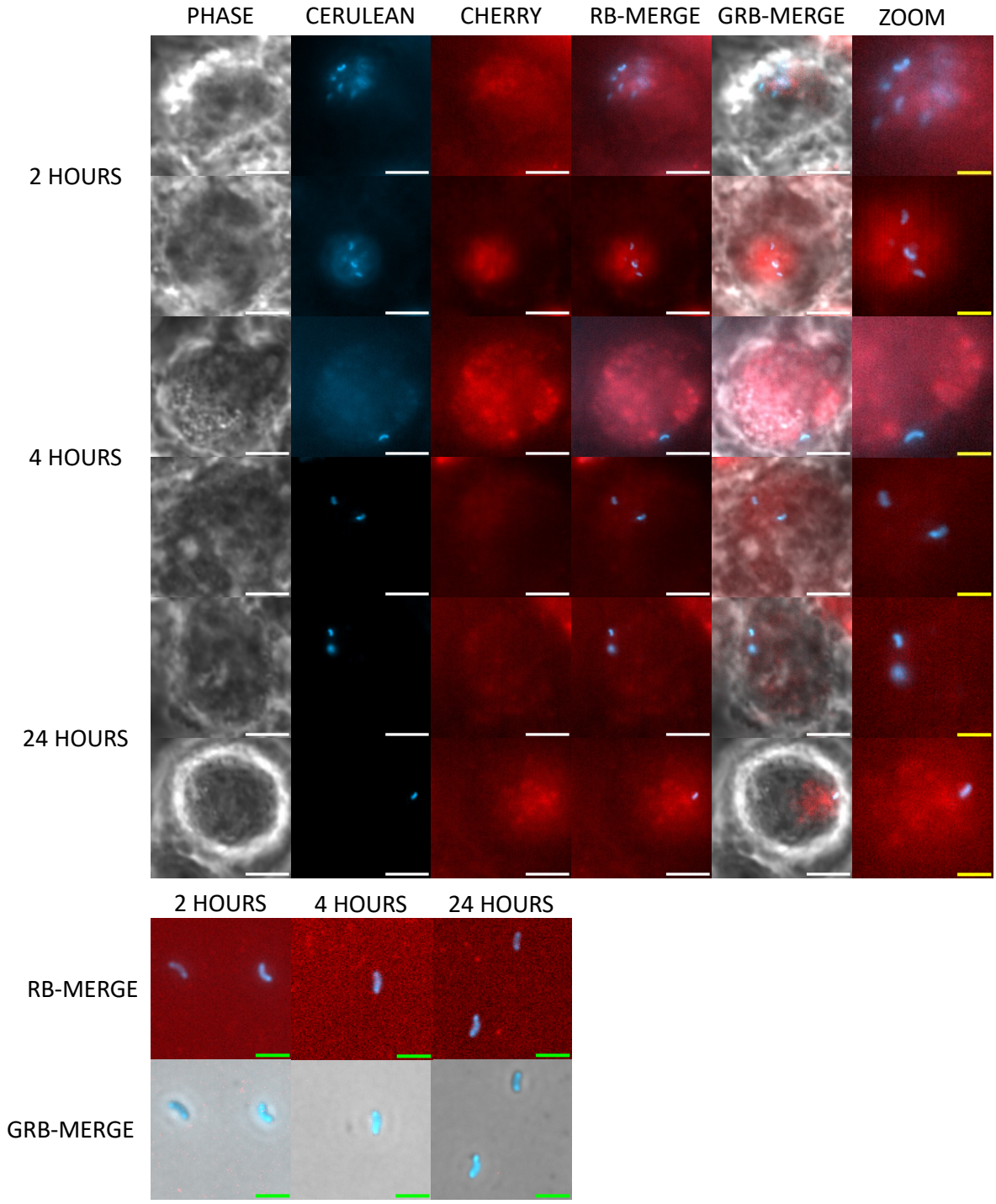

Figure 4.6.1: Bd0064mCerulean is visibly expressed by *B. bacteriovorus* throughout occupation of macrophage. *B. bacteriovorus* containing a C-terminally tagged constitutively expressed mCerulean-tagged Bd0064 protein (illuminating the cell body of the *Bdellovibrio*) were visualised via fluorescence microscopy, following uptake by macrophage, at 2-, 4- and 24-hours post-uptake. Bd0064mCerulean was expressed and fluorescent protein expression was visible throughout *Bdellovibrio* occupation of macrophage, demonstrating its suitability as a background marker of the *Bdellovibrio* cell body in combination with our fluorescently tagged proteins of interest. At least 5 fields of view were imaged from each of 2 biological replicates. Phase: Exposure 50 ms; mCerulean: Exposure 10 s, Excitation: 420-450 nm, Emission: 460-500 nm. White scale bars represent 5 μM, Yellow scale bars represent 2 μM (Zoom) and Green scale bars represent 2 μM (RPMI Controls; Lower Panel).

4.6.1. Bd0017/SurAmCherry is expressed, in some instances, by *B. bacteriovorus* at 24 hours post-uptake, whilst occupying macrophage.

To determine whether Bd0017, a SurA survival associated protein highlighted by my dual transcriptional study of *Bdellovibrio* transcription within macrophage, and by literature searches of bacterial pathogens, was expressed by *Bdellovibrio* during occupation of macrophage, Bd0017mCherry-tagged *B. bacteriovorus* were visualised following uptake by macrophage at 2-, 4- and 24-hours post-uptake. Bd0017mCherry was expressed at 24-hours post-uptake in 55.8% of cases but was not discernibly expressed at earlier timepoints (2- and 4-hours post-uptake) (Figure 4.6.2).

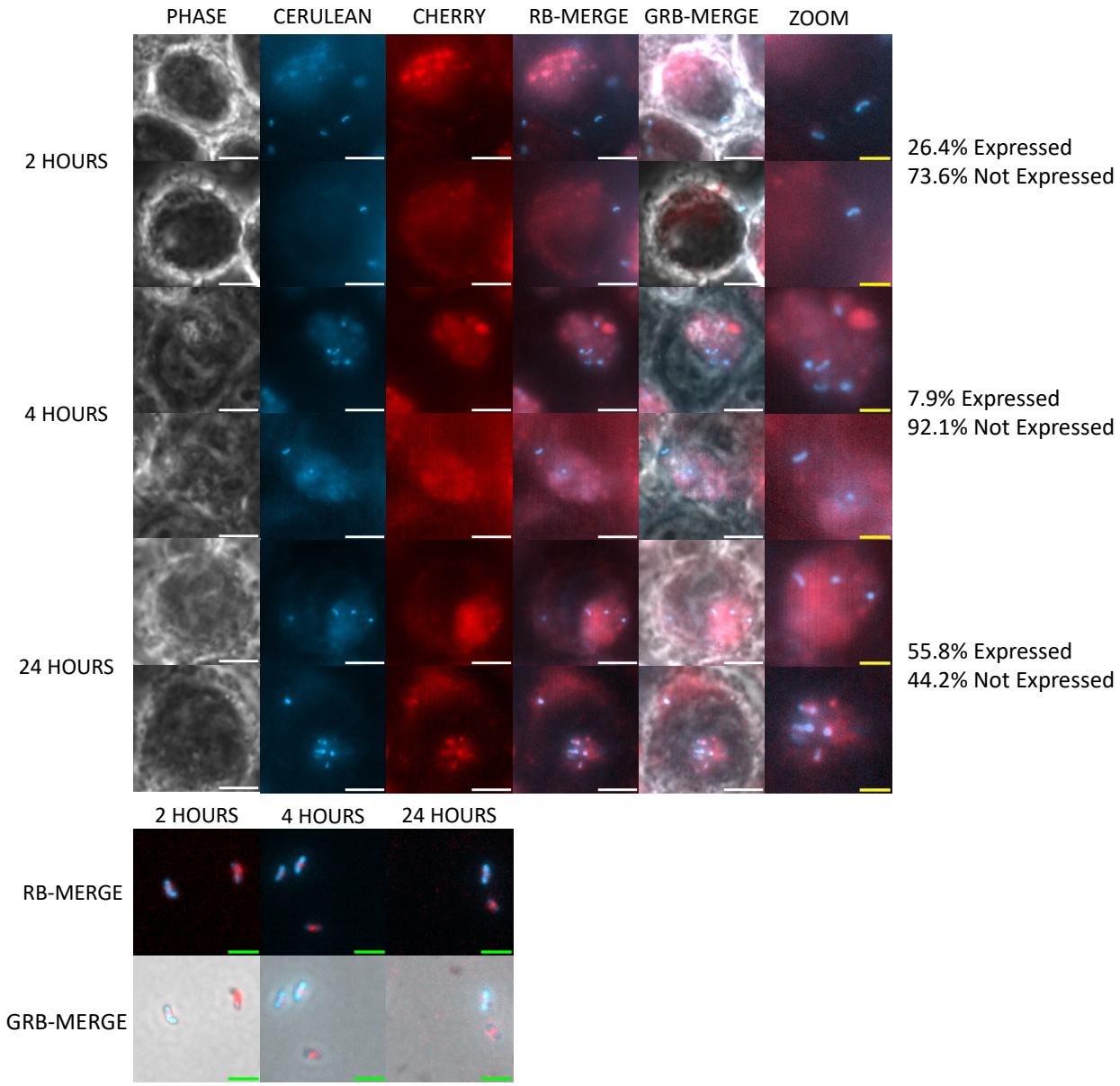

Figure 4.6.2: Bd0017mCherry is expressed, in some instances, by *B. bacteriovorus* at 24 hours post-uptake, whilst occupying macrophage. *B. bacteriovorus* containing a C-terminally tagged mCherry-tagged Bd0017 protein and a constitutively expressed mCerulean-tagged Bd0064 protein (illuminating the cell body of the *Bdellovibrio*) were visualised via fluorescence microscopy, following uptake by macrophage, at 2-, 4- and 24-hours post-uptake. In some instances, Bd0017mCherry was expressed at 24 hours post-uptake, but not at 2- and 4- hours post-uptake. At least 5 fields of view were imaged from each of 2 biological replicates. Phase: Exposure 50 ms; mCerulean: Exposure 10 s, Excitation: 420-450 nm, Emission: 460-500 nm; mCherry: Exposure 10s, Excitation: 550-600 nm Emission: 610-665 nm. White scale bars represent 5 μM, Yellow scale bars represent 2 μM (Zoom) and Green scale bars represent 2 μM (RPMI Controls; Lower Panel).

4.6.2. Fluorescently tagged Bd1401/SodC is expressed by some *Bdellovibrio* throughout macrophage occupation, whereas Bd0295/SodC is not discernibly expressed throughout *Bdellovibrio* occupation of macrophage.

4.6.2.1. Bd0295/SodC is not discernibly expressed by *B. bacteriovorus* throughout macrophage occupation.

To determine whether Bd0295, a SodC Copper-Zinc Superoxide Dismutase protein, highlighted by the initial bacterial transcriptome study in zebrafish was expressed by *Bdellovibrio* during occupation of macrophage, Bd0295mCherry-tagged or Bd0295mCerulean-tagged *B. bacteriovorus* were visualised following uptake by macrophage at 2-, 4- and 24-hours post-uptake. Bd0295mCherry and Bd0295mCerulean were not discernibly expressed throughout *Bdellovibrio* occupation of macrophage (Figures 4.6.3 and 4.6.4).

4.6.2.2. Bd1401/SodC is expressed by a small proportion of *B. bacteriovorus* throughout macrophage occupation, most frequently at 24 hours post-uptake.

To determine whether Bd1401, the other SodC Copper-Zinc Superoxide Dismutase protein in the *Bdellovibrio* genome, highlighted by literature searches and searches for SodC homologues within the *Bdellovibrio* genome, was expressed by *Bdellovibrio* during occupation of macrophage, Bd1401mCherry-tagged *B. bacteriovorus* were visualised following uptake by macrophage at 2-, 4- and 24-hours post-uptake. Bd1401mCherry was not discernibly expressed by the majority of *Bdellovibrio* throughout *Bdellovibrio* occupation of macrophage but was expressed by some *Bdellovibrio* throughout occupation, most commonly at 24-hours post-uptake (Figure 4.6.5). This would require further investigation.

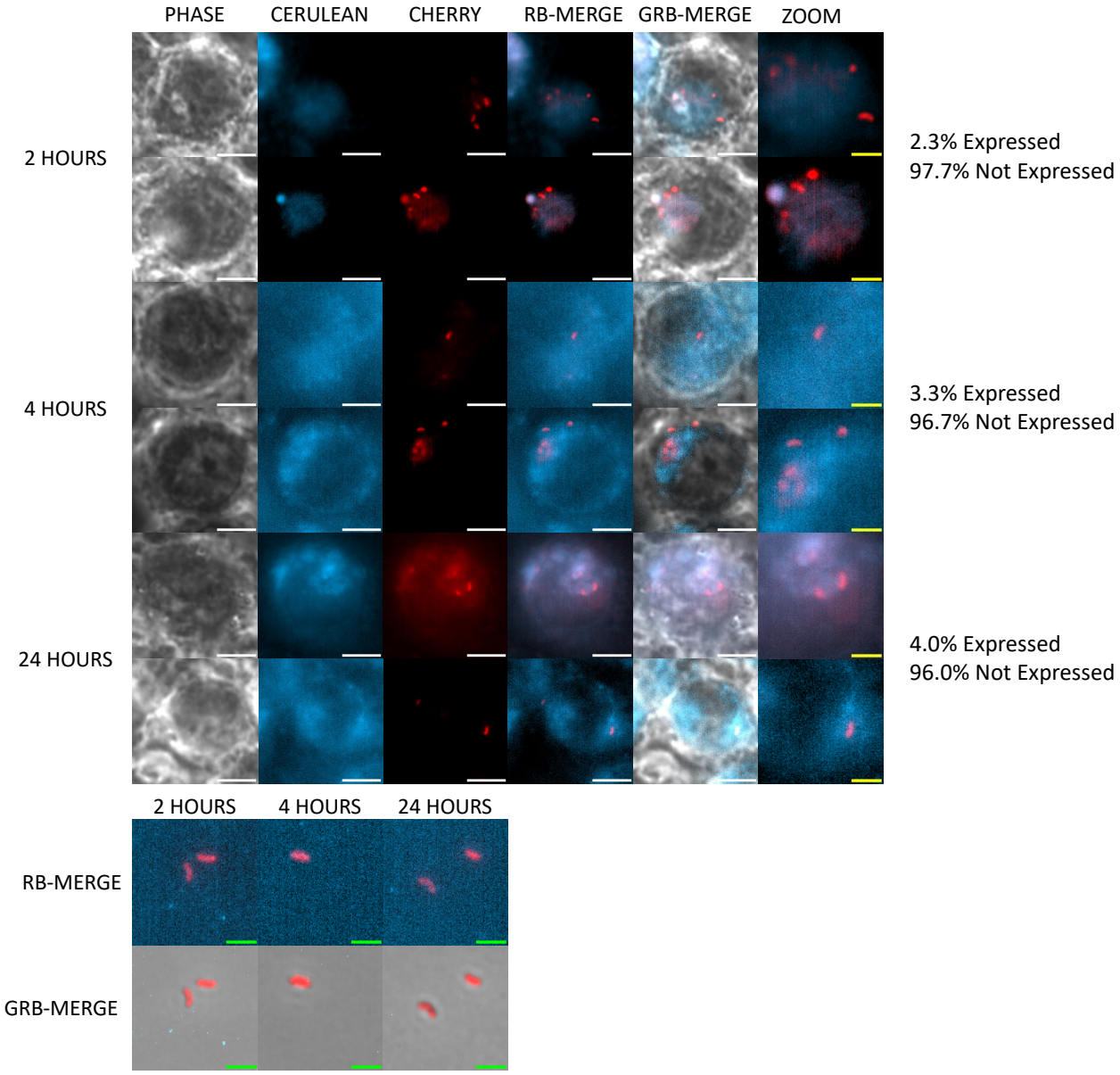

Figure 4.6.3: Bd0295mCerulean is not discernibly expressed by *B. bacteriovorus* throughout macrophage occupation. *B. bacteriovorus* containing a C-terminally tagged mCerulean-tagged Bd0295 protein and a constitutively expressed mCherry-tagged Bd0064 protein (illuminating the cell body of the *Bdellovibrio*) were visualised via fluorescence microscopy, following uptake by macrophage, at 2-, 4- and 24-hours post-uptake. Bd0295mCerulean was not discernibly expressed throughout *Bdellovibrio* occupation of macrophage. At least 5 fields of view were imaged from each of 2 biological replicates. Phase: Exposure 50 ms; mCerulean: Exposure 10 s, Excitation: 420-450 nm, Emission: 460-500 nm; mCherry: Exposure 10s, Excitation: 550-600 nm Emission: 610-665 nm. White scale bars represent 5 μM, Yellow scale bars represent 2 μM (Zoom) and Green scale bars represent 2 μM (RPMI Controls; Lower Panel).

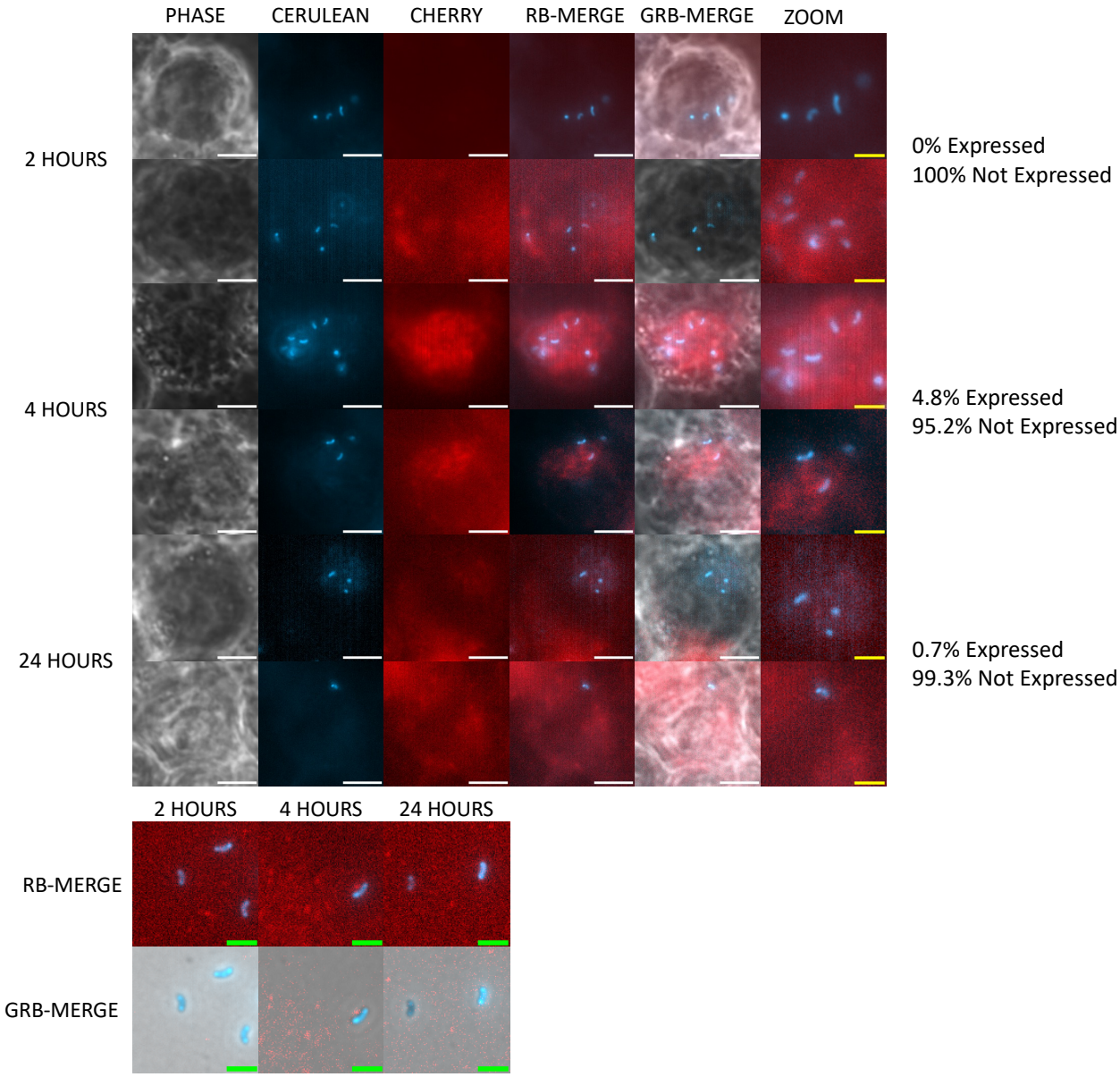

Figure 4.6.4: Bd0295mCherry is not discernibly expressed by *B. bacteriovorus* throughout macrophage occupation. *B. bacteriovorus* containing a C-terminally tagged mCherry-tagged Bd0295 protein and a constitutively expressed mCerulean-tagged Bd0064 protein (illuminating the cell body of the *Bdellovibrio*) were visualised via fluorescence microscopy, following uptake by macrophage, at 2-, 4- and 24-hours post-uptake. Bd0295mCherry was not discernibly expressed throughout *Bdellovibrio* occupation of macrophage. At least 5 fields of view were imaged from each of 2 biological replicates. Phase: Exposure 50 ms; mCerulean: Exposure 10 s, Excitation: 420-450 nm, Emission: 460-500 nm; mCherry: Exposure 10s, Excitation: 550-600 nm Emission: 610-665 nm. White scale bars represent 5 μM, Yellow scale bars represent 2 μM (Zoom) and Green scale bars represent 2 μM (RPMI Controls; Lower Panel).

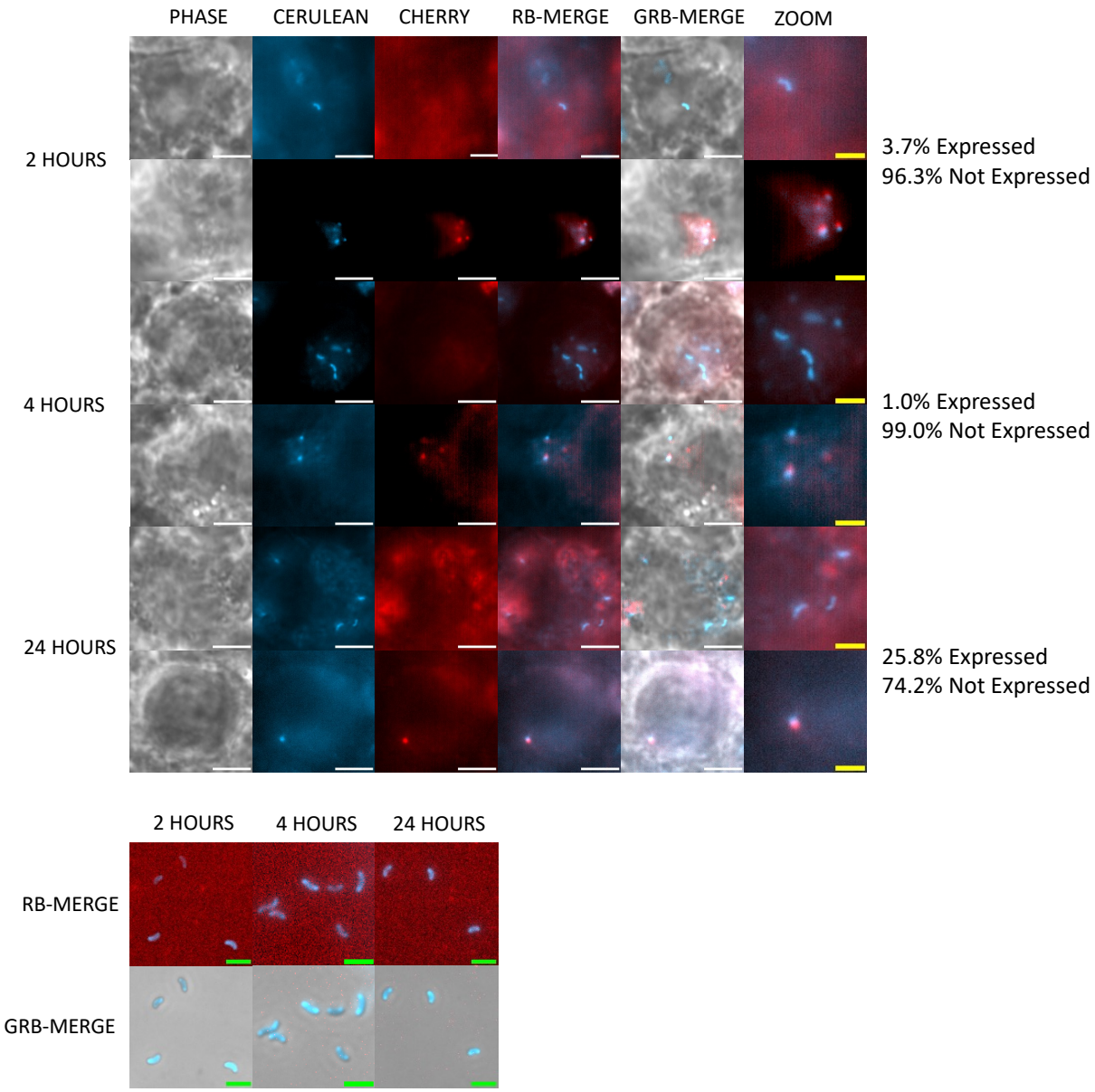

Figure 4.6.5: Bd1401mCherry is expressed by *B. bacteriovorus*, in some instances, throughout macrophage occupation, most frequently at 24 hours post-uptake. *B. bacteriovorus* containing a C-terminally tagged mCherry-tagged Bd1401 protein and a constitutively expressed mCerulean-tagged Bd0064 protein (illuminating the cell body of the *Bdellovibrio*) were visualised via fluorescence microscopy, following uptake by macrophage, at 2-, 4- and 24-hours post-uptake. Bd1401mCherry was expressed throughout *Bdellovibrio* occupation of macrophage, in some instances, with expression being most common at 24 hours post-uptake. At least 5 fields of view were imaged from each of 2 biological replicates. Phase: Exposure 50 ms; mCerulean: Exposure 10 s, Excitation: 420-450 nm, Emission: 460-500 nm; mCherry: Exposure 10s, Excitation: 550-600 nm Emission: 610-665 nm. White scale bars represent 5 μM, Yellow scale bars represent 2 μM (Zoom) and Green scale bars represent 2 μM (RPMI Controls; Lower Panel).

4.6.3. Fluorescently tagged Catalase proteins, Bd0798/CatA and Bd1154/KatA, and their Ankyrin proteins, Bd0799/AnkB and Bd1155/AnkB, are not discernibly expressed throughout occupation of macrophage by *Bdellovibrio.*

4.6.3.1. Bd0798/CatA is not discernibly expressed by *B. bacteriovorus* throughout macrophage occupation, except in some instances at 2- and 24-hours post-uptake.

To determine whether Bd0798, a catalase protein highlighted by the initial bacterial transcriptome study in zebrafish, was expressed by *Bdellovibrio* during occupation of macrophage, Bd0798mCherry-tagged or Bd0798mCerulean-tagged *B. bacteriovorus* were visualised following uptake by macrophage at 2-, 4- and 24-hours post-uptake. Bd0798mCherry and Bd0798mCerulean were not discernibly expressed by the majority of *Bdellovibrio* throughout *Bdellovibrio* occupation of macrophage, but some instances of Bd0798mCherry and Bd0798mCerulean expression were seen at 2- and 24-hours post-uptake (Figures 4.6.6 and 4.6.7).

4.6.3.2. Bd0799/AnkB is not discernibly expressed by *B. bacteriovorus* throughout macrophage occupation.

To determine whether Bd0799, a regulatory ankyrin protein, was expressed by *Bdellovibrio* during occupation of macrophage, Bd0799mCherry-tagged *B. bacteriovorus* were visualised following uptake by macrophage at 2-, 4- and 24-hours post-uptake. Fluorescent tagging of Bd0799 with an mCherry protein required the incorporation of a flexible peptide linker, as repeated attempts to tag Bd0799 directly with the mCherry tag caused mutations in the fluorescent tag and gene (Rob Till, Personal Communication), suggesting that the mCherry tag was interfering with the expression of Bd0799 in some way. Bd0799mCherry was not discernibly expressed throughout *Bdellovibrio* occupation of macrophage (Figure 4.6.8).

4.6.3.3. Bd1154/KatA is not discernibly expressed by the majority of *B. bacteriovorus* throughout macrophage occupation.

To determine whether Bd1154, a catalase protein homologous to Bd0798 and highlighted by searches of the *Bdellovibrio* genome for potential homologues, was expressed by *Bdellovibrio* during occupation of macrophage, Bd1154mCerulean-tagged *B. bacteriovorus* were visualised following uptake by macrophage at 2-, 4- and 24-hours post-uptake. Bd1154mCerulean was not discernibly expressed throughout *Bdellovibrio* occupation of macrophage (Figure 4.6.9).

4.6.3.4. Bd1155/AnkB is not discernibly expressed by *B. bacteriovorus* throughout macrophage occupation.

To determine whether Bd1155, highlighted by searches of the *Bdellovibrio* genome for potential homologues, was expressed by *Bdellovibrio* during occupation of macrophage, Bd1155mCerulean-tagged *B. bacteriovorus* were visualised following uptake by macrophage at 2-, 4- and 24-hours post-uptake. Bd1155mCerulean was not discernibly expressed throughout *Bdellovibrio* occupation of macrophage (Figure 4.6.10).

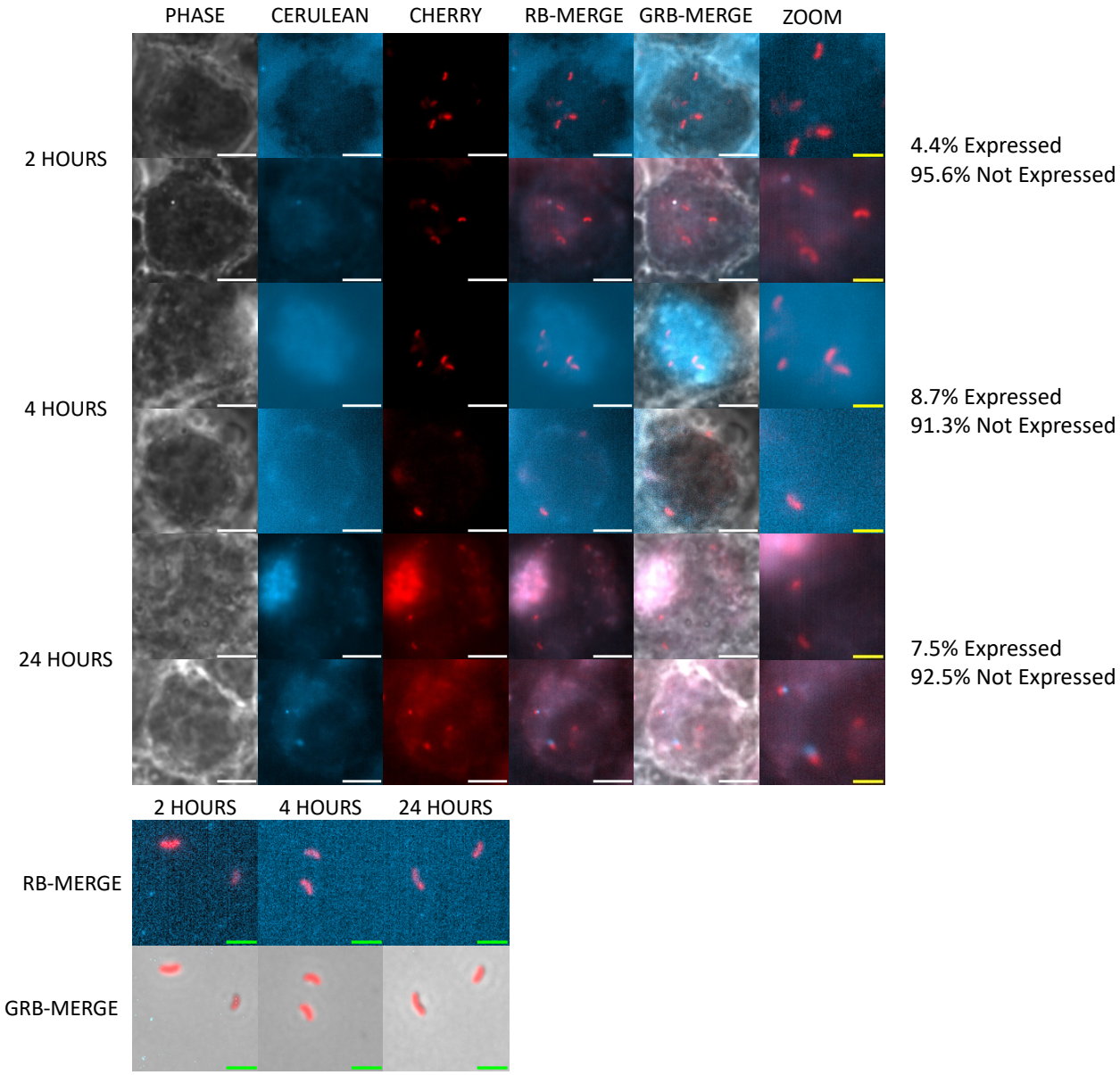

Figure 4.6.6: Bd0798mCerulean is not discernibly expressed by *B. bacteriovorus* throughout macrophage occupation, except in some instances at 24 hours post-uptake. *B. bacteriovorus* containing a C-terminally tagged mCerulean-tagged Bd0798 protein and a constitutively expressed mCherry-tagged Bd0064 protein (illuminating the cell body of the *Bdellovibrio*) were visualised via fluorescence microscopy, following uptake by macrophage, at 2-, 4- and 24-hours post-uptake. Bd0798mCerulean was not discernibly expressed throughout *Bdellovibrio* occupation of macrophage, except in some instances at 24 hours post-uptake. At least 5 fields of view were imaged from each of 2 biological replicates. Phase: Exposure 50 ms; mCerulean: Exposure 10 s, Excitation: 420-450 nm, Emission: 460-500 nm; mCherry: Exposure 10s, Excitation: 550-600 nm Emission: 610-665 nm. White scale bars represent 5 μM, Yellow scale bars represent 2 μM (Zoom) and Green scale bars represent 2 μM (RPMI Controls; Lower Panel).

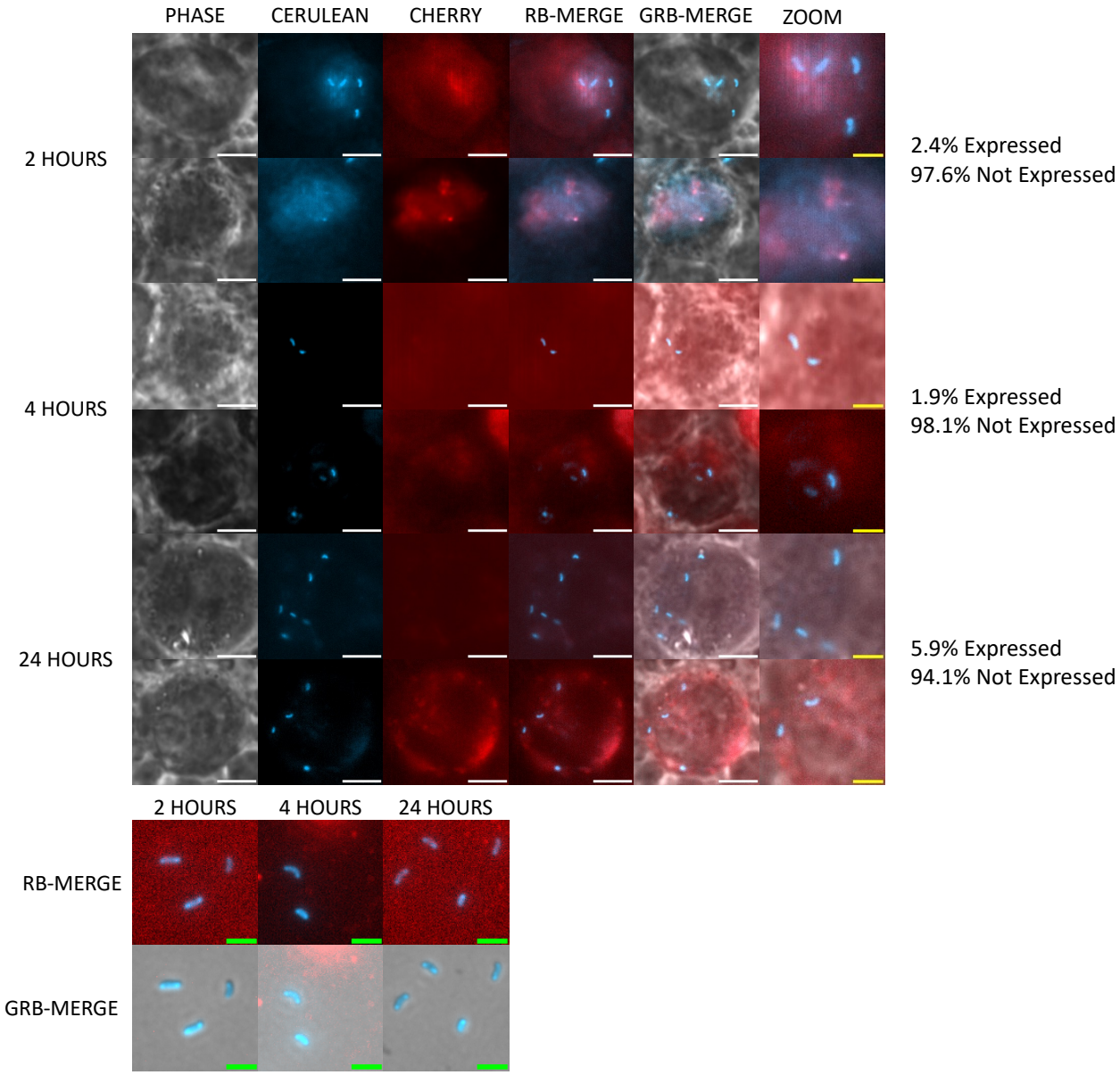

Figure 4.6.7: Bd0798mCherry is not discernibly expressed by *B. bacteriovorus* throughout macrophage occupation, except in some instances at 2- and 24-hours post-uptake. *B. bacteriovorus* containing a C-terminally tagged mCherry-tagged Bd0798 protein and a constitutively expressed mCerulean-tagged Bd0064 protein (illuminating the cell body of the *Bdellovibrio*) were visualised via fluorescence microscopy, following uptake by macrophage, at 2-, 4- and 24-hours post-uptake. Bd0798mCherry was not discernibly expressed throughout *Bdellovibrio* occupation of macrophage, except in some instances at 2- and 24-hours post-uptake. At least 5 fields of view were imaged from each of 2 biological replicates. Phase: Exposure 50 ms; mCerulean: Exposure 10 s, Excitation: 420-450 nm, Emission: 460-500 nm; mCherry: Exposure 10s, Excitation: 550-600 nm Emission: 610-665 nm. White scale bars represent 5 μM, Yellow scale bars represent 2 μM (Zoom) and Green scale bars represent 2 μM (RPMI Controls; Lower Panel).

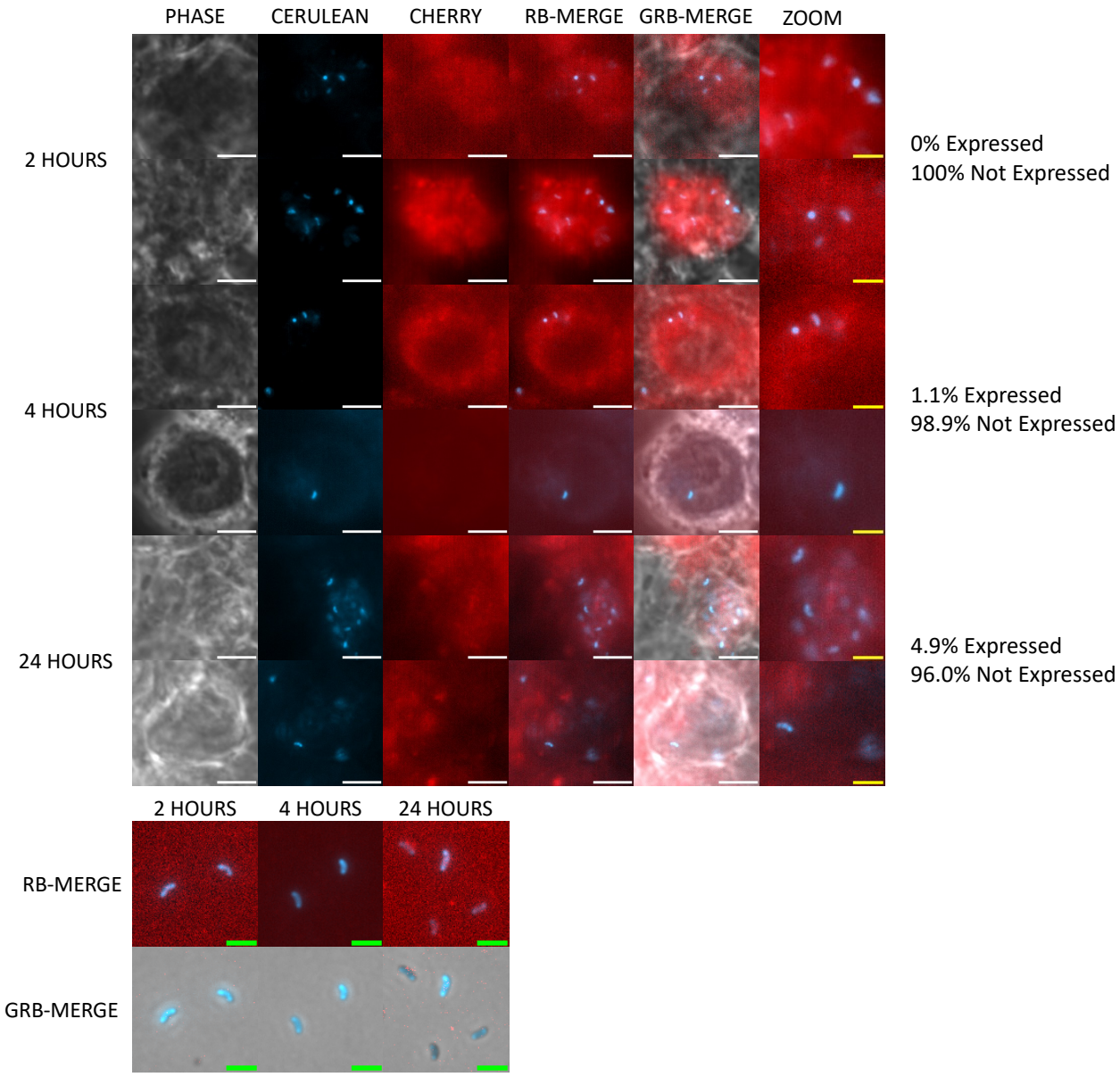

Figure 4.6.8: Bd0799mCherry is not discernibly expressed by *B. bacteriovorus* throughout macrophage occupation. *B. bacteriovorus* containing a C-terminally tagged mCherry-tagged Bd0799 protein and a constitutively expressed mCerulean-tagged Bd0064 protein (illuminating the cell body of the *Bdellovibrio*) were visualised via fluorescence microscopy, following uptake by macrophage, at 2-, 4- and 24-hours post-uptake. Bd0799mCherry was not discernibly expressed throughout *Bdellovibrio* occupation of macrophage. At least 5 fields of view were imaged from each of 2 biological replicates. Phase: Exposure 50 ms; mCerulean: Exposure 10 s, Excitation: 420-450 nm, Emission: 460-500 nm; mCherry: Exposure 10s, Excitation: 550-600 nm Emission: 610-665 nm. White scale bars represent 5 μM, Yellow scale bars represent 2 μM (Zoom) and Green scale bars represent 2 μM (RPMI Controls; Lower Panel).

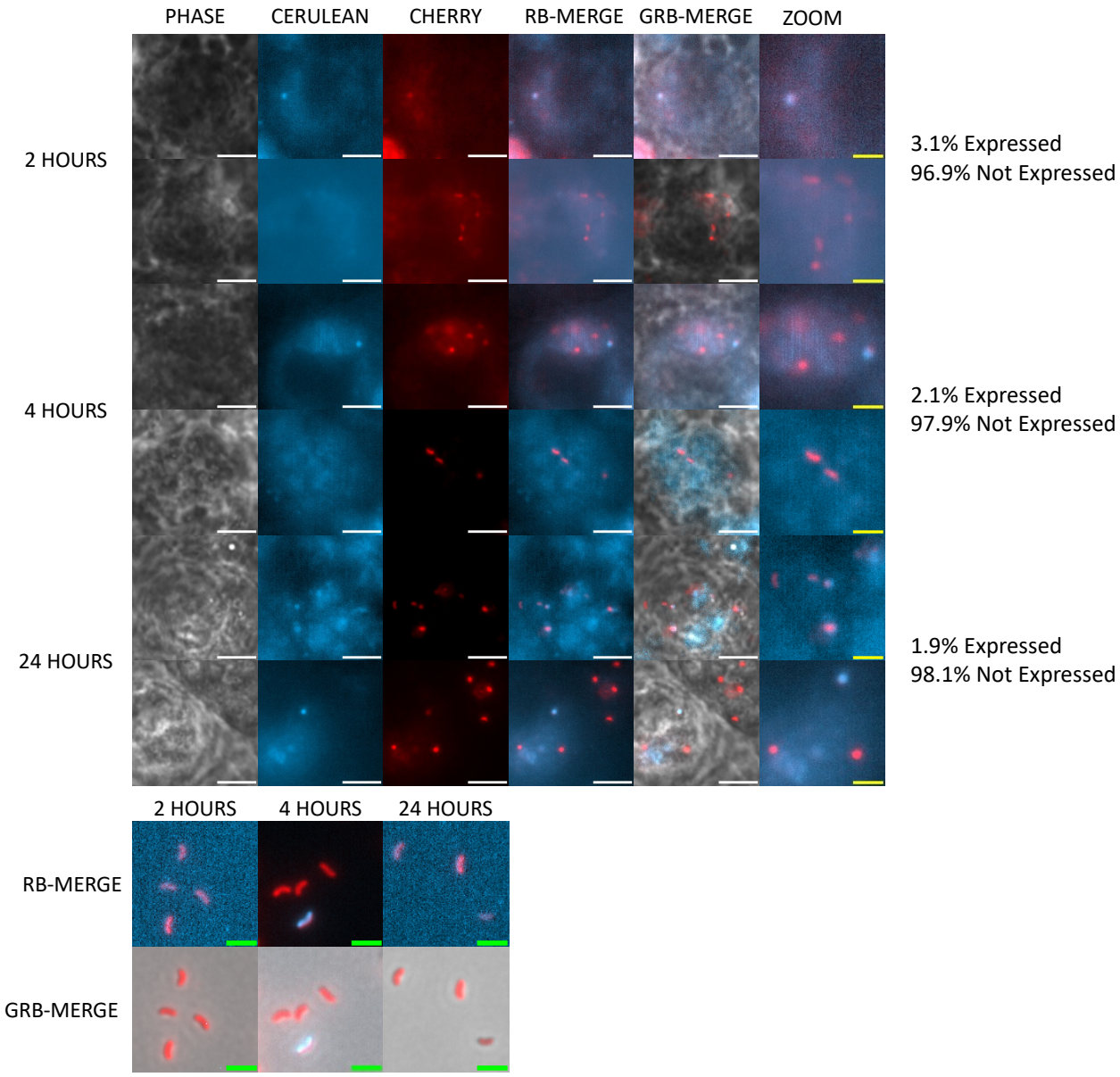

Figure 4.6.9: Bd1154mCerulean is expressed, in some instances, by *B. bacteriovorus* throughout macrophage occupation. *B. bacteriovorus* containing a C-terminally tagged mCerulean-tagged Bd1154 protein and a constitutively expressed mCherry-tagged Bd0064 protein (illuminating the cell body of the *Bdellovibrio*) were visualised via fluorescence microscopy, following uptake by macrophage, at 2-, 4- and 24-hours post-uptake. Bd1154mCerulean was expressed throughout *Bdellovibrio* occupation of macrophage, in some instances. At least 5 fields of view were imaged from each of 2 biological replicates. Phase: Exposure 50 ms; mCerulean: Exposure 10 s, Excitation: 420-450 nm, Emission: 460-500 nm; mCherry: Exposure 10s, Excitation: 550-600 nm Emission: 610-665 nm. White scale bars represent 5 μM, Yellow scale bars represent 2 μM (Zoom) and Green scale bars represent 2 μM (RPMI Controls; Lower Panel).

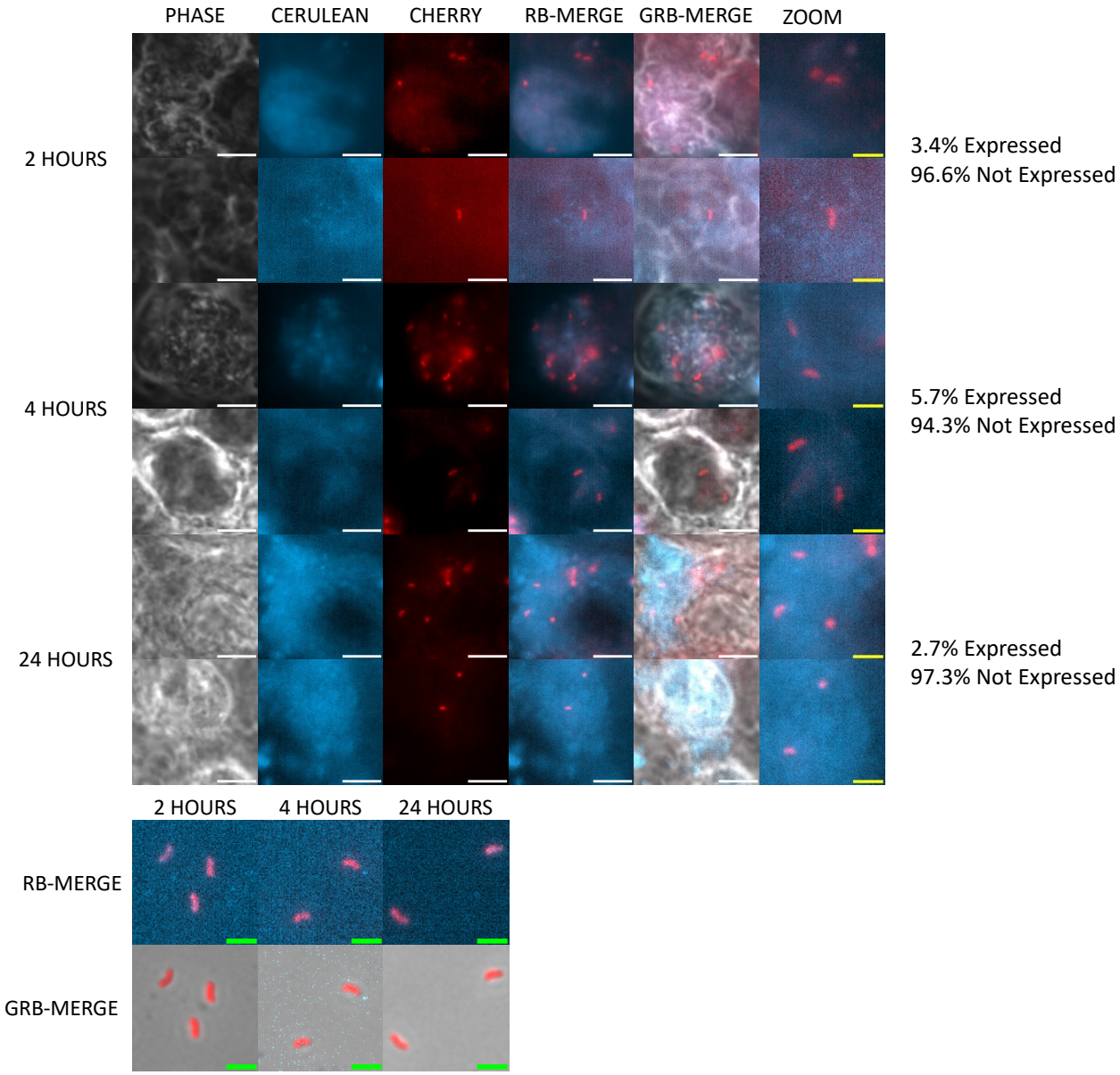

Figure 4.6.10: Bd1155mCerulean is not discernibly expressed by *B. bacteriovorus* throughout macrophage occupation. *B. bacteriovorus* containing a C-terminally tagged mCerulean-tagged Bd1155 protein and a constitutively expressed mCherry-tagged Bd0064 protein (illuminating the cell body of the *Bdellovibrio*) were visualised via fluorescence microscopy, following uptake by macrophage, at 2-, 4- and 24-hours post-uptake. Bd1155mCerulean was not discernibly expressed throughout *Bdellovibrio* occupation of macrophage. At least 5 fields of view were imaged from each of 2 biological replicates. Phase: Exposure 50 ms; mCerulean: Exposure 10 s, Excitation: 420-450 nm, Emission: 460-500 nm; mCherry: Exposure 10s, Excitation: 550-600 nm Emission: 610-665 nm. White scale bars represent 5 μM, Yellow scale bars represent 2 μM (Zoom) and Green scale bars represent 2 μM (RPMI Controls; Lower Panel).

4.6.4. Fluorescently tagged Bd1815 is expressed by a small minority of *Bdellovibrio* throughout macrophage occupation, most frequently at 24 hours post-uptake.

To determine whether Bd1815, a hypothetical protein that I hypothesise to resemble an Outer Membrane Protein or porin and highlighted by the initial bacterial transcriptome study in zebrafish, was expressed by *Bdellovibrio* during occupation of macrophage, Bd1815mCherry-tagged or Bd1815mCerulean-tagged *B. bacteriovorus* were visualised following uptake by macrophage at 2-, 4- and 24-hours post-uptake. Bd1815mCherry and Bd1815mCerulean were not discernibly expressed by the majority of *Bdellovibrio* throughout *Bdellovibrio* occupation of macrophage, but some instances of expression were seen at 4- and 24-hours post uptake, although expression is also seen in a subset of attack phase *Bdellovibrio* that have not been engulfed by macrophage (Figures 4.6.11 and 4.6.12).

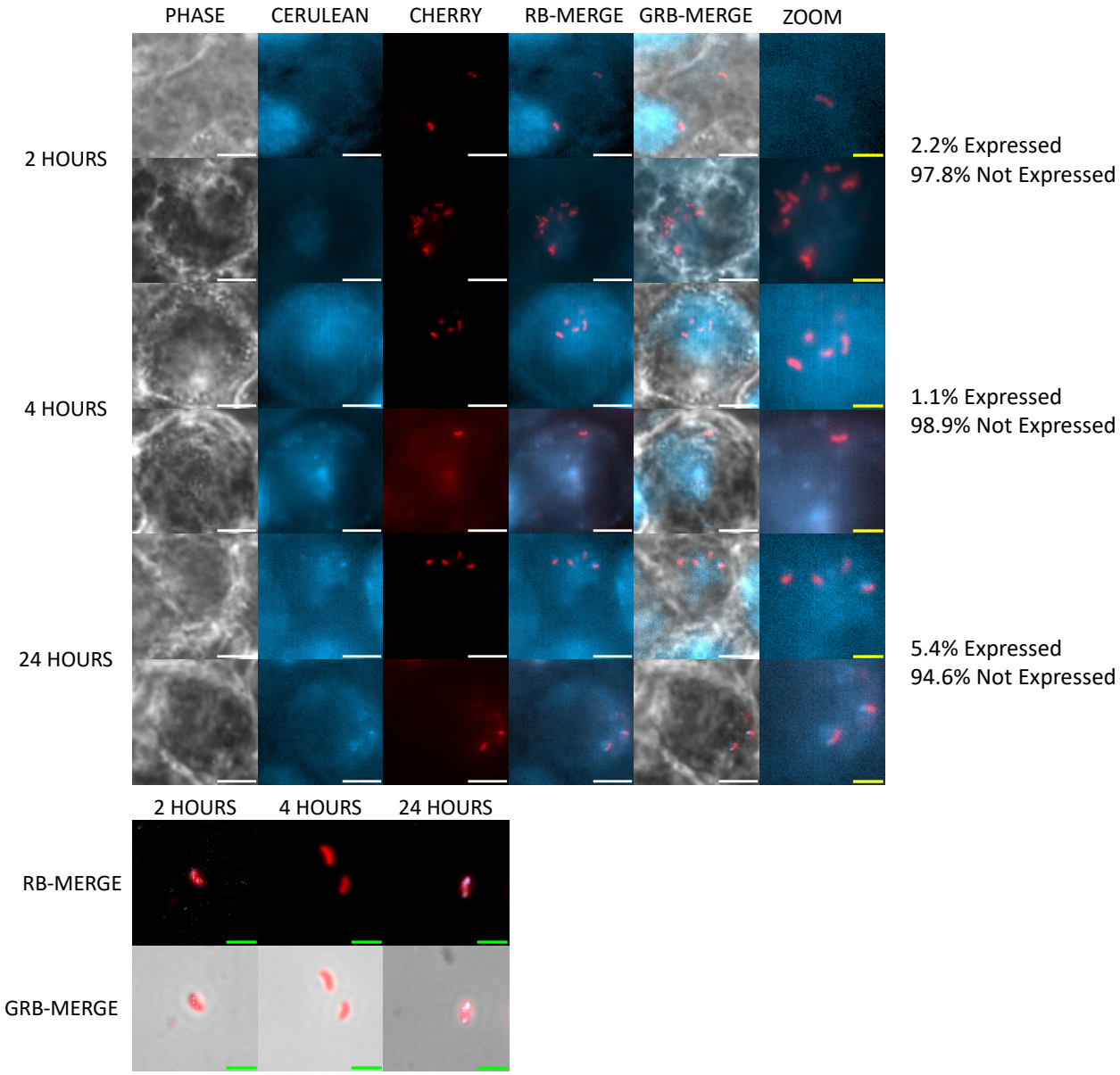

Figure 4.6.11: Bd1815mCerulean is expressed by *B. bacteriovorus*, in some instances, at 4- and 24-hours of macrophage occupation. *B. bacteriovorus* containing a C-terminally tagged mCerulean-tagged Bd1815 protein and a constitutively expressed mCherry-tagged Bd0064 protein (illuminating the cell body of the *Bdellovibrio*) were visualised via fluorescence microscopy, following uptake by macrophage, at 2-, 4- and 24-hours post-uptake. Bd1815mCerulean was expressed, in some instances, at 4- and 24- hours of *Bdellovibrio* occupation of macrophage. At least 5 fields of view were imaged from each of 2 biological replicates. Phase: Exposure 50 ms; mCerulean: Exposure 10 s, Excitation: 420-450 nm, Emission: 460-500 nm; mCherry: Exposure 10s, Excitation: 550-600 nm Emission: 610-665 nm. White scale bars represent 5 μM, Yellow scale bars represent 2 μM (Zoom) and Green scale bars represent 2 μM (RPMI Controls; Lower Panel).

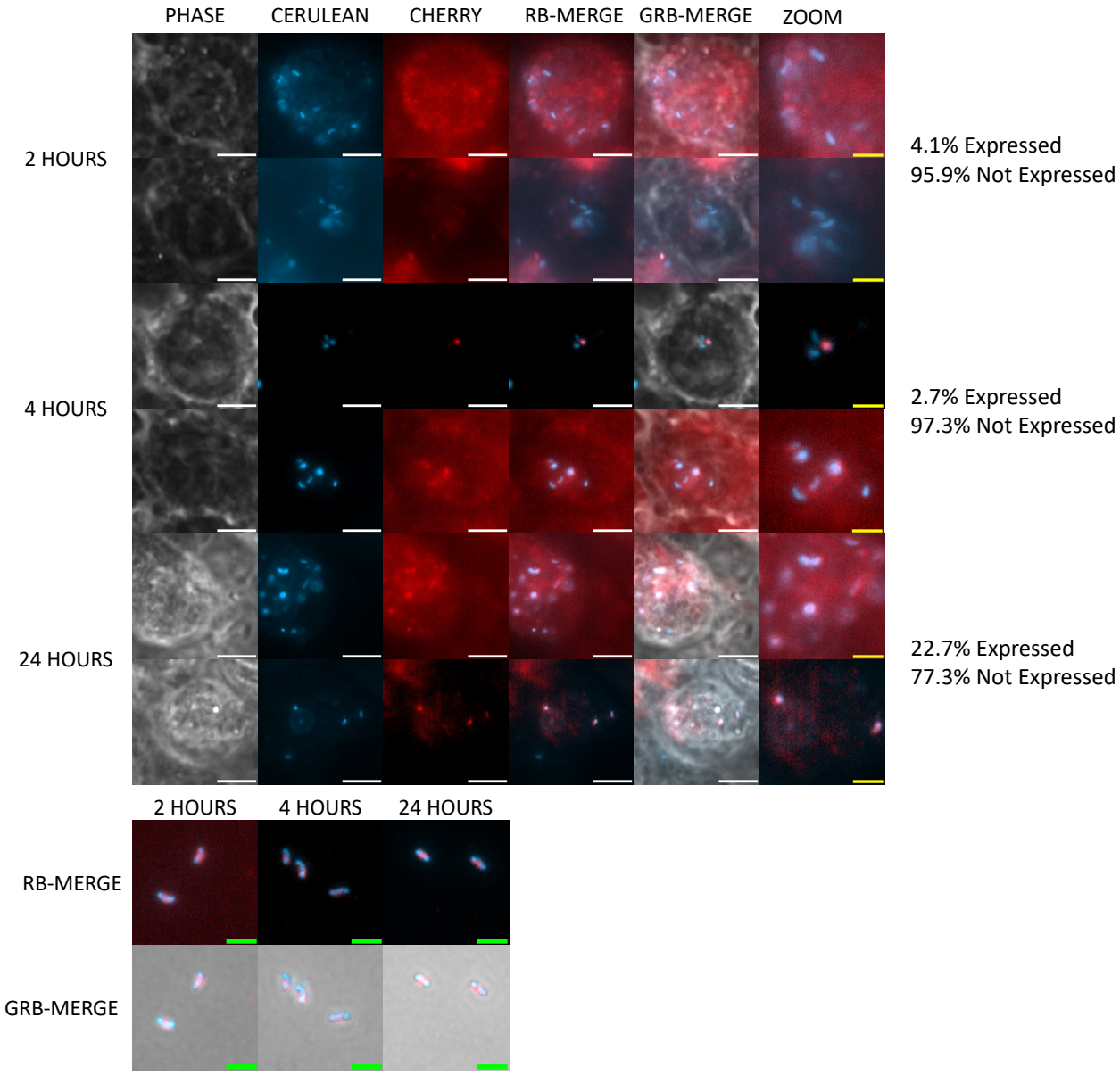

Figure 4.6.12: Bd1815mCherry is expressed by *B. bacteriovorus*, in some instances, at 4- and 24-hours of macrophage occupation. *B. bacteriovorus* containing a C-terminally tagged mCherry-tagged Bd1815 protein and a constitutively expressed mCerulean-tagged Bd0064 protein (illuminating the cell body of the *Bdellovibrio*) were visualised via fluorescence microscopy, following uptake by macrophage, at 2-, 4- and 24-hours post-uptake. Bd1815mCherry was expressed, in some instances, at 4- and 24- hours of *Bdellovibrio* occupation of macrophage. At least 5 fields of view were imaged from each of 2 biological replicates. Phase: Exposure 50 ms; mCerulean: Exposure 10 s, Excitation: 420-450 nm, Emission: 460-500 nm; mCherry: Exposure 10s, Excitation: 550-600 nm Emission: 610-665 nm. White scale bars represent 5 μM, Yellow scale bars represent 2 μM (Zoom) and Green scale bars represent 2 μM (RPMI Controls; Lower Panel).

4.6.5. Fluorescently tagged Alkyl Hydroperoxide Reductase proteins, Bd2517/AhpC and Bd2518/AhpF, are expressed throughout *Bdellovibrio* occupation of macrophage.

To determine whether Bd2517 and Bd2518, two alkyl hydroperoxide reductase proteins involved in hydrogen peroxide detoxification and highlighted by initial transcriptional studies in zebrafish, were expressed by *Bdellovibrio* during occupation of macrophage, Bd2517mCerulean-tagged or Bd2518mCerulean-tagged *B. bacteriovorus* were visualised following uptake by macrophage at 2-, 4- and 24-hours post-uptake. Bd2517mCerulean and Bd2518mCerulean were expressed throughout *Bdellovibrio* occupation of macrophage, although they are also highly expressed in attack phase cells that have not been engulfed by macrophage (Figures 4.6.13 and 4.6.14).

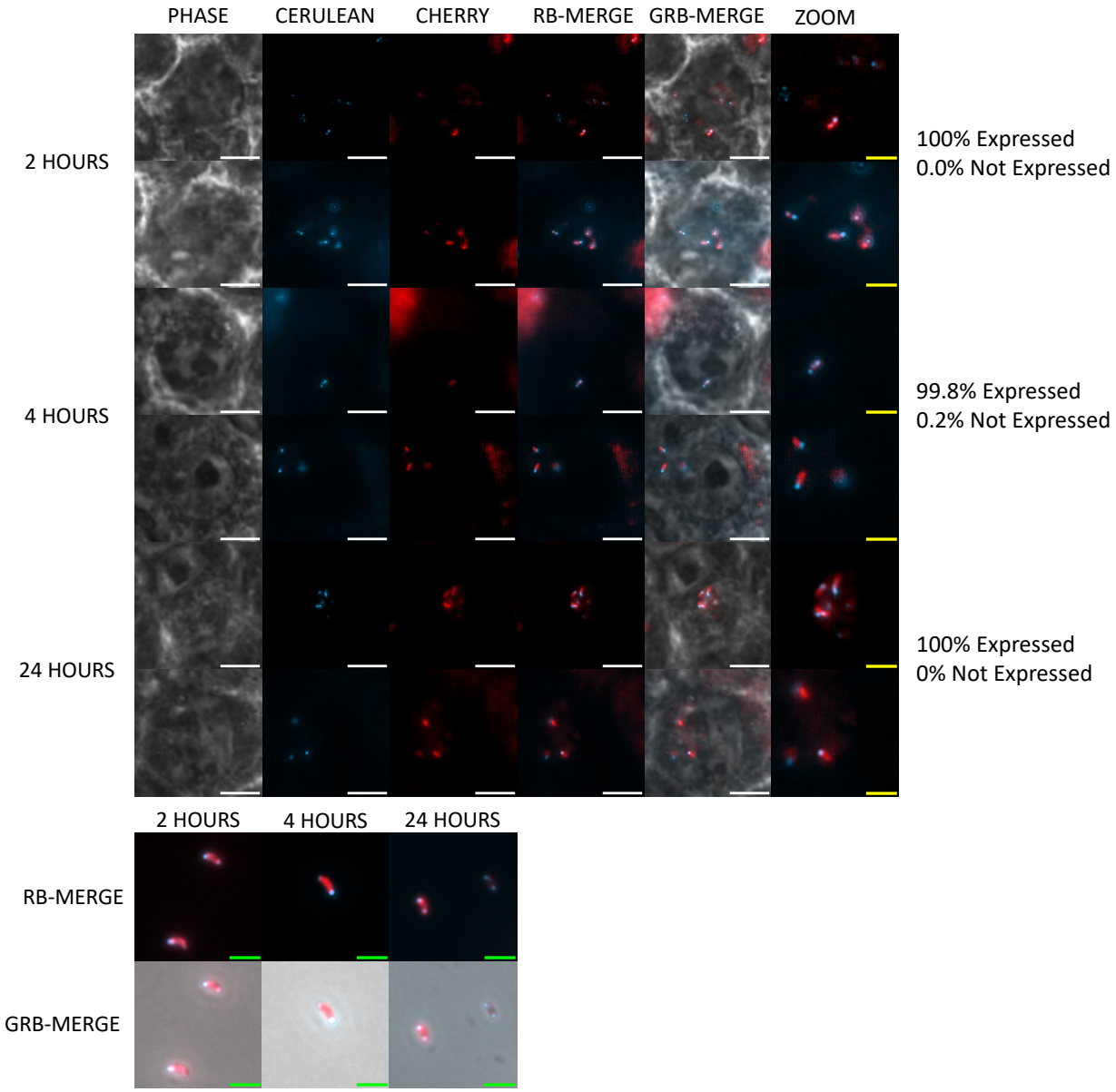

Figure 4.6.13: Bd2517mCerulean is expressed by *B. bacteriovorus* throughout macrophage occupation. *B. bacteriovorus* containing a C-terminally tagged mCerulean-tagged Bd2517 protein and a constitutively expressed mCherry-tagged Bd0064 protein (illuminating the cell body of the *Bdellovibrio*) were visualised via fluorescence microscopy, following uptake by macrophage, at 2-, 4- and 24-hours post-uptake. Bd2517mCerulean was expressed thoroughout *Bdellovibrio* occupation of macrophage. At least 5 fields of view were imaged from each of 2 biological replicates. Phase: Exposure 50 ms; mCerulean: Exposure 10 s, Excitation: 420-450 nm, Emission: 460-500 nm; mCherry: Exposure 10s, Excitation: 550-600 nm Emission: 610-665 nm. White scale bars represent 5 µM, Yellow scale bars represent 2 µM (Zoom) and Green scale bars represent 2 µM (RPMI Controls; Lower Panel).

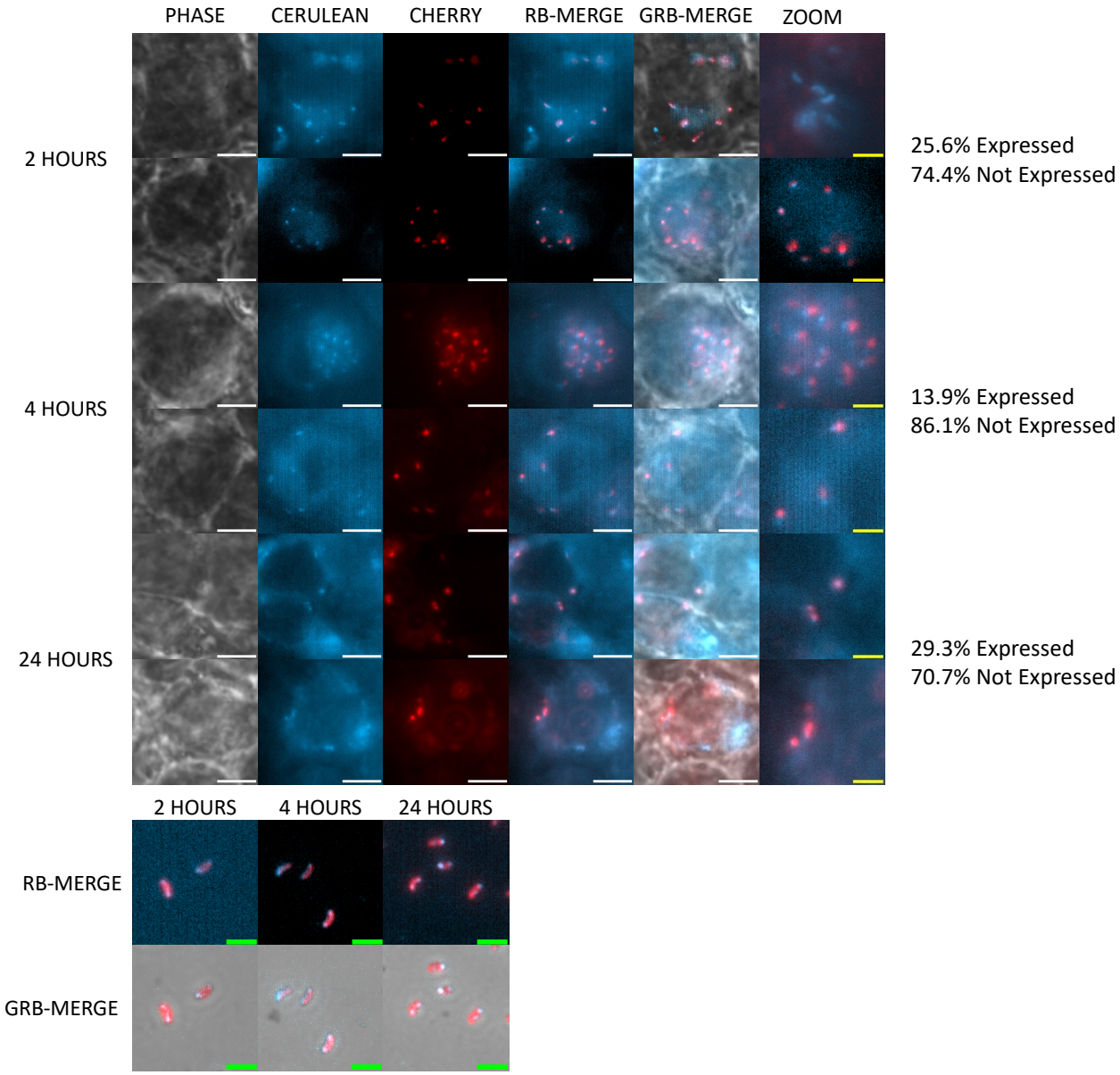

Figure 4.6.14: Bd2518mCerulean is expressed by *B. bacteriovorus* throughout macrophage occupation. *B. bacteriovorus* containing a C-terminally tagged mCerulean-tagged Bd2518 protein and a constitutively expressed mCherry-tagged Bd0064 protein (illuminating the cell body of the *Bdellovibrio*) were visualised via fluorescence microscopy, following uptake by macrophage, at 2-, 4- and 24-hours post-uptake. Bd2518mCerulean was expressed thoroughout *Bdellovibrio* occupation of macrophage. At least 5 fields of view were imaged from each of 2 biological replicates. Phase: Exposure 50 ms; mCerulean: Exposure 10 s, Excitation: 420-450 nm, Emission: 460-500 nm; mCherry: Exposure 10s, Excitation: 550-600 nm Emission: 610-665 nm. White scale bars represent 5 µM, Yellow scale bars represent 2 µM (Zoom) and Green scale bars represent 2 µM (RPMI Controls; Lower Panel).

4.6.6. Bd2620/Dps is expressed by *B. bacteriovorus* throughout macrophage occupation.

To determine whether Bd2620, a Dps DNA protection from starvation protein highlighted by initial transcriptional studies in zebrafish, was expressed by *Bdellovibrio* during occupation of macrophage, Bd2620mCerulean-tagged *B. bacteriovorus* were visualised following uptake by macrophage at 2-, 4- and 24-hours post-uptake. Bd2620mCerulean was expressed throughout *Bdellovibrio* occupation of macrophage, although it is also highly expressed in attack phase cells that have not been engulfed by macrophage (Figure 4.6.15).

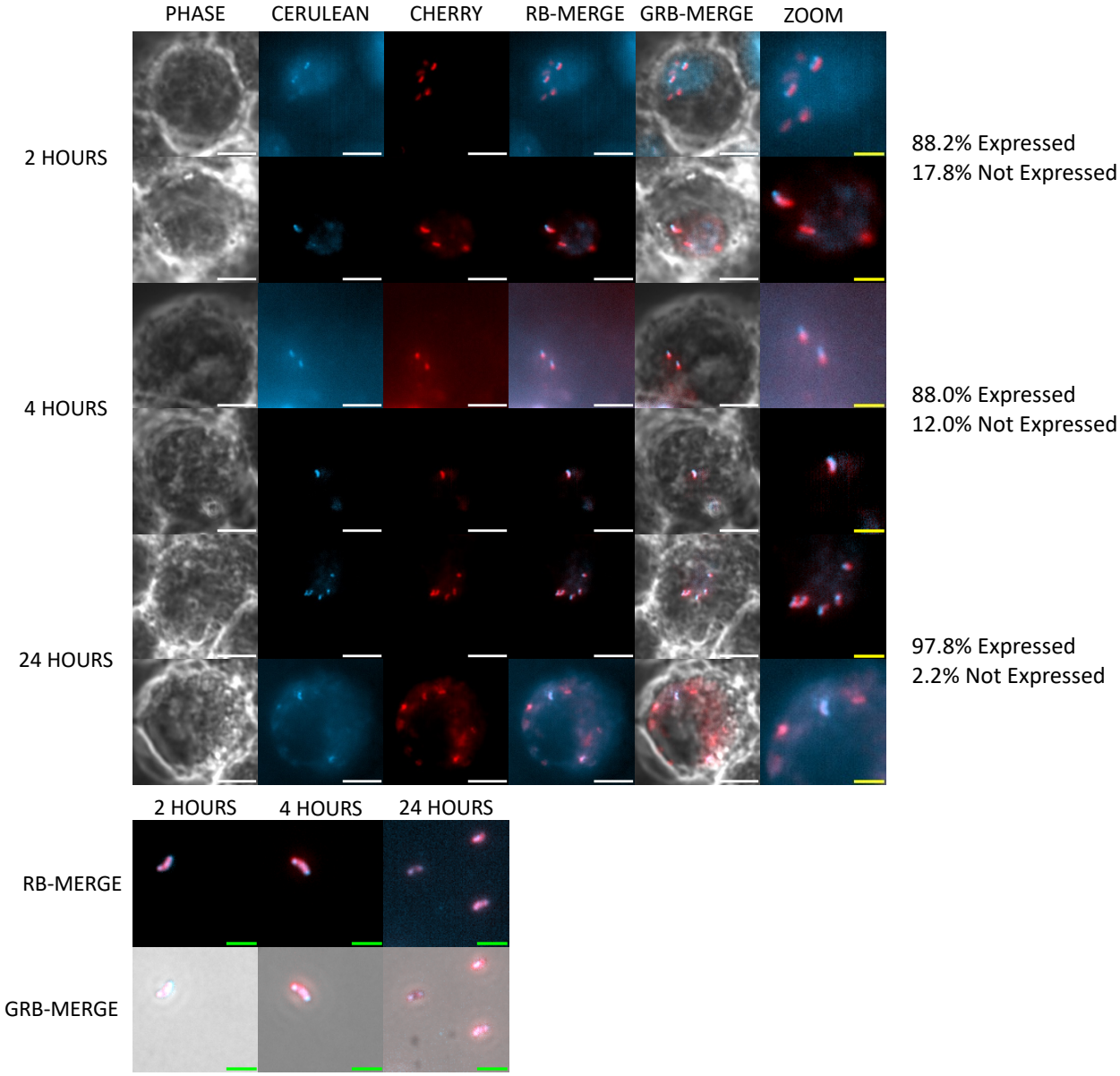

Figure 4.6.15: Bd2620mCerulean is expressed by *B. bacteriovorus* throughout macrophage occupation. *B. bacteriovorus* containing a C-terminally tagged mCerulean-tagged Bd2620 protein and a constitutively expressed mCherry-tagged Bd0064 protein (illuminating the cell body of the *Bdellovibrio*) were visualised via fluorescence microscopy, following uptake by macrophage, at 2-, 4- and 24-hours post-uptake. Bd2620 was expressed throughout *Bdellovibrio* occupation of macrophage. At least 5 fields of view were imaged from each of 2 biological replicates. Phase: Exposure 50 ms; mCerulean: Exposure 10 s, Excitation: 420-450 nm, Emission: 460-500 nm; mCherry: Exposure 10s, Excitation: 550-600 nm Emission: 610-665 nm. White scale bars represent 5 μM, Yellow scale bars represent 2 μM (Zoom) and Green scale bars represent 2 μM (RPMI Controls; Lower Panel).

4.6.7. Bd3203 is expressed by *B. bacteriovorus* throughout macrophage occupation.

To determine whether Bd3203, a hypothetical protein highlighted by initial transcriptional studies in zebrafish, was expressed by *Bdellovibrio* during occupation of macrophage, Bd3203mCerulean-tagged *B. bacteriovorus* were visualised following uptake by macrophage at 2-, 4- and 24-hours post-uptake. Bd3203mCerulean was expressed throughout *Bdellovibrio* occupation of macrophage, although it is also highly expressed in attack phase cells that have not been engulfed by macrophage (Figure 4.6.16).

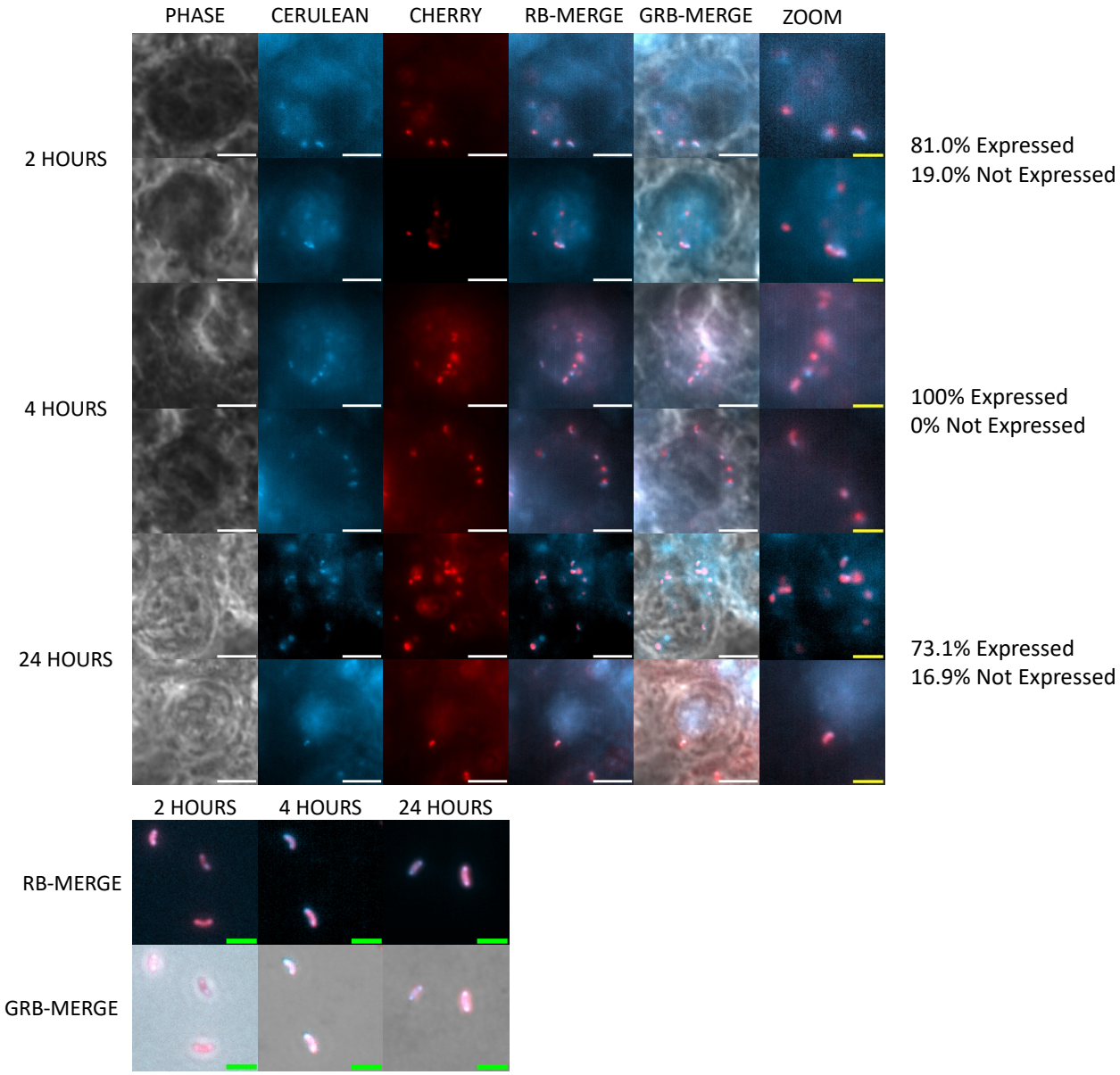

Figure 4.6.16: Bd3203mCerulean is expressed by *B. bacteriovorus* throughout macrophage occupation. *B. bacteriovorus* containing a C-terminally tagged mCerulean-tagged Bd3203 protein and a constitutively expressed mCherry-tagged Bd0064 protein (illuminating the cell body of the *Bdellovibrio*) were visualised via fluorescence microscopy, following uptake by macrophage, at 2-, 4- and 24-hours post-uptake. Bd3203 was expressed throughout *Bdellovibrio* occupation of macrophage. At least 5 fields of view were imaged from each of 2 biological replicates. Phase: Exposure 50 ms; mCerulean: Exposure 10 s, Excitation: 420-450 nm, Emission: 460-500 nm; mCherry: Exposure 10s, Excitation: 550-600 nm Emission: 610-665 nm. White scale bars represent 5 μM, Yellow scale bars represent 2 μM (Zoom) and Green scale bars represent 2 μM (RPMI Controls; Lower Panel).

4.7. Determining the importance of our candidate proteins in the predation of *E. coli* by *B. bacteriovorus*.

To determine whether the removal of our candidate gene products would affect the efficiency of predation by *B. bacteriovorus,* our gene deletion strains were incubated with *E. coli* S17-1 prey, and the OD_{600} of the predation culture measured over time. As *B. bacteriovorus* are too small to be measured accurately by optical density, the growth of *E. coli* S17-1/optical density of the predatory culture containing *E. coli* S17-1 was used as a proxy for successful predation (indicated by prey cell death and a drop in optical density).

4.7.1. Experimental considerations

At 0 hours, there was an excess of prey compared to *Bdellovibrio,* so every *Bdellovibrio* will likely have invaded a prey cell. Although entry and prey cell death occur within 20 minutes of the initiation of predation, prey cell lysis and a drop in OD_{600} does not occur until approximately 4 hours. At 4 hours, prey cells were still abundant but there were more *Bdellovibrio* predators than previously. In subsequent cycles, the number of uninvaded prey cells decreased and the number of *Bdellovibrio* increased, causing predation and the drop in OD_{600} to slow, and the rate of predation to become less efficient (Figures 4.7.1). At 18 hours, there was an excess of predator *Bdellovibrio*, but very few available prey cells (approximately $1x10^7$ c.f. $1x10^9$ at 0 hours; Figure 4.7.3) and an excess of cellular debris (Figures 4.7.2), making any further predation unlikely/minimal, and potentially explaining why the OD_{600} of the predatory culture in this assay does not equal zero (Figures 4.7.1). The remaining live *E. coli* cells are not preyed upon due to a decreased probability of collision with *Bdellovibrio* (due to cellular debris) or due to the remaining *E. coli* cells being phenotypically resistant to predation by *B. bacteriovorus* (351).

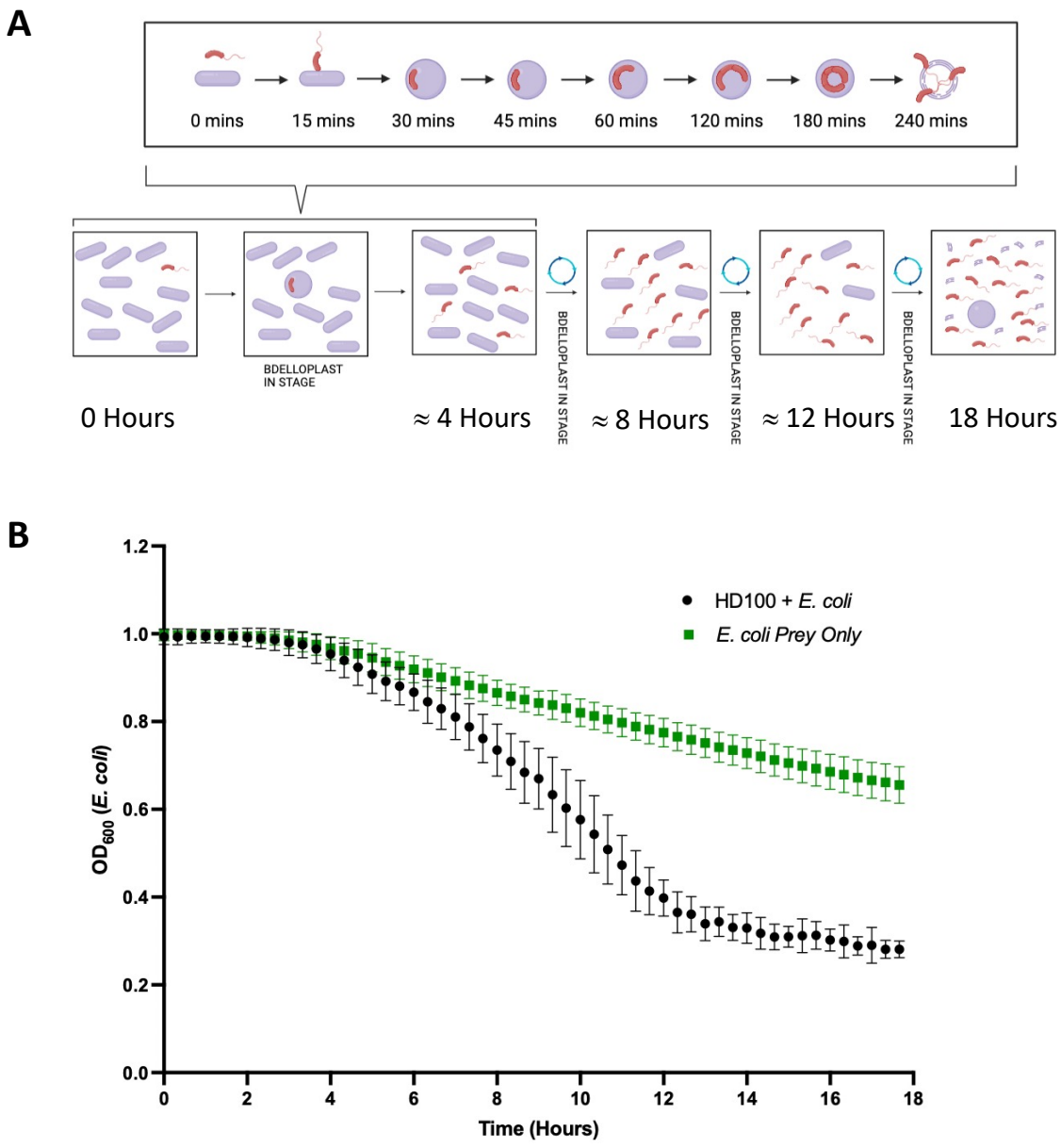

Figure 4.7.1: Predation of *E. coli* S17-1 by *B. bacteriovorus* HD100. Wildtype *B. bacteriovorus* HD100 was incubated with *E. coli* S17-1 prey over an 18-hour period, with the OD_{600} measured as a proxy for predation and prey cell bursting. At 0 hours, there is an excess of prey compared to *Bdellovibrio,* so every *Bdellovibrio* will likely invade a prey cell. Although entry and prey cell death occurs within 20 minutes, prey cell lysis and a drop in OD_{600} does not occur until approximately 4 hours. At 4 hours, prey cells are still abundant but there are more *Bdellovibrio* predators. In subsequent cycles, the number of uninvaded prey cells decreases and the number of predator *Bdellovibrio* increases, causing predation and the drop in OD_{600} to slow and become less efficient. At 18 hours, there are an excess of predator *Bdellovibrio*, but very few available prey cells and an excess of cellular debris, making any further predation unlikely/minimal. Error bars represent standard deviation. N=6, where N represents the number of biological replicates.

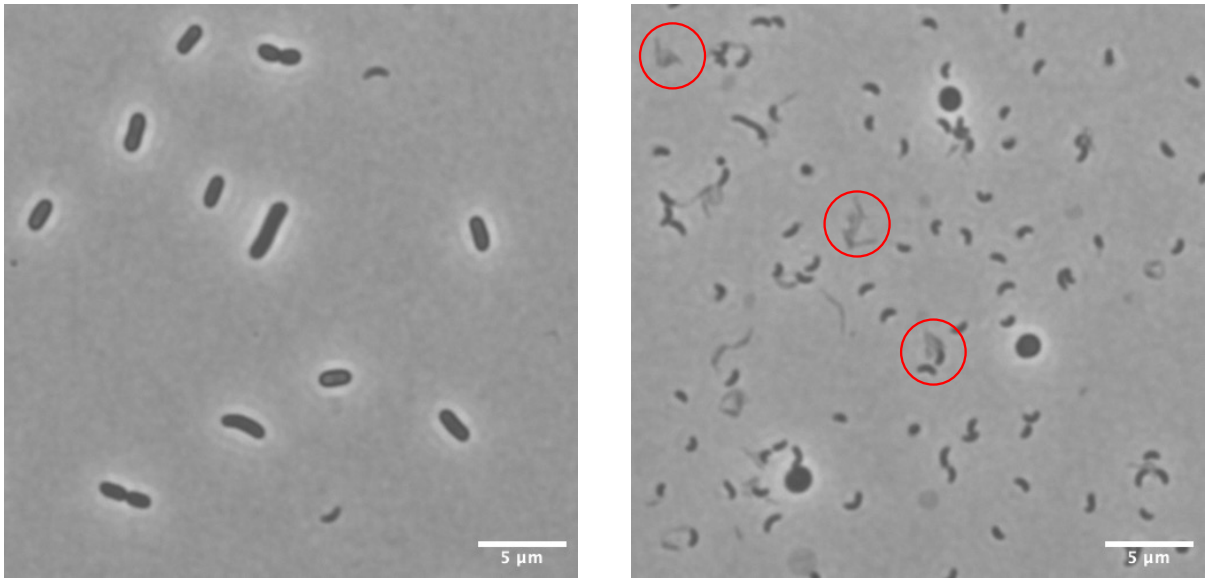

Figure 4.7.2: Microscopy images taken at 0 hours and 18 hours during the predation of *E. coli* by *B. bacteriovorus* HD100. Phase images were taken at 0 and 18 hours, during the predation of *E. coli* by *B. bacteriovorus* HD100, using an identical predation assay set-up as the assay used to test the importance of our candidate proteins in predation. At 0 hours, there is an excess of *E. coli* prey cells and very few *Bdellovibrio.* At 18 hours, there is an excess of Bdellovibrio, and very few available *E. coli* prey cells. There are also several bdelloplasts, representing stalled predation, and an excess of cellular debris (circled in red). The presence of these remaining bdelloplasts and cellular debris may explain why the OD_{600} reading never reaches zero in my assay. Scale bars represent 5 µm. Images were taken using a Nikon TiE Inverted Fluorescence Microscope. Phase: 250 ms.

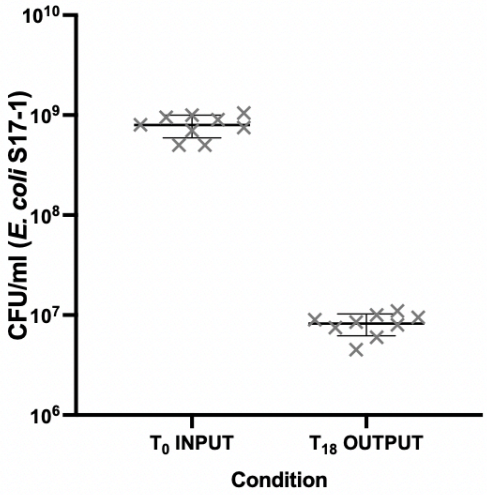

Figure 4.7.3: Comparison of the *E. coli* CFU/ml Input (T_0) and Output (T_{18}) values shows that some live *E. coli* remain after 18 hours of predation by *B. bacteriovorus* HD100. Quantification of live *E. coli* S17-1 was performed at T_0, prior to predation, and T_{18}, at the end of our predation assay (*B. bacteriovorus* HD100 incubated with *E. coli* S17-1) by CFU plating. This showed that approximately 1% of the input *E. coli* are viable and alive after 18 hours of predation. This, in combination with remaining cellular debris and bdelloplasts, may explain why the OD_{600} reading never reaches zero in my assay. Error bars represent standard deviation. N=3, where N represents the number of biological replicates.

4.7.2. Deletion of a Copper-Zinc superoxide dismutase negatively impacts predation of *E. coli* by *B. bacteriovorus.*

To investigate the role of superoxide dismutases in predation, *B. bacteriovorus* gene knockout mutants, with *bd0295* or *bd1401 sodC* genes removed, were incubated with *E. coli* prey and the OD_{600} value measured as a proxy for *E. coli* prey lysis and predation, over a course of 18 hours. Removal of *bd0295/sodC* did not alter predation (Figure 4.7.4 A), whereas removal of *bd1401/sodC* negatively impacted predation, delaying predation and decreasing prey lysis between 6 and 12 hours (P<0.05) (Figure 4.7.4 B).

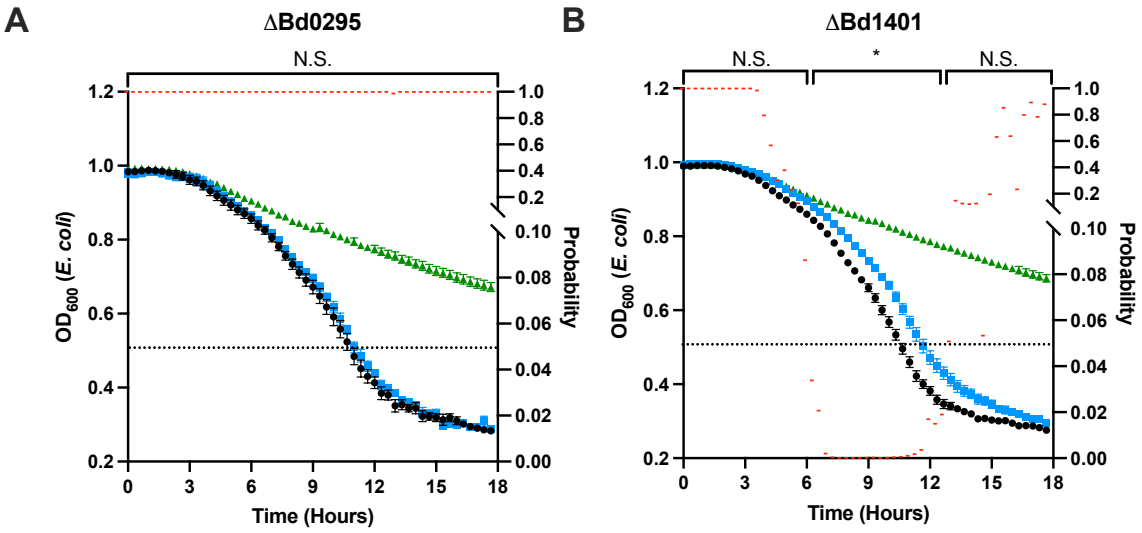

Figure 4.7.4: Removal of the *sodC* superoxide dismutase gene *bd1401* but not *bd0295* alters the ability of *B. bacteriovorus* to prey on *E. coli*. Single gene deletion mutants of *B. bacteriovorus*, with the *bd0295* or *bd1401 sodC* genes removed, were incubated with *E. coli* S17-1 prey over an 18-hour period, with the OD_{600} measured as a proxy for predation and prey cell bursting. Removal of *bd0295* did not alter the ability of *B. bacteriovorus* to prey upon *E. coli* (A). Removal of *bd1401* negatively impacted the ability of *B. bacteriovorus* to prey upon *E. coli,* represented by a decrease in prey cell lysis between 6 and 12 hours (B). Black represents Wildtype *B. bacteriovorus* HD100 (A, B). Blue represents *B. bacteriovorus* Δ*bd0295* (A) or Δ*bd1401* (B). Green represents an *E. coli* only control. Error bars represent standard error of the mean. N.S. represents non-significance at P<0.05. * Indicates significance at P<0.05. ** Indicates significance at P<0.01. Significance was assessed using a two-way ANOVA with a Sidak's multiple comparison test. N=3 (A) or N=6 (B), where N represents the number of biological replicates. Probability values for each timepoint (Test vs HD100 control) are represented by red horizontal line markers, plotted on the right x axis.

4.7.3. Deletion of catalase and ankyrin proteins does not impact predation of *E. coli* by *B. bacteriovorus.*

To investigate the role of catalases, and their regulatory ankyrins, in predation, *B. bacteriovorus* gene knockout mutants, with *bd0798/catA, bd0799/ankB, bd1154/katA* or *bd1155/ankB* genes removed, were incubated with *E. coli* prey and the OD_{600} value measured as a proxy for *E. coli* prey lysis and predation, over a course of 18 hours. Removal of *bd0798/catA* (Figure 4.7.5 A) *bd0799/ankB* (B)*, bd1154/katA* (C) or *bd1155/ankB* (D) did not alter predation efficiency or prey lysis ($P<0.05$), although there was a small visible difference in cell lysis in Figure 4.7.5 C and D. This was not (statistically) significantly different to the WT, due to the spread and natural variation of the data.

As individual gene knockout mutants in catalases and ankyrins did not alter predation, I next tested whether double knockout mutants in both catalase proteins or their two, neighbouring ankyrin proteins affected predation. *B. bacteriovorus* gene knockout mutants, with *bd0798/catA* and *Bd1154/katA* or *bd0799/ankB* and *bd1155/ankB* genes removed, denoted as ΔBd0798ΔBd1154 and ΔBd0799ΔBd1155 respectively, were incubated with *E. coli* prey and the OD_{600} value measured as a proxy for *E. coli* prey lysis and predation, over a course of 18 hours. Removal of *bd0798/catA* and *bd1154/katA* did not alter predation (Figure 4.7.5 E) ($P<0.05$). Removal of *bd0799/ankB* and *bd1155/ankB* did not alter predation efficiency ($P<0.05$) (Figure 4.7.5 F), despite an apparently significant difference in prey lysis at 17 hours.

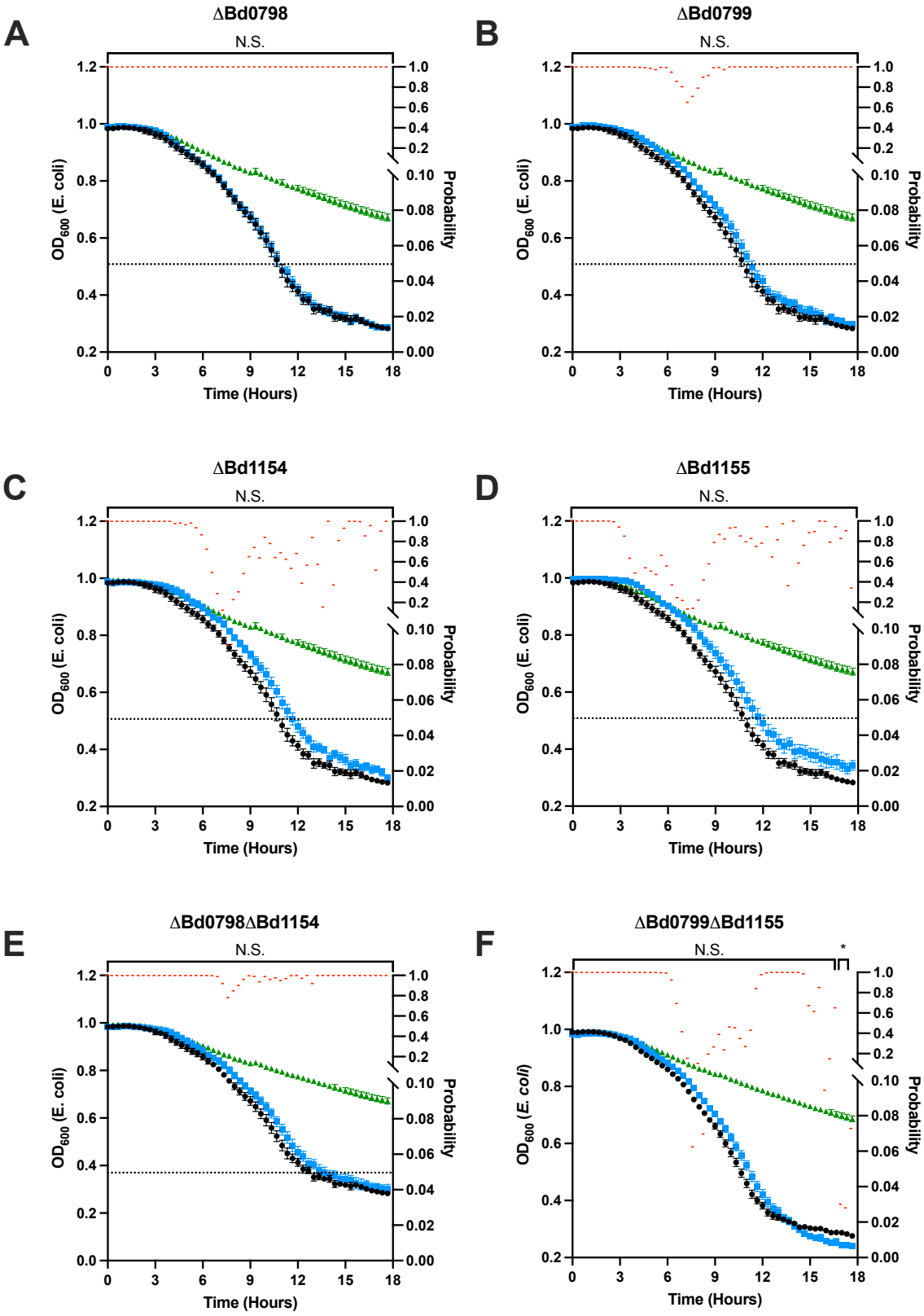
A
ΔBd0798
N.S.
B
ΔBd0799
N.S.
C
ΔBd1154
N.S.
D
ΔBd1155
N.S.
E
ΔBd0798ΔBd1154
N.S.
F
ΔBd0799ΔBd1155
N.S.
*
OD600 (E. coli)
Probability
Time (Hours)

Figure 4.7.5: Removal of the catalase genes *bd0798/catA* and/or *bd1154/katA*, or the ankyrin genes *bd0799*/*ankB* and/or *bd1155*/*ankB*, does not alter the ability of *B. bacteriovorus* to prey on *E.* coli. Single gene deletion mutants of *B. bacteriovorus*, with *bd0798*/*catA* (A), *bd0799*/*ankB* (B), *bd1154*/*katA* (C), or *bd1155*/*ankB* genes removed, or double gene deletion mutants with both Δ*bd0798* and Δ*bd1154* (E) or both Δ*bd0799* and Δ*bd1155* (F) removed, were incubated with *E. coli* S17-1 prey over an 18-hour period, with the OD_{600} measured as a proxy for predation and prey cell bursting. Removal of *bd0798* (A)*, bd0799* (B)*, bd1154* (C) or *bd1155* (D) did not alter the ability of *B. bacteriovorus* to prey upon *E. coli*. Removal of both Δ*bd0798* and Δ*bd1154* (E) or both Δ*bd0799* and Δ*bd1155* (F) did not alter the ability of *B. bacteriovorus* to prey upon *E. coli*. Black represents Wildtype *B. bacteriovorus* HD100. Blue represents *B. bacteriovorus* Δ*bd0798*/*catA* (A), Δ*bd0799*/*ankB* (B), Δ*bd1154*/*katA* (C), Δ*bd1155*/*ankB* Δ*bd0798*Δ*bd1154* (E) or Δ*bd0799*Δ*bd1155* (F). Green represents an *E. coli* only control. Error bars represent standard error of the mean. N.S. represents non-significance at P<0.05. * Indicates significance at P<0.05. Significance was assessed using a two-way ANOVA with a Sidak's multiple comparison test. N=3 (A-E) or N=6 (F), where N represents the number of biological replicates. Probability values for each timepoint (Test vs HD100 control) are represented by red horizontal line markers, plotted on the right x axis.

4.7.4. Deletion of Bd2620/Dps negatively impacts predation of *E. coli* by *B. bacteriovorus.*

To investigate the role of Bd2620 (Dps) in predation, a *B. bacteriovorus* gene knockout mutant, with the *bd2620* gene removed, was incubated with *E. coli* prey and the OD_{600} value measured as a proxy for *E. coli* prey lysis and predation, over a course of 18 hours. Removal of *bd2620/dps* negatively impacted predation, represented by a small decrease in prey cell lysis between 7 and 9 hours ($P<0.05$) (Figure 4.7.6).

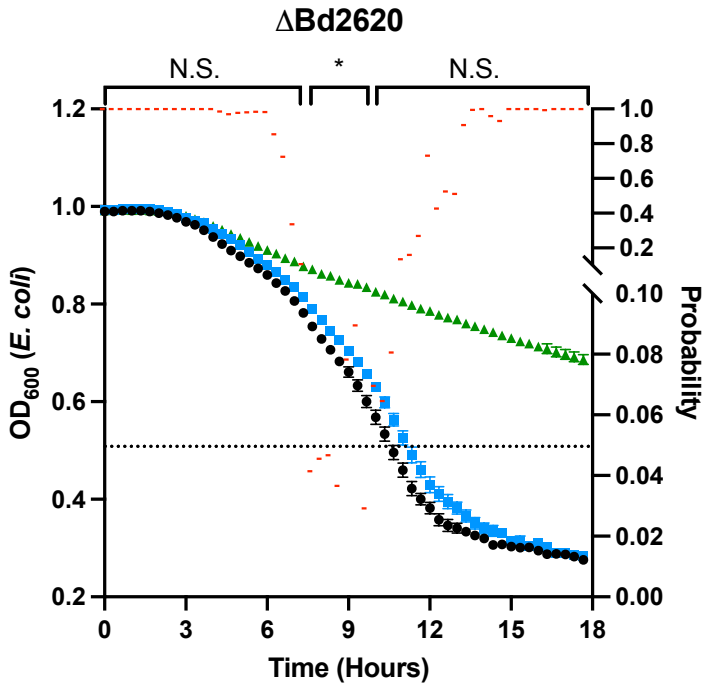

Figure 4.7.6: Removal of *bd2620/dps* alters the ability of *B. bacteriovorus* to prey on *E. coli*. A single gene deletion mutant of *B. bacteriovorus*, with the *bd2620* gene removed, was incubated with *E. coli* S17-1 prey over an 18-hour period, with the OD_{600} measured as a proxy for predation and prey cell bursting. Removal of *bd2620* negatively impacted the ability of *B. bacteriovorus* to prey upon *E. coli*. Black represents Wildtype *B. bacteriovorus* HD100. Blue represents *B. bacteriovorus* Δ*bd2620.* Green represents an *E. coli* only control. Error bars represent standard error of the mean. N.S. represents non-significance at $P<0.05$. * indicates significance at $P<0.05$. Significance was assessed using a two-way ANOVA with a Sidak's multiple comparison test. N=6, where N represents the number of biological replicates. Probability values for each timepoint (Test vs HD100 control) are represented by red horizontal line markers, plotted on the right x axis.

4.7.5. Deletion of Bd3203 (hypothetical) negatively impacts predation of *E. coli* by *B. bacteriovorus.*

To investigate the role of Bd3203 in predation, a *B. bacteriovorus* gene knockout mutant, with the *bd3203* gene removed, was incubated with *E. coli* prey and the OD_{600} value measured as a proxy for *E. coli* prey lysis and predation, over a course of 18 hours. Removal of *bd3203* negatively impacted predation, decreasing prey lysis between 7 and 11 hours 40 minutes (P<0.05) (Figure 4.7.7).

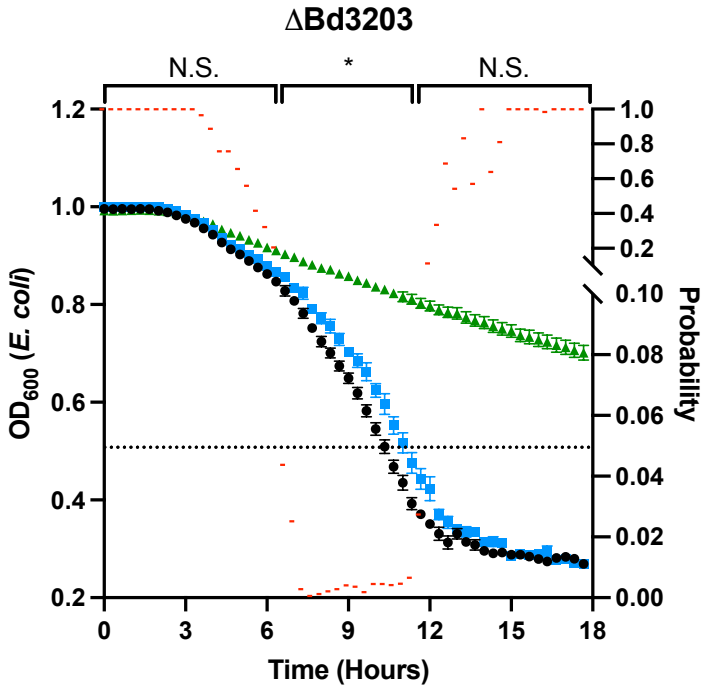

Figure 4.7.7: Removal of *bd3203* alters the ability of *B. bacteriovorus* to prey on *E. coli*. A single gene deletion mutant of *B. bacteriovorus*, with the *bd3203* gene removed, was incubated with *E. coli* S17-1 prey over an 18-hour period, with the OD_{600} measured as a proxy for predation and prey cell bursting. Removal of *bd3203* negatively impacted the ability of *B. bacteriovorus* to prey upon *E. coli*. Black represents Wildtype *B. bacteriovorus* HD100. Blue represents *B. bacteriovorus* Δ*bd3203.* Green represents an *E. coli* only control. Error bars represent standard error of the mean. N.S. represents non-significance at P<0.05. * indicates significance at P<0.05. Significance was assessed using a two-way ANOVA with a Sidak's multiple comparison test. N=6, where N represents the number of biological replicates. Probability values for each timepoint (Test vs HD100 control) are represented by red horizontal line markers, plotted on the right x axis.

4.7.6. Deletion of the hypothetical, OMP-like protein Bd1815 does not impact predation of *E. coli* by *B. bacteriovorus.*

To investigate the role of Bd1815, a hypothetical protein that I predict to have an OMP-like function, in predation, *B. bacteriovorus* gene knockout mutants, with *bd1815* removed, were incubated with *E. coli* prey and the OD_{600} value measured as a proxy for *E. coli* prey lysis and predation, over a course of 18 hours. Removal of *bd1815* did not alter predation efficiency or prey lysis (P<0.05) (Figure 4.7.8).

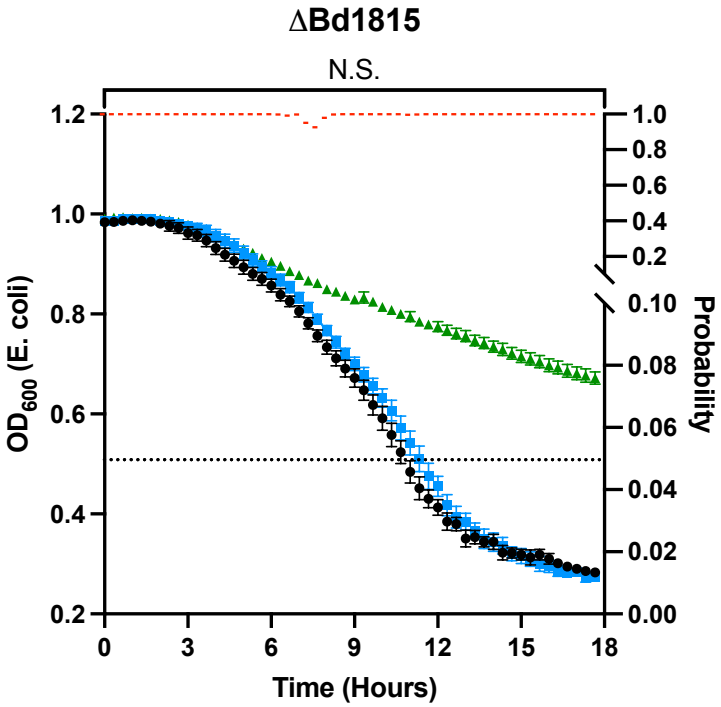

Figure 4.7.8: Removal of *bd1815* does not alter the ability of *B. bacteriovorus* to prey on *E. coli*. A single gene deletion mutant of *B. bacteriovorus*, with the *bd1815* gene removed, was incubated with *E. coli* S17-1 prey over an 18-hour period, with the OD_{600} measured as a proxy for predation and prey cell bursting. Removal of *bd1815* did not alter the ability of *B. bacteriovorus* to prey upon *E. coli*. Black represents Wildtype *B. bacteriovorus* HD100. Blue represents *B. bacteriovorus* Δ*bd1815.* Green represents an *E. coli* only control. Error bars represent standard error of the mean. N.S. represents non-significance at P<0.05, assessed using a two-way ANOVA with a Sidak's multiple comparison test. N=3, where N represents the number of biological replicates. Probability values for each timepoint (Test vs HD100 control) are represented by red horizontal line markers, plotted on the right x axis.

4.7.7. Computational analysis of *E. coli* OD_{600} curves shows that deletion of *bd1401* and *bd3203* delays predation.

Using a methodology derived from Remy et al., 2022, I, with assistance from Dr Carey Lambert, used an R-based programme, CurveR, to analyse the regression and characteristics of the *E. coli* OD_{600} curve (413) for each of the *Bdellovibrio* knockout strains. This programme fitted a regressional (predicted) curve to the OD_{600} data, with the fitness of the curve given by VEcv value. From this analysis, we compared R_{MAX} (Maximum rate of prey lysis) and S values (the time at which R_{MAX} is reached) for each of the strains. All curves, for each strain and each biological replicate, had a VEcv value of 95 or above, where 100 indicates a perfect fit between the predicted/modelled curve and the experimental data. This suggests, according to the method of Remy et al., 2022, that the curve analysis is accurate within the cut-offs used and that the values represent an accurate depiction of the data.

To determine whether the maximum rate of prey lysis (R_{MAX}) or the time at which R_{MAX} occurs (S Value) was different due to removal of certain candidate proteins, the OD_{600} of *E. coli* prey, over time, preyed upon by *B. bacteriovorus* strains with various (indicated) gene deletions was analysed using CurveR (413). The maximum rate of prey cell lysis during predation was not significantly altered by removal of any of the genes ($P<0.05$) (Figure 4.7.9A). The time at which R_{MAX} occurs was significantly delayed in *B. bacteriovorus* Δ*bd1401* ($P<0.01$) and Δ*bd3203* ($P<0.05$), indicating, by the analysis criteria suggested by Remy et al., 2022, that both gene deletion strains were delayed in lysing *E. coli* prey and in predation (Figure 4.7.9 B). This delay in lysis indicates that deletion of *bd1401* or *bd3203* impacts predator fitness, suggesting that these genes are involved in, and are important for, predation.

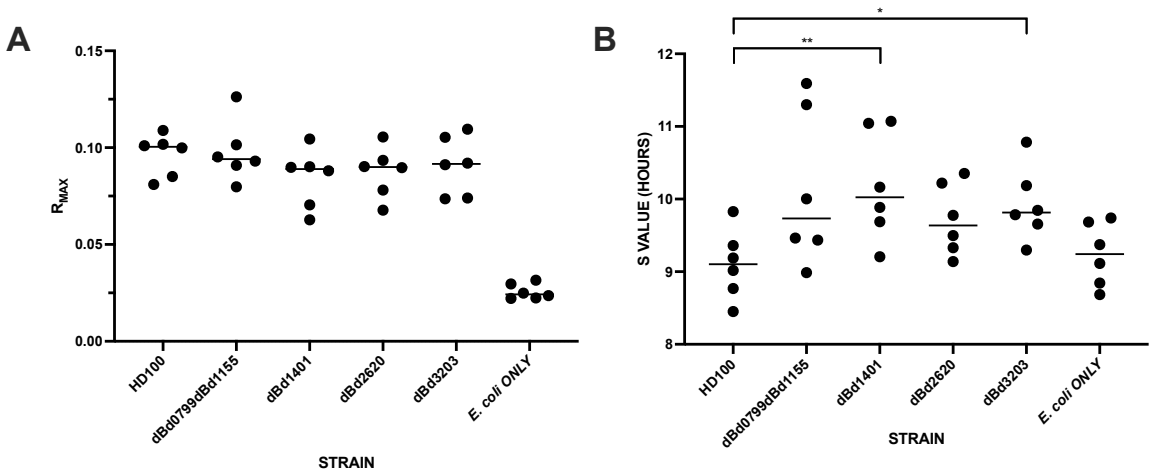

Figure 4.7.9: The maximum rate of, and timing of, *E. coli* prey lysis during two sets of three biological repeats of the predation of *E. coli* by *B. bacteriovorus* is altered by *bd1401* and *bd3203* gene deletion. CurveR software was used to analyse the OD_{600} curve of *E. coli* S17-1 prey being preyed upon by WT or gene deletion mutants of *B. bacteriovorus.* R_{MAX} represents the maximum rate of prey lysis across the whole 18-hour predation timecourse. Mean values for R_{MAX} and S are represented by black horizontal line markers. Individual biological replicates are plotted as circle markers. Despite the experimental variation between biological replicates, the trend in the data remains the same, whereby Δ*bd1401* (P<0.01) and Δ*bd3203* (P<0.05) have a higher S value (time at which R_{MAX} is reached) (Two-Way ANOVA with Dunnett's Multiple Comparisons test). The maximum rate of prey lysis was not significantly different between each of the gene deletion strains and WT *B. bacteriovorus.* * Indicates significance at P<0.05, and ** indicates significance at P<0.01, using a Two-Way ANOVA with Dunnett's Multiple Comparisons test. N=6 (A) where N represents the number of biological replicates.

4.7.8. Summary

To conclude, my data indicates that single gene deletion of *bd0295/sodC*, *bd0798/catA*, *bd1154/katA, bd0799/ankB, bd1155/ankB* or *bd1815* or double gene deletions of *bd0798/catA* and *bd1154/katA* or *bd0799*/*ankB* and *bd1155/ankB* do not impact the predation of *E. coli* S17-1 by *B. bacteriovorus* (P<0.05).

Deletion of *bd1401/sodC* negatively impacts predation, delaying predation and decreasing prey lysis between 6 and 12 hours. Deletion of *bd2620/dps* negatively impacts predation and decreases prey lysis between 7 and 9 hours (P<0.05). Deletion of *bd3203* negatively impacts predation, delaying predation and decreasing prey lysis between 7 and 11 hours 40 minutes (P<0.05). This shows that many oxidative stress response proteins are not involved in predation, but some are. This is discussed for each gene in Section 4.9.

4.8. Determining the viability of *B. bacteriovorus* gene deletion mutants in macrophage

To determine whether the removal of our candidate gene products would affect the viability of *B. bacteriovorus* in macrophage*,* our gene deletion strains were incubated with and phagocytosed by PMA-differentiated U937 cells, and their viability measured (by macrophage lysis and plaque plating) at 2-, 4-, 8- and 24-hours post-uptake.

4.8.1. Deletion of a Copper-Zinc superoxide dismutase negatively impacts the survival of *B. bacteriovorus* in macrophage.

To investigate the role of sodC Copper-Zinc superoxide dismutases in macrophage survival, *B. bacteriovorus* gene knockout mutants, with *bd0295* or *bd1401 sodC* genes removed, were incubated with macrophage and their viability measured at 2-, 4-, 8- and 24-hours post-uptake, by plating. Removal of *bd0295/sodC* did not alter viability in macrophage (Figure 4.8.1 A) whereas removal of *bd1401/sodC* did decrease the viability of *B. bacteriovorus* in macrophage at 2 hours ($P<0.05$) (Figure 4.8.1 B).

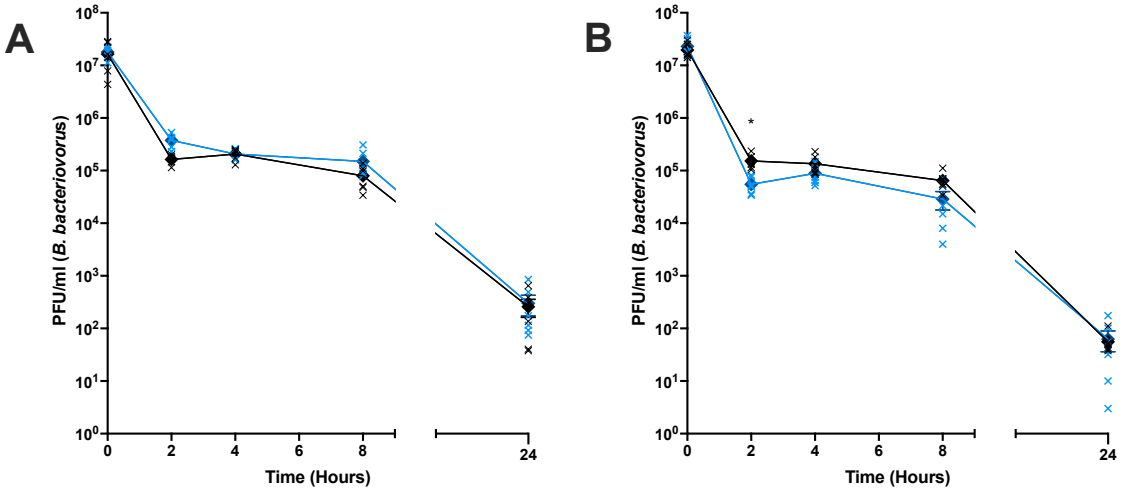

Figure 4.8.1: Removal of the *sodC* superoxide dismutase gene *bd1401* but not *bd0295* alters the survival of *B. bacteriovorus* in macrophage. Single gene deletion mutants of *B. bacteriovorus*, with the *bd0295* or *bd1401 sodC* genes removed, were phagocytosed by PMA-differentiated U937 cells and their viability measured at 2-, 4-, 8- and 24-hours post-uptake via plating. Removal of *bd0295* did not alter the viability of *B. bacteriovorus* in macrophage (A). Removal of *bd1401* negatively impacted the viability of *B. bacteriovorus* in macrophage at 2 hours post-uptake (P>0.05) (B). Black represents Wildtype *B. bacteriovorus* HD100 (A, B). Blue represents *B. bacteriovorus* Δ*bd0295* (A) or Δ*bd1401* (B). Error bars represent standard error of the mean (A, B). Significance was assessed using a two-way ANOVA with a Sidak's multiple comparison test. N=3, where N represents the number of biological replicates. * Indicates significance at P<0.05. All other comparisons between WT and mutant were non-significant at P<0.05.

4.8.2. Deletion of catalase and ankyrin proteins does not impact the survival of *B. bacteriovorus* in macrophage.

To investigate the role of catalases, and their regulatory ankyrins, in macrophage survival, *B. bacteriovorus* gene knockout mutants, with *bd0798/catA, bd0799/ankB, bd1154/katA* or *bd1155/ankB* genes removed, were incubated with macrophage and their viability measured at 2-, 4-, 8- and 24-hours post-uptake, by plating. Removal of *bd0798/catA* (Figure 4.8.2 A) *bd0799/ankB* (B)*, bd1154/katA* (C) or *bd1155/ankB* (D) did not alter the viability of *B. bacteriovorus* in macrophage.

As individual gene knockout mutants in catalases and ankyrins did not alter the viability of *B. bacteriovorus* in macrophage, I next tested whether double knockout mutants in both catalase proteins or their two, neighbouring ankyrin proteins affected survival. *B. bacteriovorus* gene knockout mutants, with *bd0798/catA* and *bd1154/katA* or *bd0799/ankB* and *bd1155/ankB* genes removed, denoted as ∆*bd0798*∆*bd1154* and ∆*bd0799*∆*bd1155* respectively, were incubated with macrophage and their viability measured at 2-, 4-, 8- and 24-hours post-uptake, by plating. Removal of *bd0798/catA* and *bd1154/katA* did not alter the viability of *B. bacteriovorus* in macrophage ($P<0.05$) (Figure 4.8.4 E). Removal of *bd0799/ankB* and *bd1155/ankB* did not alter the survival of *B. bacteriovorus* in macrophage ($P<0.05$) (Figure 4.8.4 F).

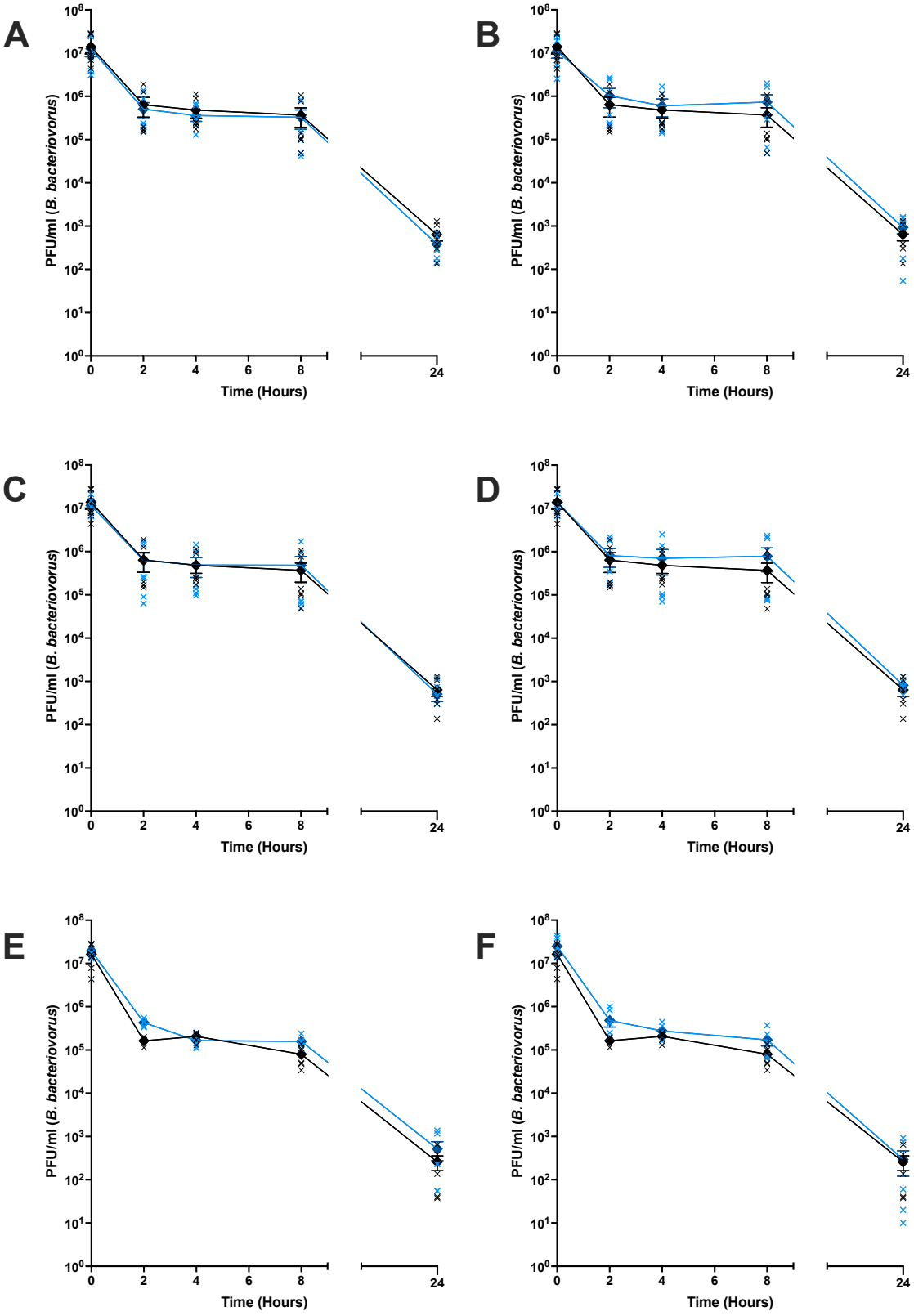
A
B
C
D
E
F
PFU/ml (B. bacteriovorus)
Time (Hours)
0
2
4
6
8
24

Figure 4.8.2: Removal of the catalase genes *bd0798/catA* and/or *bd1154/katA*, or the ankyrin genes *bd0799*/*ankB* and/or *bd1155*/*ankB*, does not alter the survival of *B. bacteriovorus* in macrophage. Single gene deletion mutants of *B. bacteriovorus*, with *bd0798*/*catA* (A), *bd0799*/*ankB* (B), *bd1154*/*katA* (C), or *bd1155*/*ankB* genes removed, or double gene deletion mutants with both ∆*bd0798* and ∆*bd1154* (E) or both ∆*bd0799* and ∆*bd1155* (F) removed, were phagocytosed by PMA-differentiated U937 cells and their viability measured at 2-, 4-, 8- and 24-hours post-uptake via plating. Removal of *bd0798* (A)*, bd0799* (B)*, bd1154* (C) or *bd1155* (D) did not alter the viability of *B. bacteriovorus* in macrophage. Removal of both ∆*bd0798* and ∆*bd1154* (E) or both ∆*bd0799* and ∆*bd1155* (F) did not alter the viability of *B. bacteriovorus* in macrophage. Black represents Wildtype *B. bacteriovorus* HD100 (A-F). Blue represents *B. bacteriovorus* *bd0798*/*catA* (A), *bd0799*/*ankB* (B), *bd1154*/*katA* (C), or *bd1155*/*ankB.* Error bars represent standard error of the mean. Significance was assessed using a two-way ANOVA with a Sidak's multiple comparison test. N=3, where N represents the number of biological replicates. All comparisons between WT and mutant were non-significant at $P<0.05$.

4.8.3. Deletion of Bd2620/Dps does not impact the survival of *B. bacteriovorus* in macrophage.

To investigate the role of Bd2620/Dps, a DNA protection from starvation and oxidative stress protein, in macrophage survival, a *B. bacteriovorus* gene knockout mutant, with *bd2620/dps* removed, was incubated with macrophage and their viability measured at 2-, 4-, 8- and 24-hours post-uptake, by plating. Removal of *bd2620/dps* did not alter the viability of *B. bacteriovorus* in macrophage (Figure 4.8.3).

4.8.4. Deletion of Bd3203 (hypothetical) does not impact the survival of *B. bacteriovorus* in macrophage.

To investigate the role of Bd3203, a hypothetical protein of unknown function, whose expression was upregulated during zebrafish infection, in macrophage survival, a *B. bacteriovorus* gene knockout mutant, with *bd3203* removed, was incubated with macrophage and their viability measured at 2-, 4-, 8- and 24-hours post-uptake, by plating. Removal of *bd3203* did not alter the viability of *B. bacteriovorus* in macrophage (Figure 4.8.4).

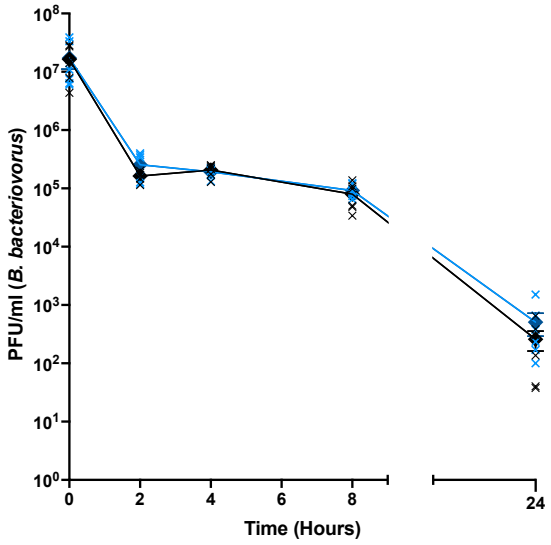

Figure 4.8.3: Removal of *bd2620/dps* does not alter the survival of *B. bacteriovorus* in macrophage. A single gene deletion mutant of *B. bacteriovorus*, with the *bd2620/dps* gene removed, was phagocytosed by PMA-differentiated U937 cells and their viability measured at 2-, 4-, 8- and 24-hours post-uptake via plating. Removal of *bd2620* did not alter the viability of *B. bacteriovorus* in macrophage. Black represents Wildtype *B. bacteriovorus* HD100. Blue represents *B. bacteriovorus* Δ*bd2620.* Error bars represent standard error of the mean. Significance was assessed using a two-way ANOVA with a Sidak's multiple comparison test. N=3, where N represents the number of biological replicates. All comparisons between WT and mutant were non-significant at P<0.05.

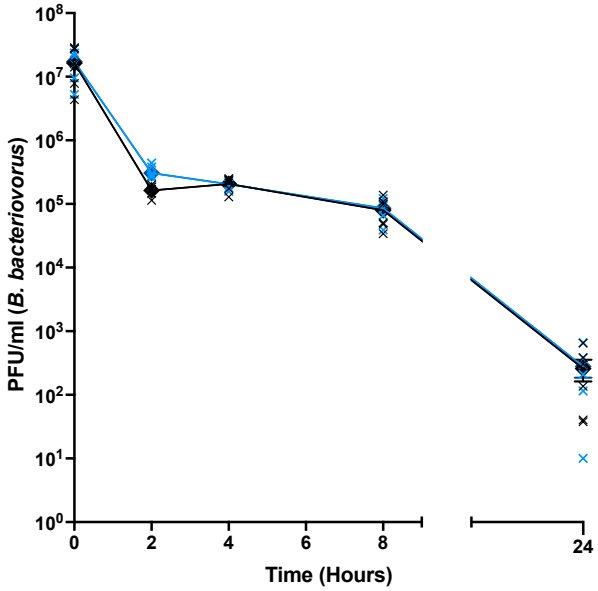

Figure 4.8.4: Removal of the gene *bd3203* does not alter the survival of *B. bacteriovorus* in macrophage. A single gene deletion mutant of *B. bacteriovorus*, with the *bd3203* gene removed, was phagocytosed by PMA-differentiated U937 cells and their viability measured at 2-, 4-, 8- and 24-hours post-uptake via plating. Removal of *bd3203* did not alter the viability of *B. bacteriovorus* in macrophage. Black represents Wildtype *B. bacteriovorus* HD100. Blue represents *B. bacteriovorus* Δ*bd3203.* Error bars represent standard error of the mean. Significance was assessed using a two-way ANOVA with a Sidak's multiple comparison test. N=3, where N represents the number of biological replicates. All comparisons between WT and mutant were non-significant at P<0.05.

4.8.5. Deletion of the hypothetical, OMP-like protein Bd1815 does not impact the survival of *B. bacteriovorus* in macrophage.

To investigate the role of Bd1815 in macrophage survival, a *B. bacteriovorus* gene knockout mutant, with *bd1815* removed, was incubated with macrophage and their viability measured at 2-, 4-, 8- and 24-hours post-uptake, by plating. Removal of *bd1815* did not alter the viability of *B. bacteriovorus* in macrophage (Figure 4.8.5).

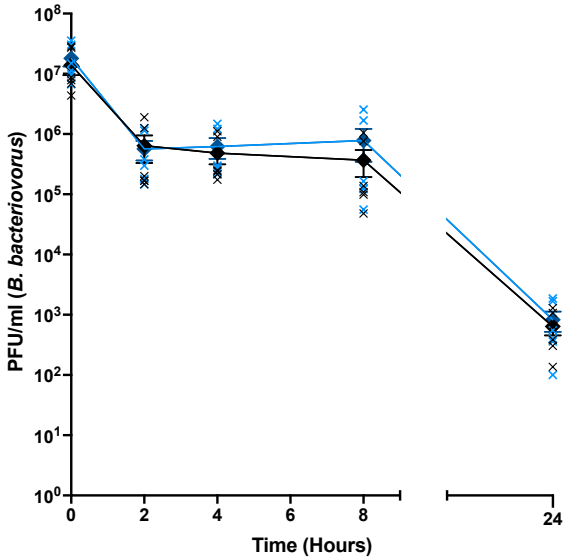

Figure 4.8.5 Removal of *bd1815* does not alter the survival of *B. bacteriovorus* in macrophage. A single gene deletion mutant of *B. bacteriovorus*, with the *bd1815* gene removed, was phagocytosed by PMA-differentiated U937 cells and its viability measured at 2-, 4-, 8- and 24-hours post-uptake via plating. Removal of *bd1815* did not alter the viability of *B. bacteriovorus* in macrophage. Black represents Wildtype *B. bacteriovorus* HD100. Blue represents *B. bacteriovorus* Δ*bd1815.* Error bars represent standard error of the mean. Significance was assessed using a two-way ANOVA with a Sidak's multiple comparison test. N=3, where N represents the number of biological replicates. All comparisons between WT and mutant were non-significant at $P<0.05$.

Table 4.8.1: Summary of the data presented in Chapter 4. N/A[1] indicates that gene deletion was not possible, owing to this gene being essential for bacterial viability.

Gene	Highlighted by…	Transcriptional expression during predation c.f. attack phase	Fluorescence throughout predation	Effect of gene deletion on predation	Transcriptional expression within macrophage	Intramacrophage fluorescence	Effect of gene deletion on survival within macrophage
surA **(*bd0017*)**	*Bdellovibrio* Macrophage transcriptional study	Downregulated between 15' and 1 hr	Expressed throughout predation (attack phase, attachment, invasion, establishment, intraperiplasmic growth and progeny release)	N/A[1]	Only detected at 24 hours post uptake.	Expressed at 24 hours post-uptake	N/A[1]
sodC **(*bd0295*)**	Zebrafish transcriptional study	Downregulated throughout	Not discernibly expressed	No effect	Highest at 2 hours	Not discernibly expressed.	No effect.
sodC **(*bd1401*)**	Homology with *bd0295*	Upregulated during intraperiplasmic growth (45' – 3hrs)	Not expressed throughout, except in rare instances	Delays predation and decreases prey lysis (6-12 hrs).	Only detected at 24 hours post uptake.	Visualised throughout, mostly at 24 hours.	Slight decrease on survival/viability at 2 hours post-uptake.
catA **(*bd0798*)**	Zebrafish transcriptional study	Downregulated throughout	Not discernibly expressed	No effect	Highly expressed throughout. Highest at 24 hours.	Not expressed throughout, except in rare instances	No effect.
ankB **(*bd0799*)**	Literature searches	Downregulated throughout	Not discernibly expressed	No effect	Highly expressed throughout. Highest at 24 hours.	Not discernibly expressed.	No effect.
katA **(*bd1154*)**	Homology with *bd0798*	Not detected	Not discernibly expressed	No effect	Only detected at 24 hours post uptake.	Not expressed throughout, except in rare instances	No effect.
ankB **(*bd1155*)**	Literature searches	Not detected	Not expressed throughout, except in rare instances	No effect	Not detected	Not discernibly expressed.	No effect.

Table 4.8.1 continued…

Gene	Highlighted by…	Transcriptional expression during predation c.f. attack phase	Fluorescence throughout predation	Effect of gene deletion on predation	Transcriptional expression within macrophage	Intramacrophage fluorescence	Effect of gene deletion on survival within macrophage
ahpC **(*bd2517*)**	Zebrafish transcriptional study	Downregulated between 15' and 45'	Expressed throughout predation	N/A[1]	Expressed throughout. Highest at 2 and 24 hours.	Highly expressed throughout intramacrophage survival. Also expressed in attack phase cells.	N/A[1]
ahpF **(*bd2518*)**	Zebrafish transcriptional study	Downregulated throughout	Expressed throughout predation	N/A[1]	Highly expressed throughout. Highest at 8 and 24 hours.	Highly expressed throughout intramacrophage survival. Also expressed in attack phase cells.	N/A[1]
dps **(*bd2620*)**	Zebrafish transcriptional study	Downregulated throughout	Expressed throughout predation	Decreases prey lysis between 7 and 9 hours	Highly expressed throughout	Highly expressed throughout intramacrophage survival. Also expressed in attack phase cells.	No effect.
bd3203	Zebrafish transcriptional study	Downregulated throughout	Expressed throughout predation	Delays predation and decreases prey lysis between 7 and 12 hours.	Highly expressed throughout	Highly expressed throughout intramacrophage survival. Also expressed in attack phase cells.	No effect.
bd1815	Zebrafish transcriptional study	Downregulated when inside prey (all timepoints except 15' and 5hrs)	Expressed throughout predation	No effect.	Expressed throughout. Highest at 2 and 4 hours.	Visualised throughout, mostly at 24 hours.	No effect.

4.9. Discussion: Testing the roles of my candidate proteins in predation and intramacrophage survival

4.9.1. Recap: Potential oxidative stresses in predation

During predation, *B. bacteriovorus* enters through the outer membrane of a Gram-negative bacterial prey cell and crosses the prey cell wall, entering the inner periplasm. The periplasm of a live Gram-negative bacterial prey cell is highly reducing, making it a region of high oxidative stress, due to the presence of oxide radicals and oxidative species (15, 346, 476-478). The prey cell is alive for the first 20 minutes of invasion by the predator and so oxidative radicals can assault the invading *B. bacteriovorus* (479). Upon prey cell death, a dysfunctional electron transport chain will also contribute oxidative radicals that may attack *Bdellovibrio* during invasion.

Furthermore, during growth of *B. bacteriovorus* within a prey cell, *Bdellovibrio* degrades nucleic acids, proteins and other macromolecules and utilises them for intraperiplasmic growth (337, 480, 481). The enzymatic degradation of prey macromolecules will also produce oxide radicals and oxidative species that, if left unchecked, would also cause oxidative damage to the *Bdellovibrio*. Upon exit of *Bdellovibrio* from prey cells, the LPS outer membrane and peptidoglycan cell wall are digested to allow for the release of *Bdellovibrio* progeny into the surrounding environment (290, 292, 311). This exit to a more aerobic external environment from inside the prey to outside represents another point of potentially high oxidative stress.

Various oxidative stress tolerance mechanisms and proteins are encoded by bacterial cells to combat these oxidative stresses; I hypothesised that possibly overlapping, or separate, oxidative stress tolerance mechanisms would be important for the entry into, and subsequent growth and exit of *B. bacteriovorus* from the periplasm of prey bacteria. Thus, deletions for such tolerance genes might affect predation.

I also hypothesised that possibly overlapping, or separate, oxidative stress tolerance mechanisms would be important for accidentally prolonged survival of *Bdellovibrio* in macrophage, allowing for the temporary tolerance of phagosomal conditions. The survival of *Bdellovibrio* within a host, and its interactions with the host immune response are important when considering the efficacy of *Bdellovibrio* as a novel antimicrobial treatment.

4.9.1.1. Potential oxidative stresses in macrophage

As outlined in Section 1.4.5.2.3, macrophages use a combination of nutrient restriction, hydrolytic enzymes (lipases, proteases, hydrolases), acidic stress and oxidative stress (peroxide and superoxide radicals) to kill bacteria within the phagosome. Upon macrophage activation, multiple oxidative species are produced that subsequently contribute to oxidative stress. Nitric oxide is produced by by Nitric Oxide Synthase complex, from NADPH, molecular oxygen, and L-arginine, usually in response to proinflammatory cytokine stimulus. Nitric Oxide subsequently reacts with other molecular species to form highly reactive oxidative species, such as NO reacting with O_2- to form peroxynitrite (482). Superoxide radicals are produced by the NADPH Oxidase complex that assembles in the phagosomal membrane of macrophage, upon activation (482). The oxidative species produced in these processes are concentrated within the phagosome at μM concentrations, reacting with proteins, lipids, and DNA to induce oxidative damage and degradation of the phagosomal cargo (482).

As *Bdellovibrio* is hypothesised to tolerate large amounts of oxidative stress throughout its predatory lifecycle, I hypothesise that some of these oxidative stress tolerance mechanisms/proteins may also confer an accidental and temporary tolerance to the highly oxidative and bactericidal conditions inside the macrophage phagosome.

This may be an unintentional bonus of the predatory lifecycle, or a relic of their soil-dwelling natural habitat, where they would encounter amoeba, which are analogous to macrophage in some contexts i.e., phagocytosis.

4.9.2. Discussing the roles of my candidate proteins

4.9.2.1. The Roles of Copper-Zinc Superoxide Dismutases in proposed tolerance to oxidative insult throughout predation and intramacrophage survival.

Bd0295 and Bd1401 are both predicted Copper-Zinc superoxide dismutase proteins that detoxify oxygen radicals of exogenous origin, to prevent DNA and protein mutation and oxidative damage to the cell, as detailed in Section 1.4.7.3.1.

Bdellovibrio are likely exposed to these exogenous ROS when they invade the periplasm of other Gram-negative cells, disrupting the prey cell electron transport chain and killing the prey cell. During intraperiplasmic growth, the enzymatic degradation of prey macromolecules is also likely a prominent source of oxidative species. Superoxides and reactive oxygen species are manufactured by macrophage and flooded into the phagosome in high abundance as a bactericidal mechanism to kill ingested bacteria, therefore superoxide dismutases may also confer a level of protection to *Bdellovibrio*, against macrophage-generated ROS.

4.9.2.1.1. Bd1401/SodC, but not Bd0295/SodC, contributes to predation of *E. coli* by *B. bacteriovorus*.

SodC (Bd0295 and Bd1401) expression was not seen throughout predation. This was unexpected, as Bdellovibrio is likely exposed to reactive oxygen species throughout predatory invasion into the prey cell periplasm, and when degrading prey cell macromolecules to repurpose them for its own intraperiplasmic growth. Transcriptional studies of *bd0295* suggested that, as it was downregulated throughout predation, $SodC_{Bd0295}$ was likely not to be involved in predation. However, *bd1401* expression is upregulated throughout intraperiplasmic growth, suggesting that $SodC_{Bd1401}$ is likely involved in predation. As to why there was an absence of discernible fluorescent protein expression is unknown.

Deletion of *bd1401* led to a delay in predation and a reduction in prey cell lysis. This is indicative of *Bdellovibrio* progeny being less fit, or more damaged by an absence of Bd1401, suggesting that it is involved in combatting reactive oxygen species within the intraperiplasmic growth phase of predation, where oxygen radicals are generated due to the hydrolysis of prey macromolecules, or upon prey cell exit, due to the hydrolysis of prey peptidoglycan and outer membrane components, to facilitate the exit of *Bdellovibrio* progeny from the prey cell, responding to and protecting the cell from a change in oxygen tension from emerging from a cell, into a wider, highly aerobic, and aerated environment. Despite this fitness cost, predation was still able to proceed, suggesting that other superoxide tolerance mechanisms exist within the *Bdellovibrio* proteosome. Deletion of *bd0295* did not impact predation, in line with the other data presented that suggests Bd0295 is not involved in predation.

$SodC_{Bd1401}$ may also contribute to survival of *B. bacteriovorus* inside, or upon exit from prey. This could be tested by enumerating *Bdellovibrio* numbers at these timepoints, or after each subsequent round of predation, to determine whether $SodC_{Bd1401}$ function impacts predator viability, predator fitness or predation efficiency.

Future work: accounting for differences between Bd0295 and Bd1401. It is interesting that Bd0295 deletion did not alter predation and yet Bd1401 deletion did, despite both genes encoding proteins of the same basic function. This may be due to differences in how transcription of *bd0295* and/or *bd1401* is initiated (at the promoter level), or any post-transcriptional or post-translational differences in their mRNA transcripts and protein production i.e. Bd0295 function may be redundant, with Bd1401, or others, being produced it its place in response to superoxide stress, whereas Bd1401 deletion may not be compensated for, owing to Bd0295 being under tighter transcriptional regulation.

The difference in impact of SodC deletion may be because one SodC enzyme is more functional or efficient than the other. This is supported by the difference in structure of these two proteins (Figure 4.3.8), where, although both proteins have the same predicted functional annotation, they have different structures and so may perform slightly different functions or with varying efficiencies or may perform these functions at slightly different locations within the cell. Bd0295 has a lipobox within its structure, suggesting it is secreted into the periplasm of the *Bdellovibrio* but remains associated with the outer leaflet of the cytoplasmic membrane whereas Bd1401 does not have a lipobox and therefore is secreted but may act in a different location within the periplasm, compared to Bd0295.

Future work: Further quantification and characterisation of superoxide stresses in predation.

Further characterisation of the oxidative stresses, and more specifically the quantification of the levels of superoxide radicals within the periplasm of the prey cell at different stages of predation would support these data and the definition of a role for Bd1401 in predation further. Commercially available kits predominantly focus on fluorescent reporter based quantification of reactive oxygen species within eukaryotic cells. However, trialling these kits in the unique scenario of bacterial predation may give us an indication of the varying oxidative stresses throughout predation.

Future work: Is Bd0295 function truly redundant? Bd1401 and Bd0295 may functionally compensate for one another. Deletion of both *bd0295* and *bd1401* simultaneously would test this hypothesised functional redundancy, where the double SodC deletion mutant could be tested for predation efficiency and macrophage survival as previously documented. If a level of functional redundancy did exist between the two SodC proteins, I would expect a poorer viability in macrophages and decreased/slower prey lysis in predation due to the fitness cost on progeny *Bdellovibrio*. If the two sodC proteins did not compensate for one another, I would expect that the ∆*bd0295*∆*bd1401* mutant would be as viable in macrophage and as efficient at predation as the single ∆*bd1401* mutant. However, a ∆*bd0295*∆*bd1401* mutant may not be viable in predation, making it impossible to construct.

Additionally, I would complement the *bd1401* gene, back into the ∆*bd1401 B. bacteriovorus* mutant, to confirm that the phenotype seen in the ∆*bd1401 B. bacteriovorus* mutant, is due to *bd1401* deletion. A plasmid had been designed (Mr Paul Radford) and is in the process of being conjugated into ∆*bd1401 B. bacteriovorus* and validated (Mr Rob Till), but completion of this was not possible due to time constraints.

4.9.2.1.2. $SodC_{Bd1401}$, but not $SodC_{Bd0295}$, contributes to survival and viability in macrophage.

The importance of SodC in bacterial pathogens and infection. The importance of SodC for the survival and virulence of bacterial pathogens in macrophage is well documented. *Burkholderia cenocepacia* SodC mutants are more susceptible to bacterial killing by exogenous superoxide, have a severe growth defect and are killed more rapidly by murine macrophages (483). In *Salmonella enterica* serovar Cholaraesuis, deletion of the two SodC proteins both impaired viability in macrophage, with each protein being of varying importance depending on the activation state and bacterial uptake pathway of the macrophage (484-486). Other studies in *Salmonella enterica* Typhimurium report no effect on susceptibility to extracellular ROS, but a defect in colonisation of murine spleen cells (487), murine macrophage and in live murine infection models (488). In *Salmonella enterica* Typhimurium, SodC deletion mutants were more susceptible to killing by the respiratory burst and nitric oxide synthase in murine infection (488). In *Brucella abortus*, deletion of SodC reduced survival and virulence in murine macrophages and murine infection (489). A defect in virulence and host survival is also reported in *Haemophilus ducreyi* (490, 491), *Neisseria meningitidis (492)*, *Mycobacterium tuberculosis* (493), *E. coli* (494) and *Burkholderia pseudomallei* (495).

Conversely, in *Legionella pneumophila*, SodC is not essential for growth and survival in macrophage (496), and *Actinobacillus pleuropneumoniae* was not impaired in virulence within an intratracheal model of infection (497). Some studies report no effect of SodC deletion in cell-line derived macrophage, but reduced virulence in murine models of infection (498).

Clearly, multiple factors surrounding the host, bacterial pathogen, activation state of the macrophage/immune response all contribute to the phagolysosomal maturation pathway and thus the outcome of infection and importance of SodC within this.

$SodC_{Bd0295}$ was not discernibly expressed by *Bdellovibrio* within macrophage, despite transcriptional studies suggesting that *bd0295* is expressed throughout intramacrophage survival, especially at 2 hours post-uptake. As transcriptional studies suggest a more important role for Bd0295, and with the limitations of the current microscopy studies, it would be pertinent to characterise Bd0295 protein content via another means e.g., quantification by Western blot analysis. However, as *bd0295* gene deletion did not affect *Bdellovibrio* intramacrophage survival, I suggest that Bd0295 does not meaningfully contribute to the superoxide tolerance response of *Bdellovibrio* whilst it temporarily resides within the phagosome of macrophage, where superoxide stress is evident and well characterised in other bacterial pathogens. Conversely, $SodC_{Bd1401}$ expression is seen at 24 hours post-uptake, in-line with transcriptional studies. Deletion of *bd1401* reduces *Bdellovibrio* survival at 2 hours post-uptake, within macrophage, suggesting that Bd1401 is important, or involved in, the initial superoxide tolerance response of *Bdellovibrio* after initial uptake, inside the macrophage phagosome. Removal of Bd1401 function makes *Bdellovibrio* more susceptible to superoxide stress and bacterial killing. The difference in importance between $SodC_{Bd0295}$ and $SodC_{Bd1401}$ may be due to a difference in subcellular localisation, as detailed in Section 4.3.

4.9.2.1.3. Summary: The roles of superoxide dismutases in predation and *Bdellovibrio* occupation of macrophage

To conclude, SodC enzymes are of varying importance in bacterial pathogens and host infection. Bd1401 is important for predation by *B. bacteriovorus*, likely in aiding the tolerance to superoxide stress during intraperiplasmic growth and exit from Gram-negative prey. Bd0295 was not important in predation.

Bd0295 also does not contribute to survival against and tolerance to reactive oxygen species stress within the macrophage phagosome, whereas Bd1401 may confer a survival benefit, in combination with other, currently unknown, factors. The differences in structure and localisation of Bd0295 and Bd1401 may also explain why deletion of Bd1401 impacted viability of *Bdellovibrio* in macrophage, but deletion of Bd0295 did not. Other superoxide/ROS detoxification mechanisms may exist within *Bdellovibrio* that may also contribute to survival and tolerance of *Bdellovibrio* to phagosome conditions within macrophage.

4.9.2.2. Tolerance of peroxide stress throughout predation and intramacrophage survival.

The periplasm of *E. coli* is a highly reducing environment (499, 500), therefore oxidative stresses, including peroxide-based species generation (15, 346, 476-478), are experienced by *Bdellovibrio* throughout invasion into the periplasm, intraperiplasmic growth (produced during the digestion of prey macromolecules) and during the digestion of prey cell wall peptidoglycan and LPS outer membrane upon progeny release and prey exit.

4.9.2.2.1. Peroxide stress tolerance throughout predation of *E. coli* by *B. bacteriovorus*.

Catalases are not important for predation of *E. coli* by *B. bacteriovorus*. Catalase (Bd0798/CatA and Bd1154/KatA) expression was not seen throughout predation. A lack of a peroxide stress response would be surprising as *Bdellovibrio* is likely exposed to peroxide stresses upon entry into the prey cell periplasm. However, transcriptional studies show that *bd0798* and *bd0799* expression was downregulated throughout predation, potentially explaining the absence of fluorescent protein expression. Deletion of *bd0798, bd0799, bd1154* and *bd1155* does not impact predation, further suggesting that these proteins are not important in predation and that another peroxide detoxifying mechanism exists. Instead, I suggest that the peroxide stress response involves Bd2517/AhpC and Bd2518/AhpF, which are both expressed throughout predation.

Bd2517/AhpC and Bd2518/AhpF are two subunits of a protein that catalyses the detoxification of hydrogen peroxide, therefore making these proteins important in the tolerance of oxidative stress and potentially, adaptation to the changes in oxygen tension and oxidative stress throughout entry into the prey cell periplasm, intraperiplasmic growth and prey cell exit.

AhpC is the peroxide reducing subunit of the protein, whereas AhpF is a flavoprotein that uses NADPH as an electron donor to reduce AhpC, increasing the peroxide-reducing capabilities of AhpC (501, 502).

Transcriptional studies show that both *bd2517* and *bd2518* are downregulated throughout predation. However, I suggest that as these proteins are involved in tolerating the initial peroxide assault upon entry into the prey cell periplasm, the expression of these genes is likely always highest in attack phase cells. This could be tested by quantifying protein levels of Bd2517 and Bd2518 throughout predation, where I would expect an abundance of protein in attack phase cells that is quicky depleted at 30 and 45 minutes onwards. I would compare the protein abundance to the amount of Bd2517 and Bd2518 protein produced in response to exogenous hydrogen peroxide (in vitro addition to culture media), to see if this also upregulated Bd2517 and Bd2518 protein production. Deletion of *bd2517* and *bd2518* was lethal, suggesting that the peroxide detoxification function of Bd2517 and Bd2518 is vital for predation.

4.9.2.2.2. Tolerance of peroxide stress in macrophage.

The importance of catalases in bacterial pathogens and infection. In other bacterial pathogens, catalase activity is essential for virulence and survival, including in *Staphylococcus aureus* (in combination with SOD) (503, 504), *Campylobacter jejuni* (505), *Helicobacter pylori* (506), *Francisella tularensis* (507, 508), *Neisseria meningitidis* (509, 510), *Legionella pneumophila* (511, 512) *, Mycobacterium tuberculosis* (513, 514).

In other bacteria, single catalase mutants were still virulent in murine macrophage and infections with *Salmonella* Typhimurium (515), *Yersinia pestis* (516), *Francisella tularensis* (517)*, Staphylococcus aureus* (518) and *Neisseria gonorrhoeae* (519). This highlights the redundancy in peroxide-detoxification mechanisms, whereby deletion of the 3 catalases and 2 Ahp subunits in *Salmonella* Typhimurium gives an increased susceptibility to Hydrogen Peroxide, reduced survival, and reduced virulence in murine macrophages. Overexpression of KatG or TsaA/Ahp restored the resistance to hydrogen peroxide (520).

The importance of alkyl hydroperoxide reductases in bacterial pathogens and infection. AhpC is the peroxide reducing subunit of the protein, whereas AhpF is a flavoprotein that uses NADPH as an electron donor to reduce AhpC, increasing the peroxide-reducing capabilities of AhpC (501, 502). Most bacterial pathogens have a AhpC protein, even if they are lacking an OxyR regulon or an AhpF counterpart, including *C. jejuni* which lacks AhpF (521) and *M. tuberculosis,* which lacks OxyR (522-525). Transcription of the *ahpF* gene is induced by the OxyR regulon, in *E. coli* and *P. aeruginosa*, along with *dps*, *katA*,a*nkB*, *ahpB* and *ahpC* (526, 527).

In *Salmonella* Typhimurium, AhpC is upregulated during macrophage infection but is not essential for virulence in a murine model of infection (528). Deletion of AhpC did increase the susceptibility of *S.* Typhimurium to Reactive Nitrogen Species (523). Removal of AhpC, in combination with KatE, KatG, KatN and TsaA, increases the susceptibility of *S.* Typhimurium to hydrogen peroxide, attenuating virulence and decreasing survival. Overexpression of KatG or TsaA (Ahp-like) rescues these defects (520). *S.* Typhimurium deficient in AhpC was more susceptible to RNI killing (523).

In *M. tuberculosis*, deletion of AhpC increases susceptibility to peroxynitrite and decreases macrophage survival (dependent on activation state)(529). Similarly, in *Francisella tularensis*, deletion of AhpC confers susceptibility to ROS and RNS, decreasing survival in macrophage. However, the function of AhpC is replaced by SodC or KatG, highlighting the functional redundancy in the oxidative stress response (530, 531). In *L. pneumophila*, AhpC is upregulated during growth in macrophage, but deletion does not impact growth, likely due to functional redundancy (532). In *S. aureus*, single gene deletions of AhpC and KatA are not susceptible to ROS or attenuated in virulence, whereas a double ∆*katA*∆*ahpC* mutant is attenuated in virulence, due to a higher susceptibility to ROS. In *E. coli,* AhpC confers resistance to RNS and protects UPEC within murine macrophage (533). In *C. jejuni,* AhpC, KatA and SodB are the important players in the oxidative stress response (534, 535).

Catalase (Bd0798/CatA and Bd1154/KatA) expression were not seen throughout intramacrophage survival of *Bdellovibrio*, despite transcriptional studies suggesting that *bd0798* and *bd0799* gene expression is high throughout, especially at 24 hours post-uptake, when significant oxidative stress and bacterial killing is occurring. Deletion of *bd0798, bd0799, bd1154* and *bd1155*, in isolation or in combination (i.e., ∆*bd0798*∆*bd1154* and ∆*bd0799*∆*bd1155*) did not affect *Bdellovibrio* intramacrophage survival. Peroxide stress is well documented within the phagosome of macrophage, therefore alternative proteins must perform this peroxide-detoxification function within the macrophage phagosome. The presence of peroxide stress likely triggers *bd0798, bd0799, bd1154* and *bd155* expression, but the role of these proteins must be redundant within the peroxide detoxification response. Instead, I suggest that Bd2517 and Bd2518, which are expressed throughout intramacrophage survival (at the transcriptional and translational level) and are essential for bacterial viability, perform this peroxide detoxification function.

This is one example of genes that are essential for bacterial viability and the predatory lifecycle of *Bdellovibrio* also potentially conferring a survival benefit to *Bdellovibrio* within the macrophage phagosome, through the tolerance of peroxide stress.

4.9.2.2.3. Summary: Peroxide detoxification within predation and intramacrophage survival.

There is a high amount of redundancy in peroxide-detoxifying mechanisms within *Bdellovibrio*, owing to the ability to detoxify hydrogen peroxide effectively and rapidly being vital in aerobically respiring cells. Catalase expression contributes to hydrogen peroxide tolerance and in infection in bacterial pathogens, but high levels of functional redundancy exist in the bacterial repertoire of peroxide detoxification. In *Bdellovibrio* deletion of both catalase proteins, and their regulatory ankyrin partners, does not impact the survival of *Bdellovibrio* within macrophage. I hypothesise that this absence of a survival defect is due to the peroxide-detoxifying proteins, Bd2517 and Bd2518, within the *Bdellovibrio* transcriptome performing this function instead. Bd2517 and Bd2518 are vital for predatory life and peroxide detoxification within *Bdellovibrio*. AhpC and AhpF also have well characterised roles in the detoxification of hydrogen peroxide in other bacteria (520, 528, 530-532, 536). I suggest that Bd2517/AhpC and Bd2518/AhpF are important in peroxide detoxification within predation and *Bdellovibrio* intramacrophage survival.

4.9.2.3. The Role of Bd2620/Dps (DNA Protection from Starvation protein) in proposed tolerance to oxidative insult throughout predation and intramacrophage survival.

Bd2620/Dps is a DNA protection from starvation protein, linked to nutrient starvation and protection from oxidative stress in *E. coli, Salmonella Typhimurium* and other bacteria (415). Bd2620/Dps was also highlighted in the initial zebrafish transcriptional study, suggesting it may be important in tolerance of the host environment.

Dps binds to DNA (via iron or magnesium binding; (537)) in the chromosome and excludes oxidative and destructive species from the chromosome, whilst the ferroxidase activity neutralises and sequesters oxidative species (538, 539), catalysing the oxidation of Fe(II) by hydrogen peroxide (into Fe(III)) (540-542). Dps is a minor component in the exponential phase of bacterial growth, but a major component in stationary phase, nucleoid associated, compacting DNA into a highly ordered and compact structure (543, 544).

In *E. coli,* Dps is a minor component in actively growing cells but is the predominant nucleoid associated protein in stationary phase cells (545), when nutrients are exhausted and growth conditions are not ideal. Dps compacts DNA into a highly ordered structure (543, 544), conferring its protective capabilities by binding to DNA and excluding oxidative species from the chromosome, or neutralizing and sequestering damaging oxidative species via its ferroxidase activity (538, 539).

Nutrients are actively restricted within the macrophage phagosome, as part of the antibacterial response to prevent bacterial growth and replication within the phagosome. Oxidative stresses are also well documented within the macrophage phagosome, as one of the primary antibacterial/bactericidal responses. This suggests that Dps would be a good candidate for aiding or benefiting *Bdellovibrio* within the macrophage phagosome, combatting damage induced by nutrient starvation or oxidative stress.

4.9.2.3.1. Bd2620/Dps, contributes to predation of *E. coli* by *B. bacteriovorus*.

Bd2620/Dps is highly expressed in attack phase *Bdellovibrio* and throughout predation, suggesting it is involved in predation. Transcriptional studies show that *bd2620* gene expression is downregulated throughout predation. As mentioned earlier, Bd2620 packages DNA to protect it from reactive species generated by oxidative stress or nutrient starvation. Active gene expression, which is high in the intraperiplasmic growth phase of *Bdellovibrio*, requires DNA to be less compact and more accessible to the transcriptional machinery. Downregulation of Bd2620 within the cell, when nutrients are abundant and large levels of gene expression are occurring, supports this role. Deletion of *bd2620* reduced prey cell lysis, indicating that predators were less able to invade and prey upon the bacterial cells due to the absence of Bd2620. If deletion of *bd2620* reduces DNA compaction, it is possible that, despite Bd2620 not being involved in, and being downregulated during, predation, Bd2620 function may be important in attack phase *Bdellovibrio,* in protecting the chromosome from reactive species generated through oxidative stress or nutrient starvation. Damage to the chromosomal DNA of *Bdellovibrio* would make it less fit, potentially impacting predation efficiency. Quantification of Bd2620 expression throughout predation, using Western blot analysis, would be very informative and could confirm the hypothesis that Bd2620 function is turned off/reduced during the intraperiplasmic growth of *Bdellovibrio*.

4.9.2.3.2. Bd2620/Dps does not significantly contribute to survival and viability in macrophage.

The importance of Dps in bacterial pathogens and infection. The ferroxidase activity of Dps protects DNA against hydrogen peroxide-mediated damage and iron-dependent killing by hydrogen peroxide in *Salmonella* Typhimurium, enhancing survival and virulence in murine macrophage, in combination with a Copper-Zinc superoxide dismutase to protect bacteria from hydrogen peroxide damage (487).

Dps mutants show increased susceptibility and cell death in response to nutrient starvation, oxidative stress, metal toxicity (546) and thermal stress (547, 548). Dps proteins are typically highly conserved between bacterial species (549).

In *Listeria monocytogenes,* Fri (a Dps-like protein) gene deletion strains are more susceptible to hydrogen peroxide and iron starvation and are defective in replication in macrophage and murine infection (550). Similar trends were seen in *Actinobacillus pleuropneumoniae* and the Dps-like protein FtpA (551), and hydrogen peroxide resistance in *Staphylococcus aureus* (552).

These studies suggest that Bd2620/Dps may be important in macrophage survival.

In our studies, Bd2620 is expressed throughout intramacrophage survival, in line with transcriptional studies. Dps protects DNA from oxidative damage due to oxidative stress or nutrient starvation, both of which will be present within the macrophage phagosome. Therefore, expression of Bd2620 throughout intramacrophage survival supports this role. This contrasts with *bd2620* expression throughout predation, where *bd2620* was downregulated throughout. Nutrients are abundant within the prey cell, whilst *Bdellovibrio* is undergoing large global changes in gene expression associated with intraperiplasmic growth, which requires the DNA to be accessible to translational apparatus. As *Bdellovibrio* is not actively growing within the macrophage phagosome, in contrast to bacterial pathogens, DNA does not need to be accessible for gene transcription, but is still susceptible to damage from oxidative species, making the function of Dps important. Deletion of Bd2620 did not impact intramacrophage survival. This may be due to bacterial killing occurring in a short timeframe (24 hours), before DNA damage can accumulate in the non-growing bacterium and have a detrimental effect. I therefore suggest that Bd2620 is involved in tolerating stress (oxidative or nutrient starvation associated) within the macrophage phagosome, but that this contribution is futile and does not ultimately prevent bacterial killing.

Longitudinal studies of Δ*bd2620 Bdellovibrio* and how its DNA accumulates mutations over time would be of great interest in the future, as there is no parallel scenario of a bacteria with a predatory lifecycle lacking Dps in the literature.

4.9.2.3.3. Concluding remarks: The importance of Bd2620/Dps in Predation and *Bdellovibrio* Occupation of Macrophage.

Dps transcription is initiated by the OxyR regulon (553), which also regulates the expression of various catalase and superoxide dismutase enzymes, therefore explaining its presence in the zebrafish transcriptional list originally, even if its function and importance in macrophage survival remains unclear. I suggest that Bd2620 is important for predator fitness, during predation, protecting the bacterial chromosome from oxidative and nutrient starvation associated stress. During intraperiplasmic growth in a nutrient rich prey cell environment, Dps is downregulated to allow transcriptional machinery to access the bacterial chromosome. As *Bdellovibrio* is not growing within the macrophage phagosome, but oxidative and nutrient starvation associated stresses are high, Dps is highly expressed and associates with the bacterial chromosome in this scenario.

4.9.2.4. The Role of Bd3203 in proposed tolerance to oxidative insult throughout predation and intramacrophage survival.

Bd3203 is a hypothetical protein of unknown/uncharacterised function, which I chose to study owing to it being highlighted as significantly transcriptionally upregulated by *Bdellovibrio* within zebrafish, where they are known to be engulfed by host leukocytes (1). As detailed in Section 4.3.1.3.6, Bd3203 contains a CBS (Cystathionine Beta Synthase) domain, which are known to be involved in the regulation of proteins and sensitivity to adenosyl carrying ligands (419, 473, 474).

4.9.2.4.1. Bd3203 contributes to predation of *E. coli* by *B. bacteriovorus*.

Bd3203 is associated with and in the same operon as Bd3200/MurD and Bd3201/MraY, a UDP-N-acetylmuramoylalanine-d-glutamate ligase involved in cell wall formation and a peptidoglycan biosynthesis protein respectively (STRING), suggesting that Bd3203 may regulate proteins involved in cell wall synthesis or modification, both of which are crucial throughout entry into, and intraperiplasmic growth of *Bdellovibrio* within prey. This suggests that Bd3203 is likely linked to predator growth or cell wall homeostasis rather than oxidative stress. Further work to characterise the interaction partners of Bd3203, via bacterial two hybrid studies, may help to assign a function and therefore a role for Bd3203 in predation. No homologues of Bd3203 were found in other bacteria, potentially suggesting a *Bdellovibrio* or predation-specific role for Bd3203.

Bd3203 is highly expressed in attack phase *Bdellovibrio* and throughout predation, suggesting it is involved in predation. Transcriptional studies show that *bd3203* gene expression is downregulated throughout predation. Bd3203 may play a role in regulating cell wall modification. During filament growth and intraperiplasmic growth, *Bdellovibrio* is actively growing and therefore extensive cell wall modification will be occurring, perhaps suggesting that Bd3203 is not required during this phase of predation. Deletion of *bd3203* delayed predation and reduced prey cell lysis. If Bd3203 has a regulatory function within predation, by the same logic as above, it is possible that deletion of *bd3203* leads to dysregulation of this function and cell damage, resulting in a fitness cost that may translate to a decrease in predation efficiency. As the role of Bd3203 is unknown these conclusions are purely speculative at this stage. Studies of the proteins that Bd3203 interacts with throughout predation, via bacterial 2 hybrid experiments, would be very informative.

4.9.2.4.2. Bd3203 does not significantly contribute to survival and viability in macrophage.

Bd3203 is expressed throughout intramacrophage survival, in line with transcriptional studies. As Bd3203 does not have an annotated function, it is difficult to speculate on its role within intramacrophage survival. Deletion of *bd3203* does not impact the survival of *Bdellovibrio* within macrophage, therefore its role is likely unimportant. Due to its association with other cell wall modifying enzymes, it likely plays a regulatory role within cell wall modification. As the cell wall of *Bdellovibrio* will be under attack from various molecular species whilst *Bdellovibrio* resides within the phagosome, it is likely that Bd3203 expression is an attempt to mitigate this. Ultimately, *Bdellovibrio* is killed so this represents a futile stress response to the bactericidal conditions present within the macrophage phagosome.

4.9.2.5. The Role of Bd1815 in proposed tolerance to oxidative insult throughout predation and intramacrophage survival.

Bd1815 is a hypothetical protein of unknown/uncharacterised function (UniProt), which I chose to study because it was highlighted as significantly transcriptionally upregulated by *Bdellovibrio* within zebrafish, where they are known to be engulfed by host leukocytes (1). Structural predictions, as outlined in Section 4.3.1.3.2, suggest that Bd1815 may function as an Outer Membrane Protein (OMP) or porin.

4.9.2.5.1. Bd1815 is not important in predation of *E. coli* by *B. bacteriovorus*.

Bd1815, to which I have ascribed an OMP-like function, is expressed throughout predation. Downregulation of *bd1815* throughout predation, despite visible (fluorescent) protein expression, except at 15 minutes and 5 hours, when *Bdellovibrio* is not inside a prey cell, suggests that this protein has a role in prey recognition or entry, or in attack phase cells, rather than throughout predation.

The same logic may also apply whereby nutrient uptake is required for intraperiplasmic growth, therefore *bd1815* gene expression is highest in attack phase to “stock” the attack phase cells with Bd1815, prior to intraperiplasmic growth. Deletion of *bd1815* did not impact predation, suggesting that, despite its expression throughout predation, its role is redundant and/or not important.

4.9.2.5.2. Bd1815 does not contribute to survival and viability in macrophage.

Bd1815 expression was seen throughout intramacrophage survival, in line with transcriptional studies. Deletion of Bd1815 did not impact *Bdellovibrio* survival within macrophage. As the role of Bd1815 is likely in nutrient uptake or growth, and *Bdellovibrio* is in a highly nutrient-restricted environment, this is feasible. As a bacterium that must efficiently uptake and re-purpose nutrients from the prey cell as part of its intraperiplasmic growth, there is likely to be a high amount of redundancy in the nutrient uptake response. Upregulation of *bd1815* throughout intramacrophage survival, and its presence within the upregulated gene dataset during zebrafish infection, likely represent a starvation response to nutrient restriction rather than playing any meaningful contribution to bacterial survival.

Bd1815 expression could represent an attempt to modify cell wall composition in response to a change in environment (and environmental stress), explaining why it is highly expressed (transcriptionally and at the protein level) in macrophage but does not contribute to macrophage survival.

4.9.2.6. The Roles of the Outer Membrane Protein Chaperone Bd0017/SurA in proposed tolerance to oxidative insult throughout predation and intramacrophage survival.

Bd0017/SurA is a survival associated chaperone protein, mostly studied in *E. coli* but also of demonstrable importance in *Yersinia pestis* (554)*, Y. pseudotuberculosis* (555)*, Pseudomonas aeruginosa* (556) *Shigella* flexneri (557), involved in regulating the correct folding of outer membrane proteins (UniProt). I chose to study Bd0017/SurA as it might well affect macrophage survival, as it does in *Yersinia pestis* (554)*, Y. pseudotuberculosis* (555)*, Pseudomonas aeruginosa* (556) *Shigella* flexneri (557), and because it was highly upregulated in an initial look at my transcriptional studies of *Bdellovibrio* gene expression inside macrophage.

4.9.2.6.1. Bd0017/SurA is essential for predation of *E. coli* by *B. bacteriovorus*.

Bd0017mCherry was expressed throughout predation, in attack phase cells and throughout attachment, invasion, establishment, intraperiplasmic growth and progeny release. As Bd0017 is a chaperone protein, related to correct protein folding within the cell, and the *Bdellovibrio* outer surface is undergoing extensive remodelling throughout predation, whilst also being attacked by reactive molecular species upon entry into the prey cell periplasm, it is highly likely that Bd0017 contributes to predation. Transcriptional studies indicate that *bd0017* expression was downregulated between 15 minutes and 1 hour. During this period, *Bdellovibrio* is attaching to and invading the prey cell, therefore various outer membrane fusion and modification events will be occurring, therefore transcriptional downregulation of *bd0017* expression during this period may reflect this dynamic outer surface remodelling. Bd0017 was essential for predator viability, suggesting that Bd0017 is indispensable for predation.

This suggests that SurA is important during the early stages of intraperiplasmic growth within the prey cell. This might be when the largest changes in outer membrane composition are occurring, or when the most exogenous species (that may damage or impact protein folding) are present within the prey cell periplasm. Alternatively, SurA may assist with the high levels of new transport protein expression and folding in the outer membrane, on the surface of *Bdellovibrio*, to take up the products of the hydrolytic enzymes secreted into prey cells by *Bdellovibrio*, to break down prey macromolecules and fuel intraperiplasmic growth.

The outer membrane and bacterial surface of *Bdellovibrio* is important throughout predation and for controlling how *Bdellovibrio* interacts with the wider environment. Initially, for interacting with the prey cell and initiating attachment, then for invasion into the prey cell periplasm, establishing itself in the prey cell periplasm and initiating intraperiplasmic growth, and finally the exit of *Bdellovibrio* progeny from the prey cell. Maintaining the correct bacterial surface, with the appropriate membrane content and fluidity, and adhesins throughout predation is crucial for successful and efficient predation and for bacterial survival under changing environmental stresses.

4.9.2.6.2. Bd0017/SurA may contribute to survival and viability in macrophage.

The importance of SurA in bacterial pathogens and infection. In *Yersinia pseudotuberculosis,* SurA is required for bacterial virulence, envelope integrity and adhesin/invasion expression and attachment to host cells (555). Similarly, ΔsurA mutants are avirulent in a murine *Y. pestis* infection model (554) and a *Pseudomonas aeruginosa Galleria mellonella* infection (556). *Salmonella* Typhimurium mutants are defective in attachment and invasion of eukaryotic cells of mice (558, 559). In *Shigella flexneri* infection, deletion of SurA abrogates cell-cell spread (557). In UPEC (Uropathogenic *E. coli*), adherence and invasion of bladder epithelial cells was decreased (560), with growth and survival within host cells decreased (561) due to Type I fimbriae biogenesis being defective (560).

Other studies show that SurA is of high importance for surface protein and virulence factor expression, contributing to bacterial establishment, survival, and infection. SurA may also regulate outer membrane composition and confer a survival advantage under changing environmental stresses. I hypothesised that SurA helps regulate this process, as it does in *Yersinia pestis* (554)*, Y. pseudotuberculosis (555), Pseudomonas aeruginosa* (556) *Shigella* flexneri (557) and other bacterial pathogens (558-561)in macrophage. This is the role that I suggest and wish to test for SurA in *Bdellovibrio* throughout predation and macrophage survival.

Bd0017 is important in attempting to control and regulate the outer membrane composition and maintain correct protein conformation in response to the oxidative species and damaging conditions present within the developing macrophage phagosome, as a last-ditch attempt for survival.

Bd0017 was expressed at 24 hours post-uptake in macrophage, in line with transcriptional data. The impact of *bd0017* gene deletion on *Bdellovibrio* survival within macrophage was not able to be tested. However, I would hypothesise that, as Bd0017 expression was evident at 24 hours post-uptake, when significant amounts of bacterial killing are occurring, and in-line with the roles of SurA in other bacterial pathogens, Bd0017 function would likely contribute to *Bdellovibrio* survival within macrophage.

4.9.3. Limitations

4.9.3.1. Fluorescent tagging

Quantification of protein expression in this study relied on fluorescent tagging and quantification of expression timings through microscopy. Fluorescent tagging of the proteins in this study may interfere with expression, folding or secretion, meaning that the fluorescent tag is then mutated or deleted under selection pressure, owing to the tag making the protein less functional. If the fluorescent tag interferes with protein folding and function, only the non-tagged, functional copy present within the *Bdellovibrio* genome would be functionally expressed, with the tagged version becoming promptly degraded.

The tagged gene construct (5'- flanking immediately upstream of the target gene, the gene itself, the fluorescent tag and the 3' flanking downstream of the target gene) were sequenced, upon assembly, to confirm that the fluorescent tag and gene were functional and intact, therefore any mutations impacting the function or expression of the gene or fluorescent tag will have occurred due to selective pressure since then.

I could test this by sequencing the *gene:mCherry* (or *gene:mCerulean*) constructs in *Bdellovibrio bacteriovorus* to confirm that the plasmid sequence is correct, before letting it undergo multiple rounds of predation and then re-sequencing the construct and seeing if any mutations had occurred. This would suggest that the fluorescent tag was under a high selective pressure to mutate and may explain a lack of visible fluorescent protein expression, with proteins that we predict to be highly expressed and important in predation or intramacrophage survival.

One example of this was that attachment of an mCherry tag to the C-terminus of Bd0799 consistently resulted in mutation of the gene whereas attachment of an mCherry tag to Bd0799 with a flexible peptide linker did not induce a frameshift mutation within the *bd0799* gene (Robert Till; Personal Communication), suggesting that the mCherry tag was sterically interfering with Bd0799 protein expression, folding or function and was therefore selected against in predatory cultures of *Bdellovibrio.*

4.9.3.2. Autofluorescence

The presence of, previously unknown, autofluorescence of prey cells and macrophage in mCerulean and mCherry channels made the interpretation of some microscopy data challenging, owing to any potential fluorescent protein expression being indiscernible from background autofluorescence in some instances. This predominantly affected diffusely or lowly expressed proteins, owing to the absence of a discrete, strong fluorescent signal. Whilst some of the proteins in this study were fluorescently tagged with multiple colours, helping me to determine whether the protein was expressed in macrophage or predation, and not visible, or not expressed, this was not possible for all of my protein candidates due to time limitations.

Bd0295 and Bd0798 were tagged with both mCerulean and mCherry tags, therefore I am confident that an absence of fluorescent protein expression is due to a lack of protein expression and not prey autofluorescence making fluorescent protein expression indiscernible. Alternatively, the fluorescent tag may have mutated under a selective pressure, owing to it interfering with protein expression, function or folding (as previously discussed).

Quantification of protein expression through Western blot analyses would be pursued in future (as documented in Section 4.6).

4.9.3.3. Z-stacks

Bdellovibrio cannot be seen within macrophage using phase contrast, making the imaging of *Bdellovibrio*-containing macrophage, with respect to focusing and getting sharp images, more difficult. It is important to remember that I was aiming to visualise an atypically small bacterium, that I could not see “live”, through the macrophage cell membrane and phagosomal membrane, of which the *Bdellovibrio* could be in any orientation, whilst visualising fluorescent protein expression. This has only been done once before, by Raghunathan and co-workers, where they used a Bd0064mCerulean tagged *Bdellovibrio* that emits a very bright fluorescent signal.

Further imaging of my fluorescently tagged strains would be useful, to make firm conclusions of protein expression. However, I have imaged large quantities of *Bdellovibrio*-containing macrophage and quantified the protein expression, making the best use of the resources I have. I would suggest that this assay, in its current format, is not optimised or suitable for further analysis of fluorescent protein expression, by *Bdellovibrio* within macrophage. Other approaches would need to be used to follow up on my findings.

The use of Z-stacking to visualise *Bdellovibrio* at set depths throughout the macrophage cell and to gain images of better focus was attempted. However, this was time-consuming and risked photo-bleaching my fluorescent tags owing to the long exposure times needed to visualise (yet undetermined) fluorescent protein expression. Attempts also did not yield any better quality of images and therefore this approach was not utilised further.

4.9.3.4. Essentiality for predation

As was suggested previously, there may be an overlap between the genes used by *Bdellovibrio* to combat oxidative stress generated by its own aerobic respiration, those encountered during predation and those encountered during intramacrophage survival.

A limitation of the approach I have used to identify these genes is that, if they are essential for *Bdellovibrio* viability, I cannot accurately test their essentiality or role in macrophage survival, as gene deletion mutants are not possible to generate. This was the case for *bd2517/ahpC, bd2518/ahpF* and *bd0017/surA.* This limits the conclusions that I can make from this study so is an important consideration.

4.9.4. Further work

Multiple oxidative stresses and cues are occurring simultaneously within the macrophage phagosome that will alter the oxidative stress response of *Bdellovibrio* and ultimately dictate its tolerance and survival. Another approach to testing the importance of these genes and oxidative stress tolerance mechanisms to isolate the individual roles of these genes, both in macrophage survival and in predation, would be to expose single gene deletion mutants to exogenously generated reactive oxygen species and peroxide species, and assess their survival to these individual mono-natured oxidative stresses.

To assess viability to peroxide-based radicals, I would firstly incubate my deletion mutants (Δ*bd0295*/*sodC*, Δ*bd1401*/*sodC*, Δ*bd0798*/*catA*, Δ*bd0799*/*ankB*, Δ*bd1154*/*katA*, Δ*bd1155*/*ankB*, Δ*bd0798*Δ*bd1154*, Δ*bd0799*Δ*bd1155* and Δ*bd2620*/*dps*) with high amounts of hydrogen peroxide and test their viability (through plating) over time. To assess viability to superoxides/ROS, I could use xanthine oxidase to generate superoxide, hydrogen peroxide and nitric oxide radicals within the cell, in each of my gene deletion mutants, as outlined in (562). It is difficult to generate superoxide molecules individually, without also generating other peroxide and nitric oxide radicals, owing to the high reactivity of oxide radicals.

I would expect to see a decrease in bacterial viability if the target protein was important in survival against peroxide radicals or superoxide radicals. This would implicate some of these genes in the response to oxidative stress and confirm or deny their importance in tolerance of peroxide-based or superoxide radicals.

However, Ransy and co-workers debate the relevance and limitations of using high amounts of hydrogen peroxide to induce oxidative/peroxide stress, suggesting that the concentrations required far exceed those physiologically relevant and present within aerobically respiring cells (563).

However, due to the high levels of functional redundancy, no single gene deletion may give this effect, subsequently requiring the deletion of different combinations of these proteins e.g. a double SodC mutant or a double Catalase, double SodC mutant, or the removal of further protein candidates e.g. Thioredoxins in combination with catalase genes.

Measurement of reactive oxygen species within *Bdellovibrio* throughout predation and in response to different external oxidative stressors would also be of great interest, to characterise the oxidative stresses that *Bdellovibrio* is exposed to/must tolerate during predation. Unfortunately, the majority of the probes commercially available are optimised for eukaryotic cells and so would not work to test our hypotheses (564).

4.9.5. Final remarks

A large subset of *Bdellovibrio* gene expression will not represent an active response to oxidative stress, but a generalised (non-specific) stress response to damaging or different environmental conditions, including changes in oxygen tension, nutrient availability, an increase in damaging oxidative species and an increased requirement for cell wall repair. Some of the genes highlighted above are highly expressed throughout *Bdellovibrio* occupation of macrophage but do not contribute to survival, or do not have a clear/characterised role/importance in macrophage survival. Other genes may be important in predation but have no discernible role in macrophage survival. I initially wished to assess whether possibly overlapping, or separate, oxidative stress tolerance mechanisms would be important for the entry into, and subsequent growth and exit of *B. bacteriovorus* from the periplasm of prey bacteria or would be important for accidentally prolonged survival of *Bdellovibrio* in macrophage, allowing for the temporary tolerance of phagosomal conditions. The survival of *Bdellovibrio* within a host, and its interactions with the host immune response are important when considering the efficacy of *Bdellovibrio* as a novel antimicrobial treatment.

Although these genes did not (solely) confer a survival advantage within macrophage, it is important to consider the original (preliminary) data that highlighted these gene candidates. *bd0295*, *bd0798*, *bd1815*, *bd2620* and *bd3203* were significantly upregulated at the transcriptional expression level when *Bdellovibrio* were inoculated into a zebrafish hindbrain, during which the host immune response was seen, suggesting that they were involved in adaptation or temporary survival within a host. Whilst some genes were expressed and potentially important in the survival of *Bdellovibrio* in macrophage and for the tolerance of oxidative stress, others were not. The latter subset may still contribute to oxidative stress tolerance within macrophage and/or predation, but their roles are functionally redundant with other proteins within the *Bdellovibrio* oxidative stress tolerance proteosome.

Bdellovibrio is under nutrient restriction and high levels of oxidative stress within the macrophage phagosome. From the data presented in Chapter 4, I surmise that Bd1401 contributes to the tolerance to superoxide stress within the phagosome. Bd2517 and Bd2518 likely contribute to the tolerance of peroxide stress within the phagosome. Dps_{Bd2620} and Bd3203 expression likely represents a stress response to intraphagosomal conditions, to protect the bacterial cell chromosome and surface. These responses are futile as bacterial killing still proceeds. This does however add further support to the hypothesis that some genes within the *Bdellovibrio* genome that aid with tolerance of oxidative stress during predation, may also confer a temporary survival benefit to *Bdellovibrio* within the macrophage phagosome, where it is able to survive for 24 hours before significant bacterial killing. I suggest that these genes are a small snapshot of a wider oxidative stress response that may benefit *Bdellovibrio* survival within macrophage, and that there are large amounts of functional redundancy within this response. The implications of this for the future potential use of *Bdellovibrio* as a novel antimicrobial therapy are that, in support of animal models that show the beneficial effects of *Bdellovibrio* on bacterial infection resolution, *Bdellovibrio* may be equipped to survive temporarily and act on pathogenic prey within this short window before significant bacterial killing occurs.

Bdellovibrio would not be present (or administered) within a host, without their being a bacterial pathogen also present. The next step in these studies would be to see how *Bdellovibrio* survival is impacted in the presence of pathogenic prey, where macrophage are likely to be more highly proinflammatory and activated by the immunogenic ligands of the bacterial pathogen cell. This adds another layer of complexity to this interaction, but it was important to obtain an initial understanding of the interactions between *Bdellovibrio* and macrophage first, before progressing our understanding further.

Chapter 5: Dual analysis of bacterial and eukaryotic gene transcription throughout *Bdellovibrio bacteriovorus* intramacrophage survival.

In this Chapter, I investigated the response of cultured U937 macrophage-like cells to *Bdellovibrio* uptake and occupation by interrogating a single run of Dual RNASeq data, which looks at host and bacterial transcription simultaneously, to identify genes and pathways of interest for further, follow-up, investigations (as in Raghunathan et al., 2019), including monitoring pathways with labelled cell strains.

By doing Dual RNASeq we also wanted to test whether it was possible to detect a *Bdellovibrio* transcriptional signal inside macrophages, bearing in mind that this might be very small and outweighed by a large eukaryotic transcriptional signal, and that *Bdellovibrio* are not pathogens, and are therefore not able to grow inside macrophages. The initial idea was that were we to detect significant *Bdellovibrio* expression we could follow up the essentiality of that by gene deletions. However as in Chapter 4 we also used our existing “in host zebrafish” transcriptional signal for such experiments. As will be seen below a significant macrophage signal, in response to *Bdellovibrio* was detected and, although follow up experimentation in the lab was not possible, I discuss the informatic data I gained from the RNASeq below.

I firstly categorise and investigate the responses of *Bdellovibrio* to residence within macrophage (Chapter 5a). I then characterise the response of host macrophage to *Bdellovibrio*, considering categories which I found to relate to innate immunity first, before expanding this to its implications for the adaptive immune response which is outside the boundaries of our experimental system (Chapter 5b).

Chapter 5a: Analysis of the transcriptional response of *Bdellovibrio* throughout macrophage occupation.

5.1. Rationale for Bacterial RNASeq Analysis

In Chapter 4, I characterised the roles and importance of a subset of proteins, mostly related to oxidative stress tolerance, on the temporary survival of, and tolerance to, macrophage occupation and phagosomal conditions. I also characterised the importance of these proteins in predation, drawing parallels between the oxidative stresses experienced by *Bdellovibrio* inside macrophage compared to those experienced when invading and growing within a Gram-negative prey cell. Whilst some candidates were important for oxidative stress tolerance in macrophage, prey or both, others were not and their functions redundant to and/or compensated for by other proteins within the *Bdellovibrio* proteosome.

In this chapter, I now ask what the wider transcriptional response of *Bdellovibrio* to macrophage occupation is. Subject to the caveats detailed previously, this is only a limited bacterial transcriptome. However, I still attempt an initial characterisation of the response of *Bdellovibrio* to macrophage occupancy.

5.2. Introduction to Bacterial RNASeq Analysis

5.2.1. Caveats surrounding bacterial RNASeq analysis.

It was initially hoped that DualSeq of both macrophage and *Bdellovibrio* transcripts might be possible, but we understood the number of *Bdellovibrio* within macrophages was small and that detection of sufficient transcripts to determine expression changes might be impossible. We have previously used transcriptomic data from *Bdellovibrio* injection into whole zebrafish were 5 x 10^4 *Bdellovibrio* per zebrafish larva were injected but, in these studies, only single numbers of *Bdellovibrio* per macrophage were engulfed. From studies performed by Raghunathan and co-workers (which we followed the exact same methodology for *Bdellovibrio* uptake by macrophage), they saw an average of 15 *Bdellovibrio* per macrophage cell at 2 hours post-uptake, and 10 *Bdellovibrio* per macrophage cell at 24 hours post-uptake, although this was highly variable (2).

FIOS genomics were unable to analyse the bacterial component of the response due to the presence of an inadequate amount of bacterial RNA. This meant that the bacterial reads present only mapped to a small number of *B. bacteriovorus* genes (216 transcripts out of the possible 3,546 transcripts in the HD100 genome), and at low counts (mostly count = 1). Bacterial RNA also failed their 6 quality control tests and was not included in any functional analysis.

This was likely due to the low bacterial titre used (10^7 plaque forming units per sample, giving a multiplicity of infection of 1:50 (macrophage:bacteria)). Raghunathan and co-workers saw approximately 15 *Bdellovibrio* per macrophage cell at 2 hours post-uptake, and 10 *Bdellovibrio* per macrophage cell at 24 hours post-uptake (2), whereas I see, from measuring the viability of *Bdellovibrio* engulfed by macrophage, that of the 10^7 PFU added to each sample, only approximately 2x 10^5 PFU are engulfed by macrophage at 2 hours post-uptake, and I know from microscopy studies that not all macrophage contain *Bdellovibrio* at 2 hours post-uptake.

The amount of bacterial RNA in the sample would have been significantly outweighed by the large quantity of eukaryotic RNA present. Another explanation is that the RNA extraction protocol was optimised for the extraction of eukaryotic RNA. However, extensive research was performed to devise the optimal procedure for isolating both bacterial and eukaryotic RNA, with great success in other studies using the same approach (565-567). A larger bacterial titre was used in these studies. The bacterial titre used in this study was beyond my control as the samples were previously generated. However, increasing the bacterial titre would have made comparisons to other collected data inappropriate and therefore alteration of the bacterial titre would not have solved this problem. Also, the bacteria used in these studies were pathogens so the uptake efficiency of these bacteria compared with *Bdellovibrio* may vary.

However, to try and get any insight into *Bdellovibrio* gene expression, I carried out a manual input of the fastq files (containing both eukaryotic and bacterial RNA reads) into the Rockhopper Bacterial RNASeq analysis pipeline (428-430), gave an analysis of bacterial gene expression. The number of reads mapped to the HD100 genome, and to known protein-coding genes, within each sample can be found in Supplementary Tables 2.5.3 and 2.5.4. Of the 4626 predicted RNAs, 951 were sense orientation. There were 1823 differentially expressed protein coding genes. This is further detailed below.

5.2.2. Comparison to other bacteria:host DualSeq studies

To assess the quality of our RNA-Seq experiment, compared to other Dual-Seq experiments involving intracellular bacteria, we needed to assess whether the percentage of reads belonging to the bacteria compared to eukaryotic genes was similar to other studies, and if the coverage and read depth were similar. In Damson et al.'s study, 11% of their reads mapped to *P. aeruginosa* compared to 64% of the reads mapping to the murine genome (567). In Pisu et al.'s study, between 0.3 and 2% of their reads mapped to the genome of *M. tuberculosis* across their samples (566). In our study, between 0.13 and 0.35% of our reads mapped to the *B. bacteriovorus* genome. Possibly explanations for the difference in reads mapping to the bacterial genome compared to the eukaryotic genome may be due to *P. aeruginosa* being an actively dividing and metabolically active pathogen in murine alveolar macrophages whereas *B. bacteriovorus* is not actively replicating within the macrophage and is significantly smaller so may be closer to the *M. tuberculosis* (a slowly dividing pathogen) end of the spectrum. We achieved a coverage of between 1.27 x and 3.46x across our samples. These data indicate that our approach has provided a sufficient quantity of RNA to study the differential gene expression occurring in both host and bacteria simultaneously.

As mentioned previously, my DualSeq study did not have sufficient depth, therefore my abundant analysis will be based on the host macrophage transcription. Despite this, I have attempted an analysis of the bacterial transcription profile throughout macrophage occupation, but this would require further work to investigate the trends and gene candidates outlined below before any firm conclusions could be drawn.

Subject to the caveats outlined above, the transcriptomic profile of *Bdellovibrio*, surviving within macrophage over a 24-hour period (until significant bacterial killing) was visualised using Rockhopper (428-430), a bacterial differential gene expression analysis pipeline. This gave a list of differentially expressed genes. I then applied a 2-fold cut-off and a q value (adjusted p value) of 0.05 to this list, to highlight genes that were differentially expressed between each timepoint. I then manually curated this list, looking for genes that belonged to certain biological or functional categories using UniProt (415) and KEGG (424, 425) for functional characterisation. I will explore these functional categories and any associations between the highlighted genes and current literature regarding bacterial infection and host survival below. These genes were not explored further due to time limitations, however I wanted to see if any trends emerged from these datasets. An initial follow up investigation before analysing these gene candidates fully would be to quantify the amount of transcript by qtPCR, throughout *Bdellovibrio* occupation of macrophage, to confirm that they are of interest, given the partial nature of the *Bdellovibrio* transcriptome in this instance.

To put my (preliminary) findings into context, I have shown the data from Raghunathan et al., 2019 and my own studies that show the viability of *Bdellovibrio* at each of the timepoints used for the RNASeq analysis (Figure 5.2.1).

a) Data taken from Raghunathan et al., 2018 b) Data from my study

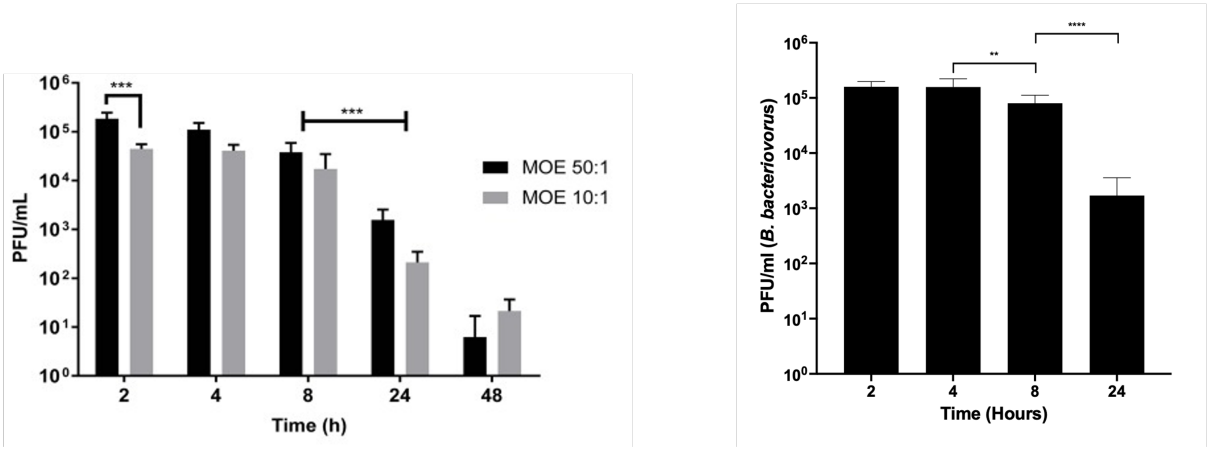

Figure 5.2.1: Viability of *B. bacteriovorus* inside PMA-differentiated U937 cells. *B. bacteriovorus* HD100 were exposed to PMA-differentiated U937 cells for two hours at an MOI (Multiplicity of Infection) of 1:50 (U937: *Bdellovibrio*). U937 cells were then lysed at 2, 4, 8, 24 (a & b) and 48 (a) hours after initial exposure, to enumerate the remaining, live *Bdellovibrio.* Error bars indicate the Standard Deviation of the dataset. a) **Graph taken from Raghunathan et al., 2019**. Data shown represents the mean value of 2 independent experiments, each set up in duplicate, with plaque counts enumerated for two technical replicates also. *** corresponds to P=0.0002, using a Mann-Whitney test. b) Data shown represents the mean value of 6 independent experiments, with plaque counts enumerated for two technical replicates also. ** corresponds to P<0.01; **** corresponds to P<0.0001, using a Mann-Whitney test.

5.3. Functional characterisation of bacterial gene expression

5.3.1. Oxidative stress tolerance

To determine whether *Bdellovibrio* expresses any further genes related to oxidative stress tolerance, whilst residing within macrophage, I curated my list of differentially expressed genes for genes related to oxidative stress tolerance (Table 5.2.1). The expression values (raw reads and Log_2 fold change) for each of these genes has been represented for each timepoint below (Figure 5.2.2). Several oxidative stress related genes, linked to the survival of various bacterial pathogens in host infection, were highly expressed throughout *Bdellovibrio* occupation of macrophage, especially at 24-hours post-uptake. This suggests that *Bdellovibrio* was experiencing high levels of oxidative stress throughout its occupation of macrophage, in line with what is known about phagosomal maturation and bacterial uptake within the host, and that these oxidative stresses were most significant at 24 hours, when significant bacterial killing occurs.

I also looked at the transcriptional expression of these (proposed) oxidative stress related genes throughout predation of *E. coli* by *B. bacteriovorus*. The Log_2 fold change of these genes, compared to attack phase expression is represented for each timepoint below (Figure 5.2.2). Whilst some genes (*bd0177*, *bd0298* and *bd0456*) were upregulated throughout predation, or at the beginning (*bd1002*) or end (*bd1425*) of predation, most genes were downregulated throughout predation, compared to attack phase expression. Of particular interest is *bd1002* which controls and activates the SoxS superoxide response regulon, as it was upregulated upon invasion and establishment in the periplasm (30 and 45 minutes), at the beginning of intraperiplasmic growth (1 and 2 hours), and after progeny release (5 hours), compared to attack phase expression. This suggests that *Bdellovibrio* is experiencing oxidative stress at each of these key points of predation.

Table 5.2.1: Oxidative stress tolerance related genes expressed by *Bdellovibrio* inside macrophage.

Gene	Synonym	Function/Associations
bd0177	peptidyl-prolyl cis-trans isomerase	Antimicrobial protein resistance; Chaperone protein; host survival; oxidative stress and pH resistance (568)
bd0298	stress-induced protein OsmC	Oxidative stress defence protein OsmC protects against organic peroxide stress in *M. tuberculosis (569)* and *E. coli (570)*
bd0456	lactoylglutathione lyase	Oxidative stress protection of *Salmonella* Typhimurium in nutrient rich environments (571) Tolerance of acidic pH in *Streptococcus mutans (572)*
bd0909	Putative redox protein; OsmC Homologous to OsmC	Oxidative stress defence protein OsmC protects against organic peroxide stress in *M. tuberculosis (569)* and *E. coli (570)*
bd0945	electron transfer flavoprotein-ubiquinone oxidoreductase	Inner mitochondrial membrane respiratory chain; fatty acid and amino acid oxidation (573)
bd1002	redox-sensing activator of soxS	Controls the superoxide response regulon. Resistance to Nitric Oxide dependent macrophage killing of *E. coli.* Not required for resistance to macrophage killing or virulence of *Salmonella* Typhimurium in mice (574) but important for oxidative stress tolerance (575)
bd1401	superoxide dismutase	Contributes to intracellular survival of *Burkholderia cenopacia* in macrophage (483) and of *Salmonella* serovars in phagocytes (494)
bd1425 *bd1451*	MarR family transcriptional regulator	Activation of both antibiotic resistance and oxidative stress resistance genes (576)
bd1805	bacterioferritin comigratory protein	Peroxiredoxin/ detoxification of hydrogen peroxide (577); oxidative stress response (578)
bd2071	TetR family transcriptional regulator	Multidrug resistance; Oxidative stress resistance (579)
bd2113	organic solvent tolerance protein	Multidrug resistance; Stress tolerance in *Yersinia pestis* (580)
bd2153	universal stress protein	Oxidative and acid stress tolerance in *Listeria monocytogenes* (581)
bd2788	peptide methionine sulfoxide reductase (msrA)	Reverses oxidative damage (582) and aids survival of *M. tuberculosis* in macrophage (583)
bd3076	transport protein (terC)	Oxidative stress tolerance; Tellurite resistance; redox modulator induced by alkaline conditions (KEGG)
bd3432	response regulator of hydrogenase 3 activity (hydG)	High Zinc tolerance; Zinc transport two-component system (584); Linked to nutrient starvation and global regulator required for intracellular replication of *Legionella pneumophila* in macrophage (585)

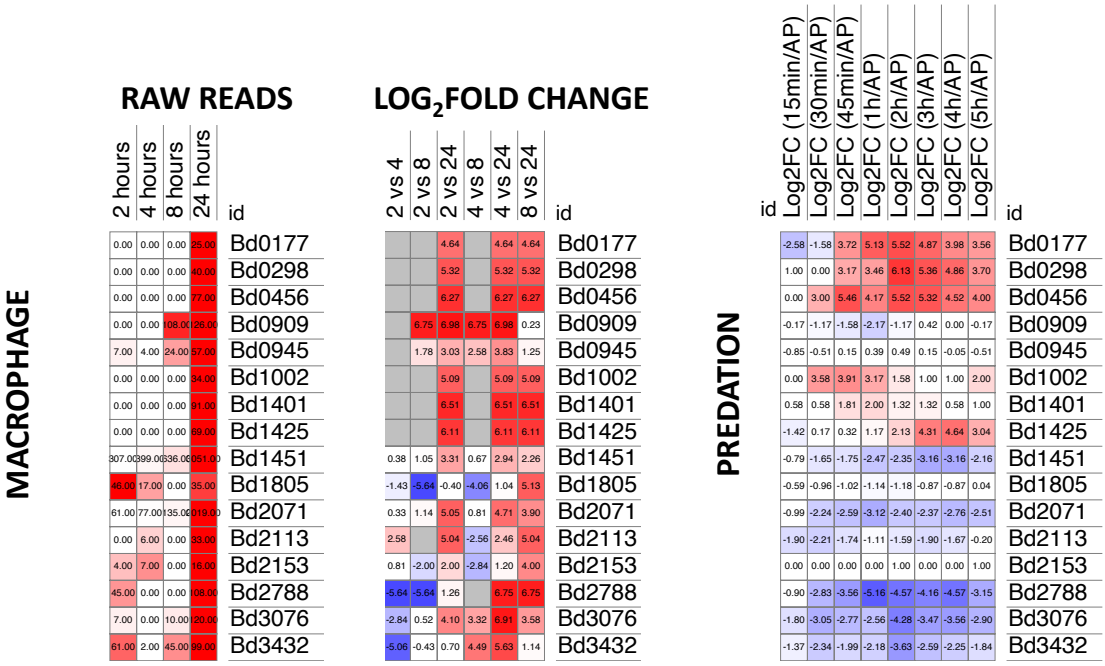

Figure 5.2.2: Genes related to oxidative stress were upregulated at 24 hours of *Bdellovibrio* occupation of macrophage but were not all upregulated throughout predation. A (limited) bacterial transcriptome from *Bdellovibrio* occupying macrophage over a 24-hour period was curated for significantly upregulated and downregulated (2x Cut off; q<0.05) genes related to the oxidative stress response. The majority of gene expression, relating to oxidative stress tolerance, was seen at 24 hours post-uptake (A). The bacterial transcriptome of *B. bacteriovorus* throughout predation of *E. coli* was interrogated for the selected genes, proposed to be involved in the oxidative stress response. Whilst some genes were upregulated throughout predation, the majority of the selected genes were downregulated throughout predation (B). Heatmaps were generated using Morpheus.

5.3.2. Host associated gene expression.

To determine whether *Bdellovibrio* expresses any genes that have been previously associated with persisting within a host (mostly by bacterial pathogens), I curated my list of differentially expressed genes for genes that had previously been documented to be differentially expressed during host infection, in literature regarding other bacterial pathogens (Table 5.2.2). The expression values (raw reads and Log_2 fold change) for each of these genes has been represented for each timepoint below (Figure 5.2.3). Several of these genes are associated (in other bacteria) with regulating virulence factor expression and modifying outer membrane composition in response to environmental and oxidative stresses. There was no significant trend within this subset of genes, with respect to the timepoints that gene expression was most highly upregulated, with individual gene expression varying widely throughout *Bdellovibrio* occupation. Some of these genes may contribute to the temporary survival of *Bdellovibrio* inside macrophage and require further investigation.

I also looked at the transcriptional expression of these (proposed) host infection associated genes throughout predation of *E. coli* by *B. bacteriovorus*. The Log_2 fold change of these genes, compared to attack phase expression is represented for each timepoint below (Figure 5.2.3). The majority of these genes were not differentially expressed throughout predation.

Table 5.2.2: Genes associated with host infection, expressed by *Bdellovibrio* inside macrophage.

Gene	Synonym	Function/Associations
bd0017	survival protein SurA precursor	Chaperone/Aids folding of Bd0018 Trafficking of outer membrane proteins and adhesins in *Yersinia pestis,* reducing attachment to eukaryotic cells and invasion (555) Chaperone to outer membrane proteins (586) Aids virulence of *Pseudomonas aeruginosa* in a *Galleria mellonella* infection model (556) Essential in murine infection, and for growth and survival at low pH in *Yersinia pestis* (554)
bd0586	isoprenoid biosynthesis protein with amidotransfera se-like domain	Glycoxylase/Hydrolase (587)
bd0665	choloylglycine hydrolase	Decreases host bile salt toxicity, affects OMP composition and bacterial internalisation in *Brucella abortus* (588)
bd0819	fusaric acid resistance protein	Fusaric acid tolerance (589)
bd0880	periplasmic protein cpxP	Envelope stress response; virulence of UPEC in murine bladder and zebrafish model; increased sensitivity to complement mediated killing (590) Negative regulator of OmpF expression and virulence in *Citrobacter rodentium* (591) Inhibits CpxA and controls pili location and kidney cell invasion in UPEC (592) Switched on by envelope stress in *Salmonella* Typhimurium to regulate Cpx operon and virulence (593) Envelope stresss under alkaline conditions in *E. coli* (594)
bd1759	two-component response regulator KdpE	Associated with EHEC (595) Potassium transport: involved in virulence and intracellular survival of *Staphylococcus aureus, Escherichia coli, Salmonella* Typhimurium*, Yersinia pestis* and *Francisella spp.* by regulating the expression of virulence associated loci (596)
bd3394	two component response regulator	ragA Outer membrane component; link to virulence in *Porphyromonas gingivalis* (597)
bd3415	serine protease	Homologous to dotA of *Legionella pneumophila;* linked to bacterial replication (598)
bd3456	ferrochelatase	Virulence and intracellular survival in *Brucella abortus* (547); nutrient acquisition; haem synthesis and iron acquisition (599)
bd3591	ABC-type transport	Virulence and lipid transport to induce immune response in *Mycobacterium tuberculosis* (600)
bd3885	methanol dehydrogenas e regulatory protein (MoxR)	Pathogen survival in equine macrophages (601) Oxidative stress resistance during infection in *Francisella tularensis* (602)

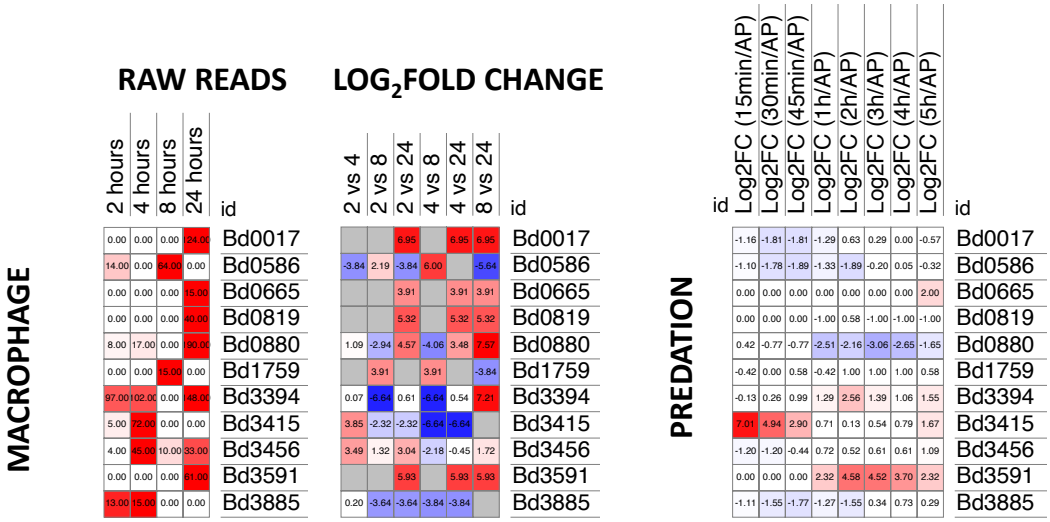

Figure 5.2.3: Genes related to host infection were upregulated throughout *Bdellovibrio* occupation of macrophage, with some also differentially expressed throughout predation. A (limited) bacterial transcriptome from *Bdellovibrio* occupying macrophage over a 24-hour period was curated for significantly upregulated and downregulated (2x Cut off; q<0.05) genes related to the host infection in other bacteria. The expression of individual genes varied throughout *Bdellovibrio* occupation of macrophage, with no significant trends. The bacterial transcriptome of *B. bacteriovorus* throughout predation of *E. coli* was interrogated for the selected genes, proposed to be related to host infection in other bacteria. Whilst some genes were upregulated or downregulated throughout predation, the majority of the selected genes were not differentially expressed throughout predation. Heatmaps were generated using Morpheus.

5.3.3. Nitrogen metabolism

Uptake of *Bdellovibrio* inside a macrophage represents a significant shift in oxygen tension, therefore, alternative anaerobic forms of respiration may dominate in this hypoxic environment, to continue ATP generation and fuel protein production and cellular metabolism. To determine whether *Bdellovibrio* expresses any genes that are associated with alternative forms of respiration and ATP generation, I curated my list of differentially expressed genes for genes that are functionally associated with nitrogen metabolism and anaerobic respiration (Table 5.2.3). The expression values (raw reads and Log_2 fold change) for each of these genes has been represented for each timepoint below (Figure 5.2.4). Most genes that are associated with anaerobic respiration and nitrogen metabolism were highly expressed at 24 hours post-uptake of *Bdellovibrio* occupation of macrophage. This suggests that *Bdellovibrio* was resorting to alternative sources of ATP generation, due to the hypoxic environment within the macrophage phagosome, at 24 hours post-uptake. This anaerobic respiration will provide ATP for protein synthesis, fuelling the stress response of *Bdellovibrio* inside the macrophage phagosome.

I also looked at the transcriptional expression of these (proposed) anaerobic respiration or nitrogen metabolism related genes throughout predation of *E. coli* by *B. bacteriovorus*. The Log_2 fold change of these genes, compared to attack phase expression is represented for each timepoint below (Figure 5.2.4). Whilst some genes were upregulated (*bd0021*, *bd0022* and *bd1955*), or downregulated (*bd2567* and *bd2591*) throughout predation, most genes were not differentially expressed throughout predation, compared to attack phase expression.

Table 5.2.3: Genes related to anaerobic respiration and nitrogen metabolism, expressed by *Bdellovibrio* inside macrophage.

Gene	Synonym	Function/Associations
bd0021	electron transfer flavoprotein subunit alpha	Electron transfer; Mitochondrial fatty acid beta oxidation; Metabolism; Growth on complex or simple carbon substrates; nitrogen fixation; essential for viability in *Burkholderia cenocepacia* in *C. elegans* infection (603) and causes rod to sphere change in morphology independent of MreB (604)
bd0022	electron transfer flavoprotein beta-subunit	Electron transfer; Mitochondrial fatty acid beta oxidation; Metabolism; Growth on complex or simple carbon substrates; nitrogen fixation; mutant led to increased ROS accumulation (605)
bd1955	protein-P-II uridylyltransferase	Nitrogen starvation (606, 607)
bd2567	pseudoazurin	denitrification; cytochrome c; electron donor; copper; nitric oxide reductase (608, 609) Denitrification may regulate virulence of *Brucella abortus* (609)
bd2591	transcription regulator	anaerobic tolerance; anaerobic regulatory protein (KEGG)
bd2592	pyruvate formate-lyase activating enzyme	
bd2593	anaerobic ribonucleoside triphosphate reductase	Metal ion binding (Uniprot); anaerobic oxidoreductase (KEGG) nucleotide metabolism; anaerobic tolerance
bd2597	norD protein	
bd2598	nitric oxide reductase NorQ protein	
bd2599	nitric-oxide reductase subunit B (norB)	Nitric oxide reductase; nitrogen metabolism (KEGG) Essential for survival and replication of *Brucella suis* in murine infection (610) Upregulated in abcesses and under iron-restriction, conferring enhanced fitness and virulence in *Staphylococcus aureus* murine infection (611)
bd2601	nitric oxide reductase, cytochrome c-containing subunit (norC)	Reduces Nitric Oxide toxicity during denitrification and pathogenesis in *Ralstonia solanacearum* (612)

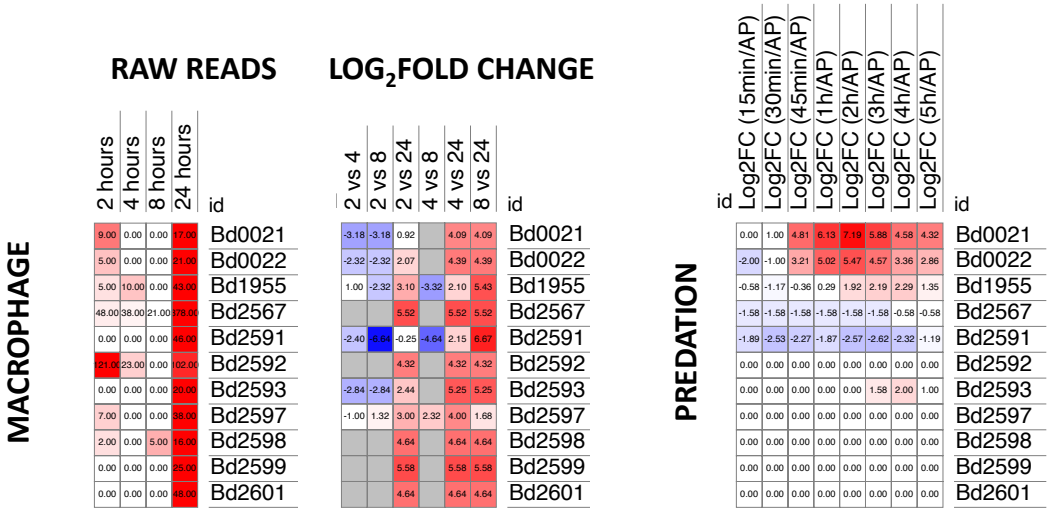

Figure 5.2.4: Genes related to anaerobic respiration and nitrogen metabolism were upregulated at 24 hours of *Bdellovibrio* occupation of macrophage. A (limited) bacterial transcriptome from *Bdellovibrio* occupying macrophage over a 24-hour period was curated for significantly upregulated and downregulated (2x Cut off; q<0.05) genes related to anaerobic respiration and nitrogen metabolism. The expression of genes varied related to anaerobic respiration and nitrogen metabolism were most highly upregulated at 24 hours of *Bdellovibrio* occupation of macrophage. The bacterial transcriptome of *B. bacteriovorus* throughout predation of *E. coli* was interrogated for the selected genes, proposed to be involved in the anaerobic respiration and nitrogen metabolism. Whilst a minority of genes were upregulated or downregulated throughout predation, the majority of the selected genes were not differentially expressed throughout predation. Heatmaps were generated using Morpheus.

5.3.4. Multidrug tolerance

Whilst inside the phagosome, *Bdellovibrio* is exposed to an arsenal of antimicrobial and bactericidal proteins and small molecules. Whilst some of these molecules may resemble antimicrobial agents typically used to treat bacterial infection, or may attack the bacterium via a similar mechanism e.g. host antimicrobial peptides attack the bacterial membrane via a similar mechanism to polymyxin antibiotics, from a cell perspective, the same cues that signal damage due to antimicrobial agents are also seen when the bacterial cell is targeted by host antimicrobial peptides and reactive oxygen species e.g. cell wall damage, lipid membrane damage, DNA mutation. Due to this, signalling pathways and gene expression patterns associated with multidrug resistance, also represent a response to bactericidal conditions present within the phagosome.

To analyse the response of *Bdellovibrio* to the bactericidal conditions within the phagosome, I curated my list of differentially expressed genes for genes that are associated with multidrug resistance/tolerance (Table 5.2.4). The expression values (raw reads and Log_2 fold change) for each of these genes has been represented for each timepoint below (Figure 5.2.5). Most genes that are associated with multidrug tolerance were highly expressed at 24 hours post-uptake of *Bdellovibrio* occupation of macrophage. This suggests that the majority of antimicrobial effectors targeting and stressing *Bdellovibrio* were abundant at 24 hours post-uptake, correlating with the significant amounts of bacterial killing seen at this timepoint.

I also looked at the transcriptional expression of these (proposed) multidrug resistance related genes throughout predation of *E. coli* by *B. bacteriovorus*. The Log_2 fold change of these genes, compared to attack phase expression is represented for each timepoint below (Figure 5.2.5).

A significant proportion of these genes were upregulated throughout predation, compared to attack phase expression. As the majority of multidrug tolerance mechanisms are focused on the bacterial surface or cell wall modification, and *Bdellovibrio* is undergoing extensive modification of its cell surface throughout intraperiplasmic growth and predation, whilst also being exposed to various harmful agents whilst occupying the prey periplasm, this may explain why a large number of multidrug tolerance related genes were upregulated throughout predation.

Table 5.2.4: Genes related to multidrug tolerance, expressed by *Bdellovibrio* inside macrophage.

Gene	Synonym	Function/Associations
bd0333	ampG protein	Beta lactam resistance; Cell wall recycling (613)
bd0360	peptide ABC transporter permease	microcin C transport system permease protein (KEGG) Operon is related to protection against acidic stress and antimicrobial peptides; Invasion, virulence, and replication of *Brucella melitensis* in mice infection (614)
bd0395	Bcr/CflA subfamily drug resistance transporter	Associated with biofilm formation in *Proteus mirabilis* (615) multidrug resistance transporter ((616); InterPro)
bd0657	tetracycline-efflux transporter	Tetracycline efflux (KEGG)
bd0707	FusA/NodT family protein	Beta lactam resistance; Cationic Antimicrobial Peptide resistance; Outer membrane protein (KEGG)
bd0708	macrolide-specific efflux protein	macrolide export protein; multidrug resistance (KEGG)
bd0797	polyketide synthase	Antibiotic biosynthesis (KEGG)
bd0888	acriflavin resistance protein	Multidrug resistance transporter; same pump in *Salmonella* Typhimurium for resistance to oxidative stress and macrophage killing (617)
bd0980	divalent cation tolerance protein	Ion tolerance (InterPro)
bd0982	dienelactone hydrolase	Chlorocatechol degradation (618)
bd1111	peptide ABC transporter ATPase	Putative Antimicrobial Peptide transporter (KEGG)
bd1113	Iron-regulated protein frpA	Iron related cytotoxin associated with pathogenesis of *Neisseria meningitidis* (619)
bd1145	acriflavin resistance protein	Multidrug resistance transporter; same pump in *Salmonella* Typhimurium for resistance to oxidative stress and macrophage killing (617)
bd1577	multidrug resistance protein	Multidrug resistance (KEGG)
bd1746	erythromycin esterase	Multidrug resistance; macrolide resistance (KEGG)
bd1751	NolG efflux transporter	Multidrug resistance; heavy metal resistance; membrane transporter (KEGG)
bd1765	organic solvent tolerance protein	Multidrug resistance; Stress tolerance in *Yersinia pestis* (580)
bd1798	NolG efflux transporter	Multidrug resistance; heavy metal resistance; membrane transporter (KEGG)
bd1972	ABC-type dipeptide/oligopeptide/ nickel transport systems	Beta lactam resistance (KEGG)
bd2034	isopenicillin N epimerase	Amino acid degradation; penicillin and cephalasporin synthesis (KEGG)
bd2036	beta-lactamase exonuclease	beta lactamase; Multidrug resistance (KEGG)
bd2170	hemolysins	Putative hemolysin; Magnesium and Cobalt exporter (KEGG)
bd2190	oligopeptide ABC transporter ATP-binding protein	Peptide/Nickel transport (KEGG)

bd2228	HAS ABC exporter outer membrane component	Metalloprotease secretion in *Serratia marcescens* (620)
bd2342	mate efflux family protein	Multidrug resistance (KEGG)
bd2357	dedA protein	Colistin resistance and Lipid A modification (621) so may confer Antimicrobial Peptide resistance also
bd2575	2-component transcriptional regulator	Copper resistance; ompR porin repression; Phosphate regulon response regulator (KEGG)
bd2709	oligopeptide transport system permease	oligopeptide transport; nickel transport; beta lactamase resistance (KEGG)
bd2710	oligopeptide ABC transporter permease	
bd3057	MarR family transcriptional regulator	Multiple antibiotic resistance protein regulator (KEGG)
bd3060	transcriptional regulator	TetR/AcrR family transcriptional regulator, Regulator of cefoperazone and chloramphenicol sensitivity (KEGG)
bd3063	transcriptional regulator	Unknown
bd3212	beta-lactamase	Beta lactam resistance; Multidrug resistance (KEGG)
bd3549	rhodanese-related sulfurtransferase	Anti-oxidative stress (622)
bd3804	ABC-type organic solvent resistance transport system, permease	Phospholipid/Cholesterol transport permease protein (KEGG)
bd3805		
bd3806	ABC-type organic solvent resistance transport system ATP-binding protein	

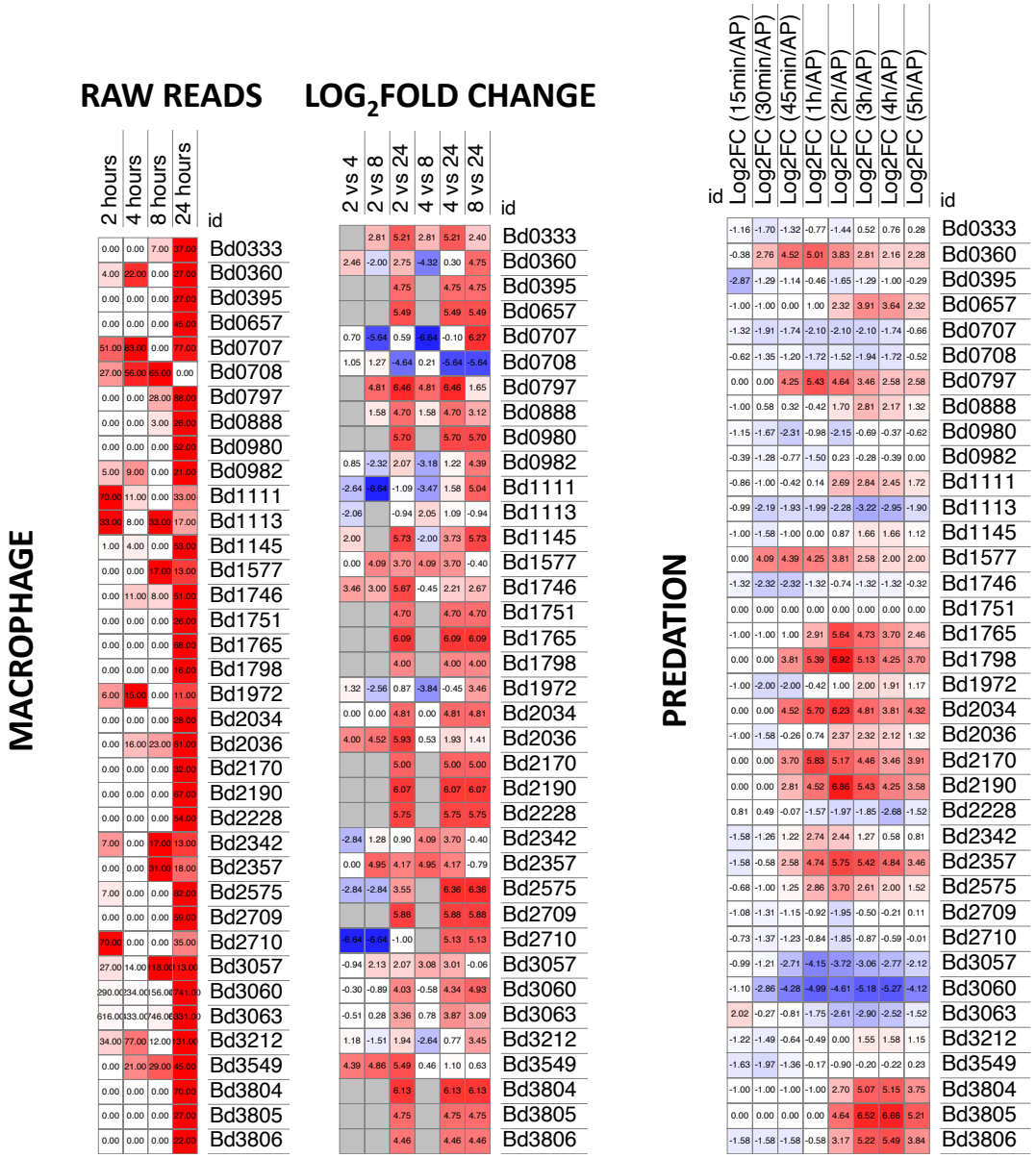

Figure 5.2.5: Genes related to multidrug tolerance were upregulated at 24 hours of *Bdellovibrio* occupation of macrophage. A (limited) bacterial transcriptome from *Bdellovibrio* occupying macrophage over a 24-hour period was curated for significantly upregulated and downregulated (2x Cut off; q<0.05) genes related to multidrug tolerance. The expression of genes varied related to multidrug tolerance were most highly upregulated at 24 hours of *Bdellovibrio* occupation of macrophage. The bacterial transcriptome of *B. bacteriovorus* throughout predation of *E. coli* was interrogated for the selected genes, proposed to be involved in multidrug tolerance. Interestingly, a significant proportion of genes were upregulated or downregulated throughout predation. Heatmaps were generated using Morpheus.

5.3.5. Nutrient starvation

Nutrients are highly restricted in the phagosome, limiting bacterial growth and preventing dissemination of bacterial infection. *Bdellovibrio* undergoes periods of nutrient starvation within its predatory lifecycle, between subsequent invasion of Gram-negative prey cells, therefore it is likely to have mechanisms associated with tolerance to nutrient starvation. To determine whether *Bdellovibrio* expresses any genes that are associated with nutrient starvation, I curated my list of differentially expressed genes for genes that are functionally associated with nutrient starvation (Table 5.2.5). The expression values (raw reads and Log_2 fold change) for each of these genes has been represented for each timepoint below (Figure 5.2.6). Most genes that are associated with nutrient starvation were highly expressed at 24 hours post-uptake of *Bdellovibrio* occupation of macrophage, although some are also highly expressed earlier on in *Bdellovibrio* occupation. This fits with the highly nutrient-restricted conditions associated with the mature phagosome and is in line with the idea that *Bdellovibrio* will undergo large changes in gene expression in an attempt to combat the bactericidal conditions in the phagosome, therefore expending large amounts of ATP and other nutrients through its upregulated protein synthesis.

I also looked at the transcriptional expression of these (proposed) nutrient starvation related genes throughout predation of *E. coli* by *B. bacteriovorus*. The Log_2 fold change of these genes, compared to attack phase expression is represented for each timepoint below (Figure 5.2.6). A subset of these genes were upregulated throughout predation. This may suggest that *Bdellovibrio* is experiencing nutrient starvation throughout predation.

Table 5.2.5: Genes related to nutrient starvation, expressed by *Bdellovibrio* inside macrophage.

Gene	Synonym	Function/Associations
bd1236	DNA-binding stress protein	Starvation-inducible chaperone protein (KEGG)
bd1454	pyoverdine biosynthesis protein PvcA	Iron acquisition; Link to host cell autophagy; Nutrient starvation and acquisition (623)
bd1455	pyoverdine biosynthesis protein PvcB	
bd2145	sulfur deprivation response regulator	Nutrient starvation (KEGG)
bd2648	outer membrane iron(III) dicitrate receptor	Nutrient starvation; iron transporter (KEGG)
bd2860	siderophore-mediated iron transport protein	Nutrient starvation; iron acquisition; membrane transport (KEGG)
bd3153	phosphoenolpyruvate synthase	Gluconeogenesis; starvation response; global signalling; Rifampicin phosphotransferase (KEGG)
bd3372	ABC-type zinc and manganese transporter ATPase component	Nutrient starvation; iron acquisition; membrane transport (KEGG)
bd3373		

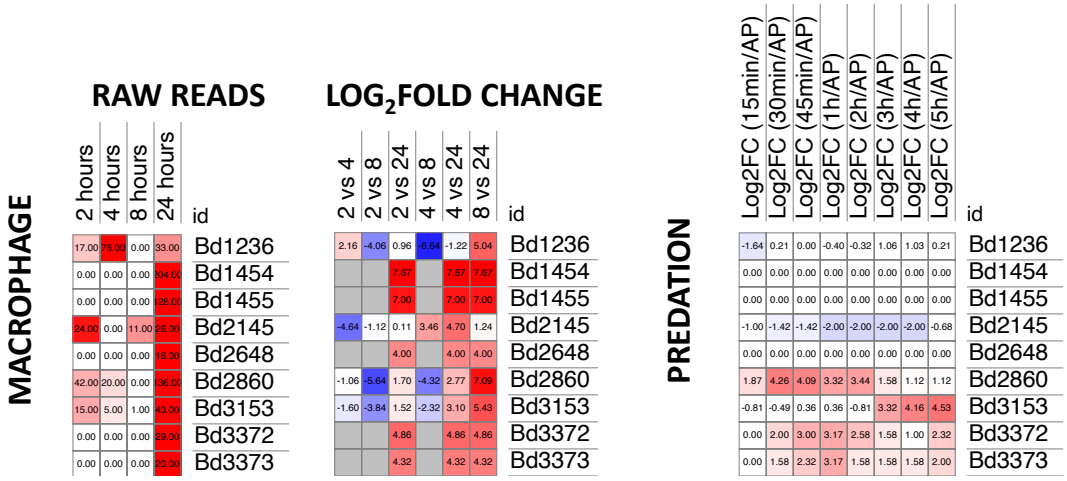

Figure 5.2.6: Genes related to nutrient starvation were mostly upregulated at 24 hours of *Bdellovibrio* occupation of macrophage, with some also upregulated throughout predation. A (limited) bacterial transcriptome from *Bdellovibrio* occupying macrophage over a 24-hour period was curated for significantly upregulated and downregulated (2x Cut off; q<0.05) genes related to nutrient starvation. The expression of genes varied related to nutrient starvation were most highly upregulated at 24 hours of *Bdellovibrio* occupation of macrophage. The bacterial transcriptome of *B. bacteriovorus* throughout predation of *E. coli* was interrogated for the selected genes, proposed to be involved in nutrient starvation. A subset of these genes were upregulated throughout predation. Heatmaps were generated using Morpheus.

5.3.6. Peptidoglycan and Outer membrane synthesis

The bacterial surface represents the first interface between the bacterial cell and the host. It is also the first barrier to host bactericidal mechanisms/effector proteins, suggesting it may be altered or repaired to avoid cell death (624). To determine whether *Bdellovibrio* expresses any genes that are associated with peptidoglycan or outer membrane lipid synthesis, I curated my list of differentially expressed genes for genes that are functionally associated with peptidoglycan or Lipid synthesis (Table 5.2.6). The expression values (raw reads and Log_2 fold change) for each of these genes has been represented for each timepoint below (Figure 5.2.7).

Most genes that are associated with Peptidoglycan and Lipid synthesis were highly expressed at 24 hours post-uptake of *Bdellovibrio* occupation of macrophage, although some are also highly expressed earlier on in *Bdellovibrio* occupation. This fits with the majority of membrane and cell wall damaging agents being abundant in the mature phagosome, at 24 hours post-uptake, prompting membrane and cell wall repair.

I also looked at the transcriptional expression of these (proposed) Peptidoglycan and Lipid synthesis genes throughout predation of *E. coli* by *B. bacteriovorus*. The Log_2 fold change of these genes, compared to attack phase expression is represented for each timepoint below (Figure 5.2.7). As expected, the majority of these genes were upregulated towards the end of predation, compared to attack phase expression, when intraperiplasmic growth and release of *Bdellovibrio* progeny from the prey cell was occurring. In attack phase, *Bdellovibrio* are not growing therefore Peptidoglycan and Lipid synthesis gene expression would be low.

Table 5.2.6: Genes related to peptidoglycan and outer membrane lipid synthesis, expressed by *Bdellovibrio* inside macrophage.

Gene	Synonym	Function/Associations
bd0448	phospholipase D	cardiolipin lipid synthesis (KEGG)
bd0585	D-alanine-D-alanine ligase	D-alanine metabolism; peptidoglycan biosynthesis; vancomycin resistance (KEGG)
bd0664	lipase LipA	Represses autolysis in *Streptococcus pneumoniae* infection; hydrolyses/frees fatty acids off membrane (KEGG;(625))
bd1516	phospholipase D family protein	cardiolipin lipid synthesis (KEGG)
bd1870	glucose-1-phosphate thymidylyltransferase	polyketide/streptomycin/o-antigen synthesis (KEGG)
bd2389	cardiolipin synthetase	cardiolipin lipid metabolism (KEGG)
bd3201	phospho-N-acetylmuramoyl-pentapeptide-transferase	peptidoglycan synthesis and degradation; vancomycin resistance (KEGG)
bd3204	UDP-N-acetylmuramoylalanyl-D-glutamyl-2, 6-diaminopimelate--D-alanyl-D-alanine ligase	
bd3205	UDP-N-acetylmuramoylalanyl-D-glutamate--2, 6-diaminopimelate ligase	

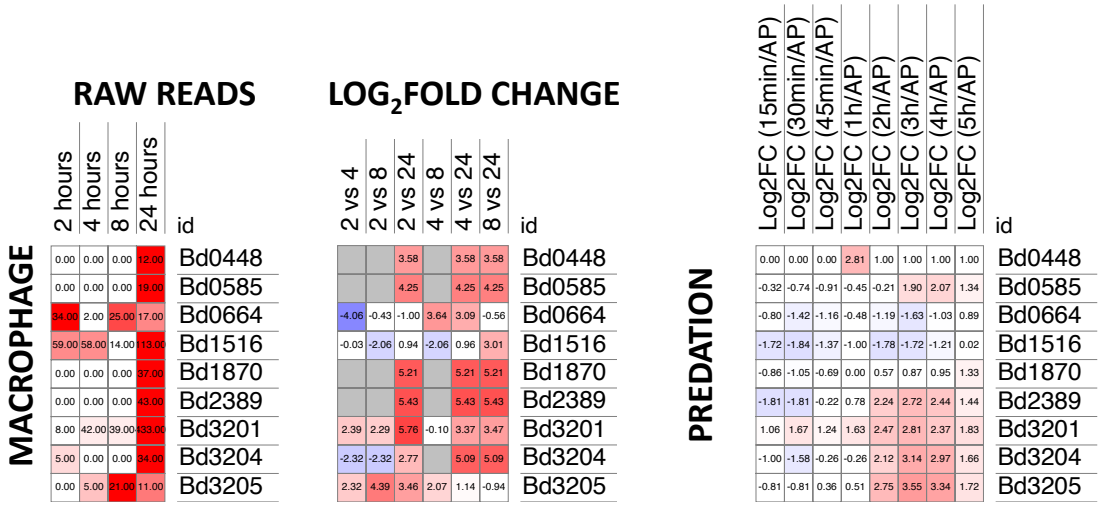

Figure 5.2.7: Genes related to peptidoglycan and lipid synthesis are mostly upregulated at 24 hours of *Bdellovibrio* occupation of macrophage, and at the later stages of bacterial predation. A (limited) bacterial transcriptome from *Bdellovibrio* occupying macrophage over a 24-hour period was curated for significantly upregulated and downregulated (2x Cut off; q<0.05) genes related to Peptidoglycan and Lipid synthesis. The expression of genes varied related to Peptidoglycan and Lipid synthesis are most highly upregulated at 24 hours of *Bdellovibrio* occupation of macrophage. The bacterial transcriptome of *B. bacteriovorus* throughout predation of *E. coli* was interrogated for the selected genes, proposed to be involved in Peptidoglycan and Lipid synthesis. The majority of genes were upregulated throughout predation. Heatmaps were generated using Morpheus.

5.3.7. Stress

To determine whether *Bdellovibrio* expresses any genes related to non-oxidative stress tolerance, whilst residing within macrophage, I curated my list of differentially expressed genes for genes related to various global stress responses (Table 5.2.7). The expression values (raw reads and Log_2 fold change) for each of these genes has been represented for each timepoint below (Figure 5.2.8). Several stress related genes, mostly linked to chaperone function and maintenance of protein folding and function, were highly expressed throughout *Bdellovibrio* occupation of macrophage, especially at 2- and 24-hours post-uptake. This suggests that *Bdellovibrio* is experiencing high levels of stress initially upon uptake and towards the end of phagosome maturation, even though other stress response related genes were expressed throughout *Bdellovibrio* occupation of macrophage. Most of these genes are related to generic stress responses, triggered by a change in environmental conditions, to maintain protein folding and function.

I also looked at the transcriptional expression of these (proposed) generic/ non-oxidative stress related genes throughout predation of *E. coli* by *B. bacteriovorus*. The Log_2 fold change of these genes, compared to attack phase expression is represented for each timepoint below (Figure 5.2.8). The majority of the selected genes were upregulated throughout predation, with the exception of *bd1287*, a heat chaperone, which was downregulated throughout predation. This suggests that *Bdellovibrio* is experiencing other stresses throughout predation.

Table 5.2.7: Genes related to stress responses, expressed by *Bdellovibrio* inside macrophage.

Gene	Synonym	Function/Associations
bd0638	SsrA-binding protein	Stalled ribosome translation rescue; Global regulation of Two component systems (Kim et al., 2022)
bd0961	desiccation-related protein	Dessication resistance (KEGG)
bd1287	heat shock protein HtpX	Heat shock chaperone protein (KEGG) upregulated by *Mycobacterium tuberculosis* in THP-1 cells (600) and *Francisella tularensis* (626)
bd1296	DnaJ protein	Chaperone; Heat shock protein (KEGG)
bd2205	cell division inhibitor SulA	cellular response to DNA damage; cell division inhibitor; SOS response and evasion of engulfment in UPEC infection (627, 628)
bd2272	spb1 gene forserine protease (AJ428902) related protein	Pilus protein secretion; stress response; link to opsonin-independent phagocytosis and intracellular of Group B Streptococcus (629) Internalisation of *Streptococcus agalactiae* (630)
bd2274		
bd2275		
bd3511	transcriptional repressor of the SOS regulon	DNA damage; DNA repair; Stress response (KEGG)
bd3727	outer membrane lipoprotein Blc	Lipid/Outer membrane modification under osmotic stress (631, 632)
bd3872	DnaJ protein	Shock/stress response; Response to hyperosmotic and heat shock; chaperone (KEGG)

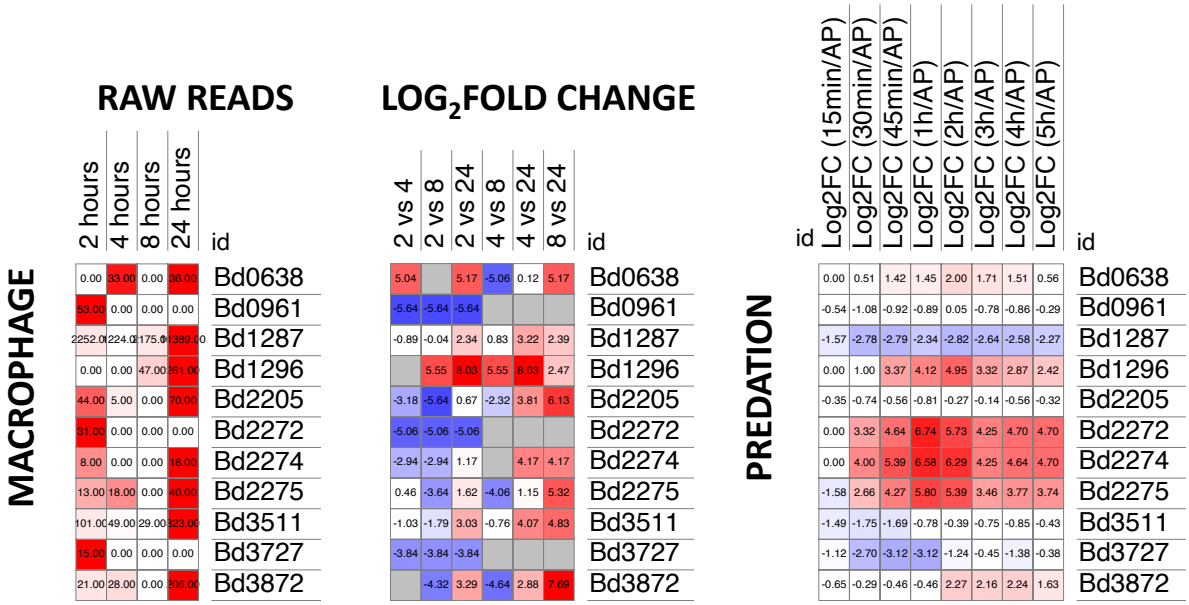

Figure 5.2.8: Genes related to Stress are upregulated throughout *Bdellovibrio* occupation of macrophage. A (limited) bacterial transcriptome from *Bdellovibrio* occupying macrophage over a 24-hour period was curated for significantly upregulated and downregulated (2x Cut off; q<0.05) genes related to various stress responses. The majority of gene expression, relating to stress tolerance, were seen throughout *Bdellovibrio* occupation of macrophage, specifically at 2- and 24-hours post-uptake. The bacterial transcriptome of *B. bacteriovorus* throughout predation of *E. coli* was interrogated for the selected genes, proposed to be involved in generic (non-oxidative) stress responses. The majority of genes were upregulated throughout predation. Heatmaps were generated using Morpheus.

Summaries of the expression of the bacterial genes within each of these functional categories can be found below, along with how these bacterial changes correlate with host interactions and phagosomal conditions. The overall trends within these data are summarised in Section 5.4.

Table 5.2.8 A summary of the data presented in Chapter 5a. N.D. indicates not detected; N.D.E. indicates not differentially expressed.

Gene(s)	Function	Intramacrophage expression (Log_2FoldChange)	Expression throughout predation	Correlation with Macrophage interactions
Oxidative stress tolerance				
bd0177	Acidic pH tolerance	Highly expressed at 24 hours	Downregulated during attachment and invasion; upregulated during intraperiplasmic growth.	Tolerance of fluctuating pH within end-stage phagolysosome
bd0456				
bd2153			N.D.E	Tolerance of acid/proton rich periplasm of prey also
bd3076	Alkaline pH response		Downregulated throughout predation	
bd1002	Superoxide response	Highly expressed at 24 hours	Upregulated throughout prey cell residency	Tolerance of high levels of oxidative stress within phagosome at 24 hours
bd1401	Superoxide dismutase			
bd1425	Transcriptional regulator of oxidative stress response and/or multidrug resistance	Highly expressed at 24 hours	Upregulated during late stage intraperiplasmic growth	
bd1451				
bd2071			Downregulated throughout predation	
bd2113				
bd0298	Organic solvent and peroxide stress response	Highly expressed at 24 hours	Upregulated throughout intraperiplasmic growth	Initial response to oxidative stress in phagosome, and high levels of oxidative stress at 24 hours (that ultimately culminate in bacterial killing).
bd0909		Highly expressed at 8 and 24 hours	Downregulated during early growth	
bd0945	Fatty acid oxidation		N.D.E.	
bd1805	Peroxide response	Highly expressed at 2 and 24 hours	N.D.E	
bd2788	Oxidative damage reversal		Downregulated throughout intraperiplasmic growth	Tolerance of initial and subsequent phagosomal conditions
bd3432	Zinc tolerance	Highly expressed at 2, 8 and 24 hours	Downregulated throughout intraperiplasmic growth	
Host infection				
bd0017	Survival associated chaperone protein	Highly expressed at 24 hours	Downregulated early in predation	In response to significant bacterial killing at 24 hours, attempts to regulate protein folding and outer membrane integrity.
bd0586	Hydrolase	Highly expressed at 8 hours	Downregulated early in predation	-

Table 5.2.8 continued…

bd0665	Bile salt resistance	Highly expressed at 24 hours	Upregulated in newly released progeny	Attempt to resist bacterial killing and bactericidal protein action within phagosome by altering outer membrane
bd0819	Fusaric acid tolerance	Highly expressed at 24 hours	N.D.E	
bd0880	Outer membrane modification	Highly expressed at 24 hours	Downregulated later in predation	
bd3591	Lipid transport	Highly expressed at 24 hours	Upregulated throughout intraperiplasmic growth	
bd1759	Transcriptional regulator	Highly expressed at 8 hours	N.D.E	-
bd3394	Transcriptional regulator	Highly expressed throughout	Upregulated throughout intraperiplasmic growth	-
bd3415	Serine protease	Highly expressed at 4 hours	Upregulated during attachment, invasion and progeny release	Initial response to phagosomal uptake
bd3456	Iron acquisition	Highly expressed at 4, 8 and 24 hours	Downregulated early in predation (15' – 30')	Response to nutrient starvation within the phagosome.
bd3885	Oxidative stress tolerance	Highly expressed at 2 and 4 hours	Downregulated throughout early predation (15' – 2 hours)	Initial response to oxidative stressors present within the phagosome
Anaerobic respiration and nitrogen metabolism				
bd0021	Electron transfer	Expressed at 2 and 24 hours; highest at 24 hours	Upregulated throughout intraperiplasmic growth	Within the anaerobic and nutrient restricted phagosome, *Bdellovibrio* attempts to use alternative electron donors to generate ATP for protein synthesis and metabolism. This is most prominent at 24 hours, where the most significant amounts of bacterial gene expression (and bacterial killing) occur
bd0022				
bd1955	Nitrogen starvation	Expressed throughout; highest at 24 hours		
bd2567	Denitrification		Downregulated throughout predation	
bd2591	Anaerobic respiration/tolerance	Highly expressed at 24 hours		
bd2592			N.D.	
bd2593			Upregulated during late growth	
bd2597	Nitrogen metabolism		N.D.	
bd2598			N.D.	
bd2599			N.D.	
bd2601			N.D.	

Table 5.2.8 continued…

Multidrug tolerance				
bd0333	Beta lactam resistance	Highly expressed at 24 hours	Downregulated throughout predation	Proteins/bactericidal immune factors that target the cell wall will also trigger the same expression responses as conventional cell-wall and membrane targeting antibiotics. Tolerance of cell-wall targeting agents, in response to hydrolytic enzymes and AMPs and bactericidal conditions within phagosome, explaining the high levels of expression at 8 and 24 hours, where most bacterial killing is seen.
bd1765	Beta lactam resistance	Highly expressed at 24 hours	Upregulated throughout intraperiplasmic growth	
bd2036	Beta lactam resistance	Expressed at 4, 8 and 24 hours; highest at 24 hours	Upregulated throughout intraperiplasmic growth	
bd1972	Beta lactam resistance	Expressed throughout	Downregulated upon invasion, upregulated during late growth	
bd3212	Beta lactam resistance	Highly expressed throughout, especially at 24 hours	Downregulated during attachment and invasion; upregulated during late growth	
bd0707	Beta lactam resistance; AMP tolerance	Expressed throughout	Downregulated throughout predation	
bd0360	AMP tolerance	Expressed at 4 and 24 hours	Upregulated throughout predation	
bd1111	AMP tolerance	Highest at 2 and 24 hours	Upregulated during intraperiplasmic growth	
bd2357	AMP tolerance	Highly expressed at 8 and 24 hours	Upregulated throughout intraperiplasmic growth	
bd0395	Multidrug transporter	Highly expressed at 24 hours	Downregulated throughout	
bd0657	Tetracycline efflux	Highly expressed at 24 hours	Upregulated during intraperiplasmic growth	
bd0708	Macrolide export	Expressed at 2, 4 and 8 hours	Downregulated throughout predation	
bd1746	Macrolide resistance	Highly expressed at 24 hours	Downregulated throughout predation	
bd0888	Multidrug transporter	Highly expressed at 24 hours	Upregulated during intraperiplasmic growth	
bd2342	Multidrug transporter	Highly expressed at 8 and 24 hours	Downregulated during attachment and invasion, upregulated during intraperiplasmic growth	
bd1145	Multidrug transporter	Highly expressed at 24 hours	Downregulated upon invasion, upregulated at late stages of predation	
bd1577	Multidrug transporter	Highly expressed at 8 and 24 hours	Upregulated throughout predation	
bd1113	Cytotoxin	Expressed throughout	Downregulated throughout predation	

Table 5.2.8 continued…

bd0797	Antibiotic synthesis	Expressed at 8 and 24 hours	Upregulated throughout predation	
bd2034	Penicillin synthesis	Highly expressed at 24 hours	Upregulated throughout intraperiplasmic growth	
bd0982	Chlorocatechol degradation	Highly expressed at 24 hours	Downregulated at points during predation	
bd2228	Metalloprotease export	Highly expressed at 24 hours	Downregulated throughout intraperiplasmic growth	
bd0980	Ion tolerance	Highly expressed at 24 hours	Downregulated throughout predation	
bd1751	Heavy metal transporter	Highly expressed at 24 hours	N.D.	
bd1798	Heavy metal resistance	Highly expressed at 24 hours	Upregulated throughout intraperiplasmic growth	
bd2170	Metal ion transporter	Highly expressed at 24 hours	Upregulated throughout intraperiplasmic growth	
bd2190	Metal ion transporter	Highly expressed at 24 hours	Upregulated throughout intraperiplasmic growth	
bd2575	Copper resistance	Highly expressed at 24 hours	Upregulated throughout intraperiplasmic growth	
bd2709	Metal ion transporter	Highly expressed at 24 hours	Downregulated during early growth	
bd2710	Metal ion transporter	Highly expressed at 2 and 24 hours	Downregulated during early growth	
bd3057	Transcriptional regulator	Highly expressed at 8 and 24 hours	Downregulated throughout predation	
bd3060	Transcriptional regulator	Highly expressed throughout, especially at 24 hours	Downregulated throughout predation	
bd3063	N/A	Highly expressed throughout, especially at 24 hours	Downregulated throughout predation; Upregulated upon attachment	
bd3549	Oxidative stress tolerance	Highly expressed at 4, 8 and 24 hours, especially at 24 hours	Downregulated during attachment and invasion	
bd3804	Phospholipid transport	Highly expressed at 24 hours	Downregulated during attachment and invasion; upregulated during late growth	
bd3805				
bd3806				

Table 5.2.8 continued…

Nutrient starvation				
bd1236	Starvation-induced chaperone	Expressed throughout, highest at 4 and 24 hours	Downregulated upon attachment	Within the macrophage phagosome, nutrients are highly restricted, therefore starvation-induce proteins are highly expressed, along with nutrient uptake transporters, especially at 24 hours, where nutrient starvation has been ongoing. Conversely, during predation, the prey cell is nutrient rich, therefore starvation proteins are downregulated, and nutrient uptake transporters are upregulated, as seen here.
bd1454	Iron acquisition/starvation	Highly expressed at 24 hours	N.D.	
bd1455			N.D.	
bd2648			N.D.	
bd2860		Expressed throughout, highest at 24 hours	Highly upregulated throughout predation	
bd2145	Nutrient/sulfur starvation	Highly expressed at 2 and 24 hours	Downregulated throughout prey cell residency	
bd3153	Gluconeogenesis	Highly expressed at 24 hours	Upregulated late in intraperiplasmic growth and in newly released progeny	
bd3372	Zinc/Manganese uptake		Upregulated throughout prey cell residency and in newly released progeny.	
bd3373				
Peptidoglycan and outer membrane synthesis				
bd0448	Cardiolipin synthesis	Expressed at 24 hours	Upregulated at 1 hour only	Attempt to modify outer membrane to resist bactericidal phagosomal conditions at 24 hours, where most bacterial killing occurs
bd1516		Expressed at 2, 4 and 24 hours, most significantly at 24 hours	Downregulated throughout predation	
bd2389	Cardiolipin metabolism	Expressed at 24 hours	Downregulated in attack phase and attachment. Upregulated during intraperiplasmic growth (3 – 5 hours)	
bd0664	Fatty acid hydrolysis	Expressed throughout.	Downregulated throughout predation	Outer membrane modification to prevent recognition (?)
bd1870	Polyketide/o-antigen synthesis	Expressed at 24 hours	Upregulated in newly released progeny	*Bdellovibrio* is not growing at 24 hours, therefore peptidoglycan synthesis and degradation represents an attempt to modify the cell in response to damage inflicted by host antimicrobial peptides and hydrolytic enzymes (most bactericidal at 24 hours)
bd0585	Peptidoglycan synthesis and degradation	Expressed at 24 hours	Upregulated at later stages of predation and growth (3 – 5 hours)	
bd3201		Expressed throughout, most highly at 24 hours		
bd3204		Expressed at 24 hours		
bd3205		Expressed most highly at 8 hours		

Table 5.2.8 continued…

Stress				
bd0638	Stalled ribosome translation rescue	Expressed at 4 and 24 hours	Upregulated during prey cell residency	N/A
bd0961	Dessication resistance	Expressed at 2 hours only	N.D.E.	No significant role
bd2205	Cell division inhibitor SulA	Predominantly expressed at 2 and 24 hours	N.D.E.	*Bdellovibrio* are not growing within the macrophage phagosome.
bd2272	Pilus secretion	Expressed at 2 hours only	Upregulated throughout predation	*Bdellovibrio* attempting to sense the environment within the phagosome. Pili are vital for predation.
bd2274		Expressed at 2 and 24 hours		
bd2275		Expressed most highly at 24 hours		
bd3727	Osmotic stress membrane modification	Expressed at 2 hours	Downregulated at beginning of predation (0' – 2 hours)	Initial response to uptake by macrophage/phagosomal conditions
bd1287	Heat shock chaperone	Highly expressed throughout, predominantly at 24 hours	Downregulated throughout predation	
bd1296	DnaJ chaperone	Expressed at 8 and 24 hours	Upregulated throughout predation	*Bdellovibrio* are under high amounts of oxidative stress (and significant bacterial killing) at 24 hours. Attempt to protect chromosome and proteins.
bd3511	DNA repair; SOS response	Expressed throughout, most highly at 24 hours	Downregulated at beginning of predation (0' - 45')	
bd3872	DnaJ chaperone	Expressed most highly at 24 hours	Upregulated during intraperiplasmic growth.	

5.4. Summary

In summary, from this (limited) bacterial transcriptomic dataset of *Bdellovibrio* gene expression, whilst it temporarily occupies macrophage, we see the transcriptional upregulation of several genes related to oxidative stress tolerance, suggesting that *Bdellovibrio* was experiencing high levels of oxidative stress throughout its occupation of macrophage, most significantly at 24 hours post-uptake. This correlates and supports our rationale for Chapter 4, where I sought to determine if *Bdellovibrio* was attempting to tolerate oxidative stresses within macrophage.

Investigating genes associated with host infection (from the literature on bacterial pathogens and infection), *Bdellovibrio* expresses various genes, predominantly at 24 hours, in an attempt to tolerate phagosomal conditions and resist bacterial killing through oxidative stress tolerance.

Bdellovibrio expresses genes related to nitrogen metabolism and aerobic respiration at 24 hours post-uptake, indicating that it is attempting to utilise alternative pathways to generate ATP and is under respiratory stress.

Genes related to nutrient starvation were most upregulated at 24 hours post-uptake, suggesting that this is when *Bdellovibrio* is under the most significant stress, correlating with the most significant levels of bacterial killing also. Of note is the increase in the expression of iron acquisition genes (*bd1454, bd1455* and *bd2648*) throughout intramacrophage survival, consistent with bacterial infection and critical for intraphagosomal survival, but who's expression are entirely absent throughout predation. This validates the experimental setup and demonstrates that *Bdellovibrio* are experiencing intraphagosomal conditions representative of those experienced by bacteria during host infection. This is also highlights one subset of genes which are important for macrophage survival but not for predation, showing a disconnect between the two scenarios (explored in Chapter 6).

Gene expression related to multidrug tolerance and peptidoglycan and outer membrane synthesis were also most prominent at 24 hours post-uptake, suggests that this was when the majority of membrane/cell wall targeting antimicrobial effectors targeting and stressing *Bdellovibrio* were present.

Clearly, as the highest levels of transcriptional upregulation occur at 24 hours post-uptake, this represents the most significant timepoint at which *Bdellovibrio* is trying to tolerate and resist the conditions within the phagosome, and is under severe stress, in response to the significant levels of bacterial killing occurring at this timepoint. Prior to this, *Bdellovibrio* is still undergoing large shifts in transcriptional expression, but fewer discernible trends emerge at earlier timepoints to suggest a co-ordinated response to intramacrophage survival.

Owing to only a partial transcriptome being available for *Bdellovibrio* throughout its occupancy of macrophage, these (preliminary) conclusions would require further testing and validation in future to fully characterise the main themes in the response of *Bdellovibrio* to intramacrophage survival and phagosomal conditions.

Chapter 5b: Analysis of the transcriptional response of macrophage to *Bdellovibrio* throughout macrophage occupation.

5.5. What is already known, or expected, regarding the host response to *Bdellovibrio*?

5.5.1. Introduction to the host transcriptional response to *Bdellovibrio*

I have chosen to look at the macrophage transcriptional response to *Bdellovibrio bacteriovorus* uptake at 4 timepoints, capturing earlier and later stages of macrophage occupation prior to (significant) bacterial killing at 24 hours. This is because previous work by Dr Dhaarini Raghunathan (2) showed that *Bdellovibrio* occupation of macrophage lasted 48 hours, with a significant viability of *Bdellovibrio* (6×10^4 PFU/ml; 33% of predicted uptake input) up until 8 hours, upon which significant killing occurred and the viability of *Bdellovibrio* decreased to 3×10^3 (1.5%) at 24 hours and dropped further (8×10^1 PFU/ml; 0.25%) at 48 hours.

The key bacterial ligands on *Bdellovibrio* which could be recognised by the host are unexplored, unlike the situation for many bacterial pathogens, and will be investigated by interrogating the host RNASeq response pathways showing altered transcription in comparison to the known macrophage responses to bacterial pathogens (see Section 1.4.3). I have considered these alternatively transcriptionally regulated pathways by mRNA sampling at 2-, 4-, 8- and 24-hour timepoints.

2 hours: At 2 hours post-exposure, *Bdellovibrio* are known from work by Raghunathan and co-workers to have been recently encountered and internalised by macrophage (2). By analogy with the known processes of bacterial pathogen engulfment (185) and also fluorescent antibody studies of *Bdellovibrio* uptake by macrophage (2), large cytoskeletal (F-actin and microtubule) rearrangements will have occurred in host cells, promoting membrane rearrangement, along with trafficking of endosomes to the phagosome after initial uptake.

Phagocytosis may be opsonic, due to cross-reacting or specific IgG antibodies present in the foetal bovine serum-containing culture media; or may be non-opsonic and initiated through the binding of host Pattern Recognition Receptors (PRRs) to *Bdellovibrio* Pathogen Associated Molecular Patterns (PAMPs)/microbial ligands.

At 2 hours, we would expect to see a non-specific and generalised response to bacterial stimuli, before further recognition later in the phagocytic pathway. We (2) know there is some *Bdellovibrio* persistence within macrophage, therefore I hypothesised that I might expect a potential delay or inhibition in recognition, which I have investigated further in this study. At 2 hours, transcriptional changes will be largely due to interactions with the surface epitopes of the *Bdellovibrio*, and potentially due to changes in oxygen abundance due to respiration of an additional cell type, alongside the macrophages.

4 hours: At 4 hours post-uptake, *Bdellovibrio* is persisting live within macrophage, inside a phagosome (2). Further sampling of the contents of the phagosome is likely occurring. Cycling of pH towards acidification is also occurring. Some non-specific lysis of *Bdellovibrio* has likely occurred, but there is no extensive bacterial killing (Figure 5.4.1) ((2); This study).

8 hours: At 8 hours post-uptake, *Bdellovibrio* is persisting, live, within macrophage but Raghunathan and co-workers and I detected some killing (approximately 3-fold drop in PFU). ELISA work showed a strong TNFα response induced throughout 4 and peaking at 8 hours, and an induced IL-6 response also (2).

24 hours: At 24 hours, Raghunathan and co-workers saw significant acidification of the phagolysosome (LysoTracker Red staining of acidified vesicles) (2), along with a 100-fold drop in viability. It is likely that digestion of microbial ligands, prior to antigen presentation on antigen presenting cells via MHC-II complexes, and amplification of the inflammatory and adaptive immune response will be readily occurring at 24 hours post-uptake.

Production of IL-1β, IL-6 and IL-8 (proinflammatory) and IL-10 (anti-inflammatory) cytokines (detected by ELISA) was also seen to increase at 24 hours (2).

I checked the persistence of *Bdellovibrio* in U937 cells using an identical methodology to Raghunathan and co-workers, comparing the viability of *Bdellovibrio* seen. I detected and saw similar values for *Bdellovibrio* viability as Raghunathan and co-workers (2).

5.5.2. What is known/expected of the macrophage response to *Bdellovibrio*?

Data from a survey of 25 randomly chosen human sera shows that although 90 % had a detectable level of anti-*Bdellovibrio* antibodies (measured by ELISA), 50-60% of these samples had a low anti-*Bdellovibrio* antibody titre (<10 μg/ml) (2). Exposure to *Bdellovibrio* was also not recent, due to the titre of IgG antibodies exceeding those of IgM (2). This suggests that exposure to *Bdellovibrio*, is uncommon or short-lived, and that there is no large circulating anti-*Bdellovibrio* antibody titre in human populations. This may indicate that in the Foetal Bovine Serum used in our tissue culture media, low levels of anti-*Bdellovibrio* antibodies may also be present because *Bdellovibrio* is a soil dwelling organism that the cow may be exposed to, although this has not been tested. Opsonic phagocytosis may also occur through the binding of other host proteins (present within Foetal Bovine Serum) to *Bdellovibrio* e.g. complement proteins.

Opsonisation of *Bdellovibrio* with human sera, prior to exposure to PMA-differentiated U937 cells, did not significantly affect uptake (at 2 hours) and viability (at 4 hours), compared to non-opsonised *Bdellovibrio* (Dr Dhaarini Raghunathan, personal communication). This suggests that, despite my comments above, non-opsonic phagocytosis may be the dominant mechanism of *Bdellovibrio* uptake and that recognition of key bacterial ligands by host PRRs is an important factor for *Bdellovibrio* uptake and processing.

Early (EEA1: Early Endosomal Antigen 1) and late (LAMP1; Lysosomal Associated Membrane Protein 1; Rab7) phagosomal marker proteins are already present on the *Bdellovibrio*-containing phagosome (Figure 5.4.2)(2) at 1-hour post-uptake suggesting the phagosome has reached a level of maturity at that point, so *Bdellovibrio* is not inducing a full delay in phagosomal maturation.

The phagolysosome will contain high levels of ROS (Reactive Oxygen Species) including superoxide and nitric oxide molecules, proteases, lipases, lysozymes, cathepsins etc. but Raghunathan and co-workers do not detect phagolysosome acidification and see minimal killing of *Bdellovibrio* at 2 hours post-uptake (Figure 5.4.1)(2).

A detailed explanation of the host Pattern Recognition Receptors expressed by the host, and which microbial ligands they recognise are detailed in Section 1.4.3. The surface ligand composition of *Bdellovibrio* is discussed in Section 1.6.2, along with the predicted immunogenicity of *Bdellovibrio* surface ligands in Section 1.6.7.2.3.

5.6. Comparing these macrophage activation events with my RNASeq results.

As documented in Section 2.5, I analysed 2 technical repeats of a single run of RNA sequencing, from a pool of nucleic acids originating from both PMA-differentiated U937 cells and internalised *Bdellovibrio* at 4 individual timepoints covering the occupation period of *Bdellovibrio.* These data were analysed and the fold-change in gene expression between timepoints calculated (see Section 2.5.3).

Lower levels of gene induction are relevant to host gene expression and infection (633) but, as I was dealing with such a large list of differentially expressed genes, I decided to focus on those that were more highly differentially expressed (2-fold up or downregulation). When discussing the biological interpretation of these data, I have also considered other genes that were not differentially expressed, where appropriate, so I do not believe that the applied cut-offs used, exclude any relevant biological findings.

5.6.1. A wider view of the host transcriptional response to *Bdellovibrio*

Firstly, I wanted to get a more global picture of the host transcriptional response to *Bdellovibrio* occupation, I looked at the differentially upregulated and downregulated Gene ontology terms associated with *Bdellovibrio* occupation of macrophage.

5.6.1.1. Upregulated gene ontology terms

Interestingly, the majority of all gene ontology terms were upregulated throughout *Bdellovibrio* occupation and reached their maxima at 24 hours post-uptake. Gene ontology terms relating to the “cell periphery” and “plasma membrane” were significantly upregulated at 24 hours, potentially representing a large amount of receptor signalling and antigen presentation at 24 hours, after significant bacterial killing, to amplify and coordinate the adaptive immune response (Figure 5.6.1).

Gene ontology terms related to “Immune response”, along with “responses to (external) biotic stimuli”, “other organisms” and “response to bacterium” were upregulated between 2 and 8 hours, peaking at 8 hours, and is then downregulated at 24 hours, potentially suggesting a resolution of the immune response, associated with significant bacterial killing (Figure 5.6.1).

Gene ontology terms relating to responses to cytokines, cytokine stimuli and cytokine-mediated signalling pathways were upregulated and reached their maxima at 4 hours, remaining high at 8 hours, and tailing off at 24 hours post-uptake (Figure 5.6.1).

Finally, responses to external stimuli, signal transduction, response to stimulus, cell signalling, and communication reach their maximum at 8 hours and remain high at 24 hours post-uptake also (Figure 5.6.1).

5.6.1.2. Downregulated Gene Ontology Terms

Gene ontology terms relating to “DNA packaging”, “nucleosome organisation and assembly”, “Protein-DNA complex assembly” and chromatin assembly and disassembly are significantly downregulated at 24 hours post-uptake, suggesting that this is when the majority of gene transcription is taking place (Figure 5.6.2).

Figure 5.6.1: A heatmap showing the upregulation of gene ontology terms throughout *Bdellovibrio* occupation of macrophage.

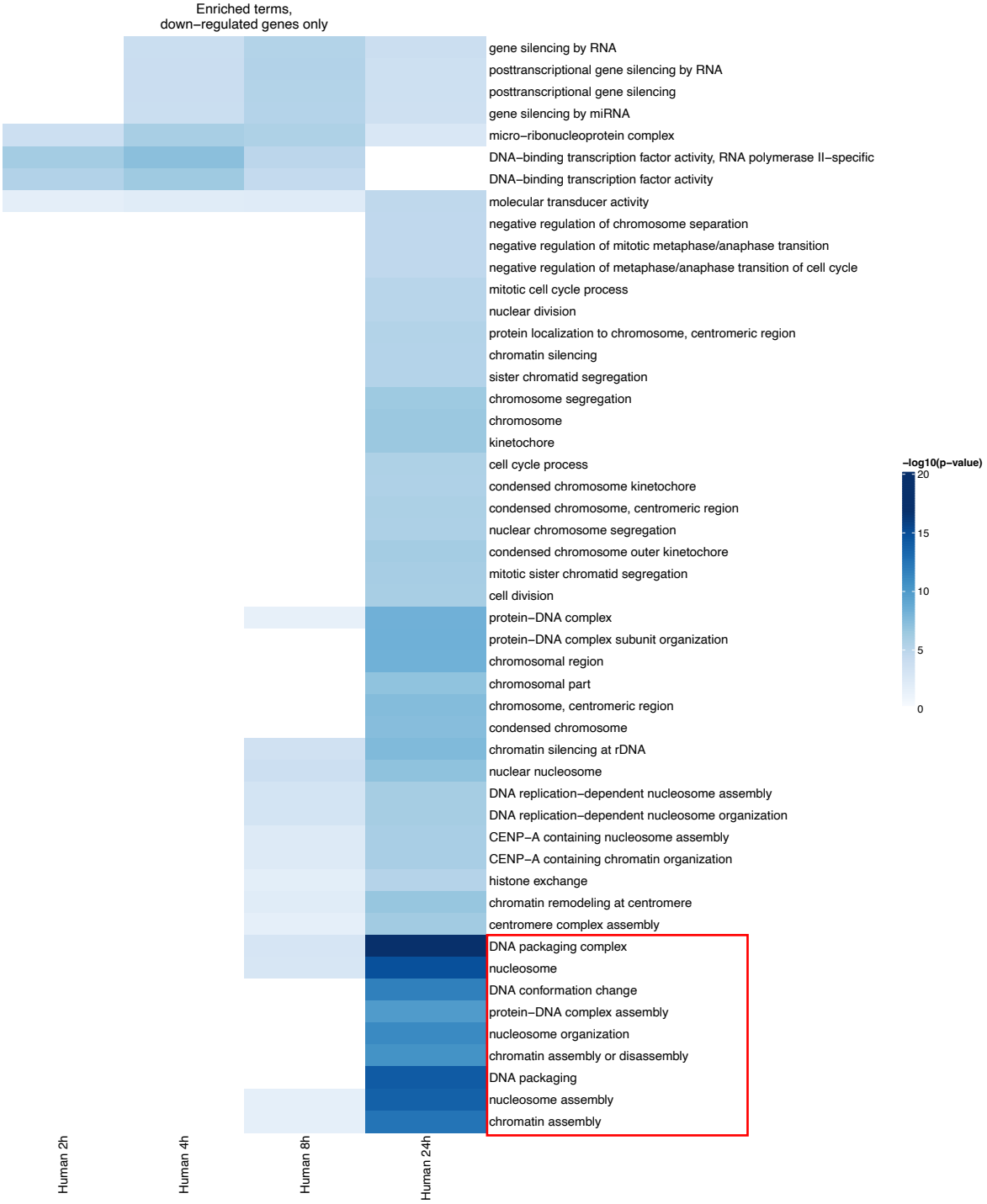

Figure 5.6.2: A heatmap showing the downregulation of gene ontology terms throughout *Bdellovibrio* occupation of macrophage.

5.6.1.3. Upregulated reactome pathways

Additionally, I also interrogated the significantly upregulated and downregulated reactome pathways throughout *Bdellovibrio* occupation of macrophage. Interferon gamma and Interferon alpha/beta signalling are upregulated at 4- and 8-hours post-uptake. G-protein coupled receptor signalling, downstream GPCR signalling, and GPCR ligand binding terms are all most prominent at 4- and 24-hours post-uptake, possibly representing the majority of endosomal sampling of bacterial ligands, and the cell-cell communication and adaptive immune response signalling occurring at 24 hours (Figure 5.6.3).

Cytokine signalling is most highly upregulated at 4 hours post-uptake, remaining high at 8 hours post-uptake also. Interleukin-10 signalling is highly upregulated throughout *Bdellovibrio* occupation of macrophage, being most prominent at 8 hours post-uptake. Signalling by interleukins, chemokine receptor binding and IL-4 and IL-13 signalling are highest at 4 hours post-uptake but remain high at 8- and 24-hours post-uptake also, representing the continued inflammatory activation of macrophage at 4 hours, and the cell-cell communication and further activation of cell types at later timepoints (Figure 5.6.3).

5.6.1.4. Downregulated Reactome Pathways

As seen with the upregulation of gene ontology terms associated with DNA packaging and assembly, relating to enhanced transcription at 24 hours post-uptake, I also see a significant downregulation of DNA methylation, a form of transcriptional regulation, at 24 hours post-uptake. Oxidative stress induced senescence is downregulated at 8 and 24 hours, prolonging cell survival and activity at these later timepoints (Figure 5.6.4).

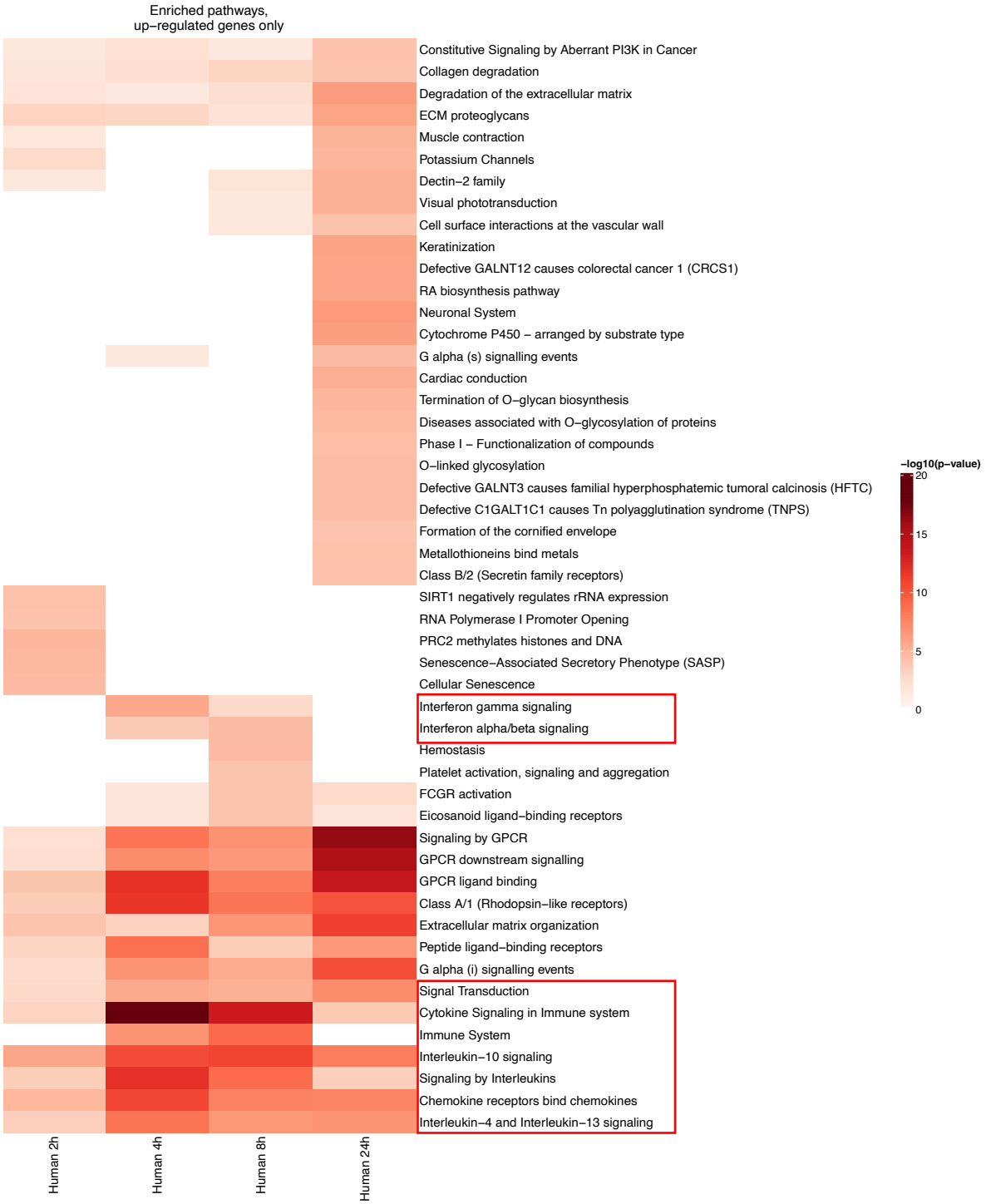

Figure 5.6.3: A heatmap showing the upregulation of Reactome terms throughout *Bdellovibrio* occupation of macrophage.

Figure 5.6.4: A heatmap showing the downregulation of Reactome terms throughout *Bdellovibrio* occupation of macrophage.

5.6.1.5. Initial Summary

In summary, a significant bacteria-associated transcriptionally encoded immune, as well as general metabolic responses are mounted towards *Bdellovibrio*, by host macrophage. Transcription associated with an immune response reached its maxima at 8 hours post-uptake before beginning to subside and give way to a more adaptive-type immune response, possibly focused on antigen presentation and cell signalling, at 24 hours post-uptake.

This has provided a wider, more global view of the host transcriptional response to *Bdellovibrio*. I will now interrogate the host transcriptional responses further. Differentially expressed genes were interrogated with specific biological questions in mind, to ask certain questions of the data and inform us of the key host gene transcription pathways occurring throughout *Bdellovibrio* occupation, helping us to gain a better understanding of the host transcriptional response to *Bdellovibrio*.

5.6.2. How is *Bdellovibrio* recognised throughout macrophage occupation?

As detailed in Section 1.4.3., Toll-like receptors (TLRs) are one of the main PRRs involved in detecting and responding to an initial microbial stimulus. Surface TLRs (TLRs -1, -2, 4, -5 and -6) detect the main surface ligands on bacteria and initiate the immune response. Once phagocytosed, endosomal TLRs (TLR -3, -7, -8 and -9) are trafficked to the phagosome where they sample the contents of the phagosome further to give a more tailored and specific immune response. The innate immune response typically gains momentum and becomes increasingly pro-inflammatory over time.

TLRs are typically expressed at low levels on unstimulated/naïve macrophage, until they are stimulated by microbial ligands or proinflammatory cytokines, upon which TLR expression is upregulated (634). The TLR expression profile is highly dependent on the macrophage subtype and local environment (634-638). For example, TLR-2 expression relatively lower on alveolar macrophage than on their peripheral monocyte progenitors, whilst TLR-4 and TLR-9 expression levels being similar and TLR-9 expression higher on alveolar macrophage (634).

The degree of downwards activation and signalling from TLRs also varies between cell types. In some cell types, TLR-2 surface expression correlates well with cytokine induction, whereas in others, similar TLR-4 surface expression levels results in different magnitudes of cytokine induction, in response to LPS stimulation (634). This highlights the crosstalk between different PRRs and the role of adaptor proteins and co-receptors in downstream signalling. TLR surface expression profiles differ between different cell types, and subtypes i.e. different tissue resident macrophage classes, influencing local host immune responses (634).

On PMA-stimulated U937 cells, the cell line used in my study, all 10 human TLRs genes are known to be expressed (measured via reverse transcriptase PCR), with TLRs -1, -3 and -6 being expressed at lower levels, relative to other cell lines, and TLRs -2 and -4 being expressed at higher levels, relative to the other cell lines tested (639).

In my study, an absence of differential expression of TLR genes does not mean that those TLRs are not recognising their specific ligands, but that the microbial ligands are not inducing an upregulation/downregulation of the specific TLR. This is indicative of a relative absence of detection but is not a conclusive determinant that the ligand has not been detected. TLR gene expression may also be induced by crosstalk through other Host Pattern Recognition Receptors, inducing proinflammatory gene expression and further TLR expression.

I discuss each relevant TLR and its potential *Bdellovibrio* ligands below.

5.6.2.1. Detection of *Bdellovibrio* peptidoglycan

5.6.2.1.1. TLR Response

TLR-2 is known to work in combination with TLR-1 and TLR-6, on professional phagocytes including macrophage, to detect triacylated and diacylated lipoproteins respectively (65, 66), along with NAG (N-acetyl glucosamine) and NAM (N-acetyl muramic acid) subunits of peptidoglycan and outer membrane proteins (65, 67). Peptidoglycan is usually masked from detection by TLR-2 due to LPS outer membrane so there is typically a delay in response to peptidoglycan after uptake, until non-specific lysis of bacteria exposes peptidoglycan fragments. The peptidoglycan of *Bdellovibrio bacteriovorus* is typical of Gram-negative bacteria in structure and composition (296), unlike the LPS of *B. bacteriovorus* which is atypical. TLR-2 is reported to also detect Outer Membrane Proteins (OMPs)(640). Therefore, it may also detect the limited OMPs present in the outer membrane of *Bdellovibrio*, prior to bacterial lysis.

In this study, I see upregulation of *tlr2* gene expression at 4-, 8- and 24-hours post-uptake, with transcription remaining high throughout (Figure 5.6.5). The gene encoding TLR-1, which works in complex with TLR-2 to detect triacylated lipoproteins/lipopeptides, is also significantly upregulated at 4, 8 and 24 hours (Figure 5.6.5). TLR-6, which works in complex with TLR-2 also, detects diacylated lipoproteins. The gene encoding TLR-6 is also significantly upregulated at 8 hours but decreases later in *Bdellovibrio* occupation (Figure 5.6.5), suggesting a delay in response to diacylated lipoproteins compared to triacylated lipoproteins. Overall, this suggests that peptidoglycan and lipoproteins are detected and recognised at approximately 4 hours post-uptake, and that peptidoglycan recognition continues throughout *Bdellovibrio* occupation, at 8 and 24 hours also (Figure 5.6.5). These data also suggest that lipoproteins are detected and recognised later in *Bdellovibrio* occupation, as *tlr1* and *tlr6* expression are downregulated initially but are upregulated at 8 hours, compared with 2- and 4-hour timepoints.

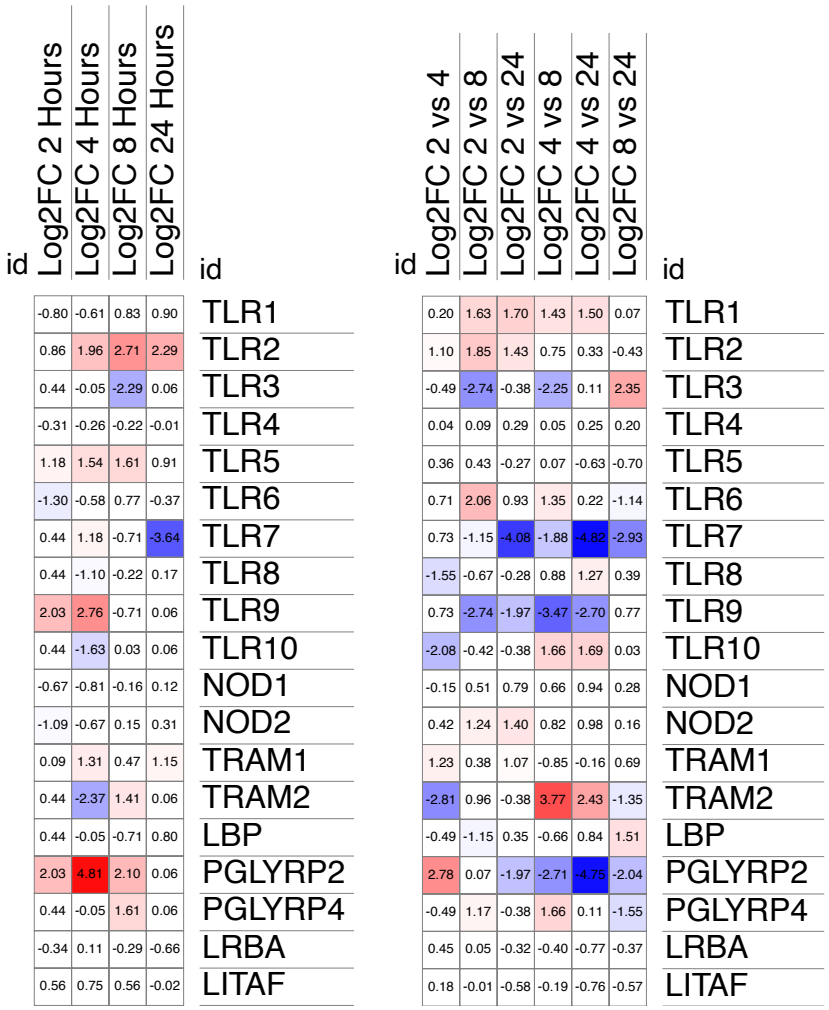

Figure 5.6.5: A heatmap visualising the expression of genes related to microbial recognition throughout *Bdellovibrio bacteriovorus* occupation within PMA-differentiated U937 macrophage-like cells. Values shown represent the Log_2 function of the ratio of gene expression values of *Bdellovibrio*-containing U937 cells, compared to cell-only controls, at 4 timepoints across a 24-hour period (left). Values shown represent the Log_2 function of the ratio of gene expression values of *Bdellovibrio*-containing U937 cells at each chosen timepoint, relative to each of the other 3 timepoints within this study (right). TLR: Toll Like Receptor; NOD: Nucleotide Oligomerisation Domain; TRAM: TLR Related Adaptor Molecule; LBP: LPS Binding Protein; PGLYRP: Peptidoglycan Recognition Protein; LRBA: LPS Responsive Beige Like Anchor Protein; LITAF: Lipopolysaccharide Induced TNF Alpha Factor. Heatmaps were generated using Morpheus.

5.6.2.1.2. NOD-Like Receptors

Peptidoglycan may also be detected by endosomal NLRs (NOD-Like Receptors) NOD-1 and NOD-2, which detect peptidoglycan within the host cell and respond to intracellular bacterial infection (68, 69, 71, 73), after peptidoglycan ligands have been internalised/ phagocytosed by host TLRs. NOD-1 and NOD-2 respond to both the amino acid DAP (D-glutamyl-meso-diaminopimelic acid) and the backbone muramic acid attached to the peptide MDP (muramyl dipeptide) respectively (69, 70, 72-74)). In other studies, NOD1 and NOD2 are highly expressed in monocytes, macrophages, and dendritic cells (80, 641, 642), with gene expression upregulated at early stages of infection, as opposed to mRNA being constitutively present and post-translationally activated for NOD1/NOD2 expression. Despite NOD1 and NOD2 being highly expressed, macrophage don't show robust upregulation of *nod1* and *nod2* gene expression to DAP or MDP alone (76, 643-646). NOD2 is documented to synergise with TLR-2 to amplify phagosomal maturation (646-648) or it may inhibit TLR-2 T-helper 1 responses (648), suggesting that NOD2 may play a feedback role in infection, rather than strong initiation of an immune response.

NOD1 and NOD2 have been shown to sense intracellular bacteria, including *S. flexneri* (70), *L. monocytogenes* (72, 75, 76), *S. pneumoniae* (77), *M. tuberculosis* (78) and a range of other Gram-negative bacteria (649, 650), but the role of NOD1/NOD2 in the resolution of infection is still poorly understood (80).

The Impact of Acetylation on Lysozyme Sensitivity and Peptidoglycan Detection.

The acetylation state of bacterial peptidoglycan is important for lysozyme susceptibility and NOD1/2 recognition; therefore, acetylation and de-acetylation of bacterial peptidoglycan is one strategy to avoid detection by the host (651-653). Most bacteria have 2' N-acetylated MDP subunits present within their peptidoglycan (653). Bacteria may modify their peptidoglycan through 6' acetylation and 2' deacetylation of MDP subunits, to prevent lysis by lyzozymes (298, 653). Lysozymal digestion of peptidoglycan post-uptake is important for recognition by NOD2 and clearance of *Streptococcus pneumoniae* infection (243). 6' acetylation does not directly impact NOD2 recognition (654), but 2' deacetylation prevents NOD2 activation, and downstream NFκB activation in *L. monocytogenes* (653). MDP is 2' N-acetylated and is recognised by NOD2 (654, 655). 2' N-glycosylation of MDP leads to higher levels of NOD2 activation (fluorescent reporter assay) and downstream NFκB activation (656, 657). More extensive N-acetylation of MDP (chemical addition) increases NOD2 and downstream NFκB activation further (656). These studies confirm that 2' N-acetylation of MDP is important for NOD2 recognition (653, 656).

Stimulation of TLRs -1, -2 and -6 and NOD1/2 by peptidoglycan induces a strong TNFα mRNA response, but without high TNFα translation. Translational repression of TNFα is derepressed when LPS/TLR-4 stimulation also occurs (644). Stimulation of NOD2 by 2' N-glycosylated MDP, but not 2' N-acetylated MDP, also induces a TNFα response (transcribed and expressed) (653, 657).

Reduction in detection by NOD1 is usually due to a decreased availability of peptidoglycan fragments due to inhibition of lysozyme action (653), although the amidylation of δ-carboxylic acid within isoglutamic acid of peptidoglycan prevents NOD1 activation (16). Reduction in detection by NOD2 is due to an absence/decreased affinity for recognition between NOD2 and MDP subunits, usually through de-acetylation (653). Detection by NOD2 is also aided by lysozymal cleavage of peptidoglycan (658).

Bdellovibrio Peptidoglycan

Bdellovibrio uses various lysozymes and peptidoglycan modifying enzymes throughout its predatory lifecycle, to modify and digest the peptidoglycan cell wall of other Gram-negative prey (290, 291, 659, 660). *Bdellovibrio* deacetylates prey peptidoglycan, making it susceptible to lysozymal action, whilst maintaining its own peptidoglycan in an acetylated state to protect itself from endogenous/self-secreted lysozymes (290, 291, 659, 660). The acetylation state of bacterial peptidoglycan is known to impact host-mediated lysozyme action and recognition by host PRRs, as I explain above (297-299, 653). Therefore, I asked "Does *Bdellovibrio* acetylation of self-peptidoglycan impact recognition of *Bdellovibrio* by the host?".

In our dataset, expression of *nod1* is unchanged throughout *Bdellovibrio* occupation (Figure 5.6.5). Expression of *nod2* is downregulated at 2 hours, post-uptake, prior to returning to pre-*Bdellovibrio* uptake levels, later in *Bdellovibrio* occupation (8 and 24 hours) (Figure 5.6.5). My data suggests that recognition of *Bdellovibrio* peptidoglycan by NOD1 and NOD2 is not significant throughout *Bdellovibrio* occupation, despite *Bdellovibrio* containing both DAP and MDP, both of which are important structural crosslinking components of its "typical" peptidoglycan cell wall, and even more so for the osmotic and enzymatic stresses encountered within its predatory lifecycle (659). *Bdellovibrio* peptidoglycan is 2' N-acetylated (MDP subunit), therefore it can activate NOD2, and downstream signalling pathways. Alternatively, *Bdellovibrio* peptidoglycan may be recognised by Host TLR-2 but does not induce an upregulation of TLR-2 expression.

To conclude, *Bdellovibrio* peptidoglycan, even in its acetylated state, can be recognised by and activate TLR-2, NOD1 and NOD-2 receptors, although *tlr2, nod1* and *nod2* gene expression are not significantly upregulated in this study. This could be clarified further by exposing U937 cells to *Bdellovibrio* peptidoglycan directly and characterising *tlr2, nod1* and *nod2* gene expression and protein expression by qtPCR and Western blot analysis respectively. *Bdellovibrio* acetylation of self-peptidoglycan does not impact recognition of *Bdellovibrio* by the host.

5.6.2.1.3. Peptidoglycan Recognition Proteins (PGLYRPs)

Macrophage also express Peptidoglycan Recognition Proteins (PGLYRPs) that recognise and bind to the peptides linking N-acetyl Muramic Acid in the Peptidoglycan backbone (81). PGLYRP-1, -3 and -4 lyse peptidoglycan and exert a bactericidal effect (81), in some cases amplifying the immune response, for example, PGLYRP1 activates TNF in *Listeria monocytogenes* infection (82), and in others, exerting a bactericidal effect but limiting the proinflammatory response to commensal microbiota (83).

pglyrp1 and *pglyrp3* are not transcriptionally upregulated in *Bdellovibrio* Macrophage occupancy. *pglyrp4* gene transcription is significantly upregulated by *Bdellovibrio* at 8 hours (Figure 5.6.5).

Peptidoglycan Recognition Protein 2 (PGLYRP2) lyses peptidoglycan into biologically inactive fragments that are less well recognised by TLRs -1, -2 and -6. PGLYRP-2 cleaves the sugar backbone from the peptide chain, thus cleaving and removing the ligands for NOD-1 and -2 (74, 84). *pglyrp2* expression is induced by TLR-2 and -5 detection of peptidoglycan and flagellin (661).

In our dataset, *pglyrp2* gene expression was highly upregulated at 2, 4 and 8 hours of *Bdellovibrio* occupation, which may explain the lack of *nod1* and *nod2* upregulation throughout *Bdellovibrio* macrophage occupancy (Figure 5.6.5). This may suggest that peptidoglycan is detected at earlier timepoints, but that recognition and immune activation is perhaps minimised in the earlier stages of occupancy, as seen in *S. typhimurium* infection where *S. typhimurium* induced PGLYRP-2 expression minimises inflammation (*pglyrp2*$^{-/-}$ mice show increased gene expression of *il-17, il-22* and proinflammatory cytokines), although this is largely independent of NOD1/NOD2 activation (662). Conversely, PGLYRP-2 played no role in *E. coli* infection suggesting that the effects of PGLYRP-2 may be dependent on the infectious agent (663). Recently, PGLYRP-2 has been shown to play a role in neutrophil recruitment in *Streptococcus pneumonia* infection, amplifying the immune response (664) and to have some, direct, bactericidal activity (665, 666). This suggests that the role of PGLYRP-2 in bacterial recognition is highly dependent on the bacterium in question. In our dataset, expression of *pglyrp2* is highly upregulated at 2-, 4- and 8-hours post-uptake, suggesting it is involved in the processing of *Bdellovibrio* by U937 cells in this scenario (Figure 5.6.5).

In conclusion, peptidoglycan may be being detected at 4 hours post-uptake and throughout *Bdellovibrio* occupation by TLRs -1, -2 and -6, whose genes are upregulated. My transcriptional study suggests that detection of peptidoglycan by NOD1/2 may not appear to play a role in *Bdellovibrio* occupation/processing, but this may be due to expression of PGLYRP-2 cleaving the peptidoglycan moieties reducing peptidoglycan recognition by NOD1/2. Peptidoglycan is one of the main ligands detected by U937 cells in response to *Bdellovibrio*. Some *Bdellovibrio* cells may be being broken down at 4 hours, through non-specific lysis, revealing the peptidoglycan formerly masked by the LPS outer membrane.

5.6.2.3. Detection of *Bdellovibrio* LPS- what is the effect of mannosylation?

In Section 1.6.2.1, I mentioned that the LPS of *Bdellovibrio* is atypical, and that this modification might reduce the recognition and binding of TLR4. Here, I consider whether transcriptional changes suggest that macrophage initiate a response to *Bdellovibrio* LPS. TLR-4, in complex with LBP (Lipopolysaccharide Binding Protein), CD14 and MD2 (Myeloid Differentiation 2) detects lipopolysaccharide (LPS) on the Gram-negative outer membrane (60). TLR-4 would usually be expected to the one of the first TLRs to detect Gram-negative bacterial exposure, owing to LPS being the major component of the outer membrane surface. TLR-4 may detect LPS at the cell surface or within endosomes, owing to it cycling between both interfaces, signalling through two separate pathways.

In our dataset, *tlr4* gene expression remained unchanged in response to *Bdellovibrio* occupancy throughout the 24-hour period (Figure 5.6.5). The U937 cells are no doubt exposed to LPS but, I propose that, due to the substitution of a phosphate group in the *Bdellovibrio* Lipid A, with an α-ð-mannose residue, (Section 1.6.2.1), this reduces the negative charge of the Lipid A molecule (301), and potentially decreases the binding affinity of Lipid A for TLR-4 significantly (60, 218) (Figure 5.6.5). This may explain why we see a lack of induction of *tlr4* transcription in *Bdellovibrio* occupancy. We also see no induction of gene expression for Lipopolysaccharide Binding Protein (*lbp*), LPS-responsive beige-like anchor protein (*lrba*) or Lipopolysaccharide Induced TNF Factor (*litaf*), reinforcing the lack of LPS response. *lbp* gene expression is downregulated at 8 hours compared to 2 hours, and then returns to pre-*Bdellovibrio*-uptake levels at 24 hours, possibly due to crosstalk with other TLRs, inhibiting *lbp* transcription (Figure 5.6.5).

ticam2 (Toll Like Receptor Adaptor Molecule 2) expression, the molecule that transduces the signal from TLRs -2 and -4, is also most highly expressed/ upregulated at 8 hours post-uptake (Figure 5.6.5), but this may be facilitating the TLR-2 response, in the absence of TLR-4 stimulation.

5.6.2.3.1. Recognition of other Gram-negative bacteria lacking LPS

Spirochetes, such as *Treponema pallidum* and *Burkholderia burgdorferi*, lack LPS therefore how they are sensed by the host immune response is of interest to us, to draw comparisons with *Bdellovibrio* and the lack of conventional TLR-4 response due to its mannosylated LPS. *T. pallidum* and *B. burgdorferi* express high amounts of lipoproteins which determine how these bacteria interact with the environment and the host immune system (667).

Despite lacking LPS (668-671), these bacteria still initiate an immune response that is highly inflammatory. This is due to the NH2-terminal lipopeptide region of the lipoprotein conferring the immunogenic activity (672). Lipoproteins are typically hidden below the surface of the bacterium; therefore, they are not directly exposed to the immune system initially. Uptake and non-specific lysis of the bacterium must occur before detection and response to bacterial lipoproteins is initiated.

The response to *T. pallidum* is mainly initiated through the peptidoglycan-sensing TLR-2 (673) and the NFκB pathway (674, 675), culminating in the production of chemokines (CCR5) (676, 677) and cytokines (TNFα, IL-1β, IL-6 and IL-12) (671, 678-680).

The macrophage response to *B. burgdorferi* is also mainly initiated through TLRs -1 and -2 (667), and the NFκB pathway (674, 675, 681, 682). It also culminates in the production of chemokines (CXCL13), (683), proinflammatory (TNFα, IL-1β, IL-6, IL-12 and anti-inflammatory (IL-10) cytokines (671, 679-681, 684-687), resulting in the production of Nitric Oxide (688, 689).

TLR-4 sensing of LPS involves the binding of CD14 and LBP (LPS Binding Protein) to enable signal transduction and TLR dimerization. Spirochaetal lipoproteins are reported to bind macrophage CD14 at the same site as LPS and activate monocytes through the TLR-4 NFκB pathway (675, 685, 690). Lipid Binding Protein (LBP), which usually aids the binding of TLR-4 to Lipid A (60)), does not mediate this interaction (669, 675).

Leptospira interrogans does have an LPS layer, which is very atypical for *Leptospira spp.,* which is detected by the host via TLR-2 and CD14 binding rather than the conventional TLR4 LPS detection pathway (691).

In summary, spirochaetal lipoproteins are recognised through TLR2, activating the NFκB pathway and upregulating macrophage production of pro-inflammatory cytokines, such as TNFα, IL-1, IL-6, IL-12 (671, 689). This is similar to the response to *Bdellovibrio*, where the types of TLR-associated gene expression induced in macrophages (namely *tlr2* and *pglyrp2*) suggests that the main surface ligands that are detected are peptidoglycan and/or lipoproteins. However, some signalling through TLR4 is seen in Spirochete recognition, which is not seen in our scenario considering how *Bdellovibrio* are recognised by macrophage.

In conclusion, U937 cells do not mount a transcriptional response suggestive of detection of *Bdellovibrio* LPS via TLR-4 or the recognised LPS-recognition pathways. *Bdellovibrio* LPS may be recognised by host TLR-4 but does not induce an upregulation of TLR-4 expression. The absence of a significant response to LPS is supported by an absence of (significant) differential gene expression of LBP and LITAF also. I suggest that this is due to the atypical LPS of *Bdellovibrio* containing an unusual α-δ-mannose group in place of the 1' and 4' phosphate groups, reducing the negative charge of Lipid A and giving a reduced binding affinity with host TLR-4 (Figure 5.6.5), subsequently not stimulating additional *tlr4* transcription. I cannot comment on whether LPS is be detected and recognised by existing surface TLR-4 molecules, throughout *Bdellovibrio* occupation. However, *Bdellovibrio* does not induce a significant upregulation of *tlr4* expression, suggesting that the response to *Bdellovibrio* LPS is minimal (Figure 5.6.5).

5.6.2.4. Detection of flagellin

TLR-5 detects conserved dipeptides at the N- and C-termini of bacterial flagellin, that are key to flagellar assembly and motility and are therefore indispensable, even if the rest of the flagellar composition is highly variable (87-89). The main recognition site on bacterial flagellins (for TLR-5 recognition) lies between amino acids 89 and 96 (36).

I aligned the 6 *Bdellovibrio* FliC proteins (FliC1-6; Q5W1M9, Q6H8R6, Q6H8R4, Q6H8R2, Q6H8R3, Q6H8R5 respectively) with *Bdellovibrio* FlaA (Q6MQQ2) and FliC from *Salmonella* Typhimurium (P06179) using Clustal Omega. The FliC N-terminal domain (Figure 1.6.2; blue bar) and FliC C-terminal domain (Figure 1.6.2; orange bar) align well with *S.* Typhimurium FliC, but the variable region in-between these two domains is much larger in *S.* Typhimurium FliC (approximately 226 Amino Acids c.f. Approximately 45 Amino acids (*Bdellovibrio* FliC1-6)), so I excluded this from my alignment. More significantly, the TLR-5 recognition domain (Amino acids 89-96; Figure 1.6.2; red box and enlarged below), is present and highly conserved in *Bdellovibrio* FliC proteins, and with *S.* Typhimurium FliC, indicating that *Bdellovibrio* flagellins should be recognised by host TLR-5.

5.6.2.4.1. Detection of flagellin in other Gram-negative bacteria

As the flagellum of *B. bacteriovorus* is sheathed by a lipid outer membrane (307, 308) and therefore, potentially masked from recognition by the host (36), we asked if we see a transcriptional TLR-5 response in bacteria where their flagellum is also masked, either by a membranous sheath or due to it being located between their inner and outer membranes.

In *Vibrio cholera* infection, TLR-5 stimulation and NFκB activation (post-translationally) by the sheathed flagellum is significantly less than stimulation/activation by the unsheathed flagellum of *S. typhimurium*, despite the individual flagellin monomers being equally immunogenic (371). Reduced TLR-5 activation is due to flagellin monomer dissociation from the flagellar fibre being greatly reduced in the sheathed flagellum of *V. cholerae*, preventing flagellin shedding and TLR-5 activation, aiding the evasion of flagellin-triggered host innate immune responses (371).

Other pathogens, *Brucella spp.* and *Helicobacter pylori,* also activate TLR-5 less due to the membranous sheath present on their flagella (372-375). Additionally, *Helicobacter pylori* flagellins are non-stimulatory (don't stimulate TLR-5 production or IL-8 protein expression) despite having a high protein sequence similarity to flagellins of other Gram-negative bacteria (692). The mechanism behind this is currently unknown, although it is suggested that steric hindrance and blocking of the N-terminal recognition site on *H. pylori* flagellins prevents recognition by TLR-5 (692).

Conversely, the flagella of *Treponema pallidum* are located in the periplasmic space, between the inner and outer membrane, potentially masking the flagellins from recognition by the host TLR-5 (693), analogous to how *Bdellovibrio* flagellins may be masked from recognition by the membranous flagellar sheath. The flagellin monomers that comprise the flagellum are highly homologous to the flagellins that make up the flagella of other Gram-negative bacteria, including *Salmonella typhimurium* and *Pseudomonas aeruginosa* (694, 695). *T. pallidum* flagellins induce IL-6 and IL-8 expression at both the mRNA and protein level (tested by qPCR and ELISA respectively), with mRNA expression peaking at 24 hours post-infection and protein levels reaching their highest at 48 hours post-infection. Flagellin detection and interleukin release occurs via TLR-5 ligation, triggering MYD88 recruitment and downstream MAPK and NFκB signalling (696-698).

Other spirochetes, for example *Leptospira spp.,* also induce a TLR5-flagellin response (699). *Borrelia burgdorferi* expresses immunogenic flagellins that bind to TLR5, however lipoprotein detection by TLRs -1 and -2 suppresses the TLR-5-Flagellin response (700, 701), demonstrating the impact of TLR crosstalk in the wider immune response.

5.6.2.4.2. Detection of flagellin in Bdellovibrio bacteriovorus occupation of macrophage

In our dataset, significant upregulation of *tlr5* transcription at 2 hours suggests that detection of *Bdellovibrio* flagellins by TLR-5 occurs within 2 hours post-uptake and remains throughout 4 and 8 hours of *Bdellovibrio* occupancy, decreasing at 24 hours (Figure 5.6.5). This suggests that flagellins are one of the predominant groups of microbial ligands detected by macrophage when recognising *Bdellovibrio*. This is unusual due to the single, polar flagellum of *Bdellovibrio* being sheathed in a lipid membrane (307), masking flagellin from TLR-5 detection. The TLR-5 mediated detection of flagellins in our dataset may be due to a dissociation of the flagellum from *Bdellovibrio,* as a reduction in TLR-5 response is seen in *V. cholerae* where the flagellum does not dissociate and trigger a TLR-5 response (371).

Alignments of *S.* Typhimurium FliC with *Bdellovibrio* flagellins shows that the region of flagellin that TLR-5 recognises is largely similar in *Bdellovibrio* when compared to the flagellins of other Gram-negative bacterial pathogens, supporting why we see a strong TLR5/flagellin response in *Bdellovibrio* occupation of macrophage (Figure 5.6.5).

Flagellins may also be detected post-internalisation by Ipaf (a NOD-like Receptor) and Naip5 (NLR Family Apoptosis Inhibitory Protein 5), triggering caspase-1 inflammasome activation, IL-1β and IL-18 maturation and cell pyroptosis (702, 703). The differential expression of *ipaf* and *naip5* genes is not captured in our data set.

CCL20 is a chemokine specifically triggered by flagellin and TLR5 ligation (704). In our dataset, we see upregulation of *ccl20* gene expression throughout *Bdellovibrio* occupation of macrophage (Figure 5.6.12), confirming the detection of *Bdellovibrio* flagellin throughout occupation.

In conclusion, TLR-5 mediated detection of *Bdellovibrio* flagellins occurs early on in *Bdellovibrio* occupation and continues throughout the early stages of infection (4- and 8-hours post-uptake). Detection of *Bdellovibrio* flagellins may be prevented by the membrane sheath surrounding the flagellum, as seen in some other Gram-negative bacteria, but non-specific lysis of *Bdellovibrio* upon uptake by macrophage may expose flagellin to TLR-5 detection early on in occupancy.

Kaplan and co-workers (309) have shown that, after entry into Gram-negative prey, the flagellum retracts into the *Bdellovibrio* upon entry. Potentially, upon entry into macrophage, *Bdellovibrio* may shed or retract their flagellum due to recognising they are inside another cell, leading to flagellar shedding and flagellin dissociation, increasing the detection of *Bdellovibrio* flagellins by TLR-5.

5.6.2.5. Detection of bacterial nucleic acids

TLR-3 typically responds to viral dsRNA. Increasing evidence suggests that TLR-3 may also detect bacterial RNA. TLR-3 is an endosomal PRR, therefore it is not involved in the initial uptake response but will sample the contents of the endosome after initial bacterial lysis, to detect bacterial RNA (52).

In our dataset, *tlr3* transcription is significantly upregulated by the presence of *Bdellovibrio* at 2, 4 and 24 hours, compared to downregulation of *tlr3* at 8 hours (Figure 5.6.5). The transcription of *ticam1* (Toll like receptor adaptor molecule 1), which transduces the signal from TLR-3 to amplify the immune response, is also upregulated at 4 and 24 hours (Figure 5.6.5).

TLR-7 responds to synthetic viral components, but may also recognise bacterial RNA in lysosomes, initiating the interferon response and targeting mitochondria to phagolysosomes to induce increased ROS production and autophagy (38, 103). Transcription of *tlr7* is upregulated at 4 hours, before decreasing at 8 and 24 hours (Figure 5.6.5), suggesting a role in amplifying the immune response and proinflammatory signalling when *Bdellovibrio* is present in the phagolysosome.

TLR-8 responds to bacterial ssRNA. Transcription is downregulated at 4 hours, in response to *Bdellovibrio*, before returning to pre-uptake levels at 24 hours (Figure 5.6.5). Despite being mainly implicated in the detection of viruses, TLR-8 has been documented to detect *Staphylococcus aureus* in monocyte-derived macrophage and induce a TNFα mediated response (705-707). However, expression is inhibited by surface TLRs, maybe explaining why transcription is downregulated at 4 hours when peptidoglycan detection (thus *tlr1, tlr2* and *tlr6* transcription) is high (Figure 5.6.5).

TLR-9 responds to unmethylated CpG containing dsDNA, therefore amplifying the response to bacteria further. In our dataset, *tlr9* gene transcription is significantly upregulated early on in *Bdellovibrio* macrophage occupancy, at 2 and 4 hours, before transcription decreases later in occupation (8 hours and 24 hours) (Figure 5.6.5). TLR-9 detects nucleotides and CpG-methylated dsDNA, therefore non-specific lysis of *Bdellovibrio* must have occurred to expose DNA to host macrophage TLR-9. TLR-9 is an endosomal PRR, suggesting lysis must occur promptly after uptake. This response is faster than the TLR-2 response to peptidoglycan, suggesting that nucleotides are one of the first major bacterial ligands to be detected by macrophage during *Bdellovibrio* occupancy.

In conclusion, U937 cells detect *Bdellovibrio* dsRNA and dsDNA at the early stages of *Bdellovibrio* occupation (2 hours post-uptake), with a sustained response to bacterial dsRNA also present later in *Bdellovibrio* occupation.

5.6.2.6. Antagonism of the immune response.

TLR-10 responds to diacylated lipopeptides and LPS ligands, whereby it forms a complex with TLR-2 and prevents NFκB activation and signalling. It is an anti-inflammatory TLR that modulates NFκB activation in response to peptidoglycan and limits TLR-2 mediated amplification of the immune response (708). In our dataset, transcription of *tlr10* is low at 4 hours, but upregulated at 8 and 24 hours, potentially curtailing the immune response at later stages of *Bdellovibrio* occupation (Figure 5.6.5).

5.6.2.8. Summary: Detection of Bdellovibrio surface ligands by macrophage

In summary, we see initial transcriptional evidence for a macrophage response to flagellin and nucleotides in *Bdellovibrio* occupancy, followed by transcriptional evidence of stronger and more sustained response to flagellin and peptidoglycan from 4 hours onwards. A response to RNA at 4 and 8 hours is also seen but is not sustained (Figure 5.6.5). The PRR recognition that prompts uptake/phagocytosis is unknown, as the surface TLRs upregulated in this study are only activated later in occupancy. As stipulated earlier, an absence of differential expression for TLR genes does not mean that the TLRs don't recognise their respective ligands throughout *Bdellovibrio* occupation of macrophage. Recognition of a bacterial ligand, without a subsequent upregulation of TLR gene expression, suggests that no significant response to that ligand is initiated. However, from work performed by Raghunathan and co-workers, we know that uptake initiated through opsonisation does not play a major role in *Bdellovibrio* uptake, therefore Pattern Recognition Receptors (and recognition) are likely to be important in the early stages of *Bdellovibrio* macrophage interactions. Most importantly, we see no transcriptional evidence of a response to LPS within *Bdellovibrio* occupancy potentially due to the diversity of Lipid A structure in *Bdellovibrio* compared to other Gram-negative bacteria, where we see an atypical mannosylated Lipid A head group (301). Whilst this has been suggested and speculated upon previously, this has never been conclusively analysed and reported and therefore warrants further investigation due to the LPS TLR-4 response being one of the key responses usually involved in the initial recognition of other Gram-negative bacteria, and which is missing in *Bdellovibrio*, which persist for longer in macrophage.

A summary of how *Bdellovibrio* is recognise by macrophage, based on these data, is depicted in Figure 5.6.6.

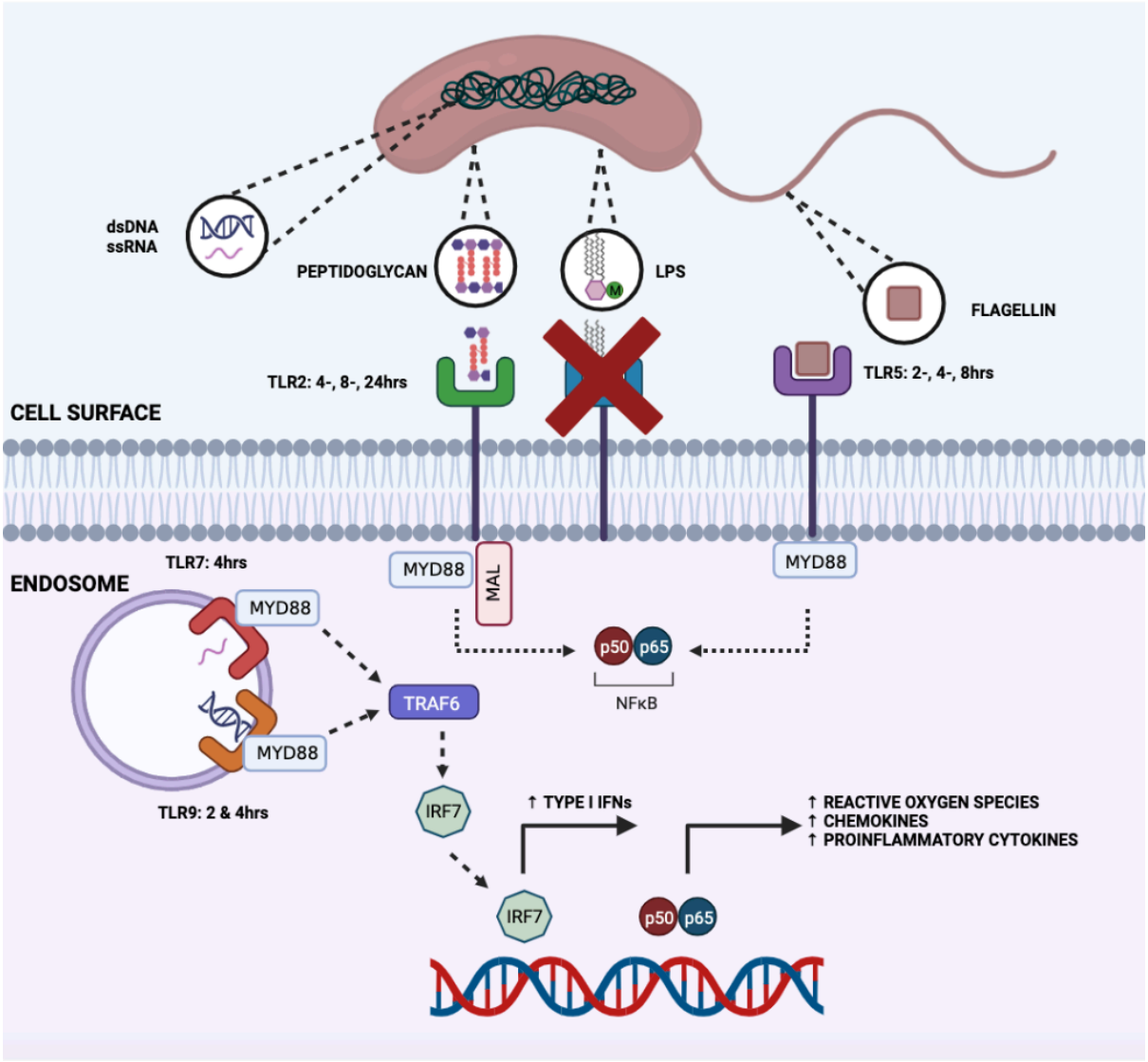

Figure 5.6.6: A schematic summarising transcriptional evidence documenting how *Bdellovibrio bacteriovorus* is, and is not, recognised by host macrophage. Initially, at 2 hours post-uptake, macrophage recognise flagellin and dsDNA (double stranded DNA) via TLR5 and TLR9 respectively. At 4 hours post-uptake, the host recognises ssRNA (single stranded RNA) and peptidoglycan, via TLR7 and TLR2 respectively, along with the continual recognition of dsDNA and flagellin. At 8 hours post-uptake, flagellin and peptidoglycan are still actively recognised, with TLR2 continuing to be upregulated for the remainder of *Bdellovibrio* occupation. Red cross indicates the lack of a typical recognition pathway.

5.6.3. What oxidative stresses are *Bdellovibrio*, and the host exposed to during macrophage occupation?

Oxidative stress is known to be increased and to contribute to antimicrobial killing in infection. The host can generate a range of reactive intermediates to combat infection but must also be able to tolerate an increase in oxidative stress itself. Reactive oxygen intermediates (ROIs) are generated as part of the normal respiratory activities of a cell, through fatty acid metabolism and the functions of the respiratory electron transport chain, therefore cells encode inherent oxidative stress tolerance pathways to detoxify and remove such radicals. ROIs are both antimicrobial and act as powerful regulatory cues for the proinflammatory response. During infection, an increased requirement for ATP and protein production to fuel membrane and cytoskeletal rearrangements and produce immunity-related and antimicrobial proteins, leads to increased mitochondrial activity and ROI production. The production of ROIs may also be purposefully upregulated to target bacteria during infection, predominantly through the action of NADPH Oxidase.

The oxidative stresses within host cells will also be altered and impacted by the oxidative activities of the in-dwelling *Bdellovibrio,* therefore we must consider the interplay between the oxidative activities of the host cell, the oxidative stresses purposefully upregulated by the host cell due to infection, and the detoxification mechanisms used by both the host and bacteria to combat oxidative stresses.

I have examined the transcription of genes within various oxidative stress related generation and tolerance pathways, within my RNASeq dataset. The various approaches to generating or combatting oxidative stress within host macrophage are detailed below.

5.6.3.1. Reactive Oxygen & Nitrogen Species

One subset of reactive oxygen intermediates that causes oxidative stress within cells are reactive oxygen species. These include oxygen radicals ($O_2^{\cdot -}$). A group of enzymes called superoxide dismutases are one means of detoxifying oxygen radicals.

5.6.3.1.1. Superoxide dismutases

As discussed earlier, superoxide dismutases convert highly reactive oxygen radicals into more toxic, but less reactive, hydrogen peroxide and diatomic oxygen. Conversion of oxygen radicals and reactive oxygen species (ROS) into hydrogen peroxide prevents oxygen radicals from reacting with host proteins and DNA, causing mutations or protein dysfunction. Superoxides may also react with other ROS to form secondary radicals. Three mammalian SODs exist. SOD1 is a cytoplasmic Copper-Zinc superoxide dismutase that breaks down reactive oxygen species that are produced as part of the normal respiratory activities of the cell. SOD2 is a Manganese superoxide dismutase that is localised to the mitochondrial matrix, at the sites of complex I, III and IV of the electron transport chain, where ROS are most highly produced (709). SOD3 is an extracellular Cu/Zn SOD located at the eukaryotic cell surface (710).

sod1 is not differentially expressed throughout *Bdellovibrio* macrophage occupancy, suggesting cytoplasmic ROS is not increased (Figure 5.6.7). *sod2* gene expression is highly upregulated throughout occupancy, with the highest expression occurring at 4 hours post-uptake (Figure 5.6.7). *sod2* transcription is within the highest 0.1% of transcriptionally upregulated genes at 8 hours also. *sod2* gene expression is upregulated through TLR-2, -3, -4, -7 and -8 activation, through the NFκB binding site present on the *sod2* promoter (711, 712), and expression of the pro-inflammatory cytokines IL-1β, TNFα (713), IL-6 (714) and IL-1 (712). P53 inhibits *sod2* expression, inducing apoptosis in some eukaryotic cells (715). SOD2 protein upregulation has been demonstrated to be important in infection (716, 717) and in the PMA-induced respiratory burst (718, 719). These data suggest that superoxide/oxygen radicals are highest at 4 hours post-uptake.

In *P. aeruginosa* infection of zebrafish, Host SOD2 acts as a proinflammatory cue, increasing leukocyte recruitment, whilst protecting phagocytes from the negative effects of ROS due to increased mitochondrial activity during infection (709). Upregulation of *sod2* gene expression (by quantitative PCR; dHL-60 Neutrophil-like and RAW264.7 murine macrophage-like cells) in response to LPS was also seen at 3, 6 and 24 hours (709). *sod2* gene expression is also shown to be upregulated in *Leishmania donovani* infection (720) and *Mycobacterium tuberculosis* infection (721, 722). In other (viral) infections, SOD2 regulates the proinflammatory immune response by upregulating (directly, or indirectly through decreased ROS levels) RIG-1 like receptor induced IFR3 and NFκB activation and signalling, resulting in a reduction in Interferon and proinflammatory cytokine production (249). It has also been suggested that the host may target mitochondrial vesicles containing SOD2 to the phagosome to enhance the conversion of oxygen radicals to the more toxic hydrogen peroxide (723).

5.6.3.1.2. NADPH Oxidase

ROS may also be produced through the NADPH oxidase complex assembly in the phagosomal membrane, catalysing the transfer of electrons to molecular oxygen to form ROS and oxygen radicals. NADPH Oxidase Activator 1 (NOXA1) induces NADPH oxidase complex formation. In our dataset, *noxa1* gene expression is upregulated in the initial stages of occupancy (2 hours post-uptake) and downregulated later (8 hours) (Figure 5.6.7). NADPH oxidase organiser 1 gene expression is downregulated during the early stages of occupancy (2 hours post-uptake) and at 8 hours, but is upregulated at 4 hours and 24 hours, with gene expression being highest at 24 hours post-uptake (Figure 5.6.7). NADPH oxidase 5 gene expression is upregulated at 2 hours and 24 hours post-uptake, but lower throughout 4- and 8-hours post-uptake (Figure 5.6.7). These data suggests that NADPH Oxidase-mediated production of ROS is upregulated initially during *Bdellovibrio* occupancy (at 2 hours), potentially as an initial bactericidal assault, and then at 24 hours post-uptake for further microbicidal killing, perhaps subsiding at 4 and 8 hours to allow for further sampling and processing of microbial antigens.

5.6.3.1.3. Nitric Oxide Synthase

Reactive Nitrogen Species (RNS) are also produced during infection, and similarly react with host and bacterial DNA and proteins causing oxidative killing. RNS are produced by the host through Nitric Oxide Synthase (NOS) complex formation. During *Bdellovibrio* occupancy, the expression of the genes encoding NOS1 and NOS3, and their associated proteins NOA1 (Nitric Oxide Associated 1), NOS1AP (Nitric Oxide Synthase 1 Adaptor Protein), NOSIP (Nitric Oxide Synthase Interacting Protein) and NOSTRIN (Nitric Oxide Synthase Trafficking) is not influenced by the presence of *Bdellovibrio* (Figure 5.6.7). The expression of the gene *nos3* is downregulated by the presence of *Bdellovibrio* at 4 and 8 hours and is upregulated at 24 hours compared to earlier timepoints (2, 4 and 8 hours) (Figure 5.6.7). Expression of *nos1ap* gene is upregulated at 8 and 24 hours compared to 2 hours and 4 hours respectively, indicating that some generation of RNS may occur (Figure 5.6.7).

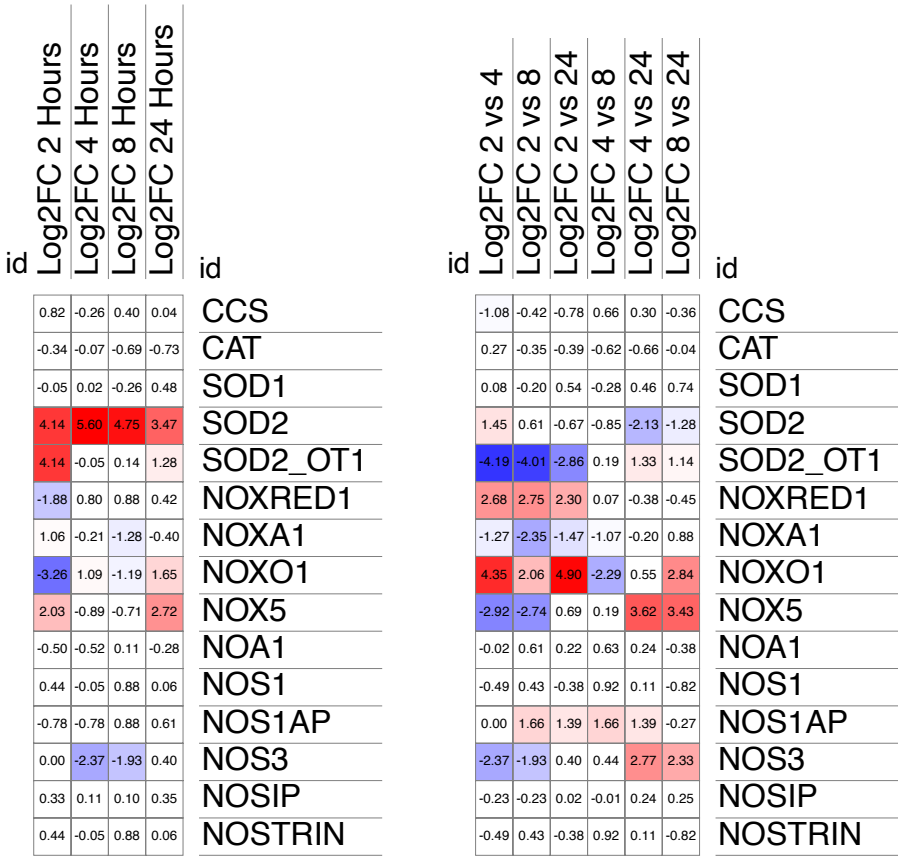

Figure 5.6.7: A heatmap visualising the expression of genes related to the oxidative stress response throughout *Bdellovibrio bacteriovorus* occupation within PMA-differentiated U937 macrophage-like cells. Values shown represent the Log_2 function of the ratio of gene expression values of *Bdellovibrio*-containing U937 cells, compared to cell-only controls, at 4 timepoints across a 24-hour period (left). Values shown represent the Log_2 function of the ratio of gene expression values of *Bdellovibrio*-containing U937 cells at each chosen timepoint, relative to each of the other 3 timepoints within this study (right). CCS: Copper Chaperone for Superoxide Dismutase; CAT: Catalase; SOD: Superoxide Dismutase; SOD2_OT1: Superoxide Dismutase 2 Overlapping Transcript 1; NOXRED1: NADP Dependent Oxidoreductase Domain Containing 1; NOXA1: NADPH Oxidase Activator 1; NOXO1: NADPH Oxidase Organiser 1; NOX5: NADPH Oxidase 5; NOA1: Nitric Oxide Associated 1; NOS1: Nitric Oxide Synthase 1; NOS1AP: NOS1 Adaptor Protein; NOS3: Nitric Oxide Synthase 3; NOSIP: Nitric Oxide Synthase Interacting Protein; NOSTRIN: Nitric Oxide Synthase Trafficking Protein. Heatmaps were generated using Morpheus.

5.6.3.2. Peroxide based stress.

Another reactive oxygen intermediate, responsible for oxidative stress within the host cell during infection is hydrogen peroxide, a highly toxic and diffusible molecule, formed by the reaction of superoxide radicals with water or other compounds, that can react with and mutate host and bacterial proteins, DNA and lipids, resulting in cell death. The host assembles organelles, termed peroxisomes, which contain multiple peroxidase enzymes, with the purpose of detoxifying hydrogen peroxide. One of the main forms of detoxifying hydrogen peroxide is via the actions of catalase enzymes.

5.6.3.2.1. Catalases

Catalases are one of the predominant anti-peroxide enzymes in the cell, localising with peroxisomes and combatting oxidative stress. Catalases contain a haem group that converts hydrogen peroxide into water and oxygen. With infection comes an increase in ROI production and oxidative stress, therefore catalase expression is typically upregulated in infection (188, 724-726).

Beyond catalysing the detoxification of hydrogen peroxide, catalases also act as a form of, and influence, immune signalling throughout infection. Catalase expression regulates polarisation of macrophage, limiting inflammation, ROS toxicity and proinflammatory cytokine production to avoid an excessive proinflammatory response (727). Overexpression of catalase has been reported to increase NFκB activation, upon LPS stimulation, leading to a hyper-inflammatory response involving increased ROS and proinflammatory cytokine production (728). Whereas catalase knockout mutants show an enhanced proinflammatory macrophage polarisation response characterised by inflammation, high levels of ROS and high proinflammatory cytokine release (727). This suggests that catalases or ROS levels do feedback into the amplification and balancing of the immune response.

In our data set, catalase gene expression is not significantly altered due to the presence of *Bdellovibrio* or throughout *Bdellovibrio* occupancy (Figure 5.6.7). This alone suggests that hydrogen peroxide stress is not increased during *Bdellovibrio* occupancy. However, the cell also detoxifies hydrogen peroxide using other peroxidase enzymes, including myeloperoxidases, perioredoxins, lactoperoxidases and glutathione peroxidases (729), which I will also explore.

5.6.3.2.2. Peroxidases

Peroxidasin is a peroxidase enzyme that detoxifies hydrogen peroxide and aids the cellular response to oxidative stress. Peroxidasin expression is induced by LPS and TNFα (730). Peroxidasin also has a direct antimicrobial effect in *P. aeruginosa* infection, where the N-terminus binds to LPS, whilst the C-terminus catalyses the conversion of hydrogen peroxide into toxic hypophalous acids (730). Peroxidasin also acts as an anti-inflammatory cue, alternatively activating macrophage in helminth infection (731).

In our dataset, the expression of the gene encoding peroxidasin is downregulated in *Bdellovibrio* occupancy at 8 hours (c.f. cell-only controls and *Bdellovibrio*-containing 2 hour and 4-hour timepoints), but is upregulated at 24 hours, indicating a role later in occupancy, potentially in *Bdellovibrio* killing (Figure 5.6.8).

Other peroxidases involved in the detoxification of hydrogen peroxide include myeloperoxidases, a family of haem-based peroxidases that produce the toxic substrate hypochlorous acid. In our dataset, expression of the gene encoding myeloperoxidase in *Bdellovibrio* occupancy is downregulated at 2, 4 and 24 hours (Figure 5.6.8). Myeloperoxidase protein expression is typically highly upregulated in inflammation (732), so this possibly suggests that the phagosome is not inflammatory at these stages. Although U937 cells are typically low expressing for myeloperoxidases (732), we see clear downregulation of expression during *Bdellovibrio* macrophage occupation (Figure 5.6.8).

Glutathione peroxidases 1-4 are also expressed in eukaryotic cells to protect against oxidative stress. Their roles in the inflammatory response are debated, with some suggestions that they are anti-inflammatory and regulate antigen presentation (733) and others suggesting that Gpx1 responds to LPS challenge by upregulating proinflammatory cytokine production (734). Potentially GPXs may fulfil both roles, fine-tuning the immune response throughout infection (735).

In our dataset, *gpx1* expression is downregulated at 4 and 8 hours compared to 2 hours, whilst *gpx3* expression is upregulated at 4 hours and downregulated at 8 hours due to the presence of *Bdellovibrio* (Figure 5.6.8). *gpx3* expression is then upregulated at 24 hours compared to 2 hours post-uptake, suggesting *gpx3* expression cycles throughout *Bdellovibrio* macrophage occupancy. *gpx4* expression is not significantly influenced by or throughout *Bdellovibrio* occupancy (Figure 5.6.8).

Lactoperoxidases are haem containing peroxidases typically found in milk, tears, saliva and in the respiratory tract mucosa (736). In our dataset, Lactoperoxidase gene expression is upregulated at 24 hours due to the presence of *Bdellovibrio*. This could indicate an increased peroxide stress due to 24-hour killing or may be a generalised response to bacterial killing and late stage phagosomal maturation (Figure 5.6.8).

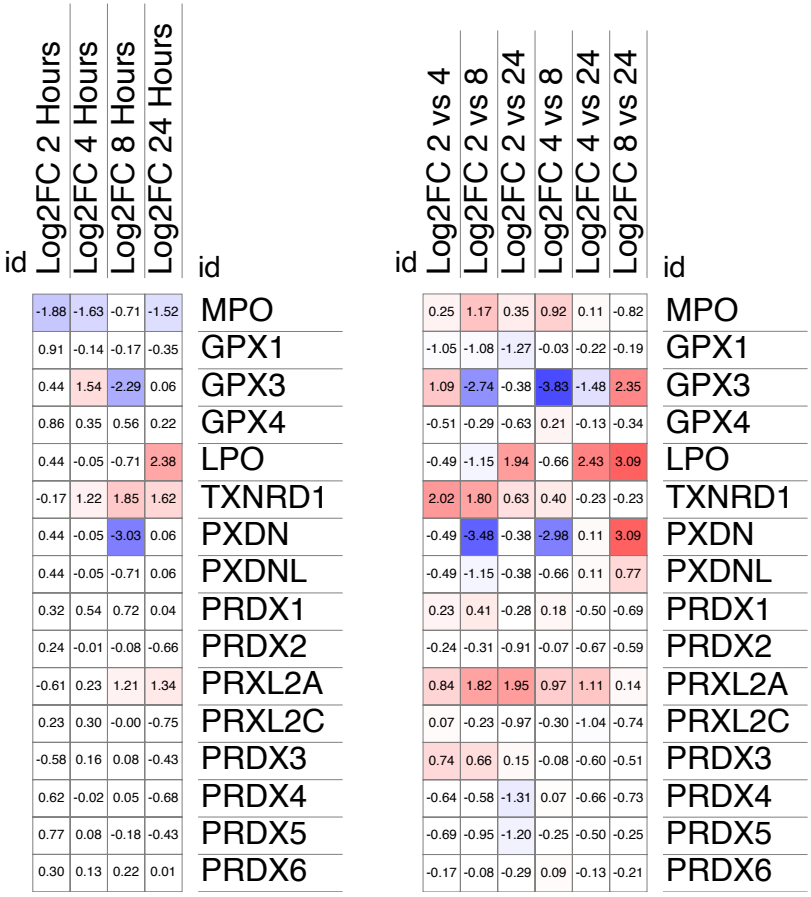

Figure 5.6.8: A heatmap visualising the expression of genes related to peroxide-related oxidative stress throughout *Bdellovibrio bacteriovorus* occupation within PMA-differentiated U937 macrophage-like cells. Values shown represent the Log_2 function of the ratio of gene expression values of *Bdellovibrio*-containing U937 cells, compared to cell-only controls, at 4 timepoints across a 24-hour period (left). Values shown represent the Log_2 function of the ratio of gene expression values of *Bdellovibrio*-containing U937 cells at each chosen timepoint, relative to each of the other 3 timepoints within this study (right). MPO: Myeloperoxidase; GPX: Glutathione Peroxidase; LPO: Lactoperoxidase; TXNRD1: Thioredoxin Reductase 1; PXDN: Peroxidasin; PXDNL: Peroxidasin Like; PRDX: Peroxiredoxin; PRXL2A: Peroxiredoxin Like 2A;. Heatmaps were generated using Morpheus.

Peroxiredoxins

Peroxiredoxins are another group of peroxidases that contribute to the tolerance of oxidative stress within the cell but may also play a role in combatting infection. Peroxiredoxins are upregulated at the mRNA and protein level in response to IFN-γ and LPS (737), and have a tripartite role in the cell, modulating redox signalling and protecting the cytoplasm of the cell during inflammation or increased ROS exposure, signalling as DAMPs (Damage Associated Molecular Patterns) to regulate inflammation through TLR binding and activation, and their direct bactericidal activity (738).

PRDX-like 2a suppresses the MAPK signalling pathway, reducing the production of proinflammatory cytokines by macrophage (739). In our dataset, the gene encoding PRDXL2a is upregulated at later stages of occupancy (8 and 24 hours) (c.f. cell-only controls and 2 hour and 4-hour timepoints respectively) (Figure 5.6.8), potentially curtailing the pro-inflammatory nature of the immune response later in *Bdellovibrio* occupation.

PDRX2Lc mediates ERK1/2 signalling and AKT1 activation, inducing the upregulation of HIF1α and enhanced glycolysis (739). In our dataset, PDRXL2c gene expression is downregulated at 24 hours post-uptake (c.f. 4 hours) (Figure 5.6.8). Combined, this may represent part of the host response to de-escalate the proinflammatory immune response after *Bdellovibrio* killing.

PDRX1 induces c-Rel and activates p38 MAPK signalling, increasing IL-12 expression and nitric oxide production, whilst decreasing arginase-1 production, shifting the activation state of the cell to a more pro-inflammatory state during *Mycobacterium tuberculosis* murine infection (740). PDRX1 also contributes to combatting *S. aureus* infection (741). Independent of the peroxidase activity, PDRX1 acts as a DAMP/stress signal and a signal of infection (activated by TLR-4: LPS binding), culminating in the upregulation of IL-6 and TNFα in macrophage, balancing the expression of immunoregulatory IL-10 (742). In our dataset, the gene encoding PDRX1 is not differentially expressed throughout occupancy, possibly due to a lack of TLR4 activation (Figure 5.6.8).

PDRX2 is ubiquitously present in most cell types, in a reduced state. LPS stimulation triggers an increase in *pdrx2* transcription via NFκB activation and triggers post-translational modification via PDRX2 glutathionylation (into its active state) and release, increasing TNFα expression. A thioredoxin substrate is also released, to aid the detoxification of hydrogen peroxide present (743). SRXN1 sulfioredoxin also activates PDRX2 by forming a transient disulphide bond and reducing the cysteine sulfenic acid residue (744, 745). In our dataset, the gene encoding PDRX2 is not differentially expressed throughout *Bdellovibrio* infection (Figure 5.6.8). However, in our dataset, expression of *srxn1* is upregulated at 4, 8 and 24 hours compared to 2 hours post-uptake (Figure 5.6.8), suggesting that PDRX2 may be present within the cell in a non-active state and that post-translational modification/activation of PDRX2 may occur at later timepoints to combat peroxide stress.

PDRX4 regulates NFκB activation in the cytosol by modulating MAP3K13 signalling and Iκβα phosphorylation respectively (746).

PDRX5 expression is upregulated by LPS: TLR binding, signalling through MAPK and the TRIF dependent/IFN independent pathway or by T-helper 1 IFNγ pathways, increasing *pdrx5* expression via MyD88 and TNF dependent pathway (747). PDRX5 also modulates the ROS signalling cascade, inducing NO production through JNK-dependent pathway, and limiting IL-6 production, signalling via the JAK/STAT pathway (748).

The expression of the genes encoding perioredoxins -1, -2, -3, -4 and -5 in *Bdellovibrio* occupancy is not significantly altered throughout stages of macrophage occupation (Figure 5.6.8), suggesting that they are not recruited/involved in bacterial killing in this scenario, or that they are constitutively present in a non-active state within the cell, and therefore mRNA levels and transcription will not increase in response to stimuli. As the majority of the peroxiredoxins are largely stimulated by LPS detection, and we see no upregulation of a TLR-4 response to *Bdellovibrio*, this may explain the lack of perioredoxin expression in this scenario.

Bioinformatic analyses revealed that SXRN1 is also co-expressed with glutathione reductase (*gsr),* Thioredoxin (*tsr*), Thioredoxin Reductase (*txnrd*) and *pdrx1-5* (STRING). The absence of differential expression for the genes encoding Peroxiredoxins 1-5 may also be explained by them potentially being present within the cell in a reduced/inactive state and are then post-translationally activated in response to infection or LPS stimulation.

When PDRX molecules react with hydrogen peroxide, the cysteine residue in the enzyme active site is weakly oxidised to disulphide or sulfenic acid. This renders PDRX inactive and unable to detoxify further hydrogen peroxide molecules. Thioredoxins reduce the cysteine residue, reactivating the PDRX enzyme, and are then themselves reduced by NADPH, in combination with thioredoxin reductase (744, 745). Reactivation of PDRX2 is the quickest of the PDRX enzymes and provides better protection against hydrogen peroxide than catalase or glutathione peroxidases. In our dataset, thioredoxin reductase 1 (*txnrd1*) gene expression is upregulated at 4-, 8- and 24-hours post-uptake (Figure 5.6.8). *txnrd2* and *txnrd3* gene expression is not significantly altered by *Bdellovibrio* occupancy (Figure 5.6.8). Thioredoxin (*tsr*) expression is not significantly altered throughout *Bdellovibrio* occupancy (Figure 5.6.8). However, it may be constitutively present within the cell, as it may play other roles within cell functioning e.g., in protein phosphorylation. The upregulation of *txnrd1* expression later in *Bdellovibrio* occupation may suggest peroxide stress is present later in *Bdellovibrio* occupancy (Figure 5.6.8).

5.6.3.3. Summary

In summary, some peroxide based oxidative stress seems to be present due to *Bdellovibrio* occupation of macrophage. The exact mechanisms through which hydrogen peroxide (or similarly toxic intermediates) are generated and tolerated throughout *Bdellovibrio* occupation remain largely unknown. Downregulation of peroxide stress tolerance/detoxifying enzymes may represent a decrease in oxidative stress, or a purposeful increase in oxidative species for bacterial killing.

5.6.4. How is cellular apoptosis differentially regulated throughout *Bdellovibrio* occupation of macrophage?

Raghunathan and co-workers (2) did not detect any significant (U937) cell death in their paper, so I will not discuss whether cellular apoptosis is transcriptionally induced/differentially regulated here, although I did consider this.

There is a large crossover and redundancy within the TNFα/TNF-Receptor signalling pathways, and within the functions of different Pellino E3 Ubiquitin Ligases, Inhibitor of Apoptosis Proteins (IAPs) and other apoptotic regulator proteins in both cell death/apoptosis signalling and the TLR/NFκB signalling pathways, therefore although some proteins were differentially regulated throughout *Bdellovibrio* Macrophage occupation, there are no distinct trends suggesting a tendency towards or away from apoptosis, in response to *Bdellovibrio*, in my dataset.

5.6.5. The roles of interferon signalling in *Bdellovibrio* macrophage occupation

Interferons are signalling proteins initially implicated in the response to viral infection, recruiting macrophages, neutrophils and dendritic cells which then mount a further, proinflammatory immune response, killing the microorganism and restoring tissue homeostasis. Their role has now been extended to bacterial infection and the wider immune response.

Three classes of interferons exist; Type I interferons include different isoforms of IFNα, a single isoform of IFNβ and other minor subtypes including IFNδ, IFNε and IFNκ.

5.6.5.1. Type I Interferons

Type I IFNs were originally believed to be predominantly produced by dendritic cells, acting via an autocrine mechanism to induce Dendritic cell activation, maturation, and migration (749). However, Type I interferons are produced by almost all cell types, including monocytes, macrophages, cells of myeloid lineage and epithelial cells. Type I IFN expression is induced by PRR- nucleic acid ligation and cytokine expression, through IRF3 and IRF7, although other IRFs may also contribute to expression. They are largely inflammatory, being produced by and acting on all cell types to enhance their function and survival (750). IFNβ is involved in the resolution of bacterial infection and inflammation, promoting cellular clearance and apoptosis when nearing the end of the immune response and upon resolution of infection (751).

In our dataset, expression of *ifnβ* is upregulated at 24 hours in *Bdellovibrio* occupation (Figure 5.6.9). Interferon epsilon is involved in immunoregulation and is typically expressed on mucosal surfaces to shield the commensal microbiota from a severe proinflammatory response (752). In our dataset, expression of *ifnε* is upregulated at 24 hours (Figure 5.6.9), potentially helping to curtail the inflammatory part of the immune response. The role if IFNκ in the immune response is largely unknown but, in our dataset, expression of *ifnκ* is upregulated at 4 and 24 hours (Figure 5.6.9).

5.6.5.2. Type II Interferons

Type II IFNs consist of IFNγ only (753). IFNγ is produced by T cells and NK cells mostly. Interferon Gamma (IFN-γ) is well characterised in the inflammatory immune response, where it primes macrophage to make them more pro-inflammatory and antimicrobial, upregulating nitric oxide production and repressing NLRP3 inflammasome activation. *ifnγ* expression is not detected in our dataset, but expression of *ifnγr1* and *ifnγr2,* the two subunits of the IFNγ receptor, are present within our dataset. Expression of *ifnγr1* is not differentially expressed throughout *Bdellovibrio* occupancy whereas expression of *ifnγr2* is upregulated at 4- and 24-hours post-uptake, potentially indicating some role for IFNγ in the immune response to *Bdellovibrio* (Figure 5.6.9). The lack of IFNγ expression in our dataset may suggest that IFNγ is constitutively present in a non-active state, or that a small transcriptional change can result in a large alteration in IFNγ protein abundance. Alternatively, the lack of a large IFNγ response by macrophage in response to *Bdellovibrio* is to be expected, as IFNγ is predominantly expressed by T cells and NK cells or may help emphasise the less-immunostimulatory nature of *Bdellovibrio.*

5.6.5.3. Type III Interferons

Type III interferons consist of IFN-λ isoforms 1-4, which are analogous to Type I Interferons in function but have a narrower cell range, with epithelial cells expressing IFNλ receptors (750). Although receptors for IFNλ are predominantly expressed on epithelial cells, IFNλ signalling still impacts macrophage function. IFNλ promotes phagocytosis, proinflammatory cytokine secretion and leukocyte recruitment through CCR5 and CXCR3 release (754). Expression of the gene encoding IFNλ is upregulated at 4 hours, whilst IFNλ receptor gene expression is downregulated at 2 hours, suggesting that the role of IFNλ begins at 4 hours post-uptake (Figure 5.6.9). Whether this has a biological or physiological effect in this system remains unknown.

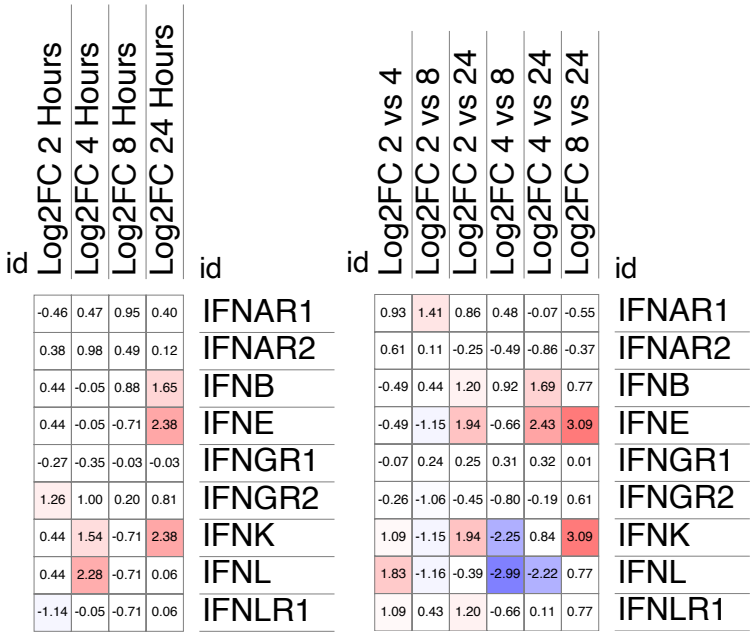

Figure 5.6.9: A heatmap visualising the expression of genes related to Interferon expression throughout *Bdellovibrio bacteriovorus* occupation within PMA-differentiated U937 macrophage-like cells. Values shown represent the Log_2 function of the ratio of gene expression values of *Bdellovibrio*-containing U937 cells, compared to cell-only controls, at 4 timepoints across a 24-hour period (left). Values shown represent the Log_2 function of the ratio of gene expression values of *Bdellovibrio*-containing U937 cells at each chosen timepoint, relative to each of the other 3 timepoints within this study (right). IFNAR1/2: Interferon Alpha and Beta Receptor Subunit 1/2; IFNB/E/K/L: Interferon Beta/ Epsilon/ Kappa/ Lambda; IFNGR1/2: Interferon Gamma Receptor 1/2; IFNLR1: Interferon Lambda Receptor 1. Heatmaps were generated using Morpheus.

5.6.5.4. Interferon Regulatory Factors

A family of interferon regulatory factors (IRFs) are also thought to have roles in regulating macrophage activation and polarisation.

IRF1 is lowly expressed in macrophage and dendritic cells, until ligation of the IFNγ receptor induces IFN1 expression. IFN1 is typically associated with the production of Type I interferons, TLR signalling via a MYD88 adaptor protein dependent pathway and proinflammatory gene expression, therefore it is associated with an M1 classical activation phenotype. IRF1 also suppresses binding of regulatory elements to the IL-4 promoter, suppressing alternative activation (755). In our dataset, the expression of the gene encoding IFN1 is upregulated at 2- and 4- hours post-uptake (Figure 5.6.10), suggesting an initiation of a M1, inflammatory activation profile.

IRF2 antagonises the actions of IRF1, competing for the IRF binding site on MYD88 and therefore negatively regulating Type I Interferon production. The downstream effects of IRF2 are context specific, where IRF2 binding decreases the release of TNFα in response to LPS, but promotes the release of IL-6, IL-12 and IFNγ, subsequently leading to reactive oxygen species generation and the iNOS-mediated oxidative burst. IRF2 also binds to STAT1 and STAT3 transcription factors, inhibiting downstream signalling that would usually culminate in caspase-1 mediated apoptosis (755). In our dataset, the expression of *irf2* is not altered throughout *Bdellovibrio* occupation (Figure 5.6.10). In our dataset, the expression of *irf2bp1* is downregulated at 4 hours post-uptake, whilst the expression of *irf2bp3* is upregulated at 8 hours post-uptake. Despite having proposed roles in the regulation of cell proliferation, apoptosis, cell differentiation, inflammation and the immune response, a clear role if IRF2BPs has not been determined (756).

IRF3 and IRF4 are typically associated with a M2 activation profile. IRF3 associates with TRIF-dependent signalling pathways (initiated by TLR3 or TLR4 ligation), inducing Type I Interferon expression and CCL5 and IFNβ expression. However, despite the production of these inflammatory signals, IRF3 expression is mainly associated with an M2, anti-inflammatory phenotype. In previous data, cytokine signalling suggests that IRF4 is a direct TLR antagonist, actively suppressing M1 proliferation. IL-4, an M2-associated cytokine, induces the expression of IRF4, which upregulates *il-10* and *il-6* transcription via a STAT6 dependent signalling pathway (755). In our dataset, the expression of *irf3* is not altered throughout *Bdellovibrio* occupation (Figure 5.6.10). *irf4* gene expression is upregulated at 24 hours (Figure 5.6.10), suggesting that TLR signalling is being largely countered and a less inflammatory response is replacing the proinflammatory response seen up until this point.

IRF5 competes with IRF4 for the MYD88 binding site, facilitating downstream signalling from TLRs that culminate in the production of the inflammatory mediators IL-6, IL-12, TNFα and other proinflammatory cytokines. Owing to its direct competition with IRF4, IRF5 downregulates the production of IL-10 also. In our dataset, expression of the gene encoding IRF5 is not altered throughout *Bdellovibrio* occupation (Figure 5.6.10).

IRF7 is one of the key regulators of monocyte-macrophage differentiation. Although a role in macrophage polarisation has not been reported, IRF7 expression has been linked to the expression of IFNα, in response to viral nucleic acids (755). In our dataset, the expression of *irf7* is upregulated at 4 hours post-uptake, downregulated at 8 hours post-uptake, then upregulated again at 24 hours post-uptake (Figure 5.6.10). As differentiation from a monocyte-derived cell line into PMA-differentiated macrophage has occurred over 48 hours prior to this experiment, I believe that the IRF7 differential gene expression shown in these data is a result of inflammatory IFNα signalling and crosstalk with other proinflammatory pathways, rather than it being a relic of monocytic differentiation.

IRF8 also drives the production of proinflammatory mediators, such as IFNβ, IL-12 and iNOS, and a M1 classical activation phenotype, in response to IFNγ and TLR stimulation (755). In our dataset, the expression of *irf8* is not altered throughout *Bdellovibrio* occupation (Figure 5.6.10).

IRF9 regulates STAT1 signalling and CXCL10 expression. IRF9 has no reported role in macrophage polarisation. In our dataset, *irf9* expression is upregulated at 8 hours, at the peak of proinflammatory signalling (Figure 5.6.10).

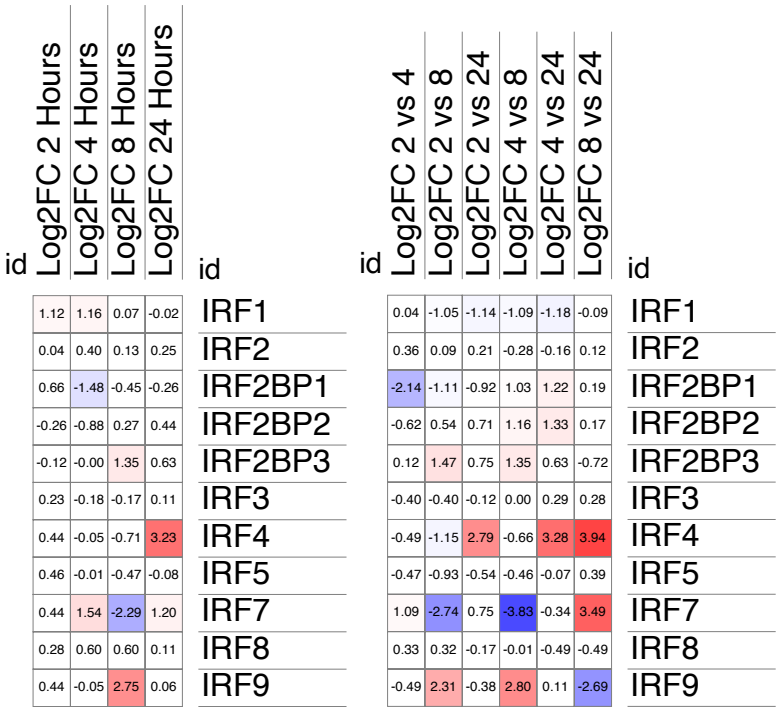

Figure 5.6.10: A heatmap visualising the expression of genes related to the Interferon Regulator Factor response throughout *Bdellovibrio bacteriovorus* occupation within PMA-differentiated U937 macrophage-like cells. Values shown represent the Log_2 function of the ratio of gene expression values of *Bdellovibrio*-containing U937 cells, compared to cell-only controls, at 4 timepoints across a 24-hour period (left). Values shown represent the Log_2 function of the ratio of gene expression values of *Bdellovibrio*-containing U937 cells at each chosen timepoint, relative to each of the other 3 timepoints within this study (right). IRF: Interferon Regulatory Factor; IRF2BP: Interferon Regulatory Factor 2 Binding Protein. Heatmaps were generated using Morpheus.

5.6.6. The roles of chemokine signalling in *Bdellovibrio* macrophage interactions

Chemokines are small messenger molecules and signals that recruit leukocytes to sites of the immune response and prompt inflammation and the initiation of an immune response. Chemokines are produced by macrophage, lymphocytes, and epithelial and endothelial cells, signalling inflammation and an amplification, or tailoring of the immune response (757). Monocytes, macrophages, and neutrophils mainly produce chemokines for the purpose of recruiting further leukocytes to the site of infection, whereas Dendritic cells produce chemokines to activate and maturate T and B cells (757).

The main chemokines released by macrophages are CXCL1, 2 and 8, which potently recruit and activate neutrophils. Macrophage also produce CCL5, CXCL9, CXCL10 and CXCL11 attract and activate T cells, Natural Killer cells and Dendritic cells, making them more relevant to the adaptive immune response (758). Other members of the chemokine family are also produced in high abundance by macrophages, along with other subsets of immune cells. Macrophage respond to a diverse range of chemokines, expressing chemokine receptors (CXCR1-4, and CCR1, 3, 5 and 7) that induce M1 polarisation and responding to chemokines CCL19, -21, -24, -25 and CXCL8 and CXCL10 (759).

Neutrophils have a similar chemokine expression profile to macrophages. They produce CXCLs 1-13, except for CXCL7, and CCL2, -3, -4, -17, -18, -19, -20 but do not produce CCL5, -7, -9, -12 and -22 (760). They respond to CXC chemokine subsets, but express very few CCL chemokine receptors, until activated by IFNγ or LPS, upon which they upregulate CCR1 and CCR3 expression (761).

Dendritic cells and T cells produce a much narrower subset of chemokines. CCL3 and CCL4 are released after antigenic stimulation, recruiting cytotoxic (CD8+) T cells (762). Dendritic cells express chemokine receptors, including CCR1, CCR2, CCR3, CCR5, CCR6 and CXCR3 and CXCR4, triggering the recruitment of DCs to inflamed tissues (763).

5.6.6.2. The Chemokine response to *Bdellovibrio*

Willis and co-workers (1) demonstrate that neutrophils are recruited in response to *Bdellovibrio* in a zebrafish model of infection, suggesting that chemokine activity is present in *Bdellovibrio* infection, although chemokine secretion was not quantified.

In our dataset, chemokines are strongly upregulated throughout *Bdellovibrio* occupancy, with some upregulated equally throughout e.g., CXCL1, 2, 3 and 8, and some upregulated and expressed (at the transcriptional level), increasing in magnitude throughout *Bdellovibrio* occupation e.g. CXCL5 and CXCL6 (Figure 5.6.11), which would result in increased neutrophil chemotaxis and activation.

CXCL9, CXCL10 and CXCL11 are most significantly upregulated at 4 hours post-uptake, suggesting an important role earlier in the immune response to *Bdellovibrio,* whereas CXCL16 is upregulated at 24 hours only, suggesting a role later in *Bdellovibrio* occupation (Figure 5.6.11). CXCL14 is upregulated early on (at 2- and 4-hours post-uptake) but downregulated at 24 hours post-uptake (Figure 5.6.11). Chemokine receptors 1 and 2 (CXCR1 and CXCR2) are downregulated at 8- and 24-hours post-uptake and 4- and 8-hours post-uptake respectively, potentially to counteract the large increase in expression of chemokine mRNA at later timepoints (Figure 5.6.11). CXCR3 is not differentially expressed throughout *Bdellovibrio* occupancy. CXCR4 and CXCR5 are upregulated at 4 hours post-uptake, and 4-, 8- and 24-hours post-uptake respectively (Figure 5.6.11).

Other chemokines (CCL type) are also largely upregulated throughout *Bdellovibrio* occupancy, promoting (in general) macrophage trafficking and inflammation (Figure 5.6.12).

CXCL3, CXCL5, CXCL10 and CCL20 gene transcription are within the highest 0.1% of transcriptionally upregulated genes at 4, 8 and 24 hours, demonstrating a key role in the response to *Bdellovibrio*.

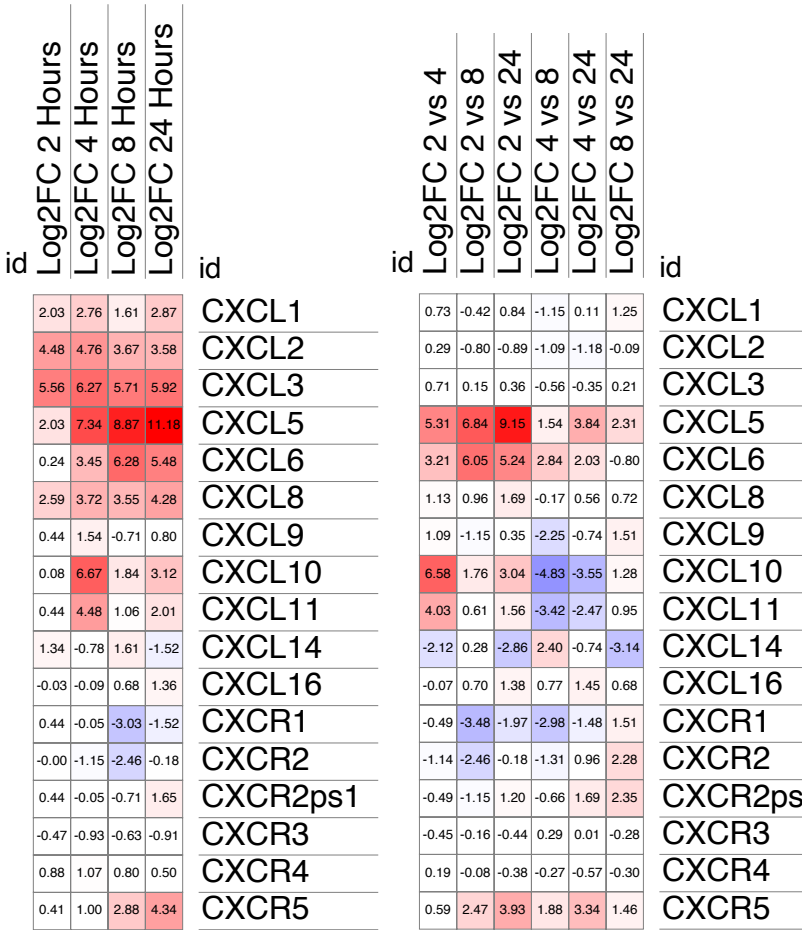

Figure 5.6.11: A heatmap visualising the expression of genes related to CXC motif Chemokine expression throughout *Bdellovibrio bacteriovorus* occupation within PMA-differentiated U937 macrophage-like cells. Values shown represent the Log_2 function of the ratio of gene expression values of *Bdellovibrio*-containing U937 cells, compared to cell-only controls, at 4 timepoints across a 24-hour period (left). Values shown represent the Log_2 function of the ratio of gene expression values of *Bdellovibrio*-containing U937 cells at each chosen timepoint, relative to each of the other 3 timepoints within this study (right). CXCL: C-X-C Motif Chemokine Ligand; CXCR: C-X-C Motif Chemokine Receptor; ps: pseudogene. Heatmaps were generated using Morpheus.

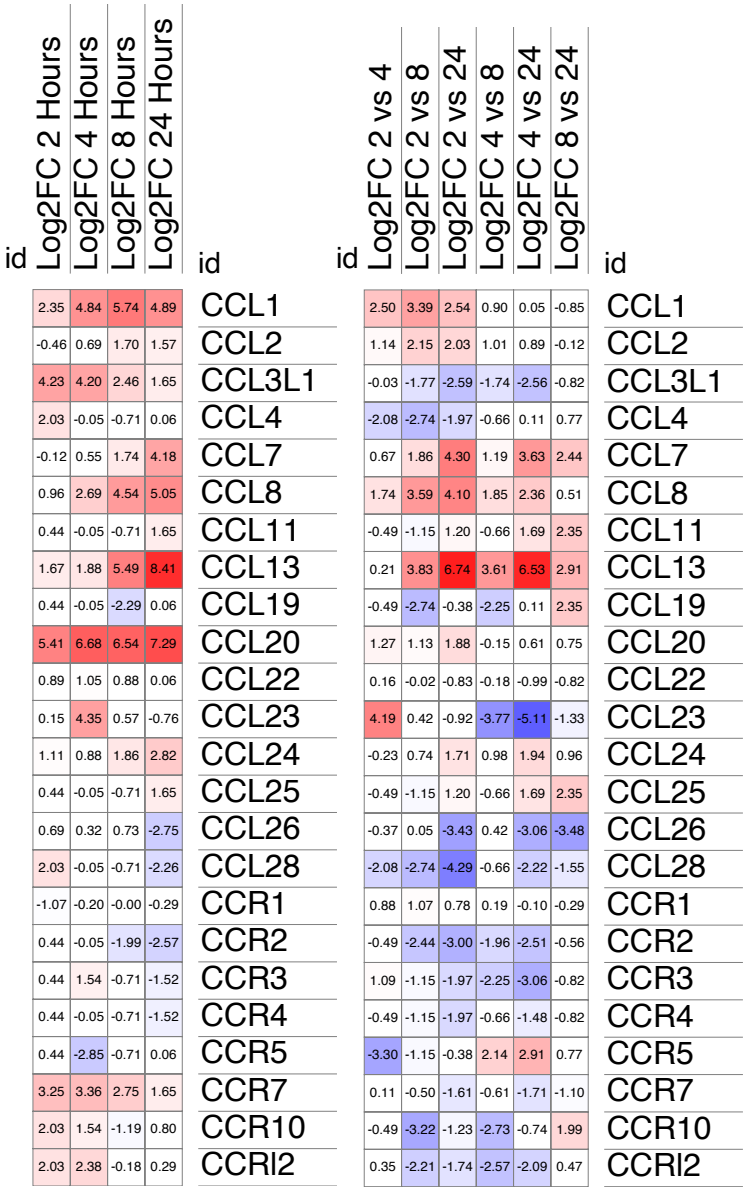

Figure 5.6.12: A heatmap visualising the expression of genes related to CCL motif Chemokine expression throughout *Bdellovibrio bacteriovorus* occupation within PMA-differentiated U937 macrophage-like cells. Values shown represent the Log_2 function of the ratio of gene expression values of *Bdellovibrio*-containing U937 cells, compared to cell-only controls, at 4 timepoints across a 24-hour period (left). Values shown represent the Log_2 function of the ratio of gene expression values of *Bdellovibrio*-containing U937 cells at each chosen timepoint, relative to each of the other 3 timepoints within this study (right). CCL: C-C Motif Chemokine Ligand; CCL3L1: CCL3 Like Protein 1; CCR: CCL Receptor; CCRl: CCR like. Heatmaps were generated using Morpheus.

5.6.7. The roles of interleukin signalling in *Bdellovibrio* macrophage interactions

5.6.7.1. Proinflammatory signalling.

The cytokine response to *Bdellovibrio* was briefly characterised by Raghunathan and co-workers (2), where they found that *Bdellovibrio* uptake and occupation within U937 cells causes upregulation of the pro-inflammatory cytokines IL-6, IL-8, and IL-1β, with protein levels at their highest later in *Bdellovibrio* occupation at 24-hours or 48-hours post-uptake. Upregulation of the anti-inflammatory cytokine IL-10 steadily increases throughout *Bdellovibrio* occupation. TNFα protein levels peak earlier in *Bdellovibrio* occupation (between 4- and 8- hours post-uptake) and decrease later in *Bdellovibrio* occupation (24- and 48- hours post-uptake). Of note is that expression of these cytokines was several folds lower than the cytokine response induced by *Salmonella* Typhimurium LT2 and *Klebsiella* pneumoniae (2).

IL-6 is a proinflammatory cytokine upregulated in acute phases of infection. In our dataset, the gene encoding IL-6 is upregulated throughout *Bdellovibrio* occupation, with gene expression being highest at 4 hours. IL-6 receptor gene expression is not differentially expressed throughout *Bdellovibrio* occupation (Figure 5.6.13). The differences between *il-6* gene expression seen in our study and IL-6 protein expression seen by Raghunathan and co-workers is likely due to post-transcriptional or post-translational regulation of IL-6 mRNA translation. Expression of IL-8 at the mRNA/transcriptional level is not captured in our dataset (Figure 5.6.13). This may be due to IL-8 mRNA transcripts being highly labile, or a small number of transcriptional events translating to a large IL-8 protein amount.

In our dataset, IL-1α gene expression is highly upregulated throughout *Bdellovibrio* occupation, with expression levels highest at 4 hours post-uptake and lowest at 8 hours post-uptake (Figure 5.6.13).

In our dataset, IL-1β gene expression is highly upregulated throughout *Bdellovibrio* occupation (Figure 5.6.13). IL-1 receptor 1 (IL-1R1) gene expression is upregulated at 2-, 4- and 8-hours post-uptake. (Figure 5.6.13) IL-1R accessory protein gene expression is upregulated at 8 hours post-uptake (Figure 5.6.13). IL-1R like 2 gene expression is upregulated throughout *Bdellovibrio* occupation, with levels significantly higher at 2 hours post-uptake (Figure 5.6.13). However, IL-1RL2 cannot bind IL-1α or IL-1β, instead acting as a receptor for IL-36 (764). Expression of the gene encoding IL-1R antagonist (IL-1RA), a decoy protein that binds to IL-1R1 and doesn't initiate signalling, hence reducing inflammation, is upregulated throughout *Bdellovibrio* occupancy, especially at 8 hours post-uptake. IL-1R2 gene expression (encoding a non-signalling IL-1 receptor) is upregulated at 4- and 24-hours post-uptake (Figure 5.6.13).

Overall, this suggests that IL-1 signalling plays an important but highly controlled role in the *Bdellovibrio* macrophage response.

Notably, *tnfa* transcriptional expression was absent from our dataset, despite TNF-α (protein) being upregulated by *B. bacteriovorus* in work performed by Raghunathan and co-workers (2). The reason for this is unknown and is under further investigation within our lab.

5.6.7.2. Anti-inflammatory Signalling

A subset of anti-inflammatory cytokines are also differentially regulated at the transcriptional level throughout *Bdellovibrio* occupancy.

IL-10 is an anti-inflammatory cytokine. *il10* expression is upregulated at 4 hours and downregulated later in infection (8 and 24 hours < 2- and 4-hours post-uptake). Expression of the genes encoding IL-10α and β receptors are not differentially expressed throughout *Bdellovibrio* occupation (Figure 5.6.13). U937 cells have been documented to secrete IL-10 following PMA differentiation (765). The differences between *il-10* gene expression seen in our study and IL-10 protein expression seen by Raghunathan and co-workers, where they see higher IL-10 protein expression later in *Bdellovibrio* occupation is likely due to post-transcriptional or post-translational regulation of IL-10 mRNA translation.

In our dataset, *il-4* expression was upregulated throughout *Bdellovibrio* occupancy, with IL-4 Receptor gene expression remaining unchanged (Figure 5.6.13). IL-13, an anti-inflammatory cytokine that skews macrophage towards an alternative/M2 activation phenotype (766) was not differentially expressed throughout *Bdellovibrio* occupation (Figure 5.6.13). IL-20 is another anti-inflammatory cytokine (767). Expression of the gene encoding an IL-20 receptor β subunit was downregulated at 8 hours post-uptake (Figure 5.6.13). IL-30 Receptor α subunit gene expression was not differentially expressed throughout *Bdellovibrio* occupation (Figure 5.6.13).

IL-37 inhibits M1 activation and NFκB pathways, reducing proinflammatory gene expression and inflammation (768, 769). In our dataset, *il-37* gene expression is downregulated at 2 hours post-uptake, de-repressing the proinflammatory response upon *Bdellovibrio* uptake, and subsequently upregulated at 24 hours post-uptake, suppressing the proinflammatory immune response (Figure 5.6.13).

IL-19 enhances proinflammatory cytokine production (IL-6 and TNFα) in response to LPS (770, 771). In our dataset, expression of the gene encoding IL-19 is not differentially expressed throughout *Bdellovibrio* occupancy, suggesting that *Bdellovibrio* LPS does not activate typical LPS detection pathways (Figure 5.6.13).

Overall, this suggests that no significant anti-inflammatory signalling is initiated in response to *Bdellovibrio* in this scenario.

Many proinflammatory cytokines are expressed in response to *Bdellovibrio*, more of which are detailed in Figure 5.6.13. The general trend is a proinflammatory cytokine response which begins at earlier timepoints and peaks at 8 hours post-uptake, beginning to subside at 24 hours where significant bacterial killing is seen.

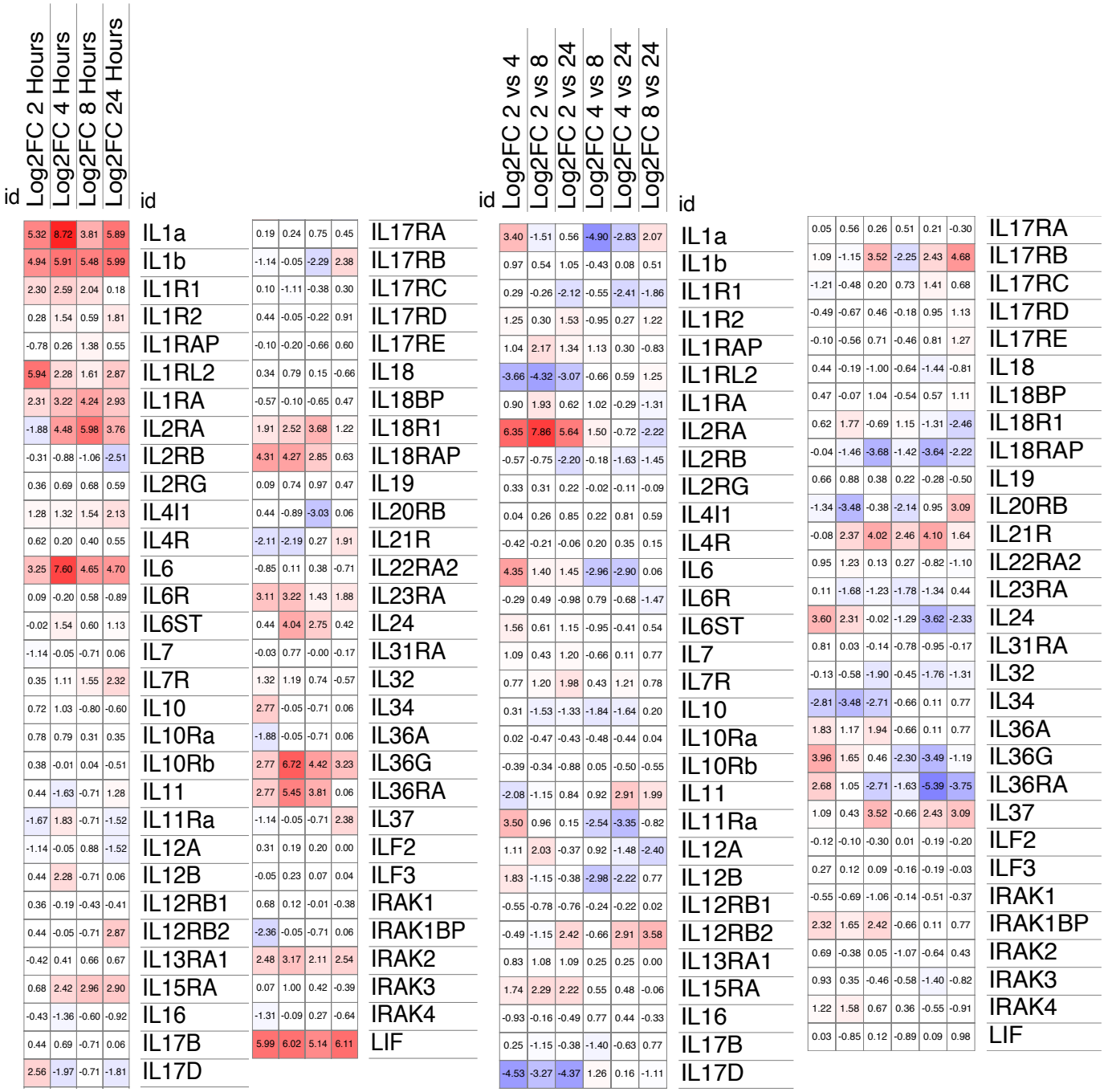

Figure 5.6.13: A heatmap visualising the expression of genes related to the Interleukin expression throughout *Bdellovibrio bacteriovorus* occupation within PMA-differentiated U937 macrophage-like cells. Values shown represent the Log_2 function of the ratio of gene expression values of *Bdellovibrio*-containing U937 cells, compared to cell-only controls, at 4 timepoints across a 24-hour period (left). Values shown represent the Log_2 function of the ratio of gene expression values of *Bdellovibrio*-containing U937 cells at each chosen timepoint, relative to each of the other 3 timepoints within this study (right). IL: Interleukin; IL_R: Interleukin _ Receptor; IL_RAP: Interleukin _ Receptor Accessory Protein; IL1RL: Interleukin 1 Receptor Like Protein; IL4I1: Interleukin 4 Interacting Protein 1; IL_ST: Interleukin _ Signal Transducer; ILF: Interleukin Enhancer Binding Factor; IRAK: Interleukin 1 Receptor Associated Kinase; IRAK_BP: IRAK Binding Protein; LIF: LIF Interleukin 6 Family Cytokine. Heatmaps were generated using Morpheus.

5.6.8. How does macrophage activation vary in response to *Bdellovibrio* occupation?

As mentioned in Section 1.4.5, macrophage activation is a complex and dynamic spectrum, therefore assessing how macrophage activation varies in response to *Bdellovibrio* occupation is not straightforward. As I am interested in whether *Bdellovibrio* induce an inflammatory immune response akin to the immune response towards other Gram-negative bacteria, I will predominantly focus on probing my transcriptional dataset for the key metabolic, cytokine and chemokine markers that are indicative of an inflammatory or anti-inflammatory/alternative activation response, taking a broad view of inflammatory macrophage activation and drawing mostly on data that I have presented so far.

The majority of the transcriptional changes highlighted relate to large changes in cytokine and interferon signalling, therefore I will use these data to help answer interrogate this question.

Chemokines

Chemokine gene expression is highly upregulated throughout *Bdellovibrio* occupation, indicative of a proinflammatory response and signalling to amplify the immune response further. For example, *cxcl10* and *cxcl11* are upregulated at 4-, 8- and 24-hours post-uptake (Figure 5.6.11). *ccl2*, an alternative activation associated chemokine ligand, is transcriptionally upregulated at 8 and 24-hours post-uptake (Figure 5.6.12), suggesting that some less inflammatory signalling is also occurring, later in *Bdellovibrio* occupation. Within a (live) host, large changes in chemokine gene expression will lead to an increase in monocyte, neutrophil and macrophage recruitment to the site, increasing the proinflammatory response towards *Bdellovibrio* and activating the immune cells further.

CCL20, which is associated with TLR-5 activation by flagellin, is highly upregulated throughout, reinforcing that detection of *Bdellovibrio* flagellin is one of the main ligands that initiates the proinflammatory immune response towards *Bdellovibrio.*

Cytokines

Cytokine signalling is another key subset in macrophage activation. Genes encoding the key proinflammatory cytokines in inflammatory activation (IL-1α, IL-1β, and IL-6) are all upregulated at a transcriptional level throughout *Bdellovibrio* occupation (Figure 5.6.13). This is supported by data from Raghunathan and co-workers (2), which also showed high induction of IL-6 and IL-1β protein expression by *Bdellovibrio* at 24 hours post-uptake.

Contrastingly, the alternative activation associated cytokine, *il4i1* gene expression, is upregulated throughout *Bdellovibrio* occupation (Figure 5.6.13). IL4I1 drives the expression of alternative activation markers and inhibits the expression of proinflammatory cytokines (772). *il1ra* gene expression is also upregulated throughout *Bdellovibrio* occupation, especially at 8 hours, with *il1r2* gene expression also being upregulated at 4- and 24-hours post-uptake (Figure 5.6.13). The anti-inflammatory cytokine IL-10 is not significantly differentially expressed (at the transcriptional level) throughout *Bdellovibrio* occupation (Figure 5.6.13).

Metabolism

A shift between metabolic states is indicative of differential macrophage activation profiles. In proinflammatory macrophage activation, a shift towards glycolysis fuels this energetically expensive process, providing ATP and metabolites required for phagocytosis and proinflammatory cytokine production, amongst other processes (773, 774). ACOD1 is a key marker in the immunometabolic switch between inflammatory and alternative activation states (775). *acod1* gene expression is induced by LPS, PAMPs and other inflammatory signalling cues, prompting itaconate synthesis and mitochondrial ROS production. *acod1* is strongly upregulated at the transcriptional level at 2, 4 and 8 hours, and is within the highest 0.1% of transcriptionally upregulated genes at 2, 4 and 8 hours, then returns to pre-exposure levels at 24 hours (Figure 5.6.14). This suggests that the proinflammatory activation state dominates at 2-, 4- and 8-hours post-uptake, before shifting towards a less inflammatory activation state at 24 hours post-uptake.

Fbp1 represents the key metabolic switch in alternative/ less inflammatory activation, enhancing gluconeogenesis. Glycolysis and oxidative phosphorylation do not dominate in human macrophage alternative activation, unlike in murine macrophage, thus gluconeogenesis is the dominant metabolic cue of alternative activation (776). In our dataset, *fbp1* gene expression is downregulated at 8 hours, at the suggested peak of proinflammatory signalling and inflammatory activation and upregulated at 24 hours indicative of a switch towards alternative activation and gluconeogenesis (Figure 5.6.14).

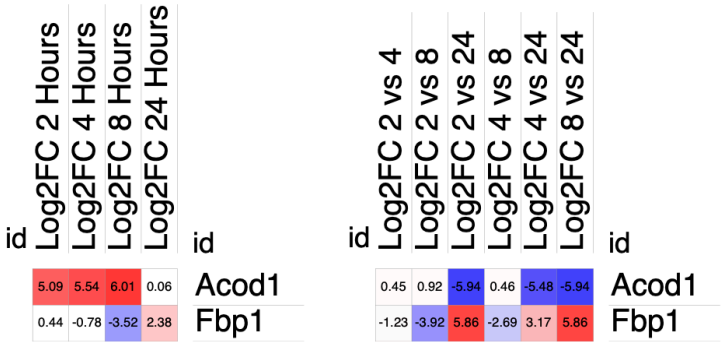

Figure 5.6.14: A heatmap visualising the expression of genes related to the immunometabolism throughout *Bdellovibrio bacteriovorus* occupation within PMA-differentiated U937 macrophage-like cells. Values shown represent the Log_2 function of the ratio of gene expression values of *Bdellovibrio*-containing U937 cells, compared to cell-only controls, at 4 timepoints across a 24-hour period (left). Values shown represent the Log_2 function of the ratio of gene expression values of *Bdellovibrio*-containing U937 cells at each chosen timepoint, relative to each of the other 3 timepoints within this study (right). Acod1: Aconitate decarboxylase 1; fbp1: fructose biphosphatase-1. Heatmaps were generated using Morpheus.

In conclusion, there is no finite switch between inflammatory and alternative activation throughout *Bdellovibrio* occupation. However, the expression of key metabolic switches, including *fbp1* and *acod1*, and general trends in cytokine and chemokine expression seem to suggest a proinflammatory response up until 8 hours post-uptake, prior to a shift towards a less inflammatory milieu at 24 hours post-uptake, with cell signalling and recruitment still dominating at this latter timepoint. The majority of gene expression represents a balance/countering the proinflammatory activation nature against a less inflammatory scenario, rather than fitting into distinct activation profiles. However, *Bdellovibrio* does induce a proinflammatory immune response akin to that of a typical Gram-negative bacterium.

5.6.9. Post-transcriptional and post-translational modification of protein expression

The host immune response is a tightly controlled, highly orchestrated process, therefore the differential expression of the proteins that contribute to the global immune response will also be tightly controlled. A balance between allowing for a rapid response to infection, and the timely shut down of the immune response is also important to prevent harm. These dynamic changes in protein expression are achieved through regulation at multiple levels: at the gene promoter level, post-transcriptionally (e.g., alternative splicing, mRNA export, mRNA stability/lability) and post-translationally (protein inhibitors or degradation).

Macrophage activation and response to bacterial stimuli is a combination of two subsets of regulation of protein expression and activity. Some proteins are always present, and then are modified, such as being phosphorylated or activated in other ways, such as by changes in pH, in response to stimuli, but won't show a large change in gene transcription in our RNASeq data. Other genes are actively transcribed only when needed and sent to the necessary location (these will show up as large changes in expression/transcription in RNASeq). This means that in some scenarios, the correlation between mRNA and protein abundance is less clear and that this difference is largely reliant on translational efficiency (777) (778, 779).

To untangle the wider response of macrophage to *Bdellovibrio* occupation, we need to be able to differentiate between genes that show no significant changes in expression because they are not involved in this specific response, from those that are not differentially expressed because they are constitutively expressed in a non-active state. To investigate this, I looked in the literature at known inhibitors and activators of certain proteins, to determine if their interaction partners may play a role in the immune response, despite not being differentiated at the level of gene expression.

Microarray analysis of U937 cells differentiated by the addition of PMA revealed that only 0.7% of genes were post-transcriptionally regulated, suggesting that post-translational regulation plays an important role in regulating gene expression in differentiation, and by extension, infection (780).

However, my focus is on transcription, therefore I can only study transcriptional modifications of activators/regulators in my dataset. I will explore NFκB regulation, as one example of this. However, other examples exist, and the roles of post-transcriptional and post-translational regulation are important considerations in the interpretation of the data in this chapter.

5.6.9.1. NFκB inhibition regulation

One common mode of regulating macrophage protein expression is translational de-repression, a process that does however involve key inducible genes (781). Activation of the NFκB pathway is repressed by a NFκBIA (NFκB inhibitor alpha) or IκBα that retains NFκB dimers in the cytoplasm. Derepression occurs when this/these inhibitor(s) are proteosomally degraded, activating NFκB and allowing for translocation to the nucleus where it activates downstream transcription pathways (782, 783). This also activates the transcription of *nfkbia* which then binds to NFκB and prevents further activation, shutting down the immune response and proinflammatory gene transcription (783). *nfkbia* gene expression is highly upregulated throughout occupation but is lowest at 8 hours post-uptake, where we see the peak of proinflammatory cytokine signalling and expression (Figure 5.6.15).

Nfkbid, another NFκB inhibitor, is significantly upregulated throughout occupation, except at 4 hours post-uptake. *nfkbie* is significantly upregulated throughout occupation, except at 8 hours post-uptake. *nfkbiz* is highly upregulated throughout occupation. Nr4a1 gene expression not significantly altered throughout. Nfkbi inhibitors all most highly upregulated at 2 hours post-uptake, *nfkbi*a and *nfkbiz* by a large margin (Figure 5.6.15), with *nfbiz* transcription being within the highest 0.1% of transcriptionally upregulated genes at 2 hours. The upregulation of these NFκB inhibitors signifies a downregulation of NFκB signalling.

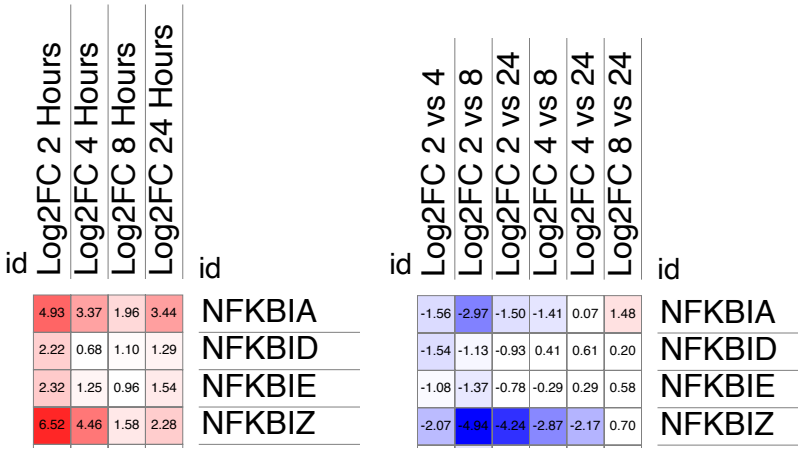

Figure 5.6.15: A heatmap visualising the expression of genes related to Transcription Factor Regulation throughout *Bdellovibrio bacteriovorus* occupation within PMA-differentiated U937 macrophage-like cells. Values shown represent the Log_2 function of the ratio of gene expression values of *Bdellovibrio*-containing U937 cells, compared to cell-only controls, at 4 timepoints across a 24-hour period (left). Values shown represent the Log_2 function of the ratio of gene expression values of *Bdellovibrio*-containing U937 cells at each chosen timepoint, relative to each of the other 3 timepoints within this study (right). NFKBA/D/E/Z: Nuclear Factor Kappa Beta Inhibitor Alpha/ Delta/ Epsilon/ Zeta; NR4A1: Nuclear Receptor Subfamily 4 Group A Member 1; DUSP1: Dual Specificity Phosphatase 1; ZFP36: Zinc Finger Protein 36; ZC3H12A: Zinc Finger CCCH-Type Containing 12A; IER3: Immediate Early Response 3; BCL2L1: BCL2 Like 1; HNRNPK: Heterogeneous Nuclear Ribonucleoprotein K. Heatmaps were generated using Morpheus.

5.6.10. Could complement pathway activation play an important role in the processing of *Bdellovibrio* by the immune response?

Previously, in this Chapter, I have mostly focused on the occupation and processing of *Bdellovibrio* by macrophage. The complement system is an important part of the non-cellular arm of the innate immune response, therefore I asked whether it played an important part in the processing and recognition of *Bdellovibrio* within the host. The complement activation pathways happen outside of a host cell, however many of the key components of the complement cascade can be produced by, or act as signals to, activated macrophage, therefore activation of the complement cascade is important in the wider host response to *Bdellovibrio*, along with the cellular/macrophage response. The complement activation pathways, along with how bacteria evade complement activation, are detailed in Chapter 1, Section 1.4.4.2.

5.6.10.1. Can macrophage initiate the complement activation pathway?

The complement system is comprised of a network of several soluble and membrane bound proteins. Most soluble complement proteins are produced by hepatocytes in the liver, whereas a wide range of cell types produce membrane-bound and a subset of soluble complement proteins outside of the liver, including C1q, FP (Factor Properdin) and Factor D (143, 784, 785). It was initially thought that the key components of the complement system (C3, C4 and MBL), were only produced by hepatocytes (786, 787). However, recent studies have shown that stimulated PMNs (Polymorphonuclear Leukocytes) can secrete complement proteins C3, C6 and C7, and complement factors FP and FB, along with membrane bound receptors CR1, CR3, CR4, C3aR and C5aR (784).

Macrophage produce C1q, C1r and Cls, which initiate the classical pathway of complement activation, along with C2 and C4. Macrophage also produce C3, FB, FD, FP and C5 of the alternative pathway. Notably, macrophage do not produce C6, C7, C8 or C9 that are required for the terminal steps of the complement activation pathway, MAC formation and bacterial lysis (784). This may mean that, unlike monocytes and dendritic cells which can produce C5-9, macrophage may be unable to complete the complement activation pathway in isolation. Membrane bound receptors that macrophage express include CR1, CR3, CR4, CRIg, C3aR, C5aR1 and C5aR2. Macrophage also express a range of soluble (C1INH, FH, FI) and membrane bound (CD46, CD55, CD59) receptors (784). The expression of complement and receptors by macrophage is highly conserved across the different types of immune cell, including dendritic cells, PMNs, monocytes, B lymphocytes and T lymphocytes, with only a few minor differences. This contrasts with the expression of complement activation proteins, of which there is a large variation between different immune cell types (143). Different macrophage activation profiles may express different complement protein activation profiles, although how this may differ remains largely unknown.

The proteins produced by each cell type are summarised in Table 5.6.1. and 5.6.2.

Table 5.6.1: Summary of Complement Pathway Proteins expressed by various immune cells. Table taken from Lubbers et al., 2017 Clinical and Experimental Immunology. PMN: Polymorphonuclear; FB: Factor B; FD: Factor D; FP: Factor Properdin.

	Classical	Lectin	Alternative	Terminal
PMN		Ficolin-1	C3, FB, FP	C6, C7
Mast Cell	C1q		C3	C5
Monocyte	C1q, C1r, C1s, C4, C2		C3, FB, FD, FP	C5, C6, C7, C8, C9
Macrophage	C1q, C1r, C1s, C4, C2		C3, FB, FD, FP	C5
Dendritic Cell	C1q, C1r, C1s, C4, C2		C3, FB, FD, FP	C5, C7, C8, C9
Natural Killer Cell				
B Lymphocyte				C5
T Lymphocyte			C3, FB, FD, FP	C5

Table 5.6.2: Summary of Complement pathway regulators and receptors expressed by various immune cells. Table taken from Lubbers et al., 2017 Clinical and Experimental Immunology. C1INH: C1 Inhibitor; C4BP: C4 Binding Protein; FH: Factor H; FH: Factor I; CR: Complement Receptor.

	Regulators (Soluble)	Regulators (Membrane Bound)	Receptors
PMN		CD46, CD55, CD59	CR1, CR3, CR4, C3aR, C5aR1
Mast Cell		CD46, CD55, CD59	CR1, CR4, C3aR, C5aR1
Monocyte	C1INH, C4BP, FH, FI	CD46, CD55, CD59	CR1, CR3, CR4, C3aR, C5aR1
Macrophage	C1INH, FH, FI	CD46, CD55, CD59	CR1, CR3], CR4, CRIg, C3aR, C5aR1, C5aR2
Dendritic Cell	C4BP, FH, FI	CD46, CD55, CD59	CR1, CR3, CR4, CRIg, C3aR, C5aR1
Natural Killer Cell		CD46, CD55, CD59	CR3, CR4, C3aR, C5aR1, C5aR2
B Lymphocyte		CD46, CD55, CD59	CR1, CR2, CR4, C5aR1
T Lymphocyte		CD46, CD55, CD59	CR1, C3aR, C5aR1

5.6.10.2. Complement protein expression in our dataset.

In our RNASeq dataset, which is from cultured PMA-differentiated macrophages, various complement proteins are differentially transcribed throughout *Bdellovibrio* occupation, whereas the expression of other genes related to the complement pathways remain unchanged.

Expression of *c1s,* which encodes one of the first proteins in the classical complement pathway is upregulated at 4- and 24-hours post-uptake, whereas *c1rl* is downregulated at 8 hours (Figure 5.6.16). The genes encoding C1qA and ClqB (two component chains of C1q protein) are upregulated at 2- and 24-hours post-uptake respectively, whereas the genes encoding the third C1q component chain (*clqc*) and the C1q Binding Protein are not differentially expressed throughout *Bdellovibrio* occupation (Figure 5.6.16).

Some complement proteins later in the classical activation pathway, that are also part of the alternative activation pathway, are also differentially expressed throughout *Bdellovibrio* occupation. Complement protein C3, one of the main complement proteins involved in both the classical and alternative activation pathways, is transcriptionally upregulated at 4-, 8- and 24-hours post-uptake (Figure 5.6.16). The gene encoding C3a receptor 1 (*c3ar1*) is not differentially expressed throughout *Bdellovibrio* occupation, whilst the gene encoding C3b receptor 1 (*cr1*) is downregulated at 24 hours post-uptake (Figure 5.6.16). Expression of the gene encoding CFD, the protein which cleaves CFB prior to C3 convertase generation, is downregulated at 2 hours post-uptake. The genes encoding complement protein 5 (C5) and C5 receptors 1 and 2 are not differentially expressed. The expression of the gene encoding CFP, which stabilises C3 and C5 convertase recruitment and MAC formation, is not differentially expressed throughout *Bdellovibrio* occupation (Figure 5.6.16).

Complement protein 7 (C7) is transcriptionally upregulated at 24 hours post-uptake. Complement protein 8 (C8) alpha chain gene expression is upregulated at 2-, 4- and 8-hours post-uptake, whereas C8 beta chain gene expression is upregulated at 2 and 24 hours but is downregulated at 8 hours post-uptake (Figure 5.6.16).

Both C8a and C8b are involved in MAC formation. C8γ gene expression is unchanged throughout *Bdellovibrio* occupation, but C8γ is not required for the bactericidal activity of C8/MAC. This is surprising, as macrophage are not thought to produce C7 or C8. However, as the cells used in this study are derived from a monocyte cell line, of which monocytes can express C7 and C8, that may explain why we see expression of C7 and C8 (at the transcriptional level) in our dataset.

Other studies of *Bdellovibrio* interactions with serum and complement factors demonstrate that *Bdellovibrio* are susceptible to the actions of complement, showing a 33% drop in viability when exposed to serum (376) and that *Bdellovibrio* are susceptible, but not eradicated, by exposure to complement, in which classical complement proteins are depleted (shown by haemolysis assay)(383).

In conclusion, the genes encoding certain proteins involved in the alternative pathway of complement activation, especially C3, are differentially expressed by macrophages throughout *Bdellovibrio* occupation whereas other genes encoding key proteins are not differentially expressed. This leaves the potential role of complement in response to *Bdellovibrio* as unresolved. Some proteins may be constitutively present within host cells, meaning no significant changes in gene expression are captured by our mRNA sampling. Conversely, expression of some genes may be in response to bacterial uptake or detection of bacterial ligands, rather than direct activation of the complement pathways. I suggest that complement activation occurs in response to *Bdellovibrio,* but the complement activation does not reach its terminal stages and culminate in significant bacterial killing, instead potentially contributing to the enhancement of the proinflammatory immune response and relying on other immune cells to produce the terminal components of the complement activation pathway that ultimately result in membrane attack complex formation and bacterial killing (Figure 5.6.17).

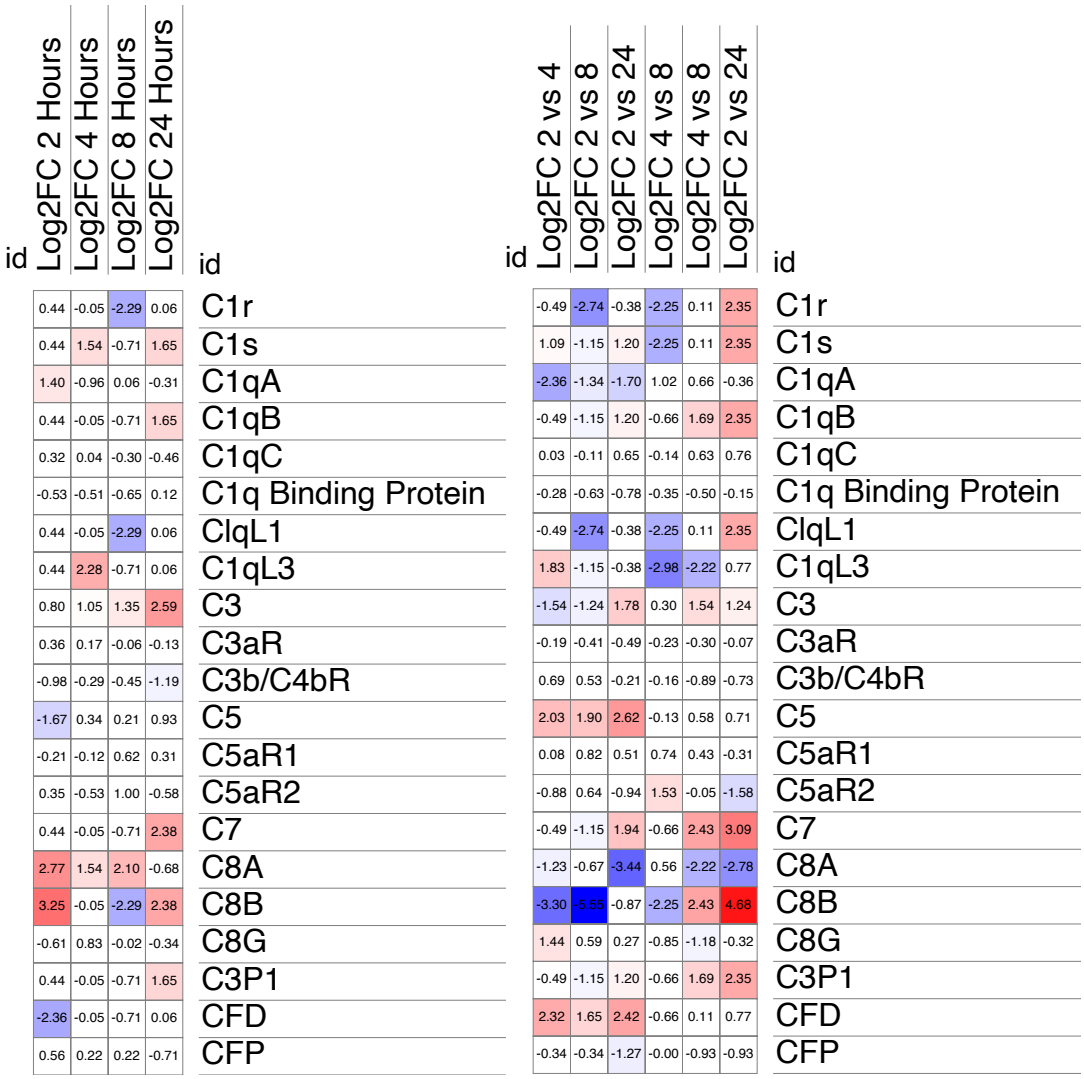

Figure 5.6.16: A heatmap visualising the expression of genes related to the Complement Activation pathway throughout *Bdellovibrio bacteriovorus* occupation within PMA-differentiated U937 macrophage-like cells. Values shown represent the Log_2 function of the ratio of gene expression values of *Bdellovibrio*-containing U937 cells, compared to cell-only controls, at 4 timepoints across a 24-hour period (left). Values shown represent the Log_2 function of the ratio of gene expression values of *Bdellovibrio*-containing U937 cells at each chosen timepoint, relative to each of the other 3 timepoints within this study (right). C1qA: Complement C1q A chain; C1qL1/3: Complement Component 1, q subcomponent-like 1/3. C3aR/C5aR: Complement component 3/5 a subunit Receptor; C3P1: Complement Component 3 Precursor Pseudogene; CFD: Complement Factor D; CFP: Complement Factor Properdin. Heatmaps were generated using Morpheus.

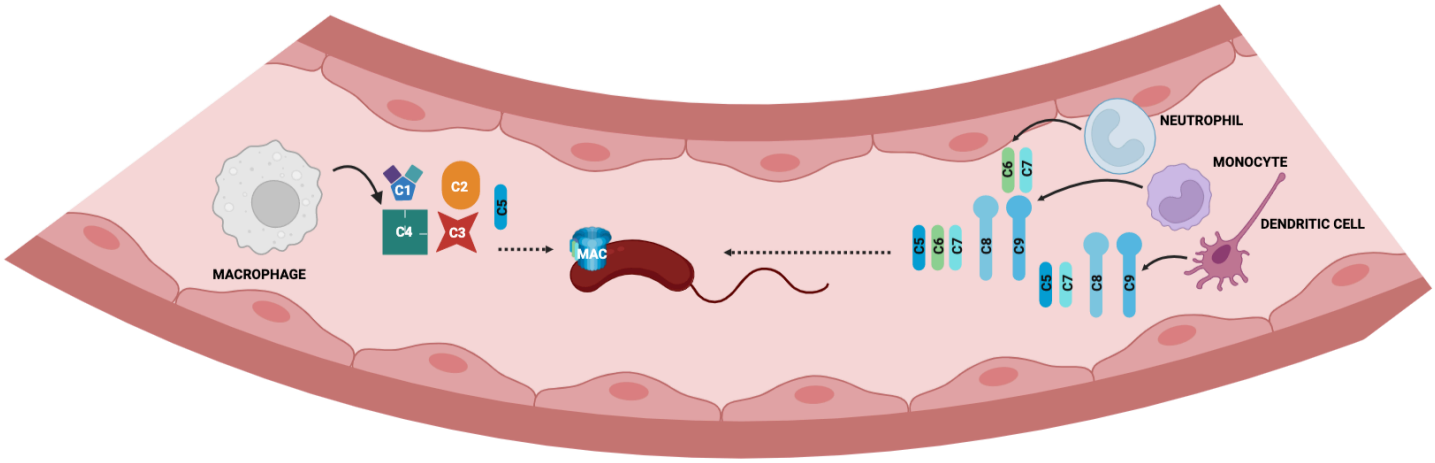

id	C1r	C1s	C1qA	C1qB	C1qC	C3	C5	C7	C8A	C8B	C8G
Log2FC 24 Hours	0.06	1.65	-0.31	1.65	-0.46	2.59	0.93	2.38	-0.68	2.38	-0.34
Log2FC 8 Hours	-2.29	-0.71	0.06	-0.71	-0.30	1.35	0.21	-0.71	2.10	-2.29	-0.02
Log2FC 4 Hours	-0.05	1.54	-0.96	-0.05	0.04	1.05	0.34	-0.05	1.54	-0.05	0.83
Log2FC 2 Hours	0.44	0.44	1.40	0.44	0.32	0.80	-1.67	0.44	2.77	3.25	-0.61
id											

Figure 5.6.17: A whole-system view of the Complement Activating pathway, detailing where the various complement proteins involved in the system originate from. Macrophages secrete C1 (a complex of C1q, C1r and C1s), C2, C3, C4 and C5, initiating the complement activation pathway, but cannot progress to form MACs (Membrane Attack Complexes) in isolation. Neutrophils secrete C6 and C7 complement proteins from the terminal pathway. Monocytes secrete C5-C9 but cannot initiate the complement pathway. Dendritic cells secrete C5, C7, C8 and C9 but not the proteins involved in the initiation of the complement activation pathway. The implications of this are that both macrophage and another cell (monocyte or dendritic cell) are required for the initiation and completion of the complement activation pathway.

Table 5.6.3: A summary of the findings of Chapter 5b. A summary of the main biological questions interrogated in Chapter 5b, with preliminary findings detailed. Some subsections have been omitted due to inconclusive results.

Biological question	Summary
How is *Bdellovibrio* recognised throughout macrophage occupation?	Peptidoglycan and triacylated lipoproteins are recognised from 4 hours post-uptake, continuing at 8- and 24-hours post-uptake (*tlr2* and *tlr1* upregulation at 4-, 8- and 24-hours). Recognition of *Bdellovibrio* peptidoglycan by NOD1 and NOD2 is not significant throughout *Bdellovibrio* occupation. LPS is not recognised (absence of change in *tlr4* and *lpb* expression) Flagellin is recognised at 2-, 4- and 8-hours post-uptake (*tlr5* upregulation and *ccl20* upregulation) Recognition of bacterial nucleic acids throughout, especially early on in occupation (*tlr3, tlr7, tlr8* and *tlr9* upregulation).
What oxidative stresses are *Bdellovibrio,* and the host exposed to during macrophage occupation?	Predominant oxidative stress is due to superoxide generation (indicated by upregulation of *sod2* throughout occupation). Some peroxide stress evident at later stages of occupation (catalase expression unchanged; myeloperoxidase expression downregulated throughout; lactoperoxidase and thioredoxin reductase expression upregulated at 24 hours, and 4-, 8- and 24-hours respectively).
What is the role of interferon signalling in *Bdellovibrio* macrophage occupation?	Biological effect is unclear, although differential regulation of interferon genes throughout.
What is the role of chemokine signalling in *Bdellovibrio* macrophage occupation?	Chemokine expression is strongly upregulated throughout *Bdellovibrio* occupancy, leading to enhanced monocyte and neutrophil chemotaxis and proinflammatory cell activation.
What is the role of cytokine signalling in *Bdellovibrio* macrophage occupation?	Cytokine expression is strongly upregulated throughout *Bdellovibrio* occupancy, leading to enhanced proinflammatory cell activation.
How does macrophage activation vary in response to *Bdellovibrio* occupation?	Macrophages are initially strongly pro-inflammatory (*acod1* expression high between 2 and 8 hours; *fbp1* expression strongly downregulated at 8 hours), followed by a slight curtailment of proinflammatory activation at 24 hours (*acod1* expression downregulated; *fbp1* expression upregulated), where a less inflammatory activation profile takes hold.

Chapter 6: Final Discussion

In my PhD, I aimed to understand and further characterise the interactions between *Bdellovibrio bacteriovorus* and the eukaryotic immune response. *Bdellovibrio bacteriovorus* represents a potential, novel antimicrobial therapy for the treatment of (Gram-negative) bacterial infection. However, despite animal studies showing successful treatment of bacterial infection by *Bdellovibrio*, we still do not understand how host immune factors, such as immune cell interactions, antimicrobial proteins or complement protein deposition, may impact the efficacy of predation within a host. We know that *Bdellovibrio* is taken up by host leukocytes and survives for 24 hours before significant bacterial killing. What is happening during this 24-hour window, whether *Bdellovibrio* is prolonging its survival within the phagosome and whether it is still able to prey upon other bacteria, are all unknown. The aim of my PhD was to further characterise how host immune factors may impact the efficacy of predation (Chapter 3) and to further characterise the 24-hour window during which *Bdellovibrio* is live within the phagosome, using transcriptional data to assess host and bacterial actions within this period (Chapters 4 and 5).

Pathogen recognition within the host. I demonstrated that host environmental factors, such as antimicrobial proteins and complement within serum, modify the susceptibility of Gram-negative pathogens to predation by *B. bacteriovorus*, with the combination of host environmental factors and predation stress inducing large changes to the outer surface components of pathogenic prey, culminating in resistance to predation through the addition of a L-Ara(4)N Lipid A modification, within the context of other large surface modifications in response to predation and host factors. Consideration of how cell surface modifications, in response to host factors, will be an important step in considering whether *Bdellovibrio* is an appropriate antimicrobial therapy to treat bacterial infection in the future.

***Bdellovibrio* recognition and processing within the host.** The mechanisms through which *Bdellovibrio* is recognised by host macrophage and how this correlates to the reduced levels of proinflammatory cytokine release seen in response to *Bdellovibrio* (compared to other, more typical Gram-negative bacteria) have never been characterised. *Bdellovibrio* is recognised initially through activation of TLR-5 receptors by flagellin, and TLRs -7, -8 and -9 by bacterial nucleic acids. Peptidoglycan and triacylated lipoprotein recognition, by TLRs -2 and -6, also contribute to *Bdellovibrio* recognition from 4 hours onwards. However, recognition of LPS by TLR-4 is not seen in *Bdellovibrio* recognition, in stark contrast to recognition of other Gram-negative bacteria, where LPS recognition is a cornerstone of Gram-negative bacterial infection. As LPS recognition significantly upregulates the proinflammatory activation of macrophage in response to Gram-negative bacteria, and we do not see this in response to *Bdellovibrio*, this may explain why we see a lower induction of proinflammatory cytokines, such as IL-6, IL-1β and TNFα, in *Bdellovibrio* infection, compared to other Gram-negative bacteria.

However, a proinflammatory response is still mounted against *Bdellovibrio,* with the majority of gene expression relating to cytokine and chemokine signalling, most of which encourages the recruitment and proinflammatory activation of monocytes and other immune cells. These data suggest that a strong proinflammatory response is mounted in response to *Bdellovibrio*, which peaks at 8 hours post-uptake, followed by a slight curtailment in proinflammatory activation but an enhancement of cell signalling at 24 hours.

Taking a wider view of the *Bdellovibrio* transcriptional response, the majority of bacterial gene expression occurs at 24 hours post-uptake, where *Bdellovibrio* is under high levels of nutrient starvation, oxidative stress and outer membrane and cell wall insult, due to the presence of reactive species, antimicrobial proteins and hydrolytic enzymes. Responses related to stress, nutrient starvation, multidrug tolerance, anaerobic respiration and outer membrane and cell wall modification are all highly upregulated at this timepoint, representing a last attempt to combat bacterial killing.

Drawing parallels between *Bdellovibrio* invasion of pathogenic bacteria, and how *Bdellovibrio* temporarily survives and tolerates phagosomal conditions within a macrophage, I aimed to investigate whether a subset of oxidative stress genes, which were transcriptionally upregulated within zebrafish infection, aided the survival of *Bdellovibrio* against phagosomal conditions, namely oxidative species. I proposed that these genes played a dual purpose within *Bdellovibrio*, conferring resistance to the oxidative stresses experienced throughout predation, where entry into a Gram-negative bacterium's periplasm and degradation of prey cell contents generates high levels of proton and reactive species stress. These proteins may also benefit *Bdellovibrio* in temporarily surviving within the phagosome of macrophage, where predation may still be possible.

Oxidative stress within predation. Upon entry into a Gram-negative prey cell, *Bdellovibrio* enters the periplasm, a highly reducing environment with a steep proton gradient, and resides within. It then kills the prey cell, leading to dysfunction of the electron transport chain and further oxidative stress. I found that Bd2517 and Bd2518, alkyl hydroperoxide reductase proteins C and F respectively, were essential for *Bdellovibrio* viability. They were highly expressed in attack phase *Bdellovibrio* and subsequently downregulated throughout predation. I suggest that these proteins detoxify reactive peroxide species upon entry into the prey cell periplasm, combatting the initial oxidative insult, therefore explaining why they are essential for bacterial survival.

A SurA chaperone protein homolog (Bd0017) is also highly expressed in attack phase and downregulated throughout predation, with its function also being indispensable for bacterial viability. As the predator surface is key to predation and initial prey recognition and entry, I suggest that Bd0017 regulates protein folding and function in response to oxidative insult, making it crucial for predation also.

During intraperiplasmic growth, *Bdellovibrio* metabolises prey cell macromolecules to re-purpose them for its own progeny growth. This involves degrading proteins and stripping the metal ions from their enzymatic active sites, generating superoxide radicals which would react with bacterial DNA and proteins and induce mutation and damage. Bd1401, a superoxide dismutase, is highly expressed during intraperiplasmic growth, with deletion resulting in a loss of predator fitness and a reduction in predation efficiency. I suggest that the function of Bd1401 is important for predation and predator fitness, neutralising superoxide radicals generated through intraperiplasmic growth and improving the fitness of progeny *Bdellovibrio* which go on to invade further bacterial prey cells.

Oxidative stress within the host. Phagocytosis and uptake into the developing phagosome of macrophage also represents a shift towards high levels of oxidative stress, along with membrane and cell wall attack by antimicrobial proteins and hydrolytic enzymes as the phagolysosome matures. The majority of oxidative stress within the phagosome occurs at 24 hours post-uptake, demonstrated by upregulation of oxidative stress genes, such as host *sod2*, which is also the time at which significant bacterial killing occurs. *Bdellovibrio* transcription reflects this, where genes related to the oxidative stress response are highly expressed at 24 hours post-uptake, including *bd0177* and *bd0456*, which are related to acidic pH tolerance, *bd1002* and *bd1401* superoxide response genes, and *bd0298, bd0909* and *bd1805*, all of which are linked to peroxide tolerance.

As Bd2517/AhpC and Bd2518/AhpF were essential for bacterial viability, I was not able to test their role within intramacrophage survival through gene deletion. However, owing to their high levels of expression at 8- and 24-hours within macrophage, I would argue that they are likely important in combatting peroxide stress within the macrophage phagosome. Bd0017/SurA, an outer membrane chaperone, was also vital for bacterial viability, making its role in intramacrophage survival unable to be tested. As it regulates protein function on the outer surface, where the majority of bactericidal insults will occur, and is upregulated at 24 hours post-uptake, Bd0017 also likely contributes to tolerating stresses within the macrophage phagosome.

Bd1401/sodC was highly expressed at 24 hours within the macrophage phagosome, and deletion of Bd1401 reduced bacterial viability at 2 hours post-uptake, suggesting that Bd1401 may play a role in tolerating superoxide stress either at 2 hours, in response to initial oxidative stresses present immediately after phagocytic uptake, or at 24 hours, where the majority of oxidative stress and bacterial killing is occurring.

Nutrient availability. Another contrast between predation and intramacrophage survival is that nutrients are abundant within the prey cell, therefore *Bdellovibrio* is actively growing. There is an absence of nutrient starvation responses within predation, compared to intramacrophage survival where nutrient starvation and stress responses, including the iron acquisition genes *bd1454, bd1455* and *bd2648*, are upregulated. This shows that nutrient restriction is ongoing within the macrophage phagosome, consistent with bacterial infection, with iron acquisition known to be critical for intraphagosomal survival. As *Bdellovibrio* is actively growing, the Dps protein Bd2620, which protects the bacterial chromosome from oxidative and nutrient starvation associated damage, is downregulated throughout predation to allow for gene transcription, protein expression and active growth. Removal of Bd2620 function decreases predation efficiency, likely due to oxidative stress induced damage to the chromosome upon prey cell entry, where DNA is usually compacted and protected from oxidative damage by Bd2620. Within the phagosome, *Bdellovibrio* is not actively growing and is undergoing extreme nutrient restriction, therefore the function of Bd2620 is likely important, hence why expression is high throughout intramacrophage survival. However, deletion of *bd2620* did not impact bacterial survival, suggesting that the function of Bd2620 may benefit *Bdellovibrio* in the short-term, but is a futile response as bacterial killing still proceeds regardless.

This highlights a disconnect between genes that are important for macrophage survival (iron acquisition genes: *bd1454, bd1455, bd2648*) and genes that are important for predation (*bd2620/dps, bd3203*) only, or some that likely contribute to both scenarios (*bd1401/sodC, bd2517/ahpC, bd2518/ahpF, bd0017/surA*), owing to the similar nature of oxidative stresses being tolerated in both.

The majority of the genes investigated in this study (*bd0295/sodC, bd0798/catA, bd0799/ankB, bd1154/katA, bd1155/ankB* and *bd1815*) do not significantly contribute to predation, or their functions are redundant to other proteins within the *Bdellovibrio* proteome. Oxidative stress tolerance is a key function within bacterial cells but is more important still in bacteria that enter other bacteria and prey upon them, or in bacteria that cause bacterial infection and encounter host immune cells. With this in mind, it is not surprising that a level of functional redundancy exists within the oxidative stress responses of *Bdellovibrio*. However, I have shown that oxidative stress tolerance contributes to survival and fitness of *Bdellovibrio* throughout predation and within the macrophage phagosome.

The actions of the immune response will impact the efficacy of *Bdellovibrio* predation, through the phagocytosis and spatial separation of predator and prey, and through the induction of modifications to the surface of pathogenic prey. These actions do not impede predation entirely, making the characterisation and understanding of the interactions between the host immune response, predator and prey all the more important, before *Bdellovibrio* can be utilised as a novel, antimicrobial therapy.

In these ways in this thesis, I have further characterised the interactions between *Bdellovibrio bacteriovorus* and the eukaryotic immune response. Taken together, my work has further characterised the interactions between predator, pathogenic prey and host macrophage, with the aim of informing us on how predation may proceed or be impeded within a host environment.

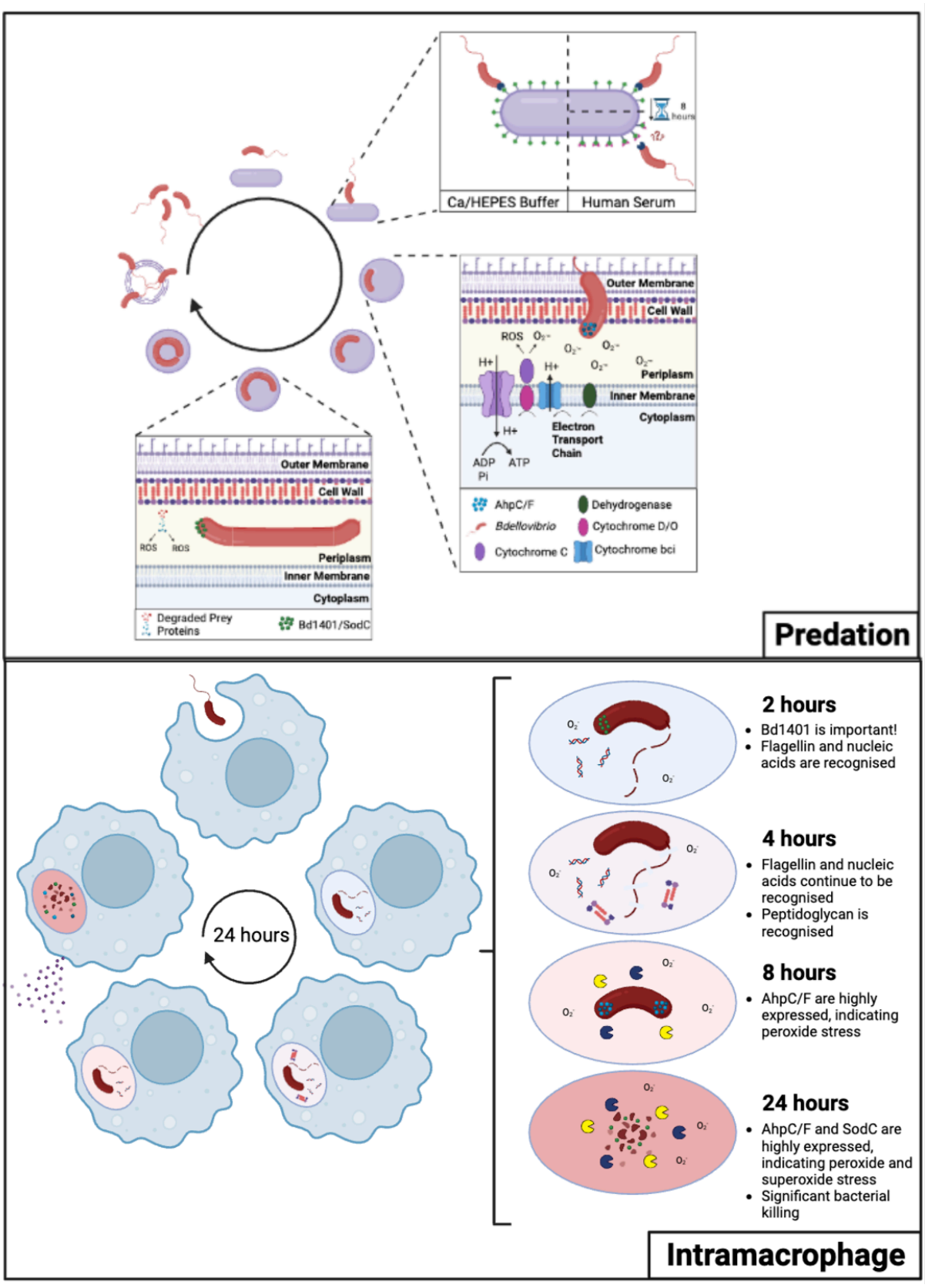

Figure 6.1: A summary of the findings of this PhD project.

Bibliography

1. Willis AR, Moore C, Mazon-Moya M, Krokowski S, Lambert C, Till R, et al. Injections of Predatory Bacteria Work Alongside Host Immune Cells to Treat Shigella Infection in Zebrafish Larvae. Curr Biol. 2016;26(24):3343-51.

2. Raghunathan D, Radford PM, Gell C, Negus D, Moore C, Till R, et al. Engulfment, persistence and fate of Bdellovibrio bacteriovorus predators inside human phagocytic cells informs their future therapeutic potential. Sci Rep. 2019;9(1):4293.

3. World Health Organisation. Monitoring Global Progress On Antimicrobial Resistance: Tripartite AMR Country Self-Assessment Survey (TRACCS) 2019-2020. World Health Organisation; 2021.

4. Centre for Disease Control and Prevention. Antibiotic Resistance Threats in the United States. USA; 2019.

5. Antibiotic Research UK. Antibiotic Resistance Breakers (ARBs) https://www.antibioticresearch.org.uk/research/antibiotic-resistance-breakers/: Antibiotic Research UK; 2021 [

6. Diseases GBD, Injuries C. Global burden of 369 diseases and injuries in 204 countries and territories, 1990-2019: a systematic analysis for the Global Burden of Disease Study 2019. Lancet. 2020;396(10258):1204-22.

7. Pendleton JN, Gorman SP, Gilmore BF. Clinical relevance of the ESKAPE pathogens. Expert Review of Anti-infective Therapy. 2013;11(3):297-308.

8. Atterbury RJ, Tyson J. Predatory bacteria as living antibiotics - where are we now? Microbiology (Reading). 2021;167(1).

9. Bertani B, Ruiz N. Function and Biogenesis of Lipopolysaccharides. EcoSal Plus. 2018;8(1).

10. Rudbach JA. Molecular Immunogenicity of Bacterial Lipopolysaccharide Antigens: Establishing a Quantitative System. The Journal of Immunology. 1971;106(4):993-1001.

11. Schromm AB, Brandenburg K, Loppnow H, Zahringer U, Rietschel ET, Carroll SF, et al. The Charge of Endotoxin Molecules Influences Their Conformation and IL-6-Inducing Capacity. The Journal of Immunology. 1998.

12. Schromm AB, Brandenburg K, Loppnow H, Zähringer U, Rietschel ET, Carroll SF, et al. The charge of endotoxin molecules influences their conformation and IL-6-inducing capacity. J Immunol. 1998;161(10):5464-71.

13. Ernst RK, Yi EC, Guo L, Lim KB, Burns JL, Hackett M, et al. Specific lipopolysaccharide found in cystic fibrosis airway Pseudomonas aeruginosa. Science. 1999;286(5444):1561-5.

14. Nikaido H. Molecular basis of bacterial outer membrane permeability revisited. Microbiol Mol Biol Rev. 2003;67(4):593-656.

15. Kadokura H, Beckwith J. Mechanisms of oxidative protein folding in the bacterial cell envelope. Antioxid Redox Signal. 2010;13(8):1231-46.

16. Wolfert MA, Roychowdhury A, Boons GJ. Modification of the structure of peptidoglycan is a strategy to avoid detection by nucleotide-binding oligomerization domain protein 1. Infect Immun. 2007;75(2):706-13.

17. Yang Y, Liu J, Clarke BR, Seidel L, Bolla JR, Ward PN, et al. The molecular basis of regulation of bacterial capsule assembly by Wzc. Nature Communications. 2021;12(1):4349.

18. Jann K, Jann B. In Escherichia coli: Mechanisms of Virulence. Sussman M, editor: Cambridge University Press; 1997.

19. Whitfield C. Biosynthesis and assembly of capsular polysaccharides in Escherichia coli. Annual Reviews Biochemistry. 2006;75:39-68.

20. Merino S, Camprubí S, Albertí S, Benedí VJ, Tomás JM. Mechanisms of Klebsiella pneumoniae resistance to complement-mediated killing. Infection and Immunity. 1992;60(6):2529-35.

21. Koval SF, Bayer ME. Bacterial capsules: no barrier against Bdellovibrio. Microbiology (Reading). 1997;143 (Pt 3):749-53.

22. Sleytr UB, Schuster B, Egelseer E-M, Pum D. S-layers: principles and applications. FEMS Microbiology Reviews. 2014;38(5):823-64.

23. Ravi J, Fioravanti A. S-layers: The Proteinaceous Multifunctional Armors of Gram-Positive Pathogens. Frontiers in Microbiology. 2021;12.

24. Koval SF, Hynes SH. Effect of paracrystalline protein surface layers on predation by Bdellovibrio bacteriovorus. J Bacteriol. 1991;173(7):2244-9.

25. Mol O, Oudega B. Molecular and structural aspects of fimbriae biosynthesis and assembly in Escherichia coli. FEMS Microbiology Reviews. 1996;19(1):25-52.

26. Proft T, Baker EN. Pili in Gram-negative and Gram-positive bacteria - structure, assembly and their role in disease. Cell Mol Life Sci. 2009;66(4):613-35.

27. Werneburg GT, Thanassi DG. Pili Assembled by the Chaperone/Usher Pathway in Escherichia coli and Salmonella. EcoSal Plus. 2018;8(1).

28. Nuccio SP, Baumler AJ. Evolution of the chaperone/usher assembly pathway: fimbrial classification goes Greek. Microbiology & Molecular Biology Reviews. 2007;71(4):551-75.

29. Thanassi DG, Bliska JB, Christie PJ. Surface organelles assembled by secretion systems of Gram-negative bacteria: diversity in structure and function. FEMS Microbiology Reviews. 2012;36(6):1046-82.

30. Lillington J, Geibel S, Waksman G. Biogenesis and adhesion of type 1 and P pili. Biochimica et Biophysica Acta. 2014;1840(9):2783-93.

31. Hospenthal MK, Costa TRD, Waksman G. A comprehensive guide to pilus biogenesis in Gram-negative bacteria. Nature Reviews Microbiology. 2017;15(6):365-79.

32. Giltner CL, Nguyen Y, Burrows LL. Type IV pilin proteins: versatile molecular modules. Microbiol Mol Biol Rev. 2012;76(4):740-72.

33. Bardy SL, Ng SYM, Jarrell KF. Prokaryotic motility structures. Microbiology (Reading). 2003;149(Pt 2):295-304.

34. Duan Q, Zhou M, Zhu L, Zhu G. Flagella and bacterial pathogenicity. Journal of basic microbiology. 2013;53(1):1-8.

35. Eckhard U, Bandukwala H, Mansfield MJ, Marino G, Cheng J, Wallace I, et al. Discovery of a proteolytic flagellin family in diverse bacterial phyla that assembles enzymatically active flagella. Nature Communications. 2017;8(1):521.

36. Andersen-Nissen E, Smith KD, Strobe KL, Barrett SL, Cookson BT, Logan SM, et al. Evasion of Toll-like receptor 5 by flagellated bacteria. Proc Natl Acad Sci U S A. 2005;102(26):9247-52.

37. Jeeves M, Knowles TJ. A novel pathway for outer membrane protein biogenesis in Gram-negative bacteria. Molecular microbiology. 2015;97(4):607-11.

38. Foley J. Mini-review: Strategies for Variation and Evolution of Bacterial Antigens. Computational and Structural Biotechnology Journal. 2015;13:407-16.

39. Osborn MJ, Wu HCP. PROTEINS OF THE OUTER MEMBRANE OF GRAM-NEGATIVE BACTERIA. Annual Reviews Microbiology. 1980;34.

40. Martinez FO, Gordon S. The M1 and M2 paradigm of macrophage activation: time for reassessment. F1000Prime Rep. 2014;6:13.

41. Mass E, Nimmerjahn F, Kierdorf K, Schlitzer A. Tissue-specific macrophages: how they develop and choreograph tissue biology. Nature Reviews Immunology. 2023.

42. Marshall JS, Warrington R, Watson W, Kim HL. An introduction to immunology and immunopathology. Allergy, Asthma & Clinical Immunology. 2018;14(2):49.

43. Davies LC, Jenkins SJ, Allen JE, Taylor PR. Tissue-resident macrophages. Nat Immunol. 2013;14(10):986-95.

44. Amulic B, Cazalet C, Hayes GL, Metzler KD, Zychlinsky A. Neutrophil function: from mechanisms to disease. Annu Rev Immunol. 2012;30:459-89.

45. Brinkmann V, Reichard U, Goosmann C, Fauler B, Uhlemann Y, Weiss DS, et al. Neutrophil Extracellular Traps Kill Bacteria. Science. 2004;303(5663):1532-5.

46. Chen T, Li Y, Sun R, Hu H, Liu Y, Herrmann M, et al. Receptor-Mediated NETosis on Neutrophils. Front Immunol. 2021;12:775267.

47. Granucci F, Foti M, Ricciardi-Castagnoli P. Dendritic cell biology. Advances in immunology. 2005;88:193-233.

48. Huang Q, Liu D, Majewski P, Schulte LC, Korn JM, Young RA, et al. The Plasticity of Dendritic Cell Responses to Pathogens and Their Components. Science. 2001;294(5543):870-5.

49. Kawai T, Akira S. The roles of TLRs, RLRs and NLRs in pathogen recognition. International immunology. 2009;21(4):317-37.

50. Kumar H, Kawai T, Akira S. Toll-like receptors and innate immunity. Biochemical and biophysical research communications. 2009;388(4):621-5.

51. Kawasaki T, Kawai T. Toll-Like Receptor Signaling Pathways. Frontiers in Immunology. 2014;5.

52. O'Neill LA, Golenbock D, Bowie AG. The history of Toll-like receptors - redefining innate immunity. Nat Rev Immunol. 2013;13(6):453-60.

53. Takeda K, Akira S. Toll-like receptors in innate immunity. International Immunology. 2005;17(1):1-14.

54. Tricker E, Cheng G. With a little help from my friends: modulation of phagocytosis through TLR activation. Cell Research. 2008;18(7):711-2.

55. Mogensen TH. Pathogen recognition and inflammatory signaling in innate immune defenses. Clin Microbiol Rev. 2009;22(2):240-73, Table of Contents.

56. Tsukamoto H, Takeuchi S, Kubota K, Kobayashi Y, Kozakai S, Ukai I, et al. Lipopolysaccharide (LPS)-binding protein stimulates CD14-dependent Toll-like receptor 4 internalization and LPS-induced TBK1–IKKε–IRF3 axis activation. Journal of Biological Chemistry. 2018;293(26):10186-201.

57. Ryu J-K, Kim SJ, Rah S-H, Kang JI, Jung HE, Lee D, et al. Reconstruction of LPS transfer cascade reveals structural determinants within LBP, CD14, and TLR4-MD2 for efficient LPS recognition and transfer. Immunity. 2017;46(1):38-50.

58. Park BS, Lee J-O. Recognition of lipopolysaccharide pattern by TLR4 complexes. Experimental & Molecular Medicine. 2013;45(12):e66-e.

59. Ciesielska A, Matyjek M, Kwiatkowska K. TLR4 and CD14 trafficking and its influence on LPS-induced pro-inflammatory signaling. Cell Mol Life Sci. 2021;78(4):1233-61.

60. Maeshima N, Fernandez RC. Recognition of lipid A variants by the TLR4-MD-2 receptor complex. Front Cell Infect Microbiol. 2013;3:3.

61. Raetz CR, Reynolds CM, Trent MS, Bishop RE. Lipid A modification systems in gram-negative bacteria. Annual review of biochemistry. 2007;76:295.

62. Maldonado RF, Sá-Correia I, Valvano MA. Lipopolysaccharide modification in Gram-negative bacteria during chronic infection. FEMS Microbiol Rev. 2016;40(4):480-93.

63. Seed KD, Faruque SM, Mekalanos JJ, Calderwood SB, Qadri F, Camilli A. Phase Variable O Antigen Biosynthetic Genes Control Expression of the Major Protective Antigen and Bacteriophage Receptor in Vibrio cholerae O1. PLOS Pathogens. 2012;8(9):e1002917.

64. Cavallo FM, Jordana L, Friedrich AW, Glasner C, van Dijl JM. Bdellovibrio bacteriovorus: a potential 'living antibiotic' to control bacterial pathogens. Critical Reviews in Microbiology. 2021;47(5):630-46.

65. Underhill DM, Ozinsky A, Smith KD, Aderem A. Toll-like receptor-2 mediates mycobacteria-induced proinflammatory signaling in macrophages. Proc Natl Acad Sci U S A. 1999;96(25):14459-63.

66. Takeuchi O, Hoshino K, Akira S. Cutting Edge: TLR2-Deficient and MyD88-Deficient Mice Are Highly Susceptible to Staphylococcus aureus Infection1. The Journal of Immunology. 2000;165(10):5392-6.

67. Oliveira-Nascimento L, Massari P, Wetzler LM. The Role of TLR2 in Infection and Immunity. Front Immunol. 2012;3:79.

68. Inohara N, Ogura Y, Chen FF, Muto A, Nuñez G. Human Nod1 Confers Responsiveness to Bacterial Lipopolysaccharides*. Journal of Biological Chemistry. 2001;276(4):2551-4.

69. Chamaillard M, Hashimoto M, Horie Y, Masumoto J, Qiu S, Saab L, et al. An essential role for NOD1 in host recognition of bacterial peptidoglycan containing diaminopimelic acid. Nature Immunology. 2003;4(7):702-7.

70. Girardin SE, Boneca IG, Carneiro LAM, Antignac A, Jéhanno M, Viala J, et al. Nod1 Detects a Unique Muropeptide from Gram-Negative Bacterial Peptidoglycan. Science. 2003;300(5625):1584-7.

71. Müller-Anstett MA, Müller P, Albrecht T, Nega M, Wagener J, Gao Q, et al. Staphylococcal Peptidoglycan Co-Localizes with Nod2 and TLR2 and Activates Innate Immune Response via Both Receptors in Primary Murine Keratinocytes. PLOS ONE. 2010;5(10):e13153.

72. Hasegawa M, Yang K, Hashimoto M, Park JH, Kim YG, Fujimoto Y, et al. Differential release and distribution of Nod1 and Nod2 immunostimulatory molecules among bacterial species and environments. J Biol Chem. 2006;281(39):29054-63.

73. Girardin SE, Boneca IG, Viala J, Chamaillard M, Labigne A, Thomas G, et al. Nod2 is a general sensor of peptidoglycan through muramyl dipeptide (MDP) detection. J Biol Chem. 2003;278(11):8869-72.

74. Girardin SE, Travassos LH, Herve M, Blanot D, Boneca IG, Philpott DJ, et al. Peptidoglycan molecular requirements allowing detection by Nod1 and Nod2. J Biol Chem. 2003;278(43):41702-8.

75. Park JH, Kim YG, McDonald C, Kanneganti TD, Hasegawa M, Body-Malapel M, et al. RICK/RIP2 mediates innate immune responses induced through Nod1 and Nod2 but not TLRs. J Immunol. 2007;178(4):2380-6.

76. Kobayashi KS, Chamaillard M, Ogura Y, Henegariu O, Inohara N, Nuñez G, et al. Nod2-Dependent Regulation of Innate and Adaptive Immunity in the Intestinal Tract. Science. 2005;307(5710):731-4.

77. Opitz B, Puschel A, Schmeck B, Hocke AC, Rosseau S, Hammerschmidt S, et al. Nucleotide-binding oligomerization domain proteins are innate immune receptors for internalized Streptococcus pneumoniae. J Biol Chem. 2004;279(35):36426-32.

78. Ferwerda G, Girardin SE, Kullberg BJ, Le Bourhis L, de Jong DJ, Langenberg DM, et al. NOD2 and toll-like receptors are nonredundant recognition systems of Mycobacterium tuberculosis. PLoS Pathog. 2005;1(3):279-85.

79. Kim JG, Lee SJ, Kagnoff MF. Nod1 is an essential signal transducer in intestinal epithelial cells infected with bacteria that avoid recognition by toll-like receptors. Infect Immun. 2004;72(3):1487-95.

80. Kanneganti TD, Lamkanfi M, Núñez G. Intracellular NOD-like receptors in host defense and disease. Immunity. 2007;27(4):549-59.

81. Royet J, Dziarski R. Peptidoglycan recognition proteins: pleiotropic sensors and effectors of antimicrobial defences. Nature Reviews Microbiology. 2007;5(4):264-77.

82. Osanai A, Sashinami H, Asano K, Li SJ, Hu DL, Nakane A. Mouse peptidoglycan recognition protein PGLYRP-1 plays a role in the host innate immune response against Listeria monocytogenes infection. Infect Immun. 2011;79(2):858-66.

83. Saha S, Jing X, Park SY, Wang S, Li X, Gupta D, et al. Peptidoglycan recognition proteins protect mice from experimental colitis by promoting normal gut flora and preventing induction of interferon-gamma. Cell Host Microbe. 2010;8(2):147-62.

84. Chaput C, Sander LE, Suttorp N, Opitz B. NOD-Like Receptors in Lung Diseases. Front Immunol. 2013;4:393.

85. Inohara N, Ogura Y, Fontalba A, Gutierrez O, Pons F, Crespo J, et al. Host recognition of bacterial muramyl dipeptide mediated through NOD2: implications for Crohn′ s disease. Journal of Biological Chemistry. 2003;278(8):5509-12.

86. Gewirtz AT, Navas TA, Lyons S, Godowski PJ, Madara JL. Cutting edge: bacterial flagellin activates basolaterally expressed TLR5 to induce epithelial proinflammatory gene expression. J Immunol. 2001;167(4):1882-5.

87. Donnelly MA, Steiner TS. Two nonadjacent regions in enteroaggregative Escherichia coli flagellin are required for activation of toll-like receptor 5. J Biol Chem. 2002;277(43):40456-61.

88. Murthy KG, Deb A, Goonesekera S, Szabo C, Salzman AL. Identification of conserved domains in Salmonella muenchen flagellin that are essential for its ability to activate TLR5 and to induce an inflammatory response in vitro. J Biol Chem. 2004;279(7):5667-75.

89. Smith KD, Andersen-Nissen E, Hayashi F, Strobe K, Bergman MA, Barrett SL, et al. Toll-like receptor 5 recognizes a conserved site on flagellin required for protofilament formation and bacterial motility. Nat Immunol. 2003;4(12):1247-53.

90. Zhou Q, Desta T, Fenton M, Graves DT, Amar S. Cytokine profiling of macrophages exposed to Porphyromonas gingivalis, its lipopolysaccharide, or its FimA protein. Infect Immun. 2005;73(2):935-43.

91. Eskan MA, Hajishengallis G, Kinane DF. Differential activation of human gingival epithelial cells and monocytes by Porphyromonas gingivalis fimbriae. Infect Immun. 2007;75(2):892-8.

92. Takahashi Y, Davey M, Yumoto H, Gibson FC, 3rd, Genco CA. Fimbria-dependent activation of pro-inflammatory molecules in Porphyromonas gingivalis infected human aortic endothelial cells. Cell Microbiol. 2006;8(5):738-57.

93. Asai Y, Ohyama Y, Gen K, Ogawa T. Bacterial fimbriae and their peptides activate human gingival epithelial cells through Toll-like receptor 2. Infect Immun. 2001;69(12):7387-95.

94. Hajishengallis G, Tapping RI, Harokopakis E, Nishiyama S, Ratti P, Schifferle RE, et al. Differential interactions of fimbriae and lipopolysaccharide from Porphyromonas gingivalis with the Toll-like receptor 2-centred pattern recognition apparatus. Cell Microbiol. 2006;8(10):1557-70.

95. Davey M, Liu X, Ukai T, Jain V, Gudino C, Gibson FC, 3rd, et al. Bacterial fimbriae stimulate proinflammatory activation in the endothelium through distinct TLRs. J Immunol. 2008;180(4):2187-95.

96. Tükel C, Raffatellu M, Humphries AD, Wilson RP, Andrews-Polymenis HL, Gull T, et al. CsgA is a pathogen-associated molecular pattern of Salmonella enterica serotype Typhimurium that is recognized by Toll-like receptor 2. Mol Microbiol. 2005;58(1):289-304.

97. Ashkar AA, Mossman KL, Coombes BK, Gyles CL, Mackenzie R. FimH adhesin of type 1 fimbriae is a potent inducer of innate antimicrobial responses which requires TLR4 and type 1 interferon signalling. PLoS Pathog. 2008;4(12):e1000233.

98. Mossman KL, Mian MF, Lauzon NM, Gyles CL, Lichty B, Mackenzie R, et al. Cutting edge: FimH adhesin of type 1 fimbriae is a novel TLR4 ligand. J Immunol. 2008;181(10):6702-6.

99. Basset A, Zhang F, Benes C, Sayeed S, Herd M, Thompson C, et al. Toll-like receptor (TLR) 2 mediates inflammatory responses to oligomerized RrgA pneumococcal pilus type 1 protein. J Biol Chem. 2013;288(4):2665-75.

100. Takahashi R, Radcliff FJ, Proft T, Tsai CJ-Y. Pilus proteins from Streptococcus pyogenes stimulate innate immune responses through Toll-like receptor 2. Immunology & Cell Biology. 2022;100(3):174-85.

101. Kawano T, Hirano T, Kodama S, Mitsui MT, Ahmed K, Nishizono A, et al. Pili play an important role in enhancing the bacterial clearance from the middle ear in a mouse model of acute otitis media with Moraxella catarrhalis. Pathogens and Disease. 2013;67(2):119-31.

102. Leonard JN, Ghirlando R, Askins J, Bell JK, Margulies DH, Davies DR, et al. The TLR3 signaling complex forms by cooperative receptor dimerization. Proceedings of the National Academy of Sciences. 2008;105(1):258-63.

103. Mancuso G, Gambuzza M, Midiri A, Biondo C, Papasergi S, Akira S, et al. Bacterial recognition by TLR7 in the lysosomes of conventional dendritic cells. Nat Immunol. 2009;10(6):587-94.

104. Rimbach K, Kaiser S, Helm M, Dalpke AH, Eigenbrod T. 2'-O-Methylation within Bacterial RNA Acts as Suppressor of TLR7/TLR8 Activation in Human Innate Immune Cells. J Innate Immun. 2015;7(5):482-93.

105. Cervantes JL, Weinerman B, Basole C, Salazar JC. TLR8: the forgotten relative revindicated. Cellular & Molecular Immunology. 2012;9(6):434-8.

106. Cervantes JL, Dunham-Ems SM, La Vake CJ, Petzke MM, Sahay B, Sellati TJ, et al. Phagosomal signaling by Borrelia burgdorferi in human monocytes involves Toll-like receptor (TLR) 2 and TLR8 cooperativity and TLR8-mediated induction of IFN-&#x3b2. Proceedings of the National Academy of Sciences. 2011;108(9):3683-8.

107. Dalpke A, Frank J, Peter M, Heeg K. Activation of toll-like receptor 9 by DNA from different bacterial species. Infect Immun. 2006;74(2):940-6.

108. Brown MS, Goldstein JL, Krieger M, Ho Y, Anderson R. Reversible accumulation of cholesteryl esters in macrophages incubated with acetylated lipoproteins. The Journal of cell biology. 1979;82(3):597-613.

109. Taban Q, Mumtaz PT, Masoodi KZ, Haq E, Ahmad SM. Scavenger receptors in host defense: from functional aspects to mode of action. Cell Communication and Signaling. 2022;20(1):2.

110. Geijtenbeek TBH, Gringhuis SI. Signalling through C-type lectin receptors: shaping immune responses. Nature Reviews Immunology. 2009;9(7):465-79.

111. Gordon S. Pattern recognition receptors: doubling up for the innate immune response. Cell. 2002;111(7):927-30.

112. Franz KM, Kagan JC. Innate immune receptors as competitive determinants of cell fate. Molecular cell. 2017;66(6):750-60.

113. Coggon CF, Jiang A, Goh KGK, Henderson IR, Schembri MA, Wells TJ. A Novel Method of Serum Resistance by Escherichia coli That Causes Urosepsis. mBio. 2018;8(3).

114. Lei J, Sun L, Huang S, Zhu C, Li P, He J, et al. The antimicrobial peptides and their potential clinical applications. Am J Transl Res. 2019;11(7):3919-31.

115. Hancock RE, Sahl HG. Antimicrobial and host-defense peptides as new anti-infective therapeutic strategies. Nature Biotechnology. 2006;24(12):1551-7.

116. Scott MG, Hancock RE. Cationic antimicrobial peptides and their multifunctional role in the immune system. Critical Reviews in Immunology. 2000;20.

117. Zasloff M. Antibiotic peptides as mediators of innate immunity. Current Opinions in Immunology. 1992;4.

118. Stolzenberg ED, Anderson GM, Ackermann MR, Whitlock RH, Zasloff M. Epithelial antibiotic induced in states of disease. PNAS. 1997;94.

119. Bevins CL. Antimicrobial peptides as agents of mucosal immunity. Ciba Foundation Symposium. 1994;186.

120. Goldman MJ, Anderson GM, Stolzenberg ED, Kari UP, Zasloff M, Wilson JM. Human b-Defensin-1 Is a Salt-Sensitive Antibiotic in Lung That Is Inactivated in Cystic Fibrosis. Cell. 1997;88.

121. Jenssen H, Hamill P, Hancock RE. Peptide antimicrobial agents. Clinical Microbiology Reviews. 2006;19(3):491-511.

122. Helander IM, Kilpelainen I, Vaara M. Increased substitution of phosphate groups in lipopoiysaccharides and lipid A of the polymyxinresistant pmrA mutants of Salmonella typhimurium- 31P-NMR study. Molecular Microbiology. 1994;11(3).

123. McPhee JB, Lewenza S, Hancock RE. Cationic antimicrobial peptides activate a two-component regulatory system, PmrA-PmrB, that regulates resistance to polymyxin B and cationic antimicrobial peptides in Pseudomonas aeruginosa. Molecular Microbiology. 2003;50(1):205-17.

124. Gunn JS, Lim KB, Krueger J, Kim K, Guo L, Hackett M, et al. PmrA–PmrB-regulated genes necessary for 4-aminoarabinose lipid A modification and polymyxin resistance. Molecular Microbiology. 1998;27(6).

125. Shafer WM, Martin LE, Spitznagel JK. Cationic Antimicrobial Proteins Isolated from Human Neutrophil Granulocytes in the Presence of Diisopropyl Fluorophosphate. Infection and Immunity. 1984;45(1).

126. Spitznagel JK. Antibiotic Proteins of Human Neutrophils. Journal of Clinical Investigation. 1990;86.

127. Anisimov AP, Dentovskaya SV, Titareva GM, Bakhteeva IV, Shaikhutdinova RZ, Balakhonov SV, et al. Intraspecies and temperature-dependent variations in susceptibility of Yersinia pestis to the bactericidal action of serum and to polymyxin B. Infection & Immunity. 2005;73(11):7324-31.

128. Peterson AA, Haug A, McGroarty EJ. Physical Properties of Short- and Long-O-Antigen-Containing Fractions of Lipopolysaccharide from Escherichia coli O111-B4. Journal of Bacteriology. 1986;165(1).

129. Williams GJ, Breazeale SD, Raetz CR, Naismith JH. Structure and function of both domains of ArnA, a dual function decarboxylase and a formyltransferase, involved in 4-amino-4-deoxy-L-arabinose biosynthesis. Journal of Biological Chemistry. 2005;280(24):23000-8.

130. Hamad MA, Di Lorenzo F, Molinaro A, Valvano MA. Aminoarabinose is essential for lipopolysaccharide export and intrinsic antimicrobial peptide resistance in Burkholderia cenocepacia. Molecular Microbiology. 2012;85(5):962-74.

131. Silipo A, Molinaro A. The diversity of the core oligosaccharide in lipopolysaccharides. Subcellular Biochemistry. 2010;53:69-99.

132. Guo L, Lim KB, Gunn JS, Bainbridge B, Darveau RP, Hackett M, et al. Regulation of Lipid A Modifications by Salmonella typhimurium virulence genes phoP-phoQ. Science. 1996;276

.

133. Vaara M, Vaara T, Jensen M, Helander IM, Nurminen M, Rietschel ET, et al. Characterization of the lipopolysaccharide from the polymyxin-resistant pmrA mutants of Salmonella typhimurium. FEBS Letters. 1981;129(1).

134. Stinavage P, Martin LE, Spitznagel JK. O-Antigen and Lipid A Phosphoryl Groups in Resistance of Salmonella typhimurium LT-2 to Nonoxidative Killing in Human Polymorphonuclear Neutrophils. Infection and Immunity. 1989;57(12).

135. Vaara M, Vaara T. Outer membrane permeability barrier disruption by polymyxin in polymyxin-susceptible and -resistant Salmonella typhimurium. Antimicrobial Agents and Chemotherapy. 1980;19(4).

136. Nummila K, Kilpelainen I, Zahringer U, Vaara M, Helander IM. Lipopolysaccharides of polymyxin B-resistant mutants of Escherichia coii are extensively substituted by 2-aminoethyl pyrophosphate and contain aminoarabinose in lipid A. Molecular Microbiology. 1995;16(2).

137. Trent MS, Ribeiro AA, Doerrler WT, Lin S, Cotter RJ, Raetz CR. Accumulation of a polyisoprene-linked amino sugar in polymyxin-resistant Salmonella typhimurium and Escherichia coli: structural characterization and transfer to lipid A in the periplasm. Journal of Biological Chemistry. 2001;276(46):43132-44.

138. Trent MS, Ribeiro AA, Lin S, Cotter RJ, Raetz CR. An inner membrane enzyme in Salmonella and Escherichia coli that transfers 4-amino-4-deoxy-L-arabinose to lipid A: induction on polymyxin-resistant mutants and role of a novel lipid-linked donor. Journal of Biological Chemistry. 2001;276(46):43122-31.

139. Sidorczyk Z, Zahringer U, Rietschel ET. Chemical structure of the lipid A component of the lipopolysaccharide from a Proteus mirabilis Re-mutant. European Journal of Biochemistry. 1983;137.

140. Hase S, Rietschel ET. The Chemical Structure of the Lipid A Component of Lipopolysaccharides from Chromobacterium violaceum NCTC 9694. European Journal of Biochemistry. 1977;75.

141. Cox AD, Wilkinson SG. Ionizing groups in lipopolysaccharides of Pseudomonas cepacia in relation to antibiotic resistance. Molecular Microbiology. 1991;5(3).

142. Acharya D, Li XR, Heineman RE-S, Harrison RE. Complement Receptor-Mediated Phagocytosis Induces Proinflammatory Cytokine Production in Murine Macrophages. Frontiers in Immunology. 2020;10.

143. Lubbers R, van Essen MF, van Kooten C, Trouw LA. Production of complement components by cells of the immune system. Clinical & Experimental Immunology. 2017;188(2):183-94.

144. Ricklin D, Hajishengallis G, Yang K, Lambris JD. Complement: a key system for immune surveillance and homeostasis. Nature Immunology. 2010;11(9):785-97.

145. Markiewski MM, Lambris JD. The role of complement in inflammatory diseases from behind the scenes into the spotlight. American Journal of Pathology. 2007;171(3):715-27.

146. Goldberg BS, Ackerman ME. Antibody-mediated complement activation in pathology and protection. Immunology & Cell Biology. 2020;98(4):305-17.

147. Gaboriaud C, Thielens NM, Gregory LA, Rossi V, Fontecilla-Camps JC, Arlaud GJ. Structure and activation of the C1 complex of complement: unraveling the puzzle. Trends Immunol. 2004;25(7):368-73.

148. Wallis R, Mitchell DA, Schmid R, Schwaeble WJ, Keeble AH. Paths reunited: Initiation of the classical and lectin pathways of complement activation. Immunobiology. 2010;215(1):1-11.

149. Chen CB, Wallis R. Two mechanisms for mannose-binding protein modulation of the activity of its associated serine proteases. J Biol Chem. 2004;279(25):26058-65.

150. Klos A, Tenner AJ, Johswich KO, Ager RR, Reis ES, Köhl J. The role of the anaphylatoxins in health and disease. Mol Immunol. 2009;46(14):2753-66.

151. Turner MW. The role of mannose-binding lectin in health and disease. Mol Immunol. 2003;40(7):423-9.

152. Lambris JD, Ricklin D, Geisbrecht BV. Complement evasion by human pathogens. Nat Rev Microbiol. 2008;6(2):132-42.

153. Fujita T. Evolution of the lectin-complement pathway and its role in innate immunity. Nat Rev Immunol. 2002;2(5):346-53.

154. Bexborn F, Andersson PO, Chen H, Nilsson B, Ekdahl KN. The tick-over theory revisited: formation and regulation of the soluble alternative complement C3 convertase (C3(H2O)Bb). Mol Immunol. 2008;45(8):2370-9.

155. Pangburn MK, Schreiber RD, Muller-Eberhard HJ. Formation of the initial C3 convertase of the alternative complement pathway. Acquisition of C3b-like activities by spontaneous hydrolysis of the putative thioester in native C3. Journal of Experimental Medicine. 1981;154.

156. Harboe M, Mollnes TE. The alternative complement pathway revisited. J Cell Mol Med. 2008;12(4):1074-84.

157. Sahu A, Kozel TR, Pangburn MK. Specificity of the thioester-containing reactive site of human C3 and its significance to complement activation. Biochemistry. 1994;302.

158. Ferreira VP, Cortes C, Pangburn MK. Native polymeric forms of properdin selectively bind to targets and promote activation of the alternative pathway of complement. Immunobiology. 2010;215(11):932-40.

159. Muller-Eberhard HJ. The killer molecule of complement. J Invest Dermatol. 1985;85(1 Suppl):47s-52s.

160. Murakami Y, Imamichi T, Nagasawa S. Characterization of C3a anaphylatoxin receptor on guinea-pig macrophages. Immunology. 1993;79(4):633-8.

161. Elsner J, Oppermann M, Czech W, Kapp A. C3a activates the respiratory burst in human polymorphonuclear neutrophilic leukocytes via pertussis toxin-sensitive G-proteins. Blood. 1994;83(11):3324-31.

162. Johnson AR, Hugli TE, Müller-Eberhard HJ. Release of histamine from rat mast cells by the complement peptides C3a and C5a. Immunology. 1975;28(6):1067-80.

163. Fischer WH, Hugli TE. Regulation of B cell functions by C3a and C3a(desArg): suppression of TNF-alpha, IL-6, and the polyclonal immune response. J Immunol. 1997;159(9):4279-86.

164. Fischer WH, Jagels MA, Hugli TE. Regulation of IL-6 synthesis in human peripheral blood mononuclear cells by C3a and C3a(desArg). J Immunol. 1999;162(1):453-9.

165. Aksamit RR, Falk W, Leonard EJ. Chemotaxis by mouse macrophage cell lines. J Immunol. 1981;126(6):2194-9.

166. Ehrengruber MU, Geiser T, Deranleau DA. Activation of human neutrophils by C3a and C5A. Comparison of the effects on shape changes, chemotaxis, secretion, and respiratory burst. FEBS Lett. 1994;346(2-3):181-4.

167. Ottonello L, Corcione A, Tortolina G, Airoldi I, Albesiano E, Favre A, et al. rC5a directs the in vitro migration of human memory and naive tonsillar B lymphocytes: implications for B cell trafficking in secondary lymphoid tissues. J Immunol. 1999;162(11):6510-7.

168. Nataf S, Davoust N, Ames RS, Barnum SR. Human T cells express the C5a receptor and are chemoattracted to C5a. J Immunol. 1999;162(7):4018-23.

169. Doorduijn DJ, Rooijakkers SHM, van Schaik W, Bardoel BW. Complement resistance mechanisms of Klebsiella pneumoniae. Immunobiology. 2016;221(10):1102-9.

170. Diao J, Bouwman C, Yan D, Kang J, Katakam AK, Liu P, et al. Peptidoglycan Association of Murein Lipoprotein Is Required for KpsD-Dependent Group 2 Capsular Polysaccharide Expression and Serum Resistance in a Uropathogenic Escherichia coli Isolate. mBio. 2017;8(3).

171. Reckseidler-Zenteno SL, DeVinney R, Woods DE. The capsular polysaccharide of Burkholderia pseudomallei contributes to survival in serum by reducing complement factor C3b deposition. Infection & Immunity. 2005;73(2):1106-15.

172. Pawlak A, Rybka J, Dudek B, Krzyzewska E, Rybka W, Kedziora A, et al. Salmonella O48 Serum Resistance is Connected with the Elongation of the Lipopolysaccharide O-Antigen Containing Sialic Acid. International Journal of Molecular Science. 2017;18(10).

173. Jessop HL, Lambert PA. The role of surface polysaccharide in determining the resistance of Serratia marcescens to serum killing. Journal of General Microbiology. 1986;132.

174. Okamura N, Nakaya R, Suzuki K, Kondo S, Hisatsune K, Imagawa Y, et al. Differences among Shigellu spp. in Susceptibility to the Bactericidal Activity of Human Serum. Journal of General Microbiology. 1988;134.

175. Porat R, Mosseri R, Kaplan E, Johns MA, Shibolet S. Distribution of Polysaccharide Side Chains of Lipopolysaccharide Determine Resistance of Escherichia coli to the Bactericidal Activity of Serum.pdf. The Journal of Infectious Diseases. 1992.

176. Clark SE, Eichelberger KR, Weiser JN. Evasion of killing by human antibody and complement through multiple variations in the surface oligosaccharide of Haemophilus influenzae. Molecular Microbiology. 2013;88(3):603-18.

177. Keo T, Collins J, Kunwar P, Blaser MJ, Iovine NM. Campylobacter capsule and lipooligosaccharide confer resistance to serum and cationic antimicrobials. Virulence. 2011;2(1):30-40.

178. Smith LM, May RC. Mechanisms of microbial escape from phagocyte killing. Biochem Soc Trans. 2013;41(2):475-90.

179. García-García E, Rosales C. Signal transduction during Fc receptor-mediated phagocytosis. J Leukoc Biol. 2002;72(6):1092-108.

180. Swanson JA. Shaping cups into phagosomes and macropinosomes. Nat Rev Mol Cell Biol. 2008;9(8):639-49.

181. Marshansky V, Futai M. The V-type H+-ATPase in vesicular trafficking: targeting, regulation and function. Curr Opin Cell Biol. 2008;20(4):415-26.

182. Kinchen JM, Ravichandran KS. Phagosome maturation: going through the acid test. Nat Rev Mol Cell Biol. 2008;9(10):781-95.

183. Babior BM. NADPH oxidase. Current opinion in immunology. 2004;16(1):42-7.

184. Jabado N, Jankowski A, Dougaparsad S, Picard V, Grinstein S, Gros P. Natural resistance to intracellular infections: natural resistance-associated macrophage protein 1 (Nramp1) functions as a pH-dependent manganese transporter at the phagosomal membrane. J Exp Med. 2000;192(9):1237-48.

185. Uribe-Querol E, Rosales C. Control of Phagocytosis by Microbial Pathogens. Front Immunol. 2017;8:1368.

186. Minakami R, Sumimoto H. Phagocytosis-coupled activation of the superoxide-producing phagocyte oxidase, a member of the NADPH oxidase (nox) family. International journal of hematology. 2006;84(3):193-8.

187. Nauseef WM. Myeloperoxidase in human neutrophil host defence. Cellular microbiology. 2014;16(8):1146-55.

188. Fang FC. Antimicrobial reactive oxygen and nitrogen species: concepts and controversies. Nature Reviews Microbiology. 2004;2(10):820-32.

189. Park YD, Williamson PR. Masking the Pathogen: Evolutionary Strategies of Fungi and Their Bacterial Counterparts. J Fungi (Basel). 2015;1(3):397-421.

190. Woolard MD, Frelinger JA. Outsmarting the host: bacteria modulating the immune response. Immunol Res. 2008;41(3):188-202.

191. Finlay BB, McFadden G. Anti-immunology: evasion of the host immune system by bacterial and viral pathogens. Cell. 2006;124(4):767-82.

192. Boyd A, Chakrabarty AM. Pseudomonas aeruginosa biofilms: role of the alginate exopolysaccharide. J Ind Microbiol. 1995;15(3):162-8.

193. Portnoy DA. Manipulation of innate immunity by bacterial pathogens. Curr Opin Immunol. 2005;17(1):25-8.

194. Kawasaki K, Ernst RK, Miller SI. 3-O-deacylation of lipid A by PagL, a PhoP/PhoQ-regulated deacylase of Salmonella typhimurium, modulates signaling through Toll-like receptor 4. J Biol Chem. 2004;279(19):20044-8.

195. Cullen TW, Giles DK, Wolf LN, Ecobichon C, Boneca IG, Trent MS. Helicobacter pylori versus the host: remodeling of the bacterial outer membrane is required for survival in the gastric mucosa. PLoS Pathog. 2011;7(12):e1002454.

196. Montminy SW, Khan N, McGrath S, Walkowicz MJ, Sharp F, Conlon JE, et al. Virulence factors of Yersinia pestis are overcome by a strong lipopolysaccharide response. Nature Immunology. 2006;7(10):1066-73.

197. Lenz LL, Mohammadi S, Geissler A, Portnoy DA. SecA2-dependent secretion of autolytic enzymes promotes Listeria monocytogenes pathogenesis. Proc Natl Acad Sci U S A. 2003;100(21):12432-7.

198. Cabanes D, Dussurget O, Dehoux P, Cossart P. Auto, a surface associated autolysin of Listeria monocytogenes required for entry into eukaryotic cells and virulence. Mol Microbiol. 2004;51(6):1601-14.

199. Sarantis H, Grinstein S. Subversion of Phagocytosis for Pathogen Survival. Cell Host & Microbe. 2012;12(4):419-31.

200. Kilian M, Mestecky J, Schrohenloher RE. Pathogenic species of the genus Haemophilus and Streptococcus pneumoniae produce immunoglobulin A1 protease. Infect Immun. 1979;26(1):143-9.

201. Fagan PK, Reinscheid D, Gottschalk B, Chhatwal GS. Identification and characterization of a novel secreted immunoglobulin binding protein from group A streptococcus. Infection and immunity. 2001;69(8):4851-7.

202. Bessen DE. Localization of immunoglobulin A-binding sites within M or M-like proteins of group A streptococci. Infection and immunity. 1994;62(5):1968-74.

203. Blake MS, Swanson J. Studies on gonococcus infection. XVI. Purification of Neisseria gonorrhoeae immunoglobulin A1 protease. Infect Immun. 1978;22(2):350-8.

204. Ryan MH, Petrone D, Nemeth JF, Barnathan E, Björck L, Jordan RE. Proteolysis of purified IgGs by human and bacterial enzymes in vitro and the detection of specific proteolytic fragments of endogenous IgG in rheumatoid synovial fluid. Mol Immunol. 2008;45(7):1837-46.

205. Gulati S, Cox A, Lewis LA, St. Michael F, Li J, Boden R, et al. Enhanced factor H binding to sialylated Gonococci is restricted to the sialylated lacto-N-neotetraose lipooligosaccharide species: implications for serum resistance and evidence for a bifunctional lipooligosaccharide sialyltransferase in Gonococci. Infection and immunity. 2005;73(11):7390-7.

206. Ram S, Sharma AK, Simpson SD, Gulati S, McQuillen DP, Pangburn MK, et al. A novel sialic acid binding site on factor H mediates serum resistance of sialylated Neisseria gonorrhoeae. The Journal of experimental medicine. 1998;187(5):743-52.

207. Kahler CM, Stephens DS. Genetic basis for biosynthesis, structure, and function of meningococcal lipooligosaccharide (endotoxin). Crit Rev Microbiol. 1998;24(4):281-334.

208. Alpuche Aranda CM, Swanson JA, Loomis WP, Miller SI. Salmonella typhimurium activates virulence gene transcription within acidified macrophage phagosomes. Proceedings of the National Academy of Sciences of the United States of America. 1992;89(21):10079-83.

209. Kier LD, Weppelman R, Ames BN. Regulation of two phosphatases and a cyclic phosphodiesterase of Salmonella typhimurium. J Bacteriol. 1977;130(1):420-8.

210. Miller SI, Kukral AM, Mekalanos JJ. A two-component regulatory system (phoP phoQ) controls Salmonella typhimurium virulence. Proc Natl Acad Sci U S A. 1989;86(13):5054-8.

211. Gunn JS, Belden WJ, Miller SI. Identification of PhoP-PhoQ activated genes within a duplicated region of the Salmonella typhimurium chromosome. Microb Pathog. 1998;25(2):77-90.

212. Belden WJ, Miller SI. Further characterization of the PhoP regulon: identification of new PhoP-activated virulence loci. Infect Immun. 1994;62(11):5095-101.

213. Guina T, Yi EC, Wang H, Hackett M, Miller SI. A PhoP-regulated outer membrane protease of Salmonella enterica serovar typhimurium promotes resistance to alpha-helical antimicrobial peptides. J Bacteriol. 2000;182(14):4077-86.

214. Fass E, Groisman EA. Control of Salmonella pathogenicity island-2 gene expression. Curr Opin Microbiol. 2009;12(2):199-204.

215. Miller SI, Ernst RK, Bader MW. LPS, TLR4 and infectious disease diversity. Nature Reviews Microbiology. 2005;3(1):36-46.

216. Lee EJ, Pontes MH, Groisman EA. A bacterial virulence protein promotes pathogenicity by inhibiting the bacterium's own F1Fo ATP synthase. Cell. 2013;154(1):146-56.

217. Bishop RE, Gibbons HS, Guina T, Trent MS, Miller SI, Raetz CR. Transfer of palmitate from phospholipids to lipid A in outer membranes of gram-negative bacteria. EMBO J. 2000;19(19):5071-80.

218. Park BS, Song DH, Kim HM, Choi B-S, Lee H, Lee J-O. The structural basis of lipopolysaccharide recognition by the TLR4–MD-2 complex. Nature. 2009;458(7242):1191-5.

219. Guo L, Lim KB, Gunn JS, Bainbridge B, Darveau RP, Hackett M, et al. Regulation of Lipid A Modifications by Salmonella typhimurium virulence genes phoP-phoQ. Science. 1996;276.

220. Trent MS, Pabich W, Raetz CR, Miller SI. A PhoP/PhoQ-induced Lipase (PagL) that catalyzes 3-O-deacylation of lipid A precursors in membranes of Salmonella typhimurium. J Biol Chem. 2001;276(12):9083-92.

221. Gunn JS, Miller SI. PhoP-PhoQ activates transcription of pmrAB, encoding a two-component regulatory system involved in Salmonella typhimurium antimicrobial peptide resistance. J Bacteriol. 1996;178(23):6857-64.

222. Tamayo R, Choudhury B, Septer A, Merighi M, Carlson R, Gunn JS. Identification of cptA, a PmrA-regulated locus required for phosphoethanolamine modification of the Salmonella enterica serovar typhimurium lipopolysaccharide core. Journal of bacteriology. 2005;187(10):3391-9.

223. Chen HD, Groisman EA. The biology of the PmrA/PmrB two-component system: the major regulator of lipopolysaccharide modifications. Annu Rev Microbiol. 2013;67:83-112.

224. Kato A, Groisman EA. Connecting two-component regulatory systems by a protein that protects a response regulator from dephosphorylation by its cognate sensor. Genes Dev. 2004;18(18):2302-13.

225. Dalebroux ZD, Miller SI. Salmonellae PhoPQ regulation of the outer membrane to resist innate immunity. Curr Opin Microbiol. 2014;17:106-13.

226. Miller SI, Pulkkinen WS, Selsted ME, Mekalanos JJ. Characterization of defensin resistance phenotypes associated with mutations in the phoP virulence regulon of Salmonella typhimurium. Infect Immun. 1990;58(11):3706-10.

227. Pulkkinen WS, Miller SI. A Salmonella typhimurium virulence protein is similar to a Yersinia enterocolitica invasion protein and a bacteriophage lambda outer membrane protein. J Bacteriol. 1991;173(1):86-93.

228. Messner KR, Imlay JA. The identification of primary sites of superoxide and hydrogen peroxide formation in the aerobic respiratory chain and sulfite reductase complex of Escherichia coli. J Biol Chem. 1999;274(15):10119-28.

229. Vanaporn M, Wand M, Michell SL, Sarkar-Tyson M, Ireland P, Goldman S, et al. Superoxide dismutase C is required for intracellular survival and virulence of Burkholderia pseudomallei. Microbiology (Reading). 2011;157(Pt 8):2392-400.

230. Cumley NJ, Smith LM, Anthony M, May RC. The CovS/CovR Acid Response Regulator Is Required for Intracellular Survival of Group B Streptococcus in Macrophages. Infection and Immunity. 2012;80(5):1650-61.

231. Rajagopal L. Understanding the regulation of Group B Streptococcal virulence factors. Future Microbiol. 2009;4(2):201-21.

232. Maisey HC, Doran KS, Nizet V. Recent advances in understanding the molecular basis of group B Streptococcus virulence. Expert Rev Mol Med. 2008;10:e27.

233. Doran KS, Nizet V. Molecular pathogenesis of neonatal group B streptococcal infection: no longer in its infancy. Mol Microbiol. 2004;54(1):23-31.

234. Seaver LC, Imlay JA. Alkyl Hydroperoxide Reductase Is the Primary Scavenger of Endogenous Hydrogen Peroxide in Escherichia coli. Journal of Bacteriology. 2001;183(24):7173-81.

235. Borlace GN, Keep SJ, Prodoehl MJ, Jones HF, Butler RN, Brooks DA. A role for altered phagosome maturation in the long-term persistence of Helicobacter pylori infection. Am J Physiol Gastrointest Liver Physiol. 2012;303(2):G169-79.

236. Basu M, Czinn SJ, Blanchard TG. Absence of catalase reduces long-term survival of Helicobacter pylori in macrophage phagosomes. Helicobacter. 2004;9(3):211-6.

237. Bryk R, Griffin P, Nathan C. Peroxynitrite reductase activity of bacterial peroxiredoxins. Nature. 2000;407(6801):211-5.

238. Evans Jr DJ, Evans DG, Takemura T, Nakano H, Lampert HC, Graham DY, et al. Characterisation of a helicobacter pylori neutrophil-activating protein. Infection and Immunity. 1995;63(6).

239. Darby EM, Trampari E, Siasat P, Gaya MS, Alav I, Webber MA, et al. Molecular mechanisms of antibiotic resistance revisited. Nature Reviews Microbiology. 2022.

240. Tomasz A. The mechanism of the irreversible antimicrobial effects of penicillins: how the beta-lactam antibiotics kill and lyse bacteria. Annual Reviews in Microbiology. 1979;33(1):113-37.

241. Cho H, Uehara T, Bernhardt Thomas G. Beta-Lactam Antibiotics Induce a Lethal Malfunctioning of the Bacterial Cell Wall Synthesis Machinery. Cell. 2014;159(6):1300-11.

242. Ragland SA, Criss AK. From bacterial killing to immune modulation: Recent insights into the functions of lysozyme. PLoS Pathog. 2017;13(9):e1006512.

243. Davis KM, Nakamura S, Weiser JN. Nod2 sensing of lysozyme-digested peptidoglycan promotes macrophage recruitment and clearance of S. pneumoniae colonization in mice. J Clin Invest. 2011;121(9):3666-76.

244. Caruso R, Warner N, Inohara N, Núñez G. NOD1 and NOD2: signaling, host defense, and inflammatory disease. Immunity. 2014;41(6):898-908.

245. Shimada T, Park BG, Wolf AJ, Brikos C, Goodridge HS, Becker CA, et al. Staphylococcus aureus evades lysozyme-based peptidoglycan digestion that links phagocytosis, inflammasome activation, and IL-1β secretion. Cell host & microbe. 2010;7(1):38-49.

246. Wolf AJ, Arruda A, Reyes CN, Kaplan AT, Shimada T, Shimada K, et al. Phagosomal degradation increases TLR access to bacterial ligands and enhances macrophage sensitivity to bacteria. The Journal of Immunology. 2011;187(11):6002-10.

247. Ganz T, Gabayan V, Liao H-I, Liu L, Oren A, Graf T, et al. Increased inflammation in lysozyme M–deficient mice in response to Micrococcus luteus and its peptidoglycan. Blood, The Journal of the American Society of Hematology. 2003;101(6):2388-92.

248. Zhang Q, Pan Y, Yan R, Zeng B, Wang H, Zhang X, et al. Commensal bacteria direct selective cargo sorting to promote symbiosis. Nature immunology. 2015;16(9):918-26.

249. Wang H, Zhang X, Zuo Z, Zhang Q, Pan Y, Zeng B, et al. Rip2 is required for Nod2-mediated lysozyme sorting in Paneth cells. The Journal of Immunology. 2017;198(9):3729-36.

250. Inamura S, Fujimoto Y, Kawasaki A, Shiokawa Z, Woelk E, Heine H, et al. Synthesis of peptidoglycan fragments and evaluation of their biological activity. Organic & biomolecular chemistry. 2006;4(2):232-42.

251. Inohara N, Ogura Y, Chen FF, Muto A, Nunez G. Human Nod1 confers responsiveness to bacterial lipopolysaccharides. J Biol Chem. 2001;276(4):2551-4.

252. Iyer JK, Coggeshall KM. Cutting edge: primary innate immune cells respond efficiently to polymeric peptidoglycan, but not to peptidoglycan monomers. The Journal of Immunology. 2011;186(7):3841-5.

253. Canton J, Schlam D, Breuer C. Calcium-sensing receptors signal constitutive macropinocytosis and facilitate the uptake of NOD2 ligands in macrophages. Nat Commun 7: 1–12. 2016.

254. Khatami A, Lin RCY, Petrovic-Fabijan A, Alkalay-Oren S, Almuzam S, Britton PN, et al. Bacterial lysis, autophagy and innate immune responses during adjunctive phage therapy in a child. EMBO Molecular Medicine. 2021;13(9):e13936.

255. Lerner TR, Borel S, Greenwood DJ, Repnik U, Russell MRG, Herbst S, et al. Mycobacterium tuberculosis replicates within necrotic human macrophages. Journal of Cell Biology. 2017;216(3):583-94.

256. Greenwood DJ, Dos Santos MS, Huang S, Russell MRG, Collinson LM, MacRae JI, et al. Subcellular antibiotic visualization reveals a dynamic drug reservoir in infected macrophages. Science. 2019;364(6447):1279-82.

257. Santucci P, Greenwood DJ, Fearns A, Chen K, Jiang H, Gutierrez MG. Intracellular localisation of Mycobacterium tuberculosis affects efficacy of the antibiotic pyrazinamide. Nature Communications. 2021;12(1):3816.

258. González-Bello C. Antibiotic adjuvants - A strategy to unlock bacterial resistance to antibiotics. Bioorg Med Chem Lett. 2017;27(18):4221-8.

259. Jansen KU, Knirsch C, Anderson AS. The role of vaccines in preventing bacterial antimicrobial resistance. Nature Medicine. 2018;24(1):10-9.

260. Doerr HW, Berger A. Vaccination against infectious diseases: What is promising? Medical Microbiology and Immunology. 2014;203(6):365-71.

261. Adam HJ, Richardson SE, Jamieson FB, Rawte P, Low DE, Fisman DN. Changing epidemiology of invasive Haemophilus influenzae in Ontario, Canada: evidence for herd effects and strain replacement due to Hib vaccination. Vaccine. 2010;28(24):4073-8.

262. Defoirdt T. Quorum-Sensing Systems as Targets for Antivirulence Therapy. Trends Microbiol. 2018;26(4):313-28.

263. Starkey M, Lepine F, Maura D, Bandyopadhaya A, Lesic B, He J, et al. Identification of Anti-virulence Compounds That Disrupt Quorum-Sensing Regulated Acute and Persistent Pathogenicity. PLOS Pathogens. 2014;10(8):e1004321.

264. Rasko DA, Sperandio V. Anti-virulence strategies to combat bacteria-mediated disease. Nature Reviews Drug Discovery. 2010;9(2):117-28.

265. García-Contreras R, Martínez-Vázquez M, Velázquez Guadarrama N, Villegas Pañeda AG, Hashimoto T, Maeda T, et al. Resistance to the quorum-quenching compounds brominated furanone C-30 and 5-fluorouracil in Pseudomonas aeruginosa clinical isolates. Pathog Dis. 2013;68(1):8-11.

266. Maeda T, García-Contreras R, Pu M, Sheng L, Garcia LR, Tomás M, et al. Quorum quenching quandary: resistance to antivirulence compounds. The ISME Journal. 2012;6(3):493-501.

267. Resch A, Rosenstein R, Nerz C, Götz F. Differential gene expression profiling of Staphylococcus aureus cultivated under biofilm and planktonic conditions. Appl Environ Microbiol. 2005;71(5):2663-76.

268. Maura D, Ballok AE, Rahme LG. Considerations and caveats in anti-virulence drug development. Curr Opin Microbiol. 2016;33:41-6.

269. Martinez JL, Baquero F. Mutation Frequencies and Antibiotic Resistance. Antimicrobial Agents and Chemotherapy. 2000;44(7):1771-7.

270. Hermoso JA, García JL, García P. Taking aim on bacterial pathogens: from phage therapy to enzybiotics. Curr Opin Microbiol. 2007;10(5):461-72.

271. Domingo-Calap P, Delgado-Martínez J. Bacteriophages: Protagonists of a Post-Antibiotic Era. Antibiotics (Basel). 2018;7(3).

272. Principi N, Silvestri E, Esposito S. Advantages and Limitations of Bacteriophages for the Treatment of Bacterial Infections. Frontiers in Pharmacology. 2019;10.

273. Briers Y, Miroshnikov K, Chertkov O, Nekrasov A, Mesyanzhinov V, Volckaert G, et al. The structural peptidoglycan hydrolase gp181 of bacteriophage phiKZ. Biochem Biophys Res Commun. 2008;374(4):747-51.

274. Briers Y, Walmagh M, Lavigne R. Use of bacteriophage endolysin EL188 and outer membrane permeabilizers against Pseudomonas aeruginosa. J Appl Microbiol. 2011;110(3):778-85.

275. O'Sullivan L, Buttimer C, McAuliffe O, Bolton D, Coffey A. Bacteriophage-based tools: recent advances and novel applications. F1000Res. 2016;5:2782.

276. Rodríguez-Rubio L, Martínez B, Donovan DM, Rodríguez A, García P. Bacteriophage virion-associated peptidoglycan hydrolases: potential new enzybiotics. Crit Rev Microbiol. 2013;39(4):427-34.

277. Lerner T, Lovering AL, Bui NK, Uchida K, Aizawa S-I, Vollmer W, et al. Specialized Peptidoglycan Hydrolases Sculpt the Intra-bacterial Niche of Predatory Bdellovibrio and Increase Population Fitness. PLoS Pathogens. 2012;8(2):e1002524-e.

278. Stolp H, Starr MP. Bdellovibrio bacteriovorus gen. et sp. n., a predatory, ectoparasitic, and bacteriolytic microorganism. Antonie van Leeuwenhoek. 1963;29(1):217-48.

279. Hobley L, Lerner TR, Williams LE, Lambert C, Till R, Milner DS, et al. Genome analysis of a simultaneously predatory and prey-independent, novel Bdellovibrio bacteriovorus from the River Tiber, supports in silico predictions of both ancient and recent lateral gene transfer from diverse bacteria. BMC Genomics. 2012;13:670.

280. Barabote RD, Rendulic S, Schuster SC, Saier MH. Comprehensive analysis of transport proteins encoded within the genome of Bdellovibrio bacteriovorus. Genomics. 2007;90(4):424-46.

281. Rendulic S, Eppinger M, Baar C, Lanz C, Keller H, Meyer F, et al. A Predator Unmasked : Life Cycle of Bdellovibrio bacteriovorus from a Genomic Perspective. Science. 2004;689(2004):689-93.

282. Hallin PF, Ussery DW. CBS Genome Atlas Database: a dynamic storage for bioinformatic results and sequence data. Bioinformatics. 2004;20(18):3682-6.

283. Tudor JJ, Davis JJ, Panichella M, Zwolak A. Isolation of predation-deficient mutants of Bdellovibrio bacteriovorus by using transposon mutagenesis. Appl Environ Microbiol. 2008;74(17):5436-43.

284. Duncan MC, Gillette RK, Maglasang MA, Corn EA, Tai AK, Lazinski DW, et al. High-Throughput Analysis of Gene Function in the Bacterial Predator Bdellovibrio bacteriovorus. mBio. 2019;10(3):e01040-19.

285. Gophna U, Charlebois RL, Doolittle WF. Ancient lateral gene transfer in the evolution of Bdellovibrio bacteriovorus. Trends Microbiol. 2006;14(2):64-9.

286. Hobley L, Fung RK, Lambert C, Harris MA, Dabhi JM, King SS, et al. Discrete cyclic di-GMP-dependent control of bacterial predation versus axenic growth in Bdellovibrio bacteriovorus. PLoS Pathog. 2012;8(2):e1002493.

287. Pan A, Chanda I, Chakrabarti J. Analysis of the genome and proteome composition of Bdellovibrio bacteriovorus: indication for recent prey-derived horizontal gene transfer. Genomics. 2011;98(3):213-22.

288. Lambert C, Hobley L, Chang CY, Fenton A, Capeness M, Sockett L. A predatory patchwork: membrane and surface structures of Bdellovibrio bacteriovorus. Adv Microb Physiol. 2009;54:313-61.

289. Mues N, Chu HW. Out-Smarting the Host: Bacteria Maneuvering the Immune Response to Favor Their Survival. Front Immunol. 2020;11:819.

290. Harding CJ, Huwiler SG, Somers H, Lambert C, Ray LJ, Till R, et al. A lysozyme with altered substrate specificity facilitates prey cell exit by the periplasmic predator Bdellovibrio bacteriovorus. Nature Communications. 2020;11(1):4817.

291. Lambert C, Cadby IT, Till R, Bui NK, Lerner TR, Hughes WS, et al. Ankyrin-mediated self-protection during cell invasion by the bacterial predator Bdellovibrio bacteriovorus. Nat Commun. 2015;6:8884.

292. Lambert C, Lerner TR, Bui NK, Somers H, Aizawa S, Liddell S, et al. Interrupting peptidoglycan deacetylation during Bdellovibrio predator-prey interaction prevents ultimate destruction of prey wall, liberating bacterial-ghosts. Sci Rep. 2016;6:26010.

293. Muller FD, Beck S, Strauch E, Linscheid MW. Bacterial predators possess unique membrane lipid structures. Lipids. 2011;46(12):1129-40.

294. Schwudke D, Linscheid M, Strauch E, Appel B, Zähringer U, Moll H, et al. The obligate predatory Bdellovibrio bacteriovorus possesses a neutral lipid a containing α-D-mannoses that replace phosphate residues. Similarities and differences between the lipid As and the lipopolysaccharides of the wild type strain B. bacteriovorus H. Journal of Biological Chemistry. 2003;278(30):27502-12.

295. Rocha DM, Caldas AP, Oliveira LL, Bressan J, Hermsdorff HH. Saturated fatty acids trigger TLR4-mediated inflammatory response. Atherosclerosis. 2016;244:211-5.

296. Lerner TR. Modification of Prey Peptidoglycan by *Bdellovibrio bacteriovorus*. Nottingham: University of Nottingham; 2012.

297. Vollmer W, Bertsche U. Murein (peptidoglycan) structure, architecture and biosynthesis in Escherichia coli. Biochim Biophys Acta. 2008;1778(9):1714-34.

298. Vollmer W, Blanot D, de Pedro MA. Peptidoglycan structure and architecture. FEMS Microbiol Rev. 2008;32(2):149-67.

299. Vollmer W, Joris B, Charlier P, Foster S. Bacterial peptidoglycan (murein) hydrolases. FEMS Microbiol Rev. 2008;32(2):259-86.

300. Kuru E, Lambert C, Rittichier J, Till R, Ducret A, Derouaux A, et al. Fluorescent D-amino-acids reveal bi-cellular cell wall modifications important for Bdellovibrio bacteriovorus predation. Nat Microbiol. 2017;2(12):1648-57.

301. Schwudke D, Bernhardt A, Beck S, Madela K, Linscheid MW, Appel B, et al. Transcriptional activity of the host-interaction locus and a putative pilin gene of Bdellovibrio bacteriovorus in the predatory life cycle. Curr Microbiol. 2005;51(5):310-6.

302. Evans KJ, Lambert C, Sockett RE. Predation by Bdellovibrio bacteriovorus HD100 requires type IV pili. J Bacteriol. 2007;189(13):4850-9.

303. Mahmoud KK, Koval SF. Characterization of type IV pili in the life cycle of the predator bacterium Bdellovibrio. Microbiology (Reading). 2010;156(Pt 4):1040-51.

304. Chanyi RM, Koval SF. Role of type IV pili in predation by Bdellovibrio bacteriovorus. PLoS One. 2014;9(11):e113404.

305. Avidan O, Petrenko M, Becker R, Beck S, Linscheid M, Pietrokovski S, et al. Identification and Characterization of Differentially-Regulated Type IVb Pilin Genes Necessary for Predation in Obligate Bacterial Predators. Sci Rep. 2017;7(1):1013.

306. Shilo M, editor Morphological and Physiological Aspects of the Interaction of Bdellovibrio with Host Bacteria1969; Berlin, Heidelberg: Springer Berlin Heidelberg.

307. Lambert C, Evans KJ, Till R, Hobley L, Capeness M, Rendulic S, et al. Characterizing the flagellar filament and the role of motility in bacterial prey-penetration by Bdellovibrio bacteriovorus. Mol Microbiol. 2006;60(2):274-86.

308. Iida Y, Hobley L, Lambert C, Fenton AK, Sockett RE, Aizawa S. Roles of multiple flagellins in flagellar formation and flagellar growth post bdelloplast lysis in Bdellovibrio bacteriovorus. J Mol Biol. 2009;394(5):1011-21.

309. Kaplan M, Chang Y-W, Oikonomou CM, Nicolas WJ, Jewett AI, Kreida S, et al. Dynamic structural adaptations enable the endobiotic predation of bdellovibrio bacteriovorus. bioRxiv. 2022:2022.06.13.496000.

310. Rittenberg SC, Shilo M. Early host damage in the infection cycle of Bdellovibrio bacteriovorus. J Bacteriol. 1970;102(1):149-60.

311. Thomashow MF, Rittenberg SC. Intraperiplasmic growth of Bdellovibrio bacteriovorus 109J: N-deacetylation of Escherichia coli peptidoglycan amino sugars. J Bacteriol. 1978;135(3):1008-14.

312. Morehouse KA, Hobley L, Capeness M, Sockett RE. Three motAB stator gene products in Bdellovibrio bacteriovorus contribute to motility of a single flagellum during predatory and prey-independent growth. Journal of Bacteriology. 2011;193(4):932-43.

313. Lu Y, Swartz JR. Functional properties of flagellin as a stimulator of innate immunity. Scientific Reports. 2016;6(1):18379.

314. Capeness MJ, Lambert C, Lovering AL, Till R, Uchida K, Chaudhuri R, et al. Activity of Bdellovibrio hit locus proteins, bd0108 and bd0109, links type IVa pilus extrusion/retraction status to prey-independent growth signalling. PLoS ONE. 2013;8(11).

315. Evans KJ, Lambert C, Sockett RE. Predation by Bdellovibrio bacteriovorus HD100 requires type IV pili. Journal of Bacteriology. 2007;189(13):4850-9.

316. Starr MP, Baigent NL. Parasitic interaction of Bdellovibrio bacteriovorus with other bacteria. J Bacteriol. 1966;91(5):2006-17.

317. Rogosky AM, Moak PL, Emmert EA. Differential predation by Bdellovibrio bacteriovorus 109J. Curr Microbiol. 2006;52(2):81-5.

318. Sockett RE. Predatory lifestyle of Bdellovibrio bacteriovorus. Annu Rev Microbiol. 2009;63:523-39.

319. Lambert C, Fenton AK, Hobley L, Sockett RE. Predatory Bdellovibrio bacteria use gliding motility to scout for prey on surfaces. Journal of Bacteriology. 2011;193(12):3139-41.

320. Jurkevitch E, Minz D, Ramati B, Barel G. Prey range characterization, ribotyping, and diversity of soil and rhizosphere Bdellovibrio spp. isolated on phytopathogenic bacteria. Applied and Environmental Microbiology. 2000;66(6):2365-71.

321. Thomashow LS, Rittenberg SC. Waveform analysis and structure of flagella and basal complexes from Bdellovibrio bacteriovorus 109J. Journal of Bacteriology. 1985;163(3):1038-46.

322. Sockett RE, Lambert C. Bdellovibrio as therapeutic agents: A predatory renaissance? Nature Reviews Microbiology. 2004;2(8):669-75.

323. Tudor JJ, McCann MP, Acrich IA. A new model for the penetration of prey cells by bdellovibrios. J Bacteriol. 1990;172(5):2421-6.

324. Kuru E, Lambert C, Rittichier J, Till R, Ducret A, Gray J, et al. Fluorescent D-amino-acids reveal bi-cellular cell wall modifications important for Bdellovibrio bacteriovorus predation. Nature Microbiology. 2018;2(12):1648-57.

325. Lambert C, Chang C-Y, Capeness MJ, Sockett RE. The First Bite— Profiling the Predatosome in the Bacterial Pathogen Bdellovibrio. PLoS ONE. 2010;5(1):e8599-e.

326. Schelling M, Conti S. Host receptor sites involved in the attachment of Bdellovibrio bacteriovorus and Bdellovibrio stolpii. FEMS Microbiology Letters. 1986;36(2-3):319-23.

327. Koval SF, Bayer ME. Bacterial capsules: no barrier against Bdellovibrio bacteriovorus. Microbiology. 1997;143(1991):749-53.

328. Rittenberg SC, Shilo M. Early host damage in the infection cycle of Bdellovibrio bacteriovorus. Journal of Bacteriology. 1970;102(1):149-60.

329. Chang CY, Hobley L, Till R, Capeness M, Kanna M, Burtt W, et al. The Bdellovibrio bacteriovorus twin-arginine transport system has roles in predatory and prey-independent growth. Microbiology (Reading). 2011;157(Pt 11):3079-93.

330. Lambert C, Sockett RE. Nucleases in Bdellovibrio bacteriovorus contribute towards efficient self-biofilm formation and eradication of preformed prey biofilms. FEMS Microbiol Lett. 2013;340(2):109-16.

331. Bukowska-Faniband E, Andersson T, Lood R. Studies on Bd0934 and Bd3507, Two Secreted Nucleases from Bdellovibrio bacteriovorus, Reveal Sequential Release of Nucleases during the Predatory Cycle. J Bacteriol. 2020;202(18).

332. Galdiero F. Membrane damage and incorporation of Escherichia coli components into Bdellovibrio bacteriovorus. Zentralblatt fur Bakteriologie, Parasitenkunde, Infektionskrankheiten und Hygiene Erste Abteilung Originale Reihe A: Medizinische Mikrobiologie und Parasitologie. 1975;230(2):203-9.

333. Matin A, Rittenberg SC. Kinetics of deoxyribonucleic acid destruction and synthesis during growth of Bdellovibrio bacteriovorus strain 109D on pseudomonas putida and escherichia coli. Journal of Bacteriology. 1972;111(3):664-73.

334. Hespell RB, Miozzari GF, Rittenberg SC. Ribonucleic acid destruction and synthesis during intraperiplasmic growth of Bdellovibrio bacteriovorus. Journal of Bacteriology. 1975;123(2):481-91.

335. Rosson RA, Rittenberg SC. Regulated breakdown of Escherichia coli deoxyribonucleic acid during intraperiplasmic growth of Bdellovibrio bacteriovorus 109J. Journal of bacteriology. 1979;140(2):620-33.

336. Hespell RB, Odelson DA. Metabolism of RNA-ribose by Bdellovibrio bacteriovorus during intraperiplasmic growth on Escherichia coli. J Bacteriol. 1978;136(3):936-46.

337. Hespell RB, Miozzari GF, Rittenberg SC. Ribonucleic acid destruction and synthesis during intraperiplasmic growth of Bdellovibrio bacteriovorus. J Bacteriol. 1975;123(2):481-91.

338. Ruby EG, McCabe JB, Barke JI. Uptake of intact nucleoside monophosphates by Bdellovibrio bacteriovorus 109J. J Bacteriol. 1985;163(3):1087-94.

339. Gray K, Ruby E. Unbalanced growth as a normal feature of development of Bdellovibrio bacteriovorus. Archives of Microbiology. 1989;152(5):420-4.

340. Eksztejn M, Varon M. Elongation and cell division in Bdellovibrio bacteriovorus. Archives of Microbiology. 1977;114(2):175-81.

341. Milner DS, Ray LJ, Saxon EB, Lambert C, Till R, Fenton AK, et al. DivIVA Controls Progeny Morphology and Diverse ParA Proteins Regulate Cell Division or Gliding Motility in Bdellovibrio bacteriovorus. Front Microbiol. 2020;11:542.

342. Fenton AK, Kanna M, Woods RD, Aizawa SI, Sockett RE. Shadowing the actions of a predator: backlit fluorescent microscopy reveals synchronous nonbinary septation of predatory Bdellovibrio inside prey and exit through discrete bdelloplast pores. J Bacteriol. 2010;192(24):6329-35.

343. Thomashow M, Rittenberg S. Developmental biology of prokaryotes. Blackwell Scientific Oxford; 1979.

344. Flannagan RS, Valvano MA, Koval SF. Downregulation of the motA gene delays the escape of the obligate predator Bdellovibrio bacteriovorus 109J from bdelloplasts of bacterial prey cells. Microbiology (Reading). 2004;150(Pt 3):649-56.

345. Varon M, Fine M, Stein A. Effect of polyamines on the intraperiplasmic growth of Bdellovibrio at low cell densities. Archives of Microbiology. 1983;136(2):158-9.

346. Arts IS, Gennaris A, Collet J-F. Reducing systems protecting the bacterial cell envelope from oxidative damage. FEBS Letters. 2015;589(14):1559-68.

347. Cotter TW, Thomashow MF. Identification of a Bdellovibrio bacteriovorus genetic locus, hit, associated with the host-independent phenotype. J Bacteriol. 1992;174(19):6018-24.

348. Capeness MJ, Lambert C, Lovering AL, Till R, Uchida K, Chaudhuri R, et al. Activity of Bdellovibrio hit locus proteins, Bd0108 and Bd0109, links Type IVa pilus extrusion/retraction status to prey-independent growth signalling. PLoS One. 2013;8(11):e79759.

349. Negus D, Moore C, Baker M, Raghunathan D, Tyson J, Sockett RE. Predator Versus Pathogen: How Does Predatory Bdellovibrio bacteriovorus Interface with the Challenges of Killing Gram-Negative Pathogens in a Host Setting? Annual Review of Microbiology. 2017;71(1):441-57.

350. Lambert C, Ivanov P, Sockett RE. A transcriptional "scream" early response of E. coli prey to predatory invasion by bdellovibrio. Current Microbiology. 2010;60(6):419-27.

351. Shemesh Y, Jurkevitch E. Plastic phenotypic resistance to predation by Bdellovibrio and like organisms in bacterial prey. Environ Microbiol. 2004;6(1):12-8.

352. Atterbury RJ, Hobley L, Till R, Lambert C, Capeness MJ, Lerner TR, et al. Effects of orally administered Bdellovibrio bacteriovorus on the well-being and Salmonella colonization of young chicks. Appl Environ Microbiol. 2011;77(16):5794-803.

353. Shatzkes K, Tang C, Singleton E, Shukla S, Zuena M, Gupta S, et al. Effect of predatory bacteria on the gut bacterial microbiota in rats. Sci Rep. 2017;7:43483.

354. Loozen G, Boon N, Pauwels M, Slomka V, Rodrigues Herrero E, Quirynen M, et al. Effect of Bdellovibrio bacteriovorus HD100 on multispecies oral communities. Anaerobe. 2015;35(Pt A):45-53.

355. Westergaard JM, Kramer TT. Bdellovibrio and the intestinal flora of vertebrates. Appl Environ Microbiol. 1977;34(5):506-11.

356. Iebba V, Santangelo F, Totino V, Nicoletti M, Gagliardi A, De Biase RV, et al. Higher prevalence and abundance of Bdellovibrio bacteriovorus in the human gut of healthy subjects. PLoS One. 2013;8(4):e61608.

357. de Dios Caballero J, Vida R, Cobo M, Maiz L, Suarez L, Galeano J, et al. Individual Patterns of Complexity in Cystic Fibrosis Lung Microbiota, Including Predator Bacteria, over a 1-Year Period. mBio. 2017;8(5).

358. Im H, Choi SY, Son S, Mitchell RJ. Combined Application of Bacterial Predation and Violacein to Kill Polymicrobial Pathogenic Communities. Sci Rep. 2017;7(1):14415.

359. Marine E, Milner DS, Lambert C, Sockett RE, Pos KM. A novel method to determine antibiotic sensitivity in Bdellovibrio bacteriovorus reveals a DHFR-dependent natural trimethoprim resistance. Sci Rep. 2020;10(1):5315.

360. Hobley L, Summers JK, Till R, Milner DS, Atterbury RJ, Stroud A, et al. Dual Predation by Bacteriophage and Bdellovibrio bacteriovorus Can Eradicate Escherichia coli Prey in Situations where Single Predation Cannot. J Bacteriol. 2020;202(6).

361. Nunez ME, Martin MO, Chan PH, Spain EM. Predation, death, and survival in a biofilm: Bdellovibrio investigated by atomic force microscopy. Colloids Surf B Biointerfaces. 2005;42(3-4):263-71.

362. Kadouri D, O'Toole GA. Susceptibility of biofilms to Bdellovibrio bacteriovorus attack. Appl Environ Microbiol. 2005;71(7):4044-51.

363. Medina AA, Kadouri DE. Biofilm formation of Bdellovibrio bacteriovorus host-independent derivatives. Res Microbiol. 2009;160(3):224-31.

364. Dashiff A, Junka RA, Libera M, Kadouri DE. Predation of human pathogens by the predatory bacteria Micavibrio aeruginosavorus and Bdellovibrio bacteriovorus. J Appl Microbiol. 2011;110(2):431-44.

365. Kadouri DE, To K, Shanks RM, Doi Y. Predatory bacteria: a potential ally against multidrug-resistant Gram-negative pathogens. PLoS One. 2013;8(5):e63397.

366. Dharani S, Kim DH, Shanks RMQ, Doi Y, Kadouri DE. Susceptibility of colistin-resistant pathogens to predatory bacteria. Res Microbiol. 2018;169(1):52-5.

367. Sun Y, Ye J, Hou Y, Chen H, Cao J, Zhou T. Predation Efficacy of Bdellovibrio bacteriovorus on Multidrug-Resistant Clinical Pathogens and Their Corresponding Biofilms. Jpn J Infect Dis. 2017;70(5):485-9.

368. Shanks RM, Davra VR, Romanowski EG, Brothers KM, Stella NA, Godboley D, et al. An Eye to a Kill: Using Predatory Bacteria to Control Gram-Negative Pathogens Associated with Ocular Infections. PLoS One. 2013;8(6):e66723.

369. Monnappa AK, Bari W, Choi SY, Mitchell RJ. Investigating the Responses of Human Epithelial Cells to Predatory Bacteria. Sci Rep. 2016;6:33485.

370. Gupta S, Tang C, Tran M, Kadouri DE. Effect of Predatory Bacteria on Human Cell Lines. PLoS One. 2016;11(8):e0161242.

371. Yoon SS, Mekalanos JJ. Decreased potency of the Vibrio cholerae sheathed flagellum to trigger host innate immunity. Infect Immun. 2008;76(3):1282-8.

372. Vijay-Kumar M, Gewirtz AT. Flagellin: key target of mucosal innate immunity. Mucosal Immunol. 2009;2(3):197-205.

373. Fretin D, Fauconnier A, Kohler S, Halling S, Leonard S, Nijskens C, et al. The sheathed flagellum of Brucella melitensis is involved in persistence in a murine model of infection. Cell Microbiol. 2005;7(5):687-98.

374. Coloma-Rivero RF, Flores-Concha M, Molina RE, Soto-Shara R, Cartes A, Onate AA. Brucella and Its Hidden Flagellar System. Microorganisms. 2021;10(1).

375. Gewirtz AT, Yu Y, Krishna US, Israel DA, Lyons SL, Peek RM, Jr. Helicobacter pylori flagellin evades toll-like receptor 5-mediated innate immunity. J Infect Dis. 2004;189(10):1914-20.

376. Im H, Son S, Mitchell RJ, Ghim CM. Serum albumin and osmolality inhibit Bdellovibrio bacteriovorus predation in human serum. Sci Rep. 2017;7(1):5896.

377. Im H, Kwon H, Cho G, Kwon J, Choi SY, Mitchell RJ. Viscosity has dichotomous effects on Bdellovibrio bacteriovorus HD100 predation. Environmental Microbiology. 2019;21(12):4675-84.

378. Hobley L, King JR, Sockett RE. Bdellovibrio predation in the presence of decoys: Three-way bacterial interactions revealed by mathematical and experimental analyses. Appl Environ Microbiol. 2006;72(10):6757-65.

379. Wilkinson MH. Predation in the presence of decoys: an inhibitory factor on pathogen control by bacteriophages or bdellovibrios in dense and diverse ecosystems. J Theor Biol. 2001;208(1):27-36.

380. Dwidar M, Nam D, Mitchell RJ. Indole negatively impacts predation by Bdellovibrio bacteriovorus and its release from the bdelloplast. Environ Microbiol. 2015;17(4):1009-22.

381. Cao H, Wang H, Yu J, An J, Chen J. Encapsulated Bdellovibrio Powder as a Potential Bio-Disinfectant against Whiteleg Shrimp-Pathogenic Vibrios. Microorganisms. 2019;7(8).

382. Boileau MJ, Mani R, Clinkenbeard KD. Lyophilization of Bdellovibrio bacteriovorus 109J for Long-Term Storage. Curr Protoc Microbiol. 2017;45:7B 3 1-7B 3 15.

383. Baker M, Negus D, Raghunathan D, Radford P, Moore C, Clark G, et al. Measuring and modelling the response of Klebsiella pneumoniae KPC prey to Bdellovibrio bacteriovorus predation, in human serum and defined buffer. Sci Rep. 2017;7(1):8329.

384. Negus D, Moore C, Baker M, Raghunathan D, Tyson J, Sockett ER. Predator Versus Pathogen How Does Predatory Bdellovibrio bacteriovorus Interface with the Challenges of Killing Gram-Negative Pathogens in a Host Setting. Annual Review of Microbiology. 2017;71.

385. Nakamura M. Alteration of Shigella pathogenicity by other bacteria. The American Journal of Clinical Nutrition. 1972;25(12):1441-51.

386. Romanowski EG, Stella NA, Brothers KM, Yates KA, Funderburgh ML, Funderburgh JL, et al. Predatory bacteria are nontoxic to the rabbit ocular surface. Sci Rep. 2016;6:30987.

387. Shatzkes K, Singleton E, Tang C, Zuena M, Shukla S, Gupta S, et al. Examining the efficacy of intravenous administration of predatory bacteria in rats. Sci Rep. 2017;7(1):1864.

388. Shatzkes K, Singleton E, Tang C, Zuena M, Shukla S, Gupta S, et al. Predatory Bacteria Attenuate Klebsiella pneumoniae Burden in Rat Lungs. mBio. 2016;7(6).

389. Silva PHF, Oliveira LFF, Cardoso RS, Ricoldi MST, Figueiredo LC, Salvador SL, et al. The impact of predatory bacteria on experimental periodontitis. Journal of periodontology. 2019(August 2018):1-11.

390. Shatzkes K, Chae R, Tang C, Ramirez GC, Mukherjee S, Tsenova L, et al. Examining the safety of respiratory and intravenous inoculation of Bdellovibrio bacteriovorus and Micavibrio aeruginosavorus in a mouse model. Sci Rep. 2015;5:12899.

391. Russo R, Kolesnikova I, Kim T, Gupta S, Pericleous A, Kadouri D, et al. Susceptibility of Virulent Yersinia pestis Bacteria to Predator Bacteria in the Lungs of Mice. Microorganisms. 2018;7(1):2-.

392. Findlay JS, Flick-Smith HC, Keyser E, Cooper IA, Williamson ED, Oyston PCF. Predatory bacteria can protect SKH-1 mice from a lethal plague challenge. Sci Rep. 2019;9(1):7225.

393. Van Essche M, Quirynen M, Sliepen I, Loozen G, Boon N, Van Eldere J, et al. Killing of anaerobic pathogens by predatory bacteria. Mol Oral Microbiol. 2011;26(1):52-61.

394. Loozen G, Boon N, Pauwels M, Slomka V, Rodrigues Herrero E, Quirynen M, et al. Effect of Bdellovibrio bacteriovorus HD100 on multispecies oral communities. Anaerobe. 2015;35:45-53.

395. Cao H, He S, Wang H, Hou S, Lu L, Yang X. Bdellovibrios, potential biocontrol bacteria against pathogenic Aeromonas hydrophila. Vet Microbiol. 2012;154(3-4):413-8.

396. PAGE JA, LUBBERS B, MAHER J, RITSCH L, GRAGG SE. Investigation into the Efficacy of Bdellovibrio bacteriovorus as a Novel Preharvest Intervention To Control Escherichia coli O157:H7 and Salmonella in Cattle Using an In Vitro Model. Journal of Food Protection. 2015;78(9):1745-9.

397. Saxon EB, Jackson RW, Bhumbra S, Smith T, Sockett RE. Bdellovibrio bacteriovorus HD100 guards against Pseudomonas tolaasii brown-blotch lesions on the surface of post-harvest Agaricus bisporus supermarket mushrooms. BMC Microbiol. 2014;14:163.

398. Jackson RW, Bhumbra S, Smith T, Sockett R, Saxon EB. Bdellovibrio bacteriovorus HD100 guards against Pseudomonas tolaasii brown-blotch lesions on the surface of post-harvest Agaricus bisporus supermarket mushrooms. BMC Microbiology. 2014;14(1):163-.

399. Youdkes D, Helman Y, Burdman S, Matan O, Jurkevitch E. Potential Control of Potato Soft Rot Disease by the Obligate Predators Bdellovibrio and Like Organisms. Appl Environ Microbiol. 2020;86(6).

400. Boileau MJ, Clinkenbeard KD, Iandolo JJ. Assessment of Bdellovibrio bacteriovorus 109J killing of Moraxella bovis in an in vitro model of infectious bovine keratoconjunctivitis. Can J Vet Res. 2011;75(4):285-91.

401. Boileau MJ, Mani R, Breshears MA, Gilmour M, Taylor JD, Clinkenbeard KD. Efficacy of Bdellovibrio bacteriovorus 109J for the treatment of dairy calves with experimentally induced infectious bovine keratoconjunctivitis. American Journal of Veterinary Research. 2016;77(9):1017-28.

402. Atterbury RJ, Hobley L, Till R, Lambert C, Capeness MJ, Lerner TR, et al. Effects of orally administered Bdellovibrio bacteriovorus on the well-being and Salmonella colonization of young chicks. Applied and Environmental Microbiology. 2011;77(16):5794-803.

403. Gomes MC, Mostowy S. The Case for Modeling Human Infection in Zebrafish. Trends Microbiology. 2020;28(1):10-8.

404. Iebba V, Totino V, Santangelo F, Gagliardi A, Ciotoli L, Virga A, et al. Bdellovibrio bacteriovorus directly attacks Pseudomonas aeruginosa and Staphylococcus aureus cystic fibrosis isolates. Frontiers in Microbiology. 2014;5(JUN):1-9.

405. Pantanella F, Iebba V, Mura F, Dini L, Totino V, Neroni B, et al. Behaviour of bdellovibrio bacteriovorus in the presence of gram-positive staphylococcus aureus. New Microbiologica. 2018;41(2):145-52.

406. Waso M, Khan S, Ahmed W, Khan W. Expression of attack and growth phase genes of Bdellovibrio bacteriovorus in the presence of Gram-negative and Gram-positive prey. Microbiol Res. 2020;235:126437.

407. Im H, Dwidar M, Mitchell RJ. Bdellovibrio bacteriovorus HD100, a predator of Gram-negative bacteria, benefits energetically from Staphylococcus aureus biofilms without predation. ISME J. 2018;12(8):2090-5.

408. Monnappa AK, Dwidar M, Seo JK, Hur JH, Mitchell RJ. Bdellovibrio bacteriovorus inhibits staphylococcus aureus biofilm formation and invasion into human epithelial cells. Scientific Reports. 2014;4:1-8.

409. Boileau MJ, Mani R, Breshears MA, Gilmour M, Taylor JD, Clinkenbeard KD. Efficacy of Bdellovibrio bacteriovorus 109J for the treatment of dairy calves with experimentally induced infectious bovine keratoconjunctivitis. Am J Vet Res. 2016;77(9):1017-28.

410. Gibson DG, Young L, Chuang R-Y, Venter JC, Hutchison CA, Smith HO. Enzymatic assembly of DNA molecules up to several hundred kilobases. Nature Methods. 2009;6(5):343-5.

411. Murdoch SL, Trunk K, English G, Fritsch MJ, Pourkarimi E, Coulthurst SJ. The opportunistic pathogen Serratia marcescens utilizes type VI secretion to target bacterial competitors. Journal of Bacteriology. 2011;193(21):6057-69.

412. Schindelin J, Arganda-Carreras I, Frise E, Kaynig V, Longair M, Pietzsch T, et al. Fiji: an open-source platform for biological-image analysis. Nature Methods. 2012;9(7):676-82.

413. Remy O, Lamot T, Santin Y, Kaljevic J, de Pierpont C, Laloux G. An optimized workflow to measure bacterial predation in microplates. STAR Protoc. 2022;3(1):101104.

414. Chaudhuri RR, Loman NJ, Snyder LAS, Bailey CM, Stekel DJ, Pallen MJ. x BASE2: a comprehensive resource for comparative bacterial genomics. Nucleic Acids Research. 2007;36(suppl_1):D543-D6.

415. Consortium TU. UniProt: the universal protein knowledgebase in 2021. Nucleic Acids Research. 2020;49(D1):D480-D9.

416. Altschul SF, Gish W, Miller W, Myers EW, Lipman DJ. Basic local alignment search tool. J Mol Biol. 1990;215(3):403-10.

417. Teufel F, Almagro Armenteros JJ, Johansen AR, Gíslason MH, Pihl SI, Tsirigos KD, et al. SignalP 6.0 predicts all five types of signal peptides using protein language models. Nature Biotechnology. 2022;40(7):1023-5.

418. Bagos PG, Nikolaou EP, Liakopoulos TD, Tsirigos KD. Combined prediction of Tat and Sec signal peptides with hidden Markov models. Bioinformatics. 2010;26(22):2811-7.

419. Mistry J, Chuguransky S, Williams L, Qureshi M, Salazar Gustavo A, Sonnhammer ELL, et al. Pfam: The protein families database in 2021. Nucleic Acids Research. 2020;49(D1):D412-D9.

420. Madeira F, Pearce M, Tivey ARN, Basutkar P, Lee J, Edbali O, et al. Search and sequence analysis tools services from EMBL-EBI in 2022. Nucleic acids research. 2022:gkac240.

421. Szklarczyk D, Gable AL, Lyon D, Junge A, Wyder S, Huerta-Cepas J, et al. STRING v11: protein-protein association networks with increased coverage, supporting functional discovery in genome-wide experimental datasets. Nucleic Acids Res. 2019;47(D1):D607-d13.

422. Szklarczyk D, Gable AL, Nastou KC, Lyon D, Kirsch R, Pyysalo S, et al. The STRING database in 2021: customizable protein-protein networks, and functional characterization of user-uploaded gene/measurement sets. Nucleic Acids Res. 2021;49(D1):D605-d12.

423. von Mering C, Huynen M, Jaeggi D, Schmidt S, Bork P, Snel B. STRING: a database of predicted functional associations between proteins. Nucleic Acids Res. 2003;31(1):258-61.

424. Kanehisa M, Furumichi M, Sato Y, Kawashima M, Ishiguro-Watanabe M. KEGG for taxonomy-based analysis of pathways and genomes. Nucleic Acids Research. 2022.

425. Kanehisa M, Sato Y, Kawashima M, Furumichi M, Tanabe M. KEGG as a reference resource for gene and protein annotation. Nucleic Acids Research. 2015;44(D1):D457-D62.

426. Dobin A, Davis CA, Schlesinger F, Drenkow J, Zaleski C, Jha S, et al. STAR: ultrafast universal RNA-seq aligner. Bioinformatics. 2012;29(1):15-21.

427. Davis MP, van Dongen S, Abreu-Goodger C, Bartonicek N, Enright AJ. Kraken: a set of tools for quality control and analysis of high-throughput sequence data. Methods. 2013;63(1):41-9.

428. McClure R, Balasubramanian D, Sun Y, Bobrovskyy M, Sumby P, Genco CA, et al. Computational analysis of bacterial RNA-Seq data. Nucleic Acids Res. 2013;41(14):e140.

429. Tjaden B. A computational system for identifying operons based on RNA-seq data. Methods. 2020;176:62-70.

430. Tjaden B. De novo assembly of bacterial transcriptomes from RNA-seq data. Genome Biology. 2015;16(1):1.

431. Taylor PW, Messner P, Parton R. EFFECT OF THE GROWTH ENVIRONMENT ON CELL-ENVELOPE COMPONENTS OF ESCHERICHIA COLI IN RELATION TO SENSITIVITY TO HUMAN SERUM. Journal of Medical Microbiology. 1981;14.

432. Raetz CR, Reynolds CM, Trent MS, Bishop RE. Lipid A modification systems in gram-negative bacteria. Annual Reviews Biochemistry. 2007;76:295-329.

433. Hejazi A, Falkiner FR. Serratia marcescens. Journal of Medical Microbiology. 1997;46.

434. Franczek SP, Williams RP, Hull SI. A survey of potential virulence factors in clinical and environmental isolates of Serratia marcescens. Journal of Medical Microbiology. 1986;22(2):151-6.

435. Aucken HM, Pitt TL. Antibiotic resistance and putative virulence factors of Serratia marcescens with respect to O and K serotypes. Journal of Medical Microbiology. 1998;47.

436. Aucken HM, Wilkinson SG, Pitt TL. Identification of capsular antigens in Serratia marcescens. Journal of Clinical Microbiology. 1997.

437. Anderson MT, Mitchell LA, Zhao L, Mobley HLT. Capsule Production and Glucose Metabolism Dictate Fitness during Serratia marcescens Bacteremia. mBio. 2017;8(3):e00740-17.

438. Hume EBH, Willcox MDP. Survival of Serratia marcescens in the Presence of Complement. Microbial Ecology in Health and Disease. 2001;13(1):55-62.

439. Clegg S, Purcell BK, Pruckler J. Characterization of genes encoding type 1 fimbriae of Klebsiella pneumoniae, Salmonella typhimurium, and Serratia marcescens. Infection and Immunity. 1987;55(2):281-7.

440. Shanks RMQ, Stella NA, Brothers KM, Polaski DM. Exploitation of a “hockey-puck” phenotype to identify pilus and biofilm regulators in Serratia marcescens through genetic analysis. Canadian Journal of Microbiology. 2016;62(1):83-93.

441. Begic S, Worobec EA. Regulation of Serratia marcescens ompF and ompC porin genes in response to osmotic stress, salicylate, temperature and pH. Microbiology. 2006;152(2):485-91.

442. Hutsul J-A, Worobec E. Molecular characterization of the Serratia marcescens OmpF porin, and analysis of S. marcescens OmpF and OmpC osmoregulation. Microbiology. 1997;143(8):2797-806.

443. Collins RF, Derrick JP. Wza: a new structural paradigm for outer membrane secretory proteins? Trends in Microbiology. 2007;15(3):96-100.

444. Drummelsmith J, Whitfield C. Gene products required for surface expression of thecapsular form of the group 1 K antigen in Escherichiacoli(O9a:K30). Molecular Microbiology. 1999;31(5).

445. Reid AN, Whitfield C. functional analysis of conserved gene products involved in assembly of Escherichia coli capsules and exopolysaccharides: evidence for molecular recognition between Wza and Wzc for colanic acid biosynthesis. Journal of Bacteriology. 2005;187(15):5470-81.

446. Paiment A, Hocking J, Whitfield C. Impact of phosphorylation of specific residues in the tyrosine autokinase, Wzc, on its activity in assembly of group 1 capsules in Escherichia coli. Journal of Bacteriology. 2002;184(23):6437-47.

447. Wugeditsch T, Paiment A, Hocking J, Drummelsmith J, Forrester C, Whitfield C. Phosphorylation of Wzc, a tyrosine autokinase, is essential for assembly of group 1 capsular polysaccharides in Escherichia coli. Journal of Biological Chemistry. 2001;276(4):2361-71.

448. Beis K, Collins RF, Ford RC, Kamis AB, Whitfield C, Naismith JH. Three-dimensional structure of Wza, the protein required for translocation of group 1 capsular polysaccharide across the outer membrane of Escherichia coli. Journal of Biological Chemistry. 2004;279(27):28227-32.

449. Rahn A, Beis K, Naismith JH, Whitfield C. A novel outer membrane protein, Wzi, is involved in surface assembly of the Escherichia coli K30 group 1 capsule. Journal of Bacteriology. 2003;185(19):5882-90.

450. Bushell SR, Mainprize IL, Wear MA, Lou H, Whitfield C, Naismith JH. Wzi is an outer membrane lectin that underpins group 1 capsule assembly in Escherichia coli. Structure. 2013;21(5):844-53.

451. Haas E. Analyses of the proteins KpsM, KpsE and KpsD in the group 2 capsular polysaccharide export complex of Escherichia coli. Manchester: University of Manchester; 2012.

452. Chamnongpol S, Dodson W, Cromie MJ, Harris ZL, Groisman EA. Fe(III)-mediated cellular toxicity. Molecular Microbiology. 2002;45(3).

453. Chamnongpol S, Groisman EA. Mg2+homeostasis and avoidance of metal toxicity. Molecular Microbiology. 2002;44(2).

454. Groisman EA, Kayser J, Soncini FC. Regulation of Polymyxin Resistance and Adaptation to Low-Mg2+ Environments. Journal of Bacteriology. 1997;179(22).

455. Bader MW, Sanowar S, Daley ME, Schneider AR, Cho U, Xu W, et al. Recognition of antimicrobial peptides by a bacterial sensor kinase. Cell. 2005;122(3):461-72.

456. Ortega XP, Cardona ST, Brown AR, Loutet SA, Flannagan RS, Campopiano DJ, et al. A putative gene cluster for aminoarabinose biosynthesis is essential for Burkholderia cenocepacia viability. Journal of Bacteriology. 2007;189(9):3639-44.

457. Lin QY, Tsai YL, Liu MC, Lin WC, Hsueh PR, Liaw SJ. Serratia marcescens arn, a PhoP-regulated locus necessary for polymyxin B resistance. Antimicrobial Agents of Chemotherapy. 2014;58(9):5181-90.

458. Fernández L, Gooderham WJ, Bains M, McPhee JB, Wiegand I, Hancock REW. Adaptive Resistance to the “Last Hope” Antibiotics Polymyxin B and Colistin in Pseudomonas aeruginosa Is Mediated by the Novel Two-Component Regulatory System ParR-ParS. Antimicrobial Agents and Chemotherapy. 2010;54(8):3372-82.

459. Gatzeva-Topalova PZ, May AP, Sousa MC. Crystal structure of Escherichia coli ArnA (PmrI) decarboxylase domain. A key enzyme for lipid A modification with 4-amino-4-deoxy-L-arabinose and polymyxin resistance. Biochemistry. 2004;43(42):13370-9.

460. Olaitan AO, Morand S, Rolain JM. Mechanisms of polymyxin resistance: acquired and intrinsic resistance in bacteria. Frontiers in Microbiology. 2014;5:643.

461. Anderson P, Johnston RB, Smith DH. Human serum bactericidal activity against Haemophilus influenzae type b. The Journal of Clinical Investigation. 1972;51.

462. Andra J, Gutsmann T, Muller M, Schromm AB. Interactions between Lipid A and Serum Proteins. Lipid A in Cancer Therapy2009.

463. Maeshima N, Fernandez RC. Recognition of lipid A variants by the TLR4-MD-2 receptor complex. Frontiers in Cellular and Infection Microbiology. 2013;3:3.

464. Wells TJ, Whitters D, Sevastsyanovich YR, Heath JN, Pravin J, Goodall M, et al. Increased severity of respiratory infections associated with elevated anti-LPS IgG2 which inhibits serum bactericidal killing. Journal of Experimental Medicine. 2014;211(9):1893-904.

465. MacLennan CA, Gilchrist JJ, Gordon MA, Cunningham AF, Cobbold M, Goodall M, et al. Dysregulated Humoral Immunity to Nontyphoidal Salmonella in HIV-Infected African Adults. Science. 2010;328.

466. Mun W, Upatissa S, Lim S, Dwidar M, Mitchell RJ. Outer Membrane Porin F in E. coli Is Critical for Effective Predation by Bdellovibrio. Microbiol Spectr. 2022;10(6):e0309422.

467. Steinman HM. Bacterial superoxide dismutases. Basic Life Sci. 1988;49:641-6.

468. Steinman HM. Construction of an Escherichia coli K-12 strain deleted for manganese and iron superoxide dismutase genes and its use in cloning the iron superoxide dismutase gene of Legionella pneumophila. Molecular and General Genetics MGG. 1992;232(3):427-30.

469. Zückert WR. Secretion of bacterial lipoproteins: through the cytoplasmic membrane, the periplasm and beyond. Biochim Biophys Acta. 2014;1843(8):1509-16.

470. Jumper J, Evans R, Pritzel A, Green T, Figurnov M, Ronneberger O, et al. Highly accurate protein structure prediction with AlphaFold. Nature. 2021;596(7873):583-9.

471. Zhang Y, Skolnick J. TM-align: a protein structure alignment algorithm based on the TM-score. Nucleic Acids Res. 2005;33(7):2302-9.

472. Bitto E, McKay DB. Crystallographic structure of SurA, a molecular chaperone that facilitates folding of outer membrane porins. Structure. 2002;10(11):1489-98.

473. Kemp BE. Bateman domains and adenosine derivatives form a binding contract. J Clin Invest. 2004;113(2):182-4.

474. Scott JW, Hawley SA, Green KA, Anis M, Stewart G, Scullion GA, et al. CBS domains form energy-sensing modules whose binding of adenosine ligands is disrupted by disease mutations. J Clin Invest. 2004;113(2):274-84.

475. Goddu RN, Henderson CF, Young AK, Muradian BE, Calderon L, Bleeg LH, et al. Chronic exposure of the RAW246.7 macrophage cell line to H2O2 leads to increased catalase expression. Free Radical Biology and Medicine. 2018;126:67-72.

476. Kashmiri ZA, Mankar SA. Free radicals and oxidative stress in bacteria. 2014.

477. Fasnacht M, Polacek N. Oxidative Stress in Bacteria and the Central Dogma of Molecular Biology. Frontiers in Molecular Biosciences. 2021;8.

478. Dubbs JM, Mongkolsuk S. Peroxide-sensing transcriptional regulators in bacteria. J Bacteriol. 2012;194(20):5495-503.

479. Lambert C, Ivanov P, Sockett RE. A transcriptional "Scream" early response of E. coli prey to predatory invasion by Bdellovibrio. Curr Microbiol. 2010;60(6):419-27.

480. Kuenen JG, Rittenberg SC. Incorporation of long-chain fatty acids of the substrate organism by Bdellovibrio bacteriovorus during intraperiplasmic growth. J Bacteriol. 1975;121(3):1145-57.

481. Matin A, Rittenberg SC. Kinetics of deoxyribonucleic acid destruction and synthesis during growth of Bdellovibrio bacteriovorus strain 109D on pseudomonas putida and escherichia coli. J Bacteriol. 1972;111(3):664-73.

482. Brune B, Dehne N, Grossmann N, Jung M, Namgaladze D, Schmid T, et al. Redox control of inflammation in macrophages. Antioxid Redox Signal. 2013;19(6):595-637.

483. Keith KE, Valvano MA. Characterization of SodC, a periplasmic superoxide dismutase from Burkholderia cenocepacia. Infect Immun. 2007;75(5):2451-60.

484. Ammendola S, Pasquali P, Pacello F, Rotilio G, Castor M, Libby SJ, et al. Regulatory and structural differences in the Cu, Zn-superoxide dismutases of Salmonella enterica and their significance for virulence. Journal of Biological Chemistry. 2008;283(20):13688-99.

485. Sansone A, Watson PR, Wallis TS, Langford PR, Kroll JS. The role of two periplasmic copper-and zinc-cofactored superoxide dismutases in the virulence of Salmonella choleraesuis. Microbiology. 2002;148(3):719-26.

486. Rushing MD, Slauch JM. Either periplasmic tethering or protease resistance is sufficient to allow a SodC to protect Salmonella enterica serovar Typhimurium from phagocytic superoxide. Molecular Microbiology. 2011;82(4):952-63.

487. Pacello F, Ceci P, Ammendola S, Pasquali P, Chiancone E, Battistoni A. Periplasmic Cu,Zn superoxide dismutase and cytoplasmic Dps concur in protecting Salmonella enterica serovar Typhimurium from extracellular reactive oxygen species. Biochimica et Biophysica Acta (BBA) - General Subjects. 2008;1780(2):226-32.

488. De Groote MA, Ochsner UA, Shiloh MU, Nathan C, McCord JM, Dinauer MC, et al. Periplasmic superoxide dismutase protects Salmonella from products of phagocyte NADPH-oxidase and nitric oxide synthase. Proceedings of the National Academy of Sciences. 1997;94(25):13997-4001.

489. Gee JM, Valderas MW, Kovach ME, Grippe VK, Robertson GT, Ng W-L, et al. The Brucella abortus Cu,Zn Superoxide Dismutase Is Required for Optimal Resistance to Oxidative Killing by Murine Macrophages and Wild-Type Virulence in Experimentally Infected Mice. Infection and Immunity. 2005;73(5):2873-80.

490. San Mateo LR, Hobbs MM, Kawula TH. Periplasmic copper–zinc superoxide dismutase protects Haemophilus ducreyi from exogenous superoxide. Molecular Microbiology. 1998;27(2):391-404.

491. Langford PR, Kroll JS. Distribution, cloning, characterisation and mutagenesis of sodC, the gene encoding copper/zinc superoxide dismutase, a potential determinant of virulence, in Haemophilus ducreyi. FEMS IMMUNOLOGY AND MEDICAL MICROBIOLOGY. 1997;17:235-42.

492. Wilks KE, Dunn KL, Farrant JL, Reddin KM, Gorringe AR, Langford PR, et al. Periplasmic superoxide dismutase in meningococcal pathogenicity. Infection and immunity. 1998;66(1):213-7.

493. Piddington DL, Fang FC, Laessig T, Cooper AM, Orme IM, Buchmeier NA. Cu, Zn superoxide dismutase of Mycobacterium tuberculosis contributes to survival in activated macrophages that are generating an oxidative burst. Infection and immunity. 2001;69(8):4980-7.

494. Battistoni A. Role of prokaryotic Cu,Zn superoxide dismutase in pathogenesis. Biochem Soc Trans. 2003;31(Pt 6):1326-9.

495. Wand ME, Müller CM, Titball RW, Michell SL. Macrophage and Galleria mellonella infection models reflect the virulence of naturally occurring isolates of B. pseudomallei, B. thailandensis and B. oklahomensis. BMC Microbiology. 2011;11(1):11.

496. St John G, Steinman HM. Periplasmic copper-zinc superoxide dismutase of Legionella pneumophila: role in stationary-phase survival. J Bacteriol. 1996;178(6):1578-84.

497. Sheehan BJ, Langford PR, Rycroft AN, Kroll JS. [Cu, Zn]-superoxide dismutase mutants of the swine pathogen Actinobacillus pleuropneumoniae are unattenuated in infections of the natural host. Infection and immunity. 2000;68(8):4778-81.

498. Farrant JL, Sansone A, Canvin JR, Pallen MJ, Langford PR, Wallis TS, et al. Bacterial copper-and zinc-cofactored superoxide dismutase contributes to the pathogenesis of systemic salmonellosis. Molecular microbiology. 1997;25(4):785-96.

499. Sen A, Imlay JA. How Microbes Defend Themselves From Incoming Hydrogen Peroxide. Front Immunol. 2021;12:667343.

500. Imlay JA. Cellular defenses against superoxide and hydrogen peroxide. Annu Rev Biochem. 2008;77:755-76.

501. Jacobson FS, Morgan RW, Christman MF, Ames BN. An alkyl hydroperoxide reductase from Salmonella typhimurium involved in the defense of DNA against oxidative damage. Purification and properties. J Biol Chem. 1989;264(3):1488-96.

502. Storz G, Jacobson FS, Tartaglia LA, Morgan RW, Silveira LA, Ames BN. An alkyl hydroperoxide reductase induced by oxidative stress in Salmonella typhimurium and Escherichia coli: genetic characterization and cloning of ahp. J Bacteriol. 1989;171(4):2049-55.

503. Das D, Bishayi B. Staphylococcal catalase protects intracellularly survived bacteria by destroying H2O2 produced by the murine peritoneal macrophages. Microbial Pathogenesis. 2009;47(2):57-67.

504. Das D, Bishayi B. Contribution of Catalase and Superoxide Dismutase to the Intracellular Survival of Clinical Isolates of Staphylococcus aureus in Murine Macrophages. Indian J Microbiol. 2010;50(4):375-84.

505. Day WA, Jr., Sajecki JL, Pitts TM, Joens LA. Role of catalase in Campylobacter jejuni intracellular survival. Infect Immun. 2000;68(11):6337-45.

506. Basu M, Czinn S, Blanchard T. Absence of Catalase Reduces Long-Term Survival of Helicobacter pylori in Macrophage Phagosomes. Helicobacter. 2004;9:211-6.

507. Shakerley NL, Chandrasekaran A, Trebak M, Miller BA, Melendez JA. Francisella tularensis Catalase Restricts Immune Function by Impairing TRPM2 Channel Activity. J Biol Chem. 2016;291(8):3871-81.

508. Melillo AA, Mahawar M, Sellati TJ, Malik M, Metzger DW, Melendez JA, et al. Identification of Francisella tularensis live vaccine strain CuZn superoxide dismutase as critical for resistance to extracellularly generated reactive oxygen species. J Bacteriol. 2009;191(20):6447-56.

509. Spence SA, Clark VL, Isabella VM. The role of catalase in gonococcal resistance to peroxynitrite. Microbiology (Reading). 2012;158(Pt 2):560-70.

510. Ieva R, Roncarati D, Metruccio MME, Seib KL, Scarlato V, Delany I. OxyR tightly regulates catalase expression in Neisseria meningitidis through both repression and activation mechanisms. Molecular Microbiology. 2008;70(5):1152-65.

511. Bandyopadhyay P, Byrne B, Chan Y, Swanson MS, Steinman HM. Legionella pneumophila Catalase-Peroxidases Are Required for Proper Trafficking and Growth in Primary Macrophages. Infection and Immunity. 2003;71(8):4526-35.

512. Bandyopadhyay P, Steinman HM. Legionella pneumophila catalase-peroxidases: cloning of the katB gene and studies of KatB function. J Bacteriol. 1998;180(20):5369-74.

513. Shi L, Sohaskey CD, North RJ, Gennaro ML. Transcriptional characterization of the antioxidant response of Mycobacterium tuberculosis in vivo and during adaptation to hypoxia in vitro. Tuberculosis (Edinb). 2008;88(1):1-6.

514. Manca C, Paul S, Barry CE, 3rd, Freedman VH, Kaplan G. Mycobacterium tuberculosis catalase and peroxidase activities and resistance to oxidative killing in human monocytes in vitro. Infect Immun. 1999;67(1):74-9.

515. Buchmeier N, Blanc-Potard A, Ehrt S, Piddington D, Riley L, Groisman EA. A parallel intraphagosomal survival strategy shared by Mycobacterium tuberculosis and Salmonella enterica. Molecular Microbiology. 2000;35(6):1375-82.

516. Han Y, Geng J, Qiu Y, Guo Z, Zhou D, Bi Y, et al. Physiological and regulatory characterization of KatA and KatY in Yersinia pestis. DNA Cell Biol. 2008;27(8):453-62.

517. Lindgren H, Shen H, Zingmark C, Golovliov I, Conlan W, Sjostedt A. Resistance of Francisella tularensis strains against reactive nitrogen and oxygen species with special reference to the role of KatG. Infect Immun. 2007;75(3):1303-9.

518. Cosgrove K, Coutts G, Jonsson IM, Tarkowski A, Kokai-Kun JF, Mond JJ, et al. Catalase (KatA) and alkyl hydroperoxide reductase (AhpC) have compensatory roles in peroxide stress

resistance and are required for survival, persistence, and nasal colonization in Staphylococcus aureus. J Bacteriol. 2007;189(3):1025-35.

519. Soler-Garcia AA, Jerse AE. Neisseria gonorrhoeae catalase is not required for experimental genital tract infection despite the induction of a localized neutrophil response. Infect Immun. 2007;75(5):2225-33.

520. Hebrard M, Viala JP, Meresse S, Barras F, Aussel L. Redundant hydrogen peroxide scavengers contribute to Salmonella virulence and oxidative stress resistance. J Bacteriol. 2009;191(14):4605-14.

521. Baillon ML, van Vliet AH, Ketley JM, Constantinidou C, Penn CW. An iron-regulated alkyl hydroperoxide reductase (AhpC) confers aerotolerance and oxidative stress resistance to the microaerophilic pathogen Campylobacter jejuni. J Bacteriol. 1999;181(16):4798-804.

522. Bryk R, Lima CD, Erdjument-Bromage H, Tempst P, Nathan C. Metabolic enzymes of mycobacteria linked to antioxidant defense by a thioredoxin-like protein. Science. 2002;295(5557):1073-7.

523. Chen L, Xie Q-w, Nathan C. Alkyl Hydroperoxide Reductase Subunit C (AhpC) Protects Bacterial and Human Cells against Reactive Nitrogen Intermediates. Molecular Cell. 1998;1(6):795-805.

524. Hillas PJ, del Alba FS, Oyarzabal J, Wilks A, Ortiz De Montellano PR. The AhpC and AhpD antioxidant defense system of Mycobacterium tuberculosis. J Biol Chem. 2000;275(25):18801-9.

525. Chiang SM, Schellhorn HE. Regulators of oxidative stress response genes in Escherichia coli and their functional conservation in bacteria. Archives of Biochemistry and Biophysics. 2012;525(2):161-9.

526. Ochsner UA, Vasil ML, Alsabbagh E, Parvatiyar K, Hassett DJ. Role of the Pseudomonas aeruginosa oxyR-recG operon in oxidative stress defense and DNA repair: OxyR-dependent regulation of katB-ankB, ahpB, and ahpC-ahpF. J Bacteriol. 2000;182(16):4533-44.

527. Seo SW, Kim D, Szubin R, Palsson BO. Genome-wide Reconstruction of OxyR and SoxRS Transcriptional Regulatory Networks under Oxidative Stress in Escherichia coli K-12 MG1655. Cell Rep. 2015;12(8):1289-99.

528. Taylor PD, Inchley CJ, Gallagher MP. The Salmonella typhimurium AhpC polypeptide is not essential for virulence in BALB/c mice but is recognized as an antigen during infection. Infect Immun. 1998;66(7):3208-17.

529. Springer B, Master S, Sander P, Zahrt T, McFalone M, Song J, et al. Silencing of oxidative stress response in Mycobacterium tuberculosis: expression patterns of ahpC in virulent and avirulent strains and effect of ahpC inactivation. Infect Immun. 2001;69(10):5967-73.

530. Alharbi A, Rabadi SM, Alqahtani M, Marghani D, Worden M, Ma Z, et al. Role of peroxiredoxin of the AhpC/TSA family in antioxidant defense mechanisms of Francisella tularensis. PLoS One. 2019;14(3):e0213699.

531. Llewellyn AC, Jones CL, Napier BA, Bina JE, Weiss DS. Macrophage replication screen identifies a novel Francisella hydroperoxide resistance protein involved in virulence. PLoS One. 2011;6(9):e24201.

532. Rankin S, Li Z, Isberg RR. Macrophage-induced genes of Legionella pneumophila: protection from reactive intermediates and solute imbalance during intracellular growth. Infect Immun. 2002;70(7):3637-48.

533. Mavromatis CH, Bokil NJ, Totsika M, Kakkanat A, Schaale K, Cannistraci CV, et al. The co-transcriptome of uropathogenic Escherichia coli-infected mouse macrophages reveals new insights into host-pathogen interactions. Cell Microbiol. 2015;17(5):730-46.

534. Flint A, Sun Y-Q, Butcher J, Stahl M, Huang H, Stintzi A. Phenotypic Screening of a Targeted Mutant Library Reveals Campylobacter jejuni Defenses against Oxidative Stress. Infection and Immunity. 2014;82(6):2266-75.

535. Oh E, Jeon B. Role of alkyl hydroperoxide reductase (AhpC) in the biofilm formation of Campylobacter jejuni. PLoS One. 2014;9(1):e87312.

536. Chen L, Xie QW, Nathan C. Alkyl hydroperoxide reductase subunit C (AhpC) protects bacterial and human cells against reactive nitrogen intermediates. Mol Cell. 1998;1(6):795-805.

537. Zeth K, Offermann S, Essen LO, Oesterhelt D. Iron-oxo clusters biomineralizing on protein surfaces: structural analysis of Halobacterium salinarum DpsA in its low- and high-iron states. Proc Natl Acad Sci U S A. 2004;101(38):13780-5.

538. Calhoun LN, Kwon YM. Structure, function and regulation of the DNA-binding protein Dps and its role in acid and oxidative stress resistance in Escherichia coli: a review. J Appl Microbiol. 2011;110(2):375-86.

539. Karas VO, Westerlaken I, Meyer AS. The DNA-Binding Protein from Starved Cells (Dps) Utilizes Dual Functions To Defend Cells against Multiple Stresses. Journal of Bacteriology. 2015;197(19):3206-15.

540. Meyer AS, Grainger DC. The Escherichia coli nucleoid in stationary phase. Advances in Applied Microbiology. 83: Elsevier; 2013. p. 69-86.

541. Ilari A, Ceci P, Ferrari D, Rossi GL, Chiancone E. Iron incorporation into Escherichia coli Dps gives rise to a ferritin-like microcrystalline core. J Biol Chem. 2002;277(40):37619-23.

542. Zhao G, Ceci P, Ilari A, Giangiacomo L, Laue TM, Chiancone E, et al. Iron and hydrogen peroxide detoxification properties of DNA-binding protein from starved cells. A ferritin-like DNA-binding protein of Escherichia coli. J Biol Chem. 2002;277(31):27689-96.

543. Frenkiel-Krispin D, Ben-Avraham I, Englander J, Shimoni E, Wolf SG, Minsky A. Nucleoid restructuring in stationary-state bacteria. Molecular Microbiology. 2004;51(2):395-405.

544. Wolf SG, Frenkiel D, Arad T, Finkel SE, Kolter R, Minsky A. DNA protection by stress-induced biocrystallization. Nature. 1999;400(6739):83-5.

545. Ali Azam T, Iwata A, Nishimura A, Ueda S, Ishihama A. Growth phase-dependent variation in protein composition of the Escherichia coli nucleoid. J Bacteriol. 1999;181(20):6361-70.

546. Thieme D, Grass G. The Dps protein of Escherichia coli is involved in copper homeostasis. Microbiol Res. 2010;165(2):108-15.

547. Almirón M, Martínez M, Sanjuan N, Ugalde RA. Ferrochelatase is present in Brucella abortus and is critical for its intracellular survival and virulence. Infect Immun. 2001;69(10):6225-30.

548. Nair S, Finkel SE. Dps protects cells against multiple stresses during stationary phase. J Bacteriol. 2004;186(13):4192-8.

549. Chiancone E, Ceci P. The multifaceted capacity of Dps proteins to combat bacterial stress conditions: Detoxification of iron and hydrogen peroxide and DNA binding. Biochimica et Biophysica Acta (BBA) - General Subjects. 2010;1800(8):798-805.

550. Olsen KN, Larsen MH, Gahan CGM, Kallipolitis B, Wolf XA, Rea R, et al. The Dps-like protein Fri of Listeria monocytogenes promotes stress tolerance and intracellular multiplication in macrophage-like cells. Microbiology (Reading). 2005;151(Pt 3):925-33.

551. Tang H, Zhang Q, Han W, Wang Z, Pang S, Zhu H, et al. Identification of FtpA, a Dps-Like Protein Involved in Anti-Oxidative Stress and Virulence in Actinobacillus pleuropneumoniae. J Bacteriol. 2022;204(2):e0032621.

552. Ushijima Y, Yoshida O, Villanueva MJA, Ohniwa RL, Morikawa K. Nucleoid clumping is dispensable for the Dps-dependent hydrogen peroxide resistance in Staphylococcus aureus. Microbiology (Reading). 2016;162(10):1822-8.

553. Altuvia S, Almirón M, Huisman G, Kolter R, Storz G. The dps promoter is activated by OxyR during growth and by IHF and sigma S in stationary phase. Mol Microbiol. 1994;13(2):265-72.

554. Southern SJ, Scott AE, Jenner DC, Ireland PM, Norville IH, Sarkar-Tyson M. Survival protein A is essential for virulence in Yersinia pestis. Microb Pathog. 2016;92:50-3.

555. Obi IR, Francis MS. Demarcating SurA activities required for outer membrane targeting of Yersinia pseudotuberculosis adhesins. Infect Immun. 2013;81(7):2296-308.

556. Klein K, Sonnabend MS, Frank L, Leibiger K, Franz-Wachtel M, Macek B, et al. Deprivation of the Periplasmic Chaperone SurA Reduces Virulence and Restores Antibiotic Susceptibility of Multidrug-Resistant Pseudomonas aeruginosa. Front Microbiol. 2019;10:100.

557. Purdy GE, Fisher CR, Payne SM. IcsA surface presentation in Shigella flexneri requires the periplasmic chaperones DegP, Skp, and SurA. J Bacteriol. 2007;189(15):5566-73.

558. Sydenham M, Douce G, Bowe F, Ahmed S, Chatfield S, Dougan G. Salmonella enterica serovar typhimurium surA mutants are attenuated and effective live oral vaccines. Infect Immun. 2000;68(3):1109-15.

559. Tamayo R, Ryan SS, McCoy AJ, Gunn JS. Identification and genetic characterization of PmrA-regulated genes and genes involved in polymyxin B resistance in Salmonella enterica serovar typhimurium. Infect Immun. 2002;70(12):6770-8.

560. Justice SS, Lauer SR, Hultgren SJ, Hunstad DA. Maturation of intracellular Escherichia coli communities requires SurA. Infect Immun. 2006;74(8):4793-800.

561. Anderson GG, Palermo JJ, Schilling JD, Roth R, Heuser J, Hultgren SJ. Intracellular bacterial biofilm-like pods in urinary tract infections. Science. 2003;301(5629):105-7.

562. Battelli MG, Polito L, Bortolotti M, Bolognesi A. Xanthine Oxidoreductase-Derived Reactive Species: Physiological and Pathological Effects. Oxid Med Cell Longev. 2016;2016:3527579.

563. Ransy C, Vaz C, Lombès A, Bouillaud F. Use of H(2)O(2) to Cause Oxidative Stress, the Catalase Issue. Int J Mol Sci. 2020;21(23).

564. Dikalov SI, Harrison DG. Methods for detection of mitochondrial and cellular reactive oxygen species. Antioxid Redox Signal. 2014;20(2):372-82.

565. Westermann AJ, Forstner KU, Amman F, Barquist L, Chao Y, Schulte LN, et al. Dual RNA-seq unveils noncoding RNA functions in host-pathogen interactions. Nature. 2016;529(7587):496-501.

566. Pisu D, Huang L, Grenier JK, Russell DG. Dual RNA-Seq of Mtb-Infected Macrophages In Vivo Reveals Ontologically Distinct Host-Pathogen Interactions. Cell Rep. 2020;30(2):335-50 e4.

567. Damron FH, Oglesby-Sherrouse AG, Wilks A, Barbier M. Dual-seq transcriptomics reveals the battle for iron during Pseudomonas aeruginosa acute murine pneumonia. Sci Rep. 2016;6:39172.

568. Unal CM, Steinert M. Microbial peptidyl-prolyl cis/trans isomerases (PPIases): virulence factors and potential alternative drug targets. Microbiol Mol Biol Rev. 2014;78(3):544-71.

569. Saikolappan S, Das K, Sasindran SJ, Jagannath C, Dhandayuthapani S. OsmC proteins of Mycobacterium tuberculosis and Mycobacterium smegmatis protect against organic hydroperoxide stress. Tuberculosis (Edinb). 2011;91 Suppl 1:S119-27.

570. Lesniak J, Barton WA, Nikolov DB. Structural and functional features of the Escherichia coli hydroperoxide resistance protein OsmC. Protein Sci. 2003;12(12):2838-43.

571. Chakraborty S, Gogoi M, Chakravortty D. Lactoylglutathione lyase, a critical enzyme in methylglyoxal detoxification, contributes to survival of Salmonella in the nutrient rich environment. Virulence. 2015;6(1):50-65.

572. Korithoski B, Levesque CM, Cvitkovitch DG. Involvement of the detoxifying enzyme lactoylglutathione lyase in Streptococcus mutans aciduricity. J Bacteriol. 2007;189(21):7586-92.

573. Watmough NJ, Frerman FE. The electron transfer flavoprotein: Ubiquinone oxidoreductases. Biochimica et Biophysica Acta (BBA) - Bioenergetics. 2010;1797(12):1910-6.

574. Fang FC, Vazquez-Torres A, Xu Y. The transcriptional regulator SoxS is required for resistance of Salmonella typhimurium to paraquat but not for virulence in mice. Infect Immun. 1997;65(12):5371-5.

575. Wang P, Zhang H, Liu Y, Lv R, Liu X, Song X, et al. SoxS is a positive regulator of key pathogenesis genes and promotes intracellular replication and virulence of Salmonella Typhimurium. Microb Pathog. 2020;139:103925.

576. Beggs GA, Brennan RG, Arshad M. MarR family proteins are important regulators of clinically relevant antibiotic resistance. Protein Science. 2020;29(3):647-53.

577. Reeves SA, Parsonage D, Nelson KJ, Poole LB. Kinetic and thermodynamic features reveal that Escherichia coli BCP is an unusually versatile peroxiredoxin. Biochemistry. 2011;50(41):8970-81.

578. Singh A, Kumar N, Tomar PPS, Bhose S, Ghosh DK, Roy P, et al. Characterization of a bacterioferritin comigratory protein family 1-Cys peroxiredoxin from Candidatus Liberibacter asiaticus. Protoplasma. 2017;254(4):1675-91.

579. Colclough AL, Scadden J, Blair JMA. TetR-family transcription factors in Gram-negative bacteria: conservation, variation and implications for efflux-mediated antimicrobial resistance. BMC Genomics. 2019;20(1):731.

580. Zhou D, Han Y, Qin L, Chen Z, Qiu J, Song Y, et al. Transcriptome analysis of the Mg2+-responsive PhoP regulator in Yersinia pestis⋆. FEMS Microbiology Letters. 2005;250(1):85-95.

581. Seifart Gomes C, Izar B, Pazan F, Mohamed W, Mraheil MA, Mukherjee K, et al. Universal stress proteins are important for oxidative and acid stress resistance and growth of Listeria monocytogenes EGD-e in vitro and in vivo. PLoS One. 2011;6(9):e24965.

582. Weissbach H, Etienne F, Hoshi T, Heinemann SH, Lowther WT, Matthews B, et al. Peptide methionine sulfoxide reductase: structure, mechanism of action, and biological function. Arch Biochem Biophys. 2002;397(2):172-8.

583. Douglas T, Daniel DS, Parida BK, Jagannath C, Dhandayuthapani S. Methionine sulfoxide reductase A (MsrA) deficiency affects the survival of Mycobacterium smegmatis within macrophages. J Bacteriol. 2004;186(11):3590-8.

584. Leonhartsberger S, Huber A, Lottspeich F, Böck A. The hydH/G Genes from Escherichia coli code for a zinc and lead responsive two-component regulatory system. J Mol Biol. 2001;307(1):93-105.

585. Al-Khodor S, Kalachikov S, Morozova I, Price CT, Abu Kwaik Y. The PmrA/PmrB two-component system of Legionella pneumophila is a global regulator required for intracellular replication within macrophages and protozoa. Infect Immun. 2009;77(1):374-86.

586. Behrens-Kneip S. The role of SurA factor in outer membrane protein transport and virulence. Int J Med Microbiol. 2010;300(7):421-8.

587. Lee C, Lee J, Lee JY, Park C. Characterization of the Escherichia coli YajL, YhbO and ElbB glyoxalases. FEMS Microbiol Lett. 2016;363(3).

588. Marchesini MI, Herrmann CK, Salcedo SP, Gorvel J-P, Comerci DJ. In search of Brucella abortus type IV secretion substrates: screening and identification of four proteins translocated into host cells through VirB system. Cellular Microbiology. 2011;13(8):1261-74.

589. Hu RM, Liao ST, Huang CC, Huang YW, Yang TC. An inducible fusaric acid tripartite efflux pump contributes to the fusaric acid resistance in Stenotrophomonas maltophilia. PLoS One. 2012;7(12):e51053.

590. Debnath I, Norton JP, Barber AE, Ott EM, Dhakal BK, Kulesus RR, et al. The Cpx stress response system potentiates the fitness and virulence of uropathogenic Escherichia coli. Infect Immun. 2013;81(5):1450-9.

591. Giannakopoulou N, Mendis N, Zhu L, Gruenheid S, Faucher SP, Le Moual H. The Virulence Effect of CpxRA in Citrobacter rodentium Is Independent of the Auxiliary Proteins NlpE and CpxP. Front Cell Infect Microbiol. 2018;8:320.

592. Zhou X, Keller R, Volkmer R, Krauss N, Scheerer P, Hunke S. Structural basis for two-component system inhibition and pilus sensing by the auxiliary CpxP protein. J Biol Chem. 2011;286(11):9805-14.

593. Subramaniam S, Müller VS, Hering NA, Mollenkopf H, Becker D, Heroven AK, et al. Contribution of the Cpx envelope stress system to metabolism and virulence regulation in Salmonella enterica serovar Typhimurium. PLoS One. 2019;14(2):e0211584.

594. Danese PN, Silhavy TJ. CpxP, a stress-combative member of the Cpx regulon. J Bacteriol. 1998;180(4):831-9.

595. Njoroge JW, Nguyen Y, Curtis MM, Moreira CG, Sperandio V. Virulence meets metabolism: Cra and KdpE gene regulation in enterohemorrhagic Escherichia coli. mBio. 2012;3(5):e00280-12.

596. Freeman ZN, Dorus S, Waterfield NR. The KdpD/KdpE two-component system: integrating K^+ homeostasis and virulence. PLoS Pathog. 2013;9(3):e1003201.

597. Potempa J, Madej M, Scott DA. The RagA and RagB proteins of Porphyromonas gingivalis. Mol Oral Microbiol. 2021;36(4):225-32.

598. Nagai H, Roy CR. The DotA protein from Legionella pneumophila is secreted by a novel process that requires the Dot/Icm transporter. The EMBO Journal. 2001;20(21):5962-70.

599. Loeb MR. Ferrochelatase activity and protoporphyrin IX utilization in Haemophilus influenzae. J Bacteriol. 1995;177(12):3613-5.

600. Fontán P, Aris V, Ghanny S, Soteropoulos P, Smith I. Global transcriptional profile of Mycobacterium tuberculosis during THP-1 human macrophage infection. Infect Immun. 2008;76(2):717-25.

601. Rahman MT, Parreira V, Prescott JF. In vitro and intra-macrophage gene expression by Rhodococcus equi strain 103. Vet Microbiol. 2005;110(1-2):131-40.

602. Dieppedale J, Sobral D, Dupuis M, Dubail I, Klimentova J, Stulik J, et al. Identification of a putative chaperone involved in stress resistance and virulence in Francisella tularensis. Infect Immun. 2011;79(4):1428-39.

603. Stietz MS, Lopez C, Osifo O, Tolmasky ME, Cardona ST. Evaluation of the electron transfer flavoprotein as an antibacterial target in Burkholderia cenocepacia. Can J Microbiol. 2017;63(10):857-63.

604. Bloodworth RAM, Zlitni S, Brown ED, Cardona ST. An electron transfer flavoprotein is essential for viability and its depletion causes a rod-to-sphere change in Burkholderia cenocepacia. Microbiology (Reading). 2015;161(10):1909-20.

605. Li Y, Zhu J, Hu J, Meng X, Zhang Q, Zhu K, et al. Functional characterization of electron-transferring flavoprotein and its dehydrogenase required for fungal development and plant infection by the rice blast fungus. Scientific Reports. 2016;6(1):24911.

606. Huergo LF, Chandra G, Merrick M. PII signal transduction proteins: nitrogen regulation and beyond. FEMS Microbiology Reviews. 2013;37(2):251-83.

607. Yurgel SN, Rice J, Mulder M, Kahn ML. GlnB/GlnK PII proteins and regulation of the Sinorhizobium meliloti Rm1021 nitrogen stress response and symbiotic function. J Bacteriol. 2010;192(10):2473-81.

608. Sam KA, Fairhurst SA, Thorneley RN, Allen JW, Ferguson SJ. Pseudoazurin dramatically enhances the reaction profile of nitrite reduction by Paracoccus pantotrophus cytochrome cd1 and facilitates release of product nitric oxide. J Biol Chem. 2008;283(18):12555-63.

609. Baek SH, Rajashekara G, Splitter GA, Shapleigh JP. Denitrification genes regulate Brucella virulence in mice. J Bacteriol. 2004;186(18):6025-31.

610. Loisel-Meyer S, Jiménez de Bagüés MP, Bassères E, Dornand J, Köhler S, Liautard JP, et al. Requirement of norD for Brucella suis virulence in a murine model of in vitro and in vivo infection. Infect Immun. 2006;74(3):1973-6.

611. Ding Y, Fu Y, Lee JC, Hooper DC. Staphylococcus aureus NorD, a putative efflux pump coregulated with the Opp1 oligopeptide permease, contributes selectively to fitness in vivo. J Bacteriol. 2012;194(23):6586-93.

612. Truchon AN, Hendrich CG, Bigott AF, Dalsing BL, Allen C. NorA, HmpX, and NorB Cooperate to Reduce NO Toxicity during Denitrification and Plant Pathogenesis in Ralstonia solanacearum. Microbiol Spectr. 2022;10(2):e0026422.

613. Zhang Y, Bao Q, Gagnon LA, Huletsky A, Oliver A, Jin S, et al. ampG gene of Pseudomonas aeruginosa and its role in β-lactamase expression. Antimicrob Agents Chemother. 2010;54(11):4772-9.

614. Wang Z, Bie P, Cheng J, Lu L, Cui B, Wu Q. The ABC transporter YejABEF is required for resistance to antimicrobial peptides and the virulence of Brucella melitensis. Sci Rep. 2016;6:31876.

615. Nzakizwanayo J, Scavone P, Jamshidi S, Hawthorne JA, Pelling H, Dedi C, et al. Fluoxetine and thioridazine inhibit efflux and attenuate crystalline biofilm formation by Proteus mirabilis. Sci Rep. 2017;7(1):12222.

616. Rao M, Liu H, Yang M, Zhao C, He Z-G. A Copper-responsive Global Repressor Regulates Expression of Diverse Membrane-associated Transporters and Bacterial Drug Resistance in Mycobacteria*. Journal of Biological Chemistry. 2012;287(47):39721-31.

617. Song S, Lee B, Yeom JH, Hwang S, Kang I, Cho JC, et al. MdsABC-Mediated Pathway for Pathogenicity in Salmonella enterica Serovar Typhimurium. Infect Immun. 2015;83(11):4266-76.

618. Schlömann M. Evolution of chlorocatechol catabolic pathways. Conclusions to be drawn from comparisons of lactone hydrolases. Biodegradation. 1994;5(3-4):301-21.

619. Thompson SA, Wang LL, West A, Sparling PF. Neisseria meningitidis produces iron-regulated proteins related to the RTX family of exoproteins. J Bacteriol. 1993;175(3):811-8.

620. Binet R, Wandersman C. Cloning of the Serratia marcescens hasF gene encoding the Has ABC exporter outer membrane component: a TolC analogue. Molecular Microbiology. 1996;22(2):265-73.

621. Panta PR, Kumar S, Stafford CF, Billiot CE, Douglass MV, Herrera CM, et al. A DedA Family Membrane Protein Is Required for Burkholderia thailandensis Colistin Resistance. Front Microbiol. 2019;10:2532.

622. Nakajima T. Roles of Sulfur Metabolism and Rhodanese in Detoxification and Anti-Oxidative Stress Functions in the Liver: Responses to Radiation Exposure. Med Sci Monit. 2015;21:1721-5.

623. Kang D, Kirienko DR, Webster P, Fisher AL, Kirienko NV. Pyoverdine, a siderophore from Pseudomonas aeruginosa, translocates into C. elegans, removes iron, and activates a distinct host response. Virulence. 2018;9(1):804-17.

624. Leseigneur C, Lê-Bury P, Pizarro-Cerdá J, Dussurget O. Emerging Evasion Mechanisms of Macrophage Defenses by Pathogenic Bacteria. Frontiers in Cellular and Infection Microbiology. 2020;10.

625. Kim GL, Luong TT, Park SS, Lee S, Ha JA, Nguyen CT, et al. Inhibition of Autolysis by Lipase LipA in Streptococcus pneumoniae Sepsis. Mol Cells. 2017;40(12):935-44.

626. Wehrly TD, Chong A, Virtaneva K, Sturdevant DE, Child R, Edwards JA, et al. Intracellular biology and virulence determinants of Francisella tularensis revealed by transcriptional profiling inside macrophages. Cell Microbiol. 2009;11(7):1128-50.

627. Horvath DJ, Jr., Li B, Casper T, Partida-Sanchez S, Hunstad DA, Hultgren SJ, et al. Morphological plasticity promotes resistance to phagocyte killing of uropathogenic Escherichia coli. Microbes Infect. 2011;13(5):426-37.

628. Clerch B, Garriga X, Torrents E, Rosales CM, Llagostera M. Construction and characterization of two lexA mutants of Salmonella typhimurium with different UV sensitivities and UV mutabilities. J Bacteriol. 1996;178(10):2890-6.

629. Chattopadhyay D, Carey AJ, Caliot E, Webb RI, Layton JR, Wang Y, et al. Phylogenetic lineage and pilus protein Spb1/SAN1518 affect opsonin-independent phagocytosis and intracellular survival of Group B Streptococcus. Microbes Infect. 2011;13(4):369-82.

630. Adderson EE, Takahashi S, Wang Y, Armstrong J, Miller DV, Bohnsack JF. Subtractive hybridization identifies a novel predicted protein mediating epithelial cell invasion by virulent serotype III group B Streptococcus agalactiae. Infect Immun. 2003;71(12):6857-63.

631. Bishop RE. The bacterial lipocalins. Biochim Biophys Acta. 2000;1482(1-2):73-83.

632. Bishop RE, Penfold SS, Frost LS, Höltje JV, Weiner JH. Stationary phase expression of a novel Escherichia coli outer membrane lipoprotein and its relationship with mammalian apolipoprotein D. Implications for the origin of lipocalins. J Biol Chem. 1995;270(39):23097-103.

633. St Laurent G, Shtokalo D, Tackett MR, Yang Z, Vyatkin Y, Milos PM, et al. On the importance of small changes in RNA expression. Methods. 2013;63(1):18-24.

634. Juarez E, Nuñez C, Sada E, Ellner JJ, Schwander SK, Torres M. Differential expression of Toll-like receptors on human alveolar macrophages and autologous peripheral monocytes. Respiratory Research. 2010;11(1):2.

635. Harju K, Glumoff V, Hallman M. Ontogeny of Toll-like receptors Tlr2 and Tlr4 in mice. Pediatric research. 2001;49(1):81-3.

636. Zarember KA, Godowski PJ. Tissue expression of human Toll-like receptors and differential regulation of Toll-like receptor mRNAs in leukocytes in response to microbes, their products, and cytokines. The journal of immunology. 2002;168(2):554-61.

637. Cario E, Podolsky DK. Differential alteration in intestinal epithelial cell expression of toll-like receptor 3 (TLR3) and TLR4 in inflammatory bowel disease. Infection and immunity. 2000;68(12):7010-7.

638. Fenhalls G, Squires GR, Stevens-Muller L, Bezuidenhout J, Amphlett G, Duncan K, et al. Associations between toll-like receptors and interleukin-4 in the lungs of patients with tuberculosis. American journal of respiratory cell and molecular biology. 2003;29(1):28-38.

639. Okamoto M, Hirai H, Taniguchi K, Shimura K, Inaba T, Shimazaki C, et al. Toll-like Receptors (TLRs) are expressed by myeloid leukaemia cell lines, but fail to trigger differentiation in response to the respective TLR ligands. British Journal of Haematology. 2009;147(4):585-7.

640. Jeannin P, Bottazzi B, Sironi M, Doni A, Rusnati M, Presta M, et al. Complexity and Complementarity of Outer Membrane Protein A Recognition by Cellular and Humoral Innate Immunity Receptors. Immunity. 2005;22(5):551-60.

641. Kapoor A, Forman M, Arav-Boger R. Activation of nucleotide oligomerization domain 2 (NOD2) by human cytomegalovirus initiates innate immune responses and restricts virus replication. PLoS One. 2014;9(3):e92704.

642. Shaw MH, Reimer T, Sánchez-Valdepeñas C, Warner N, Kim Y-G, Fresno M, et al. T cell–intrinsic role of Nod2 in promoting type 1 immunity to Toxoplasma gondii. Nature Immunology. 2009;10(12):1267-74.

643. Parant MA, Pouillart P, Contel CL, Parant FJ, Chedid LA, Bahr GM. Selective modulation of lipopolysaccharide-induced death and cytokine production by various muramyl peptides. Infection and Immunity. 1995;63(1):110-5.

644. Wolfert MA, Murray TF, Boons GJ, Moore JN. The origin of the synergistic effect of muramyl dipeptide with endotoxin and peptidoglycan. J Biol Chem. 2002;277(42):39179-86.

645. Pauleau A-L, Murray PJ. Role of Nod2 in the Response of Macrophages to Toll-Like Receptor Agonists. Molecular and Cellular Biology. 2003;23(21):7531-9.

646. Moreira LO, Zamboni DS. NOD1 and NOD2 Signaling in Infection and Inflammation. Front Immunol. 2012;3:328.

647. Schaffler H, Demircioglu DD, Kuhner D, Menz S, Bender A, Autenrieth IB, et al. NOD2 stimulation by Staphylococcus aureus-derived peptidoglycan is boosted by Toll-like receptor 2 costimulation with lipoproteins in dendritic cells. Infect Immun. 2014;82(11):4681-8.

648. Watanabe T, Kitani A, Murray PJ, Strober W. NOD2 is a negative regulator of Toll-like receptor 2–mediated T helper type 1 responses. Nature Immunology. 2004;5(8):800-8.

649. Kim GY, Kim JH, Ahn SC, Lee HJ, Moon DO, Lee CM, et al. Lycopene suppresses the lipopolysaccharide-induced phenotypic and functional maturation of murine dendritic cells through inhibition of mitogen-activated protein kinases and nuclear factor-kappaB. Immunology. 2004;113(2):203-11.

650. Zilbauer M, Dorrell N, Elmi A, Lindley KJ, Schuller S, Jones HE, et al. A major role for intestinal epithelial nucleotide oligomerization domain 1 (NOD1) in eliciting host bactericidal immune responses to Campylobacter jejuni. Cell Microbiol. 2007;9(10):2404-16.

651. Sansonetti PJ, Di Santo JP. Debugging how bacteria manipulate the immune response. Immunity. 2007;26(2):149-61.

652. Bera A, Herbert S, Jakob A, Vollmer W, Gotz F. Why are pathogenic staphylococci so lysozyme resistant? The peptidoglycan O-acetyltransferase OatA is the major determinant for lysozyme resistance of Staphylococcus aureus. Mol Microbiol. 2005;55(3):778-87.

653. Boneca IG, Dussurget O, Cabanes D, Nahori MA, Sousa S, Lecuit M, et al. A critical role for peptidoglycan N-deacetylation in Listeria evasion from the host innate immune system. Proc Natl Acad Sci U S A. 2007;104(3):997-1002.

654. Grimes CL, Ariyananda Lde Z, Melnyk JE, O'Shea EK. The innate immune protein Nod2 binds directly to MDP, a bacterial cell wall fragment. J Am Chem Soc. 2012;134(33):13535-7.

655. Mo J, Boyle JP, Howard CB, Monie TP, Davis BK, Duncan JA. Pathogen sensing by nucleotide-binding oligomerization domain-containing protein 2 (NOD2) is mediated by direct binding to muramyl dipeptide and ATP. J Biol Chem. 2012;287(27):23057-67.

656. Melnyk JE, Mohanan V, Schaefer AK, Hou CW, Grimes CL. Peptidoglycan Modifications Tune the Stability and Function of the Innate Immune Receptor Nod2. J Am Chem Soc. 2015;137(22):6987-90.

657. Coulombe F, Divangahi M, Veyrier F, de Leseleuc L, Gleason JL, Yang Y, et al. Increased NOD2-mediated recognition of N-glycolyl muramyl dipeptide. J Exp Med. 2009;206(8):1709-16.

658. Brott AS. Peptidoglycan O-Acetylation as a Virulence Factor: Its Effect on Lysozyme in the Innate Immune System. Antibiotics. 2019;8(3):94.

659. Lerner TR, Lovering AL, Bui NK, Uchida K, Aizawa S, Vollmer W, et al. Specialized peptidoglycan hydrolases sculpt the intra-bacterial niche of predatory Bdellovibrio and increase population fitness. PLoS Pathog. 2012;8(2):e1002524.

660. Lambert C, Lerner TR, Bui NK, Somers H, Aizawa S-I, Liddell S, et al. Interrupting peptidoglycan deacetylation during Bdellovibrio predator-prey interaction prevents ultimate destruction of prey wall, liberating bacterial-ghosts. Scientific Reports. 2016;6(1):26010.

661. Ma P, Wang Z, Pflugfelder SC, Li DQ. Toll-like receptors mediate induction of peptidoglycan recognition proteins in human corneal epithelial cells. Exp Eye Res. 2010;90(1):130-6.

662. Lee J, Geddes K, Streutker C, Philpott DJ, Girardin SE. Role of mouse peptidoglycan recognition protein PGLYRP2 in the innate immune response to Salmonella enterica serovar Typhimurium infection in vivo. Infect Immun. 2012;80(8):2645-54.

663. Xu M, Wang Z, Locksley RM. Innate immune responses in peptidoglycan recognition protein L-deficient mice. Mol Cell Biol. 2004;24(18):7949-57.

664. Dabrowski AN, Conrad C, Behrendt U, Shrivastav A, Baal N, Wienhold SM, et al. Peptidoglycan Recognition Protein 2 Regulates Neutrophil Recruitment Into the Lungs After Streptococcus pneumoniae Infection. Front Microbiol. 2019;10:199.

665. Bobrovsky P, Manuvera V, Polina N, Podgorny O, Prusakov K, Govorun V, et al. Recombinant human peptidoglycan recognition proteins reveal antichlamydial activity. Infection and immunity. 2016;84(7):2124-30.

666. Torrens G, Perez-Gallego M, Moya B, Munar-Bestard M, Zamorano L, Cabot G, et al. Targeting the permeability barrier and peptidoglycan recycling pathways to disarm Pseudomonas aeruginosa against the innate immune system. PLoS One. 2017;12(7):e0181932.

667. Kelesidis T. The Cross-Talk between Spirochetal Lipoproteins and Immunity. Front Immunol. 2014;5:310.

668. Haake DA. Spirochaetal lipoproteins and pathogenesis. Microbiology (Reading). 2000;146 (Pt 7)(Pt 7):1491-504.

669. Schroder NW, Eckert J, Stubs G, Schumann RR. Immune responses induced by spirochetal outer membrane lipoproteins and glycolipids. Immunobiology. 2008;213(3-4):329-40.

670. Rietschel ET, Schletter J, Weidemann B, El-Samalouti V, Mattern T, Zähringer U, et al. Lipopolysaccharide and peptidoglycan: CD14-dependent bacterial inducers of inflammation. Microb Drug Resist. 1998;4(1):37-44.

671. Radolf JD, Arndt LL, Akins DR, Curetty LL, Levi ME, Shen Y, et al. Treponema pallidum and Borrelia burgdorferi lipoproteins and synthetic lipopeptides activate monocytes/macrophages. J Immunol. 1995;154(6):2866-77.

672. Brandt ME, Riley BS, Radolf JD, Norgard MV. Immunogenic integral membrane proteins of Borrelia burgdorferi are lipoproteins. Infection and Immunity. 1990;58(4):983-91.

673. Lien E, Sellati TJ, Yoshimura A, Flo TH, Rawadi G, Finberg RW, et al. Toll-like receptor 2 functions as a pattern recognition receptor for diverse bacterial products. J Biol Chem. 1999;274(47):33419-25.

674. Norgard MV, Arndt LL, Akins DR, Curetty LL, Harrich DA, Radolf JD. Activation of human monocytic cells by Treponema pallidum and Borrelia burgdorferi lipoproteins and synthetic lipopeptides proceeds via a pathway distinct from that of lipopolysaccharide but involves the transcriptional activator NF-kappa B. Infection and Immunity. 1996;64(9):3845-52.

675. Sellati TJ, Bouis DA, Kitchens RL, Darveau RP, Pugin J, Ulevitch RJ, et al. Treponema pallidum and Borrelia burgdorferi lipoproteins and synthetic lipopeptides activate monocytic cells via a CD14-dependent pathway distinct from that used by lipopolysaccharide. The journal of Immunology. 1998;160(11):5455-64.

676. Sellati TJ, Wilkinson DA, Sheffield JS, Koup RA, Radolf JD, Norgard MV. Virulent Treponema pallidum, lipoprotein, and synthetic lipopeptides induce CCR5 on human monocytes and enhance their susceptibility to infection by human immunodeficiency virus type 1. The Journal of infectious diseases. 2000;181(1):283-93.

677. Sellati TJ, Waldrop SL, Salazar JC, Bergstresser PR, Picker LJ, Radolf JD. The cutaneous response in humans to Treponema pallidum lipoprotein analogues involves cellular elements of both innate and adaptive immunity. J Immunol. 2001;166(6):4131-40.

678. Akins D, Purcell B, Mitra M, Norgard M, Radolf J. Lipid modification of the 17-kilodalton membrane immunogen of Treponema pallidum determines macrophage activation as well as amphiphilicity. Infection and immunity. 1993;61(4):1202-10.

679. DeOgny L, Pramanik B, Arndt L, Jones J, Rush J, Slaughter CA, et al. Solid-phase synthesis of biologically active lipopeptides as analogs for spirochetal lipoproteins. Peptide research. 1994;7(2):91-7.

680. Radolf JD, Norgard MV, Brandt ME, Isaacs RD, Thompson PA, Beutler B. Lipoproteins of Borrelia burgdorferi and Treponema pallidum activate cachectin/tumor necrosis factor synthesis. Analysis using a CAT reporter construct. The Journal of Immunology. 1991;147(6):1968-74.

681. Giambartolomei GH, Dennis VA, Lasater BL, Murthy PK, Philipp MT. Autocrine and Exocrine Regulation of Interleukin-10 Production in THP-1 Cells Stimulated with

Borrelia burgdorferi

Lipoproteins. Infection and Immunity. 2002;70(4):1881-8.

682. Hirschfeld M, Kirschning CJ, Schwandner R, Wesche H, Weis JH, Wooten RM, et al. Cutting edge: inflammatory signaling by Borrelia burgdorferi lipoproteins is mediated by toll-like receptor 2. The Journal of Immunology. 1999;163(5):2382-6.

683. Rupprecht TA, Kirschning CJ, Popp B, Kastenbauer S, Fingerle V, Pfister HW, et al. Borrelia garinii induces CXCL13 production in human monocytes through Toll-like receptor 2. Infect Immun. 2007;75(9):4351-6.

684. Giambartolomei GH, Dennis VA, Lasater BL, Philipp MT. Induction of pro-and anti-inflammatory cytokines by Borrelia burgdorferi lipoproteins in monocytes is mediated by CD14. Infection and immunity. 1999;67(1):140-7.

685. Giambartolomei GH, Dennis VA, Philipp MT. Borrelia burgdorferi stimulates the production of interleukin-10 in peripheral blood mononuclear cells from uninfected humans and rhesus monkeys. Infection and immunity. 1998;66(6):2691-7.

686. Brown JP, Zachary JF, Teuscher C, Weis JJ, Wooten RM. Dual role of interleukin-10 in murine Lyme disease: regulation of arthritis severity and host defense. Infection and immunity. 1999;67(10):5142-50.

687. Diterich I, Harter L, Hassler D, Wendel A, Hartung T. Modulation of cytokine release in ex vivo-stimulated blood from borreliosis patients. Infect Immun. 2001;69(2):687-94.

688. Brightbill HD, Libraty DH, Krutzik SR, Yang R-B, Belisle JT, Bleharski JR, et al. Host defense mechanisms triggered by microbial lipoproteins through toll-like receptors. Science. 1999;285(5428):732-6.

689. Ma Y, Seiler KP, Tai K-F, Yang L, Woods M, Weis JJ. Outer surface lipoproteins of Borrelia burgdorferi stimulate nitric oxide production by the cytokine-inducible pathway. Infection and Immunity. 1994;62(9):3663-71.

690. Wooten RM, Ma Y, Yoder RA, Brown JP, Weis JH, Zachary JF, et al. Toll-like receptor 2 is required for innate, but not acquired, host defense to Borrelia burgdorferi. J Immunol. 2002;168(1):348-55.

691. Werts C, Tapping RI, Mathison JC, Chuang T-H, Kravchenko V, Saint Girons I, et al. Leptospiral lipopolysaccharide activates cells through a TLR2-dependent mechanism. Nature immunology. 2001;2(4):346-52.

692. Lee SK, Stack A, Katzowitsch E, Aizawa SI, Suerbaum S, Josenhans C. Helicobacter pylori flagellins have very low intrinsic activity to stimulate human gastric epithelial cells via TLR5. Microbes Infect. 2003;5(15):1345-56.

693. Liu J, Howell JK, Bradley SD, Zheng Y, Zhou ZH, Norris SJ. Cellular architecture of Treponema pallidum: novel flagellum, periplasmic cone, and cell envelope as revealed by cryo electron tomography. J Mol Biol. 2010;403(4):546-61.

694. Rajagopala SV, Titz B, Goll J, Parrish JR, Wohlbold K, McKevitt MT, et al. The protein network of bacterial motility. Mol Syst Biol. 2007;3:128.

695. Titz B, Rajagopala SV, Ester C, Häuser R, Uetz P. Novel conserved assembly factor of the bacterial flagellum. J Bacteriol. 2006;188(21):7700-6.

696. Xu M, Xie Y, Jiang C, Xiao Y, Kuang X, Wen Y, et al. Treponema pallidum flagellins elicit proinflammatory cytokines from human monocytes via TLR5 signaling pathway. Immunobiology. 2017;222(5):709-18.

697. Jiang C, Xu M, Kuang X, Xiao J, Tan M, Xie Y, et al. Treponema pallidum flagellins stimulate MMP-9 and MMP-13 expression via TLR5 and MAPK/NF-kappaB signaling pathways in human epidermal keratinocytes. Exp Cell Res. 2017;361(1):46-55.

698. Xu M, Xie Y, Tan M, Zheng K, Xiao Y, Jiang C, et al. The N-terminal D1 domain of Treponema pallidum flagellin binding to TLR5 is required but not sufficient in activation of TLR5. J Cell Mol Med. 2019;23(11):7490-504.

699. Holzapfel M, Bonhomme D, Cagliero J, Vernel-Pauillac F, Fanton d'Andon M, Bortolussi S, et al. Escape of TLR5 Recognition by Leptospira spp.: A Rationale for Atypical Endoflagella. Front Immunol. 2020;11:2007.

700. Dennis VA, Dixit S, O'Brien SM, Alvarez X, Pahar B, Philipp MT. Live Borrelia burgdorferi spirochetes elicit inflammatory mediators from human monocytes via the Toll-like receptor signaling pathway. Infect Immun. 2009;77(3):1238-45.

701. Cabral ES, Gelderblom H, Hornung RL, Munson PJ, Martin R, Marques AR. Borrelia burgdorferi lipoprotein-mediated TLR2 stimulation causes the down-regulation of TLR5 in human monocytes. J Infect Dis. 2006;193(6):849-59.

702. Miao EA, Andersen-Nissen E, Warren SE, Aderem A. TLR5 and Ipaf: dual sensors of bacterial flagellin in the innate immune system. Semin Immunopathol. 2007;29(3):275-88.

703. Miao EA, Ernst RK, Dors M, Mao DP, Aderem A. Pseudomonas aeruginosa activates caspase 1 through Ipaf. Proc Natl Acad Sci U S A. 2008;105(7):2562-7.

704. Sierro F, Dubois B, Coste A, Kaiserlian D, Kraehenbuhl JP, Sirard JC. Flagellin stimulation of intestinal epithelial cells triggers CCL20-mediated migration of dendritic cells. Proc Natl Acad Sci U S A. 2001;98(24):13722-7.

705. Moen SH, Ehrnström B, Kojen JF, Yurchenko M, Beckwith KS, Afset JE, et al. Human Toll-like Receptor 8 (TLR8) Is an Important Sensor of Pyogenic Bacteria, and Is Attenuated by Cell Surface TLR Signaling. Front Immunol. 2019;10:1209.

706. Eigenbrod T, Pelka K, Latz E, Kreikemeyer B, Dalpke AH. TLR8 Senses Bacterial RNA in Human Monocytes and Plays a Nonredundant Role for Recognition of Streptococcus pyogenes. J Immunol. 2015;195(3):1092-9.

707. Ehrnström B, Beckwith KS, Yurchenko M, Moen SH, Kojen JF, Lentini G, et al. Toll-Like Receptor 8 Is a Major Sensor of Group B Streptococcus But Not Escherichia coli in Human Primary Monocytes and Macrophages. Front Immunol. 2017;8:1243.

708. Fore F, Indriputri C, Mamutse J, Nugraha J. TLR10 and Its Unique Anti-Inflammatory Properties and Potential Use as a Target in Therapeutics. Immune Netw. 2020;20(3):e21.

709. Peterman EM, Sullivan C, Goody MF, Rodriguez-Nunez I, Yoder JA, Kim CH. Neutralization of mitochondrial superoxide by superoxide dismutase 2 promotes bacterial clearance and regulates phagocyte numbers in zebrafish. Infect Immun. 2015;83(1):430-40.

710. Fukai T, Folz RJ, Landmesser U, Harrison DG. Extracellular superoxide dismutase and cardiovascular disease. Cardiovasc Res. 2002;55(2):239-49.

711. Rakkola R, Matikainen S, Nyman TA. Proteome analysis of human macrophages reveals the upregulation of manganese-containing superoxide dismutase after toll-like receptor activation. Proteomics. 2007;7(3):378-84.

712. Visner GA, Dougall WC, Wilson JM, Burr IA, Nick HS. Regulation of manganese superoxide dismutase by lipopolysaccharide, interleukin-1, and tumor necrosis factor. Role in the acute inflammatory response. Journal of Biological Chemistry. 1990;265(5):2856-64.

713. Rogers RJ, Monnier JM, Nick HS. Tumor necrosis factor-alpha selectively induces MnSOD expression via mitochondria-to-nucleus signaling, whereas interleukin-1beta utilizes an alternative pathway. J Biol Chem. 2001;276(23):20419-27.

714. DOUGALL WC, NICK HS. Manganese Superoxide Dismutase: A Hepatic Acute Phase Protein Regulated by Interleukin-6 and Glucocorticoids*. Endocrinology. 1991;129(5):2376-84.

715. Drane P, Bravard A, Bouvard V, May E. Reciprocal down-regulation of p53 and SOD2 gene expression–implication in p53 mediated apoptosis. Oncogene. 2001;20(4):430-9.

716. Yu Z, He X, Fu D, Zhang Y. Two superoxide dismutase (SOD) with different subcellular localizations involved in innate immunity in Crassostrea hongkongensis. Fish & Shellfish Immunology. 2011;31(4):533-9.

717. Campa-Córdova AI, Hernández-Saavedra NY, Ascencio F. Superoxide dismutase as modulator of immune function in American white shrimp (Litopenaeus vannamei). Comp Biochem Physiol C Toxicol Pharmacol. 2002;133(4):557-65.

718. Basagoudanavar SH, Thapa RJ, Nogusa S, Wang J, Beg AA, Balachandran S. Distinct Roles for the NF-κB RelA Subunit during Antiviral Innate Immune Responses. Journal of Virology. 2011;85(6):2599-610.

719. Olsson J, Jacobson TAS, Paulsson JM, Dadfar E, Moshfegh A, Jacobson SH, et al. Expression of neutrophil SOD2 is reduced after lipopolysaccharide stimulation: a potential cause of neutrophil dysfunction in chronic kidney disease. Nephrology Dialysis Transplantation. 2010;26(7):2195-201.

720. Chaparro V, Graber TE, Alain T, Jaramillo M. Transcriptional profiling of macrophages reveals distinct parasite stage-driven signatures during early infection by Leishmania donovani. Sci Rep. 2022;12(1):6369.

721. Pisu D, Huang L, Narang V, Theriault M, Le-Bury G, Lee B, et al. Single cell analysis of M. tuberculosis phenotype and macrophage lineages in the infected lung. J Exp Med. 2021;218(9).

722. Nau GJ, Richmond JF, Schlesinger A, Jennings EG, Lander ES, Young RA. Human macrophage activation programs induced by bacterial pathogens. Proc Natl Acad Sci U S A. 2002;99(3):1503-8.

723. Abuaita BH, Schultz TL, O'Riordan MX. Mitochondria-Derived Vesicles Deliver Antimicrobial Reactive Oxygen Species to Control Phagosome-Localized Staphylococcus aureus. Cell Host Microbe. 2018;24(5):625-36 e5.

724. Mittler R, Zandalinas SI, Fichman Y, Van Breusegem F. Reactive oxygen species signalling in plant stress responses. Nat Rev Mol Cell Biol. 2022;23(10):663-79.

725. Smith JJ, Aitchison JD. Peroxisomes take shape. Nat Rev Mol Cell Biol. 2013;14(12):803-17.

726. Flannagan RS, Cosio G, Grinstein S. Antimicrobial mechanisms of phagocytes and bacterial evasion strategies. Nat Rev Microbiol. 2009;7(5):355-66.

727. Park YS, Uddin MJ, Piao L, Hwang I, Lee JH, Ha H. Novel Role of Endogenous Catalase in Macrophage Polarization in Adipose Tissue. Mediators Inflamm. 2016;2016:8675905.

728. Han W, Fessel JP, Sherrill T, Kocurek EG, Yull FE, Blackwell TS. Enhanced Expression of Catalase in Mitochondria Modulates NF-kappaB-Dependent Lung Inflammation through Alteration of Metabolic Activity in Macrophages. J Immunol. 2020;205(4):1125-34.

729. Wittmann C, Chockley P, Singh SK, Pase L, Lieschke GJ, Grabher C. Hydrogen peroxide in inflammation: messenger, guide, and assassin. Adv Hematol. 2012;2012:541471.

730. Shi R, Cao Z, Li H, Graw J, Zhang G, Thannickal VJ, et al. Peroxidasin contributes to lung host defense by direct binding and killing of gram-negative bacteria. PLOS Pathogens. 2018;14(5):e1007026.

731. Donnelly S, Stack CM, O'Neill SM, Sayed AA, Williams DL, Dalton JP. Helminth 2-Cys peroxiredoxin drives Th2 responses through a mechanism involving alternatively activated macrophages. Faseb j. 2008;22(11):4022-32.

732. Siraki AG. The many roles of myeloperoxidase: From inflammation and immunity to biomarkers, drug metabolism and drug discovery. Redox Biol. 2021;46:102109.

733. Venketaraman V, Dayaram YK, Amin AG, Ngo R, Green RM, Talaue MT, et al. Role of glutathione in macrophage control of mycobacteria. Infect Immun. 2003;71(4):1864-71.

734. Bozinovski S, Seow HJ, Crack PJ, Anderson GP, Vlahos R. Glutathione peroxidase-1 primes pro-inflammatory cytokine production after LPS challenge in vivo. PLoS One. 2012;7(3):e33172.

735. Diotallevi M, Checconi P, Palamara AT, Celestino I, Coppo L, Holmgren A, et al. Glutathione Fine-Tunes the Innate Immune Response toward Antiviral Pathways in a Macrophage Cell Line Independently of Its Antioxidant Properties. Front Immunol. 2017;8:1239.

736. Magacz M, Kędziora K, Sapa J, Krzyściak W. The Significance of Lactoperoxidase System in Oral Health: Application and Efficacy in Oral Hygiene Products. Int J Mol Sci. 2019;20(6).

737. Diet A, Abbas K, Bouton C, Guillon B, Tomasello F, Fourquet S, et al. Regulation of peroxiredoxins by nitric oxide in immunostimulated macrophages. J Biol Chem. 2007;282(50):36199-205.

738. Knoops B, Argyropoulou V, Becker S, Ferte L, Kuznetsova O. Multiple Roles of Peroxiredoxins in Inflammation. Mol Cells. 2016;39(1):60-4.

739. Guo F, He H, Fu ZC, Huang S, Chen T, Papasian CJ, et al. Adipocyte-derived PAMM suppresses macrophage inflammation by inhibiting MAPK signalling. Biochem J. 2015;472(3):309-18.

740. Matsumura K, Iwai H, Kato-Miyazawa M, Kirikae F, Zhao J, Yanagawa T, et al. Peroxiredoxin 1 Contributes to Host Defenses against Mycobacterium tuberculosis. J Immunol. 2016;197(8):3233-44.

741. Sun HN, Liu Y, Wang JN, Wang C, Liu R, Kong LZ, et al. Protective Role of Peroxiredoxin I in Heat-Killed Staphylococcus Aureus-infected Mice. In Vivo. 2019;33(3):749-55.

742. Riddell JR, Wang XY, Minderman H, Gollnick SO. Peroxiredoxin 1 stimulates secretion of proinflammatory cytokines by binding to TLR4. J Immunol. 2010;184(2):1022-30.

743. Salzano S, Checconi P, Hanschmann EM, Lillig CH, Bowler LD, Chan P, et al. Linkage of inflammation and oxidative stress via release of glutathionylated peroxiredoxin-2, which acts as a danger signal. Proc Natl Acad Sci U S A. 2014;111(33):12157-62.

744. Rabilloud T, Heller M, Gasnier F, Luche S, Rey C, Aebersold R, et al. Proteomics analysis of cellular response to oxidative stress. Evidence for in vivo overoxidation of peroxiredoxins at their active site. J Biol Chem. 2002;277(22):19396-401.

745. Chevallet M, Wagner E, Luche S, van Dorsselaer A, Leize-Wagner E, Rabilloud T. Regeneration of peroxiredoxins during recovery after oxidative stress: only some overoxidized peroxiredoxins can be reduced during recovery after oxidative stress. J Biol Chem. 2003;278(39):37146-53.

746. Masaki M, Ikeda A, Shiraki E, Oka S, Kawasaki T. Mixed lineage kinase LZK and antioxidant protein-1 activate NF-kappaB synergistically. Eur J Biochem. 2003;270(1):76-83.

747. Abbas K, Breton J, Picot CR, Quesniaux V, Bouton C, Drapier JC. Signaling events leading to peroxiredoxin 5 up-regulation in immunostimulated macrophages. Free Radic Biol Med. 2009;47(6):794-802.

748. Sun HN, Kim SU, Huang SM, Kim JM, Park YH, Kim SH, et al. Microglial peroxiredoxin V acts as an inducible anti-inflammatory antioxidant through cooperation with redox signaling cascades. J Neurochem. 2010;114(1):39-50.

749. Ali S, Mann-Nuttel R, Schulze A, Richter L, Alferink J, Scheu S. Sources of Type I Interferons in Infectious Immunity: Plasmacytoid Dendritic Cells Not Always in the Driver's Seat. Front Immunol. 2019;10:778.

750. McNab F, Mayer-Barber K, Sher A, Wack A, O'Garra A. Type I interferons in infectious disease. Nat Rev Immunol. 2015;15(2):87-103.

751. Kumaran Satyanarayanan S, El Kebir D, Soboh S, Butenko S, Sekheri M, Saadi J, et al. IFN-β is a macrophage-derived effector cytokine facilitating the resolution of bacterial inflammation. Nat Commun. 2019;10(1):3471.

752. Fung KY, Mangan NE, Cumming H, Horvat JC, Mayall JR, Stifter SA, et al. Interferon-ε protects the female reproductive tract from viral and bacterial infection. Science. 2013;339(6123):1088-92.

753. Kopitar-Jerala N. The Role of Interferons in Inflammation and Inflammasome Activation. Front Immunol. 2017;8:873.

754. Read SA, Wijaya R, Ramezani-Moghadam M, Tay E, Schibeci S, Liddle C, et al. Macrophage Coordination of the Interferon Lambda Immune Response. Front Immunol. 2019;10:2674.

755. Gunthner R, Anders HJ. Interferon-regulatory factors determine macrophage phenotype polarization. Mediators Inflamm. 2013;2013:731023.

756. Pastor TP, Peixoto BC, Viola JPB. The Transcriptional Co-factor IRF2BP2: A New Player in Tumor Development and Microenvironment. Front Cell Dev Biol. 2021;9:655307.

757. Hughes CE, Nibbs RJB. A guide to chemokines and their receptors. The FEBS Journal. 2018;285(16):2944-71.

758. Arango Duque G, Descoteaux A. Macrophage cytokines: involvement in immunity and infectious diseases. Front Immunol. 2014;5:491.

759. Xuan W, Qu Q, Zheng B, Xiong S, Fan GH. The chemotaxis of M1 and M2 macrophages is regulated by different chemokines. J Leukoc Biol. 2015;97(1):61-9.

760. Tecchio C, Cassatella MA. Neutrophil-derived chemokines on the road to immunity. Semin Immunol. 2016;28(2):119-28.

761. Capucetti A, Albano F, Bonecchi R. Multiple Roles for Chemokines in Neutrophil Biology. Frontiers in Immunology. 2020;11.

762. Thaiss CA, Semmling V, Franken L, Wagner H, Kurts C. Chemokines: a new dendritic cell signal for T cell activation. Front Immunol. 2011;2:31.

763. Tiberio L, Del Prete A, Schioppa T, Sozio F, Bosisio D, Sozzani S. Chemokine and chemotactic signals in dendritic cell migration. Cell Mol Immunol. 2018;15(4):346-52.

764. Debets R, Timans JC, Homey B, Zurawski S, Sana TR, Lo S, et al. Two novel IL-1 family members, IL-1 delta and IL-1 epsilon, function as an antagonist and agonist of NF-kappa B activation through the orphan IL-1 receptor-related protein 2. J Immunol. 2001;167(3):1440-6.

765. Lee EB, Kim A, Kang K, Kim H, Lim JS. NDRG2-mediated Modulation of SOCS3 and STAT3 Activity Inhibits IL-10 Production. Immune Netw. 2010;10(6):219-29.

766. Luzina IG, Keegan AD, Heller NM, Rook GA, Shea-Donohue T, Atamas SP. Regulation of inflammation by interleukin-4: a review of "alternatives". J Leukoc Biol. 2012;92(4):753-64.

767. Madouri F, Barada O, Kervoaze G, Trottein F, Pichavant M, Gosset P. Production of Interleukin-20 cytokines limits bacterial clearance and lung inflammation during infection by Streptococcus pneumoniae. EBioMedicine. 2018;37:417-27.

768. Zhou P, Li Q, Su S, Dong W, Zong S, Ma Q, et al. Interleukin 37 Suppresses M1 Macrophage Polarization Through Inhibition of the Notch1 and Nuclear Factor Kappa B Pathways. Front Cell Dev Biol. 2020;8:56.

769. Su Z, Tao X. Current Understanding of IL-37 in Human Health and Disease. Front Immunol. 2021;12:696605.

770. Azuma YT, Nishiyama K. Interleukin-19 enhances cytokine production induced by lipopolysaccharide and inhibits cytokine production induced by polyI:C in BALB/c mice. J Vet Med Sci. 2020;82(7):891-6.

771. Kempuraj D, Frydas S, Kandere K, Madhappan B, Letourneau R, Christodoulou S, et al. Interleukin-19 (IL-19) network revisited. Int J Immunopathol Pharmacol. 2003;16(2):95-7.

772. Yue Y, Huang W, Liang J, Guo J, Ji J, Yao Y, et al. IL4I1 Is a Novel Regulator of M2 Macrophage Polarization That Can Inhibit T Cell Activation via L-Tryptophan and Arginine Depletion and IL-10 Production. PLoS One. 2015;10(11):e0142979.

773. Van den Bossche J, Saraber DL. Metabolic regulation of macrophages in tissues. Cell Immunol. 2018;330:54-9.

774. O'Neill LA, Kishton RJ, Rathmell J. A guide to immunometabolism for immunologists. Nat Rev Immunol. 2016;16(9):553-65.

775. Wu R, Chen F, Wang N, Tang D, Kang R. ACOD1 in immunometabolism and disease. Cell Mol Immunol. 2020;17(8):822-33.

776. Galván-Peña S, O'Neill LA. Metabolic reprograming in macrophage polarization. Front Immunol. 2014;5:420.

777. Maier T, Guell M, Serrano L. Correlation of mRNA and protein in complex biological samples. FEBS Lett. 2009;583(24):3966-73.

778. Maier T, Schmidt A, Güell M, Kühner S, Gavin AC, Aebersold R, et al. Quantification of mRNA and protein and integration with protein turnover in a bacterium. Mol Syst Biol. 2011;7:511.

779. Schwanhausser B, Busse D, Li N, Dittmar G, Schuchhardt J, Wolf J, et al. Global quantification of mammalian gene expression control. Nature. 2011;473(7347):337-42.

780. Kitamura H, Nakagawa T, Takayama M, Kimura Y, Hijikata A, Ohara O. Post-transcriptional effects of phorbol 12-myristate 13-acetate on transcriptome of U937 cells. FEBS Lett. 2004;578(1-2):180-4.

781. Schott J, Reitter S, Philipp J, Haneke K, Schafer H, Stoecklin G. Translational regulation of specific mRNAs controls feedback inhibition and survival during macrophage activation. PLoS Genet. 2014;10(6):e1004368.

782. Ruland J. Return to homeostasis: downregulation of NF-kappaB responses. Nat Immunol. 2011;12(8):709-14.

783. Renner F, Schmitz ML. Autoregulatory feedback loops terminating the NF-kappaB response. Trends Biochem Sci. 2009;34(3):128-35.

784. Arbore G, West EE, Spolski R, Robertson AAB, Klos A, Rheinheimer C, et al. T helper 1 immunity requires complement-driven NLRP3 inflammasome activity in $CD4^+$ T cells. Science. 2016;352(6292):aad1210.

785. Morgan BP, Gasque P. Extrahepatic complement biosynthesis: where, when and why? Clin Exp Immunol. 1997;107(1):1-7.

786. Alper CA, Johnson AM, Birtch AG, Moore FD. Human C'3: evidence for the liver as the primary site of synthesis. Science. 1969;163(3864):286-8.

787. Morris KM, Aden DP, Knowles BB, Colten HR. Complement biosynthesis by the human hepatoma-derived cell line HepG2. J Clin Invest. 1982;70(4):906-13.

788. Cao H, Yang Y, Lu L, Yang X, Ai X. Effect of copper sulfate on Bdellovibrio growth and bacteriolytic activity towards gibel carp-pathogenic Aeromonas hydrophila. Can J Microbiol. 2018;64(12):1054-8.

789. Hanahan D. Studies on transformation of Escherichia coli with plasmids. Journal of Molecular Biology. 1983;166(4):557-80.

790. Simon R, Priefer U, Pühler A. A Broad Host Range Mobilization System for In Vivo Genetic Engineering: Transposon Mutagenesis in Gram Negative Bacteria. Bio/Technology. 1983;1(9):784-91.

791. Rogers M, Ekaterinaki N, Nimmo E, Sherratt D. Analysis of Tn7 transposition. Molecular and General Genetics MGG. 1986;205(3):550-6.

792. Schäfer A, Tauch A, Jäger W, Kalinowski J, Thierbach G, Pühler A. Small mobilizable multi-purpose cloning vectors derived from the Escherichia coli plasmids pK18 and pK19: selection of defined deletions in the chromosome of Corynebacterium glutamicum. Gene. 1994;145(1):69-73.

Appendices

Table 1.6.1: A summary of the main published animal studies interrogating *Bdellovibrio bacteriovorus* safety and efficacy *in vivo*

Main Conclusions	References
Bdellovibrio is able to prey on a range of multidrug resistant clinical isolates (polymicrobial; multidrug resistant; biofilms)	(364-367)
Bdellovibrio reduced severity and occurrence of *Shigella flexneri* induced keratoconjunctivitis on the rabbit ocular surface	(385)
Bdellovibrio was successfully used for the treatment of *Aeromonas Hydrophila* infection in fishponds	(788)
Periodontal pathogens targeted by *Bdellovibrio* in an *ex-vivo* periodontal model	(364, 393)
Treatment of *Salmonella* infection in chicks through oral administration of *Bdellovibrio* First warm-blooded animal study **Decreased *Salmonella* colonisation of gut, adverse caecal morphology, and inflammation** **No impact on gut microbiota diversity** **No impact on chick growth or wellbeing** **No spread between birds through water or faecal matter**	**Atterbury et al., 2011**
Bdellovibrio was non-cytotoxic Successful treatment of infective bovine keratoconjunctivitis mock infection on bovine kidney cells *B. bacteriovorus* 109J was not effective at treating infective bovine keratoconjunctivitis, although this required further investigation	(400, 409)
Looked at impact of *Bdellovibrio* on the intestinal microbiota	(355)
Serratia marcescens and *Pseudomonas aeruginosa* infection of *Galleria* and corneal epithelial cells *Bdellovibrio* preyed upon isolates of *S. marcescens* and *P. aeruginosa* successfully Non-cytotoxic to human corneal epithelial cells, with no increase in IL-8 or TNFα expression No adverse effects in a *Galleria* model of infection.	(368)
Bdellovibrio used to target *Pseudomonas tolasi* mushroom blight successfully	(397)
Bdellovibrio does affect overall ecology of the oral microbiome Predation efficiency decreases with increased complexity of *ex-vivo* oral models *Bdellovibrio* successfully targeted two oral pathogens in *ex-vivo* models.	(354)
Intranasal and intravenous introduction of *Bdellovibrio* showed no effect on viability or histopathology in murine mode IL-1β, IL-23 and TNFα levels in lung rose post 1 hour but decreased at 24- and 48-hour timepoints Neutrophil levels rose in blood after intravenous injection but fell again by 18 hours Increase in IL-1β, IL-23, CXCL-1, IFNγ and TNF seen but not sustained and milder than *Klebsiella pneumoniae* response.	(390)
Preharvest intervention in cattle prevented *Salmonella* and *E. coli* contamination from rumen and faeces	(396)

Bdellovibrio was non-toxic to rabbit ocular surface IL-8 but not IL-1β production initiated in response to *Bdellovibrio* *Bdellovibrio* did not inhibit wound healing	(386)
Bdellovibrio is non-toxic to human cell lines No significant elevation of proinflammatory cytokines (GM-CSF, IFN-γ, IL-10, IL-12p70, IL1β, IL-2, IL-6, IL-8 and TNF-α)	(370)
Characterised the response of human epithelial cells to *Bdellovibrio*	(369)
No adverse effects on histopathology Slight increase in cytokines (TNFα, CXCL1, IL-6, IL-13 and IL-1β) at 24 hrs but not sustained No dissemination/cleared after 10 days Intranasal administration of *Bdellovibrio* reduced *Klebsiella pneumoniae* bacterial burden in rat lung	(388)
Minimal shift in taxonomic diversity in gut microbiota, upon intrarectal inoculation of *Bdellovibrio* in rats	(353)
Injection of *Bdellovibrio* systemically into rats No adverse effects on mortality or pathology, except rise in proinflammatory cytokines (IL-1β, IL-5, IL-6, TNFα) in blood 2hrs post infection] Did not decrease *Klebsiella pneumoniae* burden in blood or dissemination suggesting *Bdellovibrio* is not appropriate for acute blood infections… *Bdellovibrio* dissemination is quickly and efficiently cleared by the host	(387)
Successful treatment of *Yersinia pestis* in mice lung model	(391)
Subcutaneous challenge with *Yersinia pestis* followed by intraperitoneal injection of *Bdellovibrio* *Bdellovibrio* treatment was protective in some mice, not others thus dependent on immune status of host *Bdellovibrio* controls spread and enhances clearance of *Y. pestis* Differential protection seen may be linked to host response to the predator in the context of prey *Bdellovibrio* survived in macrophages for a period in phagosome *Bdellovibrio* does not persist alone in vivo	(392)
Topical use of *Bdellovibrio* to treat periodontitis in rats	(389)
Mixed effects on the treatment of potato soft rot	(399)

Shigella flexneri **hindbrain infection in zebrafish larvae** ***Bdellovibrio*** **reduces** ***S. flexneri*** **numbers, with immune system proving important to eradicate infection.** ***Bdellovibrio*** **had a strong effect on improving zebrafish survival.** **Bd alone had no impact on zebrafish survival** **Bd treatment improved survival against** ***S. flexneri*** **infection due to pathogen killing** **First visualisation of active predation in vivo** **Bd are engulfed and cleared by macrophage and/or neutrophils but have sufficient dwell time to prey on pathogens** **Immune depletion shows maximum benefit comes from synergistic effect of bd with immune response, with** ***Bdellovibrio*** **contributing strongly** **Interactions with leukocytes in vivo had not previously been characterised** **Clearance was not due to enhanced immune activation of** ***Bdellovibrio*** **being present**	**Willis et al, 2016**
Quantified the interactions of live ***Bdellovibrio*** **with human phagocytic U937 cells, determining the uptake mechanisms, persistence, cytokine responses and intracellular trafficking** ***Bdellovibrio*** **is engulfed and persists (alive) for 24hrs without affecting macrophage viability** ***Bdellovibrio*** **is trafficked via the phagolysosomal pathway of degradation via F-actin and microtubule dependent methods** **Cytokine levels compared (IL-1β, TNFα, IL-6, IL-10, IL-8) to** ***S. typhimurium*** **and** ***K. pneumoniae*** **Antibody prevalence in population is high but at low levels (IgG/A: 90% but low, IgM: 50% but low)**	**Raghunathan et al., 2019**

Table 2.1.1: Bacterial strains used in the work detailed in Chapter 3

Strain	Description	Source
B. bacteriovorus HD100	Wild-type *B. bacteriovorus* Type strain NCBI Taxonomy ID: 264462 GenBank Accession: GCA_000196175.1	(281)
E. coli S17-1	Strain used as prey for *B. bacteriovorus* NCBI Taxonomy ID: 1227813 GenBank Accession: GCA_000340255.1	(789)
E. coli S17-1 λ-Pir	Strain for conjugation of mobilizable plasmids into *S. marcescens* #42 *E. coli* S17-1 with an additional donor λ-PIR plasmid, to increase conjugation efficiency owing to the suicide donor plasmid having a R6K origin of replication and low copy number.	(790)
S. marcescens #42	Clinical isolate of *S. marcescens* used for gene knockout strain generation Tetracycline (15 µg/ml) Resistant Ampicillin (500 µg/ml) Resistant	Clinical isolate obtained from Dr Mathew Diggle (Previously of EMPATH Pathology Services, Queens Medical Centre, Nottingham)
S. marcescens ΔarnA	*S. marcescens* #42 with the *arnA* lipid modification gene removed	This study
S. marcescens ΔarnT	*S. marcescens* #42 with the *arnT* lipid modification gene removed	This study
S. marcescens Δwza	*S. marcescens* #42 with the *wza* capsule exporter gene removed	This study
S. marcescens ΔFim3795-7	*S. marcescens* #42 with the *Fim3795, Fim3796* and *Fim3797* genes removed	This study
S. marcescens ΔFim4264-6	*S. marcescens* #42 with the *Fim4264, Fim4265* and *Fim4266* genes removed	This study

Table 2.1.2: Bacterial strains used in Chapter 4 & 5. CC: Callum Clark; LH: Laura Hollis (MSci Student 2021); RT: Mr Rob Till. Strains with the initials RT were kindly made by Mr Rob Till, at the request of CC. Strains with the initials “LH with CC” were made by Laura Hollis, under the supervision of CC.

Strain	Description	Source
B. bacteriovorus HD100	Wild-type *B. bacteriovorus* Type strain. Genome sequenced. NCBI Taxonomy ID: 264462 GenBank Accession: GCA_000196175.1	(278, 281)
E. coli NEB5α	*E. coli* DH5α cloning strain. Endonuclease negative.	(789)
E. coli S17-1	Strain used as prey for *B. bacteriovorus* Strain used for conjugation of mobilizable plasmids into *B. bacteriovorus* HD100. NCBI Taxonomy ID: 1227813 GenBank Accession: GCA_000340255.1	(789, 790)
E. coli S17-1 pZMR100	An *E. coli* S17-1 strain used as prey for *B. bacteriovorus* exconjugants containing the pZMR100 plasmid conferring kanamycin resistance.	(791)
B. bacteriovorus HD100 *bd0064mCerulean*	*B. bacteriovorus* containing a 3' tagged, homologous integrated *mCerulean3* tagged *bd0064* gene.	Raghunathan et al., 2019
B. bacteriovorus HD100 *bd0064mCherry*	*B. bacteriovorus* containing a 3' tagged, homologous integrated *mCherry* tagged *bd0064* gene.	Willis et al., 2016
B. bacteriovorus HD100 *bd0017mCerulean*	*B. bacteriovorus* HD100 containing an *mCerulean3* 3'- tagged *bd0017* gene. Kanamycin resistant.	This study (LH with CC)
B. bacteriovorus HD100 *bd0017mCherry*	*B. bacteriovorus* HD100 containing an *mCherry* 3'- tagged *bd0017* gene. Kanamycin resistant. Kanamycin resistant.	This study (LH with CC)
B. bacteriovorus HD100 *bd0295mCerulean*	*B. bacteriovorus* HD100 containing an *mCerulean3* 3'- tagged *bd0295* gene. Kanamycin resistant.	This study
B. bacteriovorus HD100 *bd0295mCherry*	*B. bacteriovorus* HD100 containing an *mCherry* 3'- tagged *bd0295* gene. Kanamycin resistant.	This study
B. bacteriovorus HD100 *bd0798mCerulean*	*B. bacteriovorus* HD100 containing an *mCerulean3* 3'- tagged *bd0798* gene. Kanamycin resistant.	This study
B. bacteriovorus HD100 *bd0798mCherry*	*B. bacteriovorus* HD100 containing an *mCherry* 3'- tagged *bd0798* gene. Kanamycin resistant.	This study
B. bacteriovorus HD100 *bd0799mCerulean*	*B. bacteriovorus* HD100 containing an *mCerulean3* 3'- tagged *bd0799* gene. Kanamycin resistant.	This study
B. bacteriovorus HD100 *bd0799mCherry*	*B. bacteriovorus* HD100 containing an *mCherry* 3'- tagged *bd0799* gene. Kanamycin resistant.	This study (RT)
B. bacteriovorus HD100 *bd1154mCerulean*	*B. bacteriovorus* HD100 containing an *mCerulean3* 3'- tagged *bd1154* gene. Kanamycin resistant.	This study

B. bacteriovorus HD100 *bd1154mCherry*	*B. bacteriovorus* HD100 containing an *mCherry* 3'- tagged *bd1154* gene. Kanamycin resistant.	This study (RT)
B. bacteriovorus HD100 *bd1155mCerulean*	*B. bacteriovorus* HD100 containing an *mCerulean3* 3'- tagged *bd1155* gene. Kanamycin resistant.	This study
B. bacteriovorus HD100 *bd1155mCherry*	*B. bacteriovorus* HD100 containing an *mCherry* 3'- tagged *bd1155* gene. Kanamycin resistant.	This study (RT)
B. bacteriovorus HD100 *bd1401mCherry*	*B. bacteriovorus* HD100 containing an *mCherry* 3'- tagged *bd1401* gene. Kanamycin resistant.	This study (RT)
B. bacteriovorus HD100 *bd1815mCerulean*	*B. bacteriovorus* HD100 containing an *mCerulean3* 3'- tagged *bd1815* gene. Kanamycin resistant.	This study
B. bacteriovorus HD100 *bd1815mCherry*	*B. bacteriovorus* HD100 containing an *mCherry* 3'- tagged *bd1815* gene. Kanamycin resistant.	This study
B. bacteriovorus HD100 *bd2517mCerulean*	*B. bacteriovorus* HD100 containing an *mCerulean3* 3'- tagged *bd2517* gene. Kanamycin resistant.	This study
B. bacteriovorus HD100 *bd2518mCerulean*	*B. bacteriovorus* HD100 containing an *mCerulean3* 3'- tagged *bd2518* gene. Kanamycin resistant.	This study
B. bacteriovorus HD100 *bd2620mCerulean*	*B. bacteriovorus* HD100 containing an *mCerulean3* 3'- tagged *bd2620* gene. Kanamycin resistant.	This study
B. bacteriovorus HD100 *bd3203mCerulean*	*B. bacteriovorus* HD100 containing an *mCerulean3* 3'- tagged *bd3203* gene. Kanamycin resistant.	This study
B. bacteriovorus HD100 Δ*bd0295*	*B. bacteriovorus* HD100 with the Δ*bd0295* gene removed	This study
B. bacteriovorus HD100 Δ*bd0798*	*B. bacteriovorus* HD100 with the Δ*bd0798* gene removed	This study
B. bacteriovorus HD100 Δ*bd0799*	*B. bacteriovorus* HD100 with the Δ*bd0799* gene removed	This study (RT)
B. bacteriovorus HD100 Δ*bd1154*	*B. bacteriovorus* HD100 with the Δ*bd1154* gene removed	This study (RT)
B. bacteriovorus HD100 Δ*bd1155*	*B. bacteriovorus* HD100 with the Δ*bd1155* gene removed	This study (RT)
B. bacteriovorus HD100 Δ*bd0798*Δ*bd1154*	*B. bacteriovorus* HD100 with the Δ*bd0798* and Δ*bd1154* genes removed	This study
B. bacteriovorus HD100 Δ*bd0799*Δ*bd1155*	*B. bacteriovorus* HD100 with the Δ*bd0799* and Δ*bd1155* genes removed	This study (RT)
B. bacteriovorus HD100 Δ*bd1401*	*B. bacteriovorus* HD100 with the Δ*bd1401* gene removed	This study (RT)
B. bacteriovorus HD100 Δ*bd1815*	*B. bacteriovorus* HD100 with the Δ*bd1815* gene removed	This study
B. bacteriovorus HD100 Δ*bd2620*	*B. bacteriovorus* HD100 with the Δ*bd2620* gene removed	This study
B. bacteriovorus HD100 Δ*bd3203*	*B. bacteriovorus* HD100 with the Δ*bd3203* gene removed	This study

Table 2.3.1: Primers used for gene knockout construction and validation in Chapter 3

Reference	Description	Primer sequence
arnA_UpFl_F	Gibson assembly primers for the generation of the upstream fragment of the gene knockout construct of *arnA*	tcatgtccccccccccccctgcaggGTCTTCTGTTGTGGAGTCTTTAC
arnA_UpFl_R		aagtagtccagcgCATCATTCTTCTTCCTGAGTATTG
arnA_DwFl_F	Gibson assembly primers for the generation of the downstream fragment of the gene knockout construct of *arnA*	aagaagaatgatgCGCTGGACTACTTCCTGCG
arnA_DwFl_R		gttgctgcttctacttatggtacccgggCTCATCCGGCTGCCACAG
arnA-Fl Seq F	Primer for sequencing the inserted construct (and surrounding genome) to confirm gene removal	CGCAGCTTTCTTTGCCGAAT
arnA-Fl Seq R		TTTTCGCCAAACAGCCACTG
arnT_UpFl_F1	Gibson assembly primers for the generation of the upstream fragment of the gene knockout construct of *arnT*	tcatgtccccccccccccctgcaggtacgctggactacttcctg
arnT_UpFl_R1		ttcatgcgatccacttcatgtaacgtccttac
arnT_DwFl_F	Gibson assembly primers for the generation of the downstream fragment of the gene knockout construct of *arnT*	acgttacatgaagTGGATCGCATGAACCGCC
arnT_DwFl_R		gttgctgcttctacttatggtacccgggTAGAGTCCGCCAGGCGGC
arnT-Fl Seq F	Primer for sequencing the inserted construct (and surrounding genome) to confirm gene removal	CTTCAACAACCATCCGCTGC
arnT-Fl Seq R		TGCATGTCAAAACGATCGCG
Wza_UpFL_F	Gibson assembly primers for the generation of the upstream fragment of the gene knockout construct of wza	tcatgtccccccccccccctgcaggACATATTCCGCTGGTCGG
Wza_UpFL_R		ggagttaccagttCGGCATCAAAAGAGGCAAATG
Wza_DwFL_F	Gibson assembly primers for the generation of the downstream fragment of the gene knockout construct of wza	tcttttgatgccgAACTGGTAACTCCGCAGG
Wza_DwFL_R		gttgctgcttctacttatggtacccgggAGGTCAGCTCATTGAGCTG
Wza-Fl Seq F	Primer for sequencing the inserted construct (and surrounding genome) to confirm gene removal	CGTGCTTATTCGCTGGAGGA
Wza-Fl Seq R		GCATTTTCGGTAGCGTCTGC
Fim_3795-97_UpFl_F	Gibson assembly primers for the generation of the upstream fragment of the gene knockout construct of *fim3795-7*	tcatgtccccccccccccctgcaggTTGAAAAACGGCGGCAAATC
Fim_3795-97_UpFl_R		cgtattagtcgtaAAGCATAATAAAGTCCTTTCAATAACGAATTAAC
Fim_3795-97_DwFl_F	Gibson assembly primers for the generation of the downstream fragment of the gene knockout construct of *fim3795-7*	ctttattatgcttTACGACTAATACGCCGCTTGC
Fim_3795-97_DwFl_R		gttgctgcttctacttatggtacccgggACCCCGGCGCACAGATAG
Fim 3795-97-Fl Seq F	Primer for sequencing the inserted construct (and surrounding genome) to confirm gene removal	CGATCAGGGACACGGTAAGG
Fim 3795-97-Fl Seq R		TGAACAGCAGAGCGACACAG
Fim_4264-66_UpFl_F t	Gibson assembly primers for the generation of the upstream fragment of the gene knockout construct of *fim4264-6*	catgtccccccccccccctgcaggGATTCCTTCCACAGCTTTC
Fim_4264-66_UpFl_R		cccatggccgcttATTCATAAGGCCCCTCTTG
Fim_4264-66_DwFl_F		gggccttatgaatAAGCGGCCATGGGATATC

Fim_4264-66_DwFl_R	Gibson assembly primers for the generation of the downstream fragment of the gene knockout construct of *fim4264-6*	gttgctgcttctacttatggtacccgggATAAAGGTCTCTTTCACTTCGTTC
Fim 4264-66-Fl Seq F	Primer for sequencing the inserted construct (and surrounding genome) to confirm gene removal	ATATCGTACGCGCCGTAGTG
Fim 4264-66-Fl Seq R		CGCTGATAAACGCGGCATAA

Table 2.3.2: Plasmids used in the work detailed in Chapter 3. Strains initialed with DR were made by Dr Dhaarini Raghunathan as part of a previous project in the lab.

Plasmid	Description	Source
pSC2301	A suicide vector used to introduce gene knockout constructs into *S. marcescens.* Contains an apramycin resistance cassette	Gift from Dr Sarah Coulthurst (University of Dundee)
pSC2301ΔarnA	*pSC2301* plasmid containing an *arnA* gene knockout construct for conjugation into *S. marcescens* and subsequent gene removal	This study (DR)
pSC2301ΔarnT	*pSC2301* plasmid containing an *arnT* gene knockout construct for conjugation into *S. marcescens* and subsequent gene removal	This study (DR)
pSC2301Δwza	*pSC2301* plasmid containing a *wza* gene knockout construct for conjugation into *S. marcescens* and subsequent gene removal	This study (DR)
pSC2301ΔFim3795-7	*pSC2301* plasmid containing a *Fim3795, Fim3796* and *Fim3797* gene knockout construct for conjugation into *S. marcescens* and subsequent gene removal	This study (DR)
pSC2301ΔFim4264-6	*pSC2301* plasmid containing a *Fim4264, Fim4265* and *Fim4266* gene knockout construct for conjugation into *S. marcescens* and subsequent gene removal	This study (DR)

Table 2.4.1: Primers used for fluorescent tagging of candidate genes in Chapter 4. * The same primers were used to generate mCherry tagged equivalents, using the mCherry plasmid pAKF26 as a template in place of pmCerulean3-N1.

Primer name	Description	Sequence
Bd0295mCer_F*	Gibson assembly primers for the generation of an *mCerulean3* tagged *bd0295,* amplifying the *bd0295* and *mCerulean3* genes respectively.	cgttgtaaaacgacggccagtgccaATGAAAAGAATGTTGCTTGTC
Bd0295mCer_R*		ccttgctcaccatAAGGGCCTGAATCACTCC
Bd0295mCerulean_F*		gattcaggcccttATGGTGAGCAAGGGCGAG
Bd0295mCerulean_R*		ggaaacagctatgaccatgattacgTTACTTGTACAGCTCGTCCATG
Bd0798mCer_F*	Gibson assembly primers for the generation of an *mCerulean3* tagged *bd0798,* amplifying the *bd0798* and *mCerulean3* genes respectively.	cgttgtaaaacgacggccagtgccaATGAAAAAGACACTCACAACATC
Bd0798mCer_R*		ccttgctcaccatGTCTAATCCCAATTTGGC
Bd0798mCerulean_F*		attgggattagacATGGTGAGCAAGGGCGAG
Bd0798mCerulean_R*		ggaaacagctatgaccatgattacgTTACTTGTACAGCTCGTCCATG
Bd0799mCer_F*	Gibson assembly primers for the generation of an *mCerulean3* tagged *bd0799,* amplifying the *bd0799* and *mCerulean3* genes respectively.	cgttgtaaaacgacggccagtgccaATGAGAACGTGGGCAGACTATCTTAAG
Bd0799mCer_R*		ccttgctcaccatACCTCGTGCGGGGATGAAG
Bd0799mCerulean_F*		ccccgcacgaggtATGGTGAGCAAGGGCGAG
Bd0799mCerulean_R*		ggaaacagctatgaccatgattacgTTACTTGTACAGCTCGTCCATG
Bd0799mCh_F	Gibson assembly primers for the generation of an *mCherry* tagged *bd0799* with a flexible peptide linker inbetween (as tag forced a mutation), amplifying the *bd0799* and *mCherry* gene and a flexible peptide linker.	CGTTGTAAAACGACGGCCAGTGCCAATGAGAACGTGGGCAGACTATCTTAAG
Bd0799mCh_R		CCGCCGCTACCGCCACCTCGTGCGGGGATGAAG
Bd0799mCherry_F		CCCCGCACGAGGTGGCGGTAGCGGCGGCGGT
Bd0799mCherry_R		GGAAACAGCTATGACCATGATTACGTTACTTGTACAGCTCGTCCATG
Bd1154mCer_F*	Gibson assembly primers for the generation of an *mCerulean3* tagged *bd1154,* amplifying the *bd1154* and *mCerulean3* genes respectively.	cgttgtaaaacgacggccagtgccaATGCTTAAGGGGTCGTTCAAAATTC
Bd1154mCer_R*		ccttgctcaccatATGATGGGCACTGCCACTTTC
Bd1154mCerulean_F*		cagtgcccatcatATGGTGAGCAAGGGCGAG
Bd1154mCerulean_R*		ggaaacagctatgaccatgattacgTTACTTGTACAGCTCGTCCATG
Bd1155mCer_F*	Gibson assembly primers for the generation of an *mCerulean3* tagged *bd1155,* amplifying the *bd1155* and *mCerulean3* genes respectively.	cgttgtaaaacgacggccagtgccaATGGCGACCTGGGAAGAATATAAAAAG
Bd1155mCer_R*		ccttgctcaccatAGCTTCCGGTGTTGGCCG
Bd1155mCerulean_F*		aacaccggaagctATGGTGAGCAAGGGCGAG
Bd1155mCerulean_R*		ggaaacagctatgaccatgattacgTTACTTGTACAGCTCGTCCATG
Bd1401mCh_F*		taaaacgacggccagtgccaATGTACAAAGCCCTTAGTAAAG

Bd1401mCh_R*	Gibson assembly primers for the generation of an *mCherry* tagged *bd1401,* amplifying the *bd1401* and *mCherry* genes respectively.	tgctcaccatCTTGATCACAGGCTTTGAC
Bd1401mCherry_F*		tgtgatcaagATGGTGAGCAAGGGCGAG
Bd1401mCherry_R*		cagctatgaccatgattacgTTACTTGTACAGCTCGTCCATG
Bd1815mCer_R*	Gibson assembly primers for the generation of an *mCerulean3* tagged *bd1815,* amplifying the *bd1815* and *mCerulean3* genes respectively.	cgttgtaaaacgacggccagtgccaATGAGTAAAAAGATTCTGGCTTTG
Bd1815mCer_R*		ccttgctcaccatGAAAATAAATCCGACCGTC
Bd1815mCerulean_F*		cggatttattttcATGGTGAGCAAGGGCGAG
Bd1815mCerulean_R*		ggaaacagctatgaccatgattacgTTACTTGTACAGCTCGTCCATG
Bd2517mCer_F	Gibson assembly primers for the generation of an *mCerulean3* tagged *bd2517,* amplifying the *bd2517* and *mCerulean3* genes respectively.	cgttgtaaaacgacggccagtgccaATGCAAACTATCATCAACACG
Bd2517mCer_R		ccttgctcaccatGATTTTACCAACCAGATCAAG
Bd2517mCerulean_F		ggttggtaaaatcATGGTGAGCAAGGGCGAG
Bd2517mCerulean_R		ggaaacagctatgaccatgattacgTTACTTGTACAGCTCGTCCATG
Bd2518mCer_F	Gibson assembly primers for the generation of an *mCerulean3* tagged *bd2518,* amplifying the *bd2518* and *mCerulean3* genes respectively.	cctgcaggtcgactctagagATGCTAGACTCTTCTCTTCTTG
Bd2518mCer_F		tgctcaccatAGAGTGATACATACGGTCTTC
Bd2518mCerulean_F		gtatcactctATGGTGAGCAAGGGCGAG
Bd2518mCerulean_R		cagctatgaccatgattacgTTACTTGTACAGCTCGTCCATG
Bd2620mCer_F	Gibson assembly primers for the generation of an *mCerulean3* tagged *bd2620,* amplifying the *bd2620* and *mCerulean3* genes respectively.	cctgcaggtcgactctagagTCCCTGTGCCGCAACAAAAAAG
Bd2620mCer_R		GGATTTATGACTGCGGATCATCC
Bd2620mCerulean_F		tgatccgcagtcataaatccATGGTGAGCAAGGGCGAG
Bd2620mCerulean_R		cagctatgaccatgattacgTTACTTGTACAGCTCGTCCATG
Bd3203mCer_F	Gibson assembly primers for the generation of an *mCerulean3* tagged *bd3203,* amplifying the *bd3203* and *mCerulean3* genes respectively.	cctgcaggtcgactctagagTCAAGCCGAAGCCCCAAG
Bd3203mCer_R		tgctcaccatGACGCCGGCTTGGCCTAC
Bd3203mCerulean_F		agccggcgtcATGGTGAGCAAGGGCGAG
Bd3203mCerulean_R		cagctatgaccatgattacgTTACTTGTACAGCTCGTCCATG
SurAmCh_F	Gibson assembly primers for the generation of an mCherry tagged *bd0017*	taaaacgacggccagtgccaTTGCTAGTGGCTACACCAAG
SurAmCh_R		tgctcaccatCTCATTGATACGGATGAACG
SurAmCherry_F		tatcaatgagATGGTGAGCAAGGGCGAG
SurAmCherry_R		cagctatgaccatgattacgTTACTTGTACAGCTCGTCCATG
SurAmCer_F	Gibson assembly primers for the generation of an mCerulean3 tagged *bd0017*	taaaacgacggccagtgccaTTGCTAGTGGCTACACCAAG
SurAmCer_R		tgctcaccatCTCATTGATACGGATGAACG
SurAmCerulean_F		tatcaatgagATGGTGAGCAAGGGCGAG
SurAmCerulean_R		cagctatgaccatgattacgTTACTTGTACAGCTCGTCCATG
SurA_mCh/mCerScrF		atacgtcgcatggcttgatg

Bd0295_ScrFwd*	Primer for checking construct integration into *B. bacteriovorus* exconjugants, binding approximately 50bp upstream of the target gene	gagcaaaagacaccgtggtt
Bd0798_ScrFwd*		Ggtgttatgagaacgtgggc
Bd0799_ScrFwd*		ATCGACGTAAACCTACCGCA
Bd1154_ScrFwd*		TAGAAAACGCCAGGGTCAGA
Bd1155_ScrFwd*		GCTGCTGGATAATATCGCCG
Bd1401mCherry_ScrFwd*		catccggtaagagcagcaac
Bd1815_ScrFwd*		gcttgaaatggccgctatca
Bd2517_ScrFwd		cgtattccagctgcgtcaaa
Bd2518_ScrFwd		aatacatcgctgcaaaccca
Bd2620_ScrFwd		gatcttggcatcgtcgtcac
Bd3202_ScrFwd		ccatgtaaccgatcaagccg
SurAmCer/mCh_SeqF	Primer for sequencing the inserted construct in *B. bacteriovorus* exconjugants, binding approximately 200bp upstream of the target gene and covering the whole introduced region containing the gene and fluorescent tag.	GCTCTTTGATGGATGCCGAG
Bd0295_SeqFwd*		GAAACTCTGGTGCGCGTATT
Bd0798_SeqFwd*		CGGAGGAAGACAGGACAACT
Bd0798_SeqFwdII*		TTGCTGAAGTCGAACAAGCC
Bd0799_SeqFwd*		ATCGACGTAAACCTACCGCA
Bd1154_SeqFwd*		ACCAATGATGAAGGGGCAGA
Bd1155_SeqFwd*		CGTACGCCGTCAGATCGAGG
Bd1401mCherry_SeqFwd*		agtgattcatggagccagct
Bd1815_SeqFwd*		TCAGAAACCTTCCCCATGCT
Bd1815_SeqFwdII*		gaacaagagcgcctgtttga
Bd2517_SeqFwd		GGCCGTAACGCTGATGAATT
Bd2517_SeqFwdII		tttcagggtttcaaggctgc
Bd2518_SeqFwd		CGTTGATTCTGGCGATCCTG
Bd2518_SeqFwdII		CACTGTGATGGCCCCTTCTA
Bd2620_SeqFwd		TTGAAAACCAAAGCTCCGGG
Bd3202_SeqFwd		ctgatcccctgttgtgacct

Table 2.4.2: Plasmids used in Chapters 4 & 5. CC: Callum Clark; LH: Laura Hollis (MSci Student 2021); SH: Syawal Hazanan (MSci Student 2022); RT: Mr Rob Till; PR: Mr Paul Radford. Strains with the initials RT were kindly made by Mr Rob Till, at the request of CC. Strains with the initials “LH with CC” were made by Laura Hollis, under the supervision of CC. Strains with the initials “SH with PR” were made by Syawal Hazanan, under the supervision of Paul Radford.

Plasmid	Description	Source
pmCerulean3-N1	DNA template containing *mCerulean3* gene	AddGene (#54730)
pAKF26	DNA template containing *mCherry* gene	(342)
pZMR100	Plasmid conferring kanamycin resistance	(791)
pk18mobSacB	Suicide vector used for introduction and homologous recombination of *mCerulean3* or *mCherry* tagged genes or gene knockout constructs into *B. bacteriovorus.* Contains a kanamycin resistance cassette. *lacz*α for blue-white colony selection. *sacB* for sucrose counter-selection/curing of plasmid from exconjugants.	(792)
pbd0017mCerulean	A pk18*mobSacB* plasmid containing a *bd0017* gene with *mCerulean3* fused to the 3' terminus.	This study
pbd0017mCherry	A pk18*mobSacB* plasmid containing a *bd0017* gene with *mCherry* fused to the 3' terminus.	This study
pbd0295mCerulean	A pk18*mobSacB* plasmid containing a *bd0295* gene with *mCerulean3* fused to the 3' terminus.	This study
pbd0295mCherry	A pk18*mobSacB* plasmid containing a *bd0295* gene with *mCherry* fused to the 3' terminus.	This study
pbd0798mCerulean	A pk18*mobSacB* plasmid containing a *bd0798* gene with *mCerulean3* fused to the 3' terminus.	This study
pbd0798mCherry	A pk18*mobSacB* plasmid containing a *bd0798* gene with *mCherry* fused to the 3' terminus.	This study
pbd0799mCerulean	A pk18*mobSacB* plasmid containing a *bd0799* gene with *mCerulean3* fused to the 3' terminus.	This study (SH with PR)
pbd0799mCherry	A pk18*mobSacB* plasmid containing a *bd0799* gene with *mCherry* fused to the 3' terminus.	This study (RT)
pbd1154mCerulean	A pk18*mobSacB* plasmid containing a *bd1154* gene with *mCerulean3* fused to the 3' terminus.	This study (SH with PR)
pbd1154mCherry	A pk18*mobSacB* plasmid containing a *bd1154* gene with *mCherry* fused to the 3' terminus.	This study (SH with PR)
pbd1155mCerulean	A pk18*mobSacB* plasmid containing a *bd1155* gene with *mCerulean3* fused to the 3' terminus.	This study (SH with PR)
pbd1155mCherry	A pk18*mobSacB* plasmid containing a *bd1155* gene with *mCherry* fused to the 3'terminus.	This study (SH with PR)
pbd1401mCherry	A pk18*mobSacB* plasmid containing a *bd1401* gene with *mCherry* fused to the 3' terminus.	This study (RT)
pbd1815mCerulean	A pk18*mobSacB* plasmid containing a *bd1815* gene with *mCerulean3* fused to the 3' terminus.	This study
pbd1815mCherry	A pk18*mobSacB* plasmid containing a *bd1815* gene with *mCherry* fused to the 3' terminus.	This study
pbd2517mCerulean	A pk18*mobSacB* plasmid containing a *bd2517* gene with *mCerulean3* fused to the 3' terminus.	This study
pbd2518mCerulean	A pk18*mobSacB* plasmid containing a *bd2518* gene with *mCerulean3* fused to the 3' terminus.	This study
pbd2620mCerulean	A pk18*mobSacB* plasmid containing a *bd2620* gene with *mCerulean3* fused to the 3' terminus.	This study
pbd3203mCerulean	A pk18*mobSacB* plasmid containing a *bd3203* gene with *mCerulean3* fused to the 3' terminus.	This study
pk18mobSacBΔbd0017	A pk18*mobSacB* plasmid containing a *bd0017* gene knockout construct for conjugation into *B. bacteriovorus* HD100 and subsequent gene removal	This study
pk18mobSacBΔbd0295	A pk18*mobSacB* plasmid containing a *bd0295* gene knockout construct for conjugation into *B. bacteriovorus* HD100 and subsequent gene removal	This study
pk18mobSacBΔbd0798	A pk18*mobSacB* plasmid containing a *bd0798* gene knockout construct for conjugation into *B. bacteriovorus* HD100 and subsequent gene removal	This study
pk18mobSacBΔbd0799	A pk18*mobSacB* plasmid containing a *bd0799* gene knockout construct for conjugation into *B. bacteriovorus* HD100 and subsequent gene removal	Ellie Boardman (Unpublished)
pk18mobSacBΔbd1154	A pk18*mobSacB* plasmid containing a *bd1154* gene knockout construct for conjugation into *B. bacteriovorus* HD100 and subsequent gene removal	This study (SH with PR)

pk18mobSacBΔbd1155	A pk18*mobSacB* plasmid containing a *bd1155* gene knockout construct for conjugation into *B. bacteriovorus* HD100 and subsequent gene removal	Ellie Boardman (Unpublished)
pk18mobSacBΔbd1401	A pk18*mobSacB* plasmid containing a *bd1401* gene knockout construct for conjugation into *B. bacteriovorus* HD100 and subsequent gene removal	This study (RT)
pk18mobSacBΔbd1401-COMP	A pk18mobSacB plasmid containing a WT copy of the *bd1401* gene, along with 1kb of upstream and downstream flanking, to complement *bd1401* into the Δ*bd1401* gene deletion strain	This study (RT)
pk18mobSacBΔbd1815	A pk18*mobSacB* plasmid containing a *bd1815* gene knockout construct for conjugation into *B. bacteriovorus* HD100 and subsequent gene removal	This study
pk18mobSacBΔbd2517	A pk18*mobSacB* plasmid containing a *bd2517* gene knockout construct for conjugation into *B. bacteriovorus* HD100 and subsequent gene removal	This study
pk18mobSacBΔbd2518	A pk18*mobSacB* plasmid containing a *bd2518* gene knockout construct for conjugation into *B. bacteriovorus* HD100 and subsequent gene removal	This study
pk18mobSacBΔbd2620	A pk18*mobSacB* plasmid containing a *bd2620* gene knockout construct for conjugation into *B. bacteriovorus* HD100 and subsequent gene removal	This study
pk18mobSacBΔbd3203	A pk18*mobSacB* plasmid containing a *bd3203* gene knockout construct for conjugation into *B. bacteriovorus* HD100 and subsequent gene removal	This study

Table 2.4.3: Primers used for construction of gene knockout constructs in Chapter 4.

Primer name	Description	Sequence
dBd0017Upstream_fwd	Gibson assembly primers for the generation of the upstream fragment of the gene knockout construct of *bd0017*	TAAAACGACGGCCAGTGCCAAAATAAGGATTTGATCCGATGAAATTTTC
dBd0017Upstream_rev		TTTACTCATTGCCACAGTTTTTTCCACAATC
dBd0017Downstream_fwd	Gibson assembly primers for the generation of the downstream fragment of the gene knockout construct of *bd0017*	AAACTGTGGCAATGAGTAAACTTCGAATCGC
dBd0017Downstream_rev		CAGCTATGACCATGATTACGGTTGAAACATATATCACCTCAATTA
dBd0017_ScrF	Primer for sequencing the inserted construct (and surrounding genome) to confirm gene removal	CTGTCTTTCTCGGAATGGCG
dBd0017_ScrR		GGTGCGAATAAACGGGATCC
dBd0295Upstream_fwd	Gibson assembly primers for the generation of the upstream fragment of the gene knockout construct of *bd0295*	cctgcaggtcgactctagagAAGAACTCTGCACCGGGG
dBd0295Upstream_rev		gagtttcctgTTTCATAGGGATCCCCTTTCAG
dBd0295Downstream_fwd	Gibson assembly primers for the generation of the downstream fragment of the gene knockout construct of *bd0295*	ccctatgaaaCAGGAAACTCTGGTGCGC
dBd0295Downstream_rev		cagctatgaccatgattacgGGACAGACTTTGAAGGTGAAG
dBd0295_ScrF	Primer for sequencing the inserted construct (and surrounding genome) to confirm gene removal	CGGCTGAATCCACAAAGACC
dBd0295_ScrR		GTGACTTCCATTCTGCGCTT
dBd0798Upstream_fwd	Gibson assembly primers for the generation of the upstream fragment of the gene knockout construct of *bd0798*	cctgcaggtcgactctagagTACTATTTGTATTATACCCGGAAGAC
dBd0798Upstream_rev		gttagtctaaTTTCATAAATTAACCTCGTGCG
dBd0798Downstream_fwd	Gibson assembly primers for the generation of the downstream fragment of the gene knockout construct of *bd0798*	atttatgaaaTTAGACTAACGAAAGGGCTCG
dBd0798Downstream_rev		cagctatgaccatgattacgAAGCGGGTAACGCTTTGTTG
dBd0798_ScrF	Primer for sequencing the inserted construct (and surrounding genome) to confirm gene removal	cggatggaggactcgacag
dBd0798_ScrR		ggcatctacaaatcctgggc
dBd0799Upstream_fwd	Gibson assembly primers for the generation of the upstream fragment of the gene knockout construct of *bd0799*	cgttgtaaaacgacggccagtgccaCGAAAGGGCACGAATCGC
dBd0799Upstream_rev		tgcagacggcgccTCTCATAACACCTCTCTTGCTTTCAC
dBd0799Downstream_fwd	Gibson assembly primers for the generation of the downstream fragment of the gene knockout construct of *bd0799*	aggtgttatgagaGGCGCCGTCTGCAGGCTT

dBd0799Downstream_rev		ggaaacagctatgaccatgattacgGTCGTCCTTGCAGCATCTTATCCG
dBd0799_ScrF	Primer for sequencing the inserted construct (and surrounding genome) to confirm gene removal	gggttctttgcggtcatagc
dBd0799_ScrR		agttgtcctgtcttcctccg
dBd1154Upstream_fwd	Gibson assembly primers for the generation of the upstream fragment of the gene knockout construct of *bd1154*	cgttgtaaaacgacggccagtgccaCACACCGCGATAGCTCAG
dBd1154Upstream_rev		cgccctaatgatgAAGCATAAGGACAAAGAATATTCC
dBd1154Downstream_fwd	Gibson assembly primers for the generation of the downstream fragment of the gene knockout construct of *bd1154*	tgtccttatgcttCATCATTAGGGCGGAGGATG
dBd154Downstream_rev		ggaaacagctatgaccatgattacgGGGCTTTCAAGATCGTCAG
dBd1154_ScrF	Primer for sequencing the inserted construct (and surrounding genome) to confirm gene removal	CAGAACTTGGCACCTTCCTG
dBd1154_ScrR		TGACCCGTGGATGTGATGAT
dBd1155Upstream_fwd	Gibson assembly primers for the generation of the upstream fragment of the gene knockout construct of *bd1155*	cgttgtaaaacgacggccagtgccaACTAAGTCCCGAGTCCTGCC
dBd1155Upstream_rev		gatatcaagcttcCGCCATACATCCTCCGCC
dBd1155Downstream_fwd	Gibson assembly primers for the generation of the downstream fragment of the gene knockout construct of *bd1155*	aggatgtatggcgGAAGCTTGATATCATATATAGAGAAAG
dBd1155Downstream_rev		ggaaacagctatgaccatgattacgATGTCAACCATAGGCTCTTAAAAG
dBd1155_ScrF	Primer for sequencing the inserted construct (and surrounding genome) to confirm gene removal	tgatttggtcggcaacaaca
dBd1155_ScrR		tcaaagtgaatgacggtgcg
dBd1401Upstream_fwd	Gibson assembly primers for the generation of the upstream fragment of the gene knockout construct of *bd1401*	taaaacgacggccagtgccaAGTCATACCTTTTAAACTCCATTTC
dBd1401Upstream_rev		attacttgatCTTGCACCAAGAAGAGTCAG
dBd1401Downstream_fwd	Gibson assembly primers for the generation of the downstream fragment of the gene knockout construct of *bd1401* dBd1401Upstream_fwd and dBd1401Downstream_rev were also used to generate the deleted *bd1401* gene fragment used to complement the *bd1401* gene back into the ∆*bd1401* gene deletion strain	ttggtgcaagATCAAGTAATTACTTGGCAAAGG
dBd1401Downstream_rev		cagctatgaccatgattacgGGATGATCAACTCCAAAGC
dBd1401_ScrF	Primer for sequencing the inserted construct (and surrounding genome) to confirm gene removal	tcgttggctcgcatgtaaag
dBd1401_ScrR		cttccggacgacactgagat

dBd1815Upstream_fwd	Gibson assembly primers for the generation of the upstream fragment of the gene knockout construct of *bd1815*	cctgcaggtcgactctagagTCCATTTTTTGACCGAGC
dBd1815Upstream_rev		tttagaaaatACTCATTCAACACTCCTTGTTTG
dBd1815Downstream_fwd	Gibson assembly primers for the generation of the downstream fragment of the gene knockout construct of *bd1815*	ttgaatgagtATTTTCTAAATAACAAGCAGCAGGTGATTTTAAAGGGC
dBd1815Downstream_rev		cagctatgaccatgattacgGCGGCGCTGTCGGCCAGG
dBd1815_ScrF	Primer for sequencing the inserted construct (and surrounding genome) to confirm gene removal	cgtcaggggatttggtgttg
dBd1815_ScrR		atctcccttaccgctttgcc
dBd1815_SeqF		AGTTCAGCCCTTTGATGGTG
dBd1815_SeqF2		TTTTAAAGGGCTTCCGTGTG
dBd2517Upstream_fwd	Gibson assembly primers for the generation of the upstream fragment of the gene knockout construct of *bd2517*	cctgcaggtcgactctagagTCAAAAGGAACCAAATGAC
dBd2517Upstream_rev		gatttgcctgAAAGCTTGAACTTTGAAATC
dBd2517Downstream_fwd	Gibson assembly primers for the generation of the downstream fragment of the gene knockout construct of *bd2517*	ttcaagctttCAGGCAAATCCACTCTGAAAC
dBd2517Downstream_rev		cagctatgaccatgattacgGGCCTTCGGTGTAAGTCAC
dBd2517_ScrF	Primer for sequencing the inserted construct (and surrounding genome) to confirm gene removal	ggcaaatcacagtcgcaaac
dBd2517_ScrR		ttctttctcaccttccacgc
dBd2518Upstream_fwd	Gibson assembly primers for the generation of the upstream fragment of the gene knockout construct of *bd2518*	cctgcaggtcgactctagagGCCATAACGTATTCCAGC
dBd2518Upstream_rev		gctttggcgcTAACATGTGACCTCCGTTC
dBd2518Downstream_fwd	Gibson assembly primers for the generation of the downstream fragment of the gene knockout construct of *bd2518*	tcacatgttaGCGCCAAAGCCGCCCTGG
dBd2518Downstream_rev		cagctatgaccatgattacgACGAGGCCCACAAAAGCTTTCCG
dBd2518_ScrF	Primer for sequencing the inserted construct (and surrounding genome) to confirm gene removal	tcccaaatcctcttccagct
dBd2518_ScrR		gaggtcacattcacttcggc
dBd2620Upstream_fwd	Gibson assembly primers for the generation of the upstream fragment of the gene knockout construct of *bd2620*	cctgcaggtcgactctagagAAGCTGGAAGAGGAACTG

dBd2620Upstream_rev		tggaagccgaTCTCATAATATTCCTCCTTGTC
dBd2620Downstream_fwd	Gibson assembly primers for the generation of the downstream fragment of the gene knockout construct of *bd2620*	tattatgagaTCGGCTTCCACGAAAAAGC
dBd2620Downstream_rev		cagctatgaccatgattacgCCCTTTCACCCTGGTCGTG
dBd2620_ScrF	Primer for sequencing the inserted construct (and surrounding genome) to confirm gene removal	aatacattcttgccgtcgcc
dBd2620_ScrR		ccacttcgttcggactgttc
dBd2620_ScrFII		AAAACTTGTCGATCAGGGCG
dBd2620_ScrRII		GCATCATGGCTGTCACGAAT
dBd3203Upstream_fwd	Gibson assembly primers for the generation of the upstream fragment of the gene knockout construct of *bd3203*	cctgcaggtcgactctagagCCACGTCCCCCATGAAGAC
dBd3203Upstream_rev		atcagacgccCTGACAGTGATGAGCTTTCGG
dBd3203Downstream_fwd	Gibson assembly primers for the generation of the downstream fragment of the gene knockout construct of *bd3203*	tcactgtcagGGCGTCTGATTTTTATTGTTTTTC
dBd3203Downstream_rev		cagctatgaccatgattacgTAACAATCACTGGGGTGTTC
dBd3203_ScrF	Primer for sequencing the inserted construct (and surrounding genome) to confirm gene removal	cggcgccattttgaaaactc
dBd3203_ScrR		agacaaagccaccatcctgt
dBd0295_IntFwd	A primer to check (after Sanger sequencing confirmation of gene knockout) for gene reintegration in another site of the *B. bacteriovorus* HD100 genome.	AGCGGTTCTGAAGACCATCA
dBd0295_IntRev		AATACGCGCACCAGAGTTTC
dBd0798_IntFwd		CCTTCCTGCGCTTTTCAACT
dBd0798_IntRev		GCCATAATCCGGATCGCATC
dBd0799_IntFwd		GCCGTTCGCCAAAATGACTA
dBd0799_IntRev		AGCTCATTGAACAGTCGCAC
dBd1154_IntFwd		GCGCTGAAGTTTTACACCGA
dBd1154_IntRev		CGGCGATATTATCCAGCAGC
dBd1155_IntFwd		GAAATGCGACGCTCACAGAT
dBd1155_IntRev		GATCACAGGCTTTGACTCCG
Bd1401_InternalFwd		GCGGAGGTTTGGAAATTCGT
Bd1401_InternalRev		CCAGATCCAAAGCCGTCATG
dBd1815_IntFwd		CCAATGGTGTGCTGGTGAAT
dBd1815_IntRev		AGCATGGGGAAGGTTTCTGA
dBd2620_IntFwd		AAAACGCCCATTCCCTGAAC

dBd2620_IntRev		AAAGTCACGGCACTGGTTTC
dBd3203_IntFwd		TCCCGAAAGCTCATCACTGT
dBd3203_IntRev		CAGGAGTGGGTTTGCGAAAA

Table 2.5.1: Details of the samples sent for Dual RNA Sequencing. Agilent Bioanalyser analysis of the 20 RNA samples proposed to be sent for Dual (Bacterial and Eukaryotic) RNA sequencing, consisting of 2 technical replicates for each of 5 timepoints (2-, 4-, 8-, 24- and 48-hours post *Bdellovibrio* uptake) for U937 Cell only controls and U937 + *Bdellovibrio* test samples. Samples highlighted in Red were excluded from further analysis due to a low RIN quality value.

Sample	Annotation	RNA Concentration (ng/μl)	rRNA ratio (28s/ 18s)	RNA Integrity Number (RIN)
1 (T2C)	U937s Only; 2 Hours; Replicate 1	35.0	2.0	9.8
2 (T2C)	U937s Only; 2 Hours; Replicate 2	33.0	2.0	9.0
3 (T2CBd)	U937s + *Bdellovibrio*; 2 Hours; Replicate 1	42.0	1.9	9.1
4 (T2CBd)	U937s + *Bdellovibrio*; 2 Hours; Replicate 2	42.0	2.0	9.8
5 (T4C)	U937s Only; 4 Hours; Replicate 1	22.0	1.8	9.1
6 (T4C)	U937s Only; 4 Hours; Replicate 2	44.0	2.2	9.3
7 (T4CBd)	U937s + *Bdellovibrio*; 4 Hours; Replicate 1	26.0	1.8	9.8
8 (T4CBd)	U937s + *Bdellovibrio*; 4 Hours; Replicate 2	25.0	1.9	9.2
9 (T8C)	U937s Only; 8 Hours; Replicate 1	12.0	1.8	9.9
10 (T8C)	U937s Only; 8 Hours; Replicate 2	41.0	2.1	9.8
11 (T8CBd)	U937s + *Bdellovibrio*; 8 Hours; Replicate 1	23.0	2.0	8.9
12 (T8CBd)	U937s + *Bdellovibrio*; 8 Hours; Replicate 2	56.0	1.9	9.8
13 (T24C)	U937s Only; 24 Hours; Replicate 1	32.0	1.8	9.2
14 (T24C)	U937s Only; 24 Hours; Replicate 2	45.0	1.9	9.4
15 (T24CBd)	U937s + *Bdellovibrio*; 24 Hours; Replicate 1	20.0	1.6	8.2
16 (T24CBd)	U937s + *Bdellovibrio*; 24 Hours; Replicate 2	36.0	1.6	7.5
17 (T48C)	U937s Only; 48 Hours; Replicate 1	24.0	1.8	9.0
18 (T48C)	U937s Only; 48 Hours; Replicate 2	24.0	0.0	2.5
19 (T48CBd)	U937s + *Bdellovibrio*; 48 Hours; Replicate 1	8.0	1.1	N/A
20 (T48CBd)	U937s + *Bdellovibrio*; 48 Hours; Replicate 2	33.0	1.8	9.1

Table 2.5.2: Number of reads obtained from each sequencing sample. T2C: PMA-differentiated U937 cells only; 2 hours; **T2CBd:** PMA-differentiated U937 cells with *Bdellovibrio*; 2 hours post-uptake; **T4C:** PMA-differentiated U937 cells only; 4 hours; **T4CBd:** PMA-differentiated U937 cells with *Bdellovibrio*; 4 hours post-uptake; **T8C:** PMA-differentiated U937 cells only; 8 hours; **T8CBd:** PMA-differentiated U937 cells with *Bdellovibrio*; 8 hours post-uptake; **T24C:** PMA-differentiated U937 cells only; 24 hours; **T24CBd:** PMA-differentiated U937 cells with *Bdellovibrio*; 24 hours post-uptake.

Sample Name	Sequencing File	Number of Reads
T2C	T2C_S3_R1_001.fastq.gz	47,380,238
T2CBd	T2CBd_S4_R1_001.fastq.gz	49,164,382
T4C	T4C_S5_R1_001.fastq.gz	45,893,254
T4CBd	T4CBd_S6_R1_001.fastq.gz	41,364,315
T8C	T8C_S7_R1_001.fastq.gz	45,209,959
T8CBd	T8CBd_S8_R1_001.fastq.gz	47,551,618
T24C	T24C_S9_R1_001.fastq.gz	47,906,541
T24CBd	T24CBd_S10_R1_001.fastq.gz	50,076,747

Table 2.5.3: A low number of reads successfully aligned to HD100 genome using Rockhopper software. T2C: PMA-differentiated U937 cells only; 2 hours; **T2CBd:** PMA-differentiated U937 cells with *Bdellovibrio*; 2 hours post-uptake; **T4C:** PMA-differentiated U937 cells only; 4 hours; **T4CBd:** PMA-differentiated U937 cells with *Bdellovibrio*; 4 hours post-uptake; **T8C:** PMA-differentiated U937 cells only; 8 hours; **T8CBd:** PMA-differentiated U937 cells with *Bdellovibrio*; 8 hours post-uptake; **T24C:** PMA-differentiated U937 cells only; 24 hours; **T24CBd:** PMA-differentiated U937 cells with *Bdellovibrio*; 24 hours post-uptake.

Sample Name	Sequencing File	Number of Reads	Reads successfully aligned to *Bdellovibrio* HD100 genome
T2CBd	T2CBd_S4_R1_001.fastq.gz	49,164,382	174448(0.35 %)
T4CBd	T4CBd_S6_R1_001.fastq.gz	41,364,315	106088 (0.26 %)
T8CBd	T8CBd_S8_R1_001.fastq.gz	47,551,618	63965 (0.13 %)
T24CBd	T24CBd_S10_R1_001.fastq.gz	50,076,747	99022 (0.20 %)

Table 2.5.4: Low percentage of reads mapping to HD100 genome, aligning to gene subsets. AS indicates antisense.

Sample	Percentage of HD100 mapped reads aligned to…								
	Protein coding genes		Ribosomal RNAs		Transfer RNAs		Miscellaneous RNAs		Unannotated regions
	Sense	AS	Sense	AS	Sense	AS	Sense	AS	
T2CBd	70	1	4	4	0	0	0	0	21
T4CBd	49	1	4	23	0	0	0	0	23
T8CBd	60	1	9	8	0	0	0	0	22
T24CBd	49	6	8	18	0	0	0	0	20